2008 MIDWEST LEVEE FAILURES: EROSION STUDIES

A Thesis

by

MICHELLE LEE BERNHARDT

Submitted to the Office of Graduate Studies of
Texas A&M University
in partial fulfillment of the requirements for the degree of

MASTER OF SCIENCE

December 2009

Major Subject: Civil Engineering

2008 MIDWEST LEVEE FAILURES: EROSION STUDIES

A Thesis

by

MICHELLE LEE BERNHARDT

Submitted to the Office of Graduate Studies of
Texas A&M University
in partial fulfillment of the requirements for the degree of

MASTER OF SCIENCE

Approved by:

Chair of Committee,	Jean-Louis Briaud
Committee Members,	Giovanna Biscontin
	Russell W. Jessup
Head of Department,	Mark Burris

December 2009

Major Subject: Civil Engineering

ABSTRACT

2008 Midwest Levee Failures: Erosion Studies. (December 2009)

Michelle Lee Bernhardt, B.S., Texas A&M University

Chair of Advisory Committee: Dr. Jean-Louis Briaud

The United States contains an estimated 100,000 miles (160000 km) of levees in which erosion related issues are the top priorities. Proper documentation of overtopping induced erosion is a complicated issue involving the collection and analysis of time-sensitive field data and personal observations. This thesis is a study of the performance of the Midwest Levee system during the 2008 flooding events.

The goal of the Midwest Levee investigation was to gather and analyze perishable data in an effort to provide a comprehensive overview at each breach location. To predict how a site will perform during a particular flood event, there are three main inputs: the flood conditions, the site conditions, and the soil properties. Site geometry and imperfections can greatly affect the performance of a levee system. Any low spots or potential seepage paths can concentrate the flow and be detrimental to the levee.

The vegetative cover is the single most important condition at a site. As seen in the Brevator case, vegetative armor can prevent failure of a levee comprised of less resistant soils subjected to long periods of overtopping. Recommended grasses include: Switchgrass, Smooth Brome, Reed Canarygrass, and Tall Fescue. It is also

recommended that grasses are kept at least 0.5 m tall during the flood season and to limit the presence of trees to 10 m beyond the levee toe.

The erosion resistance of the materials comprising the levee is also important. From the correlations in this study, it was determined that erodibility is influenced by grain size, relative compaction, clay content, and activity. Devices like the Torvane and Pocket Erodometer can also be used to get a quick field estimate of erosion. While these correlations and field devices give insight into an erodibility value, they are no substitute for site specific analysis with laboratory equipment such as the Erosion Function Apparatus. Soil behavior is highly nonlinear and the entire erosion function is needed to get an accurate measure of the erodibility of a soil. By combining these properties in an erosion matrix, a prediction of whether a site will withstand a given flood event can be made.

ACKNOWLEDGEMENTS

I would like to thank the members of my committee, Dr. Giovanna Biscontin, and Dr. Russell W. Jessup for their assistance throughout the course of this research. I would like to extend a special thanks to my advisor and committee chair, Dr. Jean-Louis Briaud for his guidance and support throughout the last few years. I am grateful for the encouragement he gave me to stay at Texas A&M and the effort he has made to make my graduate work a great experience.

Thanks also go to my friends and colleagues and the department faculty and staff for making my time at Texas A&M University an amazing experience. I would like to thank Stacey Tucker for help in the laboratory, Mat Leclair for his work using the EFA, Dekay Kim, Seok-Gyu Lim, and those who made up the 2008 Midwest Levee Reconnaissance team. I would also like to thank my family for their constant support.

This work was funded by both the National Science Foundation CMMI-GTE program under grant number 0842374 and the Spencer J. Buchanan Chair in the Zachry Department of Civil Engineering at Texas A&M University.

NOMENCLATURE

ASCE	American Society of Civil Engineers
ASTM	American Society for Testing and Materials
CSM	Cohesive Strength Meter
D_{50}	Mean Particle Diameter
DNR	Department of Natural Resources
EFA	Erosion Function Apparatus
ERDC	Engineering Research and Development Center
FEMA	Federal Emergency Management Agency
HET	Hole Erosion Test
HPS	Hurricane Protection System
ILIT	Independent Levee Investigation Team
ILPRC	Interagency Levee Policy Review Committee
IPET	Interagency Performance Evaluation Team
JET	Jet Erosion Test
MRGO	Mississippi River Gulf Outlet
NFIP	National Flood Insurance Program
PET	Pocket Erodometer Test
PI	Plasticity Index
RCT	Rotating Cylinder Test
SAST	Scientific Assessment and Strategy Team

UMRB	Upper Mississippi River Basin
USACE	United States Army Corps of Engineers
USCS	Unified Soil Classification System
USGS	United States Geological Survey
WRDA	Water Resources Development Act

TABLE OF CONTENTS

Page

Page

Page

Page

LIST OF FIGURES

Page

Page

Page

Page

Page

Page

Page

Page

Page

Page

Page

Page

Page

LIST OF TABLES

Page

Page

1. INTRODUCTION

In the United States alone, there are thousands of kilometers of earthen levees whose purpose is to provide flood protection. The United States Army Corps of Engineers (USACE) identifies levee overtopping as one of the top failure modes of earthen flood protection levees. Proper documentation of overtopping induced erosion is a complicated issue involving the collection and analysis of field data. It is extremely important that this time-sensitive data be collected before it is disturbed and before repairs to the levees and surrounding areas have been made. Exposed levee materials are more easily sampled and provide quantitative field data that can be used to validate empirical and numerical models, while personal observations during and after the breaching provide a qualitative explanation of the failure mechanisms.

Even with the appropriate data and documentation, the erosion phenomenon is still a complicated issue that is comprised of many different variables whose relations have yet to be fully explained. There is a need to find a link between the erosive nature of a soil and its index properties and site conditions such as, plasticity, grain size, compaction, and vegetative armor. The correct erodibility assessment of a soil is an important factor in the design and risk analysis of the world's earthen infrastructure.

The goal of the Midwest Levee reconnaissance was to gather perishable data in an effort to provide a comprehensive overview at each breach location. Laboratory

---

This thesis follows the style and format of the *Journal of Geotechnical and Geoenvironmental Engineering.*

testing was conducted to document the soil properties and site conditions and determine the erosion properties of the soils. This data was used to create an erosion matrix and a simplified method to identify potential erosion issues. Similar work done in New Orleans following Hurricanes Katrina and Rita proved that collection of this time-sensitive data is vitally important in characterizing the performance of levees. Information gained as a result of these studies can not only be used to evaluate the performance of the Midwest levee systems, but can be directly applied to the entire U.S. flood protection system and can hopefully lead to a better understanding of the failure modes of levees.

2. LEVEES AND EROSION

2.1 Earthen Embankments: What Is a Levee?

Earthen embankments can be dams, dikes, or levees. This study focuses solely on U.S. levee systems, particularly the Midwest Levee system. A levee is defined by the United States Army Corps of Engineers as an earthen embankment, or structure along a water course whose purpose is to provide flood damage reduction or water conveyance. Levees are designed to provide a specific level of temporary protection from seasonal high water for only a few days or weeks a year (USACE 2007). Contrary to what most Americans think, these levees are not designed to offer full protection. Levees can be classified as either urban or agricultural, each having different requirements. Urban levees provide flood reduction for communities, while agricultural levees provide reduced risk of flooding in lands used for agricultural purposes. According to USACE (2007), there are five main types of levees. Mainline and tributary levees are generally found parallel to the main water channel and its tributaries. Ring levees completely encircle an area from all directions. Setback levees are generally built as a second line of defense to an existing levee that has become endangered. Sublevees are constructed to control underseepage and often encircle areas landward of the main levee that are flooded. Spur levees provide protection by projecting off of the main levee and directing away river currents that could erode the main levee. Fig. 1 illustrates a common levee cross-section and some of the terminology often used to describe the various parts of a levee.

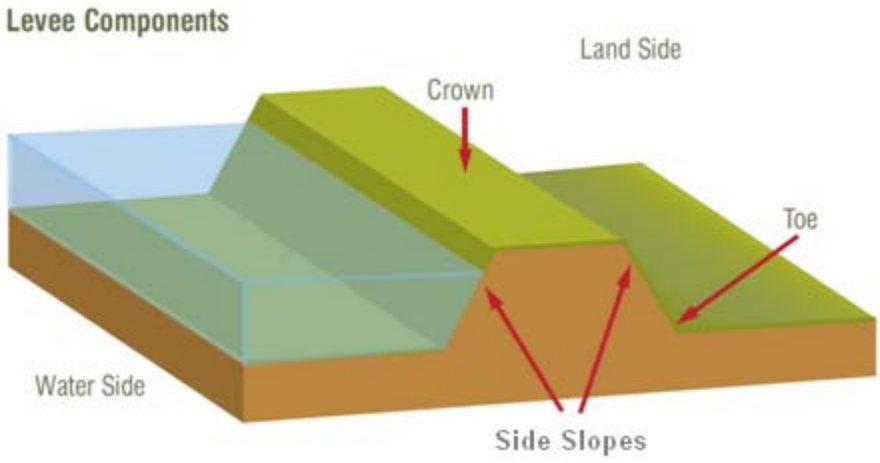

Fig. 1. Typical levee cross-section and terminology (adapted from Deretsky 2009)

There are two main types of levee construction: homogeneous and non-homogeneous. Homogeneous embankments, as shown in Fig. 1, are made of a single material, either clay or sand. The word homogeneous should be used lightly because most levees are constructed with fill taken from a borrow site and the materials are often not uniform throughout the soil deposit. Also, these types of levees are covered with some type of grass cover or vegetative armor helping to increase the surface erosion resistance. The influence of vegetation on erosion is discussed in Section 9. Non-homogeneous embankments are made of more than one material, usually a clay core with a sand shell. The preferred material for both the levee core and the homogeneous levee is a compacted cohesive clay, but the material used is often dependent on the soils available or the soils that are native to the area. Compacted clays tend to be more impermeable and more resistant to erosion than sand. The river side slopes of clay levees can range from 1:2 to 1:3 where as sand slopes must be lees steep at 1:5 (USACE

2009a). Even when soil types are closely chosen and monitored, levee systems consist of many kilometers and variability in soil and levee properties is inevitable.

2.2 Levees in the United States

In the United States alone, there are an estimated 100,000 miles (160,000 km) of levees, of which, 85 percent are locally owned and maintained (ASCE 2009). The remaining 15 percent are owned and maintained by government agencies such as the U.S. Army Corps of Engineers. Most of these levees were built many years ago in order to protect crops from flooding. These once agricultural areas have now been developed and homes and businesses are located behind the levees, increasing the risk to public health and safety. The Federal Emergency Management Agency (FEMA) estimates that approximately 22 percent of the nation's 3,147 counties contain levees (Fig. 2) and that 43 percent of the US population lives in these counties (ILPRC 2006).

Levees have been present on the North American continent even before European colonization. Native Americans built earthen mounds along rivers to protect themselves and their crops from flooding. Because water is a necessity for life, early societies developed near river banks, lakes, and coastal areas. As these communities and towns developed, seasonal river floods became an increasing issue. Primitive levees were "built" in an effort to protect these settlements from flooding, but were also developed as a way to retain flood waters so they could be used as drinking water or to irrigate crops in times of droughts (NCLS 2009).

Eventually, levees were constructed in coastal towns as well, not only to provide protection from flooding in river outlets, but to also provide protection from storm surges caused by hurricanes. At the time these levees were constructed, there was still no real design or engineering guidelines or requirements. The design was based simply on the understanding that the levee needed to be higher than the height of the flood waters (NCLS 2009).

The first recorded levee construction on the Mississippi was begun in 1717 (Mitchell 1990). The levee was 1 mi long, four ft high, and 18 ft across the crest and was erected to protect New Orleans, which was then only a small village. Levee construction was started on a large scale once Louisiana ceded to the United States and the work progressed up river and to additional basins. A large flood in 1897 proved that the levee heights were insufficient. For the first time, congress appropriated millions of dollars to improve and construct new levee structures.

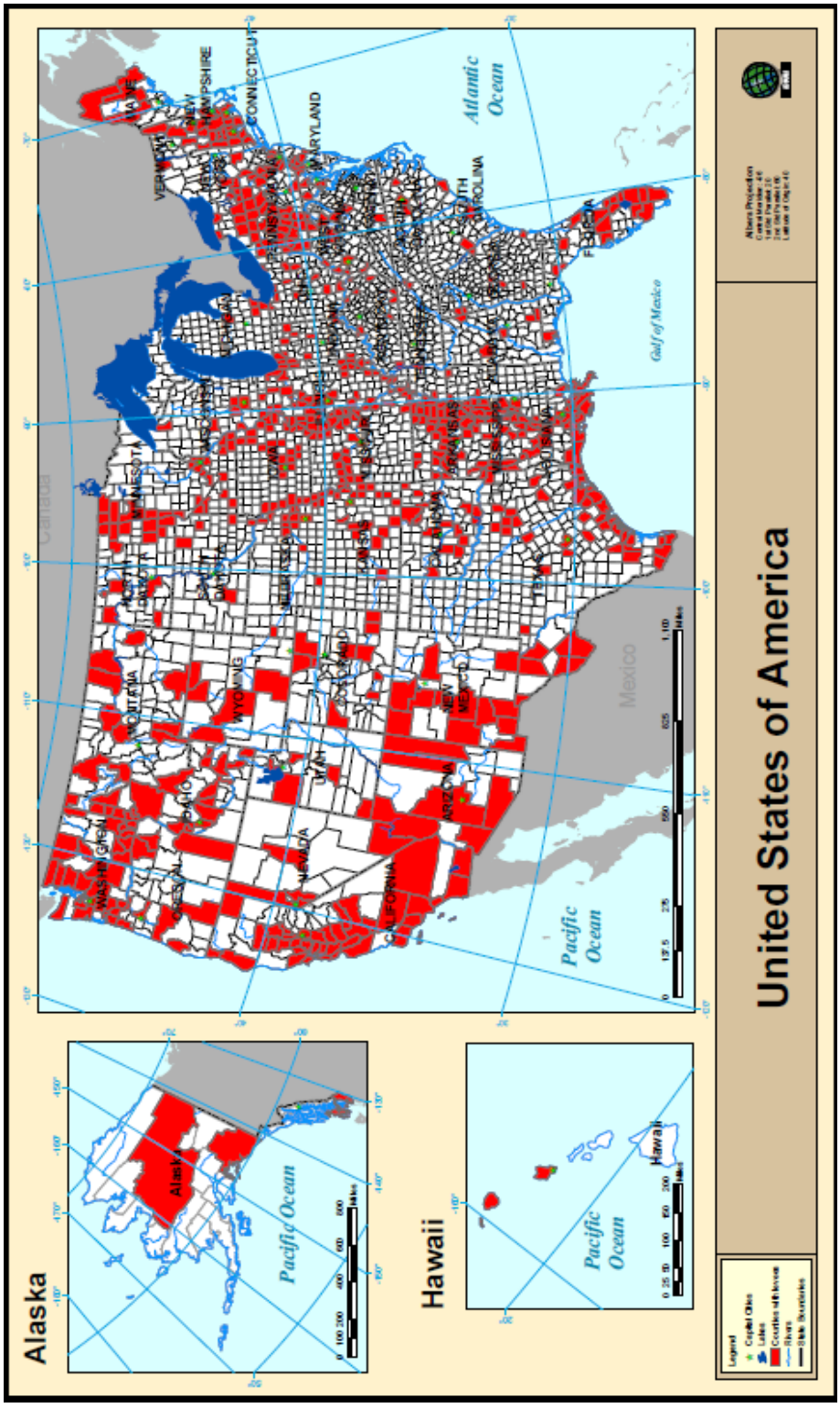

Fig. 2. Counties with levees in the U.S. (Tucker 2009)

It was not until the disastrous floods of the Mississippi and Ohio Rivers during the late 1920's and 1930's that the United States Government recognized the need for flood control policies (NCLS 2009). Fig. 3 shows Arkansas City residents camped out on the levees following the 1927 disaster. Levees were becoming more prevalent along major rivers, lakes, and coastal towns and these Flood Control Acts established federal interest in the levee design and construction executed by the Corps of Engineers at complete federal expense. Engineers often designed these structures to withstand 500 year and even 1,000 year floods estimated for that time period, which is much higher than those often found in America today (NCLS 2009).

Fig. 3. 1927 Flood victims on levee in Arkansas City, Arkansas (USACE 2009b)

The standards were lowered in 1968 when Congress enacted the National Flood Insurance Program (NFIP) (NCLS 2009). This program was created so that assistance for disastrous floods was not as heavily dependent on private insurance that most people could not afford. This act required anyone living in what was identified as a 100 year flood plain or higher to buy flood insurance; however, they would not be required to

purchase this flood insurance if the levee was "protecting" the area from a 100 year flood or less. The term "100 year flood" means there is a one percent chance that a flood event of that magnitude or more will occur in a given year, not that an event of that size will only occur every 100 years, which is the common misconception. With this policy, the NIFP unintentionally created a design standard for levees. Why build a higher levee if people didn't have to buy flood insurance if it was only built to a 100 year standard?

Limiting the height of the levee meant that it would require less material which saved the local and state governments a lot of money. Despite the disastrous flooding in California in the 1980's and the Great Flood in the Midwest in 1993, not much was done to change the levee standards. This can largely be attributed to the fact that although these floods caused billions of dollars in damage, the levees were mostly agricultural levees and there were not a lot of human casualties.

As a response to Hurricane Katrina in 2005, the U.S. Congress passed the Water Resources Development Act (WRDA) of 2007 in which they required a national levee database. Congress charged USACE with the task of building a database to inventory all federally and non-federally owned levees in the U.S. Despite current efforts, there is still no definite record of levees in the U.S. or any current condition and performance estimates, making it hard to know the most critical levees to begin remediation on. These aging levees deteriorate and require regular maintenance and upgrades which costs millions of dollars a year. Even with research efforts to improve the design and construction of new levees, riverbank soils are often complex and highly variable, hence much more uncertainty exists, yet the designers are required to provide adequate designs

with much less of a budget for exploration and testing. According to the American Society of Civil Engineers (ASCE 2009) Report Card for America's Infrastructure, levees overall in the US received a grade of "D-" and as of February 2009, results showed that approximately nine percent of levees inventoried by USACE are expected to fail in a flood event. Levees were one of only five forms of infrastructure to receive a D-, the lowest grade given. In this report card, each type of infrastructure was given a letter grade. This grade was based on condition, capacity, and funding versus need, and generally follows a traditional grading scale. The Advisory Council then reviews and adjusts the base grade to reflect positive or negative trends or the critical consequences if a catastrophic failure were to occur. ASCE also estimates the total investment needs for five years to exceed 50 billion dollars. This number is extremely large, but when compared to the damages in dollars from Katrina and the flooding events that occurred in the last two decades (Table 1), the spending appears to be justified.

Table 1. Damages in dollars from natural disasters (ASCE 2009).

Location/Year	Damages in Dollars
Midwest 1993	$272,872,070
North Dakota/Minnesota 1997	$152,039,604
Hurricane Katrina 2005	$16,467,524,782
Midwest 2008	$583,596,400

Source: National Committee on Levee Safety

For each infrastructure, the estimated five year funding requirement as well as the amount ASCE estimates will be spent in that time were compared. The investment for levees was on the low end compared to other infrastructures like roads at $380.5 billion. On the downside, ASCE predicts only 2.3 percent of the 50 billion dollars needed is expected to be appropriated and spent on levee improvements. This is the

lowest investment percentage of all other forms of infrastructure, as shown in red on the bar graph below (Fig. 4). The next lowest investment is public transit systems which are forecasted to receive up to 28 percent of its required funds. Despite warnings from ASCE and Congress getting involved in this troubling issue, the proper investment is still not being made to fix the country's levee problems. As population densities increase behind these levees, the effects of levee failures become even greater. It is important for the public to understand the risk of living near a levee and more must be done to push for local levee improvement.

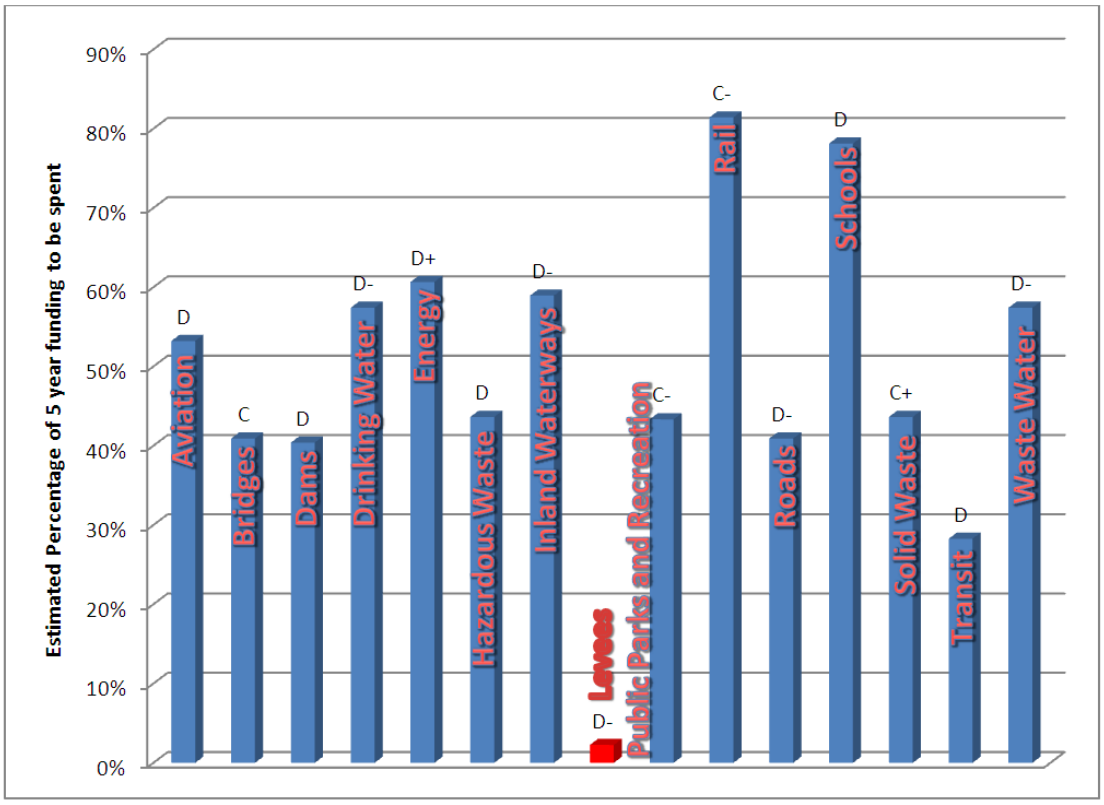

Fig. 4. Percentage of expected investment in dollars (Tucker 2009)

2.3 Failure Modes of Levees

Failure modes for earthen embankments include: excessive settlement, foundation failure, slope failure, seepage due to cracking or piping, and surface erosion. One or a combination of these can lead to breaching and failure of the levees in the event of some hazard. In the case of levees, breaching is said to have occurred when a part of the levee breaks away and flood waters are allowed to flow through. A breach can be a gradual or very sudden failure. For the purpose of this thesis, failure is defined at the point when the levee is no longer able to provide the protection that it was originally designed for. In other words, a levee that is overtopped by waters that exceed its design height is not considered a failure.

Excessive settlement over time or an inadequate levee design height can result in levee failure by allowing water to overtop the levee and flood the protected area (Phoon 2008). Excess weight from the water surcharge on either side of the levee can lead to slope instability and failure. As the slope fails, often times the crest is also removed lowering the height of the levee and allowing water to overtop, once again flooding the protected area. This slope failure leads to a reduction in levee cross-section and can allow throughseepage which weakens the levee and allows more water into the protected area. With any prolonged wetting event, there is also a threat of underseepage. This underseepage allows water through the more permeable foundation and is indicated by the presence of sand boils. Levees are often made of more high plasticity clays because of their ability to reduce seepage and resist erosion. In the hot, dry summer months these clays desiccate and cracks form. With sudden rewetting these cracks become

instant seepage paths and can also lead to slope failure. Probably the most obvious of all is surface erosion. Overtopping waters, flowing rivers, hurricane storm surges, or heavy precipitation can have detrimental effects on the surface of levees if they are not properly armored with vegetative cover.

Of the failure modes discussed above, the majority of all failures in the United States according to the US Army Corps of Engineers are due to erosion related issues. These can be one or a combination of mechanisms such as, erosion due to overtopping, internal or throughseepage erosion, or underseepage erosion. Fig. 5 shows a simplified drawing of these possible erosion failure modes.

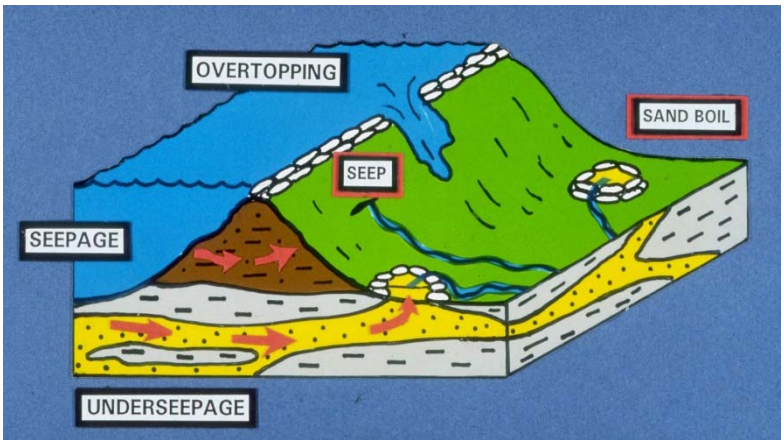

Fig. 5. Schematic of erosion failure modes (Martindale 2009)

2.4 Fundamentals of Erosion

This section presents a summary of the fundamentals of erosion as described by Briaud (2008) and Briaud et al. (2008). Every erosion problem has three main inputs: the soil, the water, and the shape or geometry of the obstruction that the water will encounter. For this study, soil is defined as an earthen element with measureable

properties such as grain size and plasticity that can be classified using the Unified Soil Classification System (USCS). Fig. 6 shows a free body diagram of the forces present on a soil particle located at the surface of the soil/water interface during no flow conditions (left), and during flow conditions (right). Notice the hydrostatic pressure around the soil particle is larger at the bottom during the flow condition, which in turn creates the buoyancy force that reduces the weight of objects under water.

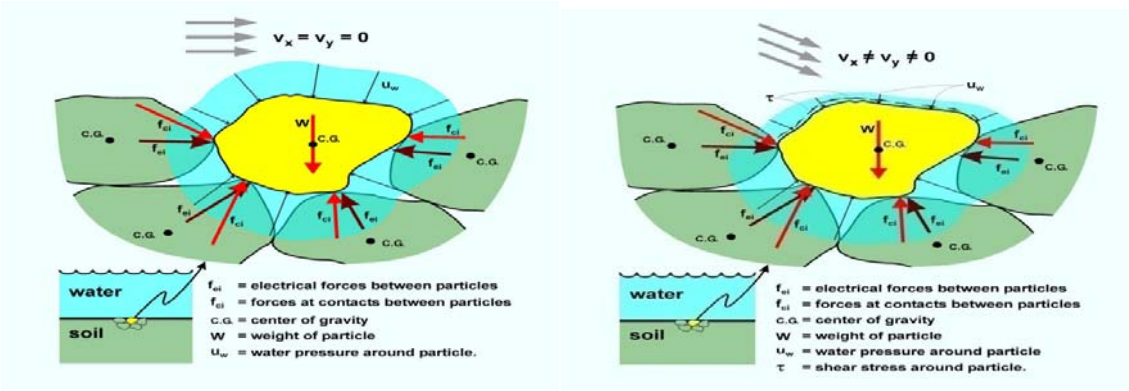

Fig. 6. No flow conditions (left), flow conditions (right) (Briaud 2008)

Under the flowing water conditions, a drag force and corresponding shear stresses appear at the interface between the soil particle and the water. Also, the normal stress on top of the particle decreases with the increasing water velocity and the normal and shear stresses located at the boundaries are also fluctuating with due to turbulence in the water. At higher velocities, the presence of such eddies, and vortices can greatly contribute to the erosion process. Note that in the cases where the soil exhibits low suction values (tensile stresses in the inter-particle water), the f_{ci} forces shown in the figures can be relatively large, at least until the presence of water decreases the suction.

Although represented in Fig. 6 as a single particle, the same mechanics hold true for a group of particles that are dislodged by the flowing water.

Erodibility is often thought about in terms of the erosion rate of a soil, Ż, that corresponds to a given velocity, υ. This definition has some problems because water velocity is a vector which varies with distance from the soil surface and is theoretically zero at the soil/water interface (Fig. 7).

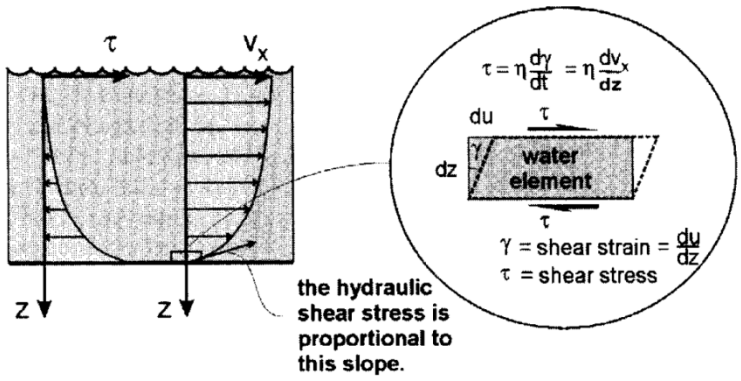

Fig. 7. Water velocity and shear stress profile (Briaud et al. 2008)

The water velocity is largest at the air/water interface and becomes zero at the soil/water interface. The corresponding shear stress created by the flowing water is largest at the soil/water interface and becomes near zero near the air/water interface. Because water is a Newtonian fluid, there is a linear relationship between shear stress and strain rate $d\gamma/dt$

$$\tau = \eta \left(\frac{d\gamma}{dt}\right) = \eta \left(\frac{dv}{dz}\right) \quad (1)$$

where η=viscosity of the water, v=water velocity, and z=depth of the water. The relationship that allows the equality with the second part of the equation is given in Fig. 7. This equation says that the shear stress is proportional to the gradient of the velocity

profile of the flow depth. This also implies that the shear stress at the water/soil interface is equal to the slope of the velocity profile at that interface. Any change in the water flow depth changes the mean water velocity, but may not change the profile at the water/soil interface, once again adding caution to the use of velocity as a tool to evaluate erosion.

Therefore, the erodibility of a soil is represented by that soil's erosion function which is defined as the relationship between the erosion rate, $\dot{Z}$, and the shear stress, τ, at the soil/water interface caused by the flowing water. This erosion function can be obtained using the Erosion Function Apparatus (EFA) or several other devices listed in a following section. The actual erosion process includes several other stress values and is given in complete form in Eq. 2:

$$\frac{\dot{Z}}{u}=\alpha\left(\frac{\tau-\tau_c}{\rho u^2}\right)^m+\beta\left(\frac{\Delta\tau}{\rho u^2}\right)^n+\delta\left(\frac{\Delta\sigma}{\rho u^2}\right)^p \quad (2)$$

where $\dot{Z}$=erosion rate (m/s), u=water velocity (m/s), τ=hydraulic shear stress, τ_c=threshold or critical shear stress below which no erosion occurs (N/m^2), ρ=mass density of water (kg/m^3), $\Delta\tau$=turbulent fluctuation of the hydraulic shear stress (N/m^2), $\Delta\sigma$=turbulent fluctuation of the net uplift normal stress (N/m^2), and all other quantities are parameters characterizing the soil being eroded. This model requires site specific determination of six variables which is highly impractical, so a more simple model is generally used:

$$\frac{\dot{Z}}{u}=\alpha\left(\frac{\tau-\tau_c}{\rho u^2}\right)^m \quad (3)$$

This model requires two parameters that can be determined by fitting the curve of the equation of the model to the erosion function. As will be discussed further in later sections, the erodibility of a soil varies for given velocities and often times there is not a single trend or regression line that can express the erosion rates for that soil at different velocities. Therefore, it is important to obtain the erosion function for each soil of interest in order to determine their erosive nature.

One of the most important values in an erosion study is the threshold value, below which no erosion occurs. This can be tracked as either a critical velocity, v_c, or critical shear stress, τ_c. These values are shown plotted versus D_{50}, or the average grain size of the soil also described as the diameter of which 50 percent of the particles are smaller (Figs. 8 and 9).

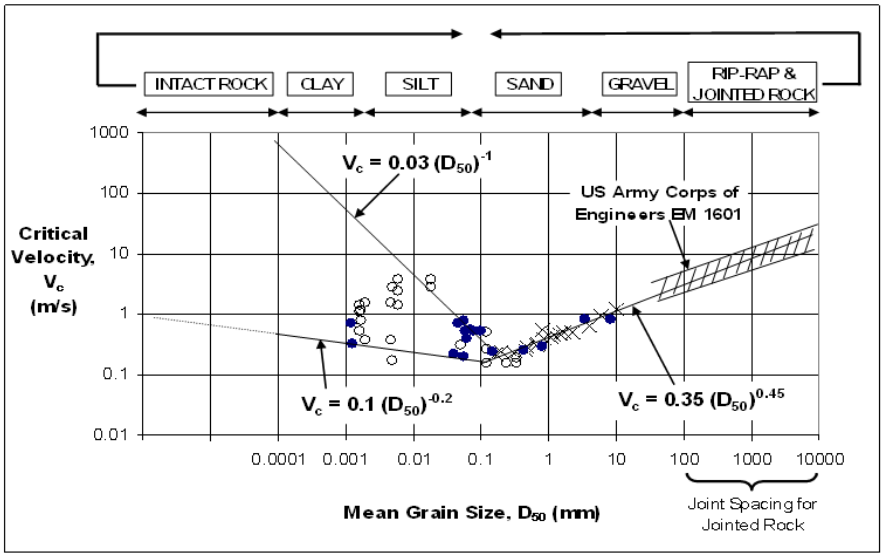

Fig. 8. Mean grain size vs. critical velocity (Briaud 2008)

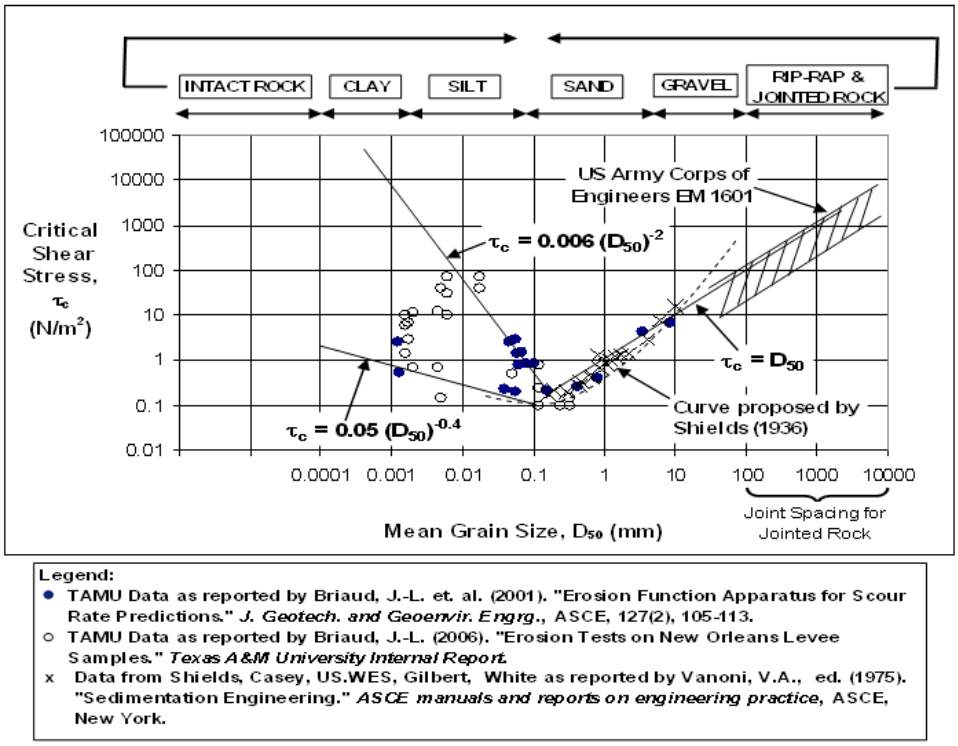

Legend:
- TAMU Data as reported by Briaud, J.-L. et. al. (2001). "Erosion Function Apparatus for Scour Rate Predictions." *J. Geotech. and Geoenvir. Engrg.*, ASCE, 127(2), 105-113.
- TAMU Data as reported by Briaud, J.-L. (2006). "Erosion Tests on New Orleans Levee Samples." *Texas A&M University Internal Report.*
- x Data from Shields, Casey, US.WES, Gilbert, White as reported by Vanoni, V.A., ed. (1975). "Sedimentation Engineering." *ASCE manuals and reports on engineering practice*, ASCE, New York.

Fig. 9. Mean grain size vs. critical shear stress (Briaud 2008)

The "V" shape of the graphs indicates that the clean fine sands are the most erodible. Increasing particle sizes to the right of 0.1 mm show an increase in erosion resistance, or higher threshold values. However, those particles with diameters less than 0.1 mm show no trend with decreasing grain size and threshold values. There are obviously other factors that come into play for fine grained soils. Many soil properties and even water properties affect a soil's erodibility. A few of these are listed in Table 2.

Table 2. Properties that affect erosion (Briaud 2008)

Soil water content	Soil dispersion ratio
Soil unit weight	Soil cation exchange cap
Soil plasticity index	Soil sodium absorption rat
Soil undrained shear str.	Soil pH
Soil void ratio	Soil temperature
Soil swell	Water temperature
Soil mean grain size	Water salinity
Soil percent passing #200	Water pH
Soil clay minerals	

Because each of these has a different influence on each soil it is impossible to determine the erodibility of a soil based on any one property and to include all of them would be extremely tedious. Several attempts to find correlations to this multi-variable problem have been made (Cao et al. 2002) and each has failed. Therefore, it is preferable to measure the erosion function directly and obtain an estimate of erosion for each flow condition.

The third input, the geometry of the obstruction, is also a concern. The geometry influences the flow of the water, the velocity of the water, and the turbulence created. Consider a pier in a river. The water flows down the river and must split and go around the pier. In order to maintain the flow rate, the water moving around the pier must accelerate. If this accelerated velocity (in some cases 1.5 times higher than the approach mean velocity) is higher than the critical velocity of the bed material, erosion also known as scour occurs around the pier. In the case of overtopping water on a levee, the geometry of the levee is such that the water is accelerated down the slope by gravity increasing the velocity of the flowing water. Depending on the height of the levee, this

velocity can reach magnitudes well over 6 m/s. This is well over the critical velocity for most typical levee soils and can result in major erosion at the toe of the levee. More explanation on determining the velocity and shear stress created by an obstacle can be found in Briaud (2008).

2.5 Erosion due to Overtopping

Overtopping waters create surface erosion by the same mechanics discussed in the preceding section. Water either from a river source or hurricane storm surge is pushed up and over the "wet" side of the levee. USACE has done many studies at their Engineer Research and Development Center (ERDC) focusing on the characteristics of overtopping waters and their effects on different slope conditions. Overtopping of levees produces fast-moving, turbulent water that moves as a sheet down the dry or land side slope and can wash away the protective grass cover and expose the soil (Fig. 10).

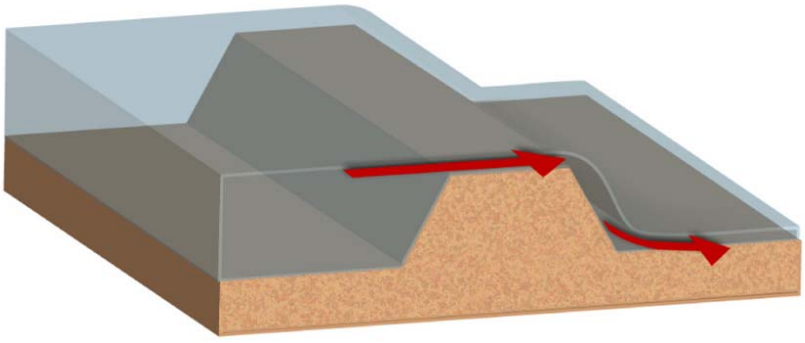

Fig. 10. Schematic of levee with overtopping flow (Deretsky 2009)

If the levee is overtopped long enough, the water may cut into the toe and erode the levee slope and perhaps the levee crest. The degree of damage is dependent on the depth and duration of the overtopping as well as the soil material properties. Erosion

and or headcutting occur at locations where there is a change in geometry or a discontinuity and progress in several stages (Fig. 11). Ralston (1987) pointed out that the headcut process is one of the key erosion mechanisms for cohesive embankments.

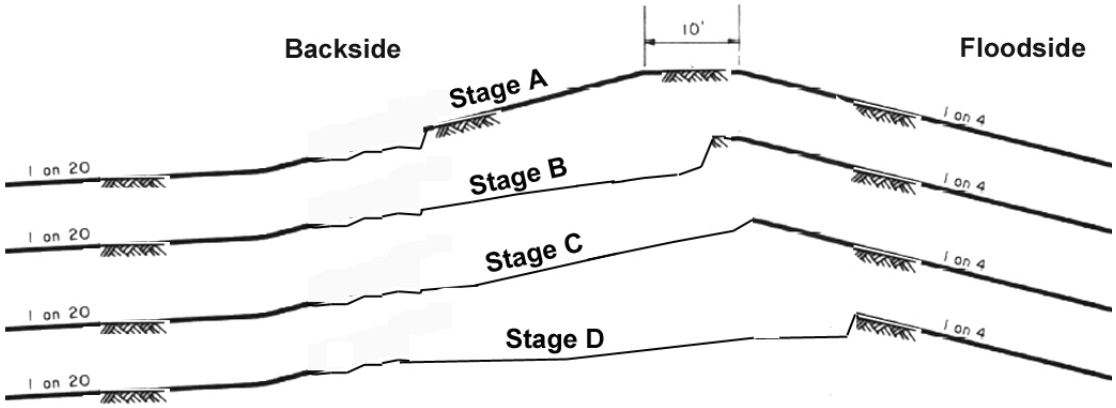

Fig. 11. Erosion and headcut progression (USACE 2009a)

Crown elevations for older levee systems may not have been designed with complete knowledge of all of the possible water elevations caused by the different hazard events. Even new levees may not be able to be constructed to withstand all extreme weather events because of a lack of funding, therefore, it is important that the land side slopes are well designed and protected by some type of vegetation or armoring. The ability to design the land side slopes requires estimates of the depth, velocities, and turbulence values of the overflowing water. USACE completed a study pertaining to the "Estimation of Combined Wave and Storm Surge Overtopping at Earthen Levees" (Hughes 2008). This work provides empirical equations that can be used in the estimation of several parameters of unsteady flow that result from a steady storm surge overflow with the addition of irregular waves for a typical levee cross-section. Hughes

and Nadal (2009) present similar work pertaining to "Shear Stress Estimates for Combined Wave and Surge Overtopping at Earthen Levees."

Extensive work has also been done on the topic in the Netherlands since the disaster of January 31, 1953 in which a storm during high tide raised the water level to record heights causing 150 levee breaches (Gerritsen 2006). The work has led to guidelines for their flood protection systems pertaining to design based on recurrence intervals, population density, soil properties, and vegetation protection (CROW 2002; Muijs 1999).

Erosion by overtopping water has been studied by many different groups. Some claim to have results that lead to correlations between the erosion rate and properties such as plasticity, unit weight, shear strength, or compaction while others prove differently. All studies, however, show that the erosion failure begins on the dry or land side of the levee. Several computer programs exist to simulate the different characteristics of levee erosion due to overtopping. These include: BREACH (Fread 1988), OVERFALL (AlQaser 1991), and SIMBA (Temple et al. 2005).

2.6 Introduction to the Erosion Function Apparatus (Briaud 2008)

As shown above, an accurate evaluation of the potential scour or erosion that can occur for a given flow rate is a critical step in levee design and risk assessment. Because of the many different factors that interact in the erosion phenomenon, it is important to be able to get a "real time" field or in situ erosion value for a given soil. Sample disturbance, density, and water content are all variables that affect the erosion rate and

must be considered before tests are performed. It is extremely important to get at least a field estimate of the erosion rate of a given soil at the time of sampling for situations in which erosion values are needed. By the time the soil has reached the lab for testing, there is a chance the some of the previously mentioned variables will have changed. Researchers have devised ways to obtain samples for testing that are as undisturbed as possible by proven sampling techniques in the field and physically going to the site to perform in situ erosion tests. The following paragraphs are summarized from information found in Leclair (2009).

In the last 20 years, several devices have been developed in an effort to quantify how erosive a soil is. The Erosion Function Apparatus (EFA) (Fig. 12) was developed in the early 1990s as a way of determining site specific erosion rates and ultimately the erosion function. ASTM standard 75 mm Shelby Tube samples are collected in the field at the site of interest within the depth of concern, brought back to the laboratory and tested in the EFA. The EFA can also be used for potential construction materials by reconstructing them in the sampling tube. The erosion rate of the material is measured at different velocities from which a chart of erosion rate versus velocity is created that also allows for the determination of an erosion category for the soil and the determination of a critical velocity and a critical shear stress for each test. These critical values can provide a quick check to determine whether or not erosion would occur for a particular event. This data can be used along with the data from a stream gage location in a computer program called the SRICOS-EFA (Scour Rate in Cohesive Soils http://ceprofs.tamu.edu/briaud/) (Briaud et al. 2004). The output results in a prediction

of the cumulative amount of erosion that would occur over time for a given event, hypothetical or real.

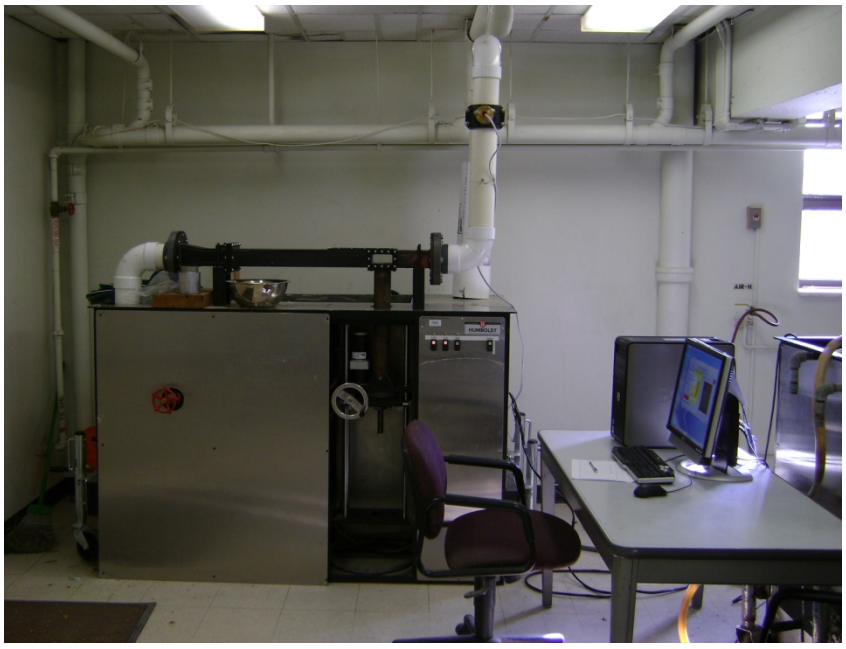

Fig. 12. Photograph of Erosion Function Apparatus (EFA)

2.6.1 How the Machine Operates

The EFA draws water through an intake in the bottom of the tank and pumps it through a gate valve and into the test section. The water flows through the pipe from left to right (Fig. 12), over the sample, and then is cycled back into the tank. The gate valve between the pump and beginning of the test section regulates the flow. A flow meter, located in the pipe, takes a measurement every second and relays them through a National Instruments Data Acquisition system to a computer. The sample is extruded into the pipe by a motorized piston which can be controlled by the operator through the

erosion program on the computer. The flow rate is converted to velocity by dividing by the cross-sectional area of the pipe and is displayed on the screen.

2.6.2 Test Procedure

Samples collected in the field using standard 75 mm Shelby Tubes and are taken back to the lab for testing in the EFA. The tube is fitted on the motorized piston base and the sample is extruded vertically out of the tube and trimmed flat to prepare it for testing. This is a critical step that is performed before each velocity stage to ensure there is only an insignificant pressure differential between the upstream and downstream ends of the sample. The base is raised so that the tube end is placed through an opening in the bottom of the rectangular cross-sectioned pipe and positioned so that the top of the tube is flush with the bottom inside surface of the pipe. The joint is sealed by a standard AS568A – 151 o-ring to prevent any leaks.

Typically, a range of velocities are determined prior to testing based on the material properties of the sample. When testing fine sand, the beginning velocity will be quite low compared to that of a high plasticity clay. Also, the site specific design flood, levee overtopping velocity, and other flow factors are taken into account when determining the most appropriate range. For most cases, the initial starting velocity of the EFA is set to approximately 0.3 m/s.

A computer data acquisition system collects the flow velocity data, the flow of water begins, and the sample is extruded 1 mm out of the tube into the flow. The sample is run until either 1 mm of erosion has occurred or 1 hour has elapsed. The test time

depends on the sample itself and the flow velocity. If the sample erodes very quickly, the sample is extruded out of the tube an extra millimeter and allowed to continue the erosion process, giving a better estimation of the amount of erosion over the period of time. The soil or rock is pushed out of the sampling tube only as fast as it is eroded by the water flowing over it. The velocity is measured by using a flow meter and is displayed on the computer screen. This procedure is repeated at several velocities, usually between 5 and 10. For each velocity, the erosion rate is measured by recording the eroded depth of the sample and dividing by the test time in hours. For instance, if the sample erodes 1 mm in 30 minutes of testing, the erosion rate is 2 mm/hr. Point by point the erosion function is obtained. When the test is complete, the sample is taken out of the EFA and discarded. The rest of the EFA data reduction uses empirically based equations of the hydraulics of closed-conduit piping and the Moody diagram to calculate the shear stress exerted by the flow of water as it flows over the soil. Several calculations must be performed in order to obtain the shear stress. The shear stress is based on the Moody Diagram and the following equation,

$$\tau = \frac{1}{8} \cdot f \cdot \rho \cdot V^2 \tag{4}$$

where τ is the hydraulic shear stress, f is the friction factor obtained from the Moody Diagram, ρ is the mass density of water (1000 kg/m^3), and V is the average velocity in the test section. The velocity is taken as the average over all of the one second interval readings taken during each velocity stage. The shear stress value is highly dependent on the velocity of the flow. Not only is the velocity component squared in the above equation, but the friction factor is also dependent on velocity through the Reynolds

Number used in the Moody Diagram. This chart pertains to closed-conduit pipe flow and uses a roughness parameter and hydraulic diameter to obtain the relative roughness. Using this parameter and the Reynolds Number,

$$\mathrm{Re} = \frac{\mu VD}{\rho} = \frac{VD}{\nu} \tag{5}$$

assuming that the kinematic viscosity of water, ν, is 1.12 * 10^{-6} m^2/s, the friction factor is determined iteratively using of the Colebrook Equation, for fully turbulent pipe flow given by

$$\frac{1}{\sqrt{f}} = -2 \cdot \log\left(\frac{\varepsilon/D}{3.7} + \frac{2.51}{\mathrm{Re}\sqrt{f}}\right) \tag{6}$$

where f is the friction factor, ε is the roughness parameter, D is the hydraulic diameter of the pipe (0.068 m for the EFA). This equation is used because the flow in the test section of the EFA is always turbulent with a Reynolds Number greater than 5000. The friction factor can then be used in Eq. 6 to determine the shear stress generated by the flowing water. Similar to the erosion function based on velocity, the corresponding shear stress data points can be plotted to obtain the erosion rate versus shear stress curve.

Figs. 13 and 14 show typical results for a given soil generated using the EFA. Fig. 13 is a plot of the erosion rate versus shear stress shown in log-log scale. Fig.14 is a similar plot only for erosion rate versus velocity. These charts can be used to find the threshold value for a soil, below which no erosion occurs. This can be tracked as either critical velocity, υ_c, or critical shear stress, τ_c. For the EFA, critical velocity is defined as the velocity at which the erosion rate is equal to 0.1 mm/hr. This value was chosen

based on the fact that the charts are used in log-log scale and the erosion rate is determined by human eye making it difficult to be any more precise than 0.1 mm/hr. It can even be argued that there is no way for this accurate of a value to be judged. In the actual determination of the critical velocity, a regression line is draw through the erosion function. Because there is much confidence in the values where the erosion is visibly larger, those points are often used for the regression line and the points with little visible erosion are not considered as heavily.

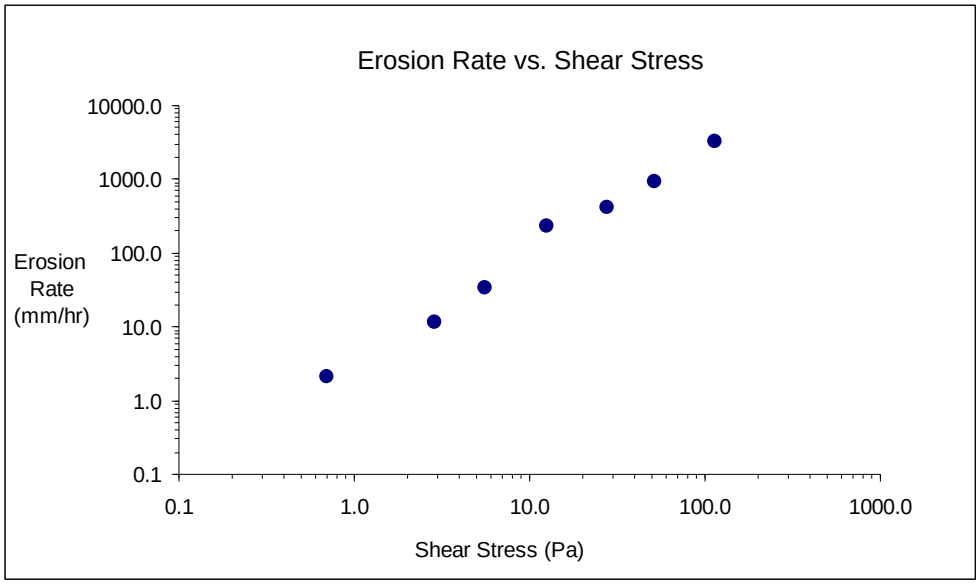

Fig. 13. EFA output of erosion rate versus shear stress

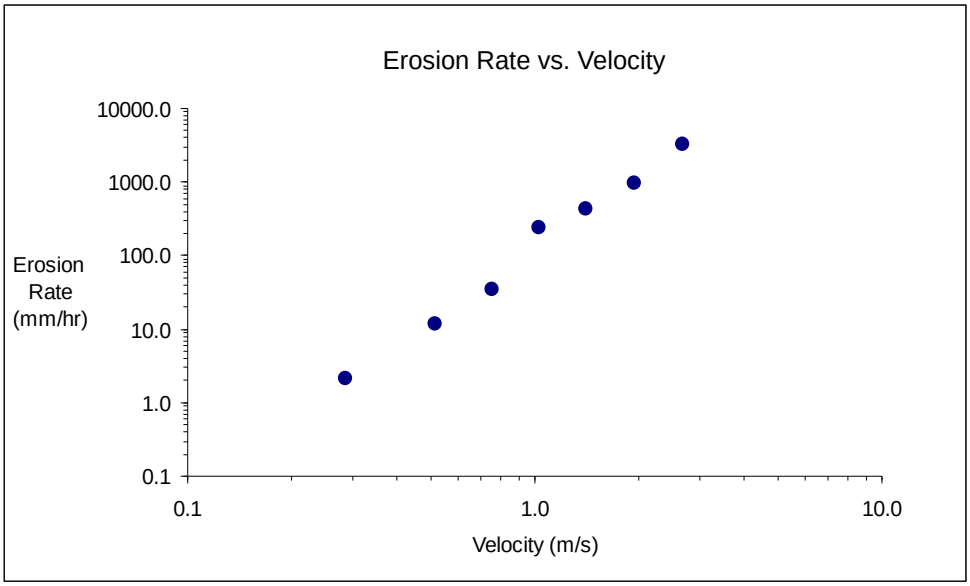

Fig. 14. EFA output of erosion rate versus velocity

An erodibility chart was developed from numerous tests conducted with the EFA (Fig.15). There are 6 categories ranging from very high erodibility (Category I) to non-erosive (Category VI). Materials showing higher erosion rates (Categories I and II) are typically sands and lower plasticity fine grained soils. Naturally occurring soils that show lower erosion rates (Categories III and IV) are usually fine grained soils exhibiting higher plastic behavior. Those that fall into Categories V and VI generally consist of hard rock such as granite, which exhibits virtually no erosion at all. A similar chart is also available for erosion rate versus velocity.

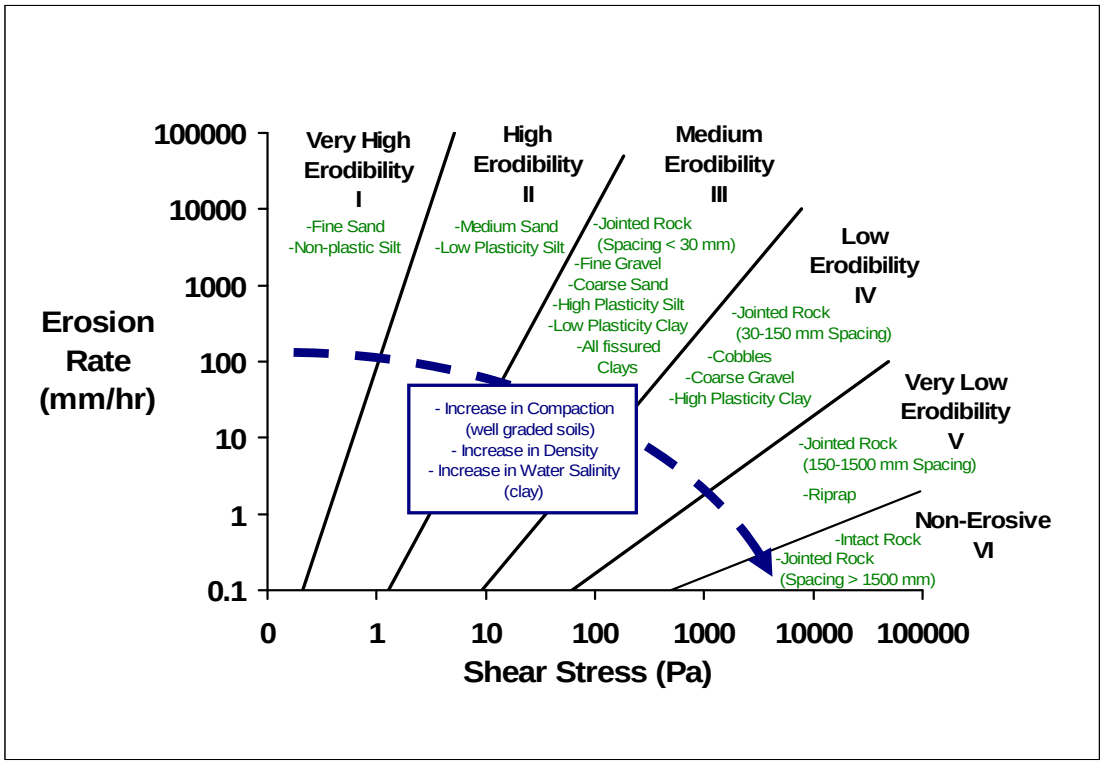

Fig. 15. Erodibility chart of the EFA (Briaud 2008)

2.6.3 Calibration

In the calibration of the EFA, the Shields' criterion was used for incipient motion of granular materials. Five tests were carried out with granular soils of known size as verification that the results obtained using the Moody Diagram correlated with the Shield's Diagram and equations (Table 3). The particles retained on each of the #10, #8, #4, 1/4", and 3/8" sieves were placed into standard Shelby tubes and compacted to a density seen in the field. The samples were tested in the EFA and the erosion functions were generated for each sample. The critical shear stress was estimated for each particle size from the erosion rate versus shear stress curve. This critical shear stress is defined as the stress exerted by the flowing water at which particles begin to erode. Using this

data, the Shield's diagram and corresponding equations were used to determine the dimensionless shear stress.

$$U = \sqrt{\frac{\tau_c}{\rho}} \tag{7}$$

where τ_c is the critical shear stress. This dimensionless value can then be used to calculate a new Reynolds Number,

$$\mathrm{Re} = \frac{Ud}{\nu} \tag{8}$$

and a non-dimensional shear stress,

$$\tau_* = \frac{\tau_o}{(\gamma_s - \gamma)d} \tag{9}$$

where γ_s is the specific weight of the soil solids, γ is the specific weight of water, and d is the particle size. The specific gravity of the sand particles used for calibration was assumed to be 2.65. This value can be compared to the dimensionless shear stress, τ_*, found on the Shield's Diagram corresponding to the value found in Eq. 4.

$$\frac{d}{\nu}\sqrt{0.1\left(\frac{\gamma_s}{\gamma} - 1\right)gd} \tag{10}$$

During the initial calibration, it was found that the dimensionless quantities calculated using EFA data compared quite closely to those found on the Shield's Diagram validating the analytical approach used with the EFA to determine the shear stress applied by the flow of water over the soil sample.

Table 3. Data from EFA calibration conducted on April 1, 2009 (Leclair 2009)

Sample	Grain Size (mm)	U_*	Re_*	Calculated Stress, τ_{*c}	Value for Shield's Diagram	Graphical τ_*	% Error
1	2	0.04	65.61	0.0417	101.60	0.041	1.7108
2	2.5	0.04	93.38	0.0432	141.99	0.045	-3.8980
3	5	0.07	292.74	0.0531	401.62	0.058	-8.3954
4	7	0.08	522.91	0.0618	665.28	0.061	1.2785
5	10	0.10	892.86	0.0618	1135.95	0.061	1.2785
		From EFA Output	τ_0 = Critical Shear Stress		G_s assumed to be 2.65		

2.6.4 Advantages and Disadvantages

The advantage of the EFA is that it can be used to estimate shear stresses and velocities for whatever material is currently in place at the site, whether it is a cohesive soil or not. Another major advantage of using the EFA is that it can be used for the evaluation of erosion potential for any site and depth sample that can be collected using Shelby tubes, while minimizing the amount of sample disturbance. The tube samples are tested and the data represents the in situ erosion conditions at the time of sampling. The test also replicates the real field phenomenon of surface erosion. The data obtained from EFA tests can be used to estimate the erosion expected for single or multiple flood events (Briaud et al. 2001).

Some of the disadvantages of the EFA include the sample and test preparation time required. For some materials, each velocity is run for one hour, which makes the complete test take at least five hours for five velocities, not including sample prep and any downtime between velocities. Also, the samples must be transported from the field

to the Texas A&M University laboratories where the EFA is housed. The shipping delays and actual time spent running the test can add up, and it could be several days before results are obtained.

2.7 Other Erosion Devices

2.7.1 Hole Erosion Test (HET) (Fell et al. 2003; Wan and Fell 2004a)

The Hole Erosion test (Fig. 16) is a method of testing internal erosion potential of earthen dams and other structures made of natural materials through the mechanism known as piping. Piping is a term used for water that flows through cracks or "pipes" in the soil. If the velocity is high enough or if it creates enough shear stress, soil particles are carried away with the water. As Fell et al. (2003) note, internal erosion has historically been the cause of failure in approximately 1 in 200 dams, so it is an important mechanism that should be quantified.

This test can be performed on existing materials or those proposed for an earthen embankment or retaining structure. Materials are first compacted to a relative density as they would be in the field. A 6 mm hole is drilled through the center of the sample, and the mold is placed between the two chambers. According to Fell et al. (2003), the flow rate is measured by allowing the water to fall into a container for a period of 10 to 20 seconds and measuring the volume accumulated. From Regazzoni et al. 2008, a v-notch weir is used as an outlet structure with known measurements. The flow rate can be calculated by measuring the height above the weir crest and plugging it into a simple equation. An increasing flow rate or the appearance of cloudy water indicates that

particles are in suspension and erosion is occurring. Because the velocity remains the same due to the constant head tank, the only way to increase the flow rate is to enlarge the hole.

As the test begins, the flow rate is measured and is later used to evaluate the initial friction factor. Throughout the test, usually between 10 and 12 flow rate readings are taken. Upon completion of the last reading, the sample is removed from the apparatus and the diameter of the hole is measured. The final friction factor can be found using the final diameter and flow rate. The completion of the test occurs when the hole diameter is so large that it reaches the side of the compaction mold or the flow rate cannot be measured accurately. From the hole diameters, erosion rate and a shear stress can be calculated and plotted.

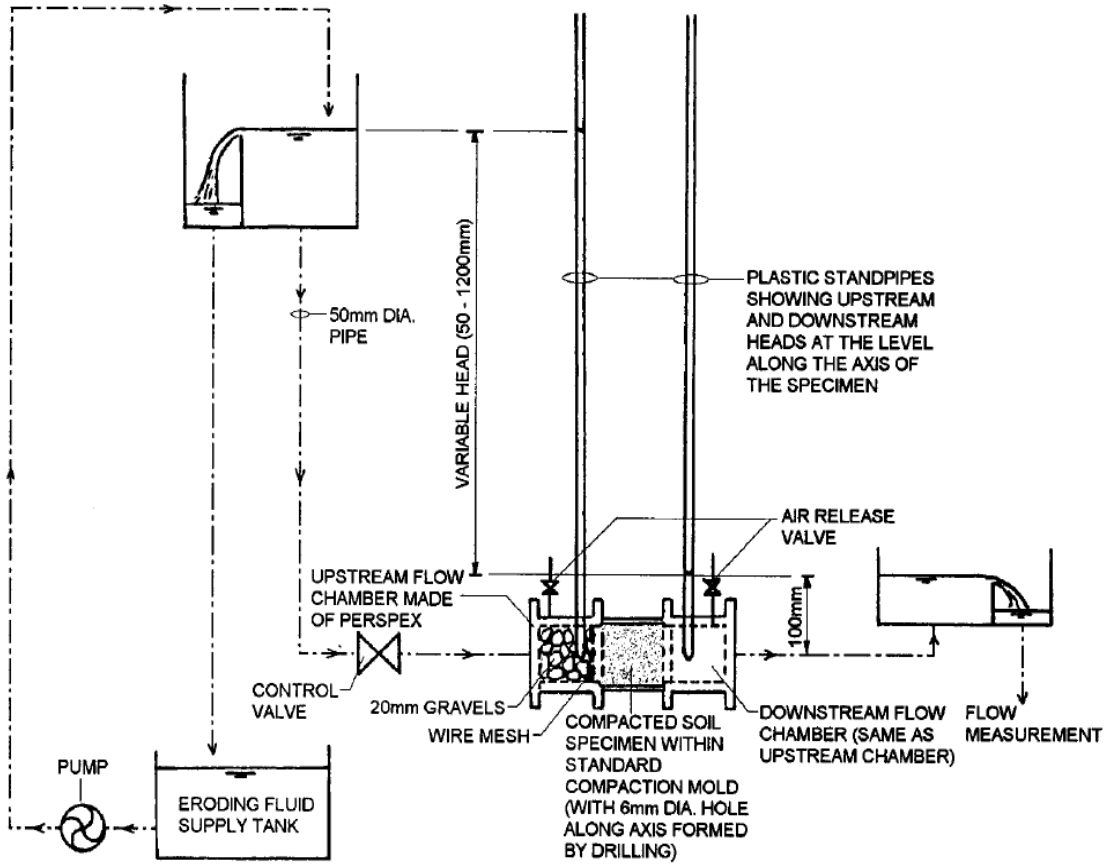

Fig. 16. Schematic of the Hole Erosion Test (Wan and Fell 2004b)

2.7.1.1 How the Apparatus Operates

A standard proctor mold housing the compacted soil specimen of interest is placed between two acrylic chambers. The upstream chamber is filled with gravel to eliminate the velocity head as the water approaches the sample and reduce the contraction of the flow as it enters the drilled hole. This ensures the hole is not eroded significantly at the entrance and that it remains relatively the same size over the width of the sample. Also, it is a smooth transition which allows the entire hole to fill with water and flow at the same velocity. This is crucial because of the assumption that the water

flows through the soil by a pressure differential rather than an energy differential. A storage tank holds the water which is then fed into a pump that gives the water sufficient head to flow into the constant head tank. The constant head tank contains an overflow outlet structure that maintains the water surface elevation. The excess water flows back into the storage tank. A 2 in pipe carries the water from the adjustable head tank through a control valve and into the upstream gravel chamber. Two air release valves, located on the upstream and downstream sides of the sample, allow the removal of air bubbles that might be present. The water flows from the gravel chamber, through the drilled hole in the sample, and exits into the downstream chamber. From the exit chamber, the water flows through an outlet structure where several methods of measuring flow rate can be used. The flow rate is found by measuring the volume of water collected in a container or with a v-notch weir at the outlet structure. The flow rate can then be calculated by measuring the height above the weir crest and using simple weir equations.

2.7.1.2 Test Procedure

The materials being tested in the HET are typically compacted soil samples in a standard proctor mold. Proposed construction materials can be compacted to the relative percent compaction of choice and tested in the HET. Also, existing soil and site conditions can be represented and tested by reconstructing a sample with properties similar to those found in the field. The mold housing the compacted soil specimen is placed between two acrylic chambers. Water fills each chamber and then the air is removed using a release valve for each compartment. Prior to beginning the test, the

downstream manometer is set to a head of 0.1 m. The upstream manometer setting is predetermined based on the shear stress that the soil would experience in the field conditions or at the operator's discretion. The upstream head has a range of 50 mm to 1.2 m above the downstream head. A 6 mm hole is drilled through the center of the sample. This hole represents a crack or seepage path that could occur in an earthen structure which retains water. As water flows through the hole, it may or may not erode the soil based on the governing shear stress inside the hole and the particular sample. An increasing flow rate or an appearance of cloudy or dark water indicates that erosion is occurring. Because of the continuity equation (Q=VA) and the fact that the velocity remains constant throughout the test because of the use of the constant head tank, the only way the flow rate can increase is by enlarging the hole.

As the test begins, the flow rate is measured and used to determine the initial friction factor for the test. Readings of the flow rate are taken and recorded and a set number of intervals, usually between 10 and 12. After the last reading, the sample is removed from the apparatus and the diameter of the hole is measured. The final friction factor is calculated using the final measured hole diameter and the final flow rate. The test completion is marked when either the hole becomes so large that it reaches the side of the compaction mold or the flow rate becomes so large that it cannot be measured accurately.

2.7.1.3 Data Reduction

The shear stress generated by the flow on the surface of the drilled hole can be determined using the pressure differential between the upstream and downstream ends of the test section, the diameter of the hole, and the length of the sample, as shown in the following equation:

$$\tau_t \cdot P_t \cdot L = \Delta p \cdot A_t \tag{11}$$

where τ is the hydraulic shear stress on the soil surface caused by the flowing water, P is the wetted perimeter of the hole, L is the length of the sample, Δp is the pressure differential between the upstream and downstream ends of the sample, and A is the area of the hole. The subscripts, t, denote the variables that are a function of time and change during the test. Assuming that the velocity at the entrance and exit of the hole is the same and that there are no head losses due to the contraction or expansion of flow, the Bernoulli Equation and static fluid pressure relationships can be used to relate the change in pressure to the head differential between the two standpipes located at each end of the sample.

$$p_{up} - p_{dn} = \gamma \cdot h_{up} - \gamma \cdot h_{dn} = \gamma \cdot \left(h_{up} - h_{dn}\right) \tag{12}$$

This equation can be reduced to:

$$\Delta p = \gamma \cdot \Delta h_t = \rho_w \cdot g \cdot \Delta h_t \tag{13}$$

where the Δh is the difference in elevation of water in the standpipes, p_w is the mass density of water (taken as 1000 kg/m^3), and g is gravitational acceleration. Combining equations 11 and 13 gives:

$$\tau_t = \rho_w \cdot g \cdot \frac{\Delta h_t}{L} \cdot \frac{A_t}{P_t} \tag{14}$$

This equation is of the same form as the shear stress for open channel flow:

$$\tau = \gamma \cdot R \cdot S_0 \tag{15}$$

where R is defined as the hydraulic radius of the channel calculated as the cross sectional area divided by the wetted perimeter (A / P), and S_0 is the bed slope. This equation assumes steady and uniform flow meaning the flow rate does not vary with time and the water depth does not cross the critical flow depth (i.e. not rapidly varied). Under these assumptions, the computations are simplified by taking the bed slope as the slope of the energy line of the flow. For the free surface channel conditions, the flow of water is governed by gravitational forces. The head loss, or change in the energy in the flow, is related to the bed slope by:

$$S_o = \frac{H_L}{L} \tag{16}$$

In the case of the HET, water is forced through the hole by a pressure differential equivalent to the head loss between two given points. This head loss divided by the length, L, between the set points gives a hydraulic gradient:

$$s = \frac{\Delta h}{L} \tag{17}$$

If the downstream standpipe is used as a datum, the head differential reduces from Δh to h and the equations for the open channel flow and the HET are the same (Eqs. 16 and 17). Equation 14 can be used for the HET and can be rewritten as,

$$\tau_t = \rho_w \cdot g \cdot s_t \cdot \frac{A_t}{P_t} \tag{18}$$

Using the relationship for the hydraulic radius of a circular conduit given by,

$$R_t = \left(\frac{A}{P}\right)_t = \frac{\frac{\pi}{4}\phi_t^2}{\pi\phi_t} = \frac{\phi_t}{4} \tag{19}$$

where φ_t is the diameter of the hole at any time, t, Equation 18 can be rewritten as

$$\tau_t = \rho_w \cdot g \cdot s_t \cdot \frac{\phi_t}{4} \tag{20}$$

This equation assumes the hole cross-section remains circular throughout the test and the density of water does not change. The density of water increases as eroded particles become suspended; however, it is assumed that this change is negligible and the density is considered constant throughout the test.

The erosion rate of the soil is derived by Wan and Fell (2004a) as the change in mass with respect to time per unit area.

$$\dot{\varepsilon}_t = \frac{1}{P \cdot L} \cdot \frac{dM}{dt} \tag{21}$$

This equation can be transformed so that it is a function of hole diameter by relating the erosion rate to the change in hole diameter as a function of time. During the test the diameter of the hole is not measured, so an analytical method was developed based on other measured quantities. Assuming again that the hole remains circular throughout the entire test, the incremental increase in the hole diameter is given by,

$$dA = 2 \cdot \pi \cdot r \cdot dr = \frac{\pi \cdot \phi \cdot d\phi}{2} \tag{22}$$

Additionally, the change in mass can be represented by,

$$dM = \rho_d \cdot L \cdot dA \tag{23}$$

where ρ_d is the dry mass density of the soil, L is the length of the hole, and dA is the incremental increase in the area of the hole. Since L is constant, LdA is essentially the change in volume. Multiplying the differential volume by ρ_d calculates an eroded mass.

Combining Equations 21, 22, and 23, and using the definition of the wetted perimeter for a pipe, P, and the circumference of the circular opening, $\pi\varphi$, the erosion rate is given by

$$\dot{\varepsilon}_t = \frac{\rho_d}{2} \cdot \frac{d\phi_t}{dt} \tag{24}$$

where $d\varphi_t/dt$ is the change in the hole diameter with respect to time. This can be approximated by $\Delta\varphi/\Delta t$ as long as the time increment is relatively small.

For closed-conduit pipes, the shear stress depends on whether the flow is laminar or turbulent. The Reynolds Number (Eq. 5) distinguishes this difference. To satisfy laminar conditions, the Reynolds Number needs to be less than 5000. Any number greater than 5000 is described as turbulent conditions. For laminar flow, the shear stress is linearly related to the average velocity through a friction factor:

$$\tau = f_{LAMINAR} \cdot V \tag{25}$$

If the flow is turbulent, the velocity term is squared.

$$\tau = f_{TURBULENT} \cdot V^2 \tag{26}$$

From the continuity equation ($Q = V \cdot A$), the mean velocity is given by,

$$V = \frac{Q}{A} = \frac{Q_t}{\frac{\pi}{4}\phi_t^2} = \frac{4Q_t}{\pi\phi_t^2} \tag{27}$$

Combining equations 20, 25, 26, and 27 gives the friction factors as a function of time for both flow conditions:

$$f_{LAMINAR,t} = \frac{\rho_w \cdot g \cdot \pi \cdot s_t \cdot \phi_t^3}{16 \cdot Q_t} \tag{28}$$

$$f_{TURBULENT,t} = \frac{\rho_w \cdot g \cdot \pi^2 \cdot s_t \cdot \phi_t^5}{64 \cdot Q_t^2} \tag{29}$$

During the analysis, the entire test is assumed to be either laminar or turbulent conditions. Most flow conditions are typically turbulent. The friction factor is assumed to be linear throughout the entire test and is interpolated using the original and final hole diameters. The diameter of the hole as a function of time can be estimated by inverting the previous two equations. For laminar flow, the hole diameter can be calculated using:

$$\phi_t = \left(\frac{16 \cdot Q_t \cdot f_{LAMINAR,t}}{\pi \cdot \rho_w \cdot g \cdot s_t} \right)^{1/3} \tag{30}$$

and for turbulent flow the hole diameter is given by:

$$\phi_t = \left(\frac{64 \cdot Q_t^2 \cdot f_{TURBULENT,t}}{\pi^2 \cdot \rho_w \cdot g \cdot s_t} \right)^{1/5} \tag{31}$$

The diameter of the hole can be calculated at the predefined intervals at which the flow rate, Q, and the change in the pressure between the upstream and downstream ends of the sample are measured. These calculated diameters can then be used to find the shear stress and erosion rate at each time step.

An example of the graphed test results is shown in Fig. 17. At the beginning of the test, the erosion rate is higher due to the removal of loose material caused by drilling the hole. This material is not considered to be a good representative of the entire sample and is not included in the linear line approximation shown. As the shear stress increases, it reaches a threshold value above which erosion occurs. Similar to the EFA, this value is defined as the critical shear stress. Fig. 17 shows a linear relation between erosion rate and shear stress.

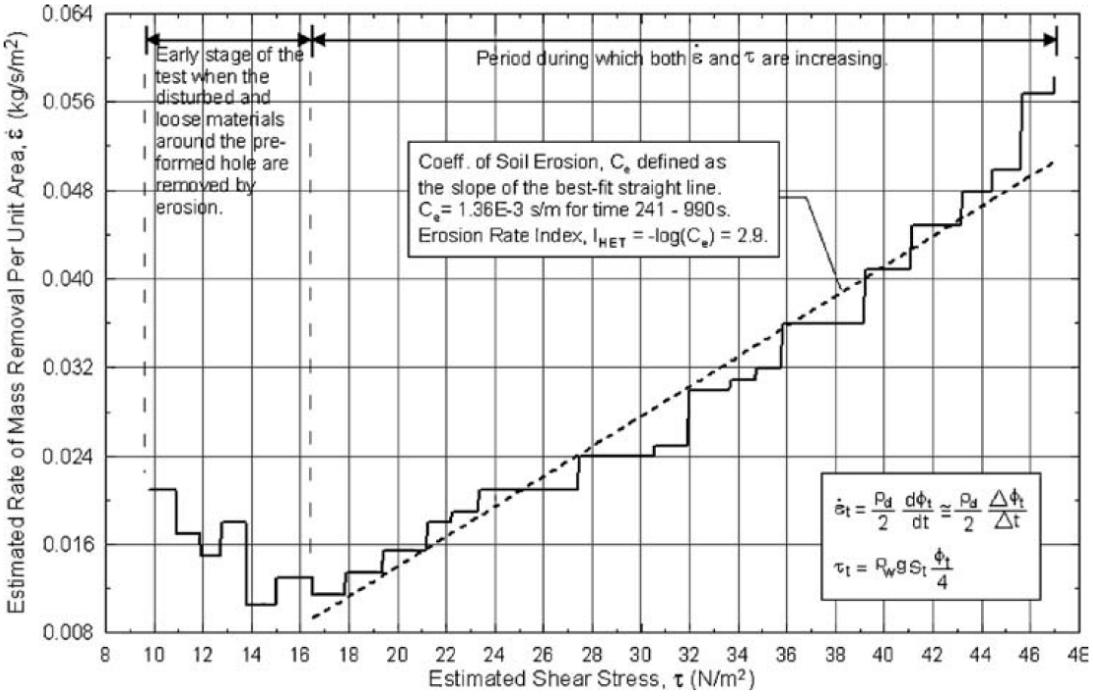

Fig. 17. Output graph from Hole Erosion Test (Wan and Fell 2004a)

2.7.1.4 Advantages and Disadvantages

This test investigates the internal erosion phenomenon. Rather than using a set of equations to calculate the erosion around a pier or along a slope, the data obtained

from the HET can be used as a predictive tool to estimate the time rate of failure for earthen embankment dams. The U.S. Bureau of Reclamation found that the potential casualties of a major dam breach are highly dependent on the amount of warning time given to citizens in the areas that could be inundated (Fell et al. 2003). The failure mechanics can be grouped into four phases: initiation, continued erosion, progression, and breach/failure as shown in Fig. 18. Identifying the rate of the erosion for a given embankment material using the HET can give a better indication of how long each phase will last and ultimately the estimated time from initiation to failure.

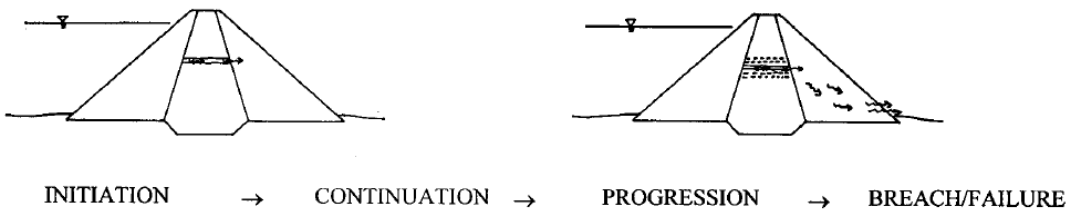

Fig. 18. Failure progression (adapted from Fell et al. 2003)

As mentioned, levee breaching can occur from one or a combination of failure modes. Often times it seems that the failure was caused from the overtopping waters, however, seepage and internal erosion may also have played a large role in the failure. Internal erosion is very difficult to detect. Sand boils and ponding of water on the dry side of the levee are warning signs that seepage is occurring, but with the presence of overtopping water, neither of these may be visible. The HET offers a way to test for the estimated time to failure due to internal erosion so that it can be compared to the time to failure due to overtopping. Table 4 relates the HET qualitative erosion time to the equivalent time until an embankment breach.

Table 4. Qualitative breach times for embankment dams (Fell et al. 2003)

Qualitative term	Equivalent time
Slow (S)	Weeks or months, even years
Medium (M)	Days or weeks
Rapid (R)	Hours (>12 h) or days
Very rapid (VR)	<3 h

The different mechanisms for elements in an embankment and the time required for a hole to develop, is shown in Table 5. These two tables can be used together to get a general and qualitative idea of internal erosion for a given material. Table 6 uses the factors affecting erosion to give more quantitative estimates of time until failure for a given soil and embankment.

Table 5. Typical initiation times (adapted from Fell et al. 2003)

Location of internal erosion	Mechanism	Usual time for development
Embankment	Backward erosion	Slow to rapid/very rapid
	Crack/hydraulic fracture	Rapid or very rapid
	High permeability zone	Slow to rapid
	Suffusion/internal instability	Slow
Adjacent or into a conduit or wall	High permeability zone, crack, or hydraulic fracture	Rapid or very rapid
	Erosion into open joints or cracks	Slow
Foundation	Backward erosion	Slow
	Backward erosion following blowout	Rapid to very rapid
	Backward erosion along a concentrated leak	Slow to rapid
	Suffusion/internal instability	Slow
Embankment to foundation	Backward erosion initiating at the contact of embankment/foundation	Slow to rapid/very rapid

Table 6: Estimation of breach times (adapted from Fell et al. 2003)

Factors Influencing the Time for Progression and Breach				
Rate of erosion	Upstream flow limiters	Breach time	Approximate likely time-qualitative	Approximate likely time-quantitative
R or VR	No	VR or R-VR	Very rapid	<3 h
R	No	R	Very rapid to rapid	3-12 h
R-M	No	VR		
R	No	R-M	Rapid	12-24 h
R-M or M	No	R		
R	Yes	R or Vr		
R	No	M or S	Rapid to medium	1-2 days
R-M or M	No	M or M-S		
R or R-M	Yes	R or R-M		
M or R-M	No	S	Medium to slow	2-7 days
R-M or M	Yes	S		
M	Yes or No	S	Slow	Weeks, months, or years

Some of the disadvantages of the HET include the sample and test preparation time required. Samples must be compacted and a hole must be drilled before the test can begin. As in the EFA test this is also a laboratory procedure and the samples must be transported from the field to a lab capable of running the test. The shipping delays and actual time spent running the test can add up, and it could be a substantial amount of time before results are obtained.

2.7.2 Jet Erosion Test (JET) (Hanson and Cook 2004; Hanson 2001)

The Jet Erosion Test (Fig. 19) allows for site specific determination of erosion rates, but unlike the EFA it is a portable device that can perform in situ tests without having to collect samples. This method eliminates any sample disturbance that would

have occurred during sampling. This device characterizes a soil in terms of its critical shear stress and a constant found in the erosion rate equation and the data obtained from each site can be used to calculate erosion quantities for design events. The JET can be used to determine erosion on earthen dams and levees, stream banks and main channels, places where core material has been exposed, and other areas where surface erosion may be a potential problem.

To begin a test, a site must be selected based on the soil of interest, but it also must be located in such a way that the slope is less than 26 degrees and it represents the channel as best as possible. Water from a nearby source is fed to the head tank where the elevation head is held constant. Similar to the EFA, approximate head settings on the mast are determined before testing to establish the range of velocities that best represent what a channel would experience in a design flood scenario. The water is ejected from the nozzle and impacts the soil surface. For a typical test, head and point gauge readings are taken every 5 to 10 minutes a total of 10 to 12 times.

Fig. 19. Jet Erosion Test (JET) during a test (Hanson and Cook 2004)

The remaining calculations are based on the hydraulic characteristics of a submerged jet and stagnation pressure. The pressure on the surface from the jet is entirely a normal stress and has no shear component, but as the water pushes against the soil surface a shear stress develops. Similar to the EFA, the JET has a categorical index where data can be plotted to give a physical meaning to the numerical data (Fig. 20). Rather than showing the categories on an erosion rate versus shear stress plot, it is presented as a coefficient, k_d, versus critical shear stress.

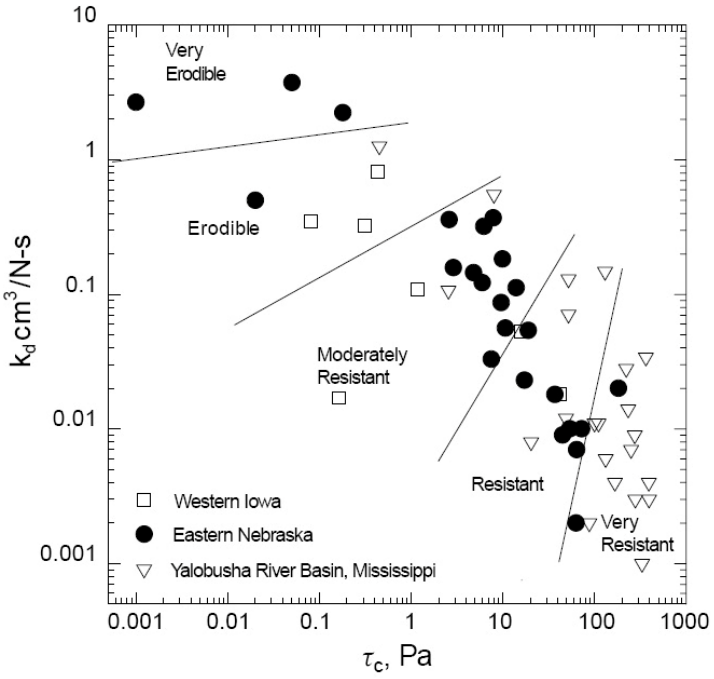

Fig. 20. Categorical chart for jet erosion testing (Hanson and Simon 2001)

2.7.2.1 How the Machine Operates

The main components of the Jet Erosion Test (JET) apparatus (Fig. 21) consist of a jet tube, nozzle, point gage, adjustable head tank and jet submergence tank. Water from a nearby water source, is pumped through a hose into a head tank where the elevation of the water is held constant for the entire test. Holding the elevation head constant ensures that the velocity and shear stress at the jet nozzle is constant. Any overflow is expelled back to the stream or original water source. Water flows from the head tank through a hose to the jet tube where it is ejected from the nozzle onto the surface of the soil (Fig. 22).

The nozzle exit is placed at the top of the water surface in the tank. Excess water in the tank is expelled out of the side of the submergence tank so that the top of water

surface remains at the same height as the nozzle exit. This ensures that there is zero gage pressure (atmospheric pressure) at the nozzle exit.

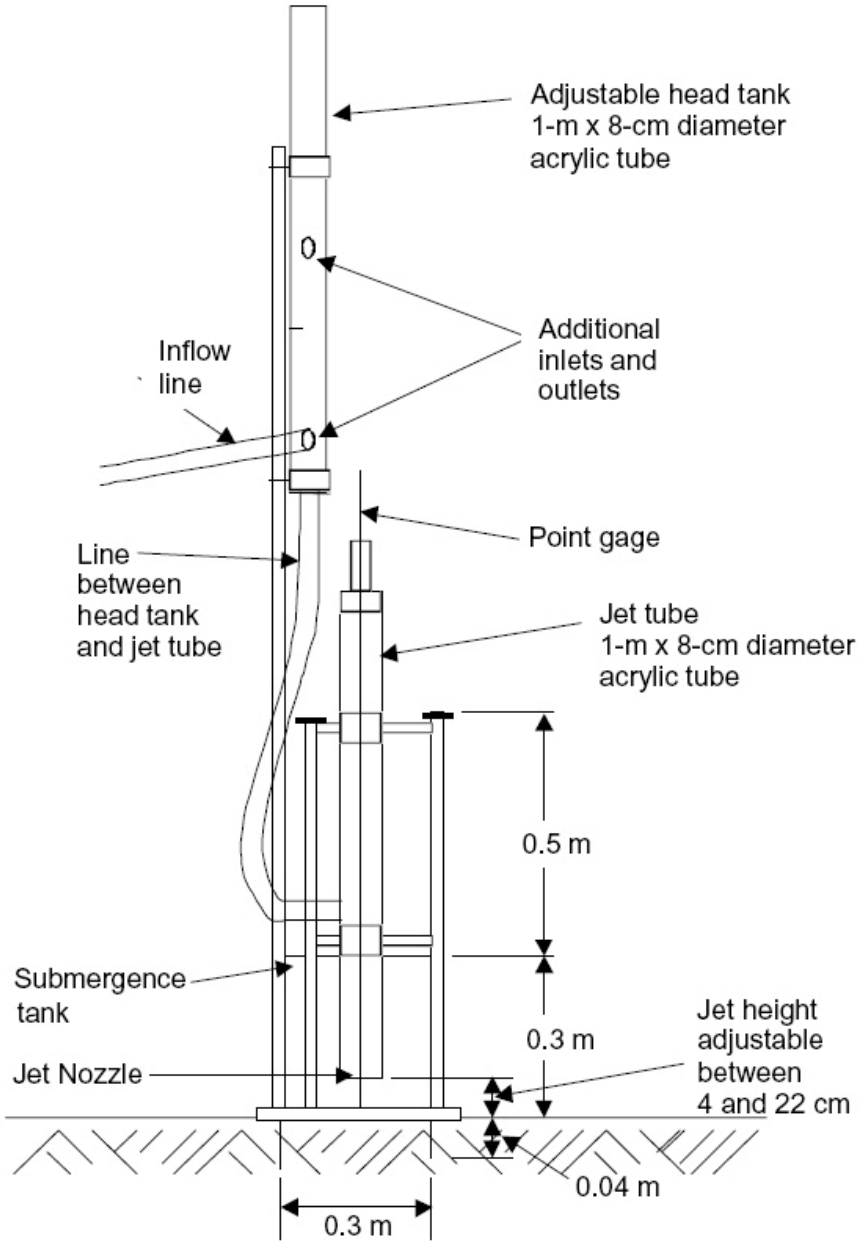

Fig. 21. Schematic of JET device (Hanson 2001)

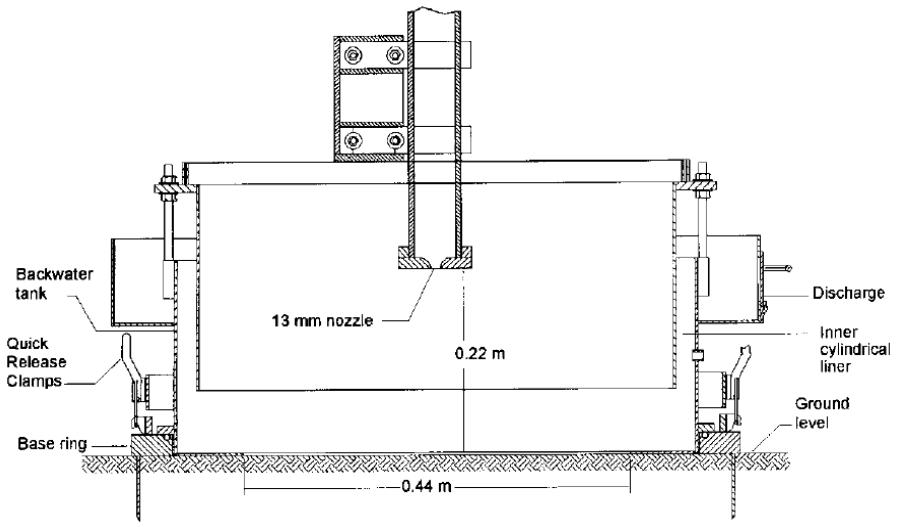

Fig. 22. Close up view of jet and soil surface (Hanson 2001)

2.7.2.2 Test Procedure

To begin an investigation, a suitable site which best represents a channel is selected for the test. The selection is based on the soil of interest making sure that the slope of the site is less than 26 degrees for the stability of the apparatus. If the material is varied, the average of several tests should be taken. If there are multiple soils types, each should be tested.

The submergence tank is pushed into the soil surface until the plate ring is flush creating a seal and allowing the tank to remain full during the tests. The jet tube and point gage are attached to the tank frame. The jet nozzle is set to a height between 6 and 35 mm, 12 nozzle diameters is generally recommended. The distance from the nozzle end to the surface of the soil is measured and recorded (J_i). The point gage is essentially a rod located in the center of the jet with the same diameter as the nozzle opening and is used to measure the distance to the soil surface. To take a reading, the point gage is

lowered through the nozzle shutting off the flow of water so that the reading can be taken. The gage is then raised back above the nozzle allowing the water to flow again.

Before beginning the test, an approximate head setting on the mast should be determined based on a range of velocity and shear stress values that the soil will experience during testing. The velocities and shear stress values chosen should be representative of an expected design flood scenario. For instance, if the approach flow velocity for a certain flood event is expected to be 2 m/s, the height of the tank should be set accordingly so that the jet velocity at the nozzle exit is as close to 2 m/s as possible.

The hoses connecting the tanks are attached next and a hose is connected from the water source to the head tank and finally from the head tank to the jet tube. A deflector plate is then placed in front of the nozzle. This plate allows the tank to be filled without causing erosion on the soil surface. The point gage is placed through the opening of the nozzle and flow to the jet tube is initiated. An air relief valve located at the top of the jet tube allows for the removal of any air that becomes trapped. Once all the air has been removed, the point gage is retrieved allowing water to flow through the nozzle, strike the deflector plate, and fill the submergence tank. Once the submergence tank is full, a reading of the supplied head is recorded. The deflector plate is removed so that the jet strikes surface of the soil. Head and point gage readings are taken at specific intervals, usually every 5 to 10 minutes with 10 to 12 readings total.

2.7.2.3 Data Reduction

Fort the JET, the erosion rate of a given material is linearly proportional to the difference in hydraulic stress and critical shear stress. For materials that erode very quickly, however, the equation can give a negative critical shear stress which is physically impossible.

$$\dot{\varepsilon} = k_d \cdot (\tau - \tau_c) \tag{32}$$

The other analytical calculations are based on the hydraulic characteristics of a submerged jet and stagnation pressure. A stagnation point is defined where the flow of water becomes zero at the surface of a solid object. At this point, the kinetic energy generated from the flow of water is converted to a pressure on the surface of the soil. This pressure is entirely a normal stress, however, as the water pushes out and away from the surface, a shear stress develops on the surface. The stress distribution is not uniform as shown in Fig. 23.

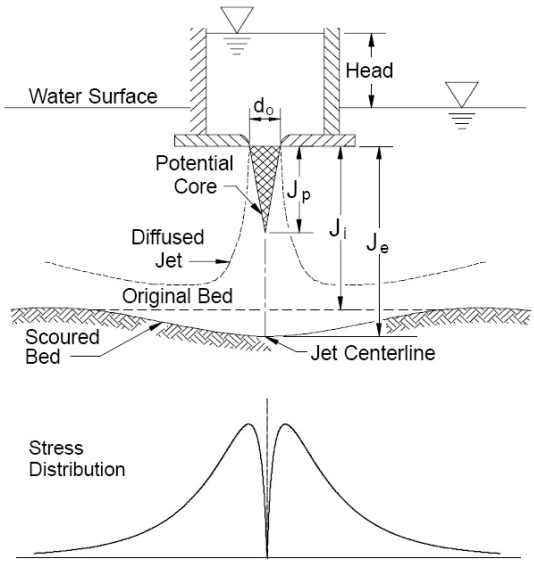

Fig. 23. Shear stress distribution of submerged jet (Hanson and Cook 2004)

The equation used to calculate the shear stress of the water at the exit of jet is given by,

$$\tau = C_f \cdot \rho \cdot U^2 \tag{33}$$

where C_f is a unit-less coefficient of friction (0.00416), ρ is the mass density of water, and U is the velocity of the water at the centerline of the jet. As the water moves from the nozzle exit the shear stress changes with the distance from the nozzle exit. The stream can be considered in two parts: the jet core, and rest of the jet. For the distance defined as the jet core, the velocity of the jet is assumed to be the same as the velocity at the orifice opening. This core has a finite length given by a coefficient multiplied by the nozzle diameter, generally six times the nozzle diameter.

$$J_p = C_d d_o \tag{34}$$

If the point gage reading taken is less than the core length, J_p, the stress exerted on the soil is said to be the stress at the nozzle exit shown by

$$\tau_o = C_f \cdot \rho \cdot U_o^2 \tag{35}$$

where τ_0 is the peak hydraulic shear stress at the nozzle exit and U_0 is the velocity of the water at the nozzle exit. U_0 is found using the following equation

$$U_o = \sqrt{2gh} \tag{36}$$

where g is the gravitational acceleration and h is the difference in elevation head between the two points of interest. The value h is calculated as the difference in the elevation of the water surface in the constant head tank and the elevation of the nozzle. In the normal exit velocity equation, there is a reduction factor of 0.62; however, the

particular nozzle used in the JET was manufactured with rounded edges so there is no reduction in the flow rate making the coefficient 1. The velocity of the jet stream is said to be inversely proportional to the distance from the jet core (Regazzoni 2008).

$$\frac{U}{U_o} = \frac{J_p}{J} \tag{37}$$

The shear stress of the jet at any distance greater than the jet core, *J*, can be calculated by combining Eq. 37 and Eq. 35:

$$\tau = C_f \cdot \rho \cdot U_o^2 \cdot \left(\frac{J_P}{J}\right)^2 \tag{38}$$

The initial stress exerted on the soil can be calculated by substituting J_i, for J (Eq. 40). If the distance to the soil surface is less than the potential core length, J_p, then the stress is said to be equal to the exiting stress.

$$\tau_i = \tau_o \left(\frac{J_p}{J_i}\right)^2 \quad \text{for } J_i > J_p \tag{39}$$

$$\tau_i = \tau_o \qquad \text{for } J_i \le J_p \tag{40}$$

The sample begins close to the nozzle and as the soil is eroded, a hole of increasing depth is created. The stress of the jet at the water/soil interface decreases as the surface of the hole becomes farther and farther from the nozzle

$$\tau_c = \tau_o \left(\frac{J_p}{J_e}\right)^2 \tag{41}$$

The critical shear stress is defined at the point and distance that the jet no longer causes the hole to deepen. This distance is measured and denoted by, J_e. The critical shear stress is determined by substituting J_e for J_i.

$$\tau_c = \tau_o \left(\frac{J_p}{J_e} \right)^2 \tag{42}$$

For some materials, the equilibrium depth may not be reached. In these cases, it can be estimated using a hyperbolic curve (Fig. 24) and equation relating erosion depth versus time developed by Blaisdell et al. (1981)

$$x = \left[(f - f_0)^2 - A^2 \right]^{0.5} \tag{43}$$

where A is defined as the distance between the conjugate axis and the vertex of the hyperbola. The other variables are given in the following expressions:

$$x = \log\left(\frac{U_0 t}{d_0} \right) \tag{44}$$

$$f = \log\left(\frac{J}{d_0} \right) - \log\left(\frac{U_0 t}{d_0} \right) \tag{45}$$

$$f_0 = \log\left(\frac{J_e}{d_0} \right) \tag{46}$$

where the J terms are defined previously, d_0 is the nozzle diameter, U_0 is defined in Eq. 36, and t is the test time.

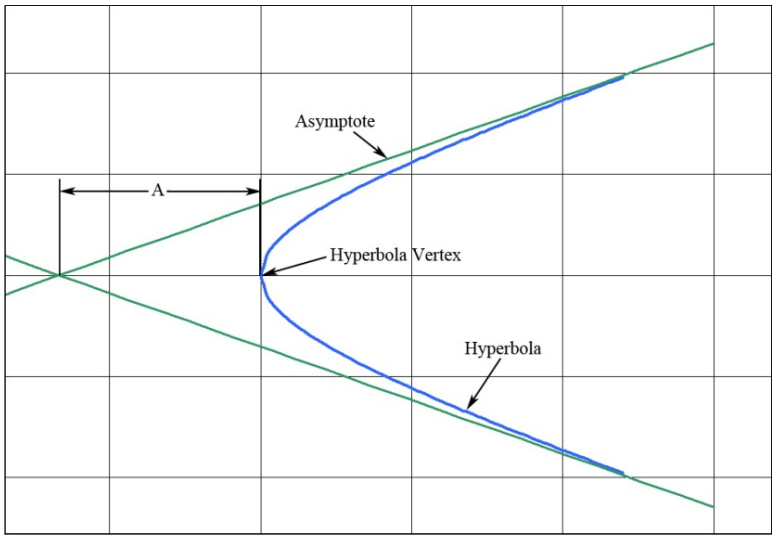

Fig. 24. Example hyperbola (Blaisdell et al. 1981)

To obtain erosion rate versus time data points, an analytically based equation is used to calculate the time:

$$t_m = T_r\left[0.5\ln\left(\frac{1+J^*}{1-J^*}\right) - J^* - 0.5\ln\left(\frac{1+J_i^*}{1-J_i^*}\right) + J_i^*\right] \quad (47)$$

where T_r is a reference time denoted as $J_e/(k_d\tau_c)$, J^* is a dimensionless term defined as J/J_e, and J_i^* is defined as J_i/J_e. In order to limit the deviations of t_m versus the measured time intervals, the value k_d is iterated. The value typically starts at 0.01 $cm^3/N{\cdot}s$, but can be specified by the user.

Similar to the EFA, the JET has a categorical index only it is presented as k_d versus critical shear stress (Fig. 20). The values can be compared and each soil can be assigned an erosion category.

2.7.2.4 Practical Application

The data obtained from a JET test can be used in several applications including: erosion of a stream bank, the centerline of a stream, and on a slope of an earthen embankment or spillway. Manning's Equation (Eq. 11) can be used to determine a flow depth in a channel for a given flow rate which can then be used to calculate the shear stress generated on a particular surface. These values can be used to calculate the erosion rate. For example, if the average k_d, τ_c, and τ_e are determined to be $1.0 \cdot 10^{-7}$ $m^3/N \cdot s$ and 1.0 Pa, and 4 Pa, respectively, the erosion rate is calculated as $3.0 \cdot 10^{-7}$ m/s or 1.08 mm/hr. Similar analysis can be performed for different flow rates and site conditions affecting the hydraulic shear stress exerted on the soil.

2.7.2.5 Advantages and Disadvantages

The test is fairly simple, the test time is short, and each test is relatively inexpensive to perform making it very feasible to perform numerous tests at a specific site in order to get a better representation of the area. Like the EFA, there is no limit to the different materials that can be tested using this apparatus, and the data obtained can be used to calculate numerous quantities such as, erosion of a stream bank, and erosion on slopes of earthen embankments.

This analysis can be performed for multiple flow rates and conditions that affect the hydraulic shear stress. The superposition rule is assumed applicable and calculated erosion depths can be added to one another to obtain the cumulative erosion.

While the actual time spent running the test may be relatively short, the time and effort required to transport the machine to the site and set it up can be substantial. Also, the apparatus requires a water source such as a river or some alternate large amount of water to be available at each testing spot. This limits the areas feasible for testing or requires the transport of large tanks of water to the site. The location of the test must also be chosen to represent channel flow as best as possible. Additionally, the slope should be less than 26 degrees to prevent overturning of the apparatus during the test. These additional constraints hinder the choice of placement substantially.

2.7.3 Cohesive Strength Meter (CSM) (Tolhurst et al. 1999)

Like the JET, the Cohesive Strength Meter (Fig. 25) is an in situ device; however, it was specifically developed to determine the temporal and spatial variations in the erosion threshold of muddy intertidal sediments. The CSM has been modified substantially since its original conception (Paterson 1989; Tolhurst et al. 1999). The current CSM controls pressure settings, pulse duration and intervals automatically with a computer and data is recorded directly and downloaded for immediate analysis. Similar to the JET, the CSM uses a submerged vertical jet of water to erode the soil's surface. The jet nozzle of the device is located in a water chamber that is pushed into the sediment. The perpendicular jet is fired at the soil surface in short pulses. The jet velocity is systematically increased throughout each experiment through pre-programmed routines. Erosion is said to have occurred when a drop in the transmission of infrared light across the chamber is found, or in other words, when the water gets

cloudy. Because the area the erosion occurs in is small, the detection of any small changes or variations is possible. Shear stresses of 12 Nm^{-2} can be imposed on the soil surface. This device allows for rapid determination of a critical entrainment stress and also provides a relative measure of erosion rate. The CSM has been used in the past for intertidal flats and salt-marsh sediment, but has been studied for cohesive soils as well.

Fig. 25. Cohesive Strength Meter during field use (Partrac 2009)

2.7.3.1 How the Machine Works

The main components of the CSM consist of a test chamber, digital panel and keypad, air supply, and fill bottles (Fig. 26). The entire system is contained in a 65x30x20 cm case and weighs 13 kg. Fig. 27 shows a schematic of the CSM and its components (Tolhurst et al. 1999).

Fig. 26. Cohesive Srength Meter (Partrac 2009)

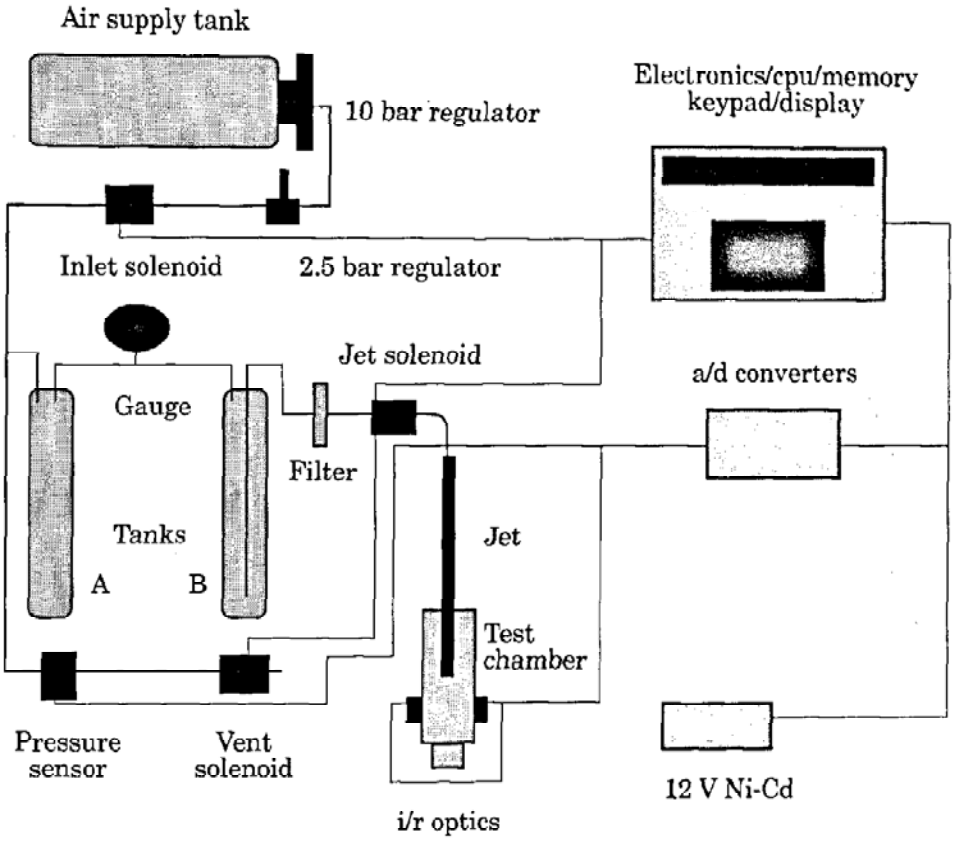

Fig. 27. Schematic of the Cohesive Strength Meter (Tolhurst et al. 1999)

The compressed air tank is a common three liter diving tank and the pressure is regulated by two standard diving regulators. The smaller regulator is connected to pressure bottle "A" and is used to provide the necessary pressure head for the test. A digital pressure gage measures the pressure in the system and it is then displayed on the LCD screen. There is also an analog pressure gage. The solenoid connected to the same line as the pressure sensor is used to vent the system if the pressure is too high. Tank "B" acts as a water reservoir. The water used should have the same salinity as the water encountered by the soil in natural conditions. Located 1cm above the soil water interface are two infrared diodes. The light transmitter emits light at a wavelength detected by a spectrally matched receiver. The test chamber is made of two plastic cylinders. The chamber contains a brass jet, the infrared transmitter, and the two aforementioned diodes. Before a test, the chamber is pushed flush with the soil surface and filled with water. The water is pumped into the test chamber and through the jet in short pulses at a given pressure. The air pressure in the CSM governs the force applied by the water jet.

2.7.3.2 Test Procedure

Several inputs must be determined before each test: pressure increment, max pressure, duration of each pulse, frequency of readings of test chamber output. There are also pre-set routines that can be chosen by using the keypad. The site and soil of interest are chosen and the apparatus is set up. The water bottle must be manually filled. The test chamber is pushed flush into the soil surface and then filled with water. The air

hoses are connected and the computer program is booted up. The rest of the test is controlled by the computer. Fig. 28 gives the steps involved in a typical test (Tolhurst et al. 1999).

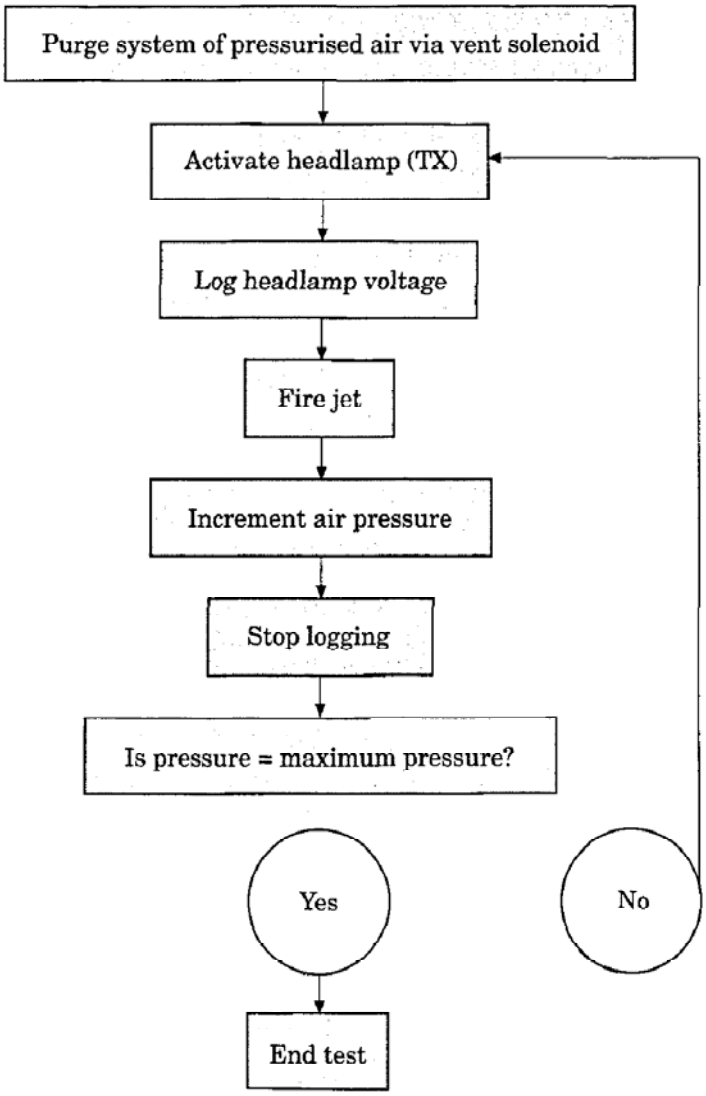

Fig. 28. CSM test procedure flow diagram (Tolhurst et al. 1999)

The air pressure during the test is brought within 6.9 kPa of the set maximum pressure and increased slightly by 0.17 kPa increments until the max is achieved. As the

pressure increases, the jet stream forms a cone with an approximate angle of 13 degrees from vertical. Photographs taken during testing show that the CSM creates a hole in the soil surface. Observations from Tolhurst et al. (1999) show that sand and larger grained particles are washed up and out of the hole by the pulses and are then re-circulated in the cell.

2.7.3.3 Data Reduction

The calculations of shear stress and erosion rate are based on the effort required to suspend the soil particles. The CSM measures water clarity and from the calibration below, the shear stresses required to suspend a particle of a given size were determined. Once a drop in transmission (decrease in clarity) is detected, the applied pressure is recorded. This pressure corresponds to an equivalent horizontal shear stress applied at the soil surface. The threshold is defined as the pressure required to suspend the particles. From this pressure, the critical shear stress and velocity can be calculated. Tolhurst et al. (1999) notes that there is no detectible difference in suspension for particles with a diameter less than 200 μm. See the calibration below for equations.

2.7.3.4 Calibration

The following calibration was taken from Tolhurst et al. (1999). A similar calibration using garnet quartz can be found in Vardy et al. (2007). For the CSM calibration to the critical suspension curve of Bagnold, a quartz sand was used. The particle sizes were determined and samples were placed in Petri dishes. The CSM test

chamber was placed over the dish and filled with distilled water. The samples were tested at 1s pulse durations at two different pressure ranges based on particle sizes. For each test, the lowest transmission was plotted for each pressure step to give an erosion profile (Fig. 29).

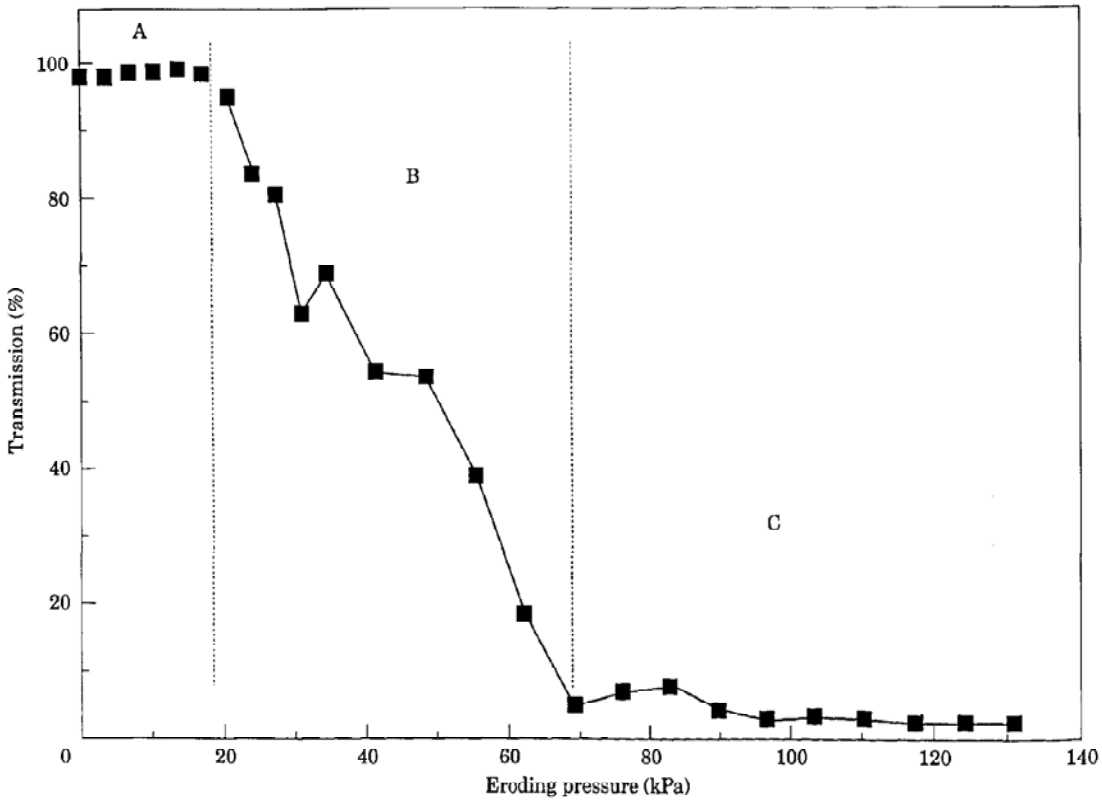

Fig. 29. Transmission data taken during CSM calibration (Tolhurst et al. 1999)

Each soil with different properties has a different transmission profile. As in the previous erosion devices, a threshold value is an important parameter for erosion analysis. For the CSM, the critical erosion threshold is defined as the pressure applied at the point when transmission drops below 90 percent. The relationship between the eroding pressure and grain size was plotted and determined to be non-linear (Fig. 30).

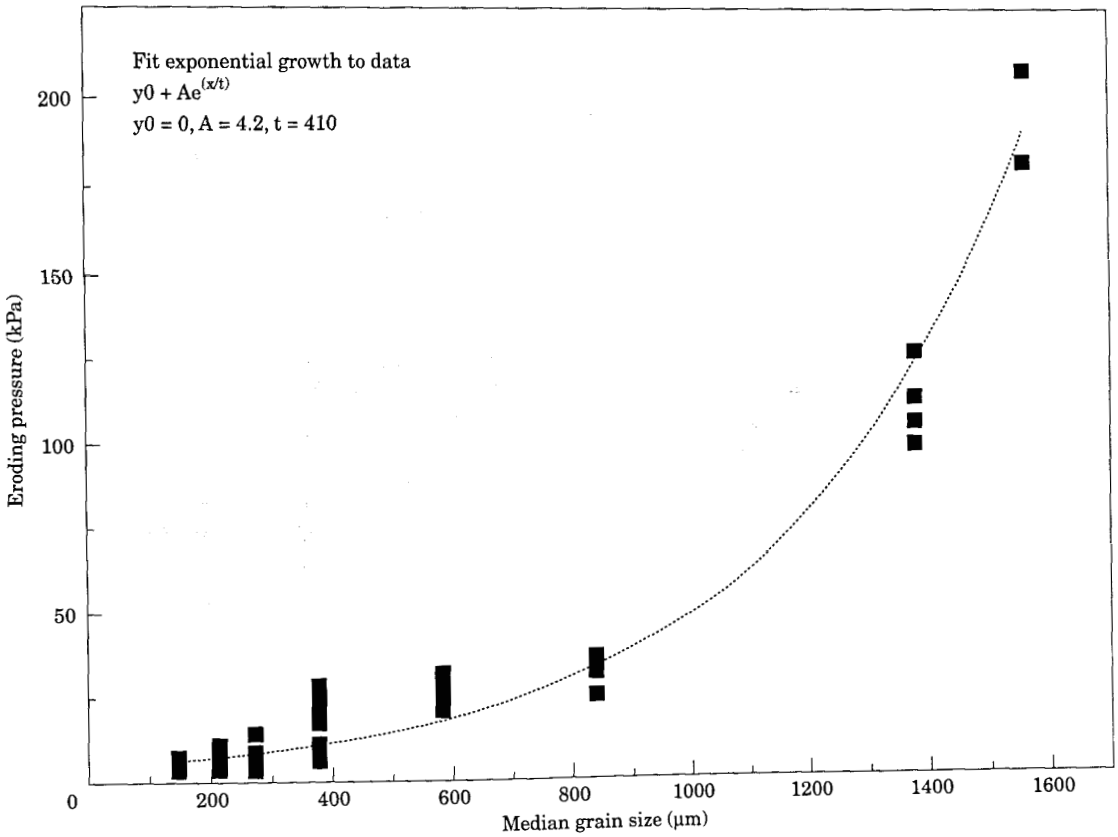

Fig. 30. Erosion pressure versus grain size (Tolhurst et al. 1999)

Similar tests run on finer grained sands indicate that the CSM cannot determine a significant difference in the erosion threshold for particles less than 200 µm. Testing also indicated that incipient motion of the soil particles is not able to be detected and it is not until they are suspended that a transmission drop can be detected. Therefore, a correlation of critical jet pressure and critical shear stress is not appropriate. Instead, the critical pressures were compared to the Bagnold equation, modified by McCave (1971), which describes sands in suspension:

$$\theta \geq \frac{CV^2}{gD} \tag{48}$$

where θ=Shield's criterion for the suspension of particles, C=0.19, V=settling velocity of particle (m/s), g=acceleration due to gravity (9.81 m/s^2), and D=grain diameter (m). Settling velocities were adjusted from Gibbs et al. (1971) to account for non-spherical shape using:

$$w_m = 0.977 {w_s}^{0.913} \tag{49}$$

where w_m=adjusted settling velocity, and w_s=settling velocity of quartz spheres. The equivalent horizontal bed stress resulting in suspension can be found using:

$$\theta = \frac{\tau_0}{(\rho_s - \rho_w) g D} \tag{50}$$

where ρ_s=sediment particle density, ρ_w=density of water (kg/m^3). An equation relating the eroding pressure to the equivalent horizontal stress was plotted and the best fit curve is given by:

$$\tau_0 = y_0 + A1 \times \left[1 - e^{(-x/t1)}\right] + A2 \times \left[1 - e^{(-x/t2)}\right] \tag{51}$$

where τ_0=equivalent horizontal erosion shear stress (N/m^2), y_0=zero, x=eroding pressure (kPa), A1=67, A2=-195, $t1$=310, and $t2$=1623. The equivalent horizontal shear stress can be converted to velocity by:

$$U = \left(\frac{\tau_0}{\rho}\right)^{1/2} \tag{52}$$

where U=shear velocity (m/s), ρ=density of water (kg/m^3), and τ_0=shear stress (N/m^2).

2.7.3.5 Advantages and Disadvantages

The compact "suitcase like" size, the fully automated device, and the short time period required for a measurement to be taken make the CSM ideal for measuring

variations in intertidal sediment erosion. However, there is still some question to the exact force or shear stress exerted on other cohesive soils during testing and how it relates to an erosion category or standard value for a flood event. The findings show a weakness in the fact that for modeling purposes a relation between the CSM results and threshold values for fine grained particles cannot be established yet (Vardy et al. 2007). As of Tolhurst et al. (1999), a detailed analysis of the turbulence effects in the CSM have not yet been made. Also, the CSM only can determine a semi-quantitative measurement of erosion rate. The test, while it is less complicated than some of the others, still involves relatively expensive and sophisticated equipment.

2.7.4 Rotating Cylinder Test (Chapuis and Gatien 1986)

The rotating cylinder test (Fig. 31) allows for the study of the fundamental mechanisms governing the steady external fluid erosion of a cohesive soil. The test can be run on either intact field samples or remolded samples. The water quality is controlled so that it is similar to the actual field and physicochemical conditions. This test also allows for the determination of the influence of factors such as water quality and physicochemical treatments of the clay.

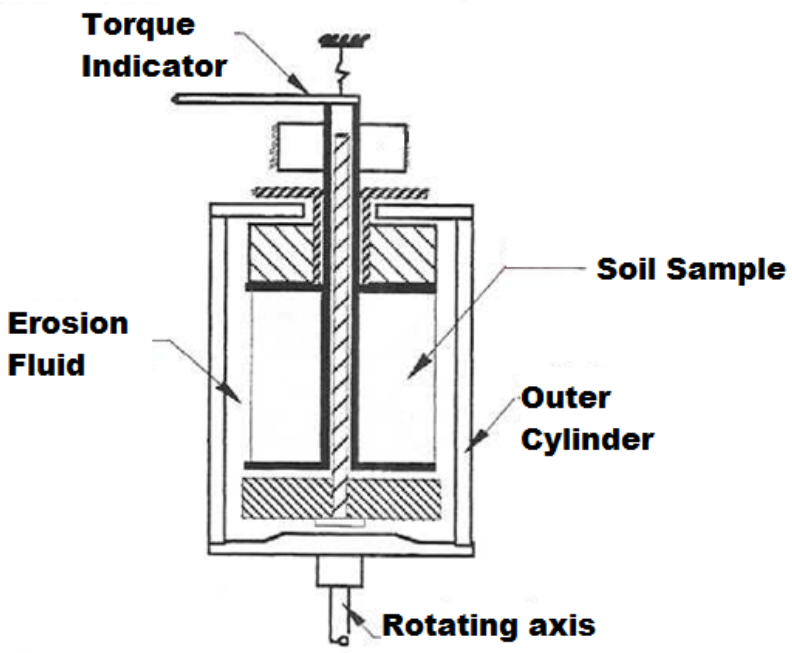

Fig. 31. Schematic of the Rotating Cylinder Test apparatus (Tarog 2000)

The principle behind the rotating cylinder apparatus is based on annular water flow between two concentric cylinders. The soil sample is contained in the inner cylinder, and is held stationary during the test. These samples can be cut from intact samples or can be remolded in a triaxial cell. It should be noted that as a general rule, the samples prepared in a triaxial cell have a smoother and less erodible surface than samples that are cut from the same intact clay for shear stresses lower than the threshold value. For intact samples, the soil is placed between two metallic cylinders guided by ball bearings. The base rotates freely relative to the outer cylinder. The outer cylinder can be rotated to impart movement of the fluid which applies a shear stress to the surface of the soil sample. For this test, the erosion rate is defined as the loss in dry weight of the sample per unit surface area and per unit time. Upon completion of each stage of a

test, the eroding fluid is emptied from the cell and the cell is rinsed. The amount of oven-dried material that exists in the collected fluid is weighed. The shear stress on the surface of the soil sample caused from the moving fluid can be directly derived from the torque required to hold the sample stationary in the apparatus. The shear stress transmitted to the clay depends on the surface roughness and is constantly changing throughout a test. The apparatus allows for the continuous measurement of the average shear stress imparted on the soil by the flowing water. The test results include a graph of shear stress versus rotation speed (Fig. 32) and a graph of erosion rate versus the contact shear stress (Fig. 33).

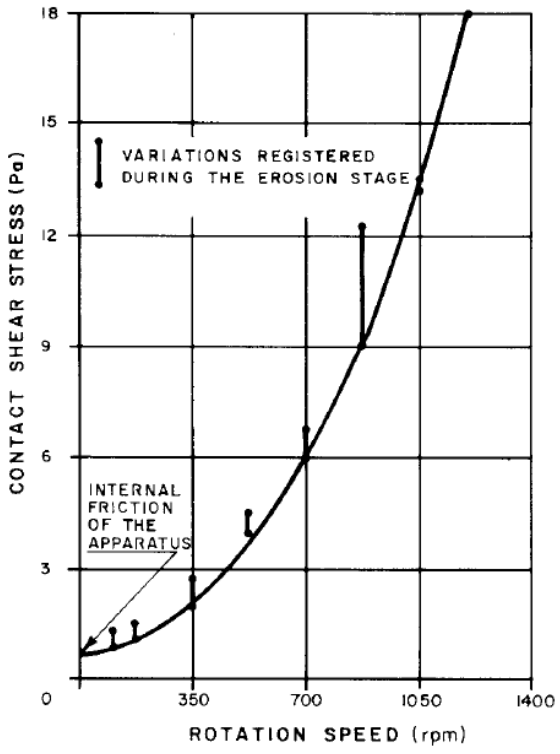

Fig. 32. Contact shear stress versus rotation speed (Chapuis and Gatien 1986)

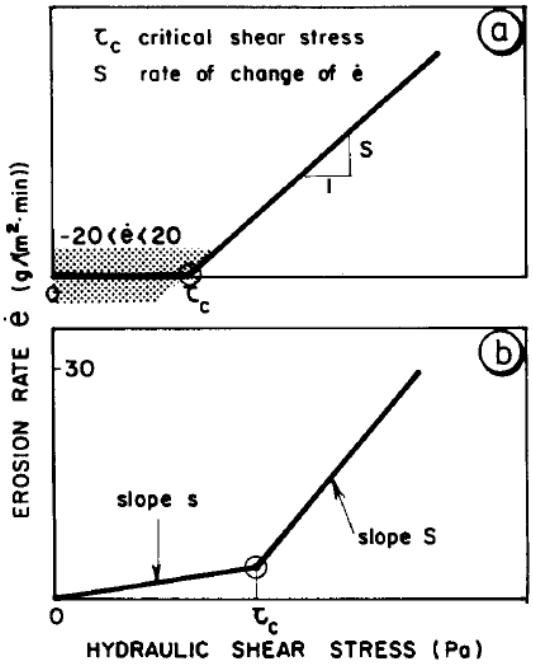

Fig. 33. Erosion rate versus shear stress (Chapuis and Gatien 1986)

2.7.4.1 How the Apparatus Operates

The apparatus allows for a cylindrical sample of soil to be placed between a base and a top metal cylinder. Both of these cylinders are guided by ball bearings. In the more recent version of the apparatus, there is no shaft within the soil sample. The base is free to rotate relative to the outer cylinder. The base can be rotated at a speed of up to 1750 rpm. The mean flow induced shear stress is directly and continuously measured. The torque required to keep the soil sample stationary is also measured. The soil sample is held stationary by a pulley and variable weight system. The more recent apparatus also has a reduced internal friction because of several mechanical improvements.

2.7.4.2 Test Procedure

An early version of the rotating cylinder only could be used for remolded clays. The clay samples were formed into a slurry and reconsolidated around a metal shaft. The shaft was then installed into the cylindrical apparatus and the sample was suspended in the erosion fluid. A more recent version of the apparatus allows for either intact or remolded samples. Reconstituted and reconsolidated samples can be formed in a triaxial cell replicating the intended field conditions. It has been noted that intact cut samples have a more rough and erodible surface than the same soil formed in the triaxial cell. The shear stresses on the surface of the triaxially formed samples are generally less than those measured on intact samples.

The clay cylinder is mounted on a circular base inside a larger transparent cylinder. This base is able to rotate at a regulated speed. The space between the soil surface and the outer cylinder is filled with water. The outer cylinder is rotated causing the fluid to also begin to rotate about the soil sample. The soil sample is held stationary. Each test consists of several stages at given rpm values. Each stage is run for 10 to 30 minutes. The shear stress imparted on the soil surface is continually measured.

Once a stage is complete, the erosion fluid is drained from the cell into a bowl and the cell is rinsed clean as the fluid is collected. The recovered fluid is oven dried and the eroded soil particles are weighed.

2.7.4.3 Data Reduction

A test report provides the eroded mass, continuous shear stress values, and rpm values for each stage. A graph of erosion rate versus the contact shear stress can be developed. A graph of contact stress versus rotation speed can also be generated (Fig. 32). Generally 6 to 10 samples are tested. Once all values are determined, it is possible to determine the threshold value for the given soil, above which the erosion rate increases considerably. A graph of mean erosion rate versus the shear stress can be made (Fig. 33).

2.7.4.4 Advantages and Disadvantages

This test can determine the influence of water quality on erodibility as well as replicate field conditions to determine the erodibility of a given soil sample. The way in which the test is run directly replicates surface erosion that can be expected under certain field flood conditions.

As discussed above, there is a difference in the contact shear stress measured based on the roughness of the sample. For the same soil, two different measures of shear stress can be expected based on whether the sample was cut from an intact piece or made in a triaxial cell.

2.8 Case History in Overtopping Erosion: New Orleans

It was not until August 2005 when Hurricane Katrina struck Southeastern Louisiana that the American public became aware of the importance of the country's levee systems. The relatively fast-moving Category 3 hurricane made landfall at 6:10 am on Monday, August 29th (van Heerden et al. 2006). Although damages were incurred throughout the south, the main focus was on New Orleans, Louisiana.

Following Hurricane Katrina, several external study teams were put together including: the Independent Levee Investigation Team (ILIT) which grew out of a UC Berkeley initiative, the Interagency Performance Evaluation Team (IPET) sponsored by USACE, and Team Louisiana which was commissioned by the Louisiana Department of Transportation and Development. Much of the information presented in this section was taken from the report prepared by Team Louisiana (van Heerden et al. 2006) because they provided an adequate review of each groups' findings. Each team conducted a thorough investigation of pre and post-Katrina conditions and levee performance. Each investigation differed in some aspects, but they generally concur on most of the failure mechanisms of the floodwalls.

Louisiana is more prone to hurricanes and flooding than any other state in the US. Prior to Katrina, over 70 percent of the population in the state lived in only 36 percent of the land. Louisiana's main attraction city, New Orleans, straddles the Mississippi River and is located in one of the world's great deltas. The city has been one of the oldest continually occupied commercial centers in American. The main portion of the city lies north of the Mississippi River, however, suburbs spread South of the river

and East and West along its banks. The entire area is surrounded by large estuarine embayments, deteriorating swamps and marshes, and lakes Pontchartrain and Borgne. Much of the city of New Orleans is at or below sea level (Fig. 34) creating water ponding areas or in essence a bowl. Even the rainwater runoff must be collected in channels and pumped out of the city. The areas below sea level are shown in dark blue. Fig. 35 shows a slightly exaggerated LIDAR scan of the elevations of New Orleans created by Dewitt Braud of the LSU Coastal Studies Institute.

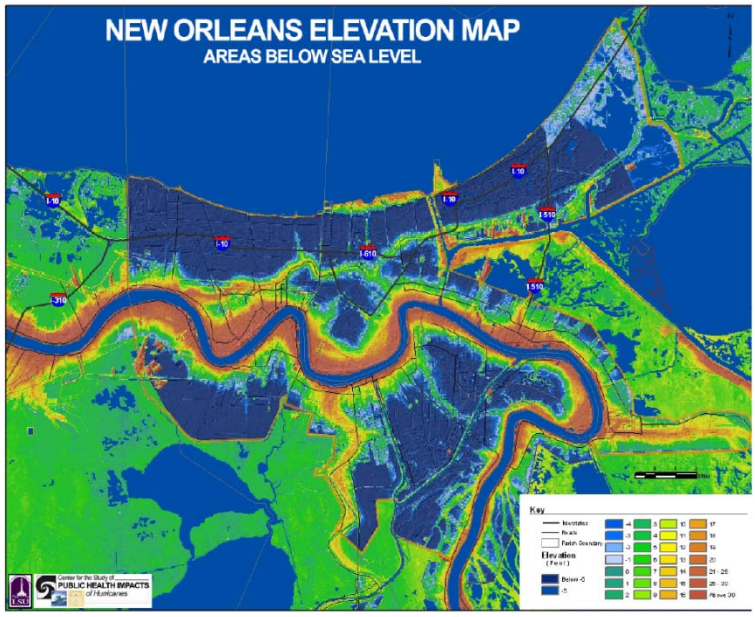

Fig. 34. LIDAR color-coded to show areas relative to sea level (HPHC 2009)

Fig. 35. LIDAR image of New Orleans by Dewitt Braud (van Heerden et al. 2006)

The city of New Orleans has been surrounded by levees since the early 18th century. These levees have allowed for the development of these subsided areas and today reach more than 25 ft (7.6 m) high in areas. As mentioned earlier, levees are designed as flood reduction systems for a specific storm or flood event and even though it was known that a large storm could overtop the flood defenses of New Orleans, the general public viewed the levees as protection system and developed the area accordingly. The hurricane brought winds and rainfall that alone dumped tremendous amounts of water into the city center. In the Greater New Orleans area alone, Interagency Performance Evaluation Team (IPET) estimated 24-hour rainfall between 9.9 in (252 mm) and 13.6 in (345 mm) beginning at about 2300 CDT on the 28th of August. The peak rate of precipitation was reported at almost 2 in/hr (51 mm/hr) between 0300 and 0400 on the 29th. Even though the winds experienced by most of the city were less than expected, the storm surge was large. The surge reached almost 20 ft

(6.1 m) against the Mississippi River levees in Plaquemines Parish and almost 30 ft (9.1 m) in some parts of Mississippi. The largest surge observed in the Greater New Orleans area was against the Mississippi River Gulf Outlet (MRGO) levee in the area formed by the convergence several levee systems. The surge penetrated 6 mi (9.7 km) into the area. Katrina's storm surge also caused the water level in the Pearl River marshes and in Lake Pontchartrain to rise. Lake Pontchartrain had been rising for about a day before Katrina made land fall, reaching about 3 ft (0.9 m) (NAVD88). With the rainfall, winds, and rising lake levels, the levees were subjected to large hydraulic loading and overtopping waters never seen before.

When the levees were breached, the storm water filled the city leaving approximately 80 percent of New Orleans Parish, 99 percent of the St. Bernard Parish, and approximately 40 percent of Jefferson Parish submerged. Because of the low lying areas, the water remained in buildings and houses and streets for weeks and even months. Over 1500 lives were lost and over 100,000 families were left homeless and many more displaced. The damages were estimated at well over 16 billion dollars (ASCE 2009). The disaster was considered the worst since the Mississippi River flood of 1927. Over 170 miles (273.6 km) of the 350 miles (563.3 km) of levees that surround New Orleans were damaged or destroyed (IPET 2006).

Fig. 36. View of New Orleans post Katrina Sept. 14, 2005 (FEMA 2005)

Several different failure modes were deemed responsible for the levee breaches. USACE identified 50 separate locations on the Greater New Orleans Hurricane Protection System (HPS) where breaches occurred from structural instability, erosion due to overtopping, or some combination of the two. Table 7 provides an example of several of the levee significant breaches and their cause.

Table 7. Summary of a portion of the significant levee breaches (van Heerden et al. 2006)

Table 3a Significant Breach Sources of Katrina Floodwater in GNO HPS							
HPS Zone	Breach Name	Type	Cause	Top Width (ft)	Sill Elev (ft)	TimeStart	Start Water Level
Orleans Metro							
Lakeview	17th St. RELee	I-Wall	Translation Slide	450	0.0	6:00-7:00	6.5
Fillmore	London North	I-Wall	Underseepage/ Rotation Slide	180	0.0	7:00-7:30	8.2
Mirabeau/ Dillard	London South	I-Wall	Underseepage	100	-4.0	6:00-7:00	7.1
City Park	Orleans Canal	Earth Levee	No Floodwall Installed	150	9.5	8:30	
Desire	IHNC West RR	RR Gate Missing	Sandbag Plug Blowout	37	5.1	4:30	9.0
Desire	IHNC West Florida Ave. North Breach	I-Wall	Overtopping Erosion	100	7.0	7:00	12.0
Desire	IHNC West Florida Ave. South Breach	Earth Levee	Overtopping Erosion	125	5.0	5:00	10.0
St. Bernard/ Lower 9th Ward							
Lower 9th Ward	IHNC East Bank North	I-Wall	Overturned/ Insufficient Levee	90	7.0	7:30	12.5
Lower 9th Ward	IHNC East Bank South	I-Wall	Overtopping Erosion Underseepage	1,000	5.0	7:30	12.5
Chalmette, Poydras, Verret	MRGO	Earth Levee	Wave Erosion Overtopping	60,000	0.0	5:00	12.0
Lower 9th Ward	IHNC/ GIWW	Wall Levee	Transitional Failure	30	4.0	6:00	11.0

Along with the investigation teams listed, a team from Texas A&M University under the direction of Dr. Jean-Louis Briaud (Briaud et al. 2008) was given the task of studying erosion due to overtopping for several areas throughout New Orleans. The

team collected thin wall steel tube samples and bag samples from the levee crests at depths less than 1m in several locations. Fig. 37 shows the locations of the samples taken.

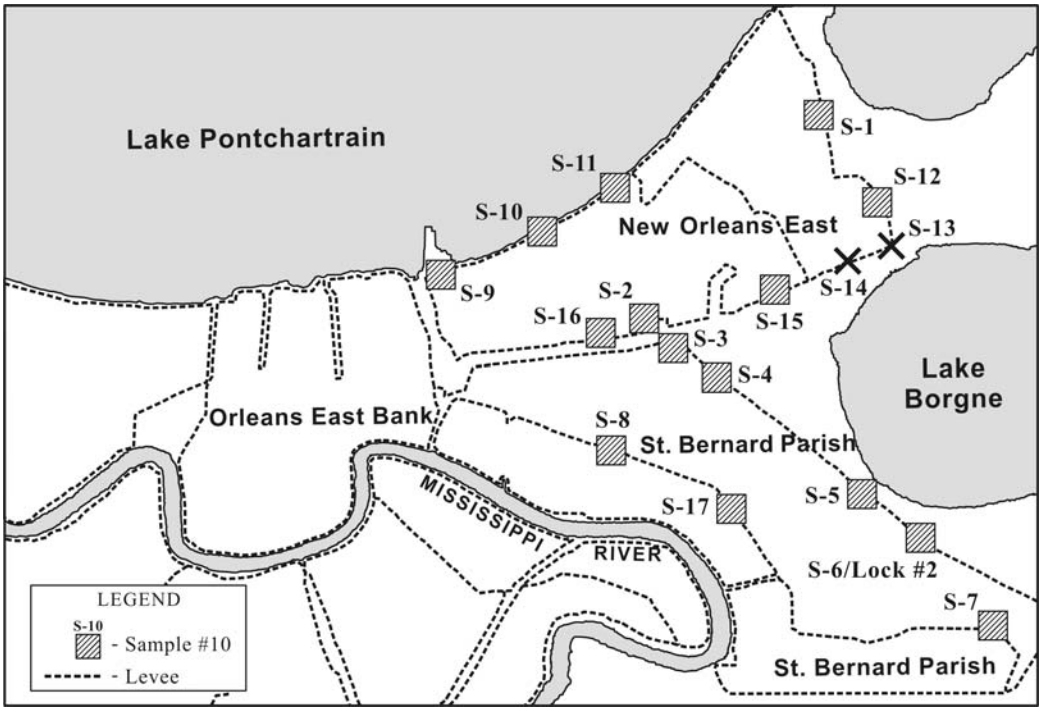

Fig. 37. Sample locations for New Orleans overtopping study (Briaud et al. 2008)

In order to get an idea of the flooding in the areas studied, the following figures are presented from van Heerden (2006). Figs. 38 and 39 show the same area as above, but are color coded. The dark blue areas show water flooding exceeding 12 ft (3.7 m) in depth. The figures also show approximate locations of the levee breaches. Figs. 40, 41, and 42 show the respective area using terminology developed by IPET to show and distinguish the different failure modes, and causes of flooding (IPET 2006).

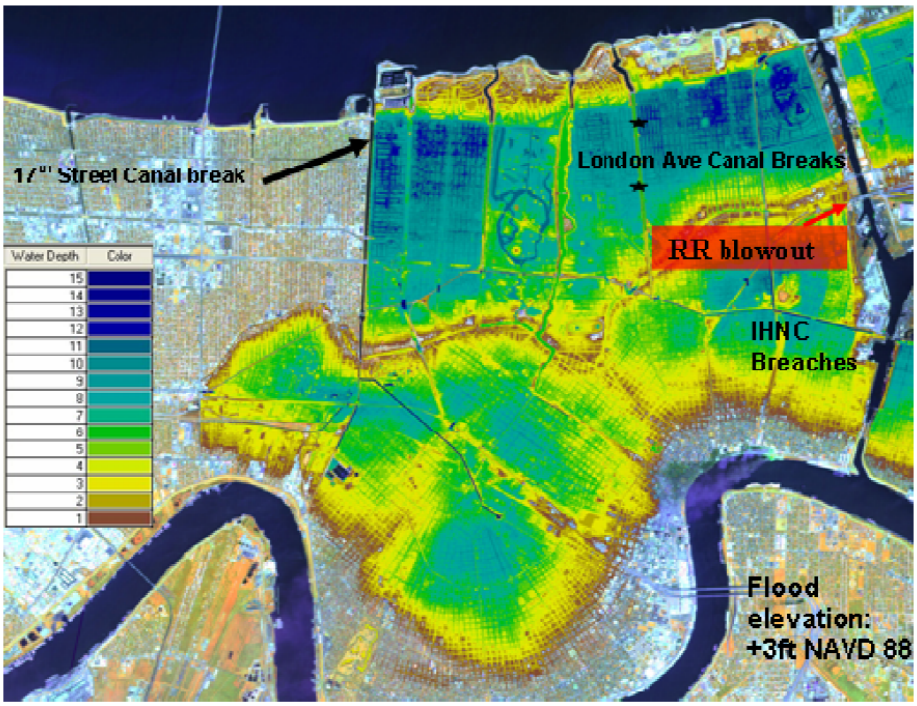

Fig. 38. LIDAR scan showing flood water depth (IPET 2006)

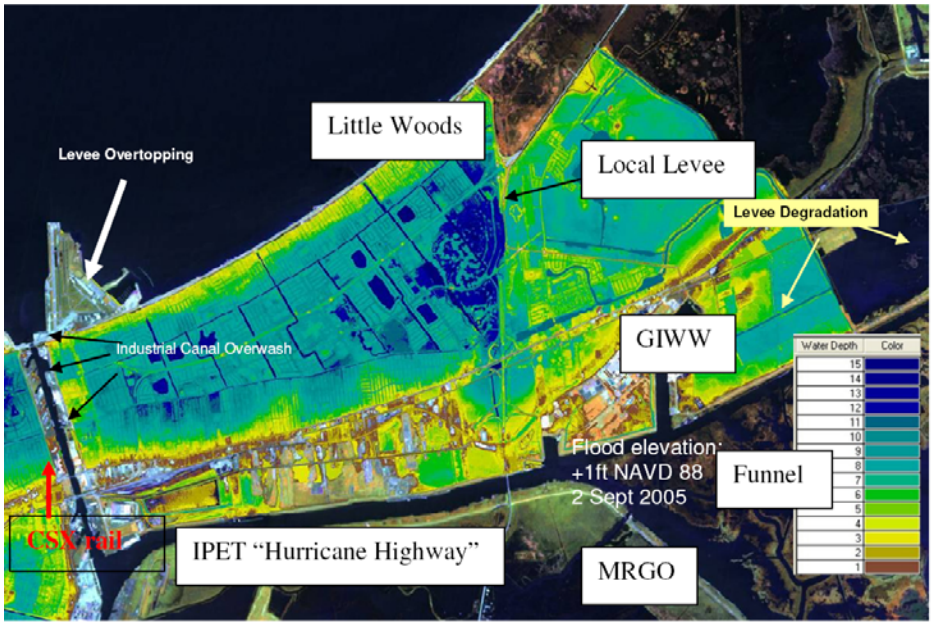

Fig. 39. LIDAR scan showing flood water depth East New Orleans (IPET 2006)

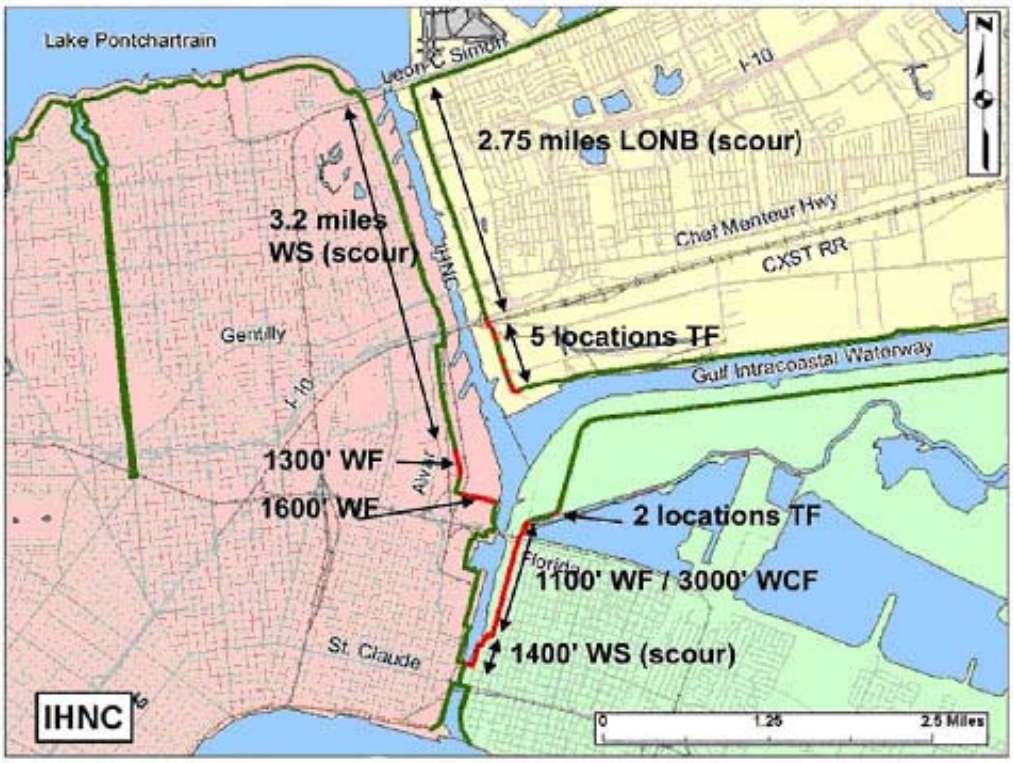

Fig. 40. Overtopping and breaching along the IHNC (IPET 2006)

Damaged areas shown: LONB= overtopped levees, no breaching, WS=Overtopped floodwalls, no breaching (stable), LOB=Overtopped levees, breaching, TF= Transition failure (floodwall to levee transition), WF= Overtopped floodwalls, breached (failure).

The IPET team determined from the assessment of the HPS for the New Orleans East area that the majority of the damage was due to erosion from overtopping waters. The lack of evidence of foundation failure led the team to believe the breaches were caused by erosion and the damage to the floodwalls was caused by a loss of soil support on the dry side because of the erosion.

Fig. 41. Overtopping and breaching in New Orleans East (IPET 2006)

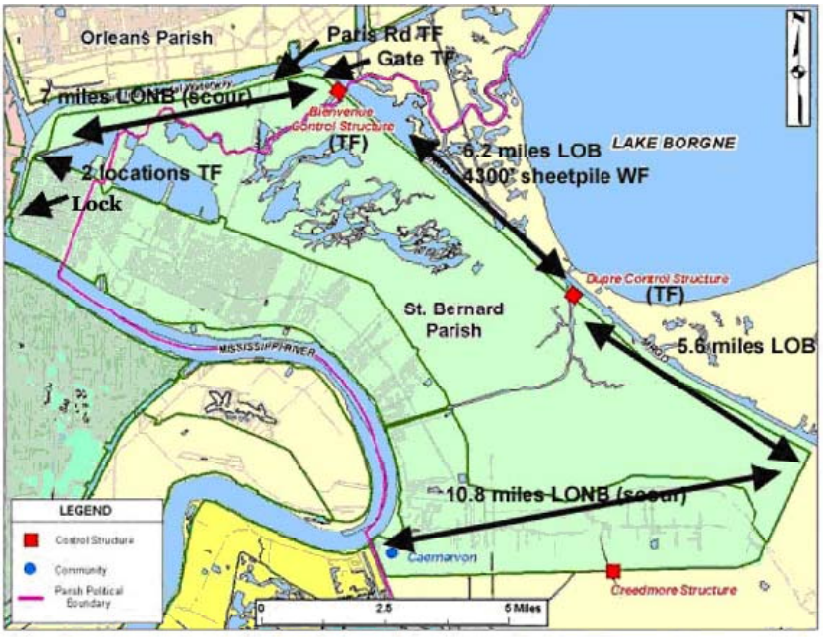

Fig. 42. IPET damage assessment on the St. Bernard HPS (IPET 2006)

The soil types sampled varied from loose fine sand to high plasticity stiff clay (Briaud et al. 2008). EFA tests were performed on each tube sample collected. The bag samples were reconstituted in Shelby Tubes at high and low compaction effort. Along with testing the different compaction effects, several of the samples were tested using tap water and several were tested using simulated sea water. The results, plotted in Fig. 43, show soils ranging from very high erodibility (Category 1) to low erodibility (Category 4).

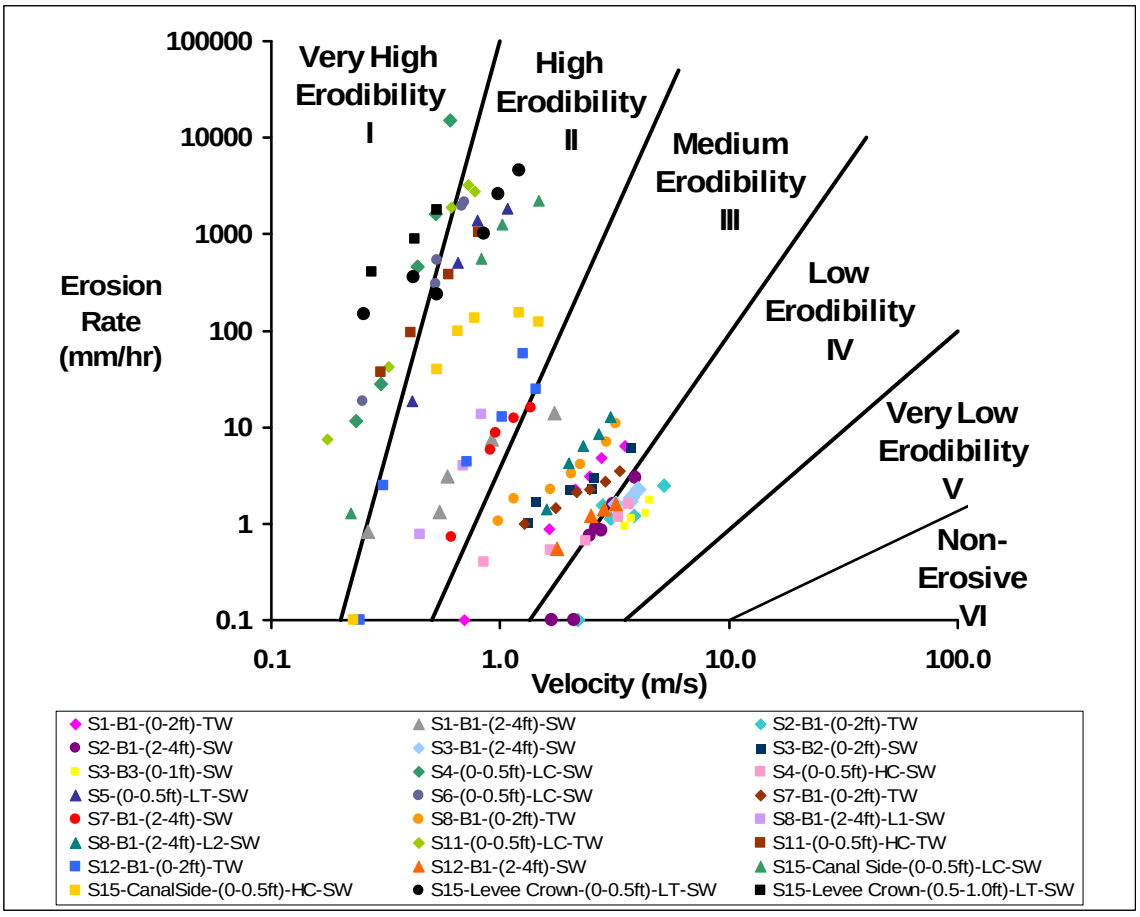

Fig. 43. EFA test results in terms of velocity (Briaud 2008)

The tests showed that erosion resistance increases with increasing compaction, however, the effect is much more significant for some soils than for others. The soils with higher fines contents seemed to be more effected by the amount of compaction. The water salinity also proved to have an influence on the erodibility of the soils; however, no general trend was recognized.

In order to relate the velocity values used in the EFA to those expected during the hurricane event, numerical simulations were conducted. The simulated levee was 5 m high with 5:1 slopes on both sides. The water height above the crest was initially set at 1 m. The water velocity determined at the bottom of the slope on the dry side reached 12 m/s while a steady state shear stress value of 35 kPa was found.

In several locations, levees were overtopped and failed while others resisted. The erosion functions for those that failed were plotted as solid circles and those that resisted were plotted as open circles (Fig. 44). There is a clearly defined division in the types of soils based on erodibility that survived the overtopping events and those that did not. These findings led to a hurricane overtopping erosion prediction chart (Fig. 45). The duration length for the overtopping considered in this chart is for a few hours at max. Longer flood overtopping events do not necessarily follow the trends found for these conditions.

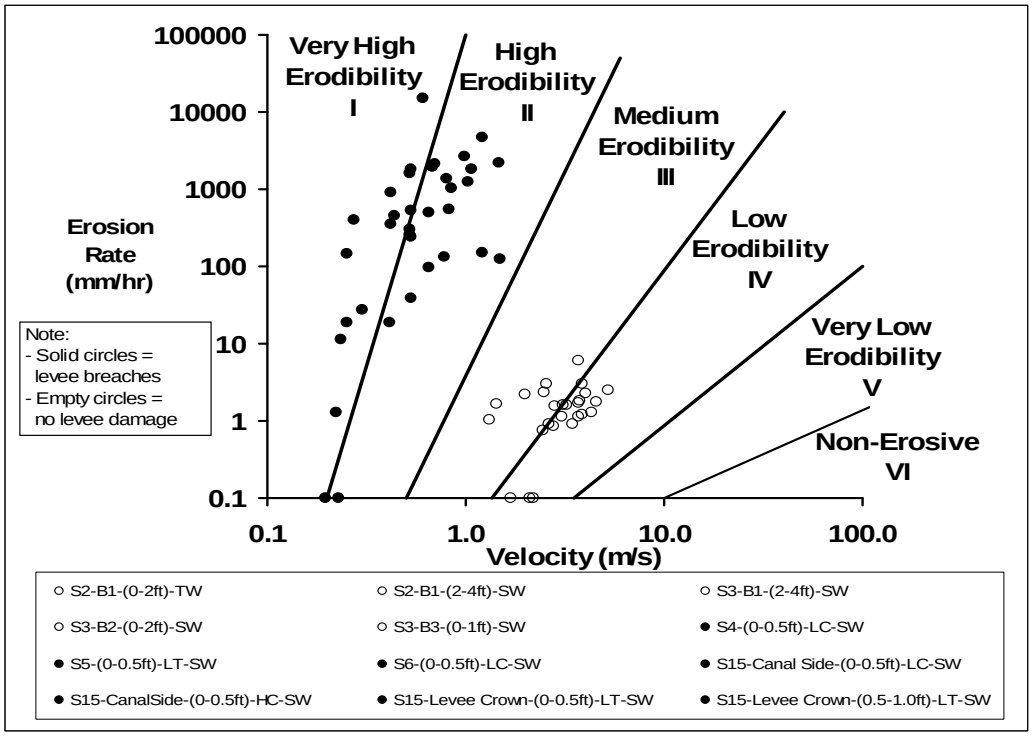

Fig. 44. EFA results plotted as pass or fail based on overtopping (Briaud 2008)

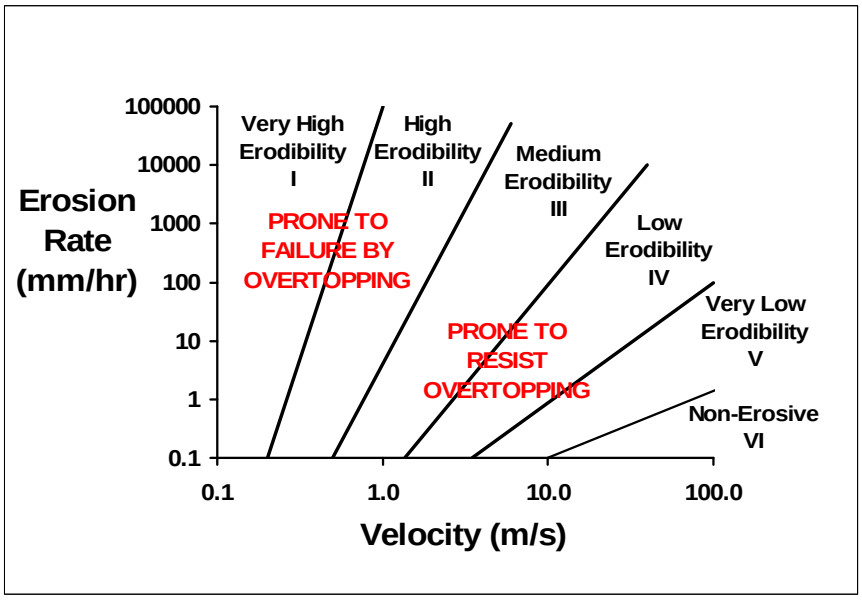

Fig. 45. Levee overtopping erosion chart for hurricane events (Briaud 2008)

3. INTRODUCTION TO THE MIDWEST LEVEE SYSTEM

3.1 America's Great River (USACE 2004; O'Brien 2002)

The Mississippi River has played more of a part in the development and expansion of the U.S. than any other river. The Mississippi River has been used continuously as a navigation and transportation channel even before the first recorded cargo was floated down the river from a Native American settlement in 1705 (USACE 2004). Its use as a transportation mode dates back thousands of years to the first American Indians in the area. They used the river to move from camp to camp with the changing seasons and later used the river as a way to get furs and other goods down river to trade with European settlers. European explorers navigated the river and its tributaries uncovering never seen before territory and settling communities along the water source, thus beginning the development along the Mississippi.

The Mississippi River has the third largest drainage basin in the world, surpassed only by the Amazon and Congo Rivers. The basin covers parts of 31 states and two Canadian provinces and reaches more than 1,245,000 square miles (3,224,535.2 km^2). The length of the Mississippi drains 41 percent of the 48 continental United States. The Mississippi River can be broken up into two main drainage sections: the lower Mississippi River Valley and the Upper Mississippi River System. The lower section begins just south of Cape Girardeau, Missouri and runs 600 miles (965.6 km) where it empties through Louisiana into the Gulf of Mexico. The Upper Mississippi River system, home to the Midwest Levee System, is a 1,300 mile (2092.1 km) waterway that links five states to the lower section and thus the Gulf Coast export markets.

For as long as the Mississippi has been in existence, it has flooded the valleys through which it flows. The first recorded flood of the Mississippi was described in 1543 by Garciliaso de la Vega, during an expedition begun by DeSoto, as severe and prolonged, beginning about March 10th and cresting about 40 days later. The river returned to its banks sometime in May after about 80 days of flooding. In the lower Mississippi valley, one flood occurs every three years on average (O'Brien 2002). These floods can last weeks and even months, such as the flood from December 1734 to June 1735 with destroyed parts of New Orleans and other places on the lower river. While the recurrent flooding left the soil along the river fertilized with nutrients, as developments and farming grew the floods destroyed buildings, equipment, crops, and even killed animals and people.

Humans have tried to control the flooding of the Mississippi for as long as they have been settling next to it. Early Native Americans and then European settlers built levees in an effort to prevent flooding (O'Brien 2002). Initially, individuals were responsible for private levee construction along their portion of land, which left the river sparsely bordered by non-engineered "mounds." It was not until the 1850's that the Mississippi Legislature authorized the creation of levee districts. Even with its creation, Louisiana, Mississippi, and Arkansas maintained different levee standards. In 1865, after the Civil War had ended, southern land owners acquired the authority to create the Board of Levee Commissioners, later known as the Mississippi Levee District. The board was able to tax land and place duty on cotton among other things to issue the funding of new levee construction projects. By 1879, the Mississippi River was in need

of much improvement, and the necessity for the coordination of engineering operations through one central office had finally been approved (USACE 2004). In that year, Congress created the Mississippi River Commission and assigned it the following tasks: "to take into consideration and mature such a plan or plans and estimates as will correct, permanently locate, and deepen the channel and protect the banks of the Mississippi river, improve and give safety and ease to navigation thereof, prevent destructive floods, promote and facilitate commerce, trade, and the postal service." Three years after the Commission was established, one of the most disastrous floods up to that point left the entire delta area devastated. Through the years as flooding continued, several other levee districts were created, until the federal government took complete control until 1917 (O'Brien 2002).

The 1927 flood had the most dramatic impact on the Mississippi River valley of any flood up to that time. The following is an excerpt taken from the PBS special Fatal Flood (2001):

> **Billy Payne, Resident:** Well, the winter of '27 it started raining early in the year that year. January, February, it rained it seemed like every day.
> **Sarah Percy, Resident:** It rained and rained and rained and rained some more. It just looked like it would never stop.
> **Mildred Commodore, Resident:** The river kept coming above flood level and it was rumored in all of the papers and things that if this levee would break we'd have a flood that would wash away from Memphis to New Orleans.

The Upper portion of the Mississippi peaked in April of 1927 and water overflowed the banks (USACE 2004). Levees bordering the river were no longer able to contain the raging waters. The breached levees allowed a wall of water to push through

the Midwestern farmlands. The flood water remained above flood stage for two months. The flood overwhelmed the lower Mississippi valley levee system, flooding approximately 26,000 square miles (67,339.7 km^2) and displacing over 600,000 people. Over 200 lives were lost and property damages reached $1.5 billion in today's prices. This disaster led to the passing of the 1928 Flood Control Act, which meant the federal government took entire control and responsibility for the management of the Mississippi River system. It also meant the U.S. Army Corps of Engineers would take over all engineering and construction along the river and it led to the Mississippi River and Tributaries Project. To date, numerous other federal sponsored improvement projects have been carried out along the Mississippi River. Each year the in place levee systems deteriorate and need repairs and as developments continue along the river, the need for more safe levees will continue to grow.

3.2 Upper Mississippi River System and the Midwest Levees

The history of Upper Mississippi River System (Fig. 46) as a navigation channel dates back to the 1820's (USGS 2007). The invention of the steamboat in the early 1800's brought a burst of river commerce and development. With the increased power of the steamboats, heavier and larger loads could be transported downstream. However, the river was inadequate in some places for this type of travel and for the larger vessels that were being used. Congress authorized the removal of any obstructions along several reaches of the river along with the construction of a canal connecting Lake Michigan and the Illinois River. Throughout the 1930's, several projects were authorized leading to

the current navigation channel. What was once rapids and waterfalls was replaced by twenty-nine locks and dams on the Mississippi and eight on the Illinois creating a stair stepped commercial and recreational waterway.

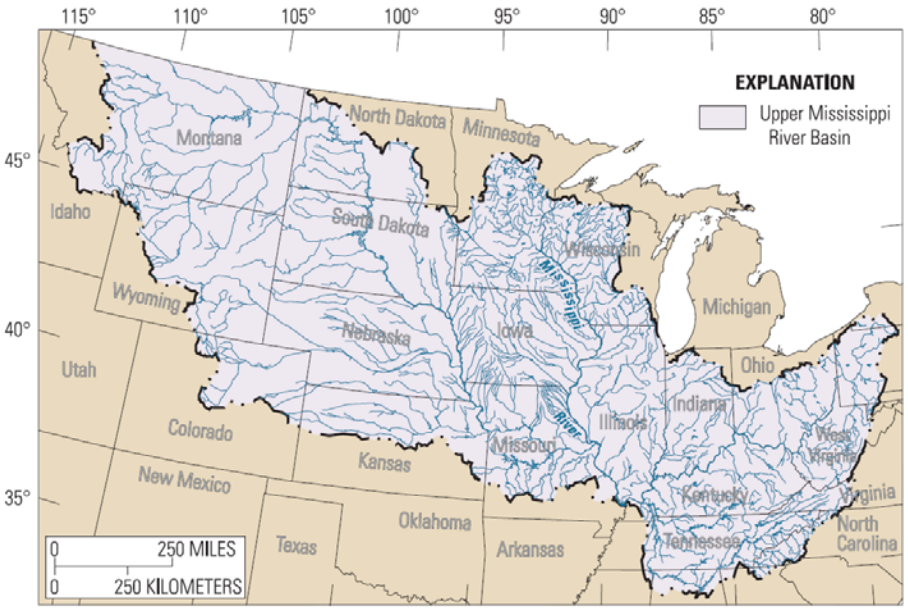

Fig. 46. Upper Mississippi River drainage basin (Johnson et al. 2003)

Today, more than 30 million of the region's residents rely on the Upper Mississippi river water for public and industrial supplies, power plant cooling, wastewater assimilation, and other uses (USGS 2007). The barge traffic is now more than ever and it will continue to grow. On average, approximately 80 million tons of cargo is shipped annually between Minneapolis and the mouth of the Missouri River. Some of the most common items shipped include: agricultural commodities, petroleum products, and coal. Farm products account for nearly half the total tonnage shipped.

The river ecosystem is home to a diverse array of fish and wildlife. A 40 mile (64.4 km) reach of the Upper Mississippi River, known as the Mississippi Flyway, is the

migration strip for approximately 40 percent of North America's waterfowl and shorebirds and the single most important inland area for migrating diving ducks in the United States (USGS 2007). The area is also important for the migration of raptors and neotropical songbirds, and the breeding and wintering birds, including the bald eagle. In the river system alone, 154 species of fish and 50 species of freshwater mussels have been recorded.

Through the years, river modifications, control projects, and floodplain development have had lasting effects on the hydrological processes that drive and maintain the floodplain ecosystem. On the Upper Mississippi River alone, nearly 60 percent of the floodplain's 1,200,000 acres (485,622.8 ha) are now used for crop and pastureland (USGS 2007). These agriculture lands are bordered by extensive levee systems that provide a reduction in the seasonal flooding risk. Sedimentation along the river system has become a serious issue. The lock and dam construction has changed the natural sedimentation process allowing erosion rates in the basin to exceed the rate of soil formation which has resulted in an increase of sediments in the Mississippi River itself. The sediments are deposited within the river and in backwater areas. This sedimentation will eventually degrade the surrounding habitat and transform the aquatic environment that presently provides fish, wildlife, and plants life to a terrestrial habitat. The Upper Mississippi River System is the only inland river in the United States to be designated by Congress as both a nationally significant ecosystem and navigation system. The National Research Council's Committee on Restoration of Aquatic

Ecosystems recently targeted the Upper Mississippi River and the Illinois River for restoration.

USACE reports that on the main stem of the Mississippi River alone, there are over 1,600 miles (2575 km) of levee in place (USACE 2007). A typical cross-section of the type of levee found along the Mississippi River is shown in Fig. 47. This diagram is mostly representative of the homogeneous levees found in Missouri and the states south along the river. Levees in the areas North of Missouri, Illinois and Iowa particularly, are multi-material zoned embankments. These levees often consist of a clay core and a clean sand shell of approximately 1 to 1.5 m. Note that the side slopes shown are a general design and are actually dependent on many variables including the land right-of-way available.

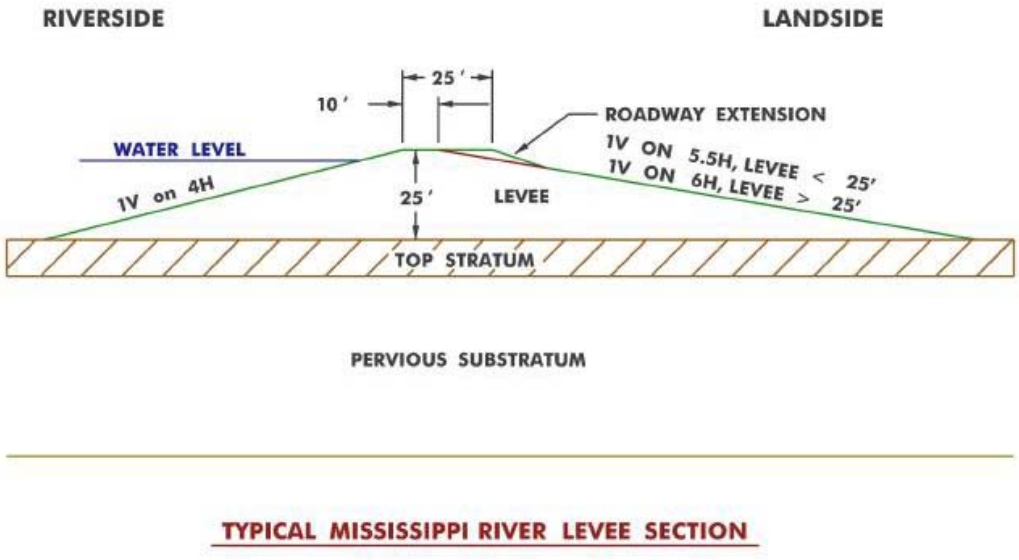

Fig. 47. Typical levee cross-section from USACE Memphis District (USACE 2007)

The Upper Mississippi River Levee System can be broken in to three main reaches (Fig. 48). A reach is defined as the length of levee comprised of similar

geomorphology, vegetation cover, and land use practices (USGS 2007). The first reach stretches from Minneapolis, Minnesota to Lock and Dam 13 near Clinton, Iowa. On this portion of the river, only 3percent of the floodplain is located behind the agricultural levees. Reach 2 stretches from Lock and Dam 13 to Lock and Dam 26. Approximately 53 percent of the floodplain in this section of the Mississippi River is located behind agricultural levees. This reach was the primary focus in the 2008 Midwest Levee Failure Investigation covered in this thesis. The third reach stretches from Lock and Dam 26 to where it meets the Ohio River. In this section of the river, approximately 82percent of the floodplain is located behind agricultural levees. A further breakdown of each reach and the pools that comprise them can be found at the USGS website.

Fig. 48. USGS Upper Mississippi River reaches (USGS 2007)

3.3 General Geology of the Area

The following section gives a general introduction into the historical geology of three of the Midwest states studied during the flood investigation. The information was gathered from several websites from government agencies and universities as well as geologists' personal sites. Further information and maps can be found at each of the sites listed.

3.3.1 Missouri (Missouri DNR 2009; Schaper 2009)

The state of Missouri contains surface bedrock deposits from several different time periods. Fig. 49, from the Missouri Department of Natural Resources (DNR), shows a generalized map of these bedrock deposits. The red and orange shades denote the oldest rocks and the younger formations are shown in the blue and green shades. The most recently deposited soils are shown in yellow and mainly consist of alluvial deposits. Those soils which have been deposited very recently are not shown on this map.

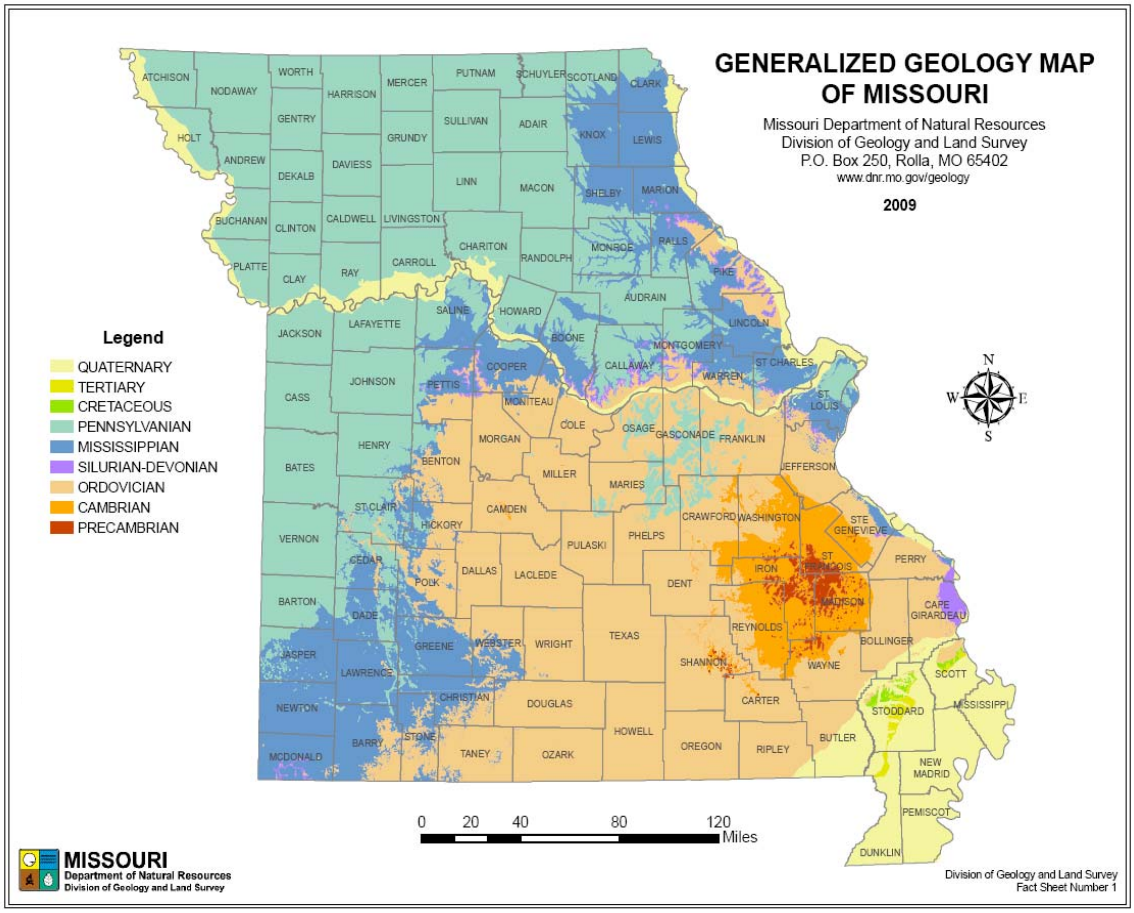

Fig. 49. Geologic map of Missouri (adapted from Missouri DNR 2009)

The following paragraphs summarize a more extensive overview of the geology of Missouri written by Jo Schaper (Schaper 2009). Geologists believe the earth, as it is known today, began 2.5 billion to 544 million years ago in what was termed the Proterozoic Eon. Fossils from some of the first shelled animals have been uncovered and date back to the period beginning 544 million years ago, called the Phanerozoic Eon. The Phanerozoic Eon is further divided into three eras: the Paleozoic, Mesozoic and Cenozoic. Each of these Eras are then subdivided into even smaller units known as Periods. With the exception of the Precambrian Era, the geological map of Missouri

shown above is based on Period names. It must be noted that geological maps at the scale shown above are very generalized and should be treated as such. This type of map only shows the rocks located at the surface of the state of Missouri. More detailed maps of smaller areas are available from the United States Geological Survey and the Missouri Department of Natural Resources GS-RAD, but this accuracy was deemed appropriate to provide a general geologic overview of the area of interest during the 2008 Midwest Levee investigation.

Generally speaking, the oldest rocks are deposited first, and then successive layers are added, most of the time in a horizontal manner. These layers can be deformed and translated by faults, or the top layers can be transported or changed by weathering and erosion. For simplification, only the age and deposition of the rocks will be considered in this discussion. Three of the common geological periods are not shown in the above map because rocks of the Permian, Triassic, and the Jurassic periods have not been found in the state of Missouri. However, rocks from the Cretaceous age were just recently correctly identified, but it seems unlikely that a large quantity of rocks of these three missing ages will be discovered. A brief discussion of each of the geologic eras and periods on the map is presented and should be referenced for the similar periods shown on the maps of the other two states.

3.3.1.1 Proterozoic or Precambrian

The Proterozoic or Precambrian Era, which dates from 1.5 billion to 544 million years ago, is one of the most studied in the state of Missouri. The oldest rocks which

have been found during drilling date back to approximately 1.8 billion years ago. These rocks are igneous and metamorphic base left in Northern Missouri by the Central Plains Orogen. The Central Plains Orogen is defined as an episode of mountain building believed to be the episode which stuck the ancient sub-continent onto already existing proto-North America. The geology in Missouri is interesting in the fact that only slightly younger rocks are still left exposed. For instance, the St. Francois Mountain area consists of several igneous rocks such as granites, rhyolites, ignimbrites, and felsites which date back 1.48 to 1.38 billion years ago. A similar sort of igneous rocks underlie a wide part of the Midwest, but are only exposed in the St. Francois Mountains and a small area of Oklahoma.

A geologist's job consists of locating similar rocks and minerals and trying to explain how they all fit together, but still today much of geology remains a puzzle. Although there are several possible hypotheses, the most accepted explanation for the formation of the Ozarks and therefore, much of Missouri, is that the St. Francois Mountain area was a volcanic hotspot. This explanation is similar to that describing the formation of Yellowstone. The characteristic rock of Yellowstone is a type of volcanic lava much like that found in the Ozarks.

However the St. Francois area was developed, the fact is that it was through erupting hot magma that the lava plateau was created. This lava cooled quickly on the surface as fine grained or porphyritic rhyolite, felsite, and ignimbrite and below ground as shallow granite "plutons". After many years of weathering, something caused the deep

mantle magmas to rise filling the fissures that were previously formed and causing new ones to form.

3.3.1.2 Cambrian Period

Cambrian Rocks found in Missouri are estimated to date back 544 to 505 million years ago. These rocks reveal the time period when Missouri was covered by a shallow continental sea and also show that the highest igneous mountains were more than likely not underwater. The Cambrian Age rocks found in Missouri are all sedimentary in nature and were formed from other rocks after weathering transport, deposition and lithification. At this time, the shape of the North American continent differed from what is today and it is likely that the deeper ocean waters were much closer. It is estimated that nearly all of the sediments in Missouri were deposited under shallow conditions.

The Lamotte Sandstone, which dates to this period, is comprised of cemented rock fragments. This sandstone is made up of angular quartz, feldspar, and dark minerals in the lower portions and the upper layers consist of less fragments and mostly rounded quartz. Just above the sandstone are the Bonne Terre Formation, the Davis Formation, and the Derby-Doe Run, Potosi and Eminence Dolomites. The Bonne Terre Formation consists of limestone/dolomite, sands, and shale. The Davis Formation consists of dark shale and rip-rap conglomerate. These types of rocks indicate the carbonates were formed in deeper seas and the shales can either be formed in shallow tidal flats or in deep sea mud.

3.3.1.3 Ordovician Period

Ordovician age rocks date back 505 to 441 million years ago and are abundant in Missouri. These rocks consist of mostly carbonates, thin shales, and three sandstones: the Gunter, the Roubidoux, and the St. Peter glass sand. The Ordovician rocks found in Missouri show inconsistent deposition indicating that the water was shallower and more varied than the previous sea. The difference in thickness of some of the layers varies tremendously at different locations. The Gunter sandstone at the base alone varies from several meters thick to a small almost unrecognizable seam over the region.

Exposed carbonates were eroded, followed by the Tippecanoe transgression during the mid Ordovician. The first Tippecanoe deposit is the St. Peter sandstone. This layer of "beach" sand marks the second inundation of the Ordovician. Above the sand is a distinct yellow dolomite known as the St. Joachim dolomite. During the mid Orodvician, the Ozark Dome, what would be southern Missouri today, experienced minor uplift. Above these layers is the Kimmswick Formation. This formation consists of limestone with a bentonite band between 0.15 and 0.3 m thick. Bentonite clay is decomposed volcanic ash and believed to mark the beginning of the Taconic Orogeny. The Taconic Orogeny is defined as the mountain building episode that occurred approximately 450 million years ago which created the Appalachian Mountains. The end of the Ordovician is marked by limestones and shales which were created as the seas retreated.

3.3.1.4 Silurian/Devonian Period

Silurian and Devonian rocks date back 441 to 362 million years ago and rather scarce throughout Missouri. The true reason they are scarce is not well known. One idea is they only existed around the Ozark fringes and another idea is they were eroded over the course of time before the middle Devonian. During this time there is evidence that the Ozarks moved upward as a result regional warping. Silurian rocks are found at the surface in several locations in Missouri near Hannibal, and Cape Girardeau. Similar rocks are also found subsurface in the northwestern corner of the state. These rocks consist of thin limestones, shales, and several dolomites.

The Silurian layers were deposited as the regressing Tippecanoe Sea revisited the area. The returning waters were local and river-like flowing through narrow paths and low lying areas. Some suggest this as the beginnings of the Mississippi River Valley.

Rocks from the Devonian age are spread across the state. The few early Devonian rocks are believed to be the last of the Tippecanoe sea deposits, while middle Devonian rocks were created during the first Kaskasia flooding stage. These rocks consist mostly of limestones. The late Devonian rocks consist of shales and sandstone with a small amount of limestone. Also formed in the Devonian age is the Chattanooga Shale. This black shale was formed in deep waters and extends from the southwest into Arkansas and Tennessee.

3.3.1.5 Mississippian Period

Between 362 and 320 million years ago, the Kaskaskia Sea returned to Missouri marking the beginning of the Mississippian age. The inundation began as a silica base, but is found as a sandstone or shale in the northeast and southwestern parts of Missouri. The Mississippian sequence is further broken down into four series: the Kinderhookian, Osagean, Meramecian and Chesterian. The different layers vary greatly throughout the state and approximately one fourth of the exposed surface is made up of rocks from this age. Most of the layers consist of certain types of limestone interbedded with thin shale layers. The Mississippian sea covering much of Missour, may have begun clear, but progressively turned muddy due to the Acadian orogeny. The most common layer is the Burlington Limestone, which is a crystalline and extremely fossiliferous limestone. This strata covers a majority of the state extending into Iowa and Arkansas. The Keokuk limestone lies just above the Burlington and is known for its geodes. These geodes are formed when mineralized water is trapped in lime muds, or gaps in the limestone and the minerals crystallize on the wall. As the Kaskaskian sea was retreating, it left silica rich muds and sands which were exposed and began to weather, marking the end of the Mississippian age.

3.3.1.6 Pennsylvanian Period

Rocks from the Pennsylvanian Period date back 320 to 286 million years ago. Although Missouri is not known as a coal producing state, the coal from this period fills northern and southwestern Missouri. The coal in Missouri , however, is high in sulfur

and much less desirable due to environmental concerns. The Absaroka sea, the final transgressive sea covering much of the state rose and fell 5 times leading to the following series of rocks: the Morrowan, the Atokan, the Desmoinsian, the Missourian and the Virgilian. Most of these consist of shales, sandstones, clays, thin limestones, and coals. The Pennsylvanian rocks are the most common north of the Missouri River and in the Osage Plains region, but they usually form thin bedded layers called *cyclothems*. A cyclothem results from wave like action as a sea moves in and out and often consists of sandstone, silty shale or siltstone, limestone, underclay, and shales.

Some evidence of rock faulting has been found that suggests that southern Missouri rose during this time period. The retreating Absarokan sea marks the end of the Pennsylvanian age and sedimentary deposition came to a close. The remainder of time has consisted of reshaping the existing formations.

3.3.1.7 Cretaceous Period

Cretaceous age rocks date back 144 to 66 million years ago and are exposed in southeast Missouri. During this time, sea levels around the world rose likely due to a decrease in volume capacity because of lava spreading across the sea floor. The New Madrid Rift Zone was reactivated depositing igneous diatremes in St. Francois and Ste. Genevieve counties. The present day Gulf of Mexico reach far north near Cape Girardeau, depositing sands, sandstones, and clay over the Rift Zone. This area, known as the Mississippi Embayment, later subsided, resulting in up to 500 ft (152.4 m) of buried Cretaceous deposits. The Cretaceous age, a period of Mesozic, is the only one to

have deposits in Missouri. The Mesozic age is also known as the Age of the Dinosaurs. Many Dinosaur fossils dating back to approximately 80 million years ago have been found across Missouri, particularly Bollinger County.

3.3.1.8 Tertiary/Quaternary Period

The Tertiary and Quaternary Periods ranging from 66 million years ago to the present, consists of alluvial clays, sand, gravels, glacial tillites, eolian clays, and loess. The large yellow area shown on the map is alluvial deposits from the Mississippi Embayment. The deposits shown along the major rivers are stream and wind deposited.

Only two of the classical glacial periods are believed to have left glacial deposits in Missouri: the pre-Illinoian (Nebraskan-Kansan) and Illinoian. The pre-Illinoian is credited with changing the course of the Missouri River to its present location, scouring and filling Northern Missouri's topography, and leaving extensive outwash gravels. Even though the Ozarks were not glaciated in the relatively recent past, Pleistocene loess of varying thicknesses cover most of the state with the exception of the higher portions of the Ozarks. Two mastodon fossil finds located in present day Jefferson County are of the Quaternary period as well.

The current era is known as the Cenozoic and is in an epoch known as the Holocene. Although the major formations have already been laid down, soil, clay, and rock fragments are continuously weathered and redeposited by water and wind and other transportation methods constantly changing the surrounding geology.

3.3.2 Illinois (Illinois SGS)

Similar to what was presented for Missouri, Figs. 50 and 51 show the bedrock exposed and the corresponding time period it was deposited. The eras shown on the maps are the same as those discussed above for Missouri. The following information and maps were found at the Illinois State Geological Survey (SGS) site.

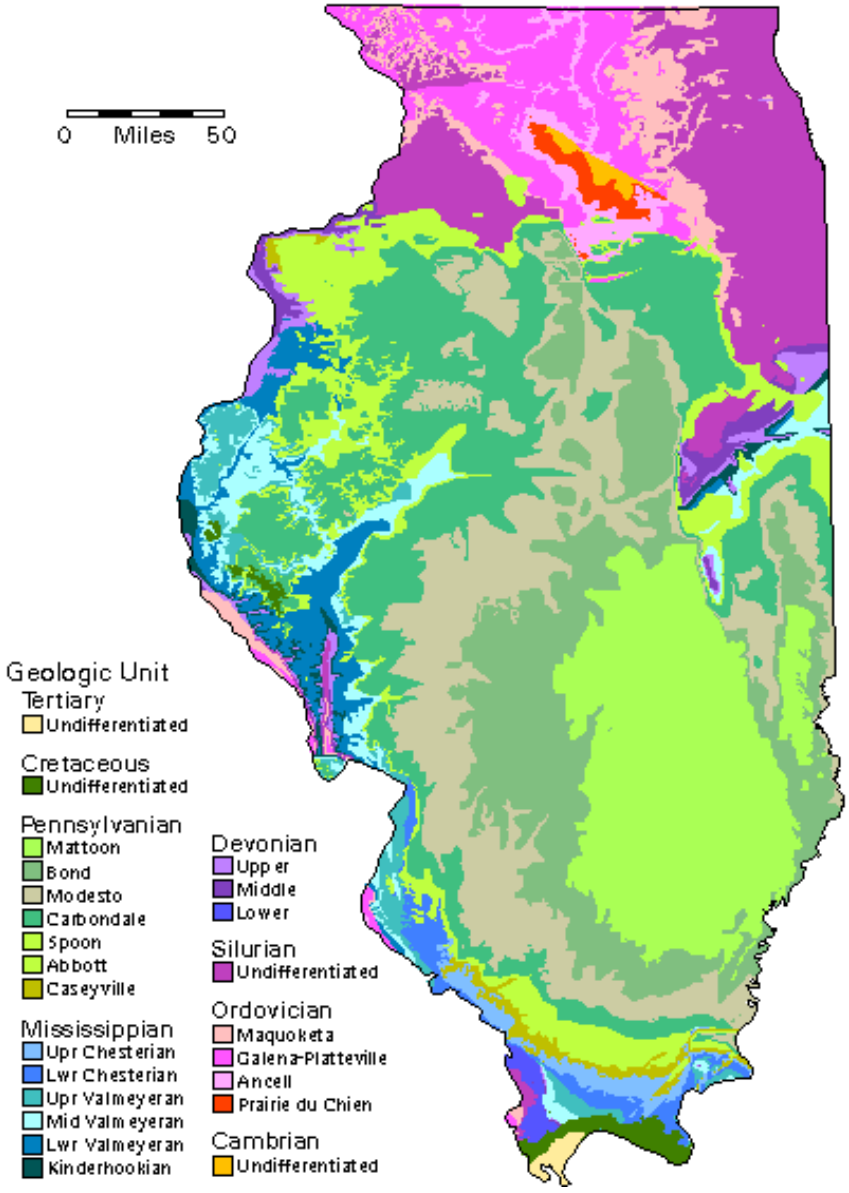

Fig. 50. Bedrock geologic map of Illinois (Illinois SGS 2009)

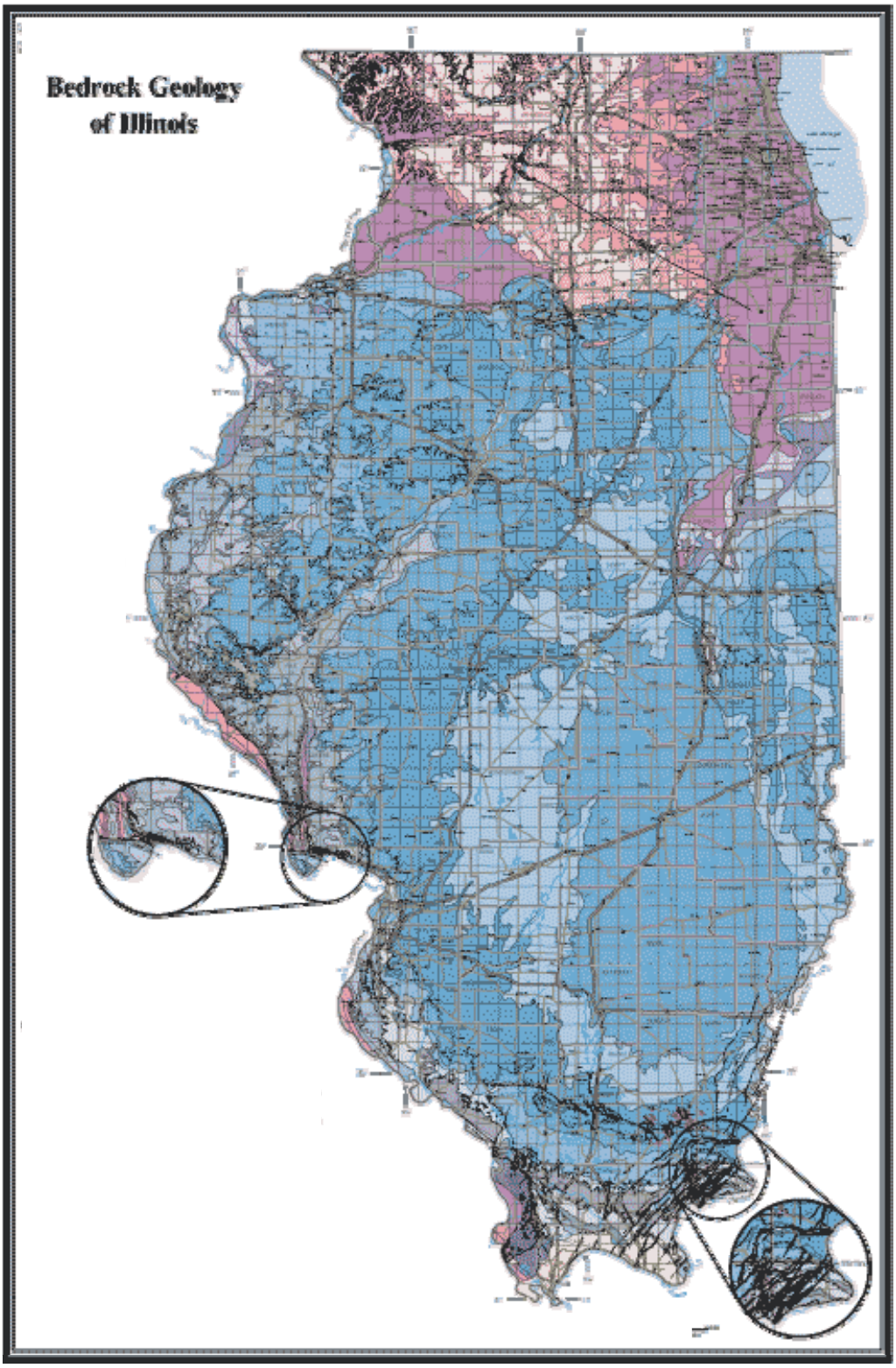

Fig. 51. Illinois bedrock geology (adapted from Illinois SGS 2009)

Unlike Missouri, very little bedrock is exposed at the surface in the state of Illinois. A small amount can be seen on the maps at the south end, northwest corner, and along the Mississippi River on the west side of the state. Like many of the states in the Midwest, most of Illinois is covered with glacial deposits from the Pleistocene ice ages. These deposits are broken down further on the Quaternary map shown in Fig. 52.

Just below the most recent sediments, much of Illinois consists of limestone and shale deposited during the mid Paleozoic Era, in shallow-water and coastal environments. The southern end, the Illinois Basin, is characterized by younger central strata overlaying older beds around the rim. The newer layers have been eroded away in the northern sections exposing older deposits dating back to the Ordovician Period. Throughout the entire state, the bedrock of Illinois is richly fossiliferous, containing trilobites and many other classic Paleozoic life forms.

As mentioned above, most of the exposed surface of Illinois is relatively new deposits. Fig. 52 shows the Quaternary deposits and the corresponding episodes. These soils mainly consist of glacial tills and moraines. Tills are defined as soils or rock fragments that are directly deposited by the glacier. Moraines are defined as areas of accumulated unconsolidated soils and rock fragments formed by glaciers.

Fig. 53 shows a form of transported sediments known as loess. Loess are defined as Aeolian soils created from wind-blown soils, such as silts, small grained sands, and clays. When wet, loess are highly erodible and unstable. They can create deep, narrow gullies, which can quickly increase in size during rain and flood events and can lead to serious hazards. The area bordering the Mississippi River has over 6.1 m of loess

deposits in some areas. These areas were of primary interest in the erosion studies presented in this thesis. In flood conditions like those experienced in 2008, these highly erodible soils increase the vulnerability of the entire area.

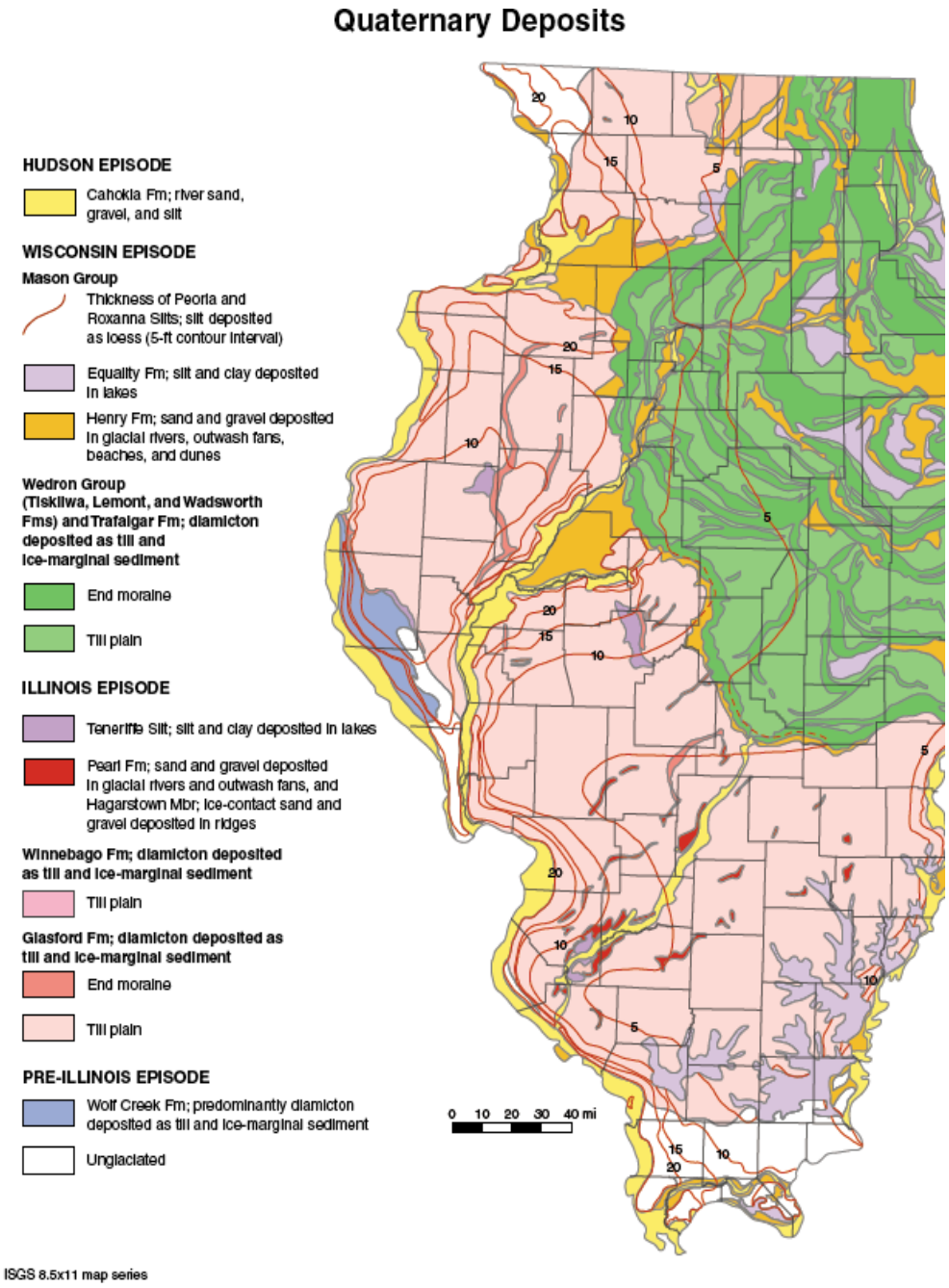

Fig. 52. Illinois quaternary deposits (Illinois SGS 2009)

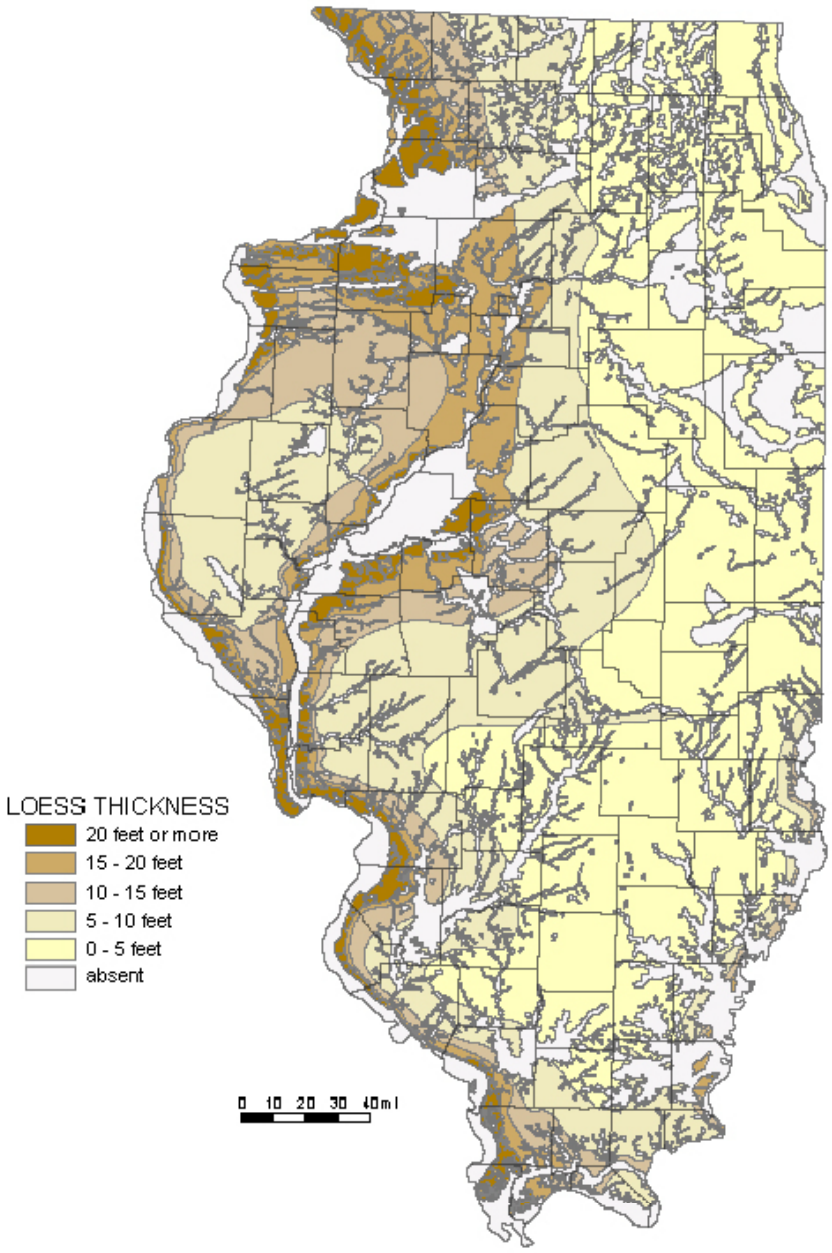

Fig. 53. Illinois loess deposits (Illinois SGS 2009)

Fig. 54 gives a common stratigraphy found in Illinois. This is similar to a hole boring logged when drilling a well. Each deposit is shown at a given depth along with the general types of rocks found.

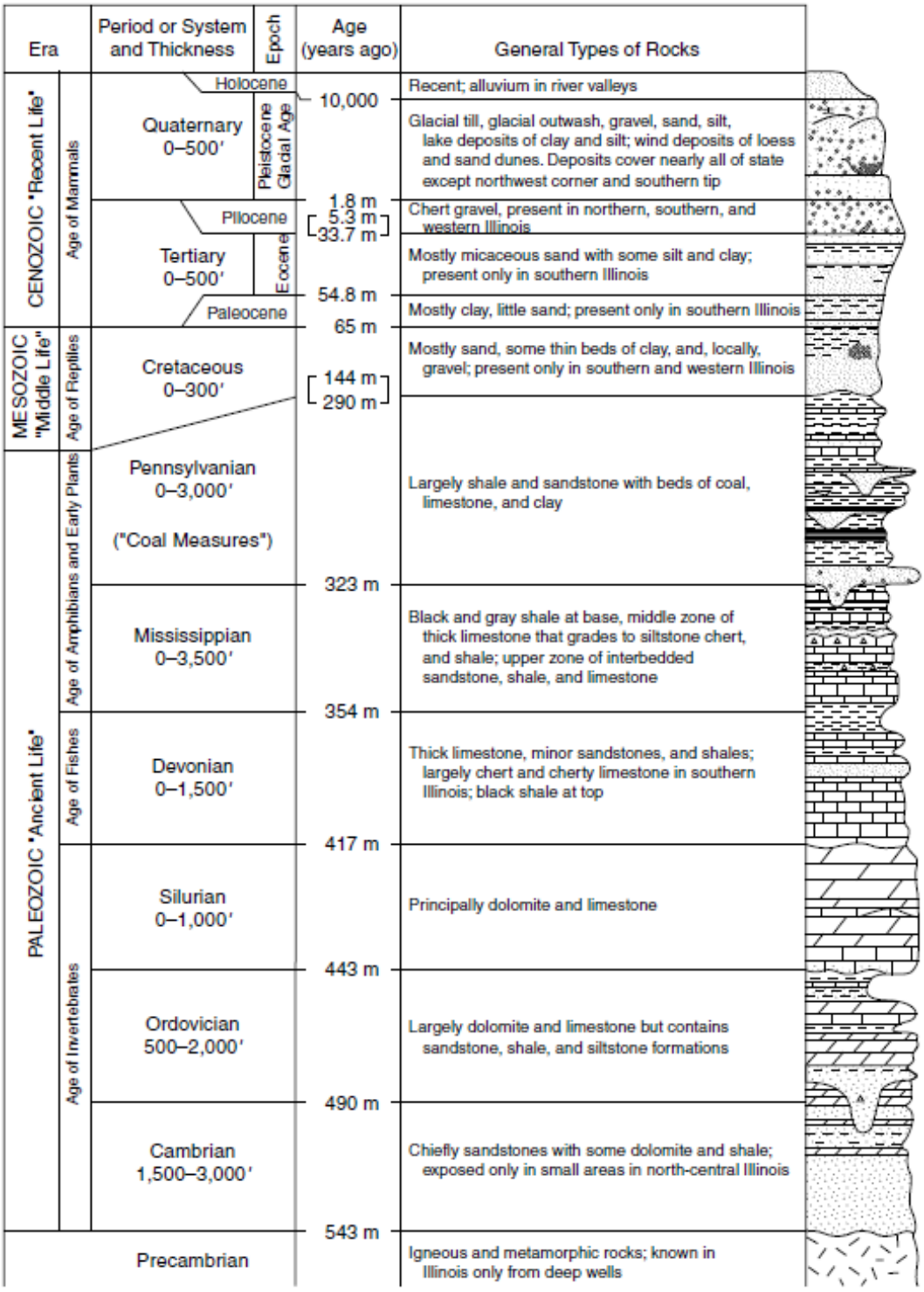

Fig. 54. General geologic stratigraphy for Illinois (Illinois SGS 2009)

3.3.3 Iowa (Iowa DNR 2009)

The following paragraphs summarize a more extensive explanation of the geology of the state of Iowa. Further information and maps can be found on the Iowa Department of Natural Resources website http://www.igsb.uiowa.edu/service/geology.htm.

Iowa's underground strata consist mostly of sedimentary rocks such as sandstone, limestone, dolomite and shale, which formed between the Cambrian and Cretaceous ages. Over time, the sediments hardened into the rock formations discussed in previous sections. The majority of the state's surface is covered with more recent glacial materials except in river valleys, and the occasional roadcut or quarry. Similar to the sections presented above, Fig. 55 shows the exposed bedrock and corresponding depositional era for the state of Iowa.

The map shows rocks from younger periods overlapping older rocks in several areas. Remnants of the Precambrian age cut through newer Cretaceous deposits in the farthest northwest point of the state. Similar scattered outcrops of silica-cemented sandstone and Sioux Quartzite, dating back to approximately 1.6 billion years ago, are the oldest exposed bedrock in Iowa. The buried Precambrian rocks found in other locations throughout the state are usually igneous and metamorphic. The circular feature shown on the map is known as the Manson Impact Structure. This 23 mile (7 m) diameter circle is the location of a meteor impact which occurred approximately 74 million years ago. The impact caused a major disruption of the Cretaceous and other bedrocks and even forced deeply buried Precambrian granite to the surface. The highly

faulted crater has since been covered with glacial deposits and sediment and is not visible on the surface.

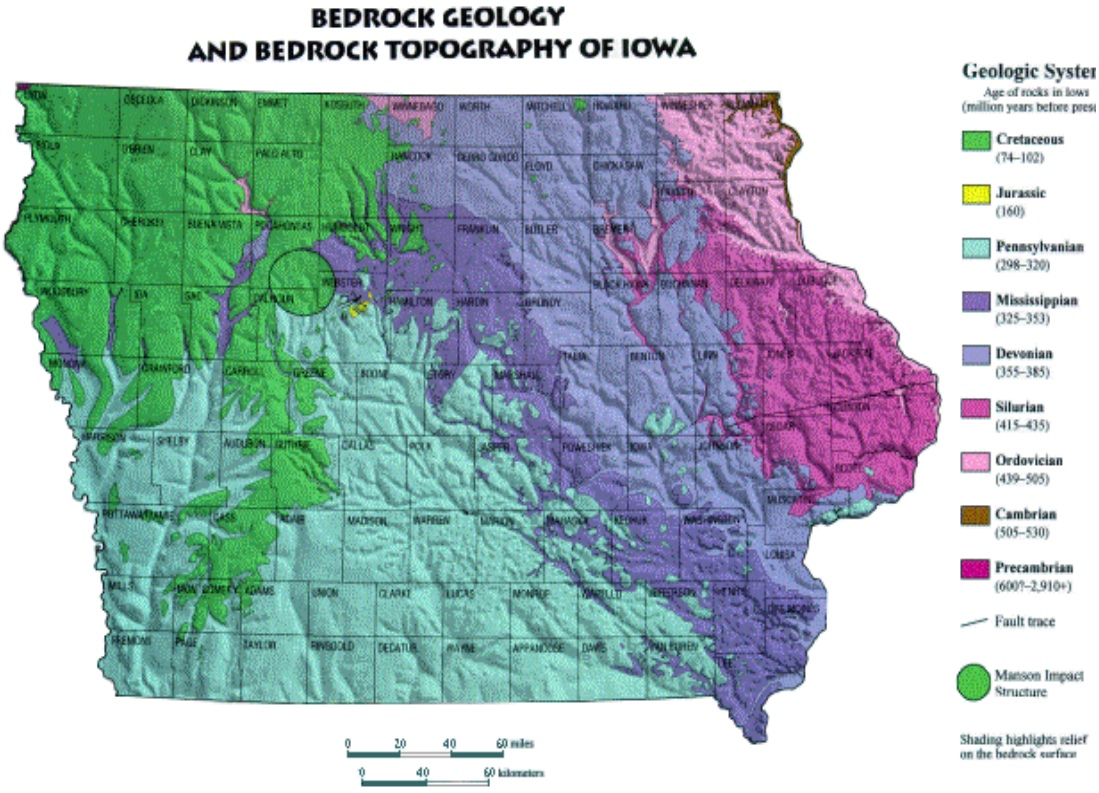

Fig. 55. Iowa's exposed surface bedrock map (Iowa DNR 2009)

The majority of the surface of Iowa is covered by loose sediments deposited in the recent past. These Quaternary sediments were deposited during several glacial events between 2.5 million and 10,000 years ago. The soils consist of pebbly clay, sand, gravel, and silt, which originated from ice sheets, melt-water streams, and winds. Through the years, these deposits have been weathered into loamy soils. These loamy soils, while well suited for farming, are easily eroded during rain and flood events. The last known glacier estimated to enter Iowa between 14,000 and 12,000 years ago directly caused the formation of the Des Moines Lobe region (Fig. 56). The melting ice sheets

left numerous wetlands and moraine ridges throughout the state. Numerous wetlands are also the direct result of a stagnant disintegrating ice sheet. The older glacial deposits dating back 2.5 million to 500,000 years ago have since been eroded and carved into rolling terrain known today as the Southern Iowa Drift (Fig. 56). The Loess Hills and much of the loess distributed across Iowa were deposited during intense erosional activity in which the silts from the river floodplains were blown all across the landscape. The loess are highly erodible and unstable when wet.

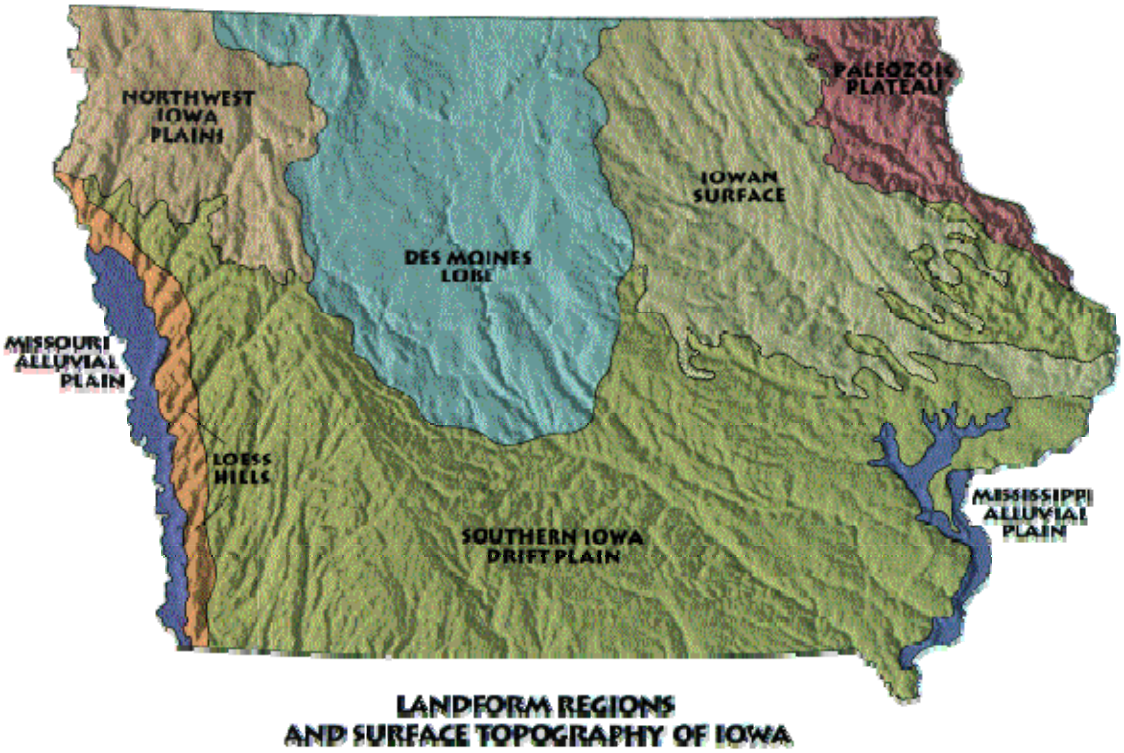

Fig. 56. Iowa topography and land regions (Iowa DNR 2009)

The geological process in the recent past and that which is still occurring today is due to river flow and erosion. These flowing rivers erode the surface and transport the material to another location. The valleys and alluvial plains shown in Fig. 56 spread

much further than the rivers which run through them, indicating that they were carved by floods from melting ice during the thawing of the glaciers. The gravel deposits and other "separated" deposits show the depositional mechanisms of the flowing water. As the water slows, the larger grain materials fall out of suspension and are deposited in a given location. Even present day floods demonstrate these erosion principles. The surface materials are eroded from one portion of a valley, sorted by flowing water, and re-deposited downstream. These ongoing events continuously change the surface topography and therefore the geologic history of Iowa.

The main area of interest in the state of Iowa during the 2008 Midwest Levee failure investigation was the Mississippi Alluvial Plain (Fig. 56). This area was created by the same processes described above. The rivers created from the melting ice sheets eroded and deposited the alluvium along the adjacent plains. These alluvium are made up of gravels, sands, silts, and some clay. The depositional characteristics of the soils depend on the velocity and movement of the river at a given location. Fast moving rivers erode the surficial soils and transport them until the velocity slows allowing particles of certain diameter to fall out of suspension. The smaller the particle size, the farther down river it is transported. The Mississippi River, also called the Big Muddy, transports large amounts of sediment into the Gulf each year (USGS 2008). Even with the lock and dams and other restraints that have been built across it, the Mississippi River still ranks sixth or seventh in the world pertaining to the amount of sediment discharged into the ocean. It is estimated that an average of 230 million tons of sediment are washed down the Mississippi and into the Gulf of Mexico every year. This statistic

dates back quite some time; however, it shows the enormous erosion and transportation power of the river.

Similar to the figure presented for Illinois, Fig. 57 gives an example of the common stratigraphy found in Iowa. The depositional age is shown at the corresponding depth along with the general types of rocks found for each.

In 1992, a National Geologic Mapping Act was passed with the goal of creating a detailed geologic mapping of the U.S. During the early stages of the program, the Iowa Geological Survey mapped a portion of the Mississippi River valley. The area mapped covered southern Muscatine and northern Louisa counties. This area is shown in the boxed area of Fig. 58. Satellite images were used to locate the boundaries between different geologic deposits and were overlaid with other geographic information. Fig. 59 shows the satellite image obtained for the area.

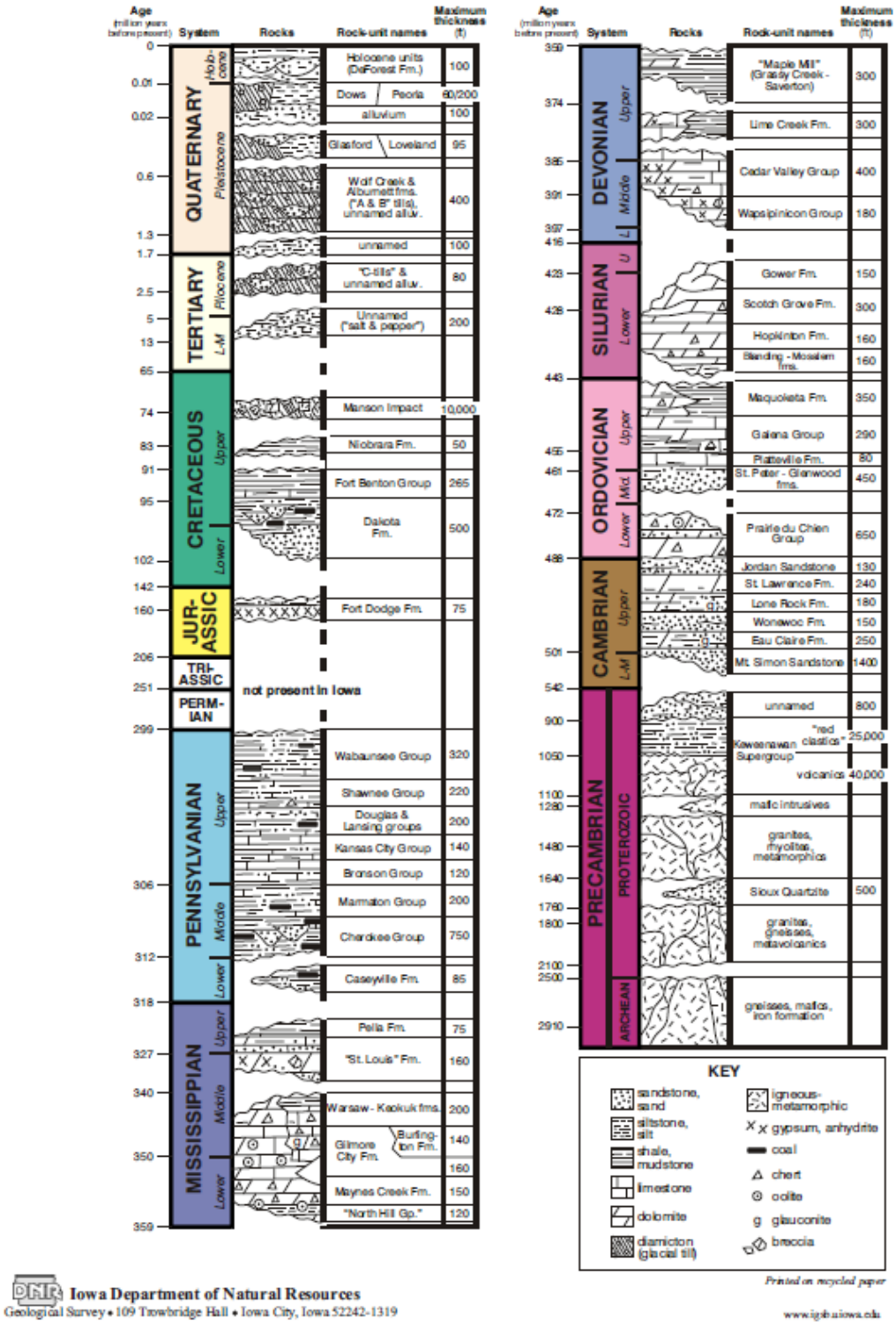

Fig. 57. Common stratigraphy for Iowa (Iowa DNR 2009)

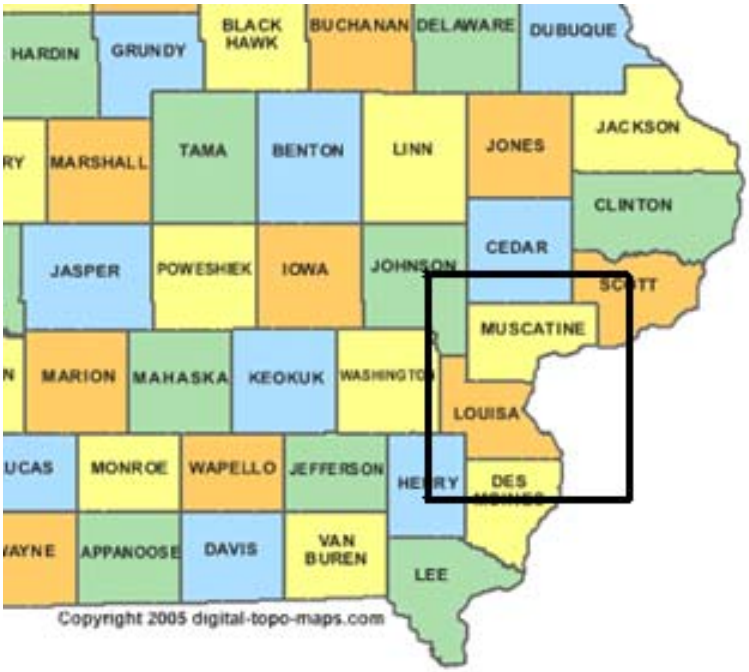

Fig. 58. Iowa county map showing area of interest (Digital Map Store 2005)

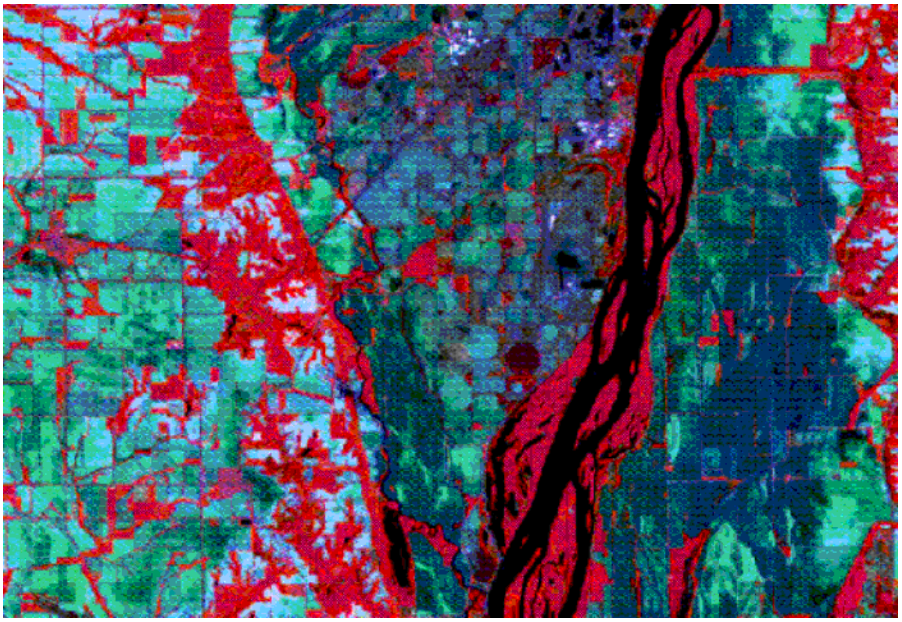

Fig. 59. Satellite image of Mississippi River valley May 27, 1989 (Iowa DNR 2009)

The satellite image shown in Fig. 59 is a color-infrared Landsat TM image of the Mississippi River valley provided by the Iowa Geological Survey. The image shows many different features such as vegetative cover, bare soil, dry or wet soil, and open water. The areas covered with vegetation are displayed in red, while the bare soil is shown in the light blue-green shades. The darker blues and blue-greens indicate wet soil and the rivers and open waters are shown in black. The areas which are generally more sandy better drained materials are shown in purple. These maps are useful in identifying geologic formations, transported deposits, and soil characteristics at given locations. This information is valuable to scientists and engineers for a number of different reasons. The maps provide an outline of geologic information that can be used for general knowledge, engineering design and understanding, and many different resource and environmental issues.

The Letts and Blanchard Island quadrangles contain approximately 285 km^2 of the Mississippi Valley and adjacent lands. The completed maps of these areas provide a layout of the geologic materials to a depth of five meters. The area contains a portion of the Upper Mississippi River navigation system. This section of river is farther north than that studied in the extents of this thesis, but the maps provide a similar geologic material layout to what is expected in the lower portion of the river. Subsurface information was compiled from water well records, engineering boring records, monitoring well records, and published soil surveys. This data was compared to landscape patterns and surface photos and satellite images in order to construct the maps.

Fig. 60 shows two of the maps completed for the Letts and Blanchard Island quadrangles along the Mississippi River Valley as a part of the STATEMAP program.

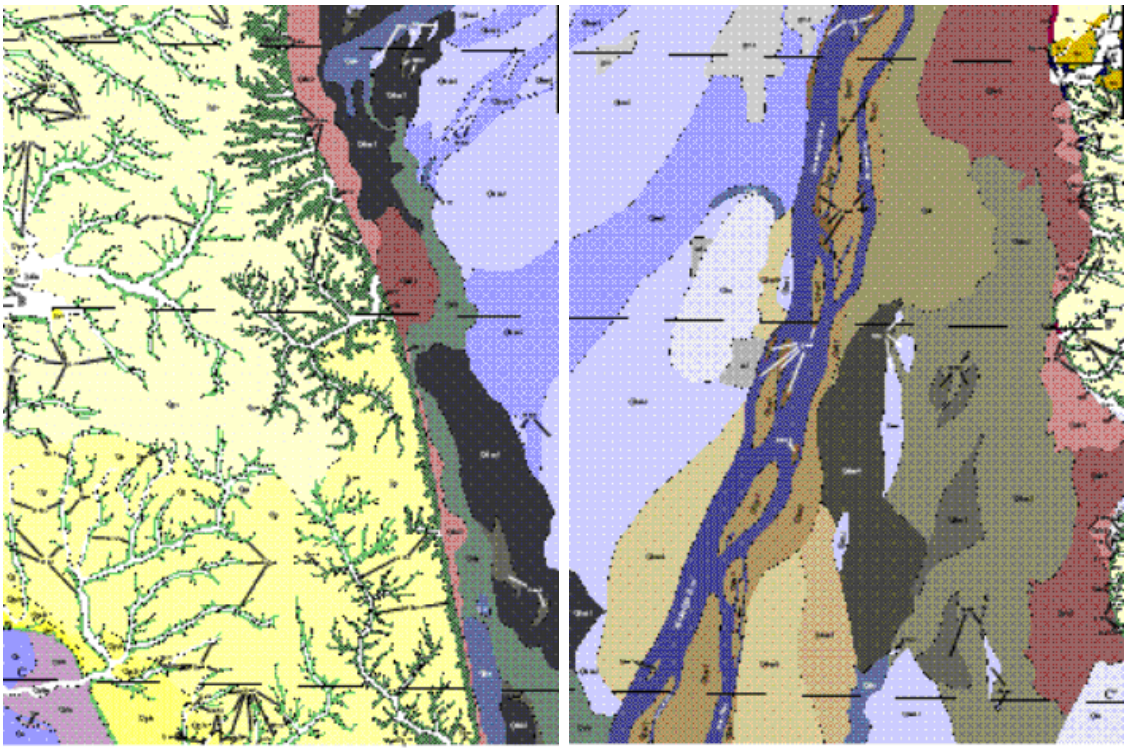

Fig. 60. Maps of the Letts and Blanchard Island quadrangles (Iowa DNR 2009)

In the above figure, two major groups of glacial Quaternary deposits are shown. The sediments left by glacial ice and wind are displayed by the yellow and green areas. Deposits left by rivers and streams throughout the valley are shown in blue, brown, and rose. These river deposits are shown by the elliptical, smooth-edged areas. The branched areas shown in the glacial sediment areas represent loess that have been eroded by younger stream deposits along the drainage paths. Maps of quadrangles similar to those shown above can provide useful information needed to address specific environmental problems such as drainage and groundwater contamination, suburban expansion in areas of sinkholes, and landfill planning.

3.4 Brief History of the 1993 Flood (Johnson et al. 2003)

The Great Flood of 1993 was marked as the costliest flood in the history of the Mississippi River Basin in the Midwestern United States (Johnson et. al 2003). Extremely large amounts of precipitation fell on the upper Midwest in the summer of 1993. Atmospheric conditions perfect for causing rainfall persisted across the entire central part of the Nation. The months of June, July, and August recorded approximately 200-350 percent above normal cumulative rainfall. Over 30 cm were recorded in parts of 10 upper Midwest states, over 60 cm fell in portions of Kansas, Missouri, Iowa, Minnesota, and Nebraska, and 96 cm were recorded in parts of east-central Iowa. The summer rainfall was determined to be 75- to 300-year frequencies (Stallings 1994). Many locations throughout the Midwest experienced more than twice as many rain days as normal in July, and in some parts rain fell every day from late June to late July (Johnson et al. 2003). Cool dry air from Canada moved south, while warm moist air from the Gulf of Mexico moved north. As the air mixed, it resulted in intense long lasting, and overwhelming rain events which flooded nearly 150 major rivers and tributaries.

The saturated soils forced runoff into overflowing streams and river channels and eventually into the Mississippi River. The river crested on July 12 near St. Louis at about 43 ft (13.1 m), and then even higher further down river. Record flow in the Missouri River added to the already full Mississippi River resulting in another record crest of 49.58 ft (15.1m) and a record flow of over 1 million ft^3/s (28316.8 m^3/s) on August 1st at St. Louis. Record flood levels were measured on every stream flow gage

station on the Mississippi River from Rock Island, Illinois to Thebes, Illinois. At one particular time, over 500 river forecast points were above the flood stage. River banks and channels were severely eroded, and as the rushing water slowed sediment was deposited over large a large area of the Midwest floodplain. Thousands of acres of land were inundated from the flooding. On June 7th, the first levee was overtopped, followed by over 1,000 more that were either topped or failed (Larson 1996).

The extreme flooding resulted in the loss of over 48 lives. (Interagency Floodplain Management Task Force 1994). Over 16,000 square miles (41439.8 km^2) in nine states was flooded, mostly in the Upper Mississippi due to the less than average inflow from Lower Mississippi basin. The damages were estimated at $20 billion (National Oceanic and Atmospheric Administration 1994). The breached levees destroyed farmland, businesses, roads, and more than 50,000 homes (Josephson 1994). Even those whose homes were not damaged were at risk of contaminated drinking water and non-functioning waste water treatment plants for many months following the flooding. Fig. 61 shows the land area affected in both the 1927 and 1993 floods. Table 8 provided by (PBS) gives a comparison of the 1927 and 1993 floods.

Fig. 61. Maps of the 1927 and 1993 floods - Upper Mississippi River (PBS 2001)

Table 8. Statistics of 1927 and 1993 floods (PBS 2001)

	1927 FLOOD	1993 FLOOD
Human Loss of Life	246	47
Displaced People	700,000	74,000
Financial Loss	$347,000,000 in 1927 = $4.4 billion in 1993 dollars	$7,500,536,000
Structural Damage	137,000 buildings destroyed or damaged	47,650 buildings destroyed or damaged
Flooded Area	27,000 square miles	15,600 square miles
River Volume	2,500,000 cubic feet of water per second	1,000,000 cubic feet of water per second (USGS)

Data from the U.S. Army Corps of Engineers except where noted

In the aftermath of the flooding, many agencies have been formed for the sole purpose of flood recovery. The Scientific Assessment and Strategy Team (SAST) was formed to provide supplemental scientific advice and flood recovery assistance to officials in the upper Mississippi River basin. They help with every portion of information management from developing, compiling, organizing, and supplying information to support the decision making processes for river basin management. The goal of the effort was to identify the best flood control approaches, to address specific flood recovery problems, and to develop a plan for long-term protection. Maps available on the website show base resource information and specific locations that are vulnerable to flooding. Much of the data presented in these sections, as well as more detailed maps and files are available on the USGS SAST site.

Also established after the 1993 flood was a Presidential Commission whose task was to determine the cause of the flooding and make recommendations to reduce the occurrence of similar events in the future (Martindale 2009). The Commission produced a report known as the "Galloway Report." Findings from the report included the need to repair and update existing levees, provide a better outreach notification to those residents living behind levees, require residents behind levees to purchase flood insurance, among several other recommendations.

3.5 Overview of the 2008 Flood

During the spring of 2008, water levels in the Mississippi River began to rise. Above average rainfall left the saturated ground unable to absorb any more water and the

runoff emptied into the river. The Mississippi rose 14 ft (4.3 m) above the normal level, at a rate fast enough to fill one and a half Olympic size swimming pools every second (Discovery Channel 2009). The levees bordering the river could no longer contain the raging waters. Although very few casualties resulted from the disastrous flood waters, an estimated $2.5 billion in property damages and dead livestock occurred from the breached levees.

Record floods were recorded across the Midwest. USGS flood gages show the progression of the flooding through the month of June (Figures 62, 63, 64, 65, 66). The black triangles show the flood gages where the river was above the flood level. As the month progressed the concentration of the flood gages above flood level grew, until it peaked sometime after about June 19th.

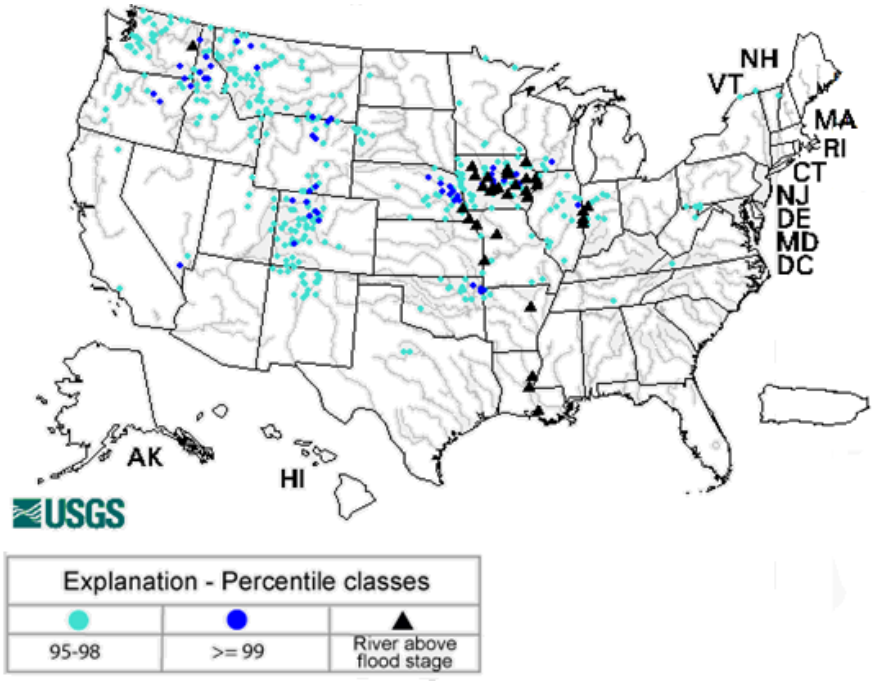

Fig. 62. USGS flood gage readings June 1, 2008 (USGS 2009)

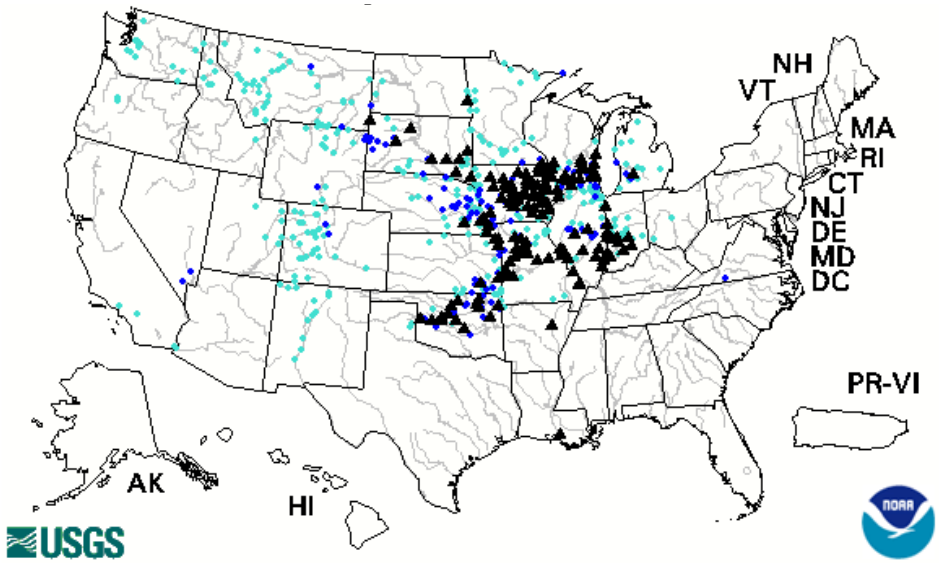

Fig. 63. USGS flood gage readings June 9, 2008 (USGS 2009)

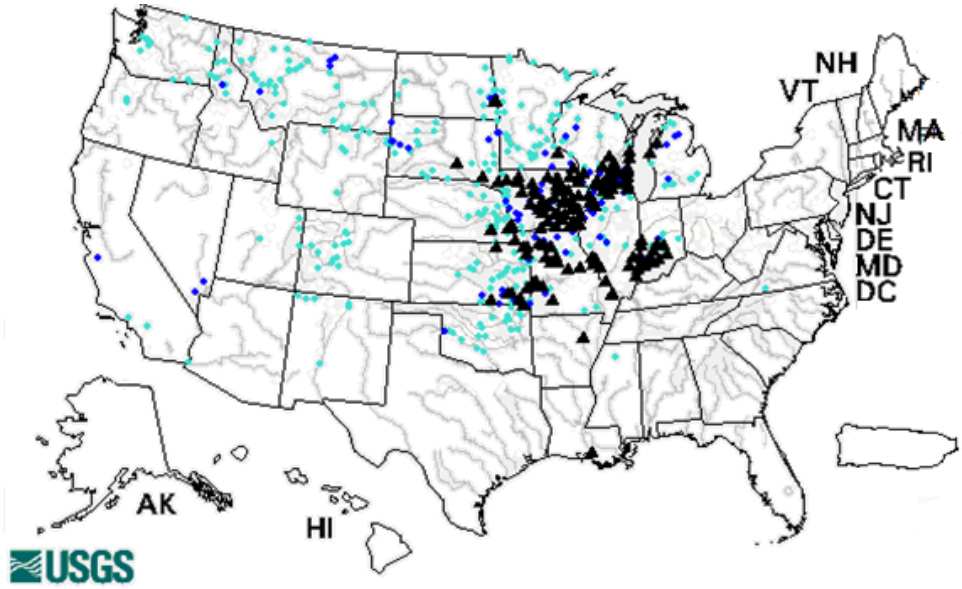

Fig. 64. USGS flood gage readings June 13, 2008 (USGS 2009)

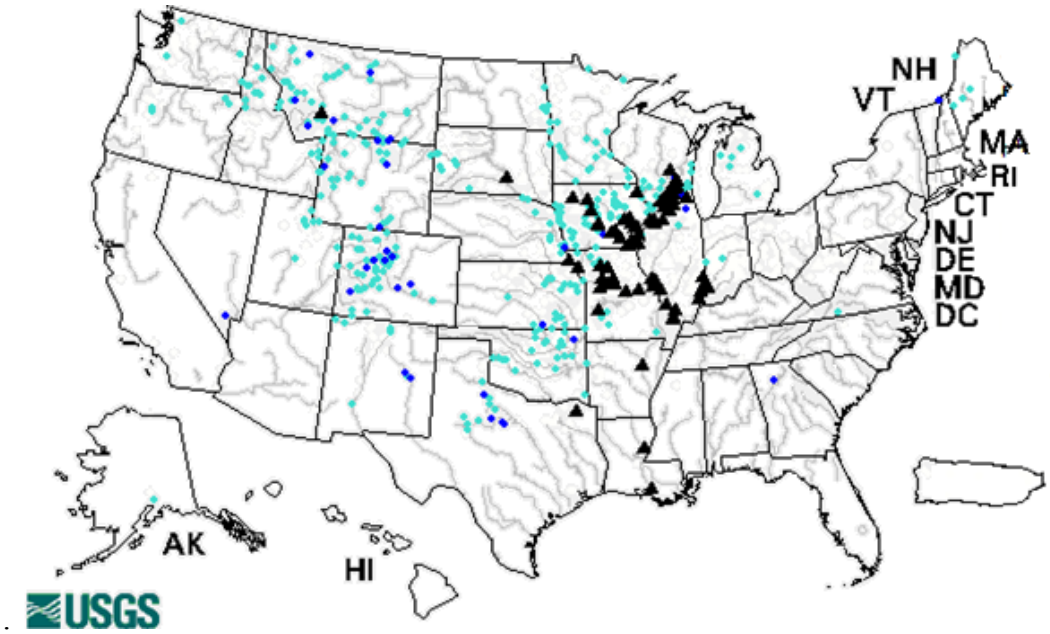

Fig. 65. USGS flood gage readings June 20, 2008 (USGS 2009)

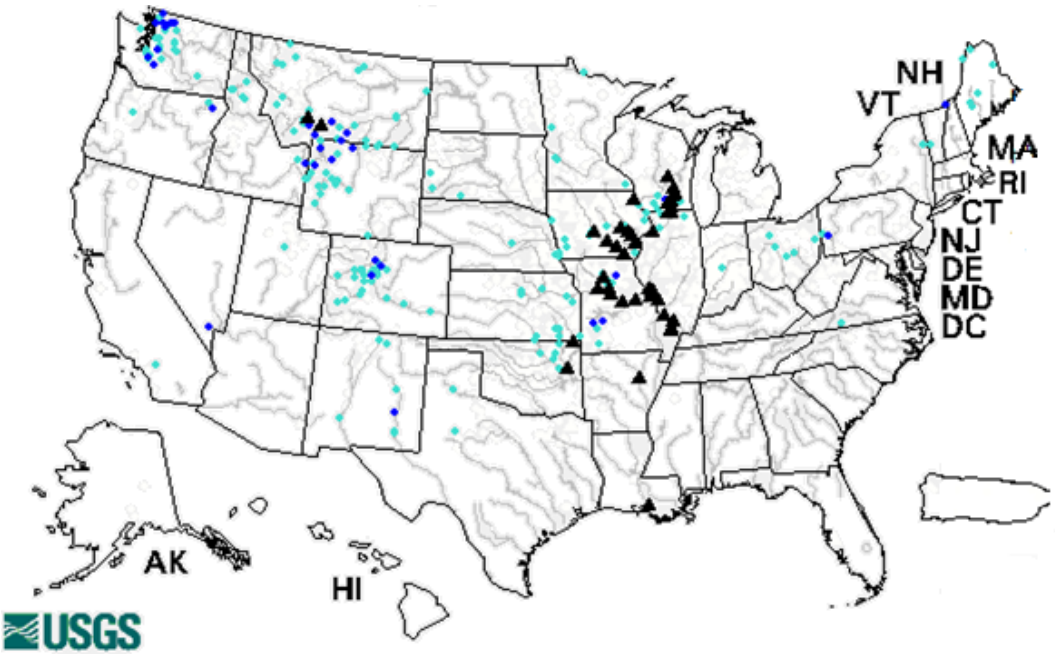

Fig. 66. USGS flood gage readings June 30, 2008 (USGS 2009)

The precipitation during the month of June added large amounts of water to an already full river system (Fig. 67). In early June, nearly 0.3 m of rain fell in parts of southern Indiana, Ohio, Wisconsin, and Iowa. The rain continued to pound the area for days and another round of storms followed. These flash floods producing thunderstorms occurred over a wide area leading to widespread river flooding in over 58 locations. The large spatial drainage basins dumped record amounts of water into the Mississippi River.

The raging waters overpowered any efforts made to contain them. Communities were covered forcing residents to evacuate. Cedar Rapids, Iowa evacuated over 25, 000 residents as the water inundated hundreds of city blocks. The water climbed 11 ft (3.4 m) higher than the previously recorded record. The Iowa River swelled as it carried waters further south. Damages in Iowa alone are estimated at $1.5 billion with even more in crop damages. A more detailed explanation is given in the Hydrological study in Section 4.

The levees were no match for the amount of water dumped on the area. Fig. 68 shows the US Army Corps of Engineers map of each particular levee system along the Mississippi and the corresponding overtopping status during the flooding events.

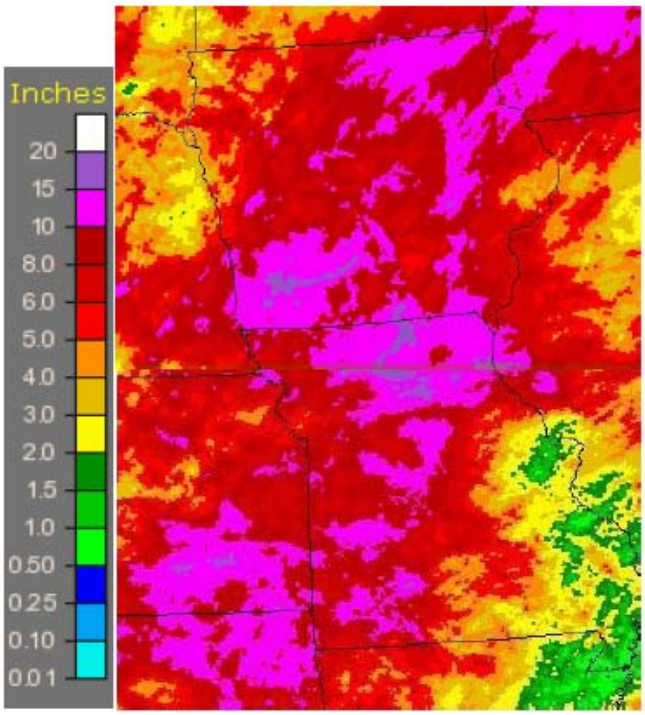

Fig. 67. Heavy rainfall during June 2008 (Rogers 2009)

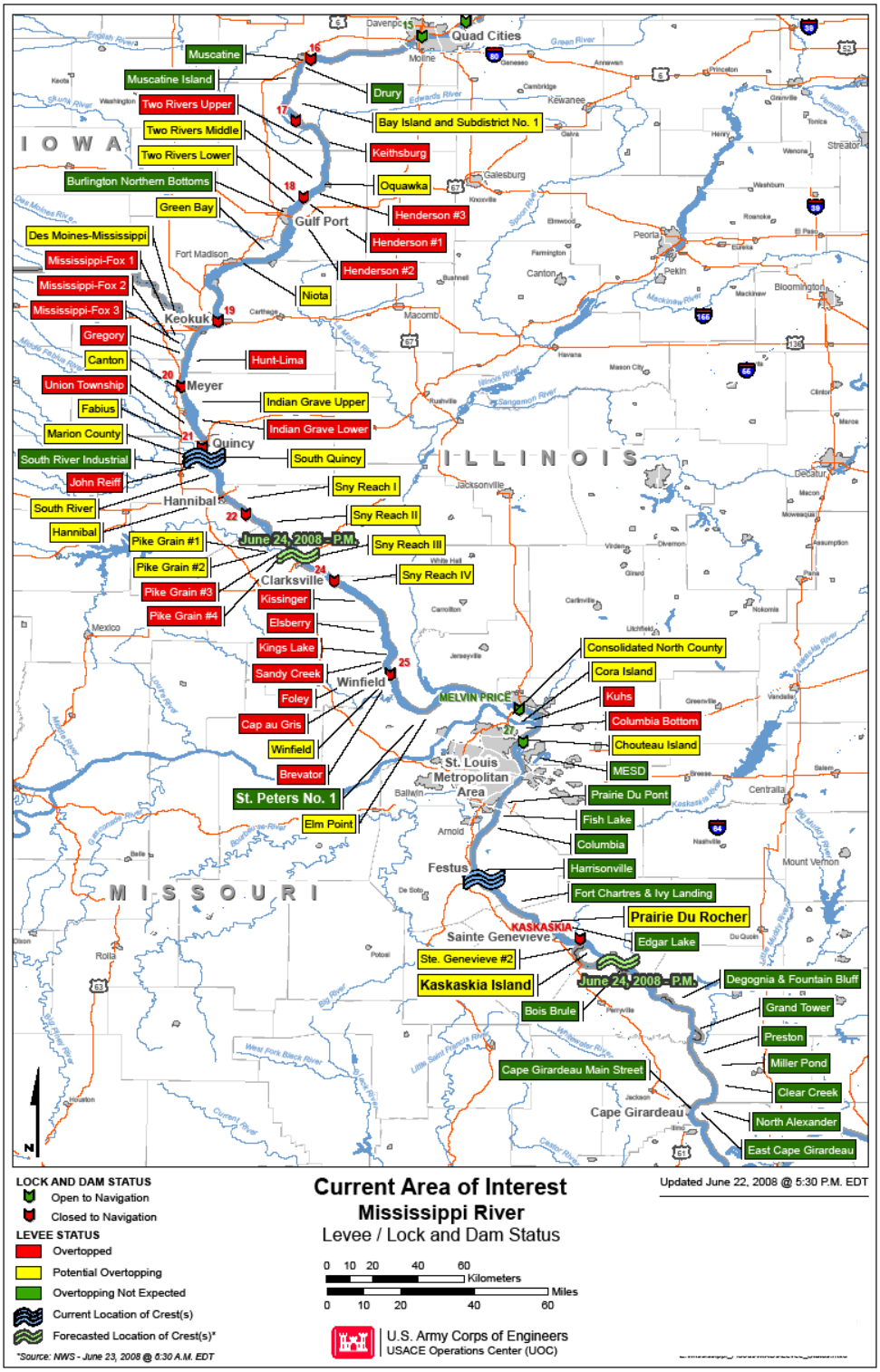

Fig. 68. Overtopping status of UMRS (adapted from USACE 2008)

The first site visited during the 2008 Midwest Levee reconnaissance was the Winfield-Pin Oak site near Winfield, Missouri. The levee breached on June 19, 2008. Approximately a 150 m gap was created in the levee from the rushing waters. Fig. 69, taken by the St. Louis District USACE, shows an aerial view as two homes were knocked off their foundations by the force of the water. Fig. 70 shows the same site on September 29th during the Midwest Levee reconnaissance. It should be noted that the breach shown in Fig. 70 was contained between the blue and white houses shown in Fig. 69 even though overtopping was also occurring further down levee. The "million dollar" question is why does a levee like the one shown fail in one location and not the other? This site is just one example out of many breaches that occurred in the Midwest region. A more in-depth description of each site visited by the reconnaissance team is presented in Section 5.

Fig. 69. Winfield-Pin Oak breach (USACE St. Louis District 2008)

Fig. 70. Winfield-Pin Oak site, Missouri

3.6 Motivation and Methods for 2008 Study

As discussed above, there are thousands of kilometers of earthen levees throughout the US whose purpose is to provide flood protection. The United States Army Corps of Engineers identifies levee overtopping as one of the top failure modes of earthen flood protection levees. Proper documentation of overtopping induced erosion is a complicated issue involving the collection and analysis of time-sensitive field data. Even with the appropriate data and documentation, the erosion phenomenon is still a complicated issue that is comprised of many different variables whose relations have yet to be fully explained. The erodibility of a soil is an important factor in the design and risk analysis of the world's earthen infrastructure.

Similar work done in New Orleans following Hurricanes Katrina and Rita proved that collection of this time-sensitive data is vitally important in characterizing the performance of levees. There are lessons to be learned from the engineers and personnel who observed the levee breaching and performed or oversaw the repairs. It is important that these lessons be effectively transmitted to future levee repair experts, emergency planners, and risk assessment experts.

Information gained as a result of these studies can not only be used to evaluate the performance of the New Orleans and Midwest levee systems, but can be directly applied to the entire U.S. flood protection system and can hopefully lead to a better understanding of the failure modes and future recommendations for levee improvements.

Following the 2008 summer flooding events, a Midwest Levee Investigation team was formed combining the efforts of the University of California at Berkeley, Texas A&M University, Missouri University of Science and Technology, and several members of USACE. The project was supported by the National Science Foundation under grant nos. CMMI-0842801, CMMI-0842659, and CMMI-08242374. The purpose of the Midwest reconnaissance mission was to collect sensitive and time-dependent perishable data in an effort to characterize several select levee breach locations. This data can later be used to calibrate subsequent numerical analyses and further develop the fields understanding of levee performance. The project breakdown provided by Rune Storesund with UC Berkeley (Storesund et al. 2009) consisted of:

1. An initial field reconnaissance to visit known breach sites along the Mississippi River between St. Louis, Missouri and Davenport, Iowa to document (via photographs) site conditions, collect eyewitness accounts, and develop a list for detailed site-specific analyses.
2. Conduct high-detail laser imaging surveys (Terrestrial LiDAR) of breach and erosion/scour features in the levees. These surveys will be used to validate future numerical simulations that predict the final scour/erosion profile for specified overtopping conditions.
3. Characterize the vegetative/grass cover on the earthen levee side slopes to determine erosion-resistance provided. This levee characteristic is frequently omitted from field characterization studies, yet is very important in the performance of the levee during overtopping conditions.
4. Characterize the levee soil materials, including the United States Soil Classification (USCS) soil types, plasticity (Atterberg Limits), grain size distribution (sieve sizes), in situ density, maximum dry density, Erosion Function Apparatus (EFA) erodibility characterization; and
5. Document the river stage at the locations of the levee breachs based on eyewitness accounts as well as available USGS Stream gage data. This data is essential to correctly evaluate overtopping depths and durations and associated water velocities on the ‘protected side’ of the flood protection levee.

Texas A&M's contribution to the comprehensive investigation consisted of several phases as follows:

1. Field reconnaissance - Information was gathered through photographs and eye witness accounts. Soil and vegetation samples were taken at each site for later analysis.
2. Hydrological investigation - Precipitation gages, antecedent soil-moisture conditions, and flow gages were all studied to get a better understanding of the flood event. A detailed description of the flood from a precipitation perspective is given by NCDC.
3. Soil Analysis - Laboratory testing and characterization of the soils at each site including: in situ densities, classification of the levee soil materials using the USCS, plasticity, grain size distribution, compaction curves for each site, and erosion testing in the Erosion Function Apparatus (EFA).
4. Vegetation - Identification of the vegetation discovered at each site, as well as a study of the influence that vegetation has on erosion.
5. Comprehensive Analysis – Combining the gathered field and lab data to determine the erodability of the materials present at each site. Erosion charts developed from previous work using the EFA will be used to classify the materials' erodible nature.

While the focus of this thesis is primarily the work done by Texas A&M, the complete characterization of the Midwest levees depends on the collection and documentation of the entire works completed by the project team. A complete collection

of the data and analysis findings will be available through the Midwest Levee Investigation team website provided by the University of California, Berkeley. This information will be made available to the public through a website portal.

4. HYDROLOGICAL STUDY

A precipitation and overall hydrological study were a crucial first step in identifying the soil conditions at the time of flooding and the magnitude of the floods the levees were subjected to. Precipitation maps used show the moisture conditions in the months leading up to the flood events as well as during the heavy rainfall and flash flood periods. The USGS flow gages give an indication of how the water drained to the river systems and traveled downstream. The data from these gages was used in a flood frequency analysis. These sections present work completed by Dekay Kim at Texas A&M.

4.1 Precipitation

According to the report of the National Climatic Data Center, the Upper Mississippi River flood that occurred during June 2008 was caused not only by the extreme precipitation which broke historical records at 15 rain gages across the Midwest, but also by the extremely wet antecedent soil-moisture conditions which had a recurrence interval of approximately 40 years over a large proportion of the Upper Mississippi River Basin (UMRB). Fig. 71 shows the accumulated rainfall for the month of March. The spring rains left the entire area fully saturated and unable to absorb any more water. The rain that fell during the months prior to June kept the ground wet and the streams funneled the runoff into rivers and ultimately into the Mississippi River.

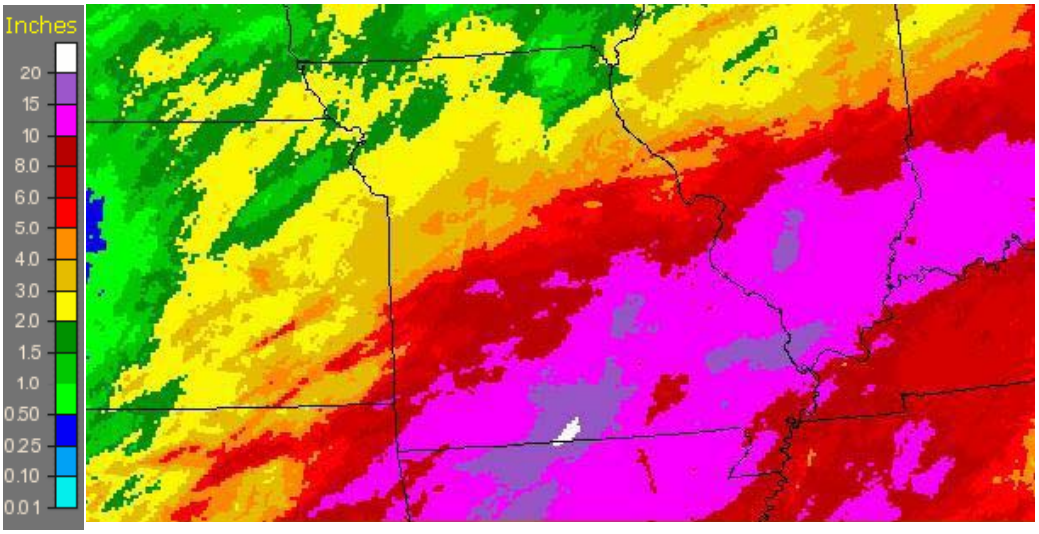

Fig. 71. Heavy rainfall in March (Rogers 2009)

The map showing accumulated rainfall before and during the flooding period best explains the cause of the June 2008 flood (Fig. 72). It is estimated from this figure that rain storms containing vast amounts of water with a spatial extent of several hundreds of kilometers covered the major portion of the UMRB during the flooding period.

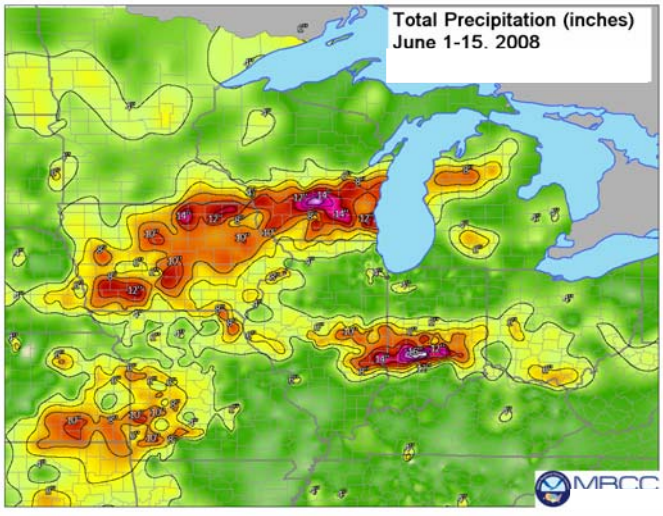

Fig. 72. Contour of accumulated rainfall (adapted from NCDC 2009)

It was also important to determine the concentration of precipitation over time. This plays a significant role in determining the magnitude of the flow peaks. A total of 15 rain gages in the area broke the historical 24-hour precipitation records (Fig. 73). The size of the circle in the figure represents the depth of the rainfall (in.) recorded at the corresponding location in the map. Most of the rainfall depths were recorded between June 7th & 8th except for the two events which occurred in the states of Missouri (June 25) and Kansas (June 27). While the map cannot represent the complicated space-time process of precipitation that occurred during the flooding period, it can be conjectured that the rainfall was concentrated between June 7th & 8th causing a higher flood peak than if it had been concentrated over a longer period of time.

Soil-moisture conditions before precipitation events play a very important role in the generation of floods. The report of the National Climatic Data Center (NCDC) indicates that the UMRB was in an extremely wet condition before the June precipitation occurred. The report states that the antecedent soil moisture conditions of eastern Iowa and southern Wisconsin had a return period of 25 years. It also indicates that the accumulated depth of the precipitation that occurred the six months previous to the flood (December 2007 to May 2008) is the second highest since the recording of the precipitation began in 1895. The color coded NCDC precipitation graph (Fig. 74) gives an indication of how wet the area was between January 2008 and June 2008. Most of the watershed of interest is represented as the darkest color, meaning the area received the highest recorded rainfall in history.

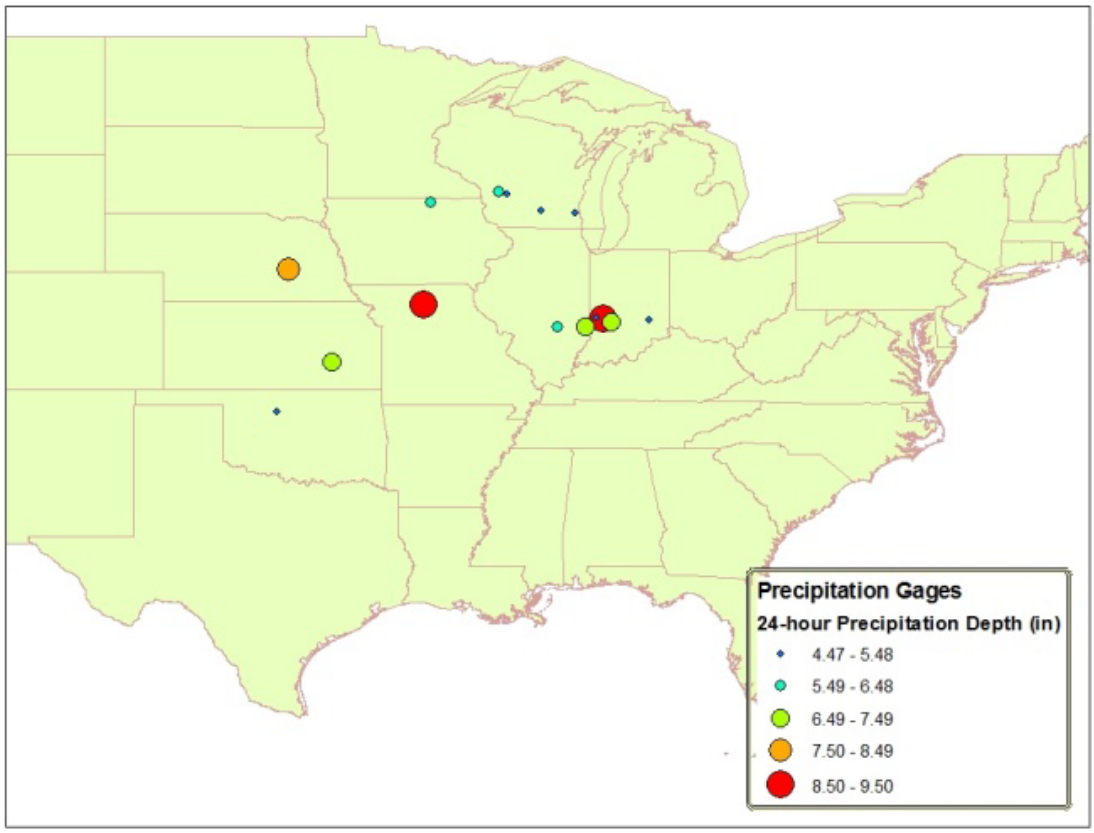

Fig. 73. 15 NCDC rainfall gages, historical 24-hour precipitation records were broken during June 2008 (NCDC 2009)

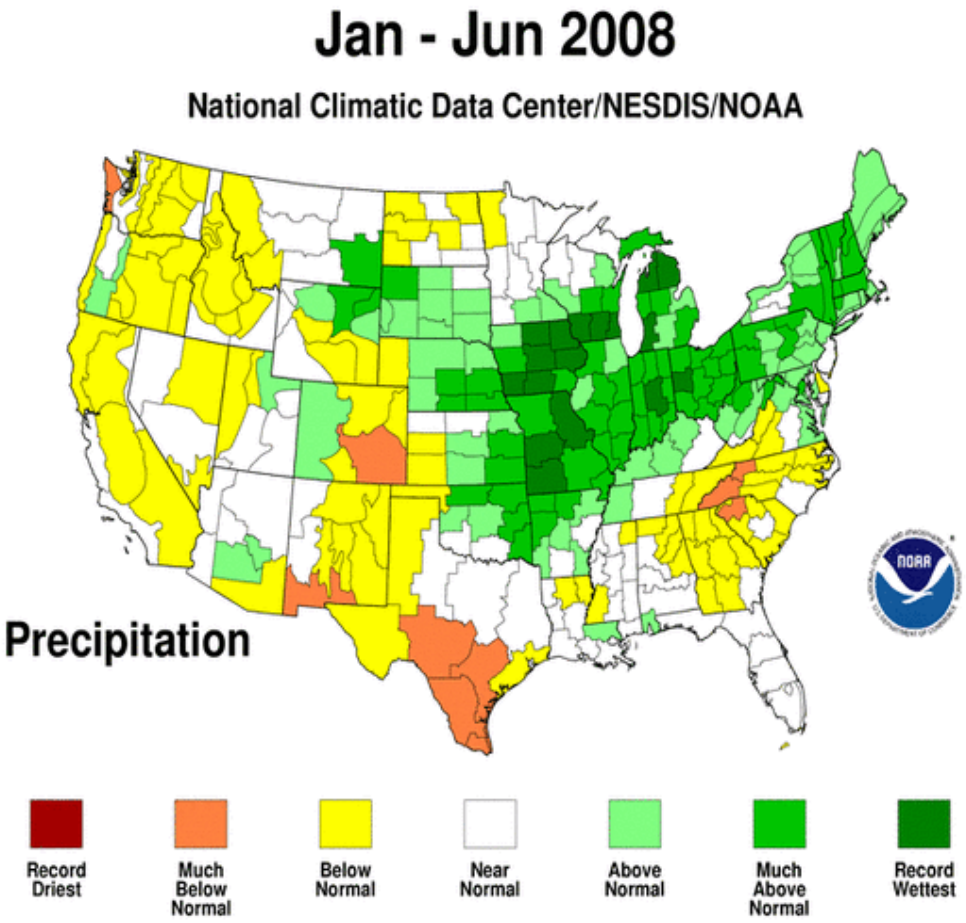

Fig. 74. Antecedent soil-moisture conditions (NCDC 2009)

4.2 Flow Frequency Analysis

The investigation on flow generally provides a more direct clue on the cause of the breaches than the investigation on rainfall does. A frequency analysis was performed on the flow data recorded at select flow gages. For the given study area, the data for six USGS flow gages was available on the main stream of Upper Mississippi River system (Fig. 75). The numbers next to the gage icons represent the USGS gage ID number. Only the gages located on the main stream of the river were chosen for the investigation

because the breaches visited occurred along or close to the main stream. The geographic properties and the availability of flow peaks of these stations as of 12/19/2008 was also available (Table 9).

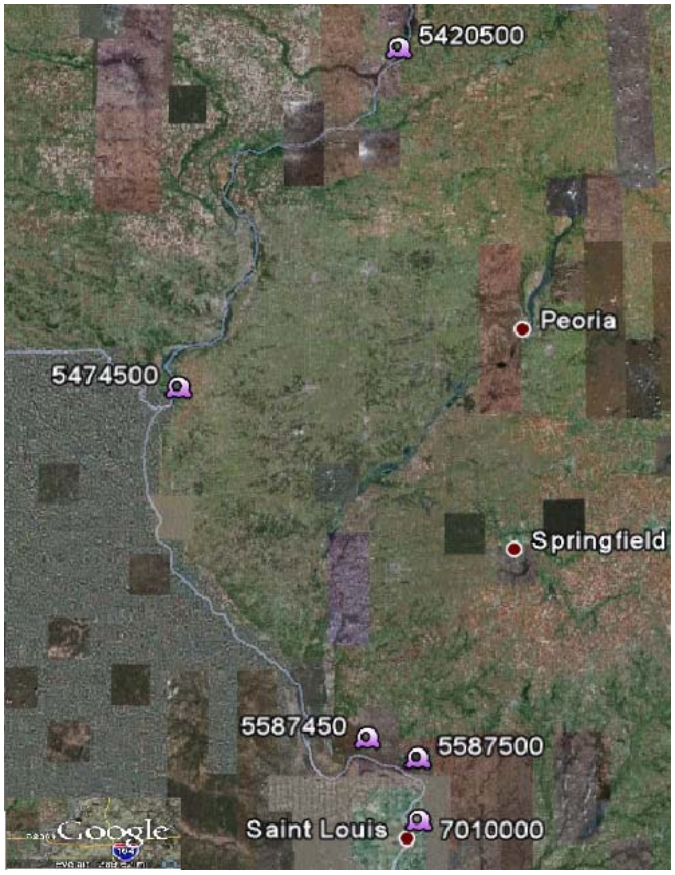

Fig. 75. Locations of the USGS flow gages used (Google Earth)

Gages 05416100 and 05587500 were excluded from the analysis because of a lack of data. However, the gage 05587450 can be a good surrogate for the excluded gage 05587500 because they are located close to one another, indicated by a difference in drainage areas of only 0.1 percent. In summary, the 4 gages shaded in Table 9 were chosen for the frequency analysis. The yearly peak flow values were not available for some gages, so the record daily average during the flooding event was used. The

frequency analysis results for each gage are presented below. Table 10 gives the dates of records used in the analysis.

Table 9. Geographical properties and flow values of the USGS flow gages

USGS ID	Latitude*	Longitude*	Drainage Area (km^2)	Type of record used	2008 Flood Peak Flow values (cms)
05416100	42.2608	-90.4230	213,400	None	None
05420500	41.7805	-90.2519	221,700	Daily Average	5,700
05474500	40.3936	-91.3742	308,200	Peak	12,400
05587450	38.9678	-90.4289	443,700	Daily Average	12,400
05587500	38.8850	-90.1808	444,200	Daily Average	12,700
07010000	38.6306	-90.1175	1,805,200	Daily Average	20,300

*WGS1984 Geographic Datum

Table 10. Dates of records used during the analysis

USGS ID	Records of flow peaks starts from	Records of flow peaks ends at	Length of records	2008 Flood Data Availability
05416100	04-15-1997	04-15-1997	1	No
05420500	05-17-1847	04-05-2007	134	Yes
05474500	06-06-1851	08-28-2007	130	Yes(Provisional)
05587450	04-01-1933	04-16-2007	22	Yes(Provisional)
05587500	06-xx-1858	05-23-1986	60	No
07010000	06-27-1844	05-11-2007	108	Yes

4.2.1 Gage 05420500

The gage is located on the edge of the Mississippi River near Clinton, Iowa (Fig. 76). This was the northern most gage used in the analysis.

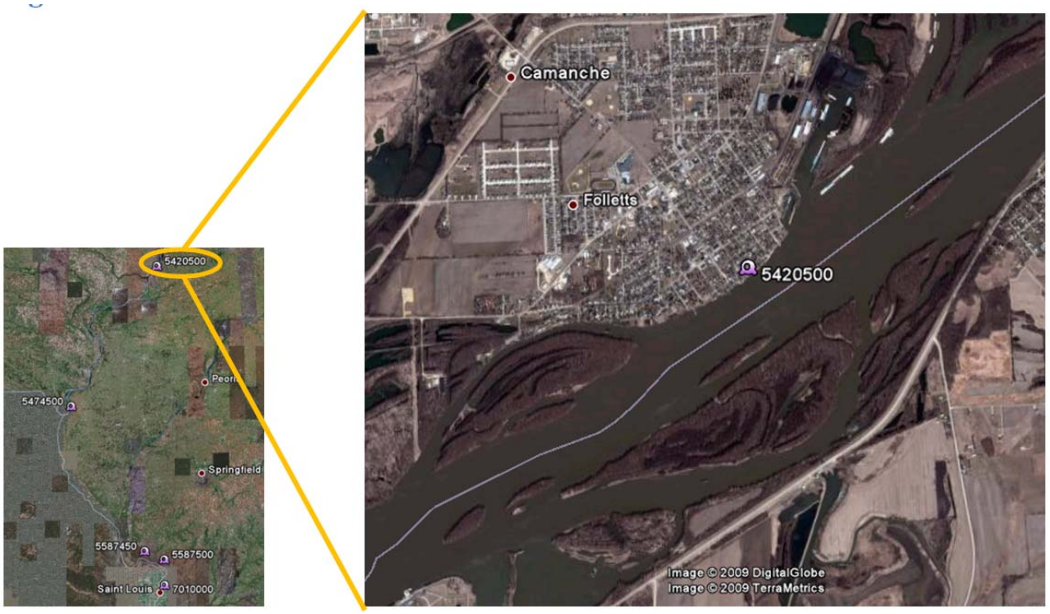

Fig. 76. Gage 05420500 location and detailed view (Google Earth)

The frequency analysis requires the records of yearly flow peaks for its basis (Fig. 77). The flow peaks influenced by human intervention (e.g. flood prevention structures) should be excluded from the flood frequency analysis. This data was recorded from 1940 until 2007. The remaining data which started in 1874 and ended in 1939 was used as the basis for the flow frequency analysis.

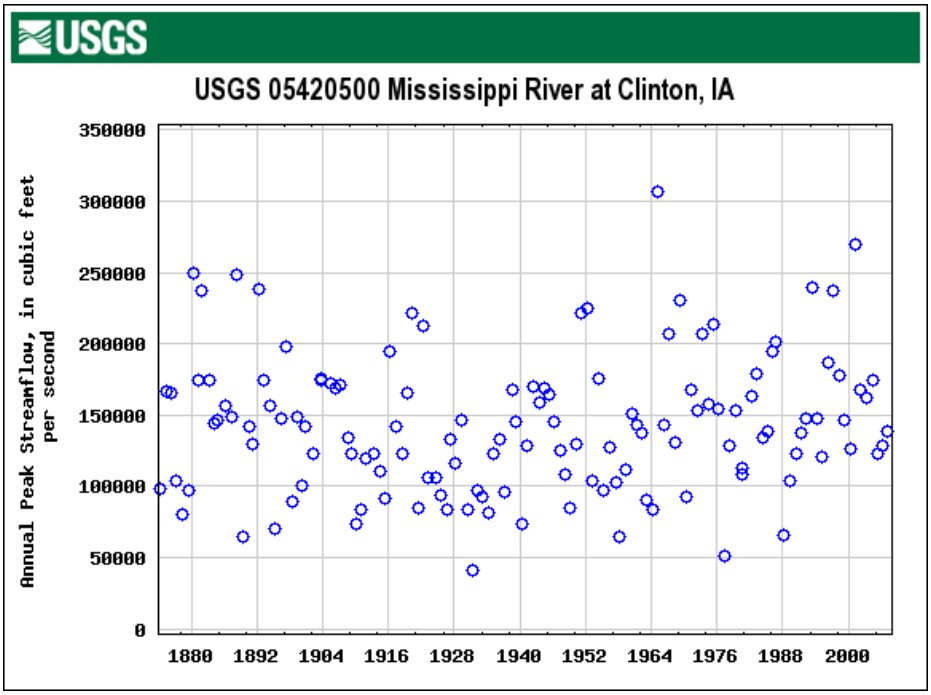

Fig. 77. Time series of yearly flow peaks at gage 05420500 (USGS 2009)

A graph was then made for the recurrence interval versus the flow (Fig. 78). The "+" signs show the observed flow peaks (y) and their recurrence interval based on a non-parametric flow frequency analysis. The dotted line, darker solid line and the other solid line represent the relationship between the observed flowpeaks and their recurrence interval based on GEV-LMOM, Bulletin 17B and GEV-MLE flood frequency analyses, respectively.

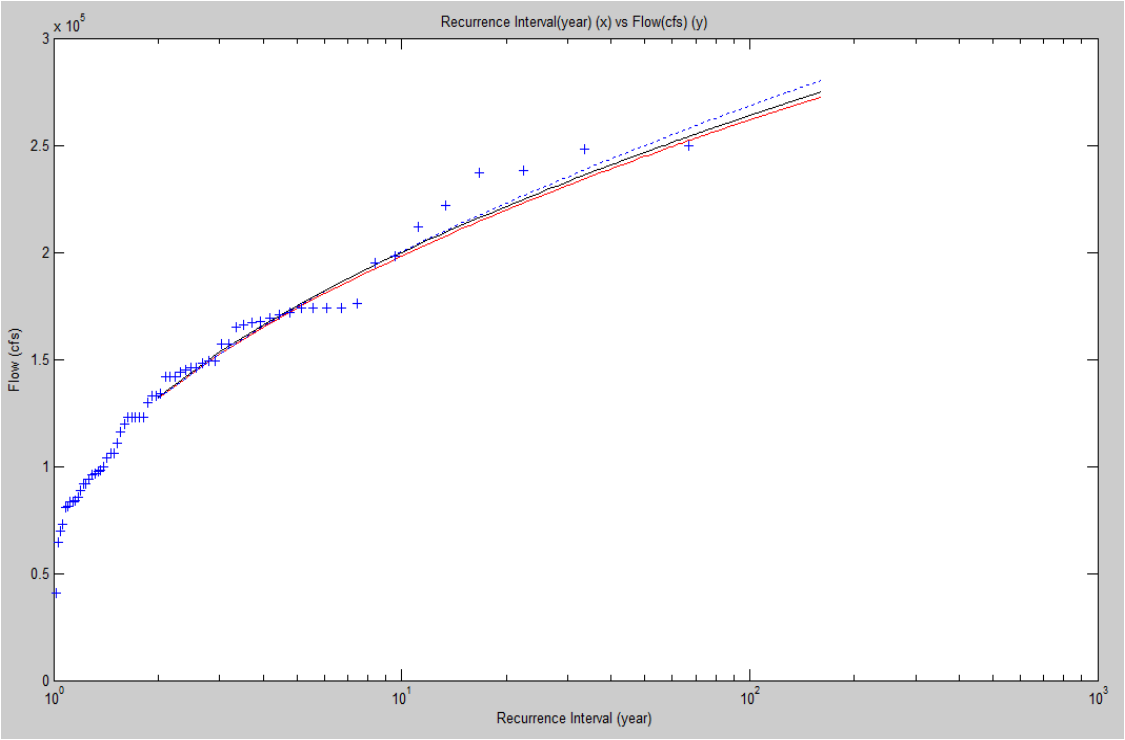

Fig. 78. Observed flow peaks versus recurrence interval at gage 05420500

The daily flow hydrograph during the 2008 flood observed at the USGS gage 05420500 is shown below (Fig. 79). Along with the hydrograph, 10 and 50 year floods based on Bulletin 17B flood frequency method are shown. The highest flow that occurred was 5,200 cms which has approximately a 7 year recurrence interval. The gage is located on the upstream of the flooded area, which explains why the flow magnitude at this location is not very large.

Due to USGS data availability, the flow to which the recurrence interval is assigned for this gage is not the yearly flow peak, but the daily average flow. Because the cross-section of the river is so large, the peak flow values and the daily average should be very close. The recurrence interval of the flow peak, as opposed to the daily average, will actually be higher than the value suggested by this report. However, it

does not seem that the difference in the two cases will be significant because the drainage area of the watershed is fairly large.

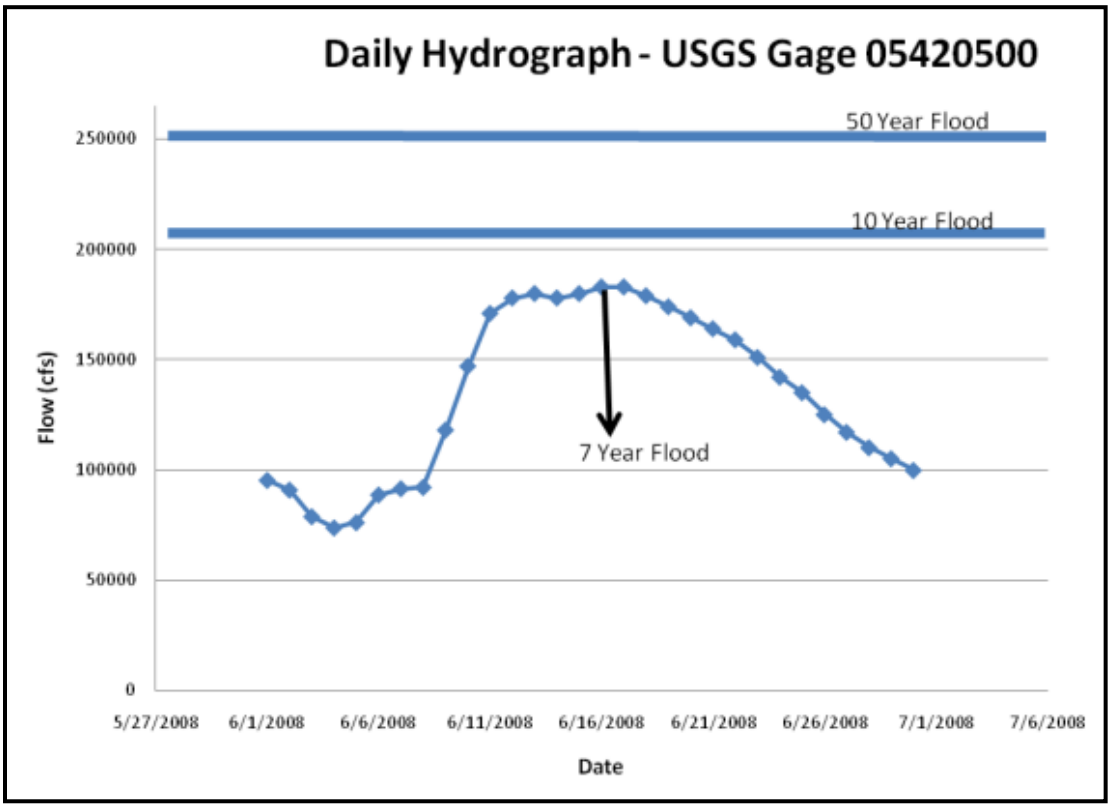

Fig. 79. Daily flow hydrograph during the 2008 flood at USGS gage 05420500

The 10 and 50 year floods shown on the hydrograph are estimated flood recurrence intervals for that location. This is often misunderstood by the public leading them to underestimate the risk of living near a levee. The term "100 year flood" means there is a 1percent chance that a flood event of that magnitude will occur in a given year. While it seems like an infrequent event, ASCE reports that there is actually an over 26 percent chance that a 100 year flood will occur during a 30 year home mortgage. Even with a "200 year flood" there is almost a 15 percent chance that the flood event will occur during the time of 30 years.

4.2.2 Gage 05474500

The gage is located on the edge of the Mississippi River just across the bank from Hamilton, Illinois in Keokuk, Iowa (Fig. 80).

Fig. 80. Gage 05474500 location and detailed view (Google Earth)

Once again, the frequency analysis requires the records of yearly flow peaks for its basis (Fig. 81). Those influenced by human intervention should be excluded from the flood frequency analysis. Such data was recorded from 1938 to 2007. The remaining data which started in 1851 and ended in 1937 was used as the basis of the flow frequency analysis.

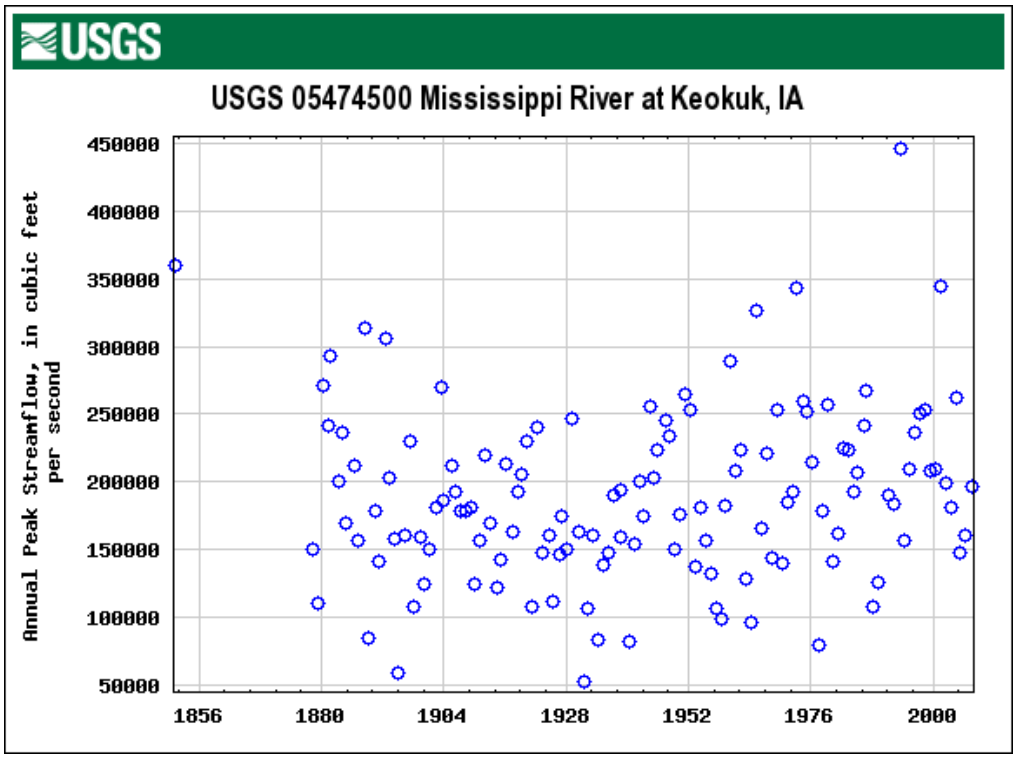

Fig. 81. Time series of yearly flow peaks at gage 05474500 (USGS 2009)

A graph was then made for the recurrence interval versus the flow (Fig. 82). The "+" signs show the observed flow peaks (y) and their recurrence interval based on a non-parametric flow frequency analysis. The dotted line, darker solid line and the other solid line represent the relationship between the observed flowpeaks and their recurrence interval based on GEV-LMOM, Bulletin 17B and GEV-MLE flood frequency analyses, respectively.

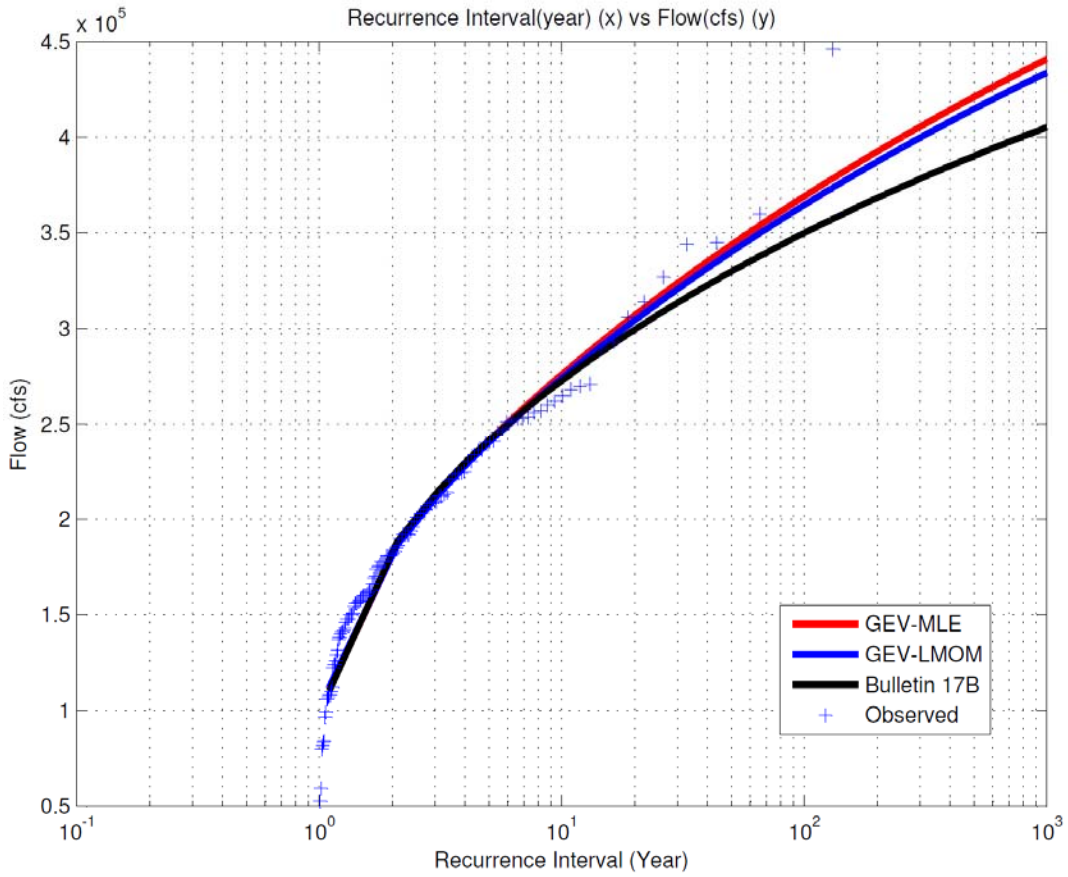

Fig. 82. Observed flow peaks versus recurrence interval at gage 05474500

The daily flow hydrograph during the 2008 flood observed at the USGS gage 05474500 is shown below (Fig. 83). Along with the hydrograph, 100 and 1000 year floods based on Bulletin 17B flood frequency method are shown. The highest flood that occured was 438,000 cfs, which has approximately a 5,500 year recurrence interval. The instantaneous flow peak and the daily average flow were same for this gage.

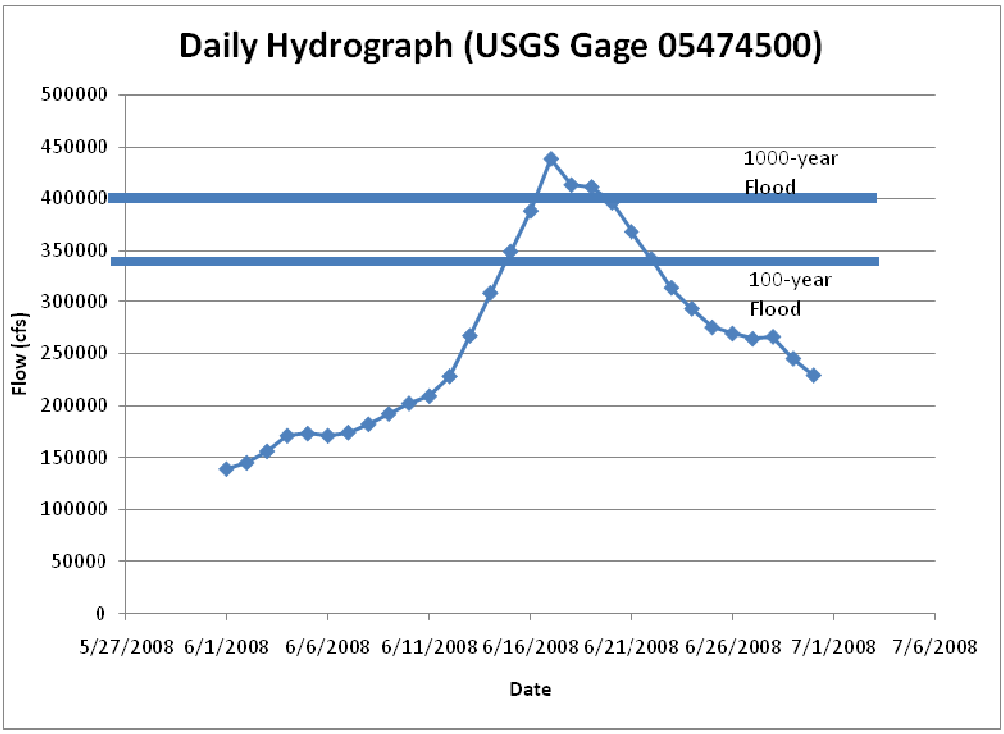

Fig.83. Daily flow hydrograph at USGS Gage 05474500

The flow recurrence interval of 5,500 year based on Bulletin 17B method does not seem to be accurate. There is a discrepancy between the estimated recurrence interval and the length of records used for the flood frequency analysis. As this discrepancy increases, the methods used in the analysis are forced to extrapolate further, introducing possible errors. The recurrence interval estimates shown are based on GEV-LMOM, which has shown in the past to yield more stable results. The calculated recurrence interval based on this method was 1200 years. This value also differs significantly from the length of the flow peaks. Without more data, the general conclusion is that the gage experienced an extremely large flood of which the return period is between several hundred years to thousand years.

4.2.3 Gage 05587450

The gage is located on the edge of the Mississippi River near Grafton, Illinois (Fig. 84).

Fig. 84. Gage 05587450 location and detailed view (Google Earth)

The frequency analysis requires the records of yearly flow peaks for its basis (Fig. 85). There were only 21 flow peaks available for the gage. This small amount of data can adversely affect the accuracy of the frequency analysis result. Gage 05587500 is located in Alton, just a short distance downstream of 05587450, with a difference in drainage area of less than 1percent. For this reason, the flow peaks observed at 05587500 were also used as the basis of the flood frequency analysis for Gage 05587450 (Fig. 86). None of the data was indicated to be influenced by human intervention. Therefore, all points were used in the flood frequency analysis.

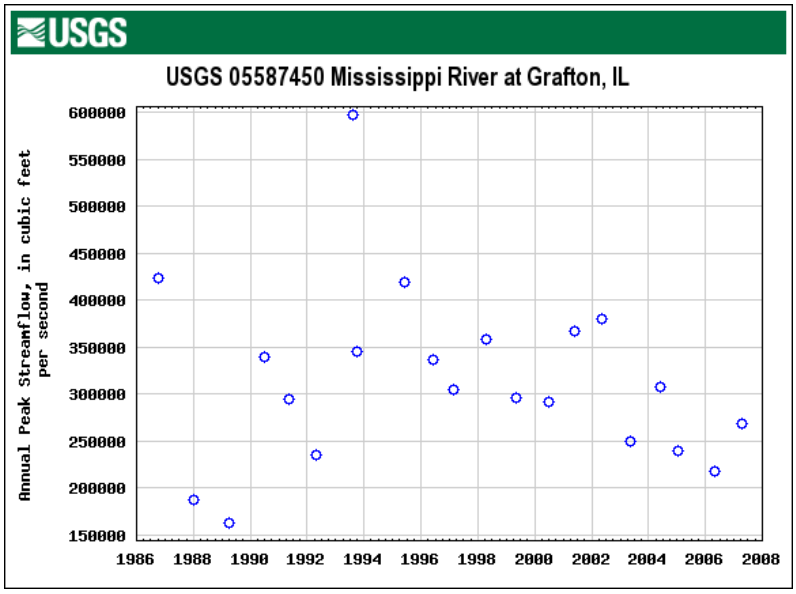

Fig. 85. Time series of yearly flow peaks at gage 05587450 (USGS 2009)

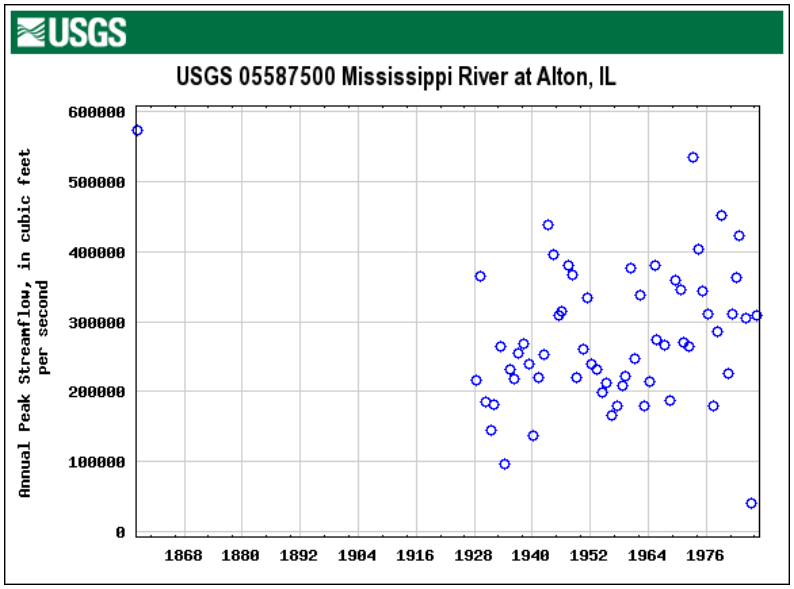

Fig. 86. Time series of yearly flow peaks at gage 05587500 (USGS 2009)

A graph was then made for the recurrence interval versus the flow (Fig. 87). The "+" signs show the observed flow peaks (y) and their recurrence interval based on a non-

parametric flow frequency analysis. The dotted line, darker solid line and the other solid line represent the relationship between the observed flowpeaks and their recurrence interval based on GEV-LMOM, Bulletin 17B and GEV-MLE flood frequency analyses, respectively.

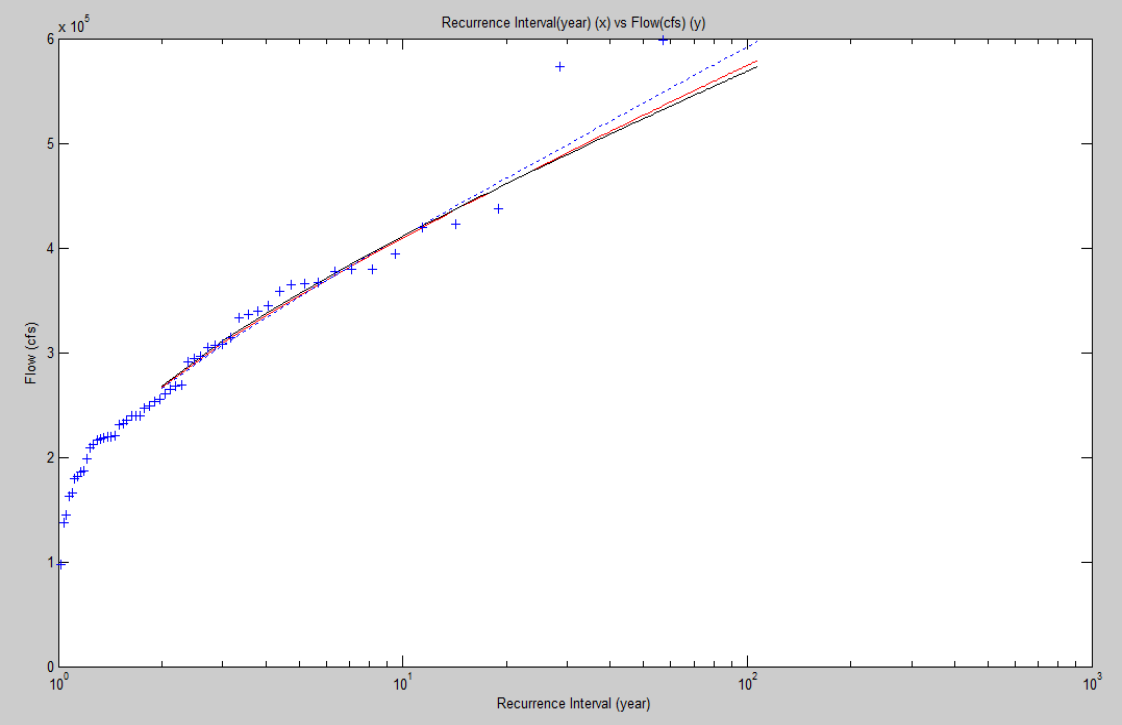

Fig. 87. Observed flow peaks versus recurrence interval at gage 05587500

The daily flow hydrograph during the 2008 flood observed at the USGS gage 05587450 is shown below (Fig. 88). It should be noted that the data used to generate the flow hydrograph is provisional, meaning it has not been approved by USGS for official use. This data can be inaccurate and is subject to a significant modification, which adds uncertainties to the accuracy of the results of the preliminary frequency analysis for this gage.

Along with the hydrograph, 10 and 50 year floods based on the Bulletin 17B flood frequency method are shown. The highest flood which occurred was 431000 cfs, which has approximately a 13 year recurrence interval. For this particular analysis, the recurrence interval was based on daily average values rather than instantaneous yearly peaks. Using daily average values has a general tendency to increase the recurrence interval.

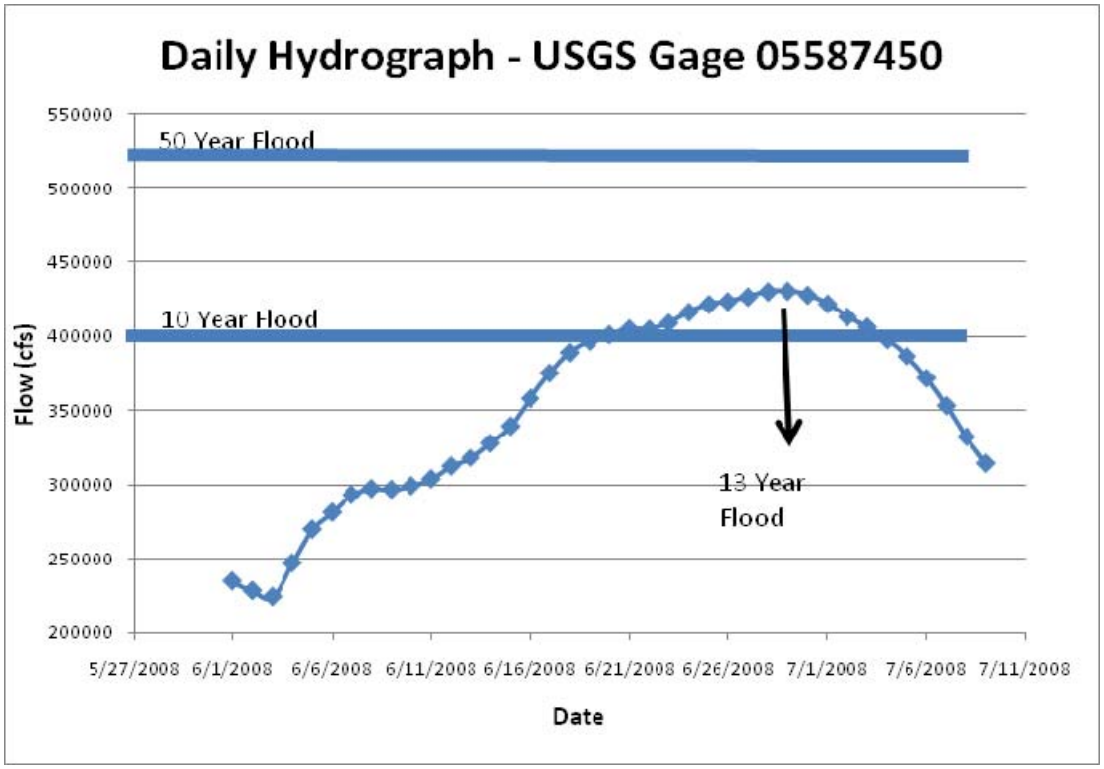

Fig. 88. Daily flow hydrograph during the 2008 flood at USGS gage 05587450

4.2.4 Gage 07010000

The gage is located on the edge of the Mississippi River near St. Louis, Missouri (Fig. 89). This was the southernmost gage used in the analysis.

Fig. 89. Gage 07010000 location and detailed view (Google Earth)

The frequency analysis requires the records of yearly flow peaks for its basis (Fig. 90). No flow data was indicated to be influenced by human intervention. Thus, all flow peaks were used in the frequency analysis.

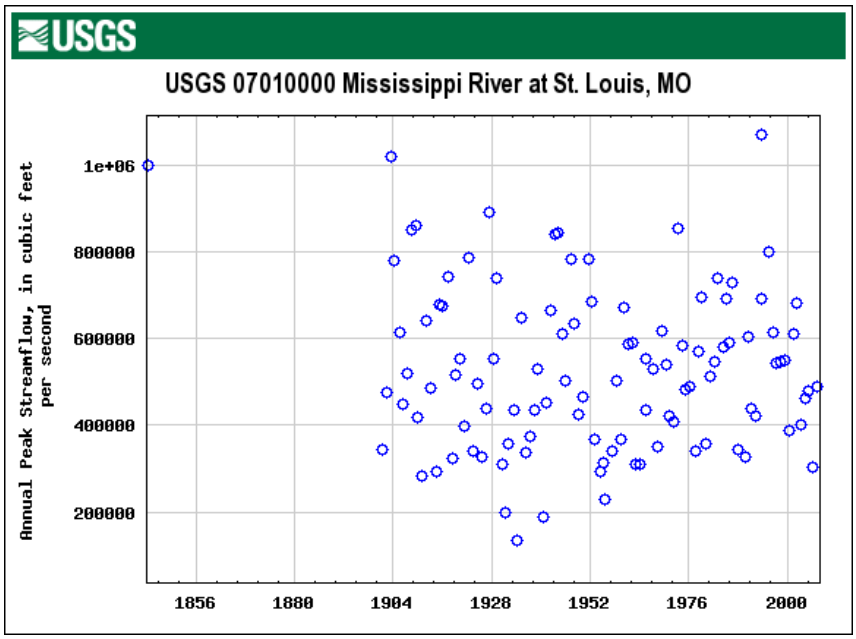

Fig. 90. Time series of yearly flow peaks at gage 07010000 (USGS 2009)

A graph was then made for the recurrence interval versus the flow (Fig. 91). The "+" signs show the observed flow peaks (y) and their recurrence interval based on a non-parametric flow frequency analysis. The dotted line, darker solid line and the other solid line represent the relationship between the observed flowpeaks and their recurrence interval based on GEV-LMOM, Bulletin 17B and GEV-MLE flood frequency analyses, respectively.

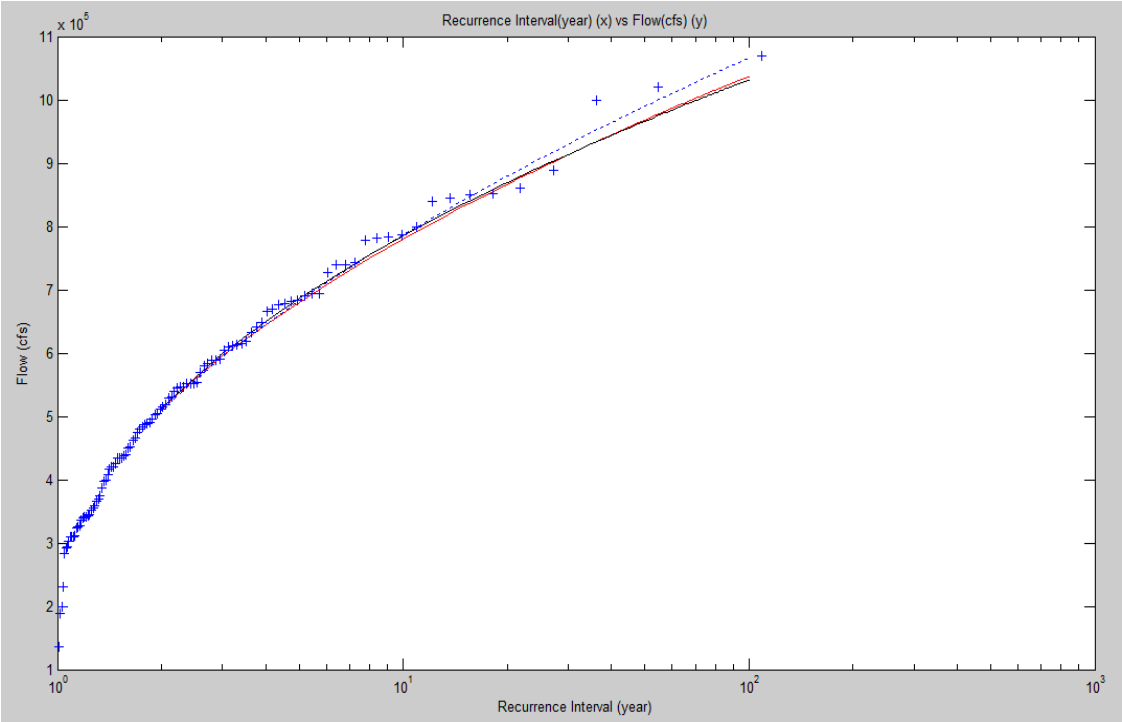

Fig. 91. Observed flow peaks versus recurrence interval at gage 07010000

Fig. 92 shows the daily flow hydrograph during the 2008 Flood observed at the USGS gage 07010000. Along with the hydrograph, a 10 year flood based on Bulletin 17B flood frequency method is shown. The highest flood which occurred was 716000 cfs, which has an approximate recurrence interval of 6 years. Similar to the previous

gage, the recurrence interval was based on daily average values instead of instantaneous yearly peak values. This could lead to an increased recurrence interval.

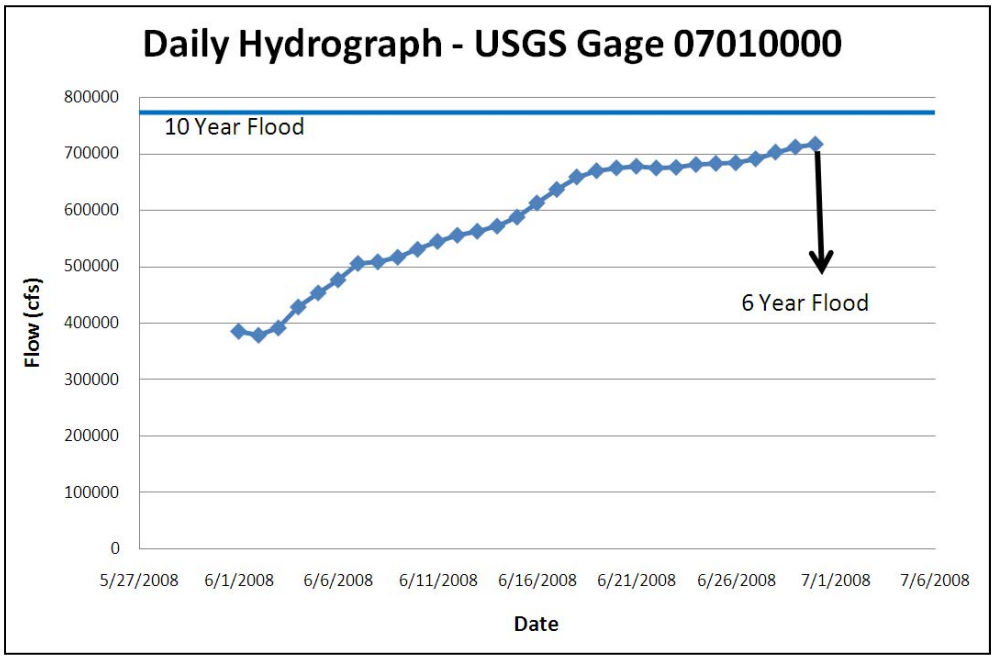

Fig. 92. Daily flow hydrograph during the 2008 flood at USGS gage 07010000

4.3 Drainage Basin Analysis

The above hydrographs show a discrepancy in the magnitude of the flow values observed at two locations along the main stream of Upper Mississippi River. According to the previous analysis, the upstream gage 05420500 experienced a 7 year flood whereas the gage located 240kilometers downstream (USGS 05474500) experienced a 300 plus year flood, 1000 year flood if the extrapolated value is used. Below this gage the flood returns to a 13 year flood. The official flow peak data for the last June flood for both locations were released by USGS. The results of the flood frequency analysis

based on several different methods (GEV-MLE, GEV-LMOM, and Bulletin 17B) shows significant difference in the recurrence intervals (Table 11).

Table 11. Flood frequency analysis results for gages 05420500 and 05474500

USGS ID	Latitude (degree)	Longitude (degree)	Drainage Area (mi^2)	Flow Peak June 2008 Flood (cms)	Date of Peak	Recurrence Intervals		
						USGS method Bulletin 17B	GEV-MLE	GEV - LMOM
05420500	41.7805	-90.2519	85,600	5,700	6/16/08	8.1	8.2	8.1
05474500	40.3936	-91.3742	119,000	12,400	6/17/08	5470	905	1178

Considering the data used for the analysis is official and has been released by the USGS, the most probable explanation for the discrepancy is that there must be a large water input between the two locations. By looking at the area draining into the river, we can get an idea of the amount of water entering at different points along the river (Fig. 93). The green area shown covers the basin that drains into the upstream gage (USGS 05420500) and the orange area covers the basins of the rivers and streams that drain into the main section of the Upper Mississippi River between the two gages. The color surface in the background represents the depth of the precipitation that occurred from June 1 to June 15, 2008. The basins were delineated based on stream networks provided by Google Earth.

The basin draining into the river between the two locations (orange area) experienced large amounts of rainfall. The entire portion of the basin experienced rainfall which broke the historical record in many locations. While further hydrologic analysis based on numerical modeling is necessary to pin-point the sources of the large flood, the vast spatial coverage of the rainfall along with the large rainfall depth seems to

have played a significant role in the generation of the flood. The basin draining to the upstream gage (USGS 05420500) also experienced large rainfall depths, but the spatial coverage of this area is not as wide as the previous case, causing a recurrence interval of only 8 years.

In summary, the difference in recurrence intervals between gage 05420500 to the north (7year flood) and gage 05474500 to the south (larger than 1000 year flood) is that a large amount of precipitation over a large area drained into the Mississippi River between these gage locations. The extreme flood caused breaches in several locations between gage 05474500 to the north (more than 1000 year flood) and gage 05587450 to the south (13 year flood). Because the water in the river drained to the flood plain through the breaches, the flood intensity was reduced at the downstream gage.

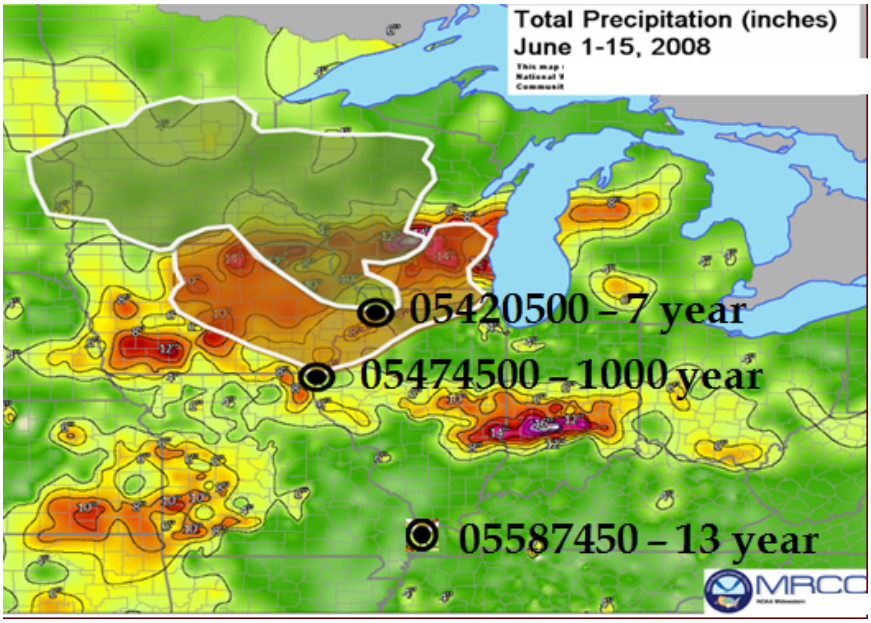

Fig. 93. Basin drainage area between two gages (adapted from NCDC 2009)

4.4 Accuracy of the Data

Several factors could possibly have an adverse affect on the accuracy of the frequency analysis results:

1. Provisional data: USGS indicates that the 2008 flood data at the gage 05420500 and 05587450 are currently posted as provisional, and can be highly inaccurate and subject to significant modification. This adds uncertainties to the accuracy of the results of the frequency analysis at each gage.
2. Length of flow peak record: Extrapolation in the flood frequency analysis (i.e. determining a design flood of which recurrence interval is greater than the length of the flow peak records) has always been an issue. Therefore, the results should be interpreted with caution if the assigned recurrence interval on a 2008 flow peak is greater than the length of the flow peak records at the gage.
3. Flood frequency analysis method: While the method suggested by the Bulletin 17B is considered to be standard way of flood frequency analysis, many recent studies argue that other methods can better model the frequency of the floods. This study provides the results based on three different methods of frequency analysis including the one suggested by the Bulletin 17B. In general, the result should be similar regardless of the type of the applied method if the flow peak record is long and accurate enough to represent the unknown previous long-term time series of the flow peaks.
4. Yearly flow peaks versus Daily flow values: Flow frequency is usually assigned to the observed instantaneous flow peak value. However, the flow peaks are not

yet available at all the stations. The author of this report received correspondence from USGS personnel stating that the flow peaks for the 2008 Flood will be available around March 2009. For this analysis, the recurrence interval used the daily observed flow values instead of flow peaks, which could potentially add inaccuracy to the results of the analysis. However, it is shown from numerous former studies that the difference between the instantaneous flow peak and the daily average flow is almost negligible for large watersheds like the ones investigated in this study.

4.5 Flood Frequency Analysis Method

The method of flood frequency analysis can be categorized by parametric and non-parametric approaches. In the non-parametric approach, the flow records of N observations are ranked in descending order with the highest value assigned a rank 1 and the smallest assigned a rank N. The probability, P_m, that the observation with rank m is equaled or exceeded is then estimated as:

$$P_m = \frac{m}{N+1} \tag{53}$$

This value of P_m and the corresponding flow value are plotted on the probability graph to find out the general tendency of the flow records. This plot is used to extrapolate and interpolate for the flow with a given recurrence interval. The non-parametric approach can provide reasonably accurate estimates of the flow with a given recurrence interval (or the recurrence interval of a given flow) within the range covered by the observations,

but the estimated values located outside of the observed range can be highly inaccurate (Wurbs and James 2002) .

In the parametric approach, the record of observed flow is assumed to behave according to a given probability distribution. Based on this assumption, the parameters of the distribution are estimated using the recorded flow peaks. Then, the recurrence interval of a given flow or the flow with a given recurrence interval is estimated based on the distribution with a set of determined parameters. As opposed to non-parametric approach, the parametric approach can provide more accurate estimates of flow or recurrence interval for values located beyond the observed data range.

In this study, the following combinations of probability distribution and parameter estimation methods were applied to assign the recurrence interval to the 2008 flood.

1. Generalized Extreme Value distribution – method of maximum likelihood (GEV-MLE)
2. Generalized Extreme Value distribution – method of L-moments (GEV-LMOM)
3. Log-Pearson Type III distribution – method of moment (Bulletin 17B)

A detailed description of each methodology is beyond the scope of this report. A document detailing each methodology can be obtained by e-mailing dekaykim@gmail.com.

5. 2008 MIDWEST LEVEE FIELD INVESTIGATION

5.1 Field Investigation

The aim of the field investigation conducted by TAMU was to document the conditions of the remaining breach areas and gather samples for index property testing and erosion testing in the EFA. A variety of flood protection system configurations (design flood return period, levee material type(s), etc.) were chosen based on past and present flood conditions and performance (levees that breached without overtopping, levee breaching as a result of overtopping, seepage-induced breaching, and levees that sustained extensive overtopping without experiencing seepage or overtopping induced breaching). The focus was placed on locations that have failed repeatedly and also those that sustained continuous overtopping for days and even weeks without failure. Recommendations were also taken from the USACE St. Louis and Rock Island Districts. All sites were situated between the USACE St. Louis District and USACE Rock Island District. These sites (Two Rivers, Indian Graves, Bryants Creek, Kickapoo, Elsberry, Kings Lake, Winfield, and Brevator) reflected a wide range of levee loadings and performance. Fig. 94 shows the study area along with the levee areas that were previously breached in the 1993 flood and those that were not.

The goal of the Midwest Levee reconnaissance was to gather perishable data in an effort to provide a comprehensive overview at each breach location. Personal observations and photographs, along with a table of samples taken are given for each site. A detailed sample log is given in Appendix 1.

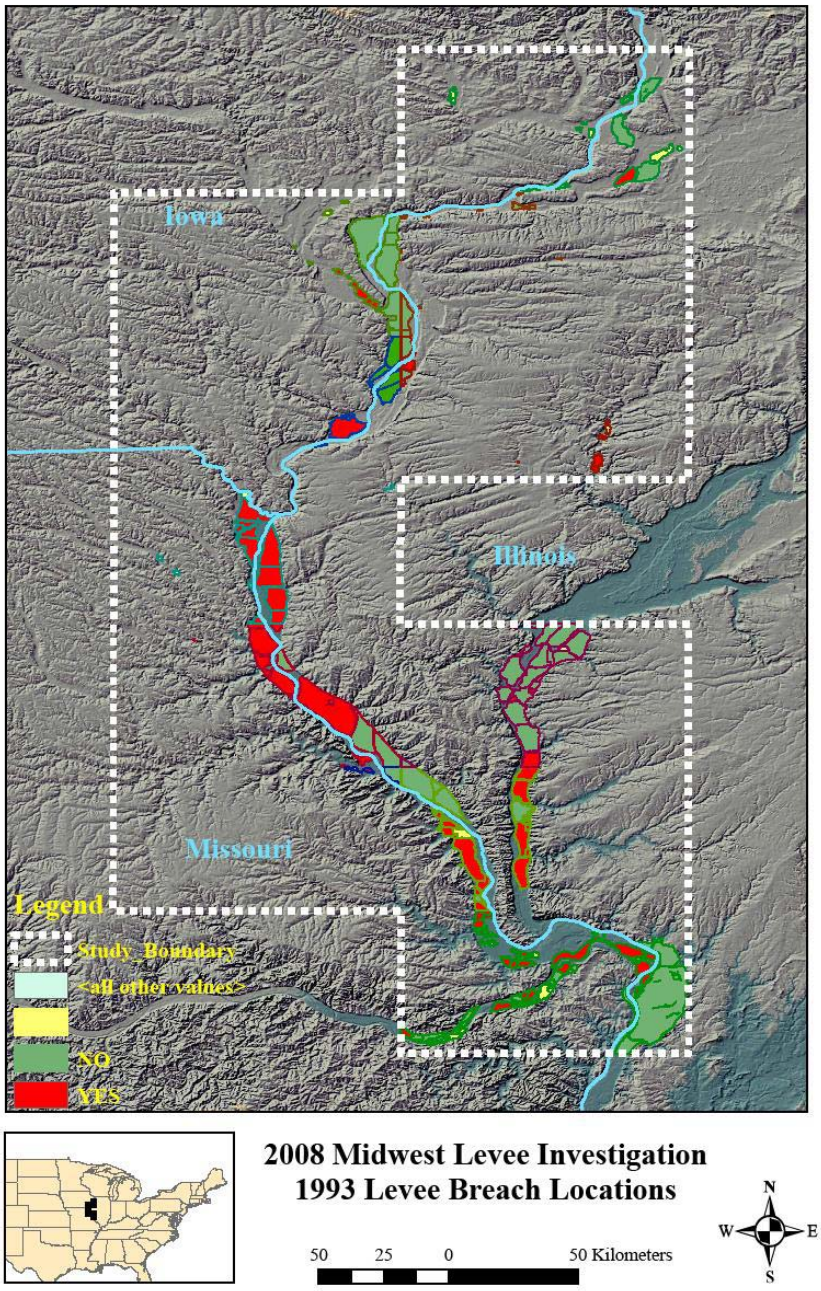

Fig. 94. 1993 flood breach locations (Rogers 2009)

Samples were collected at eight sites (Table 12). In the Google map shown in Fig. 95, the red box outlines the study area. These sites are shown in black on Fig. 96.

Sampling techniques along with a more detailed description of each site are presented in the following sections.

Table 12. Summary of sites visited during 2008 Midwest Levee Investigation

Site Name	Latitude*	Longitude*	Levee District
Winfield	38.9882	-90.6818	Cap au Gris Drainage & Levee District
Bryants Creek	39.2514	-90.7711	Elsberry Drainage District
Brevator	38.9622	-90.7114	Brevator Drainage & Levee District
Kickapoo	39.1850	-90.7427	Elsberry Drainage District
Norton Woods	39.1353	-90.7206	Elsberry Drainage District
Indian Graves	40.0011	-91.4499	Indian Graves Drainage District
Two Rivers	41.0939	-91.0687	Iowa Flint Creek Levee District No. 16

*WGS1984 Geographic Datum

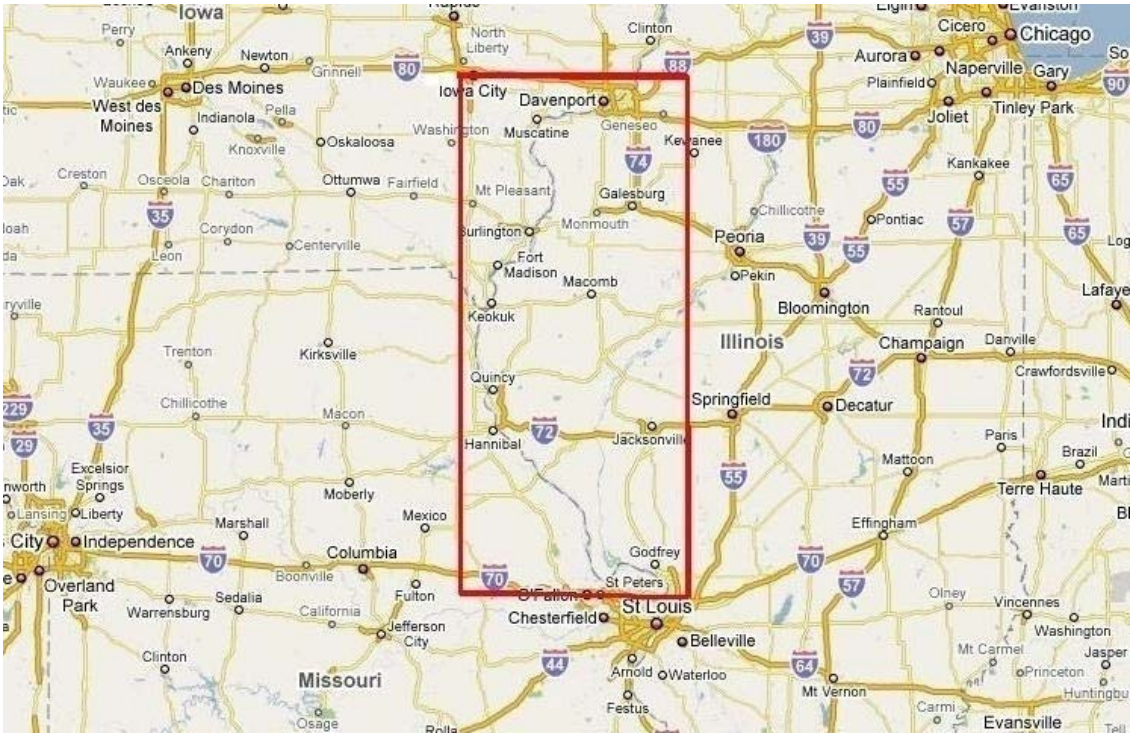

Fig. 95. Location map showing the study area outlined in red (Google maps)

Fig. 96. Map of sites visited (Storesund 2009)

5.2 Sample Collection

Because the site conditions did not allow for the use of CPT or conventional drilling rigs, surficial samples were collected. At sites were breaching had occurred, samples were taken at various locations within the breached area, in the sides of the

exposed remaining levee, and in the remaining core material. In situ samples were collected using modified thin walled Shelby Tubes approximately 154 mm long with a diameter of 76 mm and a wall thickness of 2 mm. Bulk samples were collected at each location for particle size determination and Atterberg Limits determination in order to characterize the soils according to the Unified Soil Classification System (USCS). Samples were also collected in order to determine compaction curves and max densities for each site. These values were then compared to the in situ densities calculated from the recovered tubes. The Geotechnical testing results are presented in Section 6.

The same overall sampling techniques were used at each site. The area of interest was cleared of any surface vegetation and the Shelby tubes were then pushed evenly into the soil using a wooden 2x6. If the tube was unable to be pushed flush with the surface, a wooden 4x4 was used to carefully drive the remainder of the tube in. Samples were then extracted using a shovel to remove the soil around the tube. Each sample was labeled, wrapped in plastic wrap and foil, placed in airtight plastic bags, and then placed in a cooler. Care was taken to ensure little if any water content change occurred in the samples during the remainder of the trip.

The nomenclature used refers to the site and boring/sample number. For example, S1B4 refers to site 1 and the fourth sample. The sample numbers are cumulative throughout the sites. The specified sampling depth was estimated relative to the levee crest. Most of the samples were oriented vertically (Fig. 97) and labeled with a "V." Some locations, however, required samples to be driven horizontally (Fig. 98). The samples driven horizontally into the side of the exposed levees were labeled with an

"H." A hand auger was used at the Two Rivers site in an effort to obtain a sample from the levee core (Fig. 99).

Fig. 97. Vertical sample orientation "V"

Fig. 98. Horizontal sample orientation "H"

Fig. 99. Hand auger – Two Rivers S8B35

When driving the tubes, the recovery was not always 100 percent (Fig. 100). The tubes were pushed flush with the soil surface; however, the soil plug inside did not always fill the entire length of the tube. Simplified calculations were used to evaluate possible explanations. By using general soil strength values, the force per area was calculated for both end bearing and side friction similar to what is done in calculations for piles. The soil strength in end bearing was much less than that calculated in side friction. This gives evidence that the limited recovery was the result of a bearing capacity failure of the soil below the tube once the tube became plugged, however, some compression of the samples may have also occurred due to the friction on the inside walls of the Shelby tubes.

Fig. 100. Recovery less than 100 percent

5.3 In situ Testing

Torvane (Fig. 101) and Pocket Penetrometer (Fig. 102) tests were carried out next to each sample location. The Pocket Penetrometer was used to get a quick estimate of the in situ unconfined compressive strength in units of kg/cm^2 with a range of 0.0-4.5 kg/cm^2. The Torvane was used to estimate the in situ shear strength of the cohesive soils present at each location. This device also has units of kg/cm^2. Care was taken to ensure that the materials used for these tests represented those collected in the corresponding samples. Several readings were taken to minimize variability.

Fig. 101. Torvane testing

Fig. 102. Pocket Penetrometer testing

5.4 Winfield – Pin Oak

At 10:40 am on Monday, September 29, 2008, the Midwest levee investigation team arrived at the Winfield-Pin Oak site near Winfield, Missouri. The Winfield-Pin Oak levee is maintained by the Cap Au Gris Drainage and Levee District. The levee system is estimated to reduce the risk of flooding of approximately 493 ha up to a 14-year return period flood event on the Mississippi River (Fig. 103). This area failed during the 1993 floods, however, the specific location of the breach (or breaches) was not documented (USGS 2006). This site was overtopped for an extended period beginning on June 18th. This breach was a result of overtopping induced erosion.

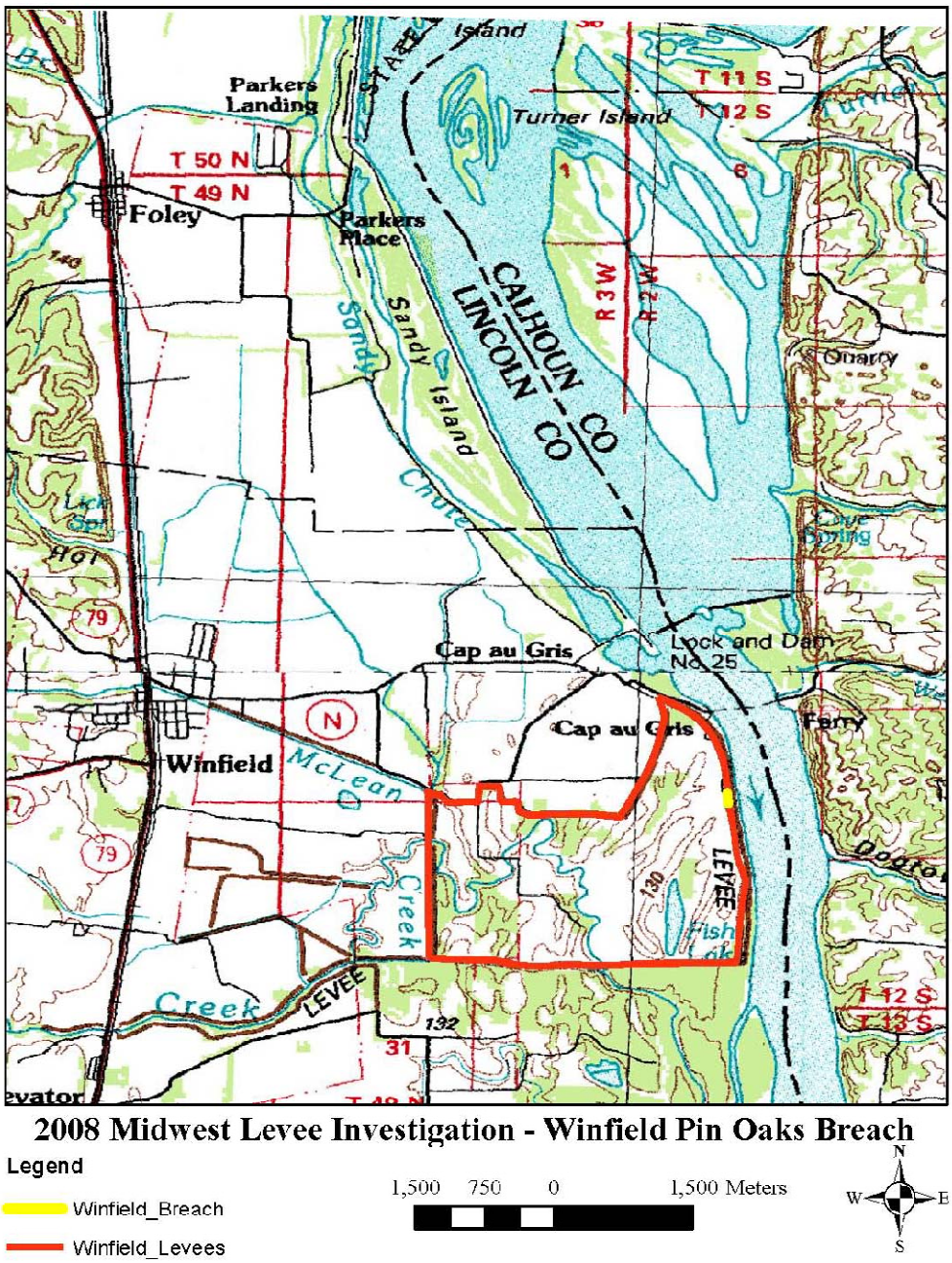

Fig. 103. Location of the Winfield Pin-Oak levee breach (Storesund 2009)

From visual inspection, the Winfield breach was estimated to be around 100 m in length. Five samples were taken from various locations within the breach (Fig. 104).

Table 13 provides a summary of the sample locations as well as Torvane and Penetrometer readings.

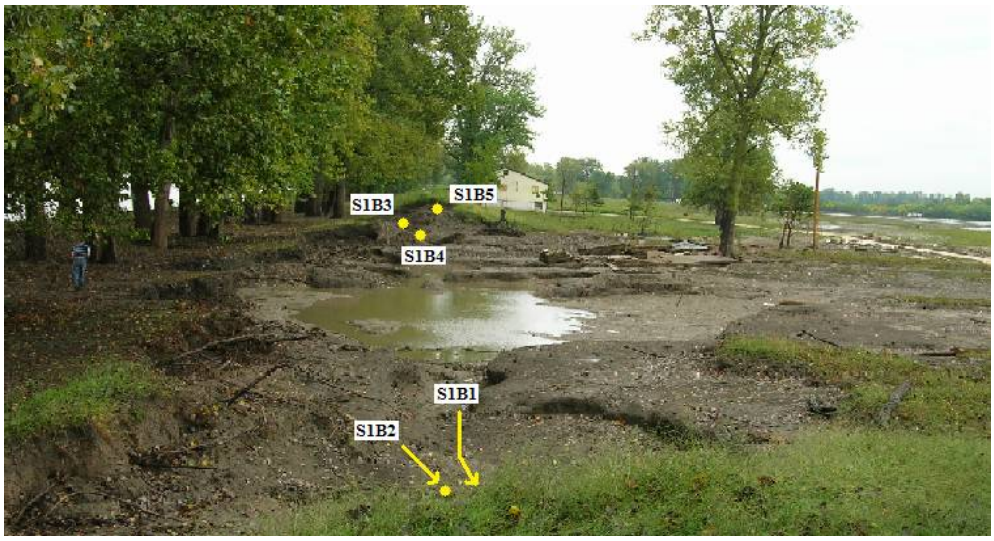

Fig. 104. Boring locations Winfield – Pin Oak breach looking South

Table 13. Winfield – Pin Oak sample log

Sample No.	Direction	Latitude*	Longitude*	Pocket Pen (kg/cm^2)	Torvane (kg/cm^2)	Depth and Location
S1B1	Horizontal	--	--	1.0, 1.1	0.45, 0.47	1.04m, crest centerline
S1B2	Vertical	--	--	0.45, 0.4, 0.35	0.15, 0.14	2.31m, slightly east of center
S1B3	Horizontal	--	--	1.75, 2.1	0.30, 0.29	2.69m, east of center
S1B4	Vertical	--	--	1.2, 1.3	0.21, 0.30	3.96m, slightly east of center
S1B5	Horizontal	--	--	0.6, 0.7	0.15, 0.2, 0.11	0.86m, crest centerline
S1Bag1	Bulk	--	--			--
S1Bag2	Bulk	--	--			--

*WGS1984 Geographic Datum

Samples B1 and B2 were taken at the North end of the existing levee. Fig. 105 shows B1 taken from a position, perpendicular to the exposed face of the existing levee,

and Fig. 106 shows B2 taken vertically from slightly east of center and lower within the core.

Fig. 105. Winfield – S1B1

Fig. 106. Winfield – S1B2

Fig. 104 shows a pond area around the center of the breach. This was the main scour point resulting from the overtopping waters. After returning to the site two days later, the pond was noticed to be almost completely dry. This indicates a somewhat sandy or silty material and quick subsurface drainage. Based on visual observations, the

levee is comprised mainly of lean clays (CL) and silts (ML) with a moderate grass covering.

The Mississippi River runs from North to South at this location. The levee borders the West river bank while the East bank is bordered by natural cliffs which provide a barrier for the flood waters and force the rising water into the levees. The water line on the trees that border the river side of the levee (Fig. 107) was somewhat higher than the existing levee crests indicating that the water was overtopping the levee by almost 1 m.

Fig. 107. High water marks on trees bordering levees

Extensive root networks and crawfish tunnels were present throughout the existing levee and breached area (Fig. 108). These encroachments often encourage the formation of seepage paths through embankments.

Fig. 108. Root networks and crawdad tunnels throughout the levee

Several homes, once standing adjacent to the river, were washed away by the floodwaters (Fig. 109). Remnants of foundation structures and debris were found across the site (Fig. 110).

Fig. 109. Home washed away by the raging flood waters

Fig. 110. Water line and debris near levee breach

5.5 Bryants Creek

The team arrived to the Bryants Creek site around 2:50 pm on September 29, 2008. The Elsberry levee at Bryants Creek is maintained by the Elsberry Drainage District. This system's estimated protection level was not identified by SAST. The levee system borders Bryants Creek until it joins the main stem of the Mississippi River just to the east of the area investigated (Fig. 111). This system failed during the 1993 floods, however, the specific locations were not documented (USGS 2006). This was one of three breaches visited within the Elsberry levee system. This breach occurred at the location of an adjacent duck pond.

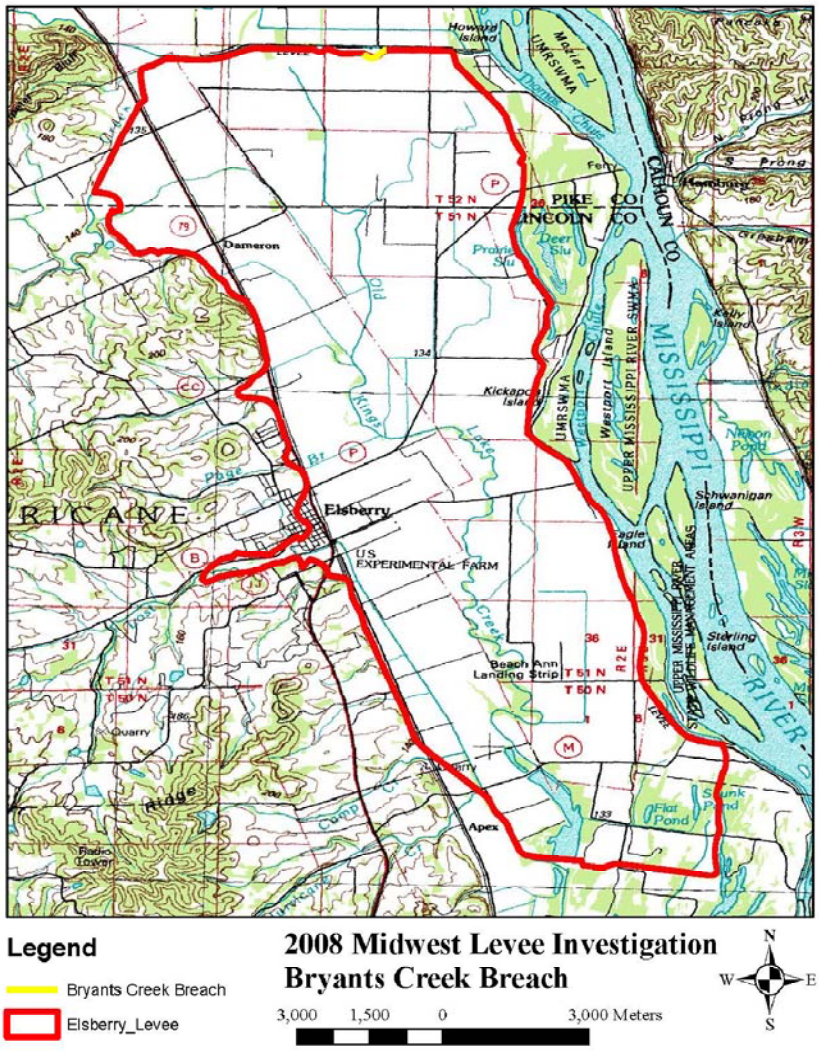

Fig. 111. Elsberry Levee System and Bryants Creek breach (Storesund 2009)

Four samples were taken from various locations within the breach. Fig. 112 shows a schematic of the boring locations and Table 14 gives the sample logs for this site.

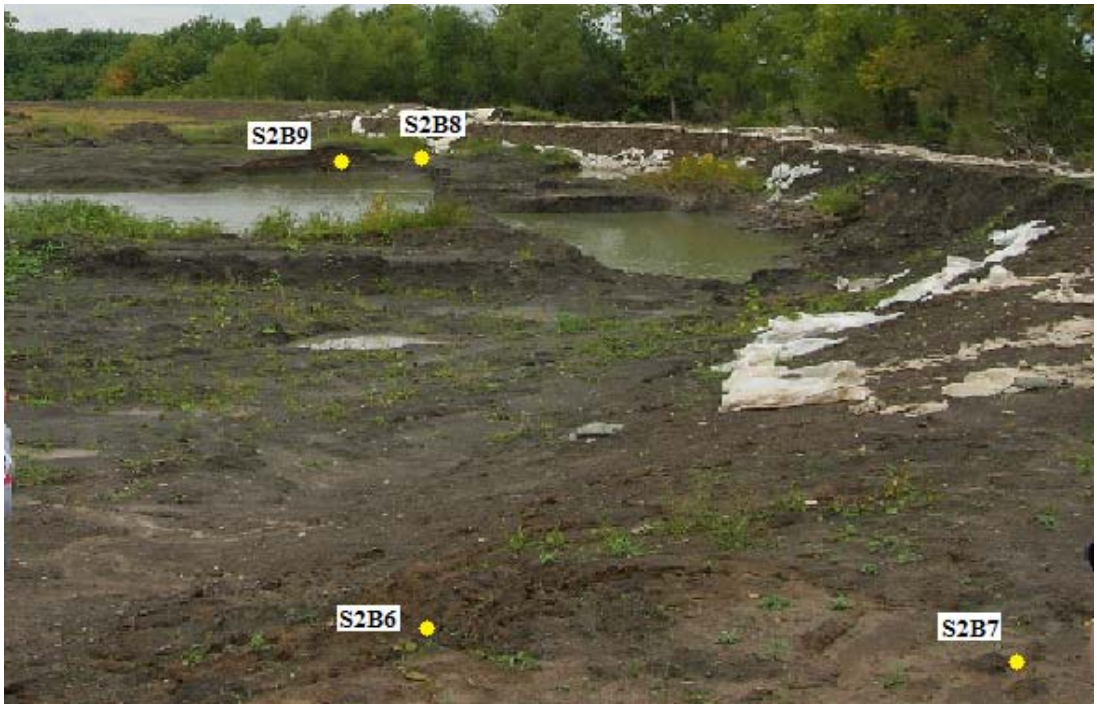

Fig. 112. Bryants Creek boring locations

Table 14. Bryants Creek sample log

Sample No.	Direction	Latitude*	Longitude*	Pocket Pen (kg/cm^2)	Torvane (kg/cm^2)	Depth and Location
S2B6	Horizontal	39.25225	-90.77829	1.9, 1.55	0.75, 0.59	1.47m, south of crest
S2B7	Vertical	39.25229	-90.77817	0.75, 1.0, 1.2	0.60, 0.80	0.46m, surface
S2B8	Vertical	--	--	1.6, 1.0	0.46, 0.51	3.05m, estimated core
S2B9	Horizontal	--	--	1.45, 1.55	0.60, 0.56	3.05m, side of core

*WGS1984 Geographic Datum

Based on visual observations, the levee is comprised mainly of lean clays (CL) with more sticky high plasticity clays in areas (CH). This site also had moderate to substantial grass covering.

After the original levee breached at this site, the US Army Corps of Engineers constructed a temporary levee in order to minimize the free-flow of water into the area during the prolonged flooding event. Onsite materials were used in combination with plastic sheeting to construct the temporary embankment.

During the initial investigation, the temporary levee was very muddy and even sticky, indicating a more clayey material. After returning to the levee two days later, the levee had dried out a substantial amount, indicating the presence of sand or silt in the clayey material. Fig. 113 shows this levee as well as the east end of the remaining levee.

Fig. 113. Bryants Creek temporary levee looking East

Remnants of the original levee structure and foundation materials were found within the breach zone. Samples B8 and B9 were located about halfway between the two ends of the remaining original levee. The samples were taken in what was believed to be the core of the original levee (Fig. 114).

Fig. 114. Remaining eroded original levee and temporary levee

This location represents the major breach location. Fig. 115 shows the breach while standing on the temporary levee looking towards the river. The leaning and pushed over vegetation indicates extremely high water velocity and volume flow. Also, the largest pool of water and scour depth was opposite this location.

Fig. 115. Trees uprooted and pushed over from the rushing waters

Fig. 116 shows some of the original levee. The darker gray material is more clayey, while the brown material contains some silt. This type of pattern could be evidence that the drag line method was used in the initial construction of the levees.

Fig. 116. Bryants Creek original levee material

5.6 Brevator

The team arrived at the Brevator site at 10 am on Tuesday, September 30, 2008. The Brevator levee is maintained by the Brevator Drainage and Levee District. The levee system is estimated to reduce the risk of flooding for approximately 745 ha for up to a 14-year return period flood event. The levee is offset over 2,000 m west of the river bank of the main stem of the Mississippi (Fig. 117). This system also failed during the 1993 flood, however, the specific location of the breach (or breaches) was not documented (USGS 2006).

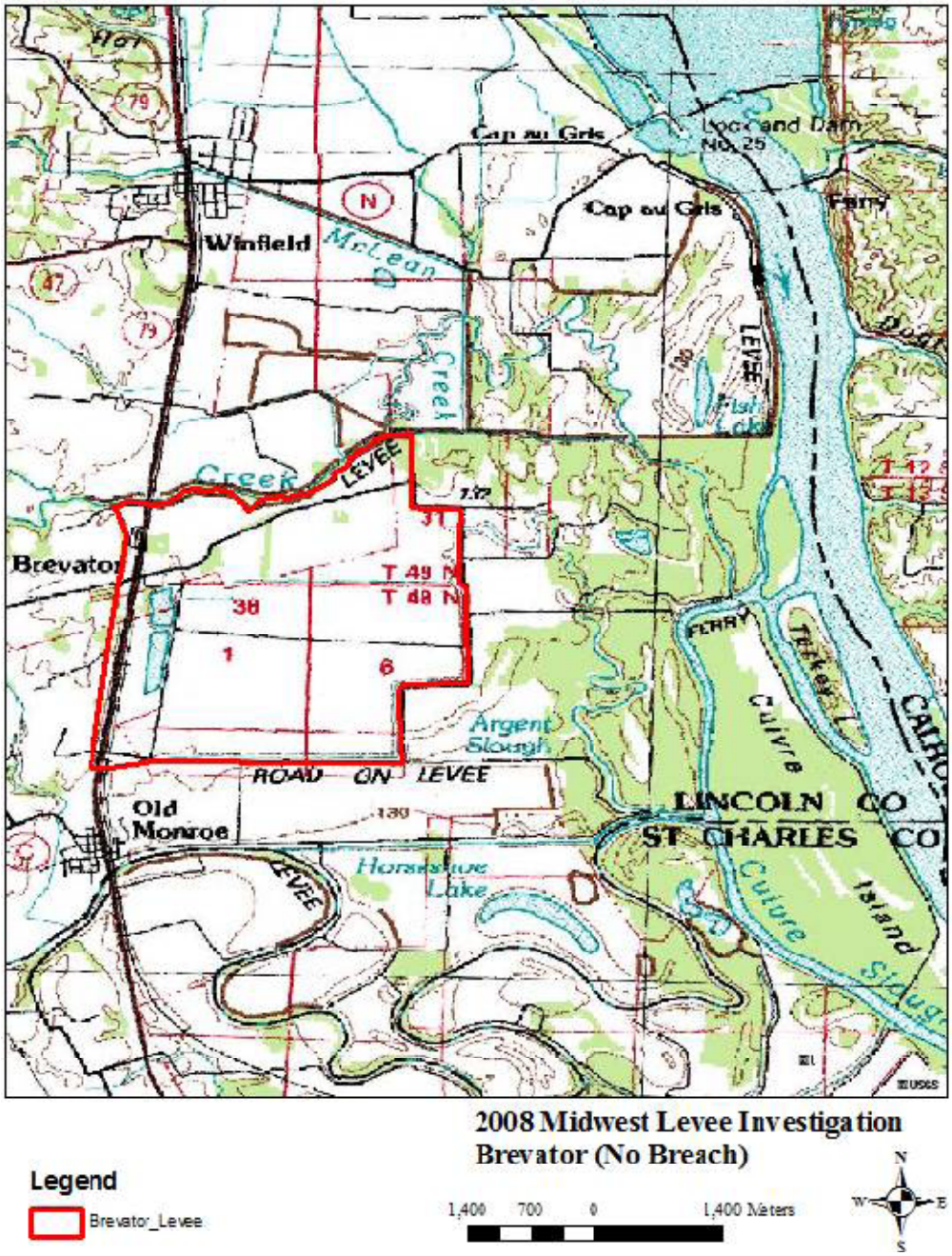

Fig. 117. Brevator Levee System (Storesund 2009)

Four samples were collected from various locations along the levee. Fig. 118 shows a schematic of the boring locations and Table 15 gives the sample logs for this site.

Fig. 118. Brevator boring locations

Table 15. Brevator sample log

Sample No.	Direction	Latitude*	Longitude*	Pocket Pen (kg/cm^2)	Torvane (kg/cm^2)	Depth and Location
S3B10	Vertical	38.96272	-90.71165	2.35, 2.6	1.075, 1.025	Surface, crest centerline
S3B11	Vertical	38.96272	-90.71171	1.2, 1.3	0.33, 0.43	3.05m, West toe
S3B12	Vertical	38.95773	-90.71169	1.75, 1.75	0.7, 0.86	Surface, crest centerline
S3B13	Vertical	38.95773	-90.71176	1.1, 1.0	0.56, 0.7	3.05m, West toe
S3Bag5	Bulk					Taken at S3B10
S3Bag6	Bulk					Taken at S3B11
S3Bag7	Bulk					Taken at S3B12
S3Bag8	Bulk					Taken at S3B13

*WGS1984 Geographic Datum

The overtopping waters were trapped in the guarded area. Fig. 119 shows the high water marks on a barn at location "A" shown on Fig. 120. While the levee did not fail, the overtopping water still flooded the surrounded area. As the water on the dry side of the levee rose, the force of the downhill running water was more than likely dissipated by the standing water. This could have added to the increased performance in the levee. At some point, the ponding water would have created a buffer to the erosive power of the overtopping water and any additional erosion at the toe would have

subsided. Substantial damages were still incurred even though the performance of the levee was celebrated. The design height of the levee should be raised to avoid similar flooding in the future.

Fig. 119. High water marks on barn

Fig. 120. Brevator Levee System and relevant locations (Storesund 2009)

This site was unique in the fact that there was no actual breach. A local resident (Mr. James Pieper) informed the team that the levee was overtopped by over half a meter of water for three days and never failed. The only sign of erosion was at a box culvert that was cracked allowing water and soil to seep through. Fig. 121 shows this seepage area.

Fig. 121. Brevator levee seepage area at box culvert

Based on visual observations and sampling, the levee was comprised of low (CL) and high plasticity clays (CH). Because there was no actual breach, only surficial samples were taken. These samples were much harder to obtain and the soil seemed to be much more stiff than at the previous sites.

At the time of overtopping, there was substantial vegetative cover. The grass was reported to be Reed Canary grass approximately 1 m in height. This type of grass survived the continuous flowing water and is suspected to have had a positive impact on preventing erosion. Also, there were no trees on or around this levee. A further vegetation investigation is presented in a later section.

5. 7 Kickapoo

At 12:40 pm, the team arrived at the Kickapoo site. The Kickapoo site is maintained by the Elsberry Drainage District. The estimated protection level for the levee system was not identified by SAST. This levee system borders the Mississippi River on the eastern perimeter (Fig. 122). This area also failed during the 1993 floods, however, the specific location of the breach was not documented (USGS 2006). Local residents reported that this breach may have been the result of throughseepage in a lower roadway section that traversed the levee crest.

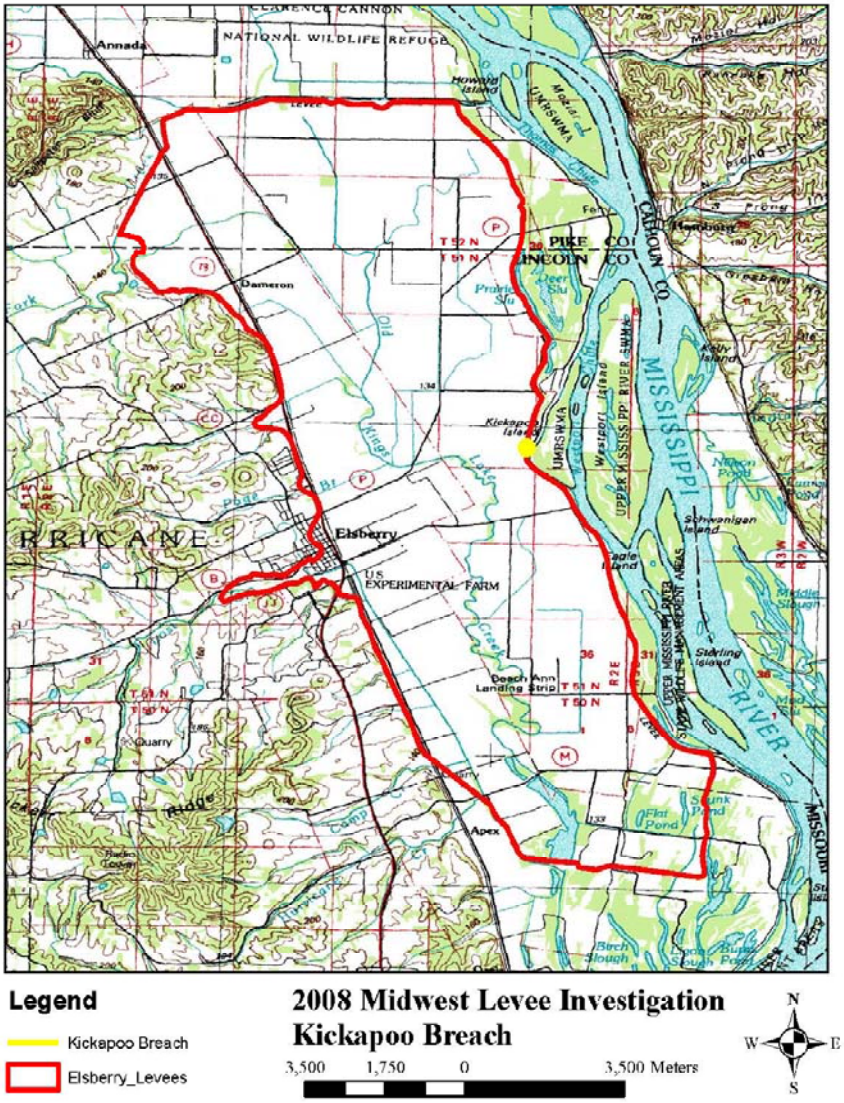

Fig. 122. Elsberry Levee System and Kickapoo breach location (Storesund 2009)

The breach was approximately 17 m in length. Five tube samples and five bulk samples were taken from various locations on each side of the remaining ends of the levee. Fig. 123 shows a schematic of the boring locations and Table 16 gives the sample logs for this site.

Fig. 123. Kickapoo breach boring locations

Table 16. Kickapoo sample log

Sample No.	Direction	Latitude*	Longitude*	Pocket Pen (kg/cm^2)	Torvane (kg/cm^2)	Depth and Location
S4B14	Vertical	39.18476	-90.74287	2.1, 1.75	0.61, 0.6	Surface, crest centerline
S4B15	Vertical	39.18481	-90.74298	1.1, 0.85	0.41, 0.45	2.75m, West toe
S4B16	Horizontal	39.1848	-90.74282	1.1, 1.25	0.6, 0.65	1.88m, crest centerline
S4B17	Vertical	39.18522	-90.74290	2.1, 2.0	0.72, 0.64	Surface, crest centerline
S4B18	Vertical	39.18522	-90.74293	2.5, 2.8	0.45, 0.5	2.75m, West toe
S4Bag9	Bulk					Taken at S4B14
S4Bag10	Bulk					Taken at S4B15
S4Bag11	Bulk					Taken at S4B16
S4Bag12	Bulk					Taken at S4B17
S4Bag13	Bulk					Taken at S4B18

*WGS1984 Geographic Datum

The extents of levee erosion were generally limited to the pre-breach roadway alignment. Based on our visual observations we found that the levee is comprised mainly of lean clays (CL) and silts (ML) with a moderate to substantial grass covering. Samples B14, B15, and B16 were taken from the south side of the breach, while B17 and B18 were taken from the north side. Sample B16 was taken in a more clayey material near the middle of the cross-section of the existing levee material.

This site was said to have initially breached at the road crossing overtop the levee. This roadway was lower than the levee on either side creating a channel for the water to flow along and ultimately cause the failure. The road crossing was also made of gravel road base which allowed quick infiltration of water and seepage through the porous material. The grass covered area north the breach was also overtopped, but it did not fail. This gives the indication that the porous roadway material had an impact on the amount of erosion in that area. Fig. 124 shows the north end of the remaining levee. The temporary road is also shown; once again lower than the levee on either side. It can also be seen in the picture that trees are both on and along the levee.

Fig. 124. Kickapoo north end of breach

Another note taken in the field was the presence of an elevated house on the river side of the levee seen in Fig. 125. The idea of elevating the house seemed to be a reasonable and well designed structure, but even at this height it was later found out that the water had risen into the home. The home was inundated as a result of wind-generated waves from the 'lake' formed inside the area bordered by the levee.

Fig. 125. Elevated house on river side of levee

5.8 Norton Woods

The team arrived to the Norton Woods site around 3:30 pm on September 30, 2008. The Norton Woods levee (Fig. 126) is maintained by the Elsberry Drainage District. The estimated protection level for the levee system was not identified by SAST. This area also failed during the 1993 floods, however, the specific location was not documented (USGS 2006). It is not clear if the breach was the result of through-seepage or overtopping induced erosion. Water marks found indicate that the floodwaters did not exceed the general levee crest elevation.

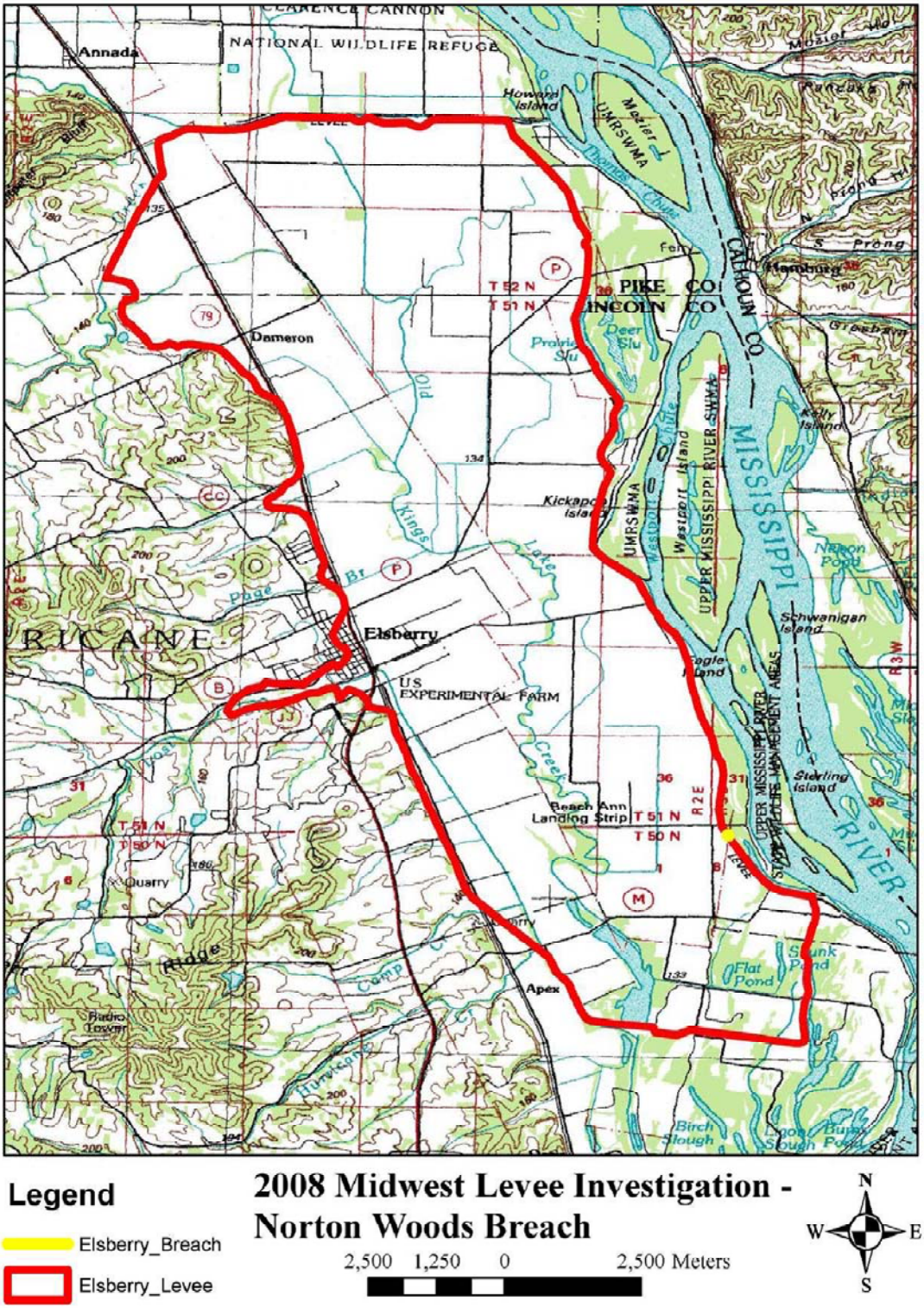

Fig. 126. Elsberry Levee System and Norton Woods breach (Storesund 2009)

The breach was approximately 23 m in length. Five tube samples and five bulk samples were taken from various locations around the breach. Fig. 127 shows a schematic of the boring locations and Table 17 gives the sample logs for this site.

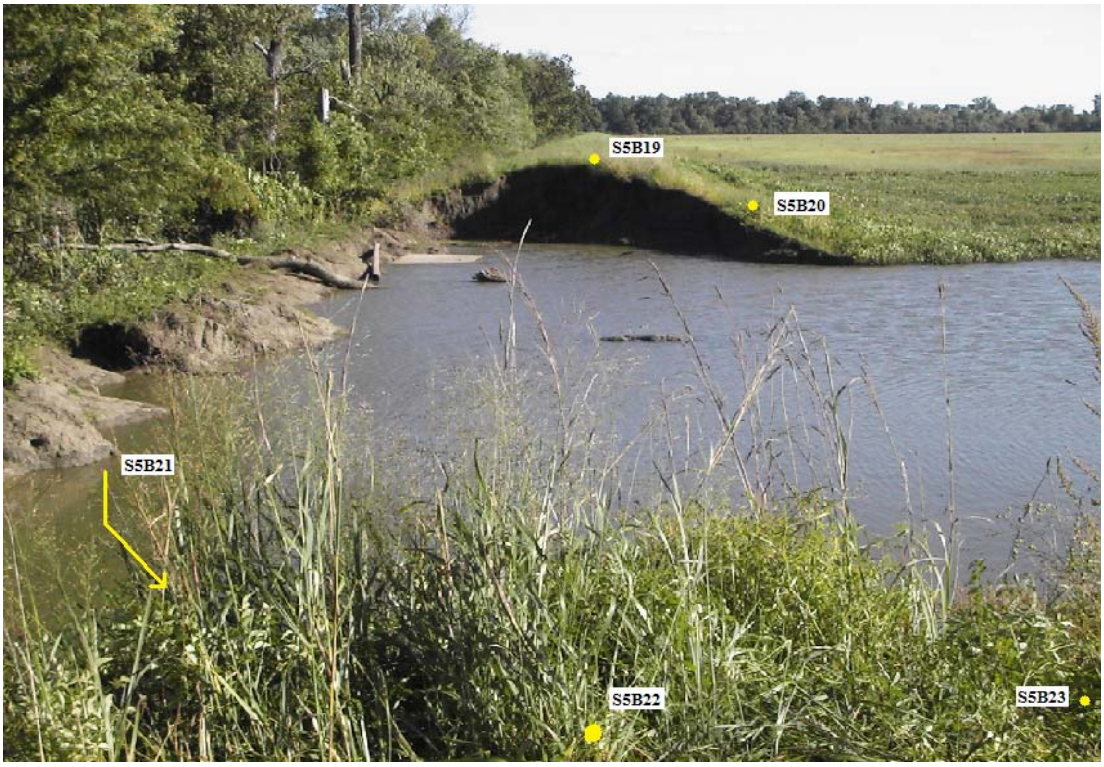

Fig. 127. Norton Woods breach boring locations

Table 17. Norton Woods sample log

Sample No.	Direction	Latitude*	Longitude*	Pocket Pen (kg/cm^2)	Torvane (kg/cm^2)	Depth and Location
S5B19	Vertical	39.13479	-90.72020	2.75, 2.3	0.875, 0.75	Surface, crest centerline
S5B20	Vertical	39.13475	-90.72027	1.25, 1.2	0.4, 0.39	3.05m, West toe
S5B21	Horizontal	39.13531	-90.72055	1.5, 1.45	0.65, 0.65	1.68m, east of center
S5B22	Vertical	39.13533	-90.72061	1.35, 1.25	0.5, 0.51	Surface, crest centerline
S5B23	Vertical	39.13533	-90.72066	1.4, 1.5	0.37, 0.41	3.05m, West toe
S5Bag14	Bulk					Taken at S5B19
S5Bag15	Bulk					Taken at S5B20
S5Bag16	Bulk					Taken at S5B21
S5Bag17	Bulk					Taken at S5B22
S5Bag18	Bulk					Taken at S5B23

*WGS1984 Geographic Datum

Based on visual observations, the levee is comprised clays with some silt in locations with moderate to substantial grass covering at the time of sampling. There was a large scour pool on the protected side of the levee (Fig. 128), with depths up to 2 m. The existing core was not as accessible at this site as it was at the others. Samples B19 and B20 were taken from the south side of the breach, while B21, B22, and B23 were taken from the north side. Sample B21 was taken horizontally, into the estimated existing mid cross-section.

Fig. 128. Norton Woods breach

Fig. 129. Norton Woods remaining levee toe

The above figure shows the material remaining from the original levee toe. The material appeared to be a clay material with some silt.

5.9 Indian Graves North

At 3:30 pm on Wednesday, October 1, 2008, the team arrived at the Indian Graves Main breach site near Quincy, Illinois. The Indian Graves Levee system is maintained by the Indian Graves Drainage District. The levee is estimated to provide flood reduction for approximately 2,800 ha for up to a 50-year return period flood event. The Mississippi River is located just west of the levee system. The levees have been previously breached on numerous occasions, including: 1888, 1929, 1947, 1965, 1973, 1993, however, the locations were not documented (USGS 2006). The 2008 breach occurred on June 18th likely as a result of underseepage rather than overtopping (Rogers 2009). The North breach was over 500 m in length, inundated approximately 6700 acres (27.1 km^2) of farmland, and displaced approximately 1.3 million m^3 of earth and sand materials onto the adjacent land. There were three breach sites along the entire levee system, labeled as the North, Middle, and South breaches (Fig. 130).

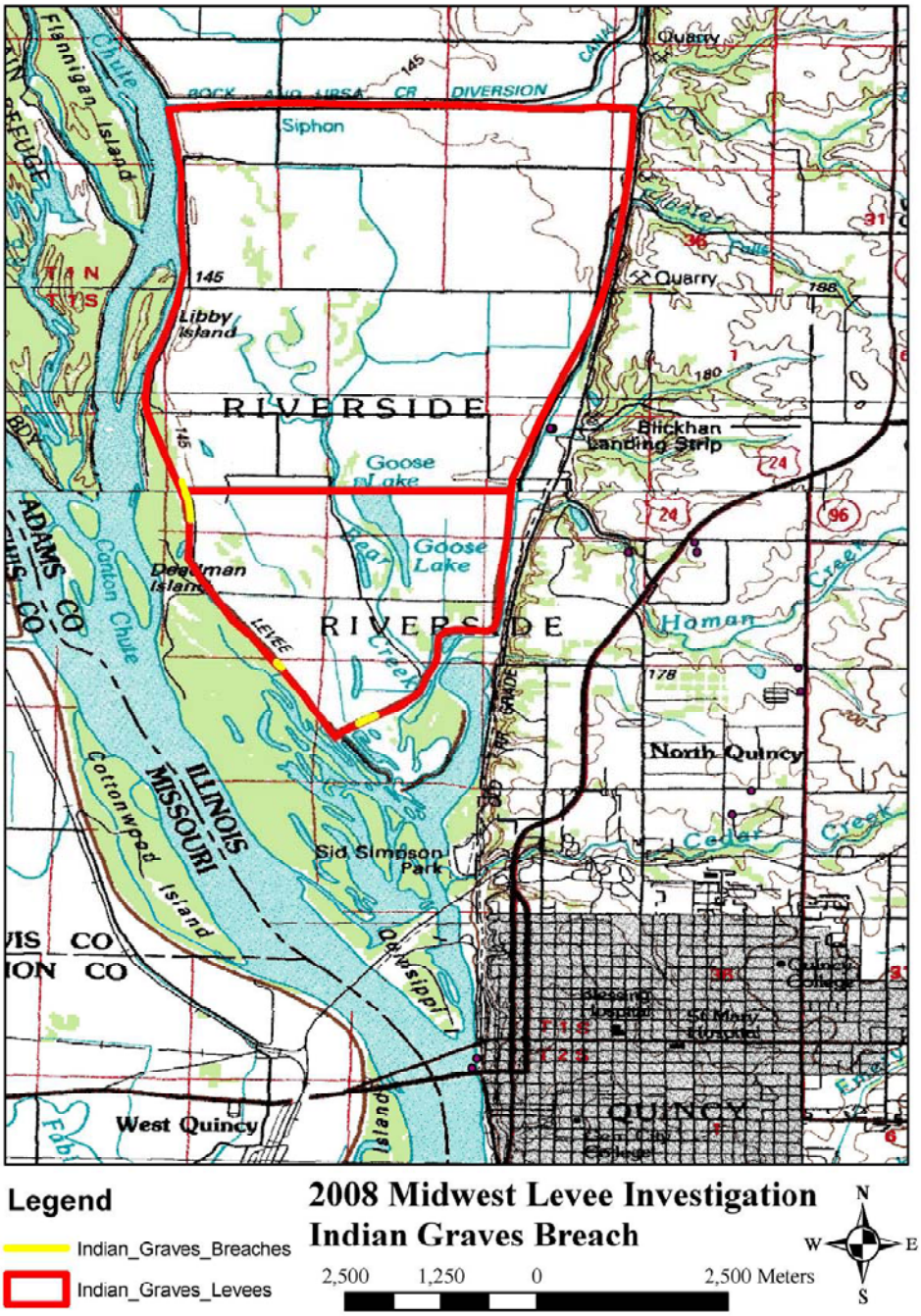

Fig. 130. Indian Graves Levee system and breaches (Storesund 2009)

Based on visual observations, all of the breached levees appeared to be sand shell with a clay core. These agricultural levees have been built up over the last 125 years.

Following the 1929 floods, dragline excavators and scrappers were employed to build up the levees in 1930-31. After breaching occurred again in 1965, the Corps of Engineers placed dredged sand shells over the clay, to add height and increase the cross-section (Rogers 2009). The sand core levees are reported to be lower maintenance than clay levees because there is no vegetation that must be established and then mowed. Also, the sand materials are abundant, cheap, and easily placed. Fig. 131 shows a schematic of a typical levee cross-section for this type of construction.

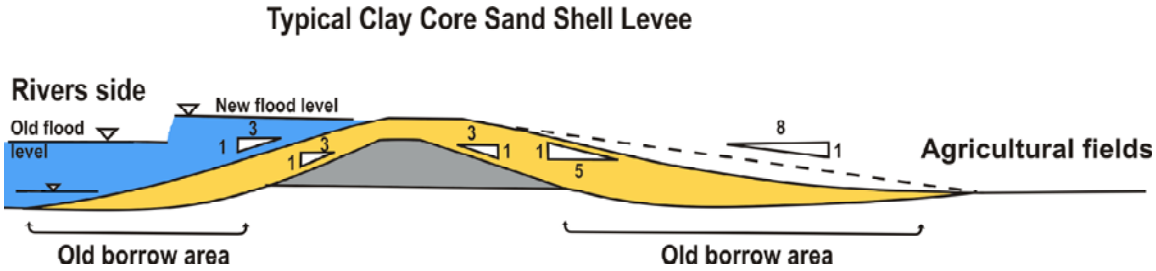

Fig. 131. Typical clay core sand shell levee cross-section (Rogers 2009)

The North or Main breach investigated in this system was approximately 507 m in length. The Middle breach was 80 m in length, and the South breach (described in Section 5.11) was approximately 196 m in length. Three tube samples and three bulk samples were taken from the North side of the Main breach at various locations. On the second day at the site, the team continued sampling and collected two tube samples from the South side of the Main breach. The materials on both ends looked similar, so bulk samples were not taken on the South side.

This site was the first levee investigated with a clay core and sand shell. The sand shell was estimated to range from approximately 1 to 1.5 m thick. During emergency flood fighting operations, a technique known as “push-up” (paid for by

FEMA) was used to raise the levee crest elevation approximately another 1 to 1.2 m for the increased water levels expected. Material from the dry side of the levee was pushed up with bulldozers to form an extra peak of protection. This technique, although it provides temporary increased overtopping protection, it changes the designed cross-section of the levee and makes it vulnerable to through-seepage and hydraulic loading during future flood events. It should also be noted that FEMA does not pay for the "push-down" or for any of the efforts taken to fix the levee back to its original cross-section. The sampling depths are given relative to the levee crest not including the push up. Fig. 132 shows a schematic of the boring locations and Table 18 gives the sample logs for this site.

Fig. 132. Indian Graves North/Main breach boring locations

Table 18. Indian Graves sample log

Sample No.	Direction	Latitude*	Longitude*	Pocket Pen (kg/cm^2)	Torvane (kg/cm^2)	Depth and Location
S6B24	Vertical	40.00128	-91.45029	1.75, 1.6	0.45, 0.4	1.88m, west of centerline
S6B25	Vertical	40.00135	-91.45022	Sand	Sand	0.30m, east of centerline
S6B26	Vertical	40.00119	-91.45047	2.0, 2.5, 2.25	0.87, 0.7	4.57m, West toe
S6Bag19	Bulk	--	--			Taken at S6B24
S6Bag20	Bulk	--	--			Taken at S6B25
S6Bag21	Bulk	--	--			Taken at S6B26
S6B27	Vertical	--	--	1.25, 1.5	0.5, 0.53	2.44m, west of centerline

*WGS1984 Geographic Datum

The remaining eroded North end of the levee is shown below in Fig. 133. Some vegetation is shown. This vegetation was transported by the flood waters and has extremely shallow root systems and provides no benefit in erosion resistance to the sand. Sample B24 was taken in the exposed levee clay core (Fig. 134). Sample B25 was taken from the sand shell by pushing the tube and capping the end with tape. A shovel was used to dig out the tube and was then slid under the tube in an effort to keep the sand within the tube. The sample was then flipped over and the other end was taped. Sample B26 was taken in the clay core of the exposed North end of the breached levee. Sample B28 was taken in the sand shell as explained previously.

Fig. 133. Indian Graves existing levee cross-section North end

Fig. 134. Clayey material at B24

Remnant sand ripples and valleys went on for hundreds of meters outside the scour zone (Fig. 135). These features show where the sand materials from the levee were transported and deposited onto the adjacent farmland by the flowing waters. The sand from the levee permanently damaged approximately 40 ha of farmland covering it

in an average depth of 1 m. The sand levees also appeared to be susceptible to wave-induced erosion. Fig. 136 shows distinct wave-cut ridges as the flood waters were pumped out of the area. As the water on the flooded side subsided and drained, wind created waves across the "lake" and the wave action formed the ridges in the sand.

Fig. 135. Sand ripples due to the rushing waters (Storesund 2009)

Fig. 136. Ridges cut in the sand by wave action (Storesund 2009)

The local farmer that owned the land flooded by the breach said he initially saw the water coming through near the South end and then it moved north. Work conducted by Dr. David Rogers, indicated that the failures were a result of seepage rather than overtopping. The underseepage slowly cut away at the dry side toe. Some overtopping may have also occurred making the combination of the erosion mechanisms detrimental to the levee. Fig. 138 shows the remaining foundation and slab from a farm workshop that was destroyed by the wall of inrushing water from the levee breach.

Fig. 137. Indian Graves Main breach – South side of breach looking North

Fig. 138. Debris left from barns and equipment destroyed by the floodwaters

5.10 Indian Graves South (Pump House)

During the main breach investigation on Thursday, several of the members visited the South site located near the pump house at around 3:00 pm. The Indian Graves Drainage District pump house (Fig. 139) was inundated during the flooding leaving three diesel pumps non-operational. Temporary pumps were put in place while repairs were made. This particular pump house was flooded in the previous 1965 and 1993 floods. A resident's house was also located near the site that had been elevated and reconstructed after the 1993 floods according to the revised FEMA elevation guidelines. Unfortunately, the recommended design elevation was not high enough to keep the home from being flooded and the home was inundated with about 1m of water. Two tube samples were taken at the South breach site. Table 19 gives the sample logs for this site.

Table 19. Indian Graves South sample log

Sample No.	Direction	Latitude*	Longitude*	Pocket Pen (kg/cm^2)	Torvane (kg/cm^2)	Depth and Location
S7B29	Vertical	--	--	1.5, 1.75	0.8, 0.7	0.91m, east of centerline South-pump house
S7B30	Vertical	--	--	Sand	Sand	South-pump house

*WGS1984 Geographic Datum

Fig. 139. Indian Graves South – pump house (Storesund 2009)

Fig. 140. Indian Graves South breach looking East (Storesund 2009)

5.11 Two Rivers

At 9:30 am on Friday, October 3, 2008, the team arrived at the Two Rivers breach site in Two Rivers, Iowa. The levees provide flood reduction for approximately 7,100 ha and were categorized by SAST for a 100-year return period flood. The levee system is west of the Mississippi and situated immediately South of the Iowa River (Fig. 141). This area did not fail during the 1993 floods (USGS 2006). The breach was the largest seen and was approximately 1,450 m long.

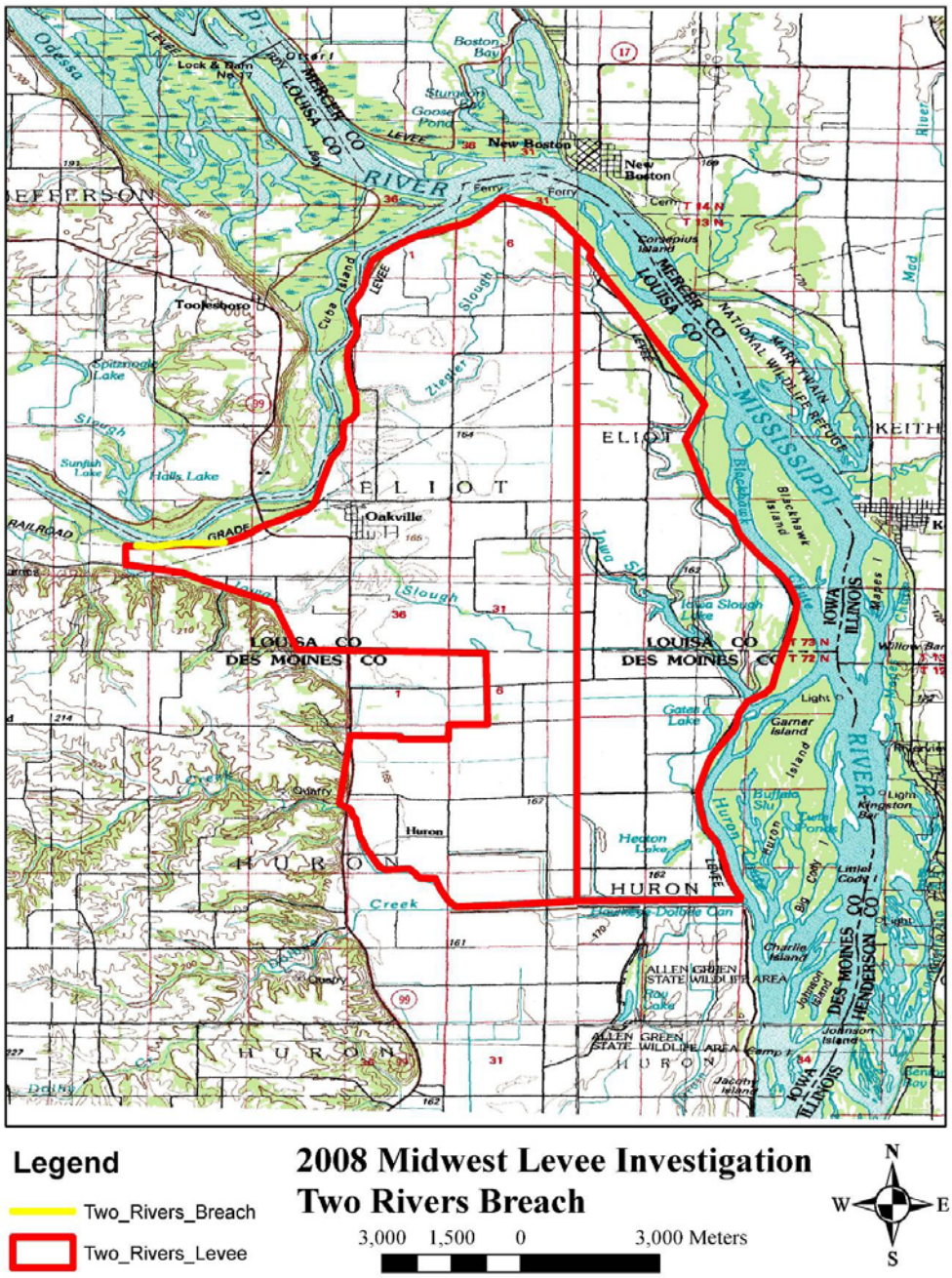

Fig. 141. Two Rivers Levee System and breach location (Storesund 2009)

Similar to the levees at the Indian Graves site, this levee also was a sand shell with approximately a 1 m push up. Similar to the Indian Graves site, the breached levees were covered in a sand shell. It was also assumed that the levees had a clay core,

but due to the extensive scour, the team was unable to determine the extents of any clay core within the levee. There was little trace of any of the original levee. An emergency rock dike had also been constructed (Fig. 142) to keep the water in the already flooded area from connecting with the Mississippi River and carving a new channel. The end of the remaining original levee was also capped in the same rock making it impossible to see the levee cross-section. Fig. 143 shows the breach area looking West, and the rock cap.

Fig. 142. Two Rivers temporary rock levee

Fig. 143. Two Rivers breach looking West

Within the levee breach limits, the erosion and scour was catastrophic. An empty corridor where the levee used to run was all that remained. The sand from the levees was transported and deposited through the breach onto the adjacent farm lands. The far west end of the levee also showed signs that the push-up technique was used. The breached levee cross section at this end showed no traces of clay core and implied that no clay core was present in these levees. By observation of the scour holes and eroded foundation area, it appeared that the levee was constructed on top of an abandoned river channel.

Five tube samples along with three bulk samples were taken at various locations within the breach and on the existing levee in an effort to find any traces of more clayey core material. Fig. 144 shows a schematic of the boring locations and Table 20 gives the sample logs for this site.

Fig. 144. Two Rivers breach boring locations

Table 20. Two Rivers sample log

Sample No.	Direction	Latitude*	Longitude*	Pocket Pen (kg/cm^2)	Torvane (kg/cm^2)	Depth and Location
S8B31	Vertical	41.09392	-91.06867	Sand	Sand	Surface, south of crest centerline
S8B32	Vertical	41.09387	-91.06850	Sand	Sand	1.83m, South toe
S8B33	Vertical	41.0938	-91.07021	2.5, 2.5	0.25, 0.375	4.52m, North of centerline
S8B34	Vertical	41.09378	-91.07007	0.75, 0.7	0.15, 0.15	5.18m, crest centerline
S8B35	Vertical	41.09395	-91.06843			East side of breach, 3.25m below crest surface, Hand auger
S8Bag31		--	--			Taken at S8B31
S8Bag32		--	--			Taken at S8B32
S8Bag33		--	--			Taken at S8B33

*WGS1984 Geographic Datum

Sample B31 was taken from the sand shell on the south side of the push up on the east end of the existing levee crest (Fig. 145). Sample B32 was taken east of the temporary on the south remaining levee toe. Samples B33 and B34 were taken out in the breach area.

Fig. 145. Two Rivers sand shell B31

Sample B33 was taken slightly north of the estimated crest centerline approximately 80 m from the East end of the remaining levee. The material resembled a compressed clay or shale (Fig. 146) and it was suspected to be native foundation material rather than material that comprised the levee itself.

Fig. 146. Clayey material at B33

Fig. 147. Sample of clayey material at B33

Sample B34 (Fig. 148) was taken near the estimated centerline approximately 65 m from the East end of the existing levee. This material was a sandy or silty clay, but may also be native material rather than material from the breached levee.

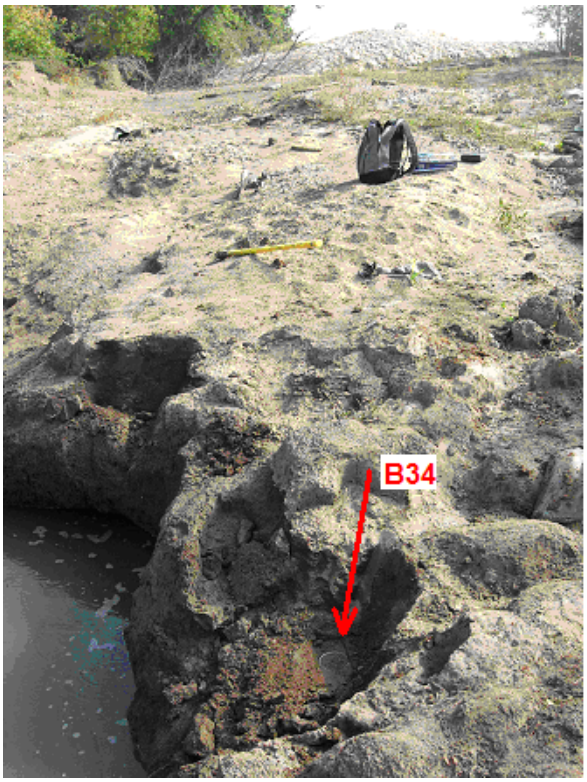

Fig. 148. Two Rivers breach area looking East

Sample B35 was taken east of the temporary rock levee. The goal was to use the hand auger to get through the sand shell and into the core material. A more clayey material was encountered around a depth of 3.5 m, but it was suspected this was also native material. Overall, no clay or separate core material was located.

6. INDEX PROPERTIES

The goal of the geotechnical laboratory work was to characterize the levee soil materials according to the Unified Soil Classification System (USCS), in situ water content, in situ density, particle size, Atterberg Limits, and maximum dry density for approximately twenty of the samples collected. Compaction curves were also found for each of the sites visited.

6.1 In situ Moisture Content and Density

The in situ water content and density were found from the tube samples prior to running the EFA tests. The water content was determined per ASTM D 2216 (ASTM 1998). The density was calculated by dividing the mass of recovered soil by the recovered volume. Values for each sample are shown below in Table 21. A more detailed data sheet can be found in Appendix 2.

6.2 Particle Size Determination

Particle size analysis was done according to ASTM D 422 (ASTM 1998). Because the percentage of fines was high for most samples, hydrometer analyses were run to determine the diameter size of the particles. Once the hydrometer data was collected, the solution was poured through the No. 200 sieve. The portion retained was dried and then run through the No. 10, 40, 80, 100, and 200 sieves. The results from the hydrometer and sieve analysis were combined to give the gradation curve for each sample. These curves were used to find the diameter of the particles of which 50 percent

are smaller, d_{50}. This parameter was then used to compare critical erosion velocity with grain size. For the sand shell samples, the standard sieve analysis was done. Each coarse grained sample had less than 5 percent fines classifying them as clean sands in which Atterberg Limit analyses were not required. The gradation data was used along with the Atterberg Limit results to determine the classification of each sample based on the USCS. Values for each sample are shown below in Table 21. The lab result sheets are given in Appendix 3.

6.3 Atterberg Limits

For the fine grained samples, Atterberg Limits were found using the multipoint method per ASTM D 4318 (ASTM). Soil was mixed with a small amount of water and run through a blender for several minutes until it was a "milkshake-like" consistency. The slurry was passed through the No. 40 sieve onto a plaster bowl where it was allowed to dry until it was at the moisture content where the liquid limit test could be run. Some of the sample was set aside and allowed to continue to dry for the plastic limit test. The results for the index properties tests run are summarized below (Table 21). The soils were classified according to the United Soil Classification System (USCS). Casagrande's plasticity chart was employed as the method of classification for the fine portion of the samples. The classification for each sample is given in Table 21. The lab result sheets are given in Appendix 4.

6.4 Index Property Test Results

Table 21. Soil index properties

Sample No.	w%	2 μm	-200	% Clay Fraction	Activity	d_{50} (mm)	LL	PL	PI	USCS
S1Bulk1	--	--	--	--	--	0.0705	NP	NP	NP	--
S1Bulk2	--	--	--	1977.6	--	0.0232	55	25	30	--
S1B1	16.58	1732.78	1486.29	1982.7*	74.96	--	--	--	--	ML
S1B2	26.76	1842.40	1453.42	1982.7*	73.31	0.0276	--	--	--	CH
S1B3	19.65	1946.47	1626.78	1982.7*	82.05	--	--	--	--	--
S1B4	24.04	2126.10	1714.02	1987.8	86.23	--	--	--	--	--
S1B5	25.98	1894.28	1503.62	1982.7*	75.84	--	--	--	--	--
S2B6	29.52	1857.59	1434.26	1875.6	76.47	0.0038	71	22	49	CH
S2B7	30.91	1850.61	1413.60	1875.6*	75.37	0.0019	78	24	54	CH
S2B8	44.84	1774.25	1224.99	1732.9*	70.69	--	--	--	--	--
S2B9	34.90	1879.80	1393.43	1732.9	80.41	0.0041	88	26	62	CH
S3B10	20.43	1832.85	1521.97	1876.6*	81.10	0.0136	41	20	21	CL
S3B11	28.60	1666.68	1296.02	1876.6*	69.06	0.0162	50	23	27	CL
S3B12	32.23	1471.52	1112.87	1876.6	59.30	0.0054	66	26	40	CH
S3B13	31.85	1743.97	1322.66	1876.6*	70.48	0.0093	64	24	40	CH
S4B14	36.88	1590.49	1161.95	1804.3*	64.40	0.0114	64	28	36	CH
S4B15	37.51	1755.22	1276.43	1804.3*	70.74	--	--	--	--	--
S4B16	31.76	1870.35	1419.50	1804.3*	78.67	0.0030	81	24	57	CH
S4B17	35.44	1687.22	1245.70	1804.3*	69.04	--	--	--	--	--
S4B18	28.65	1717.37	1334.93	1804.3	73.99	0.0302	57	24	33	CH
S5B19	28.41	1861.57	1449.72	1692.2*	85.67	0.0163	55	22	33	CH
S5B20	42.73	1574.98	1103.46	1692.2*	65.21	0.0141	70	28	42	CH
S5B21	26.23	1858.32	1472.18	1906.2	77.23	--	--	--	--	--
S5B22	29.46	1708.29	1319.50	1692.2*	77.98	--	--	--	--	--
S5B23	22.11	1414.06	1002.89	1692.2	59.27	0.0179	72	27	45	CH
S6B24	28.74	1799.96	1398.18	1814.5*	77.06	--	48	20	28	ML/CL
S6B25	6.39	1672.88	1572.41	--	--	0.3927	NP	NP	NP	SP
S6B26	28.27	1882.94	1467.92	1814.5	80.90	0.0112	60	25	35	CH
S6B27	18.47	1715.52	1448.07	1814.5*	79.81	--	--	--	--	--
S6B28	1.82	1639.85	1610.51	1814.5*	88.76	--	--	--	--	--
S7B29	25.99	1742.36	1382.89	2008.2	68.86	0.0189	54	18	36	CH
S7B30	26.06	1642.43	1302.94	--	--	0.6238	NP	NP	NP	SP
S8B31	3.37	1683.36	1628.41	--	--	0.8602	NP	NP	NP	SP
S8B32	3.74	1628.24	1569.61	--	--	0.7375	NP	NP	NP	SP
S8B33	21.10	1953.48	1613.17	--	--	0.0261	50	23	27	CH
S8B34	19.99	1975.16	1646.14	--	--	--	--	--	--	--
S8B35	Hand	Augur		--	--	0.1921	28	18	10	CL

6.5 Compaction Curves

Compaction curves were determined for each site according to ASTM D1557 (ASTM 1998) with a small volume mold rather than the standard 4 in diameter mold. This method was needed because of the limited sample sizes obtained during the site visits. Equivalent energy was applied per layer and for the overall sample. Prior to testing the Midwest Levee samples, a calibration was run to compare the small volume mold results with those from a Modified Proctor ASTM specified mold. From these curves, max densities were determined and used to approximate relative compaction at each sample location (Table 22). Only a few of the samples were used obtain the compaction curves. The soils chosen represented a certain type of soil or location in the levee. Those not tested were assumed to have similar max densities as the samples that were tested for that specific site location or soil type. Values for each sample are shown in Table 22. The lab result sheets are given in Appendix 5.

Once the curves were determined for each site, the in situ points were plotted in comparison to the compaction curves. Figs. 149 through 155, show the results for the sites visited. A compaction curve for the Two Rivers site was not developed because most of the samples collected were determined to be foundation soils rather than levee construction material. The in situ moisture contents were much higher than the optimum water content, which is why the points are to the far right of the curves.

Table 22. Soil density properties

Sample No.	**In situ Density (kg/m^3)**	**In situ Dry Density (kg/m^3)**	**Max Dry Density (kg/m^3)**	**Relative Compaction %**
S1Bulk1	--	--	--	--
S1Bulk2	--	--	1977.6	--
S1B1	1732.78	1486.29	1982.7*	74.96
S1B2	1842.40	1453.42	1982.7*	73.31
S1B3	1946.47	1626.78	1982.7*	82.05
S1B4	2126.10	1714.02	1987.8	86.23
S1B5	1894.28	1503.62	1982.7*	75.84
S2B6	1857.59	1434.26	1875.6	76.47
S2B7	1850.61	1413.60	1875.6*	75.37
S2B8	1774.25	1224.99	1732.9*	70.69
S2B9	1879.80	1393.43	1732.9	80.41
S3B10	1832.85	1521.97	1876.6*	81.10
S3B11	1666.68	1296.02	1876.6*	69.06
S3B12	1471.52	1112.87	1876.6	59.30
S3B13	1743.97	1322.66	1876.6*	70.48
S4B14	1590.49	1161.95	1804.3*	64.40
S4B15	1755.22	1276.43	1804.3*	70.74
S4B16	1870.35	1419.50	1804.3*	78.67
S4B17	1687.22	1245.70	1804.3*	69.04
S4B18	1717.37	1334.93	1804.3	73.99
S5B19	1861.57	1449.72	1692.2*	85.67
S5B20	1574.98	1103.46	1692.2*	65.21
S5B21	1858.32	1472.18	1906.2	77.23
S5B22	1708.29	1319.50	1692.2*	77.98
S5B23	1414.06	1002.89	1692.2	59.27
S6B24	1799.96	1398.18	1814.5*	77.06
S6B25	1672.88	1572.41	--	--
S6B26	1882.94	1467.92	1814.5	80.90
S6B27	1715.52	1448.07	1814.5*	79.81
S6B28	1639.85	1610.51	1814.5*	88.76
S7B29	1742.36	1382.89	2008.2	68.86
S7B30	1642.43	1302.94	--	--
S8B31	1683.36	1628.41	--	--
S8B32	1628.24	1569.61	--	--
S8B33	1953.48	1613.17	--	--
S8B34	1975.16	1646.14	--	--
S8B35	Augured		--	--

*****Used max density from other sample tested at same site.

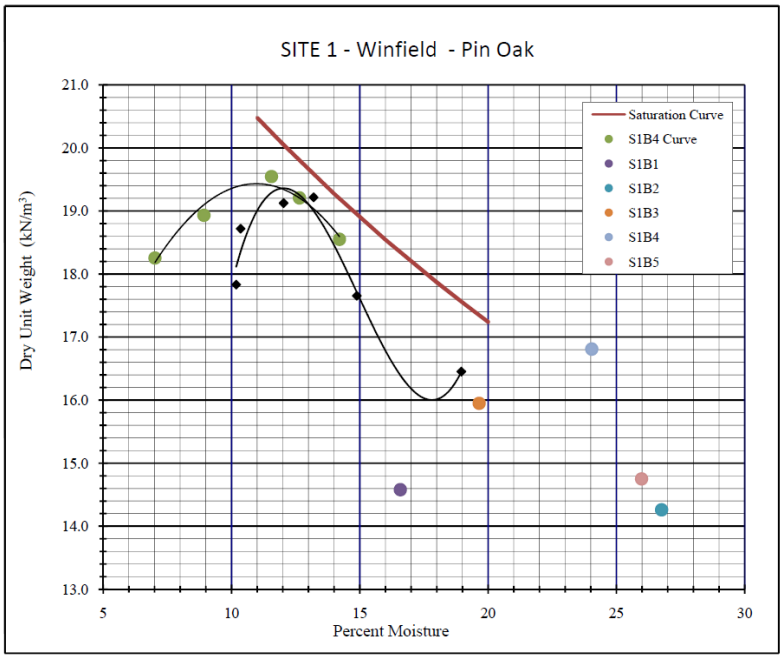

Fig. 149. Compaction curve and in situ densities – Winfield Pin Oak site

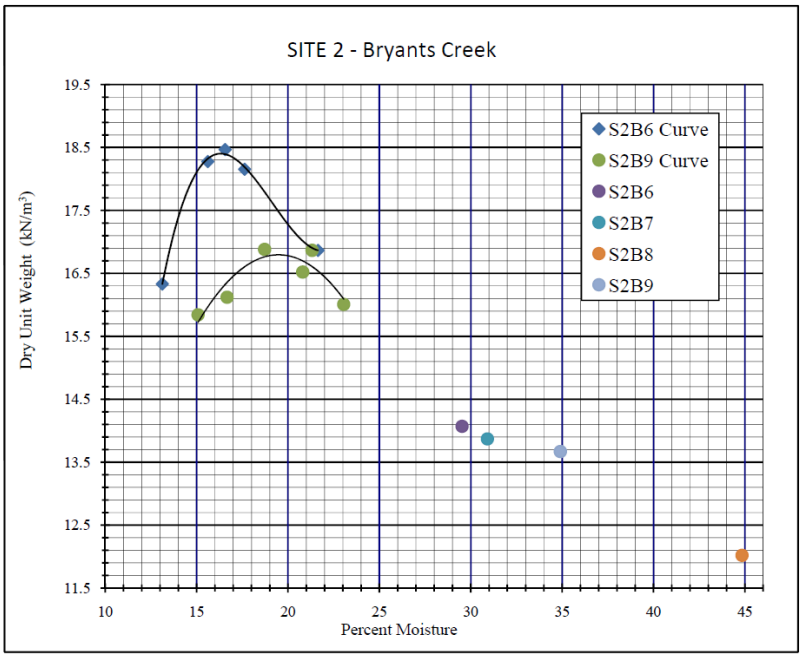

Fig. 150. Compaction curve and in situ densities – Bryants Creek site

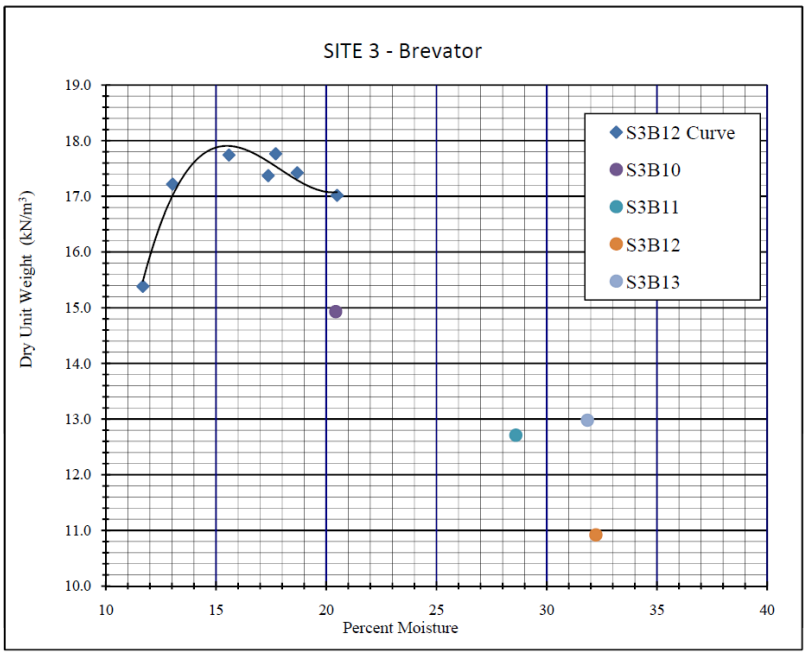

Fig. 151. Compaction curve and in situ densities – Brevator site

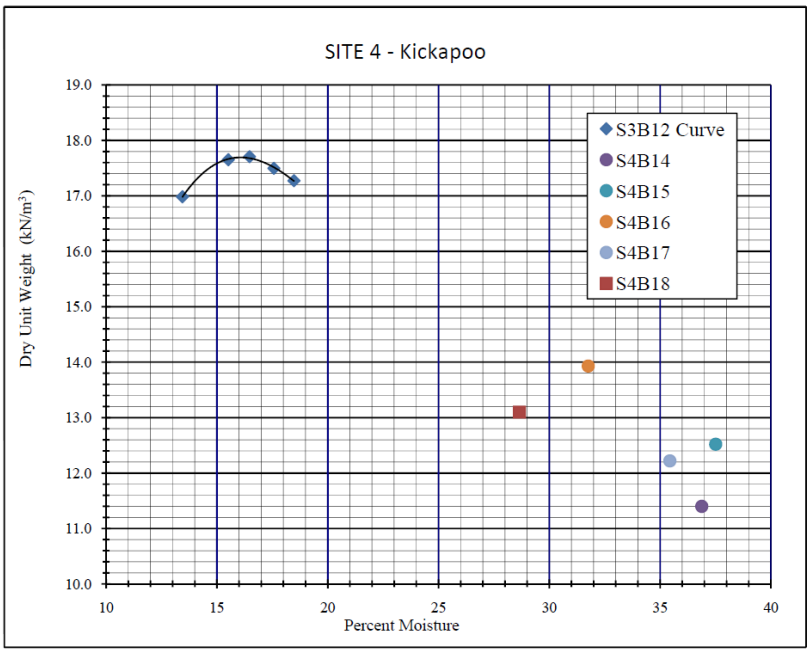

Fig. 152. Compaction curve and in situ densities – Kickapoo site

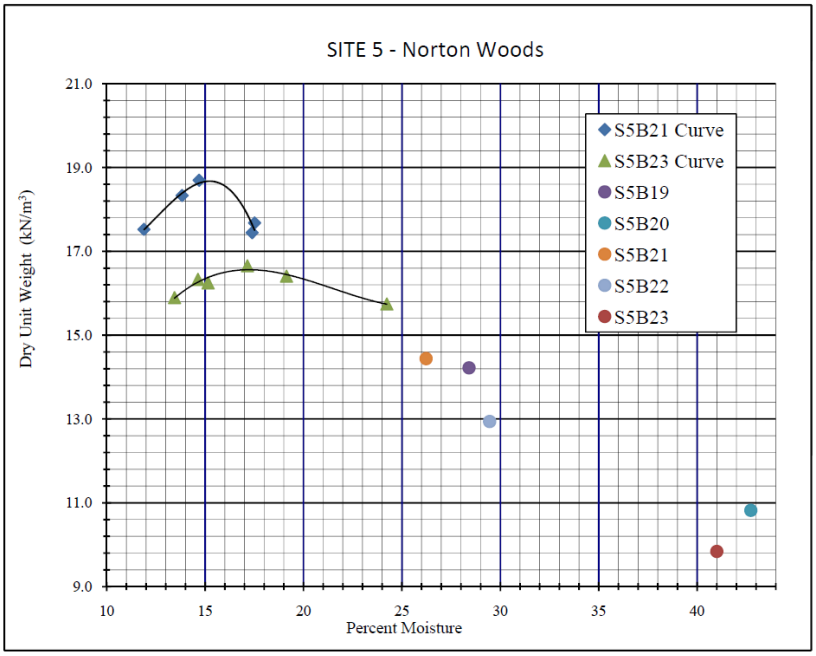

Fig. 153. Compaction curve and in situ densities – Norton Woods site

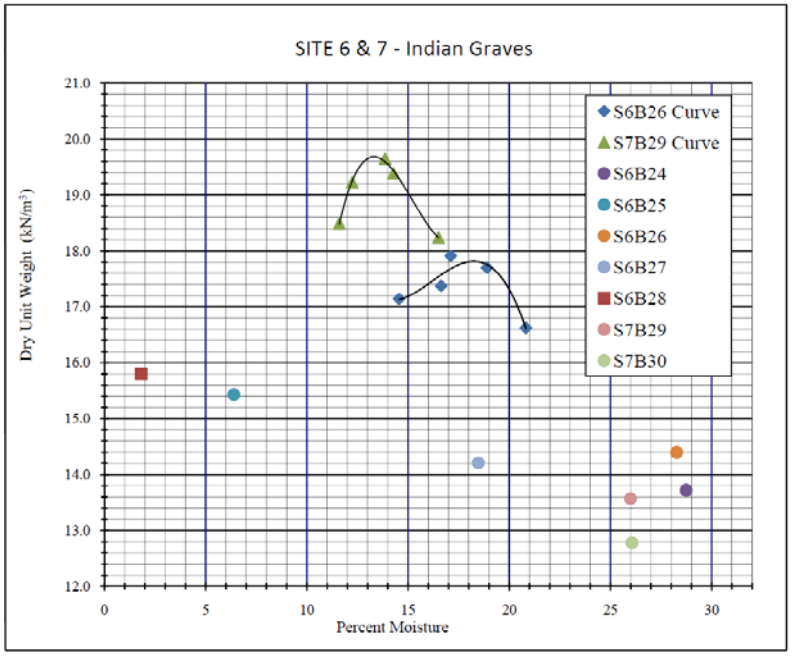

Fig. 154. Compaction curve and in situ densities – Indian Graves sites

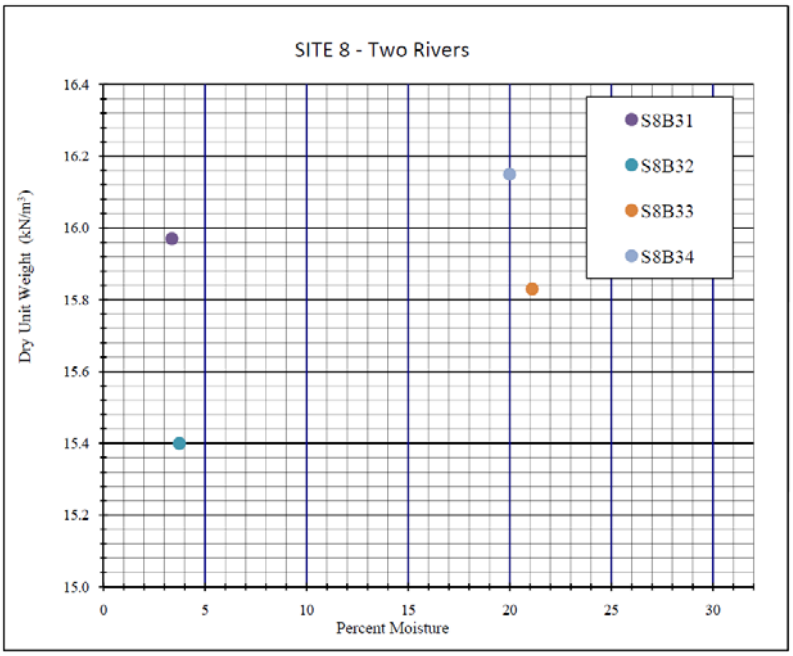

Fig. 155. Compaction curve and in situ densities – Two Rivers site

6.6 Specific Gravity

Because the hydrometer calculations require a specific gravity value for each soil, specific gravity tests were run on a few of the samples in various locations and of various soil types following ASTM D854 (ASTM 1998) procedures. As a calibration means, the test was first run on ASTM C778 graded Ottawa sand to check that the specific gravity obtained was 2.65. The values obtained for the levee samples were also checked by plotting the zero air voids line on the compaction curve charts to make sure they agreed and were above the obtained points. The lab result sheets are given in Appendix 6.

7. EROSION PROPERTIES

The erosion aspect of this project consisted of taking samples collected in the field and testing them in the Erosion Function Apparatus (EFA) to determine the erosiveness of the material at different velocities. The values obtained in the EFA were then used find the threshold critical velocity for each sample tested. Several correlations with regards to properties such as plasticity, grain size, and relative compaction were also compared in an effort to determine their influence on erosion.

7.1 Erosion Function Apparatus Results

The EFA was used to obtain the erosion functions for 20 Midwest Levee samples. The samples tested were chosen in an effort to encompass a variety of material types, locations within the levee, and performance. For example, the Brevator site was one of major interest because it was the only site that did not fail. Therefore, all four samples were tested from that site. The samples taken at Two Rivers were most likely foundation materials and not of major concern, so only two samples at that site were tested. Two of the extreme samples were chosen as an example of the erosion functions found using the EFA. Fig. 156 shows a high plasticity clay which was one of the most resistant to erosion of all the samples tested. Fig. 157 shows an example of a highly erosive clean sand taken from the levee shell. The results for all the samples tested are given in Appendix 7.

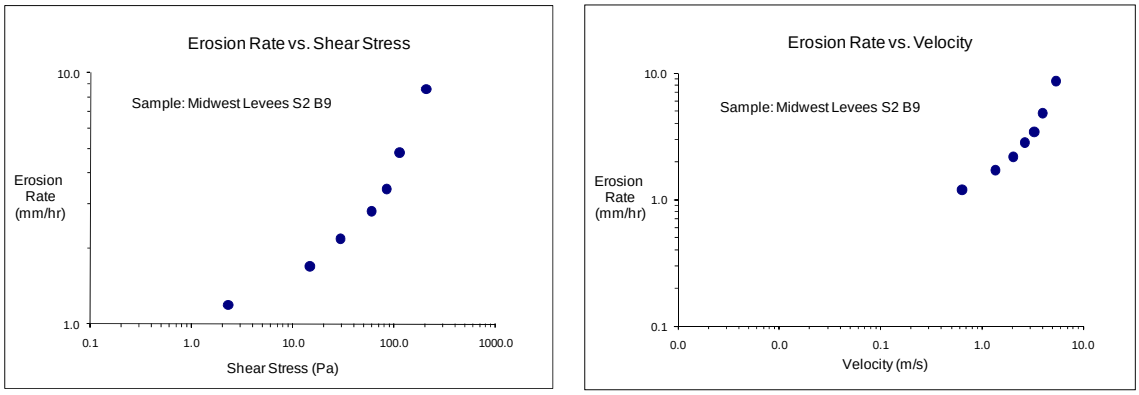

Fig. 156. EFA results for high plasticity clay taken at S2B9

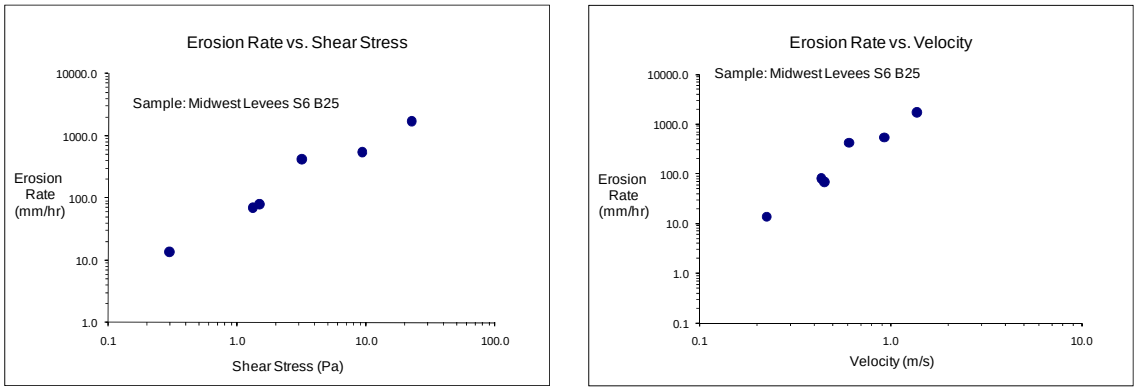

Fig. 157. EFA results for a clean sand taken at S6B25

7.2 Erosion Rate vs. Shear Stress

In order to compare the erosion functions for each sample, the EFA values were all plotted in terms of shear stress on the same graph (Fig. 158). This graph also shows the erosion categories that had been developed in previous studies.

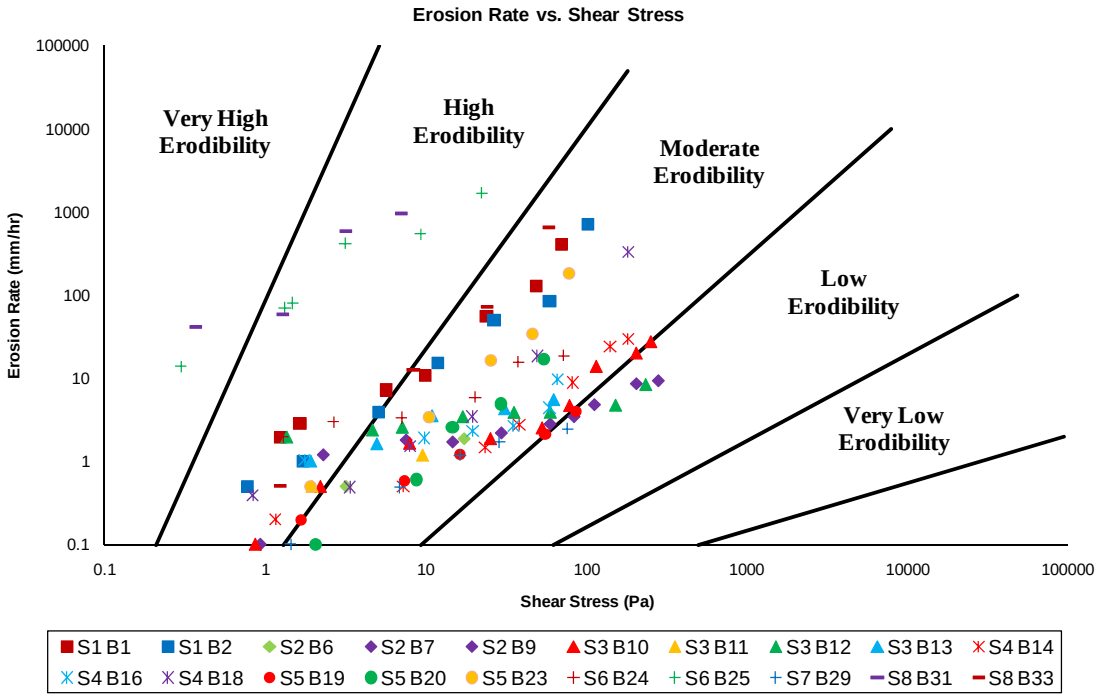

Fig. 158. Erosion rate versus shear stress for the Midwest Levee samples

There are two ways of obtaining the erosion category for a soil. One way, the erosion category corresponds to the space in which the most plotted points for that sample lie. For example, in the graph above the erosion category for S6B25 would be high erodibility. This method becomes somewhat irrelevant when looking at several of the other samples. For instance, sample S2B9 is scattered across three categories with most of the points falling in the low erodibility category even though the sample is just slightly across the boundary line. Another problem with this method is that there is no further distinction between samples that fall in the same category. As seen above, most of the samples fall in the moderate erodibility category even though the erosion rate values may vary greatly for two different samples at the same shear stress.

The method used to define the erosion category for each sample in this analysis consisted of assigning a number value of 1 through 5 to the categories. The very high erodibility category was labeled 1, while the very low erodibility was labeled 5. These values were defined halfway between each of the current boundaries. The boundary lines were labeled with half units ranging from 1.5 to 5.5. The values in-between were interpolated. For each sample, a regression line was drawn through the points of the erosion function. The distance halfway between the first point and the last point was marked on the line. This point was used to determine the erosion category in numerical terms. In a sense, the value represents the average erosion category over a range of velocities. One problem with this method is that it depends on the range of velocities tested. For this set of samples, the range of velocity was similar for each sample, so the problem was not a major issue. This erosion category value was then used in further analysis and correlations in Section 7.7. The values obtained for each sample run in the EFA are shown in Table 23.

Table 23. EFA erosion categories

Sample No.	EFA Erosion Category
S1B1	2.6
S1B2	2.7
S2B6	3
S2B7	2.6
S2B9	3.4
S3B10	3.2
S3B11	3
S3B12	3.2
S3B13	2.8
S4B14	3.3
S4B16	3
S4B18	2.9
S5B19	3.2
S5B20	3.1
S5B23	2.8
S6B24	2.8
S6B25	1.7
S7B29	3.2
S8B31	1.7
S8B33	2.6

7.3 Erosion Rate vs. Velocity

In order to compare the erosion functions for each sample, the EFA values were all plotted in terms of velocity on the same graph (Fig. 159). This graph also shows the erosion categories that had been developed in previous studies. Comparing the samples in terms of velocity makes more practical sense and it is easier to get a feel for the actual erodibility of the soil.

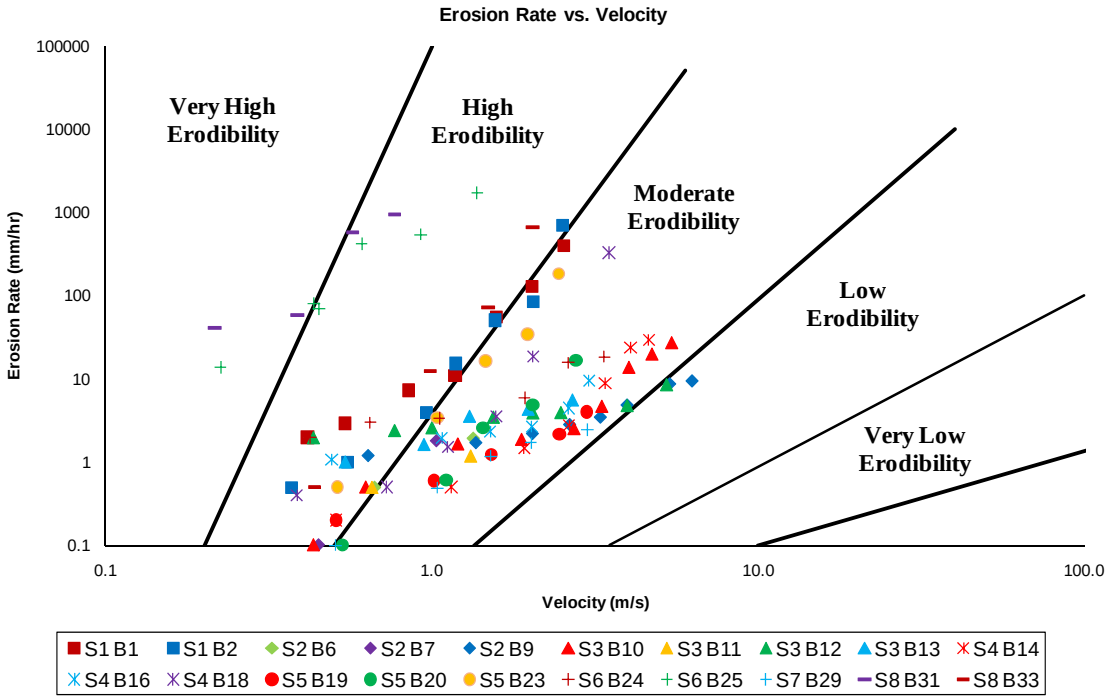

Fig. 159. Erosion rate versus velocity for the Midwest Levee samples

Because the relationship between erosion rate and velocity is nonlinear, every point of the erosion function is important. In other words, comparing two samples at 1 m/s does not necessarily say anything about the same samples at 5 m/s. The erosion rate is highly dependent on the velocity. This is shown in the above curve as several of the samples tend to become more horizontal as the velocity increases. For example, when comparing S2B9 and S5B23 at the lowest velocity, it appears that S5B23 is more resistant to erosion, but at around 3 m/s S2B9 is orders of magnitude more resistant. Therefore, it is important to know the flow conditions that the samples will be subjected to for a certain event in order to obtain the best idea of erodibility. With that said, it is possible to compare the erosion rates of samples at a given velocity if the velocity of a specific event is known.

However, it is not always reasonable to run every correlation for every point in the erosion function. This is the benefit of a threshold value. While critical shear stress and critical velocity can both be found, critical velocity was chosen for the comparisons in this analysis. The critical velocity is defined at the point when the erosion rate is 0.1 mm/hr or essentially negligible. To obtain this value, regression lines were drawn through each erosion function and the value of velocity was chosen where the line crossed the 0.1 mm/hr mark. The shape of the curves requires some judgments to be made in order to determine the critical velocity. The values at higher velocities generally have higher erosion rates that are more reasonably judged by the human eye while running the test. These values were held in higher regards compared to the very small erosion rates. These threshold values, while they simplify the analysis, they are not perfect. Using S2B9 as an example again, because the line is more horizontal, the critical velocity is lower even though it may be more resistant to erosion than another sample at a certain velocity. This proves the point again that erosion cannot be determined by a single parameter.

The slope of the line shows the dependence on velocity for a given sample. Lines with a steep slope have a large change in erosion rate for a small change in velocity. Lines that are more horizontal have little change in erosion rate for a large change in velocity. Even though reasons sated above warn against it, erosion rates are compared at a velocity of 3 m/s in another section of the analysis. A velocity of 3 m/s was chosen because it is a large enough value to judge by eye while running the EFA tests and most of the samples have taken a more linear slope at that point. Also, most

overtopping flood conditions, especially near the toe of the levee, are at higher velocities. At the higher velocities, the samples have a tendency to be slightly more predictable on the log scale.

Regression lines were used for samples that did not have a point near 3 m/s. Most overtopping events involve flood waters at velocities higher than 3 m/s. The results are also a good qualitative judge of erosion and are another piece of information in a larger analysis.

7.4 Critical Velocity versus D_{50}

Previous comparisons have been made for critical velocity versus D_{50}, or average particle diameter. Table 24 lists the critical velocity values determined for the Midwest samples and Fig. 160 shows the plotted comparison. Fig. 161 shows the data plotted on a chart developed in previous studies. Fig. 162 shows the Midwest Levee values plotted with values obtained in previous testing by others. The values seem to follow the trend set by the previous data; however, several of the samples are just outside the boundaries. The Midwest data overall seems to be more erosive than some of the other data plotted.

Table 24. Critical velocity and D_{50} values for Midwest Levee data

Sample	Critical Velocity (m/s)	D_{50}
S1B1	0.32	0.0276
S1B2	0.48	0.0276
S2B6	0.29	0.0038
S2B7	0.45	0.0019
S2B9	0.4	0.0041
S3B10	0.6	0.0136
S3B11	0.5	0.0162
S3B12	0.2	0.0054
S3B13	0.2	0.0093
S4B14	0.9	0.0114
S4B16	0.16	0.003
S4B18	0.73	0.0302
S5B19	0.33	0.0163
S5B20	0.6	0.0141
S5B23	0.5	0.0179
S6B24	0.16	0.0112
S6B25	0.1	0.3927
S7B29	0.11	0.0189
S8B31	0.11	0.8602
S8B33	0.6	0.0261

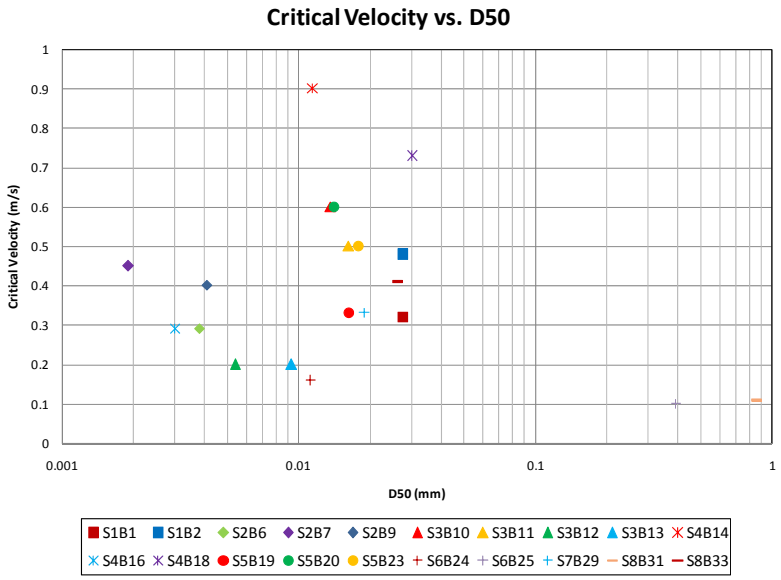

Fig. 160. Critical velocity vs. D_{50} for Midwest Levees

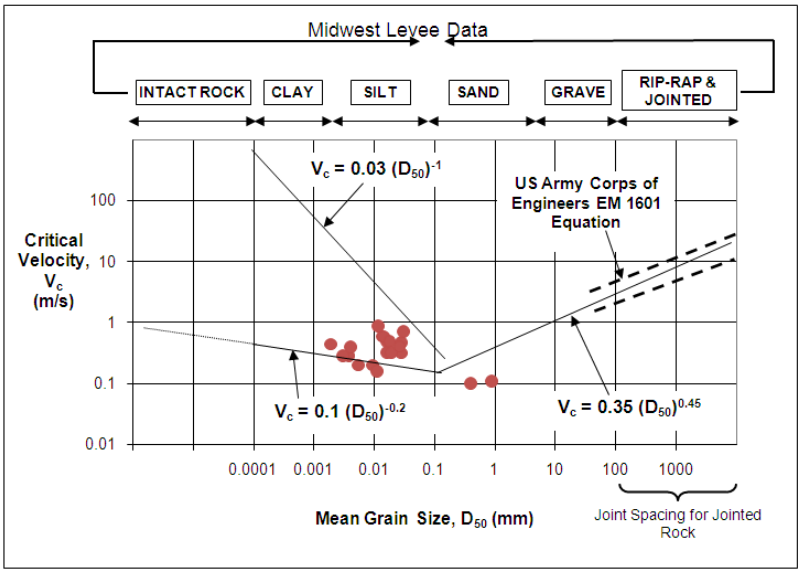

Fig. 161. Critical velocity vs. D_{50} for Midwest Levees

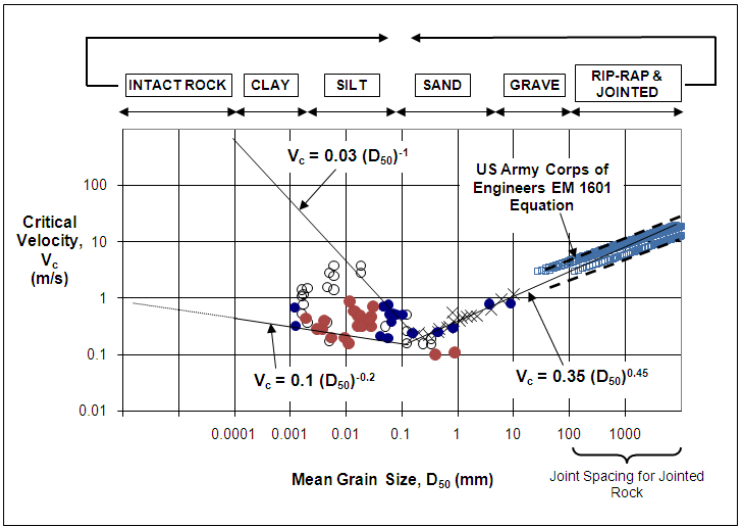

Legend:
- TAMU Data as reported by Briaud, J.-L. et. al. (2001). "Erosion Function Apparatus for Scour Rate Predictions." *J. Geotech. and Geoenvir. Engrg.*, ASCE, 127(2), 105-113.
- TAMU Data as reported by Briaud, J.-L. (2006). "Erosion Tests on New Orleans Levee Samples." *Texas A&M University Internal Report.*
- X Data from Shields, Casey, US.WES, Gilbert, White as reported by Vanoni, V.A., ed. (1975). "Sedimentation Engineering." *ASCE manuals and reports on engineering practice,* ASCE, New York.
- □ Data points from simulation using U.S. Army Corps of Engineers EM 1601 Riprap Design Equation (U.S. Army Corps of Engineers 1995).
- TAMU Midwest Levee Data

Fig. 162. Critical velocity vs. D_{50} combined results

These plots visually show the difference in cohesive and non-cohesive embankment erosion. The two points plotted to the right of 0.1 mm are levee shell material and are clean sands. These points follow a more predictable trend mostly based on gravity and particle size and weight. The points to the left are much more scattered and unpredictable and show the complexity of the cohesive soils erosion phenomenon. Clean sands are considered to have a critical velocity of 0.1 m/s. Larger granular materials as well as cohesive materials are considered to have critical velocities higher than that of clean sands.

7.5 Critical Velocity Correlations

Fig. 162 shown above is the culmination of several previous studies on the relationship between particle size and critical velocity. There is a well defined trend moving from diameter sizes of 0.1 mm and larger, but the particles smaller than 0.1 mm have a scattered pattern. As the particles decrease in size the scatter seems to grow larger. In an effort to try and identify any possible relationship that could explain this scatter, graphs were plotted for critical velocity and several other variables. These included: plasticity index (Fig. 163), relative compaction (Fig. 166), maximum dry density (Fig. 167), in situ water content (Fig. 168), excess water above optimum (Fig. 169), in situ dry mass density (Fig. 170), percent clay content (Fig. 171), percent passing the No. 200 sieve (Fig. 172), percent clay fraction (Fig. 173), and activity (Fig. 174).

Most studies agree that there is a general trend in plasticity with erosion rate. More plastic soils generally erode less than lower plasticity soils under the same

conditions. Similarly, many studies have proven a relationship between compaction and erosion rate. For the same soil, Powledge and Dodge (1985) showed that even slightly increasing compaction results in much less erosion for small embankments in flume tests. This brings up the first difficulty in comparing the Midwest Levee data. None of the samples were at the same conditions. The soils were of varying plasticity, relative compaction, water contents, and particle sizes. Every sample was at different conditions, each of which has an effect on erodibility. In other words, if plasticity was compared for samples all having the same water content, relative compaction, etc., the existence of a trend would be much easier realized. Because these samples were at all different in situ conditions, many different correlations were plotted in an effort to find any relation.

Categories were created for each parameter of interest. The sample results were color coded based on their plasticity index to determine if any defined trend existed. It appears in Fig. 160, that in general as PI increases the critical velocity decreases, however, the scatter is too great to consider this a real trend. This also does not agree with the critical velocity graphs from the previous section. There was some initial thought that the scattered area might be further broken down based on plasticity, but from the graph (Fig. 161) it appears that the data does not follow any real horizontal trends. The higher plasticity soils shown in red do; however, tend to plot to the far left which is expected.

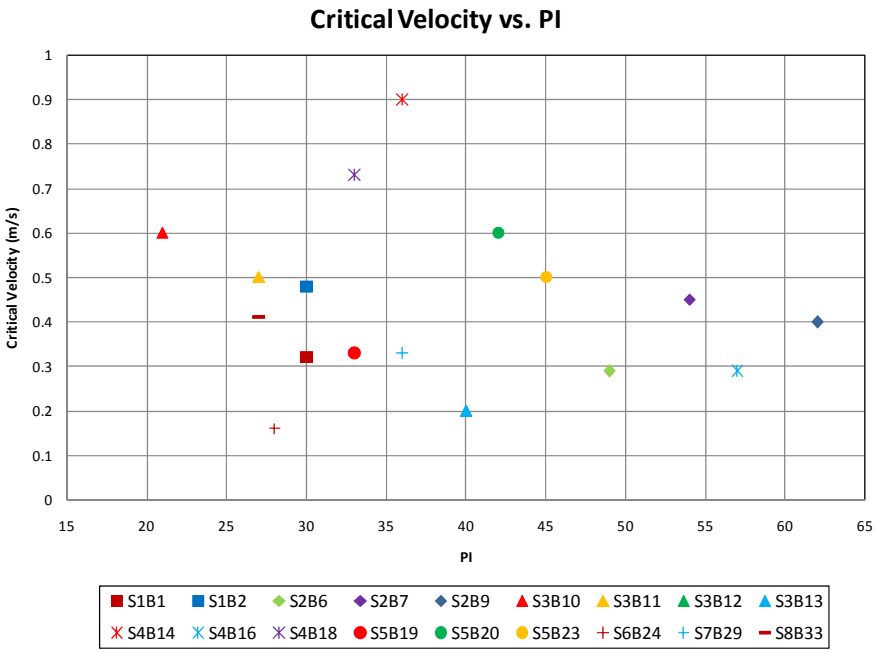

Fig. 163. Critical velocity vs. PI

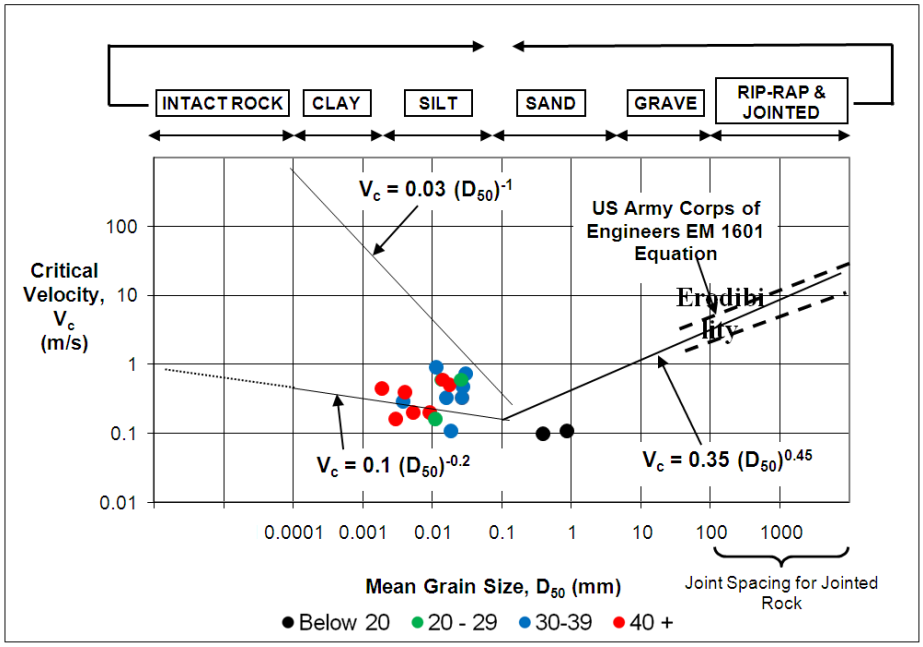

Fig. 164. Critical velocity vs. D_{50} for Midwest Levees comparing PI

Relative compaction is a property that has been proven to effect erosion. Hassan et al. (2004) showed that increases in compactive effort and water content led to an increase in erosion resistance. Part of the issue with the following plots is the relationship between critical velocity and erosion rate. The critical velocity does not necessarily have a direct relation with erodibility. Fig. 165 shows no relation between critical velocity and erosion rate at a velocity of 3 m/s. So while it may look like there is some trend in the following figures, there is really no way of relating that trend to an expected erosion rate value. The critical velocity is only a judge of the value of velocity where erosion begins to take place.

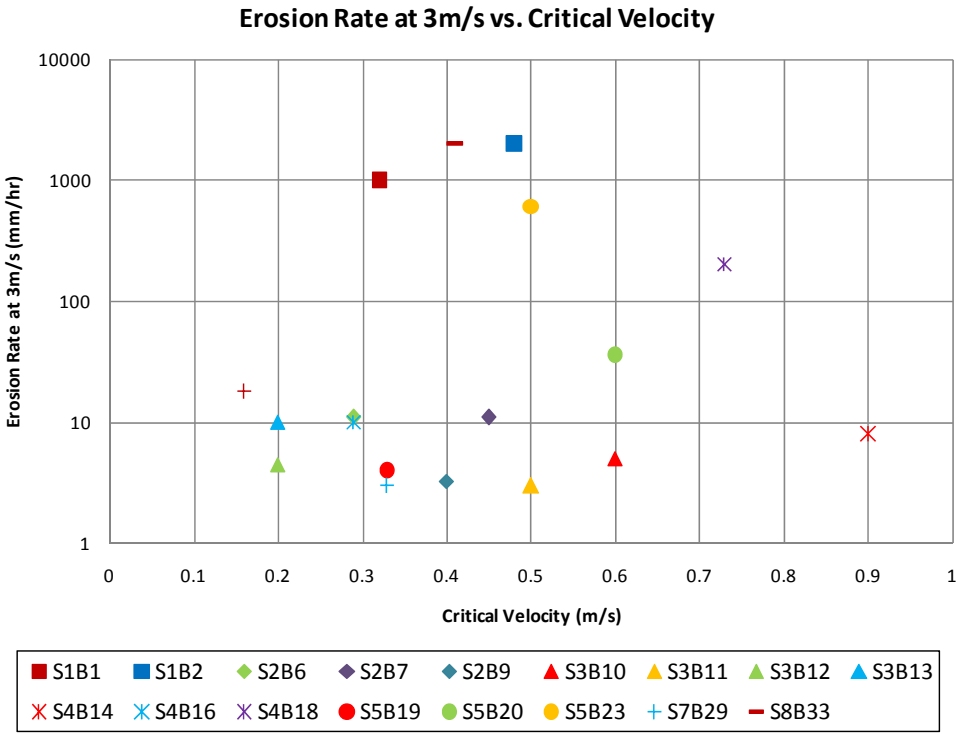

Fig. 165. Erosion rate at 3 m/s vs. critical velocity

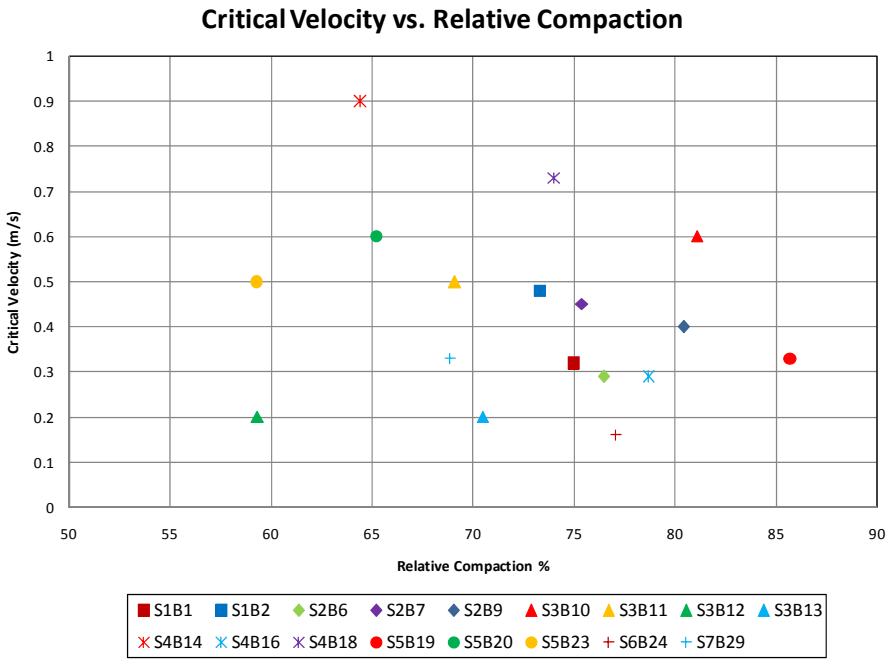

Fig. 166. Critical velocity vs. relative compaction

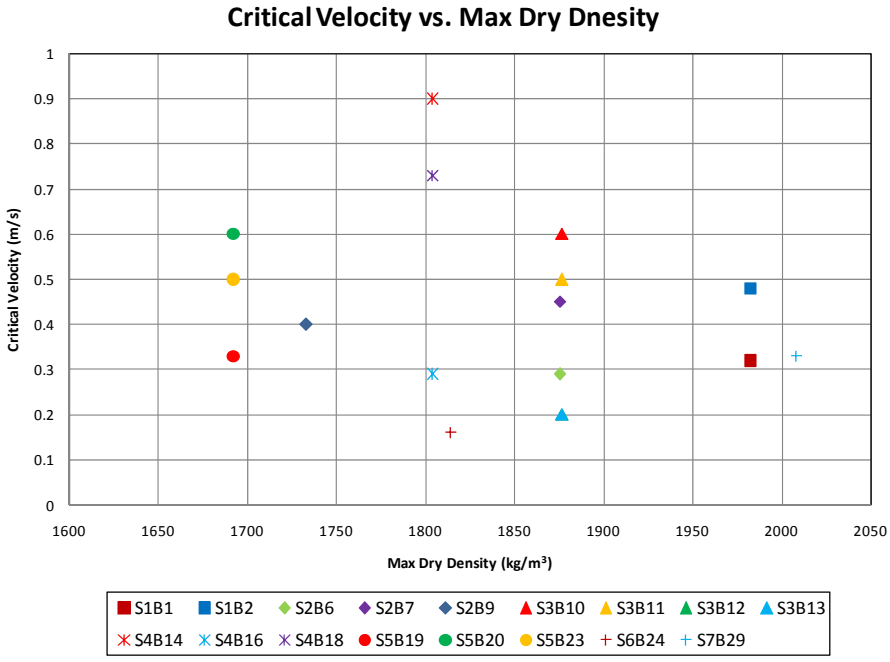

Fig. 167. Critical velocity vs. maximum dry density

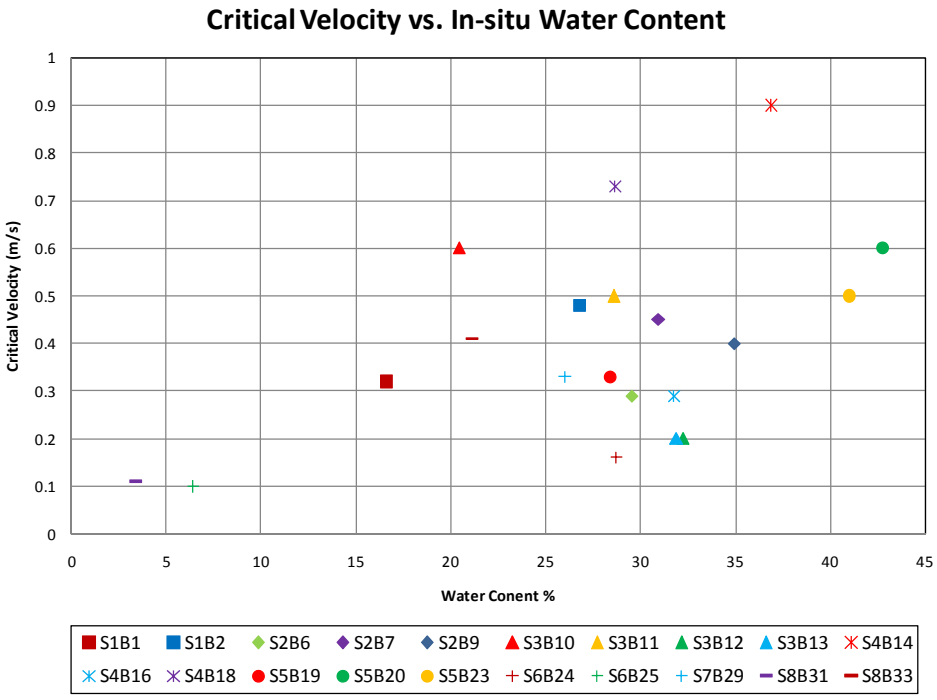

Fig. 168. Critical velocity vs. in situ water content

For the data in Fig. 169, the optimum water content found using the compaction curves was subtracted from the actual in situ water content. There was an initial assumption that excess water could reduce the resistance to erosion. If the samples were similar in every way except water content this may have been able to be proven, but because they are not, the results are inconclusive. With that said, there does seem to be a general trend with in situ water content shown in Fig. 168 above.

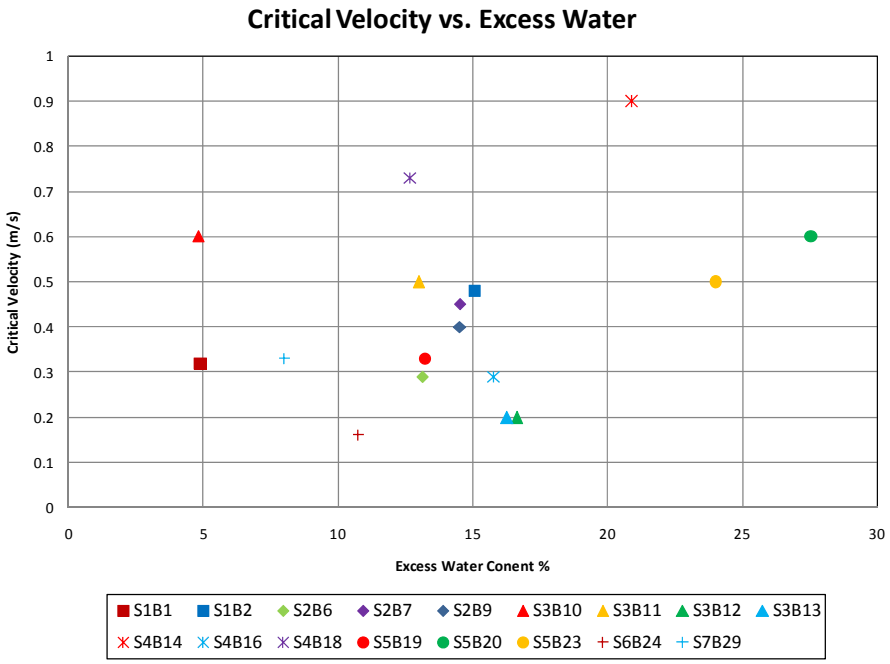

Fig. 169. Critical velocity vs. excess water content above optimum

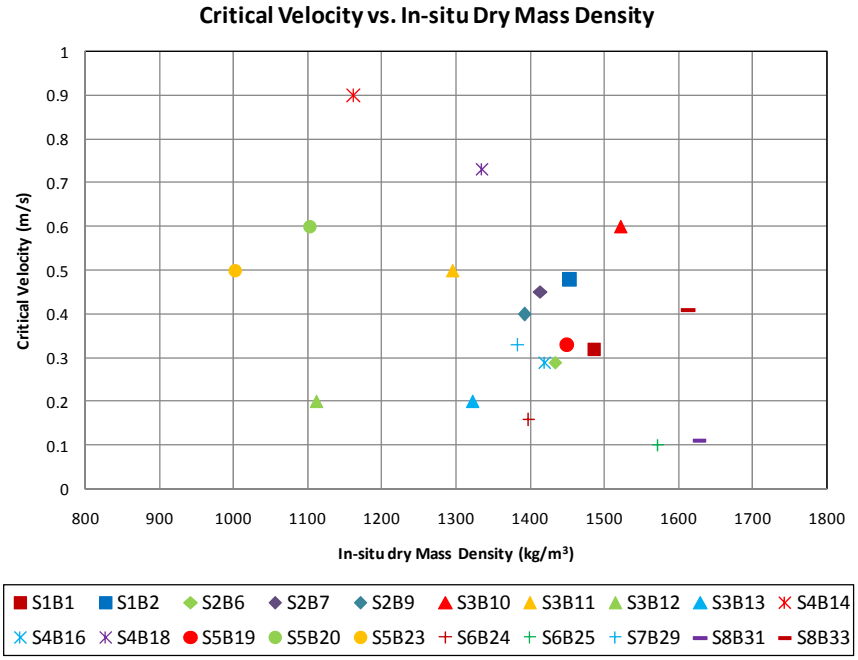

Fig. 170. Critical velocity vs. in situ dry mass density

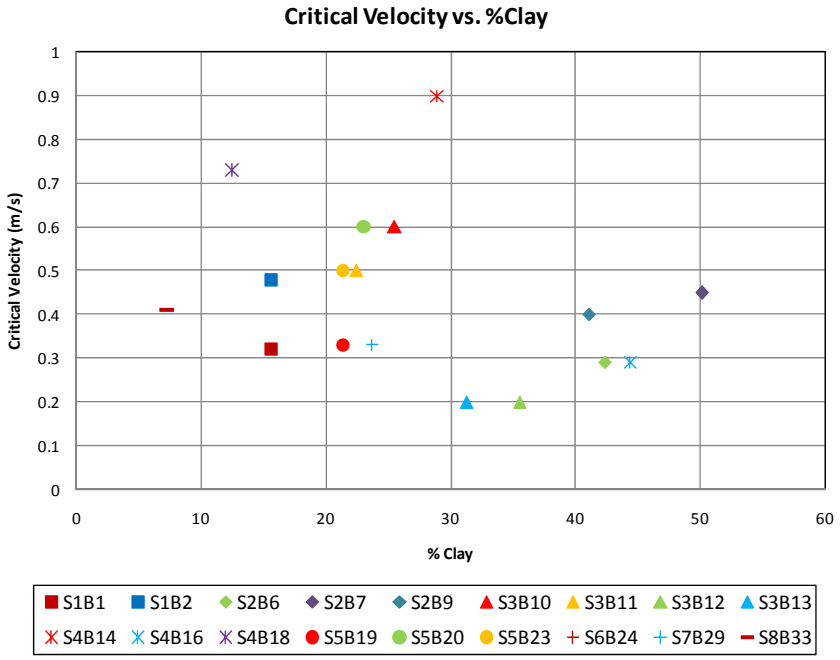

Fig. 171. Critical velocity vs. percent clay

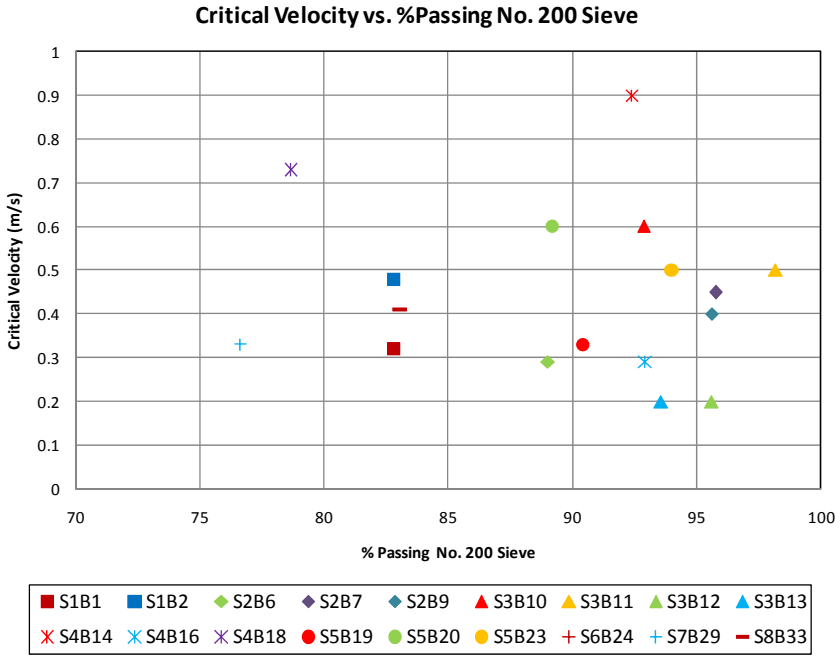

Fig. 172. Critical velocity vs. percent passing the No. 200 sieve

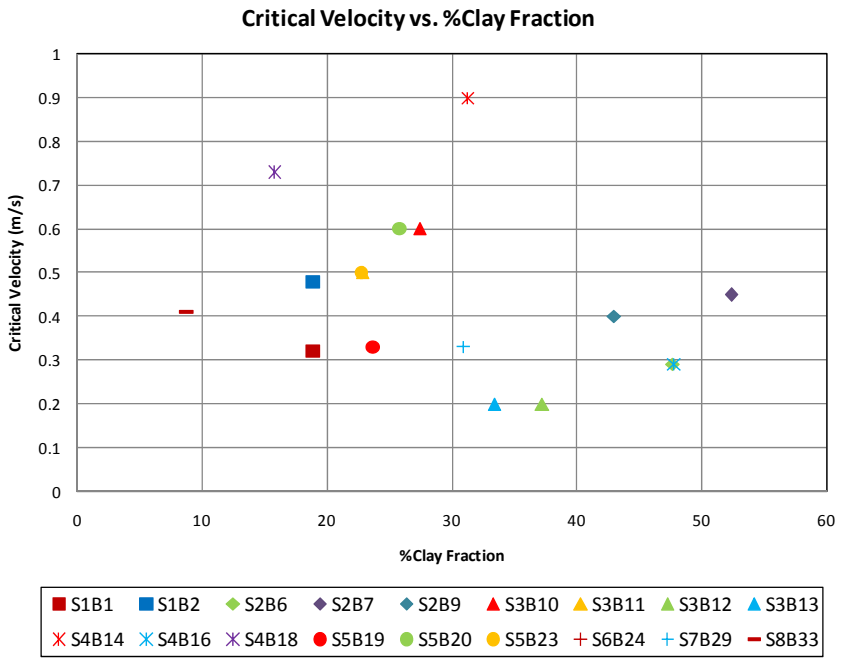

Fig. 173. Critical velocity vs. percent clay fraction

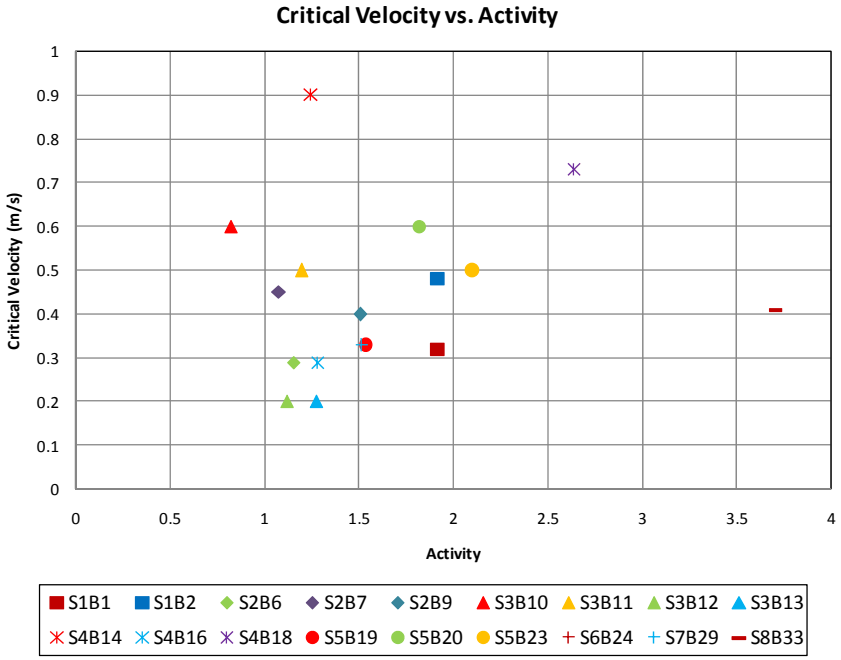

Fig. 174. Critical velocity vs. activity

Because the data was available, D_{60}, D_{10}, D_{30}, coefficient of uniformity (C_u), and coefficient of curvature (C_c) were plotted versus critical velocity. The following figures show the results, respectively.

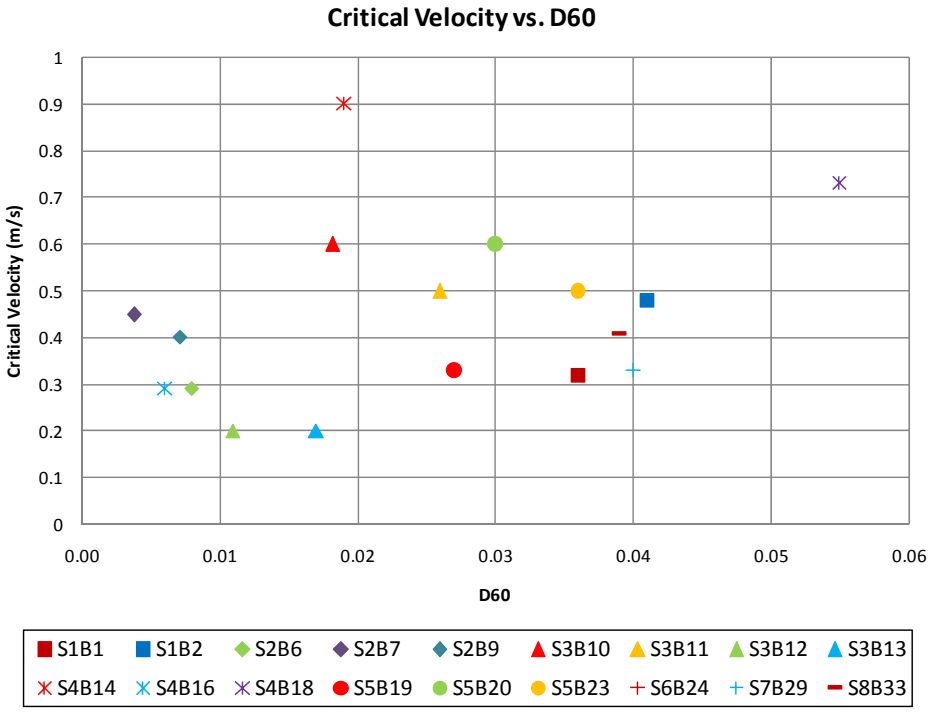

Fig. 175. Critical velocity vs. D_{60}

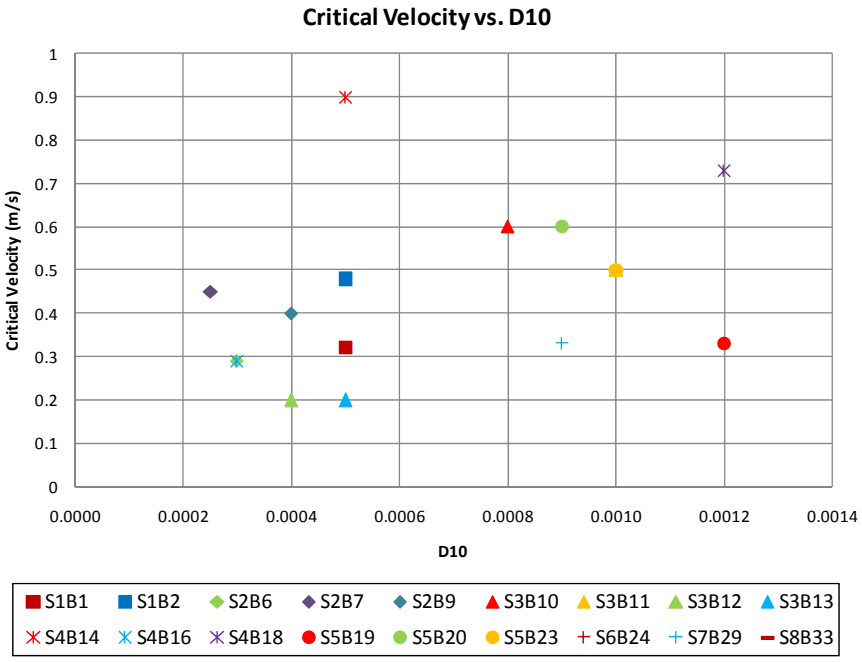

Fig. 176. Critical velocity vs. D_{10}

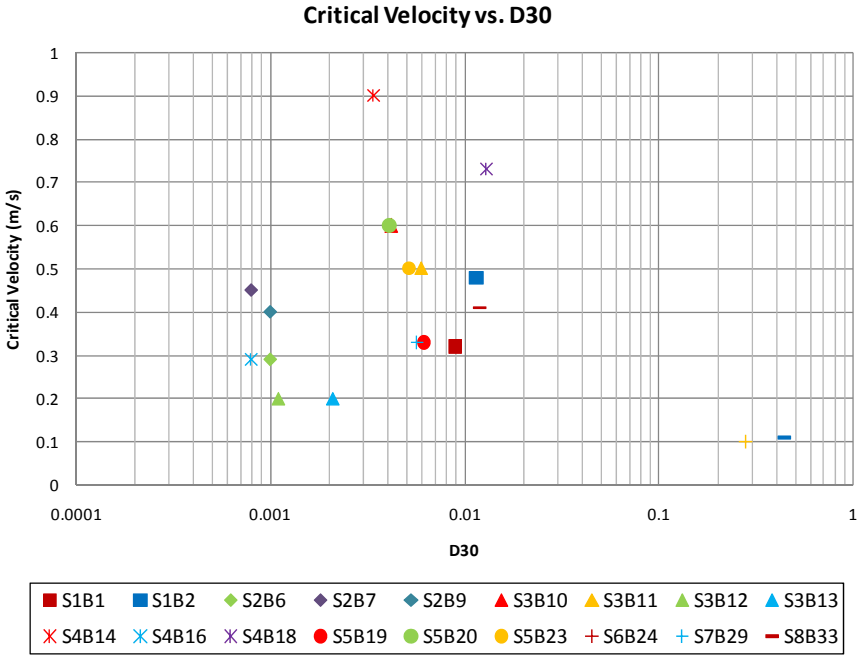

Fig. 177. Critical velocity vs. D_{30}

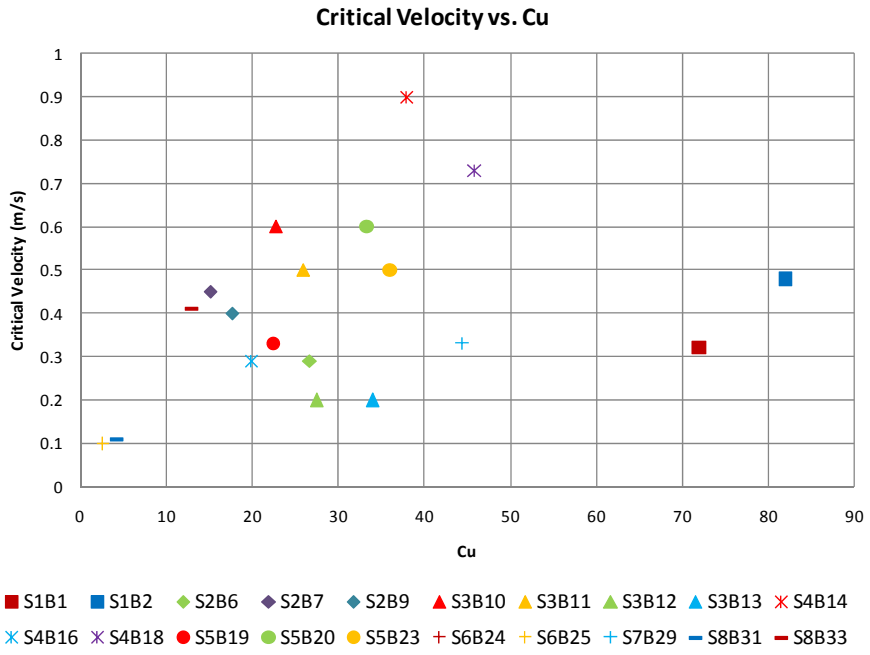

Fig. 178. Critical velocity vs. C_u

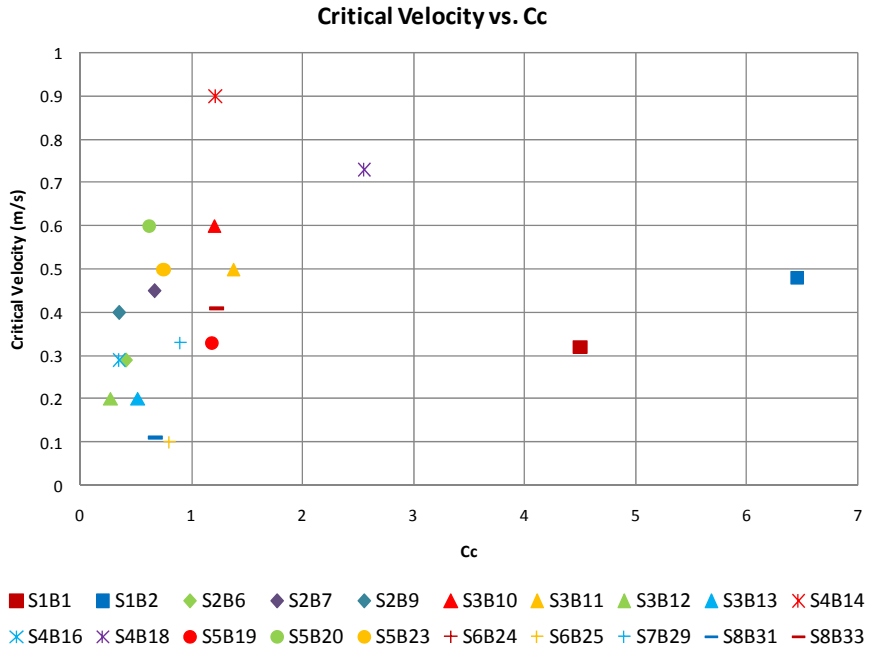

Fig. 179. Critical velocity vs. C_c

No real trends were found for the above data, but once again, critical velocity may not be unique for two soils with very different erodibilities. The entire erosion function can provide a much better clue to the relations studied.

7.6 EFA Correlations – Pass versus Fail

The first step in the comparison was to plot the same charts as above including whether the site was breached or not (Figs. 180 and 181). The sites where a breach occurred are shown in a solid shape while the Brevator site that did not breach is shown with the outlined shapes. Similar charts were produced for the Hurricane Katrina analysis (Briaud et al. 2008).

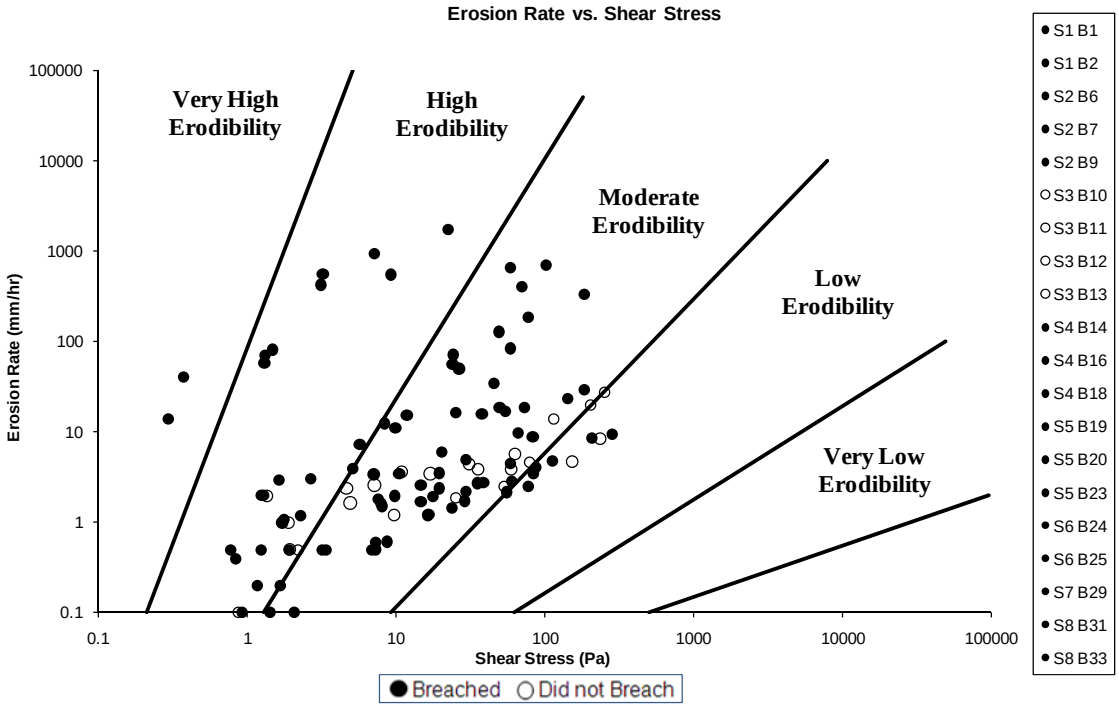

Fig. 180. EFA comparison – pass vs. fail in terms of shear stress

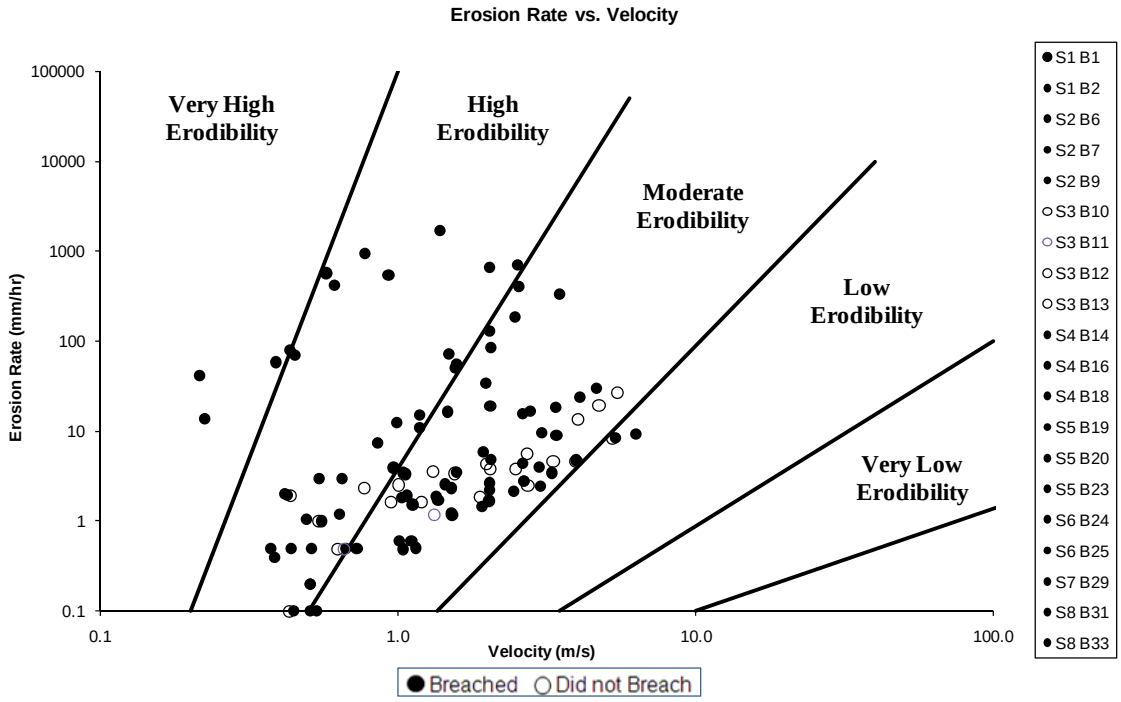

Fig. 181. EFA comparison – pass vs. fail in terms of velocity

Looking at the graphs of pass vs. fail for the Midwest Levee samples, it seems that there is no clear cut division leading to a conclusion of a critical pass/fail category or trend like what was seen in the Katrina data. Comparing the sites that failed to the sites that did not fail based on the plotted points is somewhat deceptive because the EFA only tests the bare soil and does not account for any of the site conditions, such as vegetation or other variables that may have influenced whether or not the actual site failed. If the four sites labeled as not failed were taken off the plot or moved to the right by including the effects of vegetative cover, the soils would be mostly confined to the first three categories (Very High Erodibility, High Erodibility, and Moderate Erodibility). A similar chart was produced for hurricane type events, only all the data which failed was contained in the first two categories. For longer periods of

overtopping, very resistant materials are needed in order to keep an embankment from failing. Fig. 182 shows a chart of the recommended soil categories for long periods of overtopping.

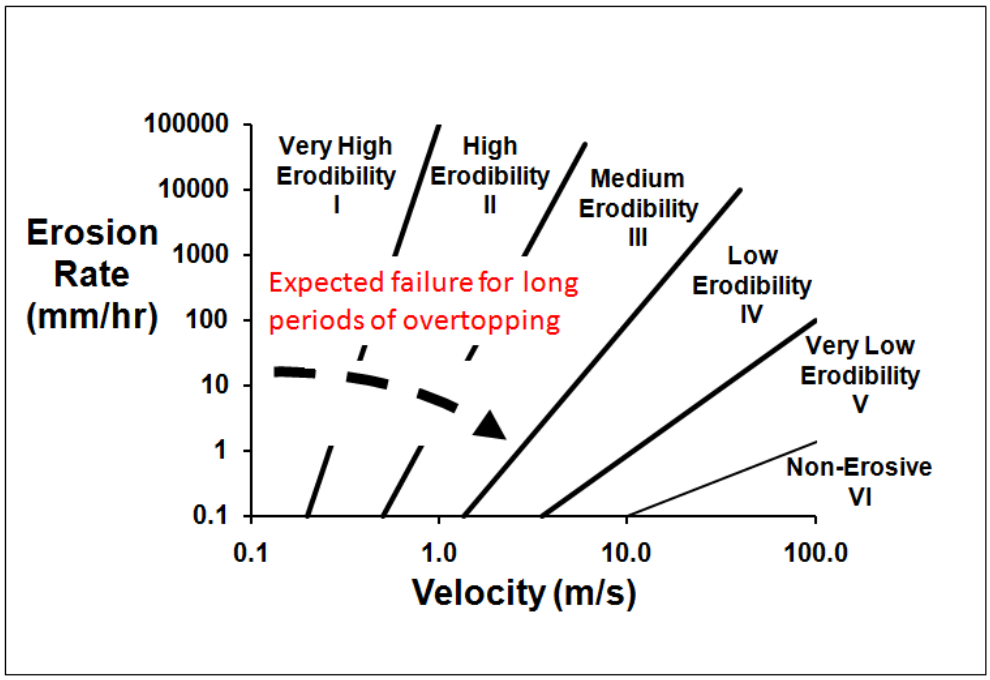

Fig. 182. Expected failure chart for long periods of overtopping

Furthermore, many of the samples tested were collected from the remaining material that did not erode during the flood events. While the site may have failed, the actual soil at the location sampled may have resisted quite well. These charts were recreated to show only the samples that were sampled within the breach locations as failed (Figs. 183 and 184). Those that were outside the breached area are shown in the open circles.

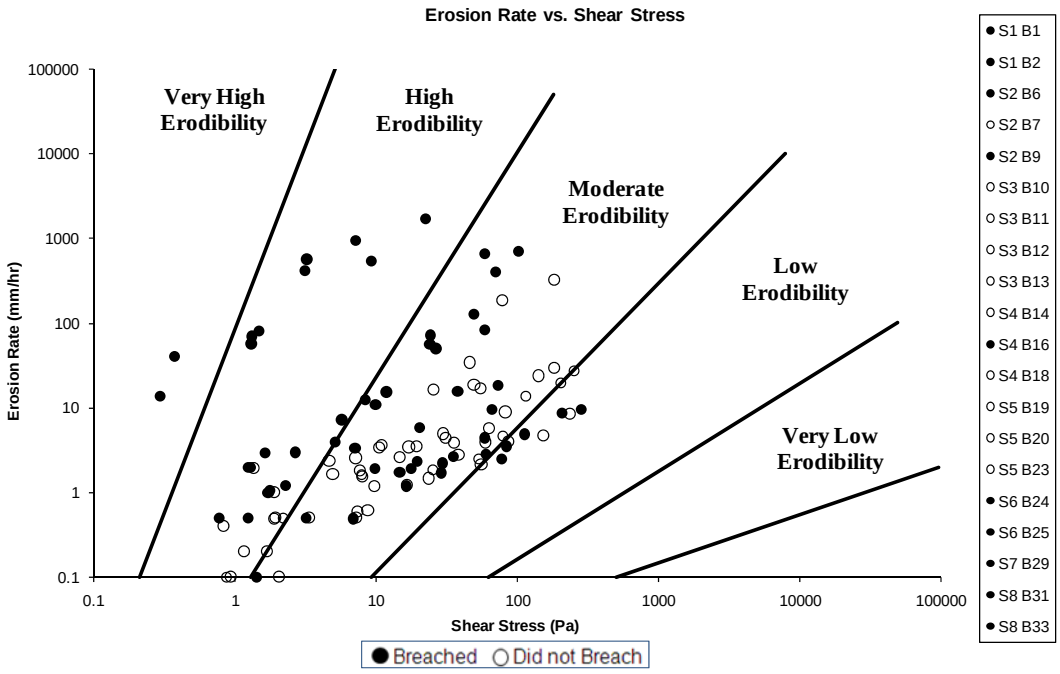

Fig. 183. Sample specific pass vs. fail in terms of shear stress

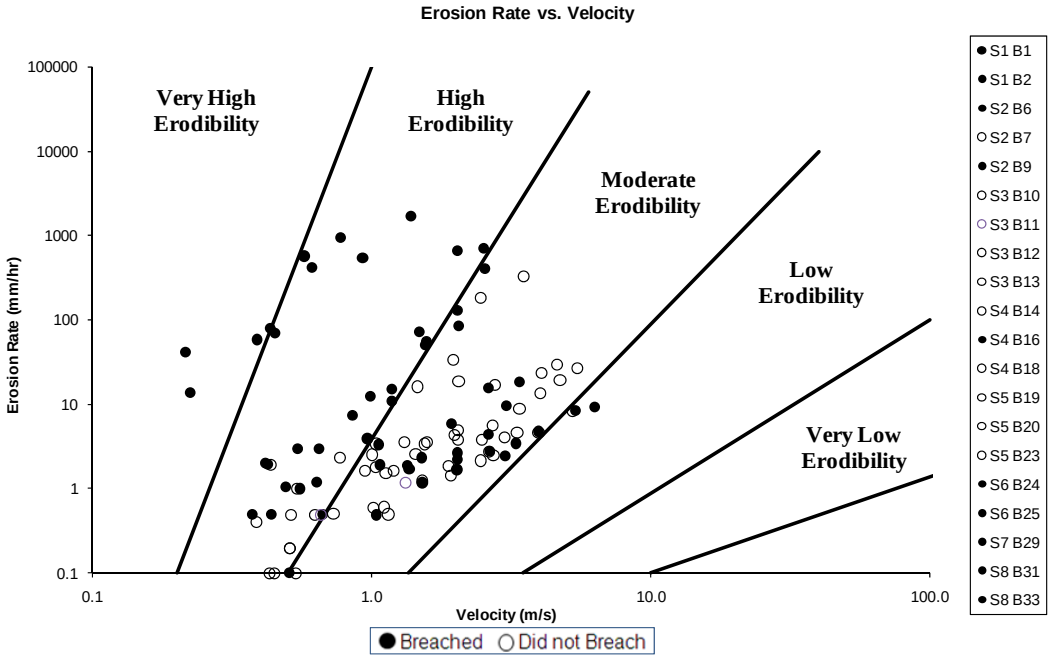

Fig. 184. Sample specific pass vs. fail in terms of velocity

These graphs are inconclusive in terms of a clear cut division between soils that failed and those that resisted. Many of the samples were taken in the existing material beside the breaches because it was impossible to get samples from inside the area or there simply were not any traces of original material left. However, these locations were less than 1 m away from the breached areas and it is unlikely that the conditions would have changed drastically in just a short distance. The samples were chosen because they were similar to those expected in the failure zones, so plotting the pass or fail on a sample specific basis is really not that helpful.

A few of the samples that were taken in the failure zones still show higher resistance in the above plots yet they still failed, once again proving the importance of the analysis of vegetative cover and other variables. The EFA results show no influence in vegetation, except for the chance of root fibers in some of the samples taken more close to the surface. A certain site or location may have had more dense vegetative cover which protected soils that would have normally failed. This is seen in the Brevator case (Fig. 181). While the soils at the site were moderately resistant, they were not the most resistant soils tested, however there was little or no sign of erosion at the sites. The grass was said to be approximately 1 m high at the time of flooding. The waters rushed over the grass and laid it down forming a protective barrier over the soil. Also, the EFA results are all tested in similar conditions. These sites experienced a variety of overtopping and in some cases seepage conditions not considered in the above plots. Some of these include: different periods of overtopping, the added influence of piping, wave action, configuration of rivers. The actual periods of overtopping

experienced at each site is one of the major pieces of information missing. There is no real data at this time with the exception of eye witness accounts that gives the length of time or height of the overtopping water at each location. A site with more resistant soils may have failed if it was overtopped for a longer period of time. It is also hard to account for seepage. At the time of flooding and overtopping, any signs of seepage are hidden to the eye and then most traces are washed away. Those sites with large tree roots, crawdad tunnels, and sites with sand shells may have also been influenced by seepage. This is once again proof of the complications involved in trying to understand the phenomenon of erosion due to overtopping in real field conditions.

It is important to understand that the EFA was only used as a judge of the erosiveness of the soils. Knowing the quantified erodibility of the soils at the site is the main piece of information needed to analyze a site. Also, for a preliminary comparison, the EFA provides a great qualitative evaluation of one soil to another. By picking a given shear stress and drawing a vertical line, soils with different properties can be evaluated. For example, at 10 Pa (Fig. 180), the soils at which the site did not fail are generally much more resistant to erosion or generally have a lower erosion rate. For reasons discussed above, this type of comparison should be used with caution and treated as more of a qualitative judge of erosion for the samples.

7.7 EFA Correlations – Plasticity Index, D_{50}, Relative Compaction

Laboratory data such as plasticity index, D_{50}, and relative compaction were divided into categories and combined with the EFA results to obtain several comparison charts. Atterberg Limit results were used to obtain the Plasticity Index (PI) for each of the samples tested. The ranges of PI's were divided into four categories. The EFA results were plotted according to their corresponding PI, with the Brevator site shown again in the open circles (Figs. 185 and 186).

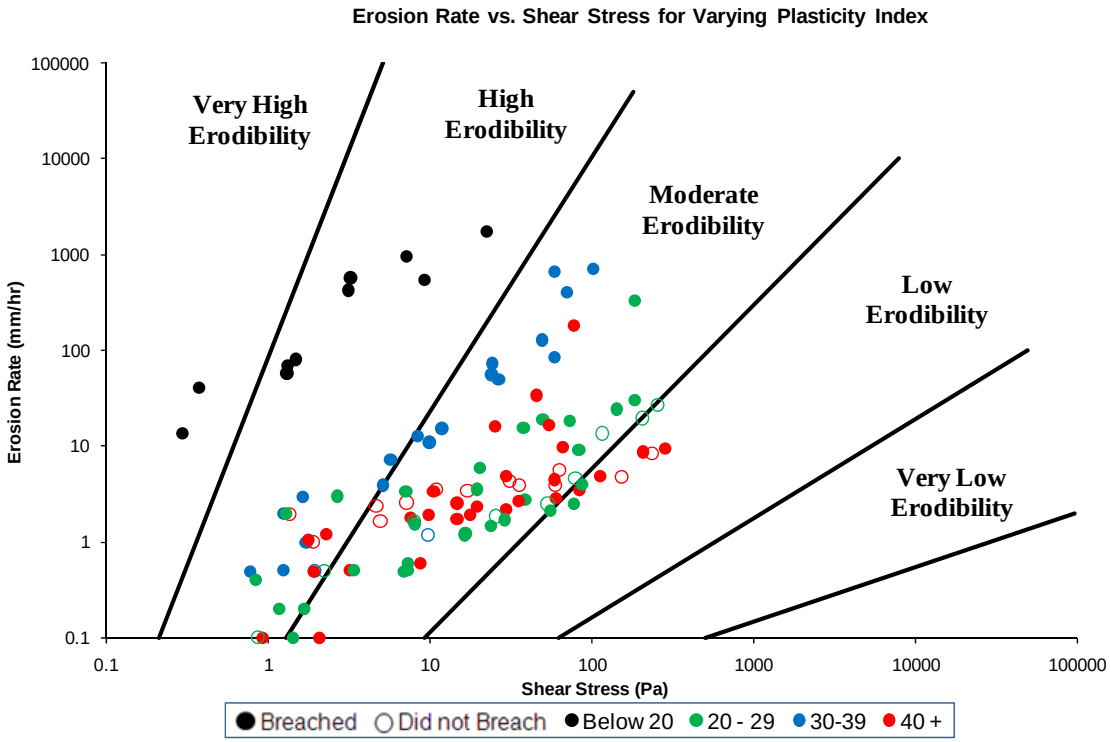

Fig. 185. EFA comparison for shear stress – plasticity index

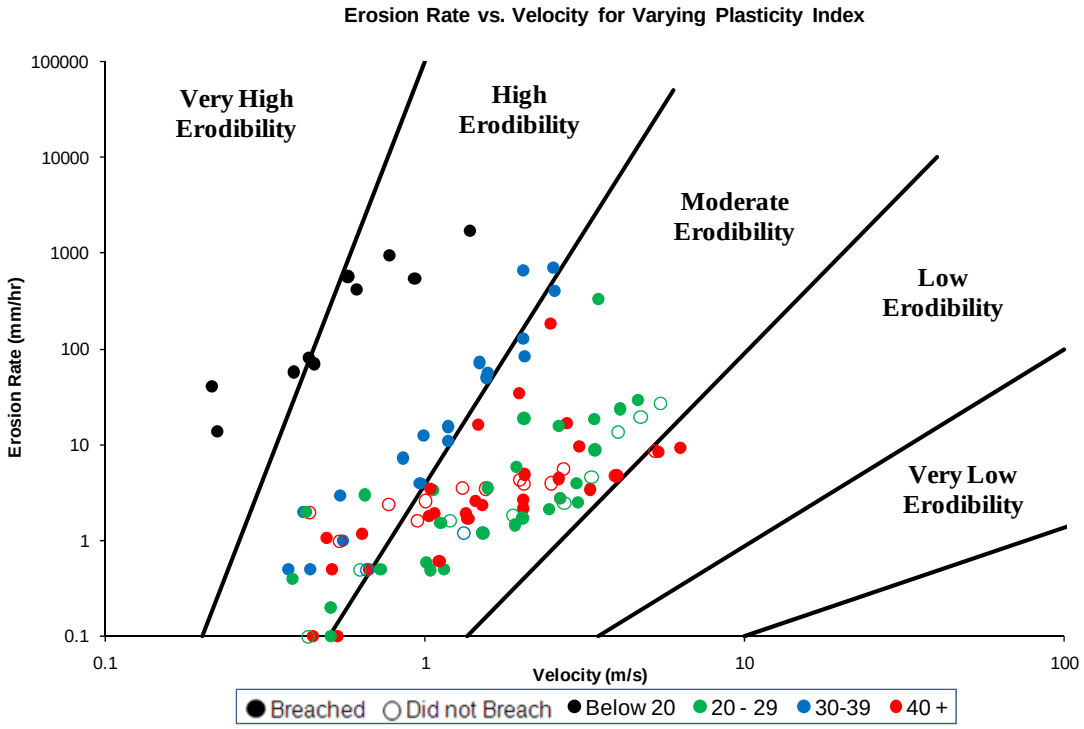

Fig. 186. EFA comparison for velocity – plasticity index

Past testing results have shown a general trend in the higher plasticity soils being more resistant to erosion. The term "general trend" is used because while many of the soils increase erosion resistance with increasing PI, there are several samples that do not. Fig. 186 shows several samples in green that are lower plasticity yet still are among the most resistant. Also, one of the highest plasticity soils and several of the samples from the blue range are on the border of being categorized as high erodibility. These soils could be dispersive clays. Dispersive clays are often found in floodplain areas and are highly erodible no matter what the plasticity. There are standardized tests that can be run to check for dispersiveness, however, for this analysis the label of dispersive or non-dispersive was not an important factor. The above plots also prove that erosion cannot

be determined by plasticity alone. Also, part of the problem with the plots above is that plasticity was not the only condition that varied for the soils. Therefore, the plot does not single out the influence of plasticity.

The same charts were constructed for average particle size, D_{50}, or the diameter at which 50 percent of the particles are smaller (Figs. 187 and 188). The D_{50} values were obtained from the hydrometer and sieve analyses.

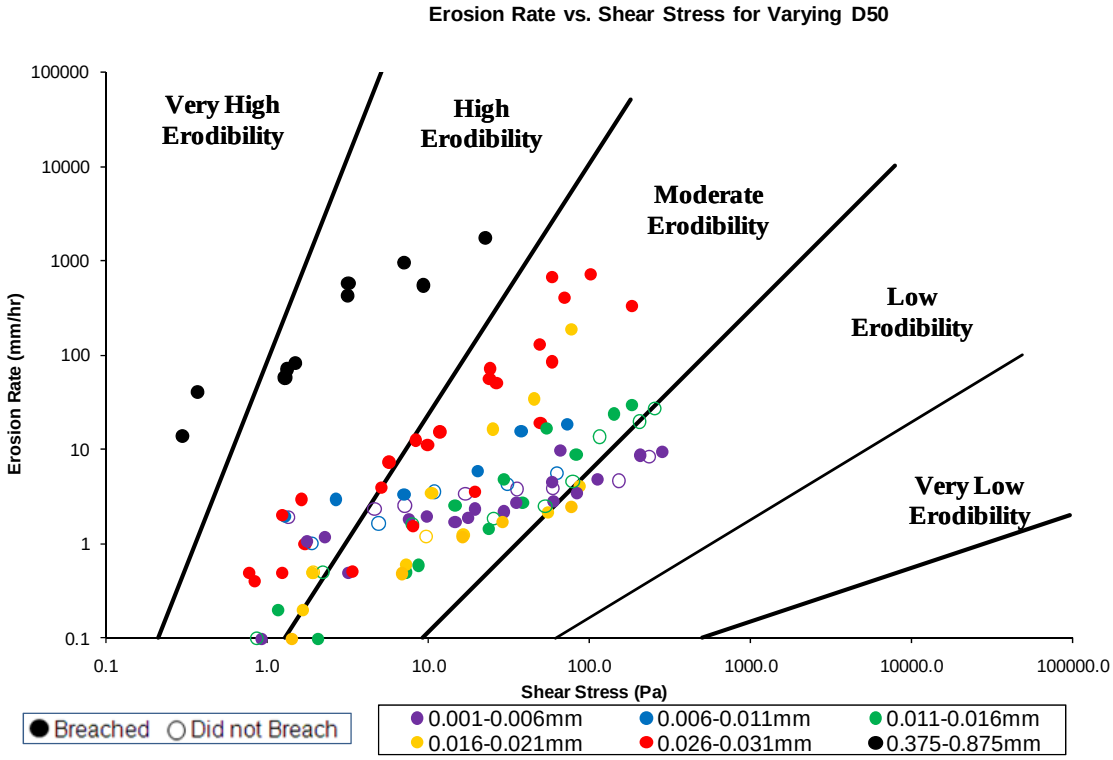

Fig. 187. EFA comparison for shear stress – D_{50}

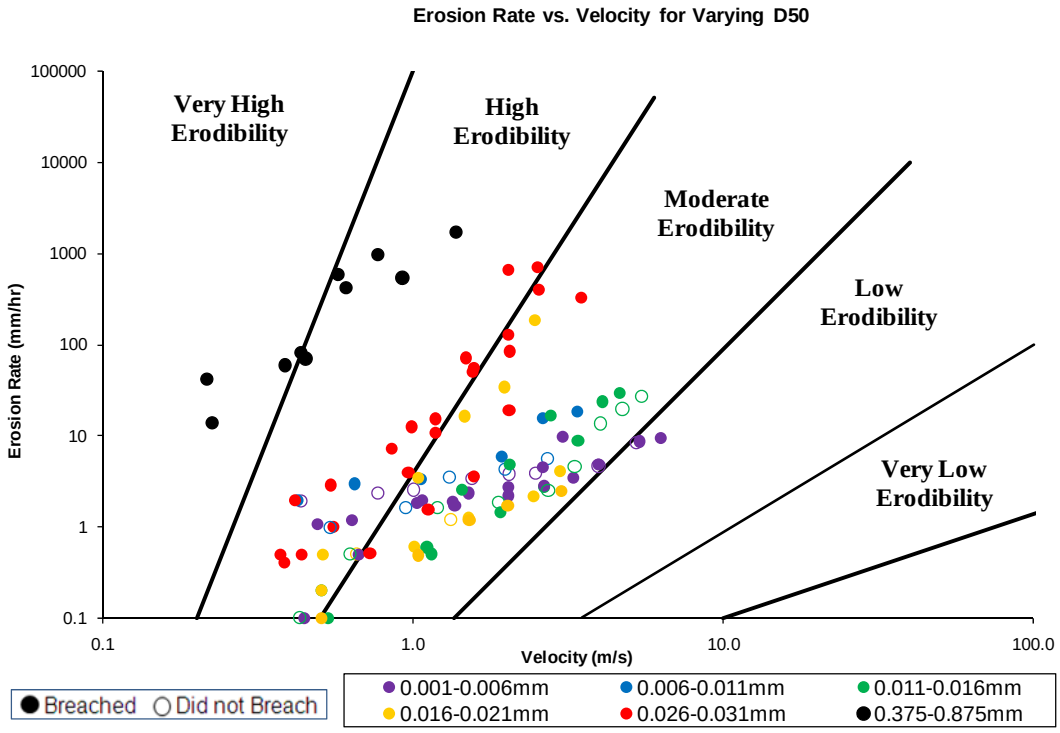

Fig. 188. EFA comparison for shear stress – D_{50}

This correlation shows a fairly consistent trend. The smallest particle sizes, shown by the purple circles are some of the more resistant soils. However, there are still several samples that do not fit the trend of resistance to erosion increasing with decreasing particles. The circles shown in red are also some of the smallest particle sizes yet they are much more erodible. These soils also correspond to those previously determined to be higher plasticity soils. The possibility that they are dispersive clays still applies and may explain why they are so erosive and why they do not follow the general trends. So once again, erodibility cannot be determined by particle size alone.

Looking now at relative compaction (Figs. 189 and 190), it seems the higher percent compaction leads to more resistant soils in general. This has been proven in previous EFA tests as well as by the Federal Highway Administration and others.

Hassan et al. (2004) showed that the erosion resistance was increased for the same materials compacted at higher water contents and higher degrees of compaction. However, the trend with the degree of compaction only holds for each soil individually. Comparing two different soils at different relative compactions is inconclusive. One soil may change drastically with slightly higher compaction values, while another may only slightly increase in resistance with a large increase in relative compaction. If these soils are of different plasticity and other conditions, the aforementioned trend may not prove true.

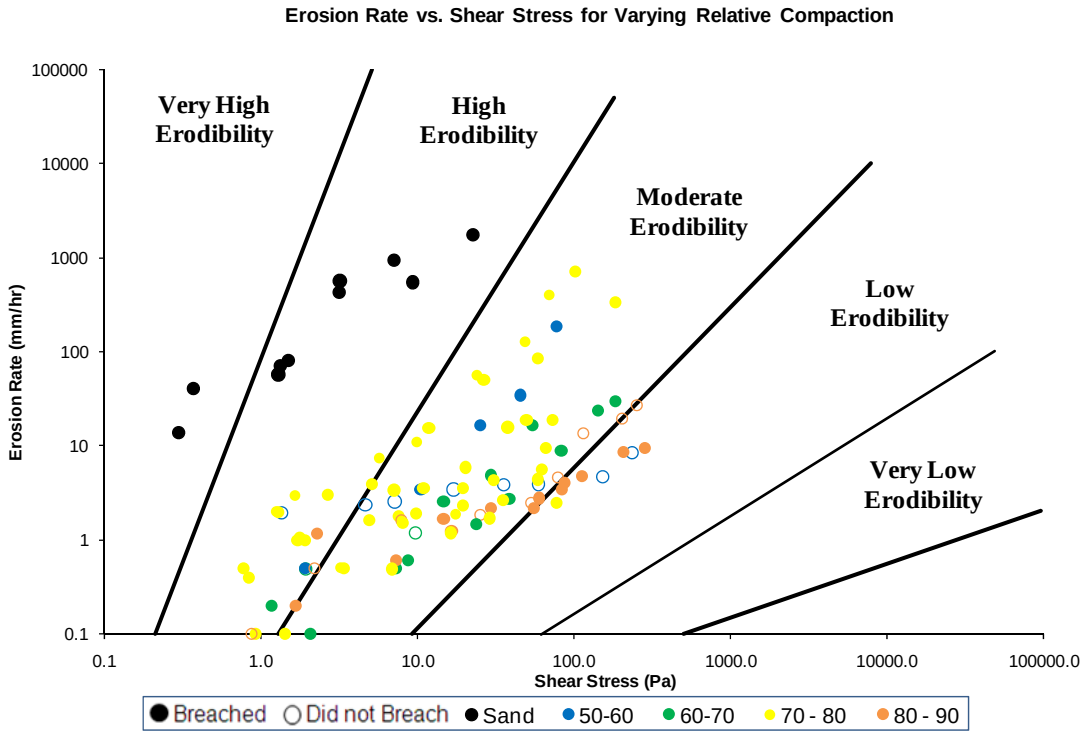

Fig. 189. EFA comparison for shear stress – percent relative compaction

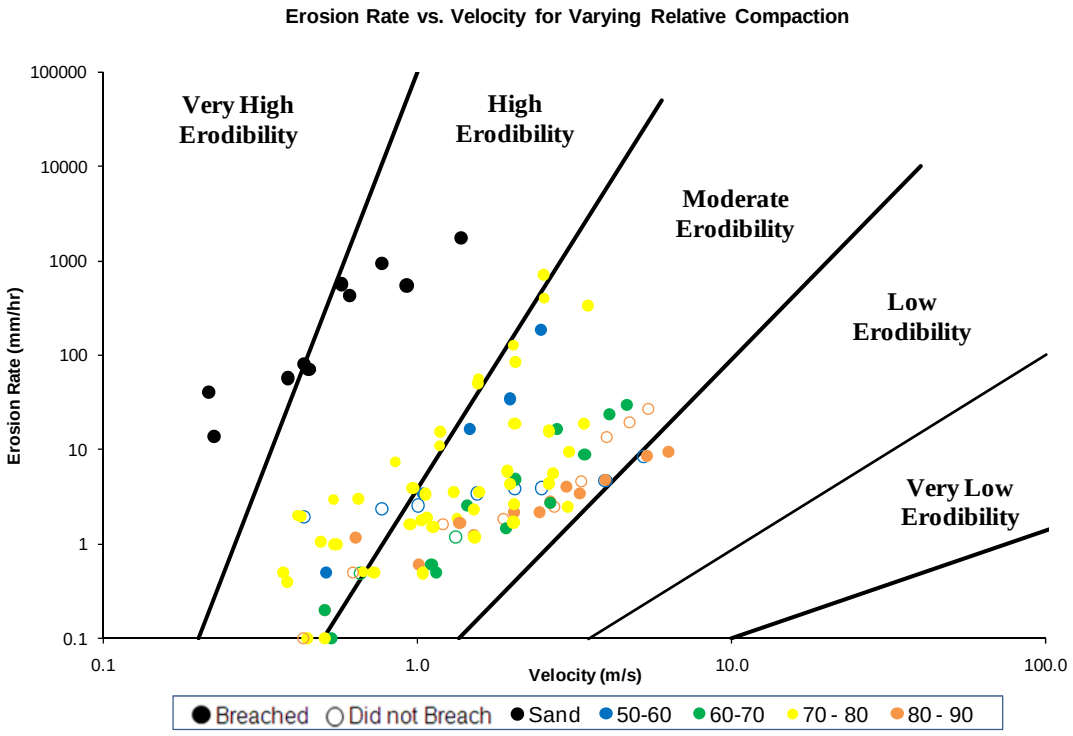

Fig. 190. EFA comparison for velocity – percent relative compaction

Once more there are soils that go against the trend. While the highest compacted soils (shown in orange) seem to be the most resistant, there are a few samples with much lower compaction (shown in green) that are still resistant. While the importance of compaction is shown, its use as an erodibility indicator is still un-justified.

For most levee construction, relative compactions higher than 90 percent are desired and even required. No sample collected had an in situ value above this threshold. Some of the samples were taken at the surface and may represent top soil used for vegetation establishment which are not expected to have a high degree of compaction. The surface must be compacted at a lesser extent so that grasses will root and spread. The calculation methods used were also simplified and could be to blame

for the lower values; however, they were adequate for use as a comparison method. Also, due to field conditions, sampling techniques were not as accurate as those used in conventional drill rigs and may have led to underestimated in situ densities. It is recommended that the field compaction values be checked with the proper density equipment before any claims are made that the sites were highly under-compacted.

While using a single correlation or parameter as an erodibility indicator is not justified, the information gained from each is important for the overall analysis. The erodibility of a soil is defined by a combination of the soil properties and site conditions. The erosion phenomenon due to overtopping may be better understood by looking at all the different variables and their relationship to the erosiveness of a soil.

These few cases prove that erosion is complicated and site specific analysis is definitely warranted. Some of the issues involved in relating this data are due to the variability in the soil properties across a site. The nature of geotechnical engineering requires the characterization of a site with using only a few scattered samples and limited data. A simple plot (Fig. 191) developed by Alexander Cheng of the University of Mississippi shows the increase in uncertainties that occur when sampling is limited over the course of several kilometers of levee. There is no way to interpolate the missing data without assuming it is similar to the points sampled. The chance of sampling extreme cases increases the uncertainties that exist and makes interpretation of the data very difficult. The soils sampled all were at unique water contents, relative compactions, clay fractions, etc. making it very difficult to compare overall soil properties with erodibility.

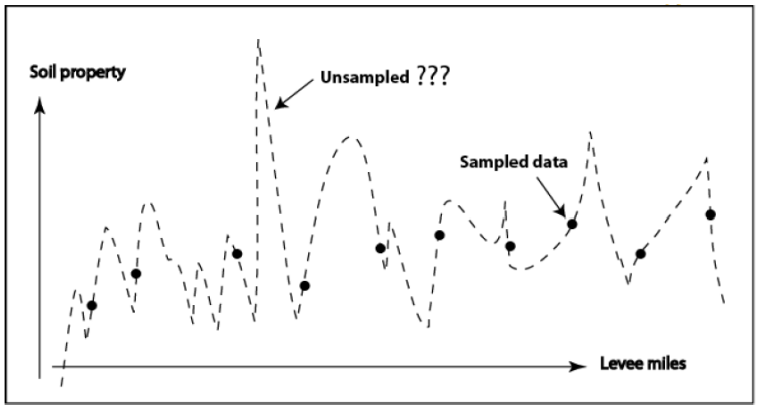

Fig. 191. Sampling variability along levees (Cheng 2008)

7.8 EFA Erosion Category Correlations

The method used to define the erosion category for each sample in this analysis was discussed in Section 7.2. The EFA categories found ranged from 1.7 to 3.4, with 1 being very high erodibility and 5 being very low erodibility. This category represents an average estimate of the erodibility based on the entire erosion function. In an effort to check for possible correlations, each erodibility category value was plotted with corresponding parameters such as PI, D_{50}, and relative compaction. The resulting plots are shown in Figs. 192, 193, and 194, respectively.

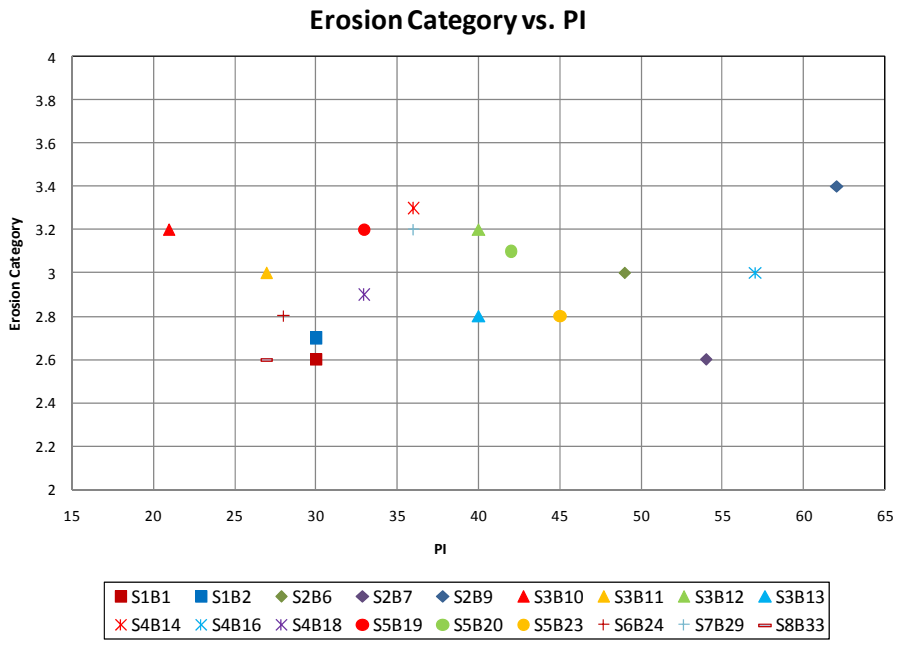

Fig. 192. Erosion category vs. PI

The plot of erosion category versus PI shows no noticeable trend. The method used to obtain the erosion categories is somewhat flawed in the fact that a soil which has several points in the low erodibility category could still have an average category value of moderate erodibility. Another sample with all the points in the moderate erodibility category would also average to be a moderately erodible soil. For this reason, it is important to look at all of the data and correlations obtained. A similar plot was obtained for erosion category versus D_{50}.

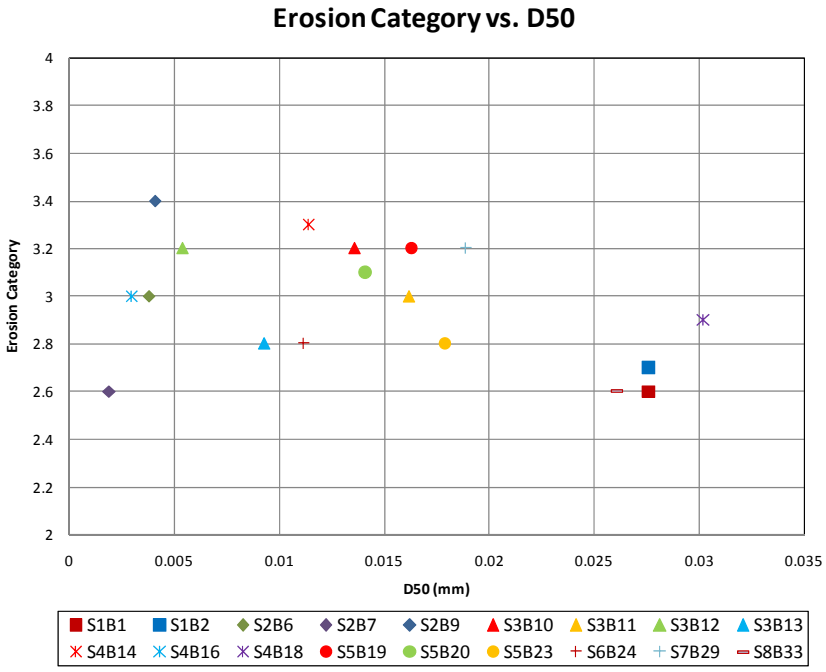

Fig. 193. Erosion category vs. D_{50}

The values for the sand samples are not shown on the above plot. The scale needed to include all the values is large and any trend becomes unreadable. The above graph shows a general trend of decreasing category value with increasing particle size, meaning that as the diameter of the particles becomes larger the soils become more erodible. In theory, this would make sense up to a point. A fine grained soil would never be more resistant that a large rock, for instance. At some point, gravity becomes the controlling factor and the erodibility would decrease with an increase in size and weight of the larger particles. This is the same idea as what was seen in plot of critical velocity versus D_{50} in Section 7.4. In Fig. 193, S2B7 has a much lower erosion category than the other soils with similar D_{50}'s. During testing, only a few erosion points were obtained for this sample. The sample was small and "plucked" out of the tube as the

velocity was increased. Several other samples had a similar problem. With only two velocity points, as in the case of S2B7, the erosion category is highly underestimated. It is more likely that this sample would have an erosion category similar to that of S2B9.

Similar plots were produced for comparison with both relative compaction (Fig. 194) and maximum dry density (Fig. 195). The plot of relative compaction does not follow the expected trend. Only those points past 70 percent relative compaction show that the erosion resistance of a soil increases as it is compacted to higher degrees. As previously explained, this graph is somewhat misleading because it does not separate out only the effects of compaction.

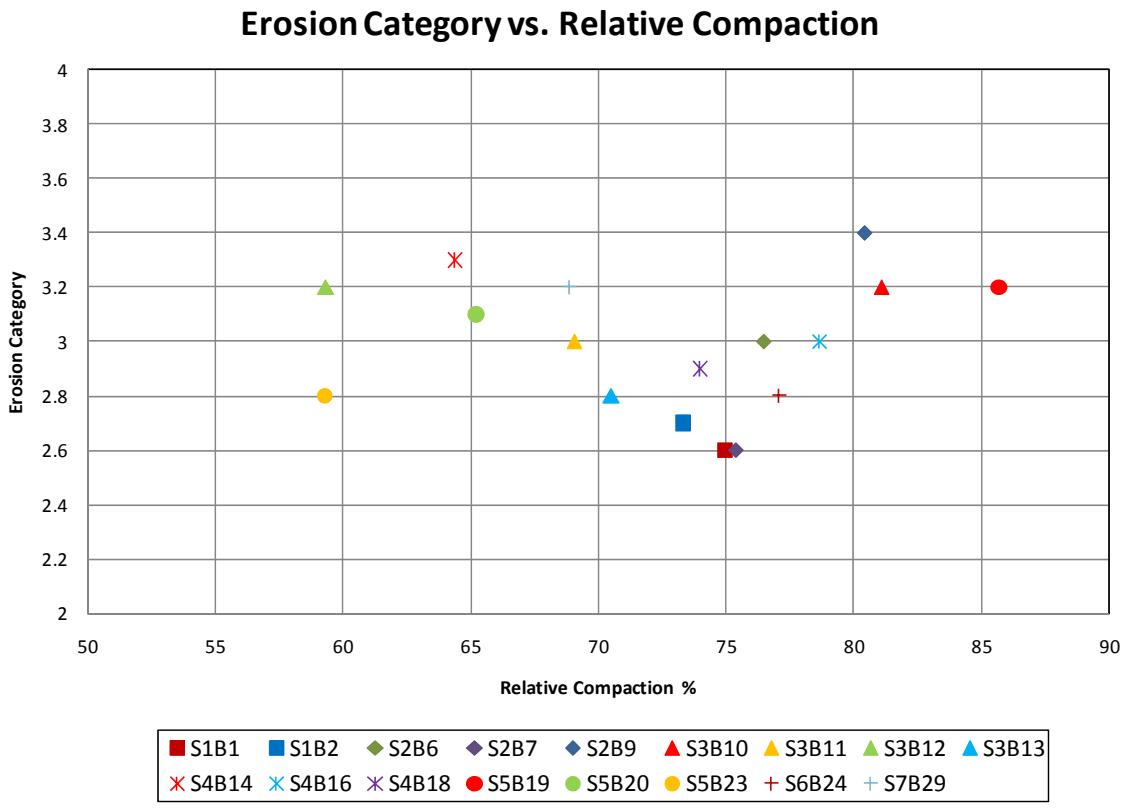

Fig. 194. Erosion category vs. relative compaction

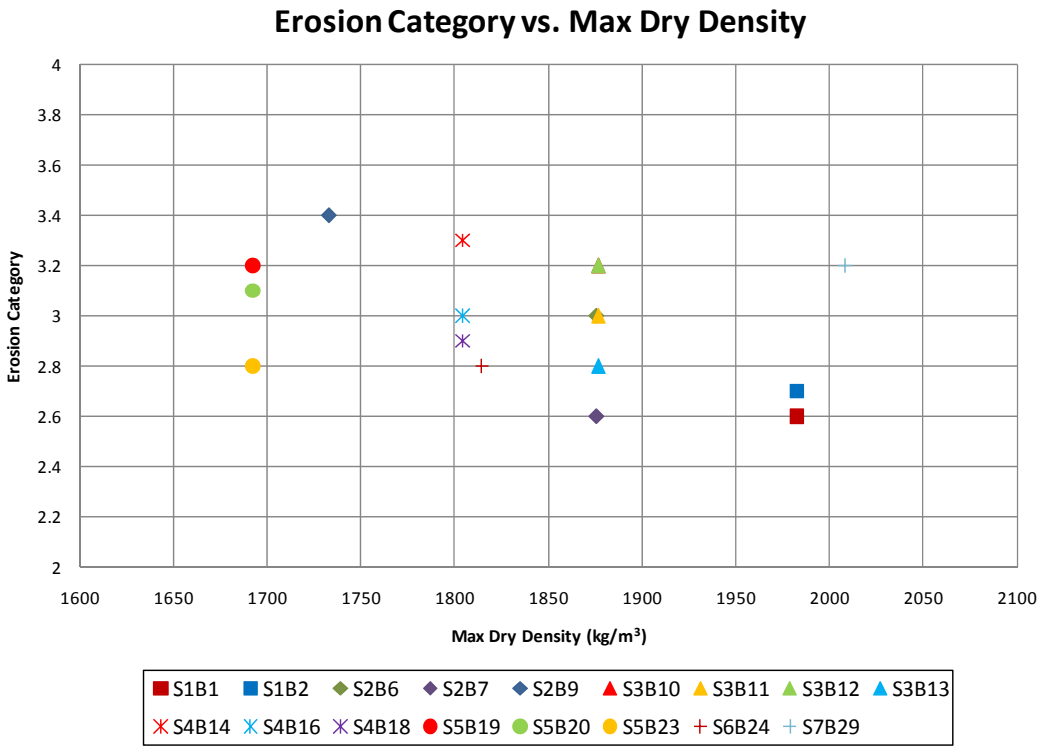

Fig. 195. Erosion category vs. maximum dry density

The graph of erosion category versus maximum dry density seems to follow a general sloping trend. As max dry density increases, the erosion category decreases. This makes sense because more sandy soils have higher max dry densities and lower erosion categories meaning they erode more. This trend is similar to the D_{50} plot, but might be a bit misleading because compaction curves were only found for a few of the samples and all of the others were assumed to be similar. Because there is a dependence on density, it was assumed that there may be some connection with water content. As a check, erosion category versus in situ dry density was plotted (Fig. 196). Erosion category was also plotted versus excess water (Fig. 197). The excess water was found

by subtracting the optimum water content on the compaction curve from the in situ water content. No real trend was found. In situ dry mass density was also plotted (Fig. 198). It appears that as density increases the erodibility category decreases. This agrees with the max density plot above.

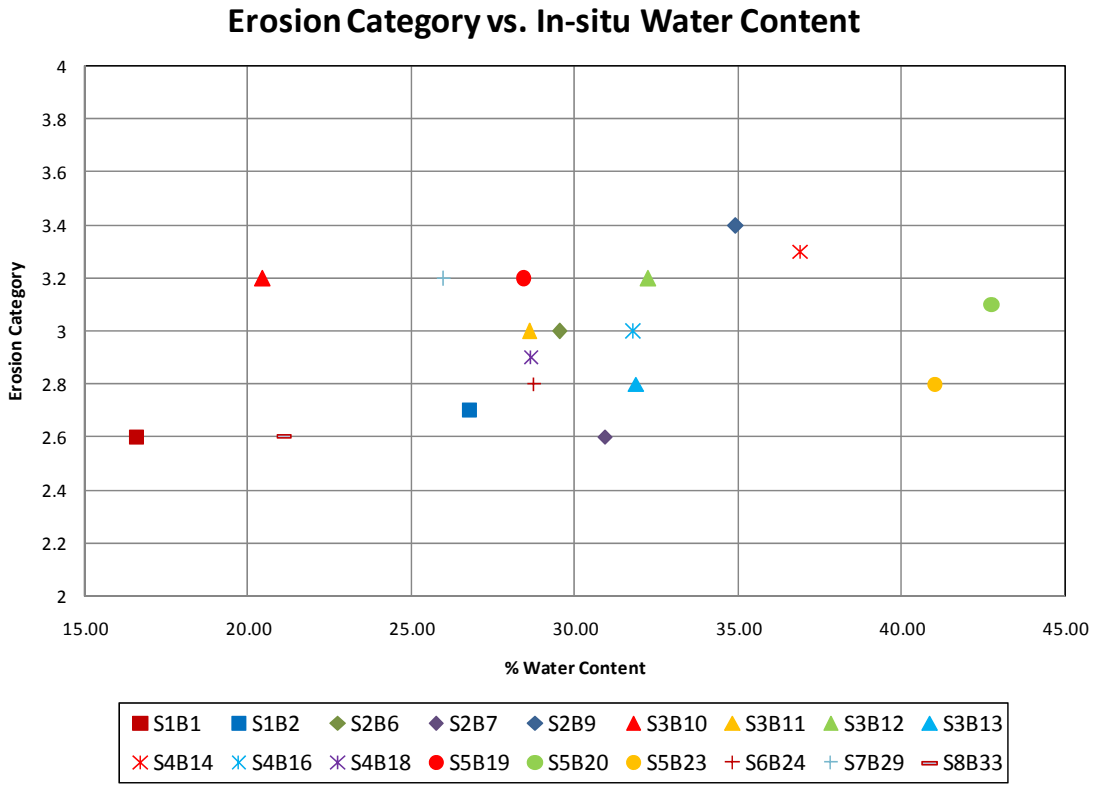

Fig. 196. Erosion category vs. in situ water content

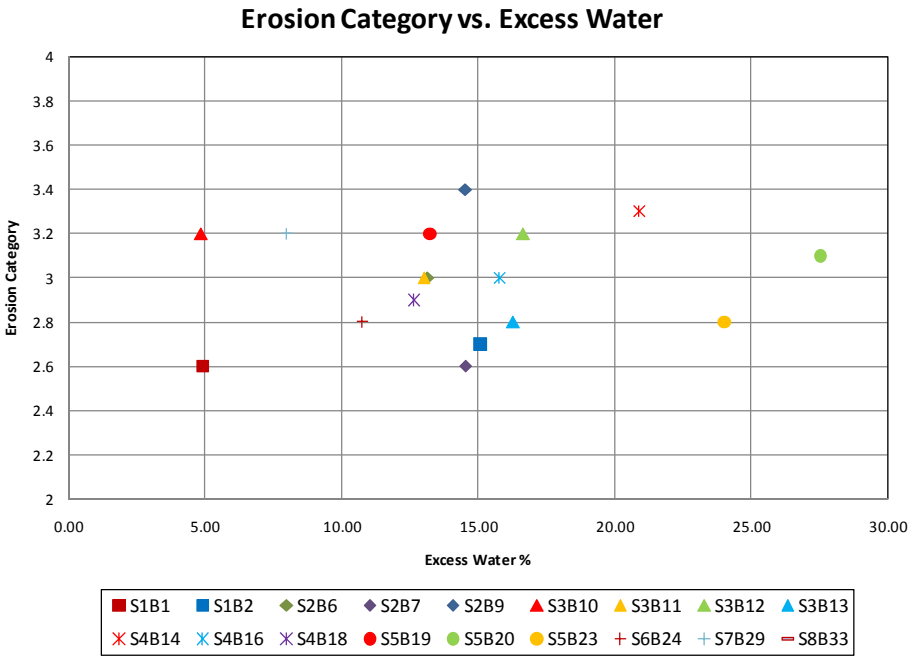

Fig. 197. Erosion category vs. excess water content above optimum

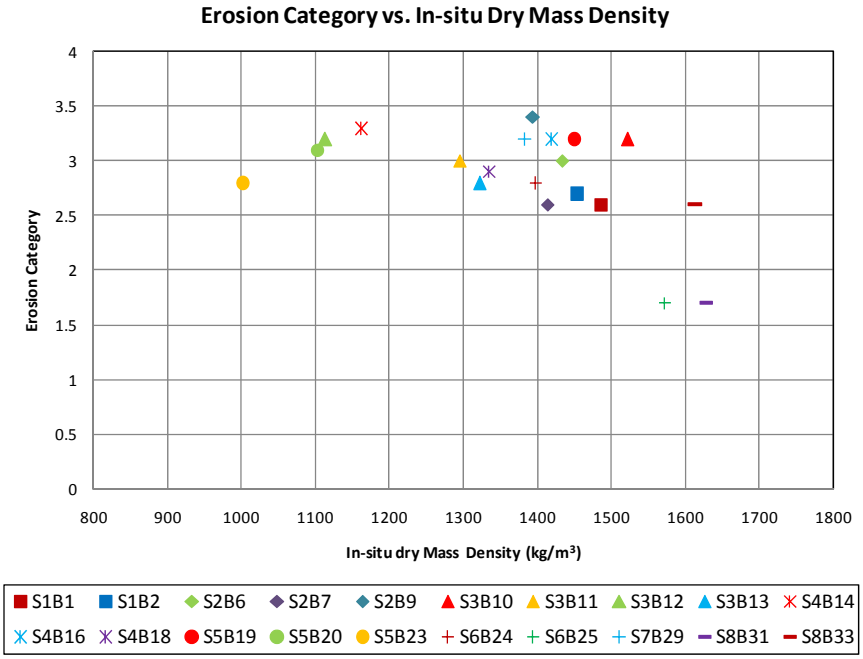

Fig. 198. Erosion category vs. in situ dry mass density

White and Gayed (1943) observed that variations in the results several laboratory overtopping tests could be traced to percent clay and percent water. Several other plots were made to test this statement. These include: percent clay (Fig. 199), percent passing the No. 200 sieve (Fig. 200), percent clay fraction (Fig. 201), and activity (Fig. 202).

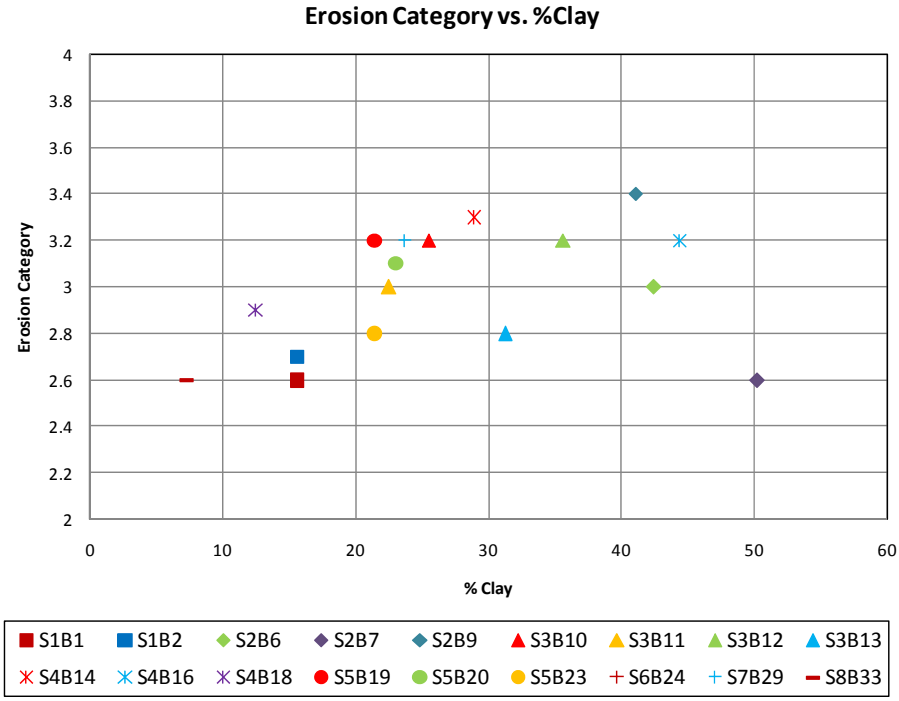

Fig. 199. Erosion category vs. percent clay

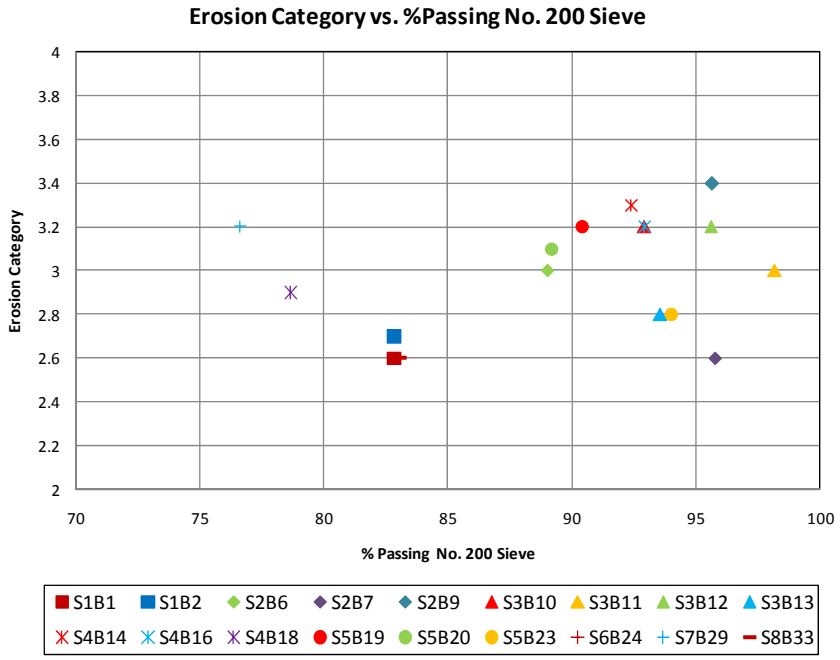

Fig. 200. Erosion category vs. percent passing No. 200 sieve

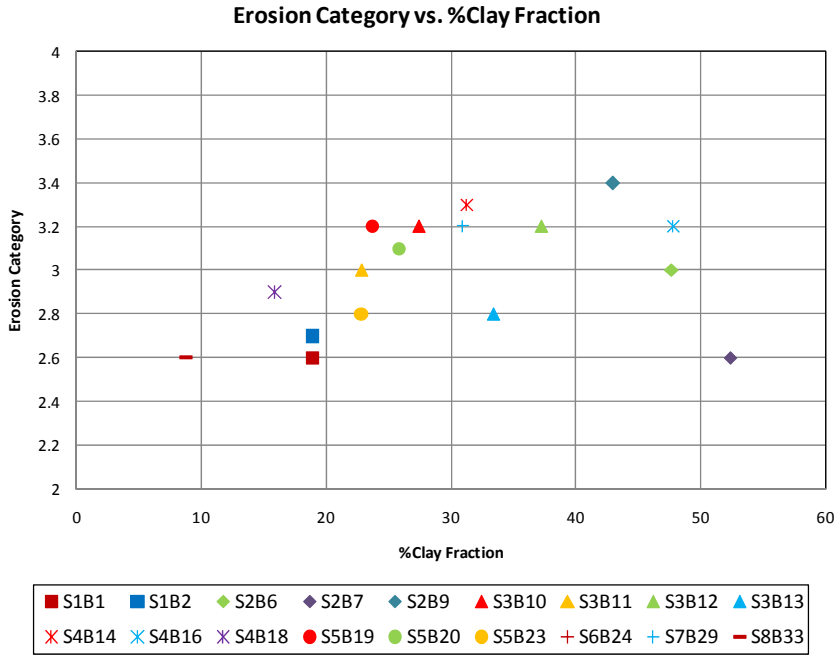

Fig. 201. Erosion category vs. clay fraction

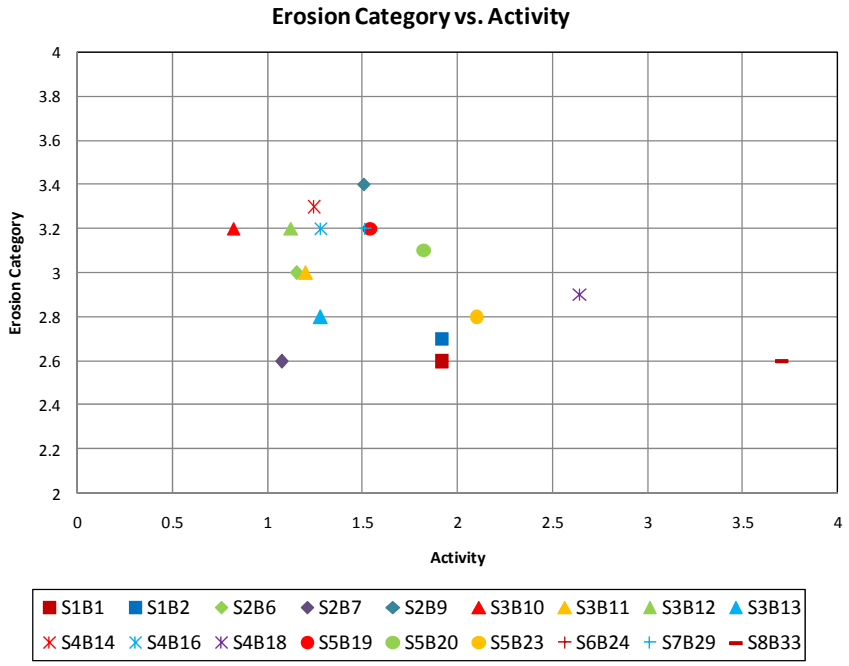

Fig. 202. Erosion category vs. activity

As the findings of White and Gayed (1943) suggest, the above plots show a trend with the percent clay content and erosion category. With the exception of the point S2B7, Figs. 199 and 201 show that as the clay content increases the erosion category increases meaning the soils are more resistant to erosion. The clay size particles were defined as 2 μm, but other previous studies have shown correlations with larger particles. Because the data was available, erodibility category was plotted versus percent smaller than 5 μm (Fig. 203), D_{60} (Fig. 204), D_{10} (Fig. 205), D_{30} (Fig. 206), C_u (Fig. 207), and C_c (Fig. 208). Only the fine grained materials are shown. Fig. 203 shows a trend similar to that of percent clay, only more concentrated. The particle size chosen for percent clay was 2 μm.

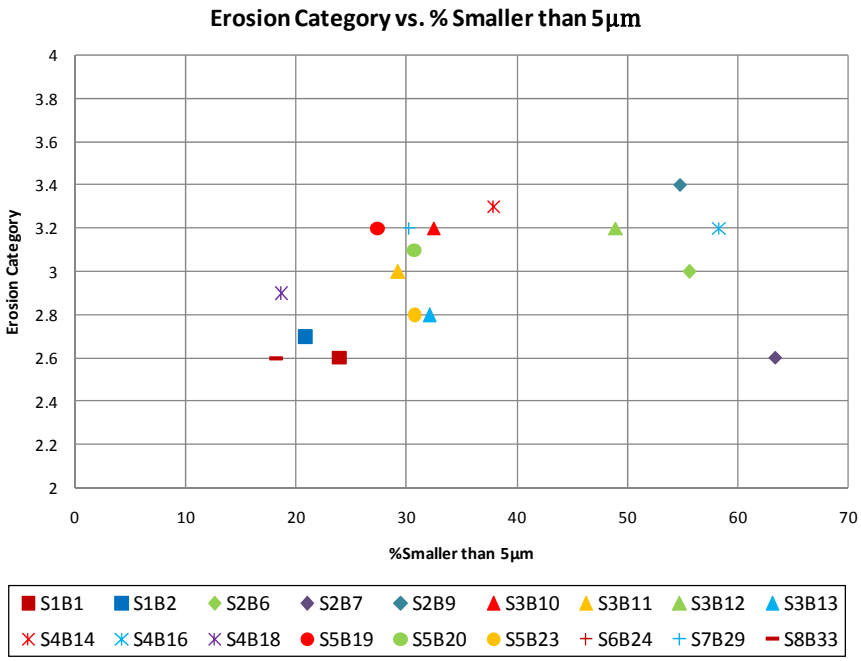

Fig. 203. Erosion category vs. percent smaller than 5 µm

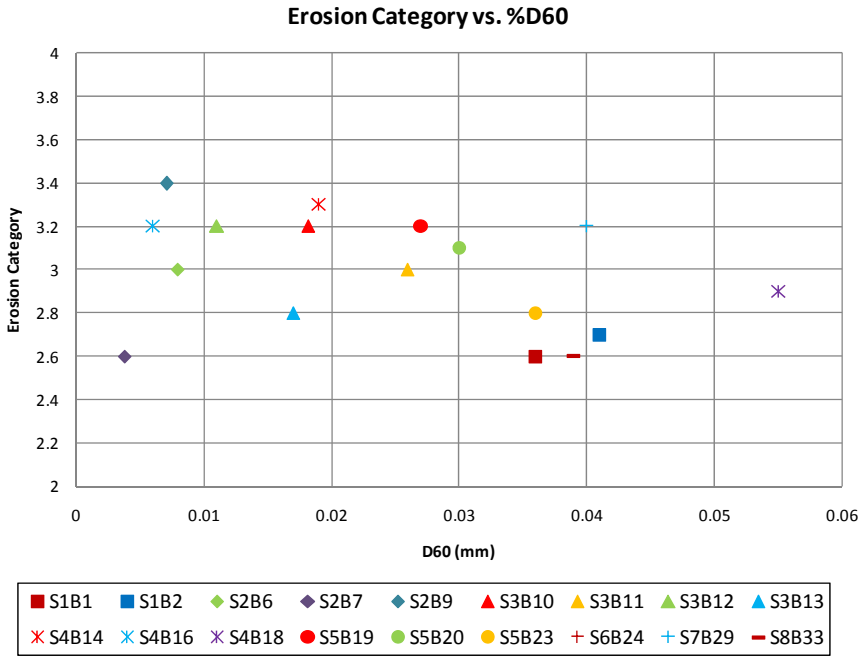

Fig. 204. Erosion category vs. D_{60}

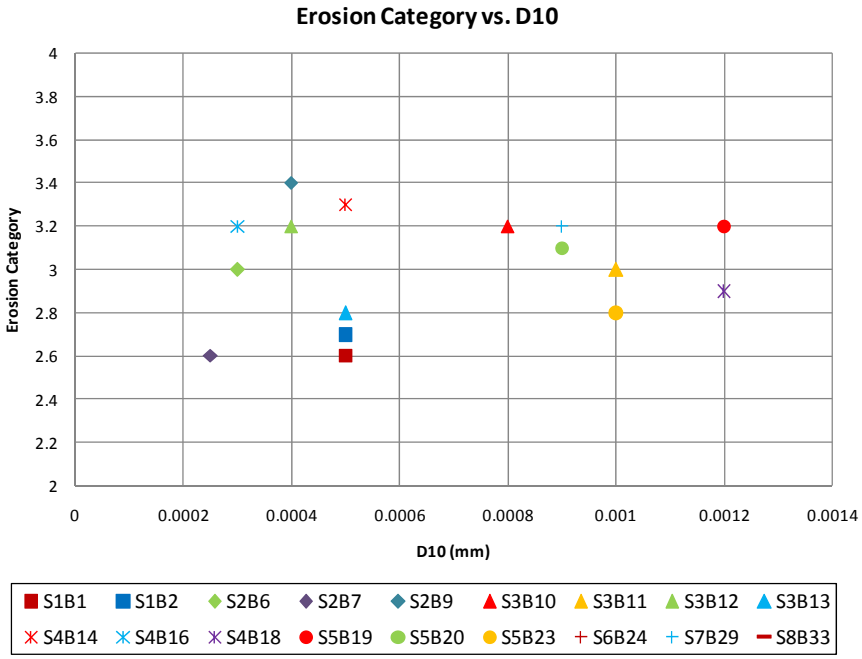

Fig. 205. Erosion category vs. D_{10}

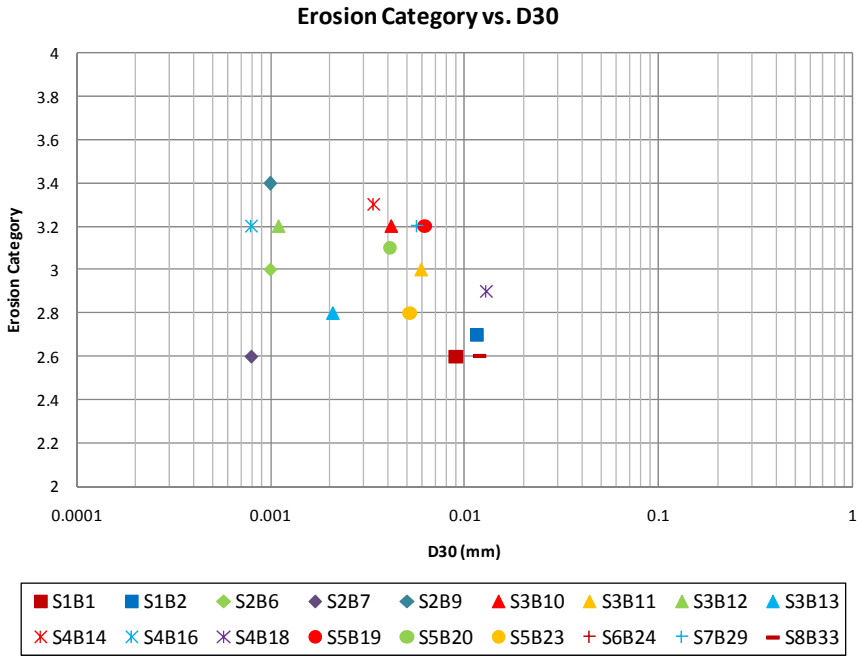

Fig. 206. Erosion category vs. D_{30}

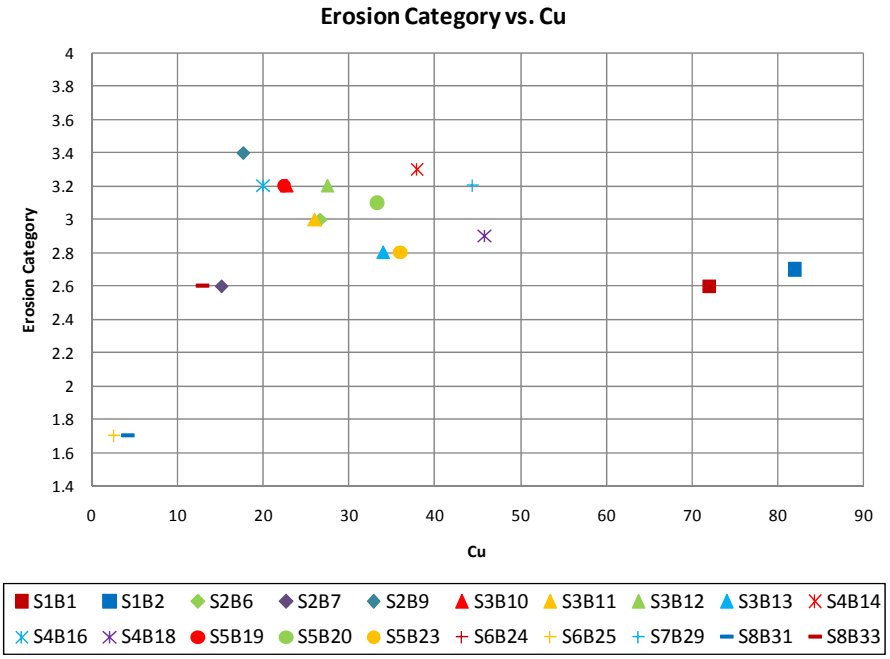

Fig. 207. Erosion category vs. C_u

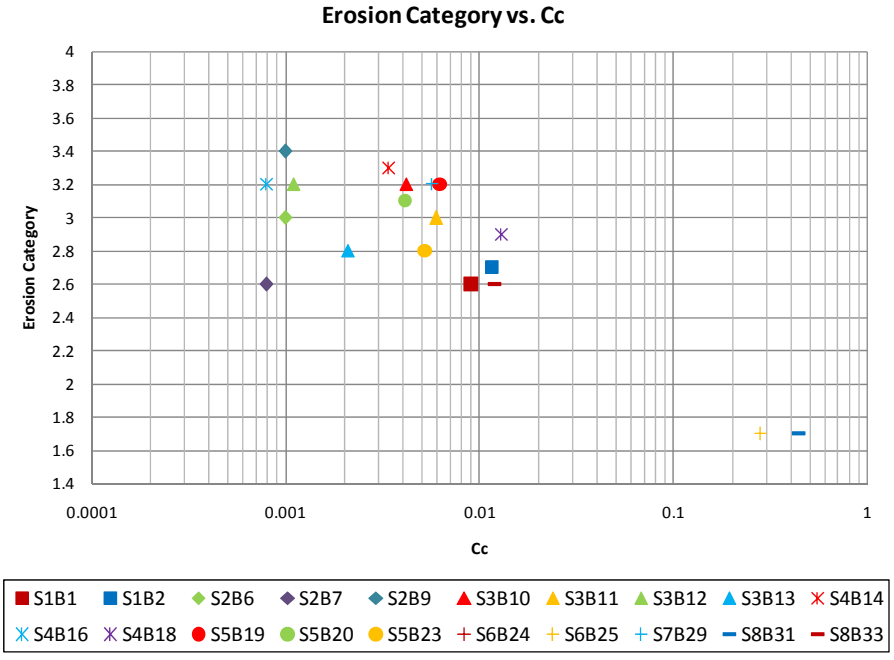

Fig. 208. Erosion category vs. C_c

The plots of Cu and Cc for the fine grained materials show that as these values increase, the erosion categories decrease. The coefficient of uniformity, Cu, and the coefficient of curvature, Cc, describe how well or poorly graded a material is. These are normally found as a classification means for granular materials.

7.9 EFA Erosion Rate at 3 m/s Velocity Correlations

As mentioned previously, the use of one point of the erosion function should be used with caution. However, correlating the various parameters with the erosion rate at 3 m/s can give an insight into how each one affects erosion. The erosion rate at 3 m/s velocity for each sample was plotted versus D_{50} (Figs. 209 and 210), PI (Fig. 211), relative compaction (Fig. 212), max dry density (Fig. 213), in situ water content (Fig. 214), excess water (Fig. 215), and in situ dry mass density (Fig. 216). The erosion rate value was extrapolated with the regression lines used to find critical velocity for those samples that were not tested near 3 m/s velocity. Erosion rate versus D_{50} was plotted at two different scales to show the results with the inclusion of the sand shell soils.

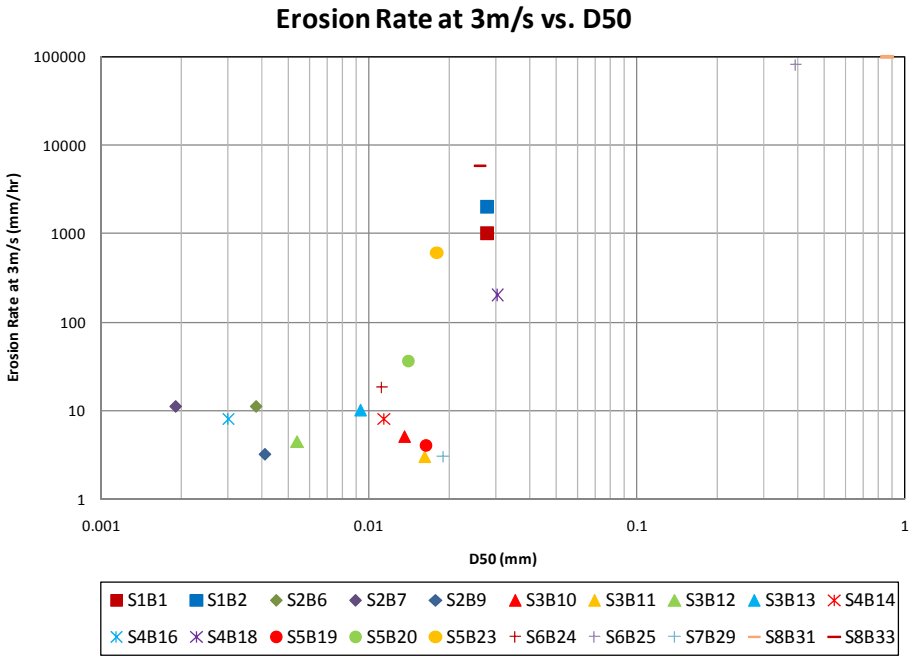

Fig. 209. Erosion rate at 3 m/s vs. D_{50}

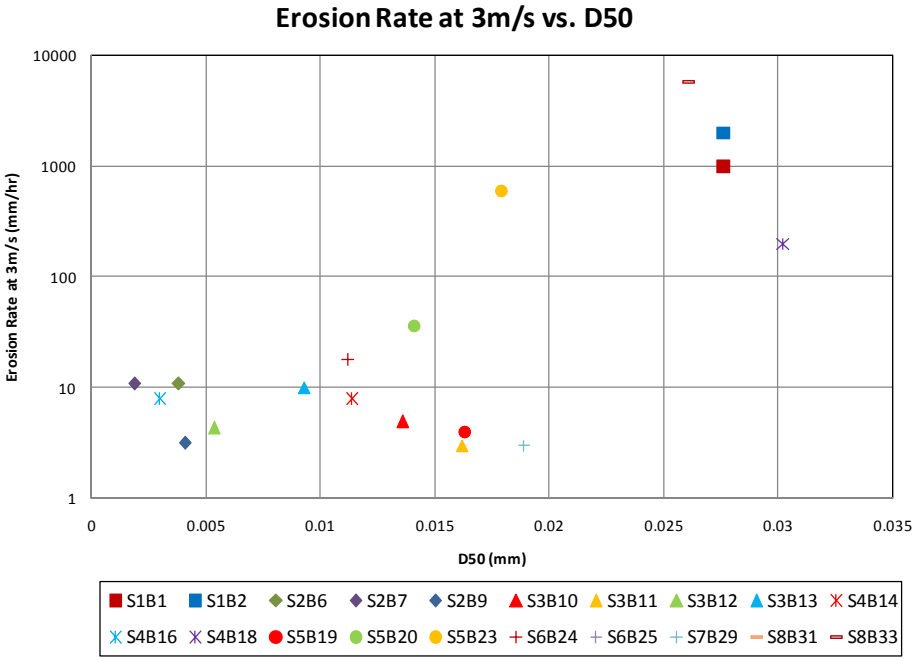

Fig. 210. Erosion rate at 3 m/s vs. D_{50} – fine grain soils only

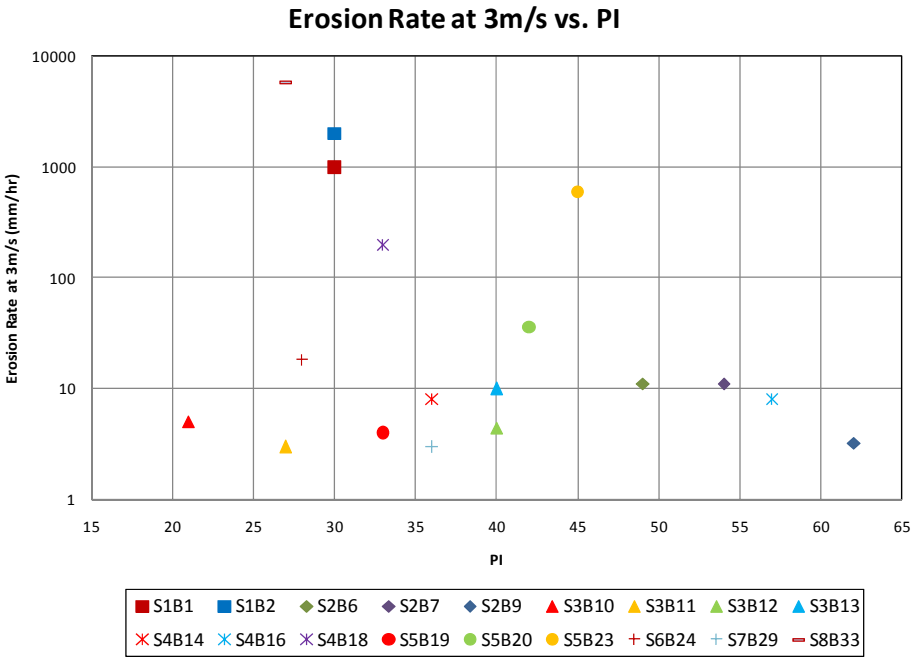

Fig. 211. Erosion rate at 3 m/s vs. PI

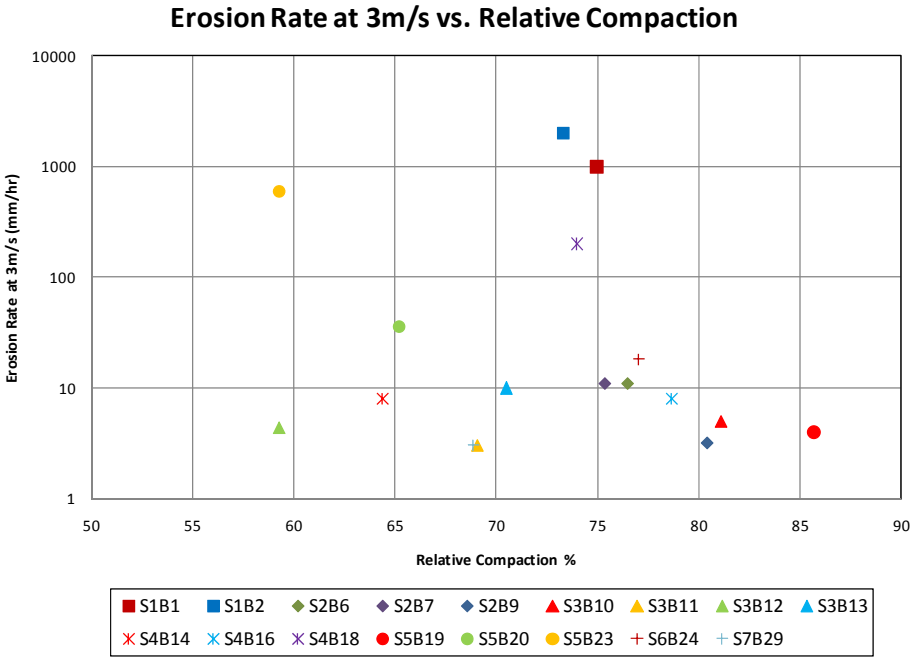

Fig. 212. Erosion rate at 3 m/s vs. percent relative compaction

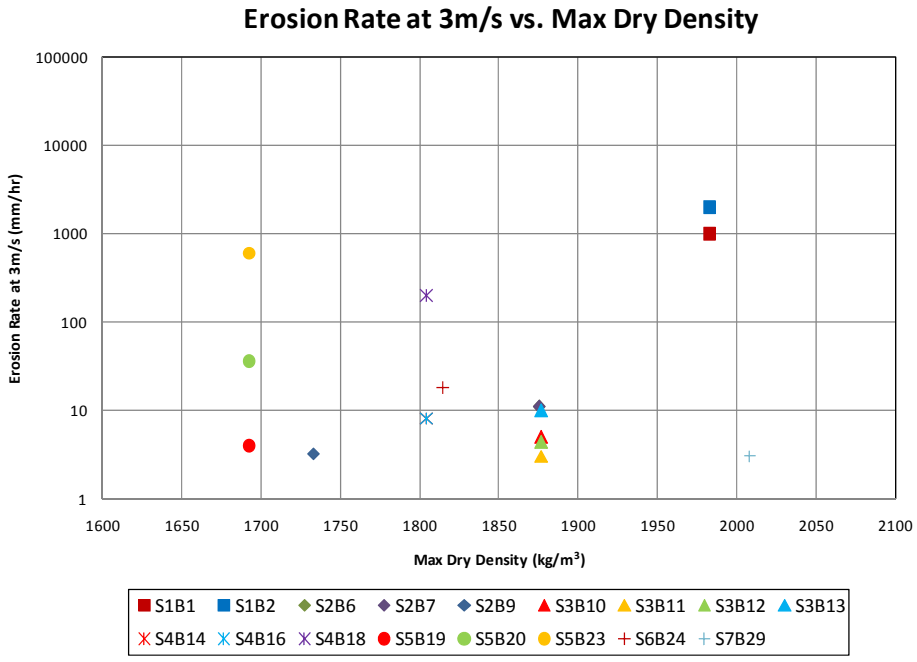

Fig. 213. Erosion rate at 3 m/s vs. max dry density

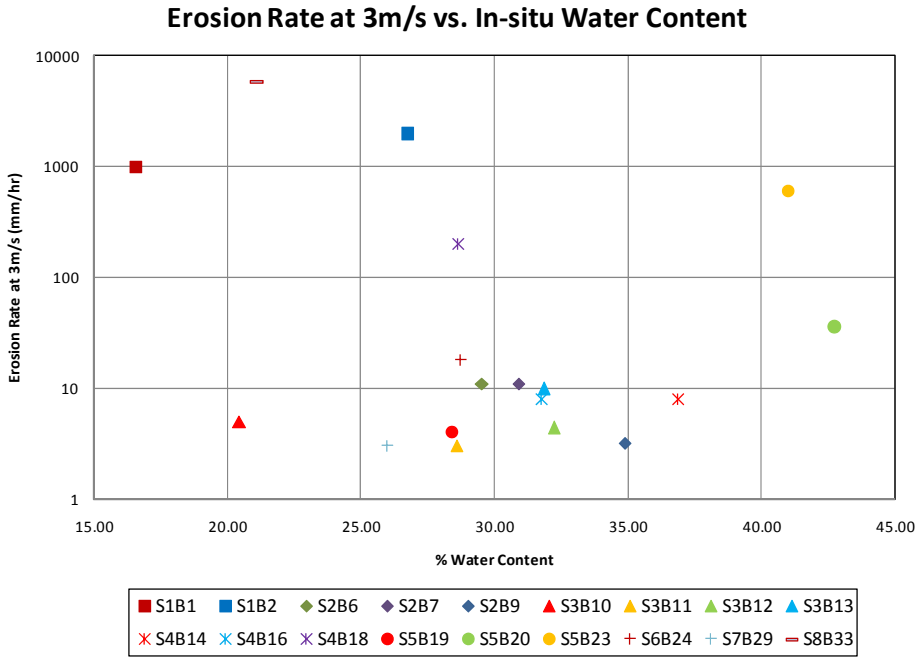

Fig. 214. Erosion rate at 3 m/s vs. in situ water content

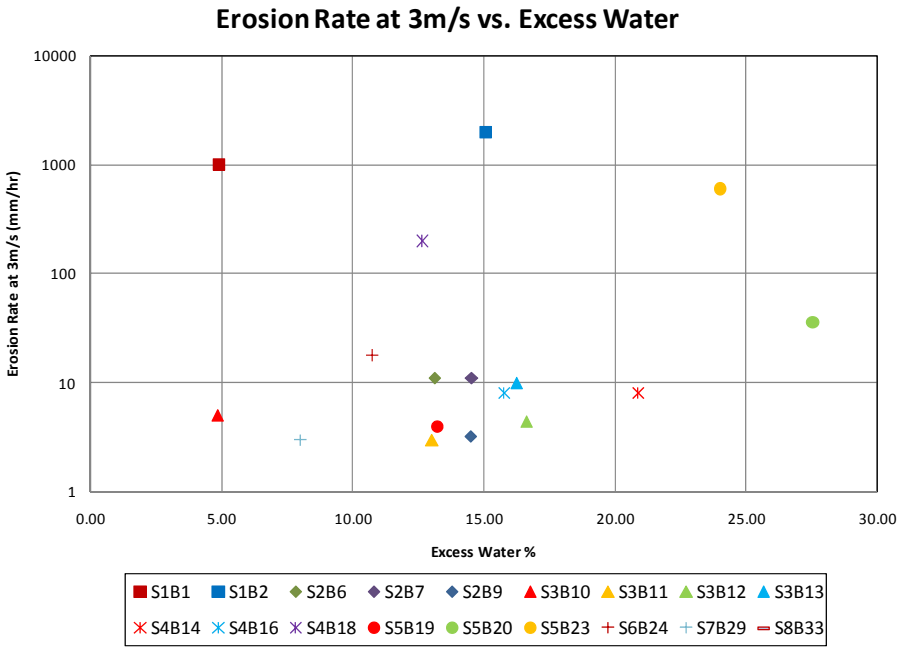

Fig. 215. Erosion rate at 3 m/s vs. excess water

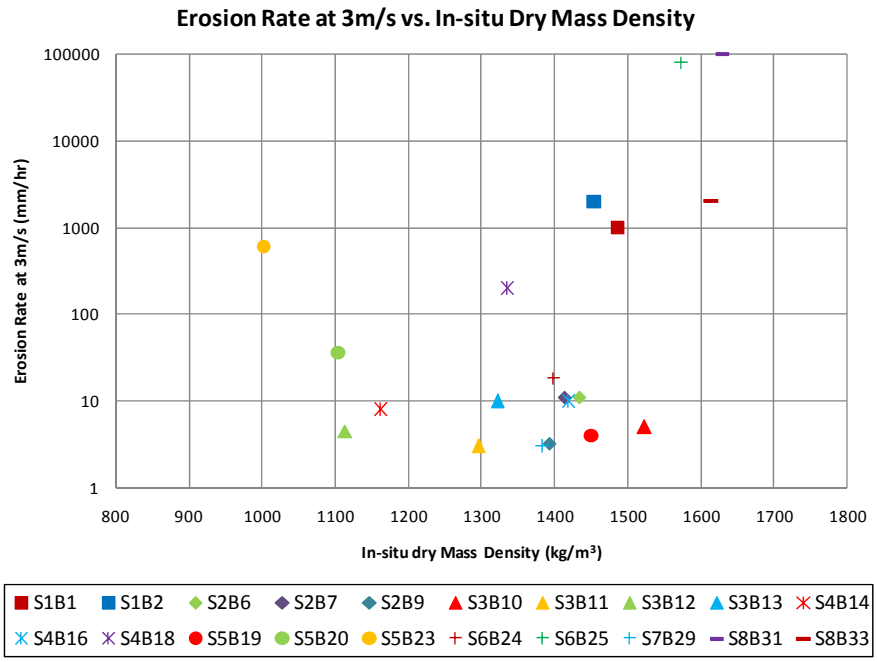

Fig. 216. Erosion rate at 3 m/s vs. in situ dry mass density

The correlation with D_{50} holds the trend expected from the other previous results. While there is quite a bit of scatter, the plot of in situ dry mass density shows that as the dry mass density increases, the erosion rate increases (Fig. 216). More sandy particles have higher dry mass densities and also erode more quickly. Similar to the previous analyses, several other comparisons were made including: percent clay (Fig. 217), percent passing the No. 200 sieve (Fig. 218), percent clay fraction (Fig. 219), and activity (Fig. 220).

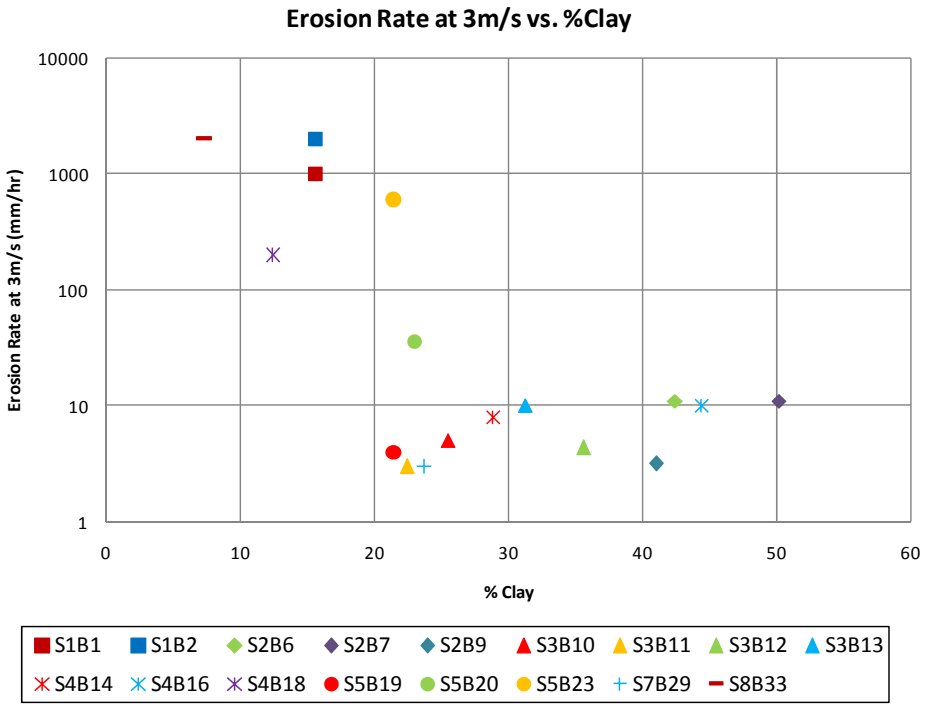

Fig. 217. Erosion rate at 3 m/s vs. percent clay

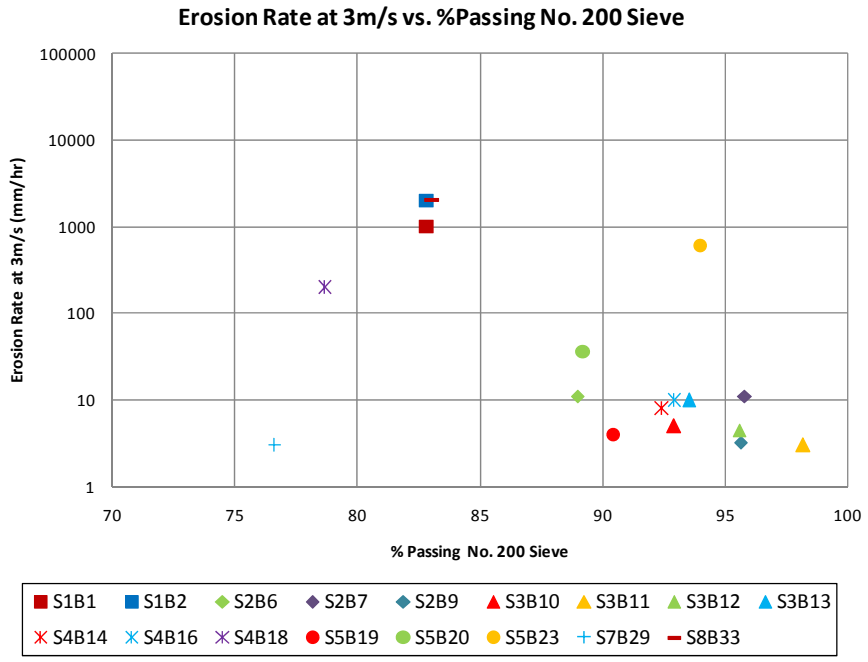

Fig. 218. Erosion rate at 3 m/s vs. percent passing No. 200 sieve

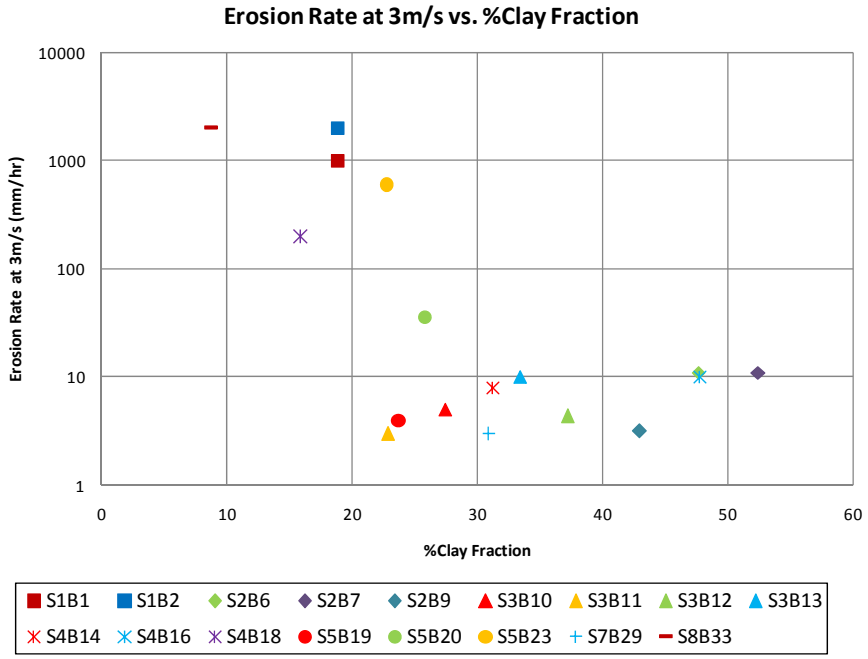

Fig. 219. Erosion rate at 3 m/s vs. percent clay fraction

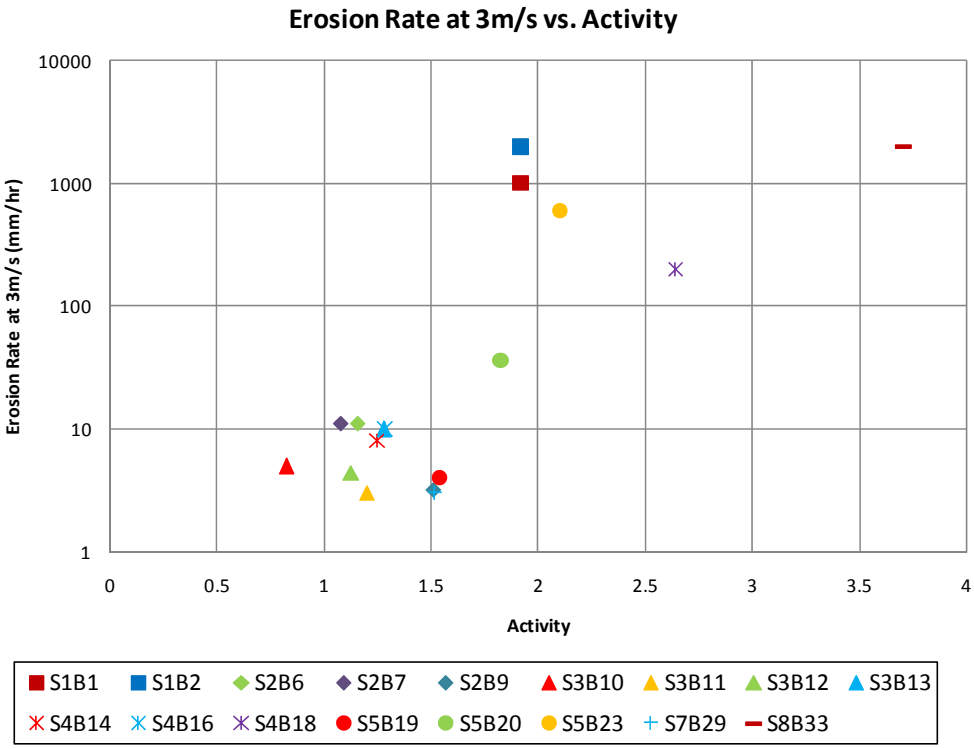

Fig. 220. Erosion rate at 3 m/s vs. activity

Once again, these plots show that as the clay content increases, the erodibility of a soil is decreased. A noticeable trend is shown in the plot of erosion rate versus activity. As activity increases, so does the erosion rate. Activity is a measure of how active the clay in the soil is. For soils with low clay content and a higher PI, the activities are large. This plot combines the effects of clay content and plasticity. Soils that might be highly plastic, but do not have high clay contents (high activities) are not necessarily resistant to erosion. However, a low plasticity clay with high clay content (low activity) may resist erosion quite well. This means that erodibility is tied mostly to clay content and particle size which agrees with the previous erosion category findings.

Because the data was available, erosion rate at 3 m/s was also plotted versus percent of particles smaller than 5µm (Fig. 221), D_{60} (Fig. 222), D_{10} (Fig. 223), D_{30} (Fig. 224), C_u (Fig. 225), and C_c (Fig. 226).

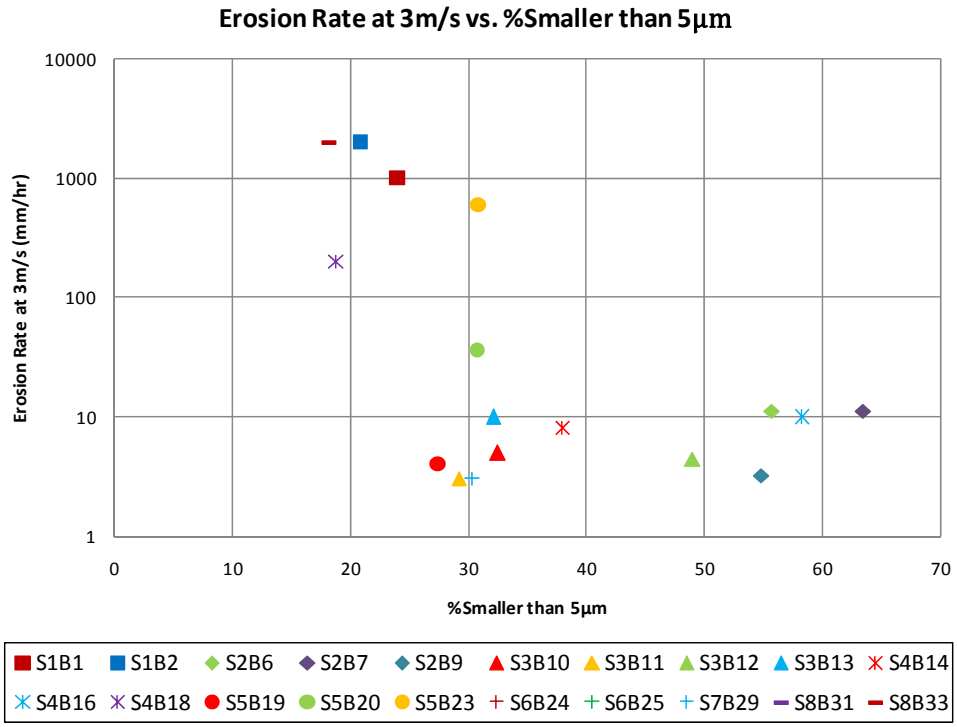

Fig. 221. Erosion rate at 3 m/s vs. percent smaller than 5µm

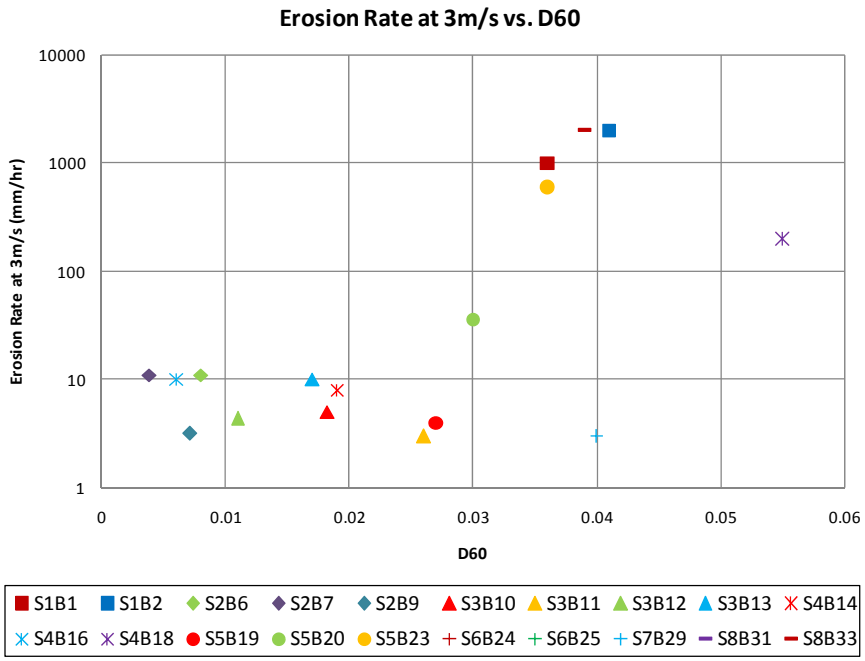

Fig. 222. Erosion rate at 3 m/s vs. D_{60}

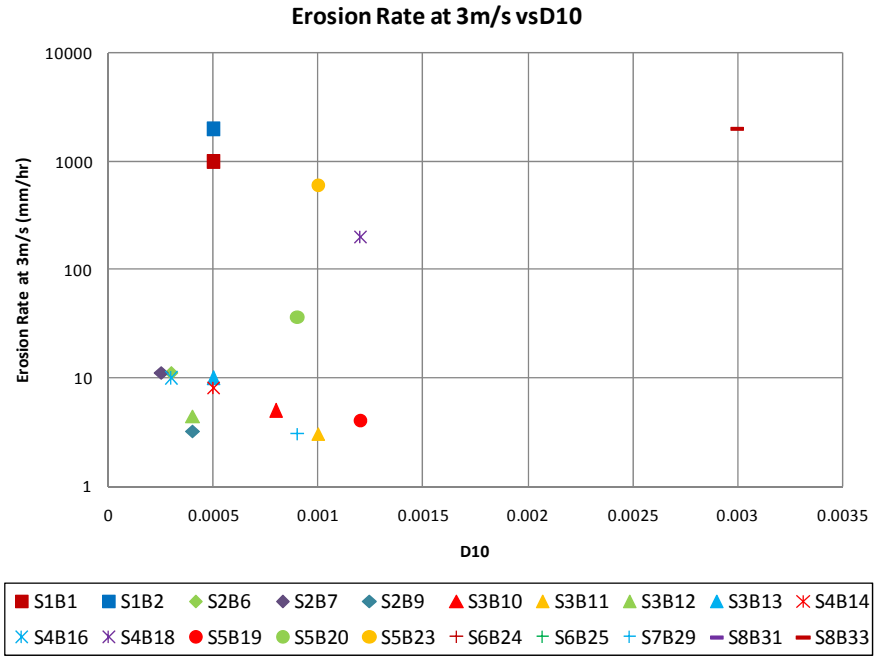

Fig. 223. Erosion rate at 3 m/s vs. D_{10}

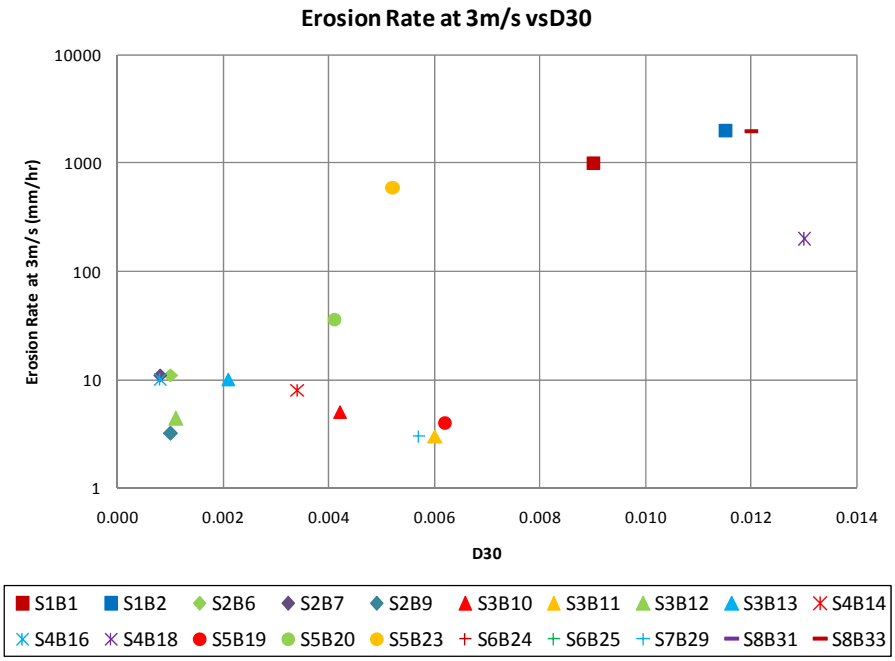

Fig. 224. Erosion rate at 3 m/s vs. D_{30}

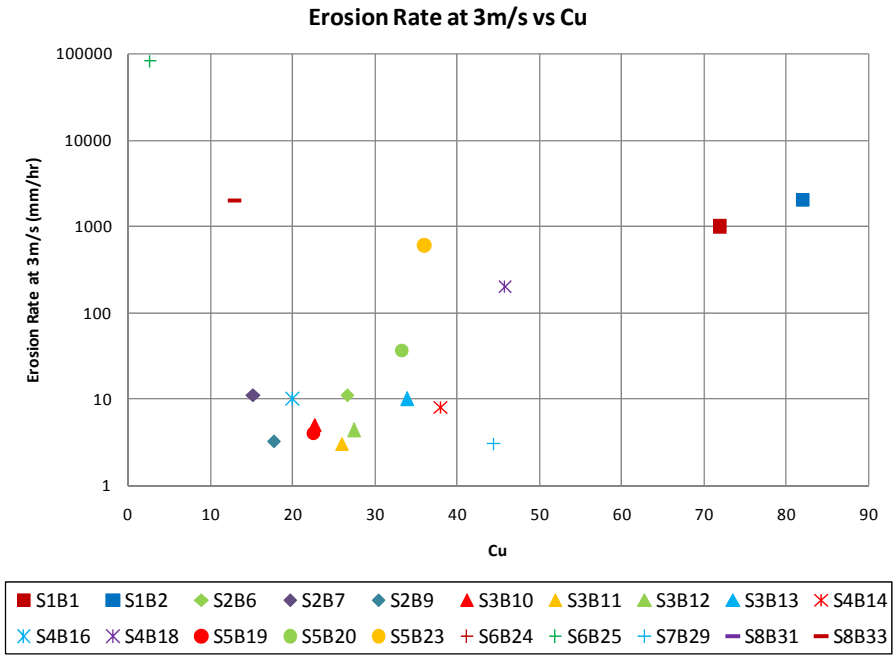

Fig. 225. Erosion rate at 3 m/s vs. C_u

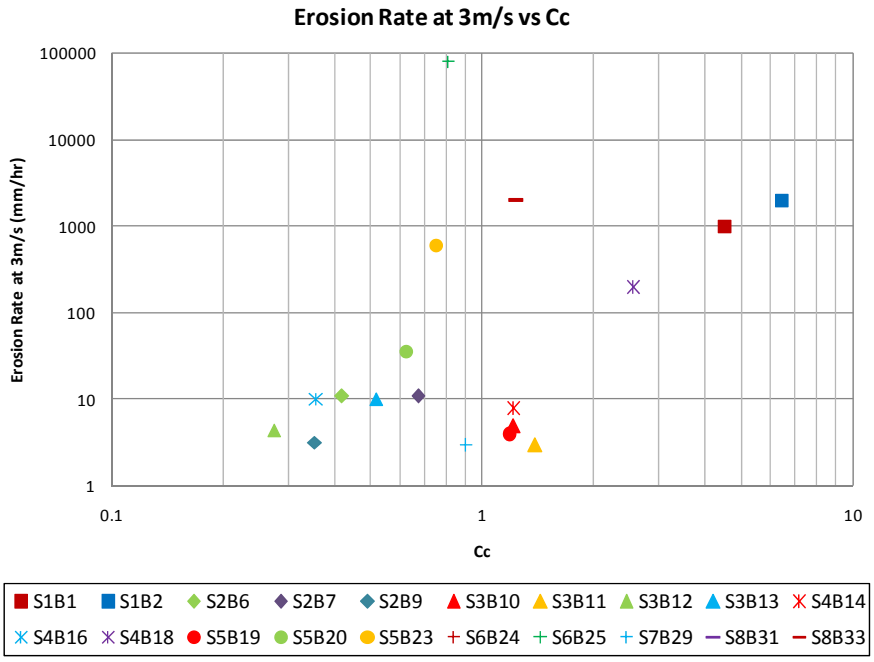

Fig. 226. Erosion rate at 3 m/s vs. C_c

With the exception of a couple of points, the plots of C_u and C_c are similar to those presented in the erosion category section. As C_u and C_c increase, the erosion rate also increases.

7.10 Pocket Penetrometer and Torvane Correlations

At the sites visited during the field reconnaissance, Pocket Penetrometer and Torvane values were determined in each location a sample was taken. These values were plotted versus critical velocity, erosion category, and erosion rate at 3 m/s velocity to see if erodibility related to any existing field tests. Figs. 227 through 232 show these graphs.

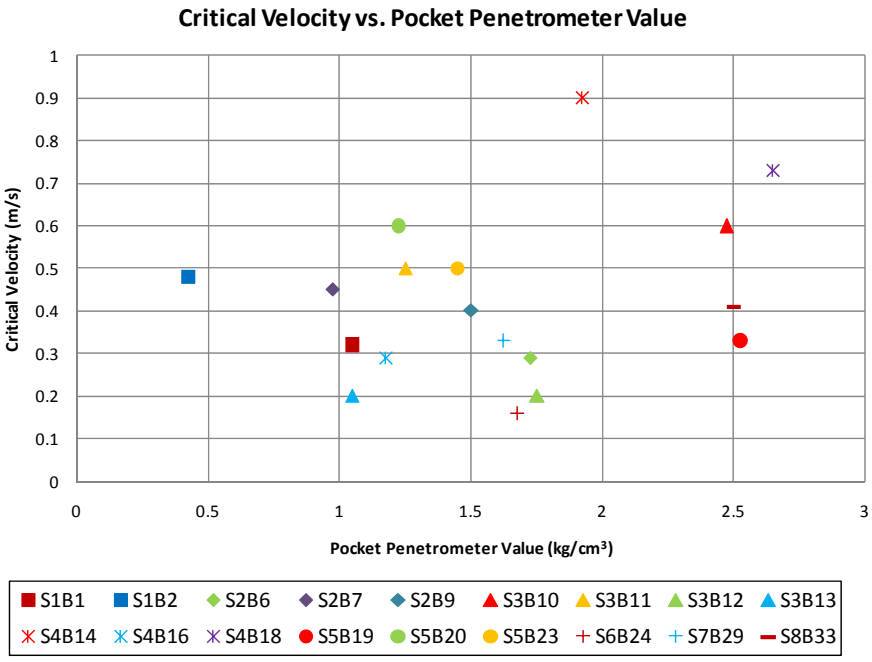

Fig. 227. Critical velocity vs. Pocket Penetrometer values

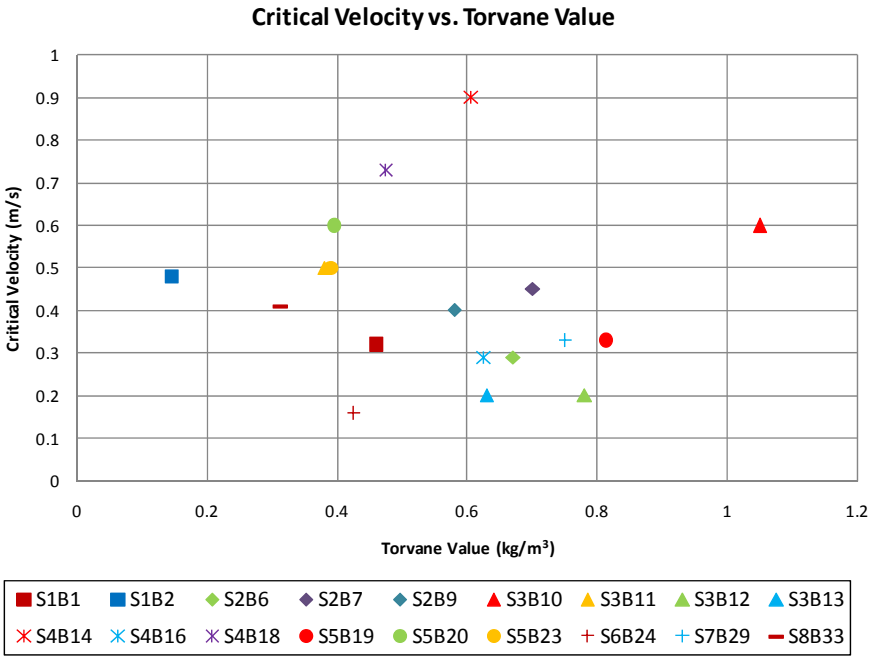

Fig. 228. Critical velocity vs. Torvane values

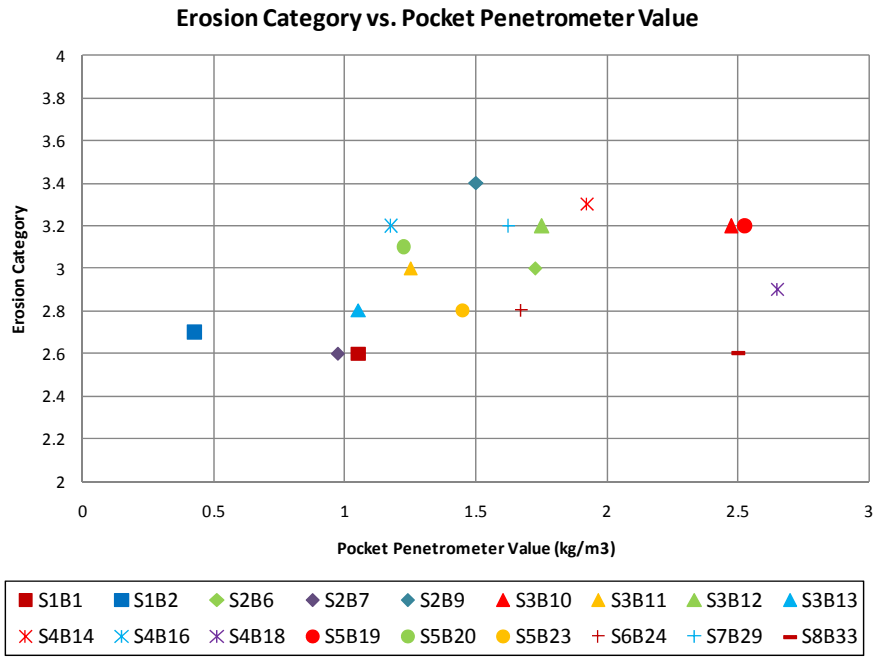

Fig. 229. Erosion category vs. Pocket Penetrometer values

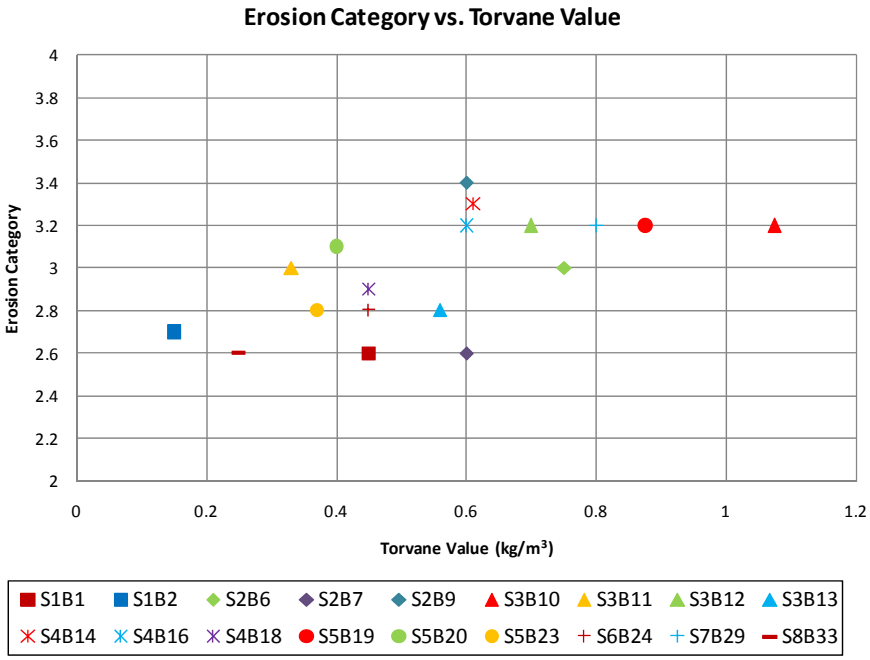

Fig. 230. Erosion category vs. Torvane values

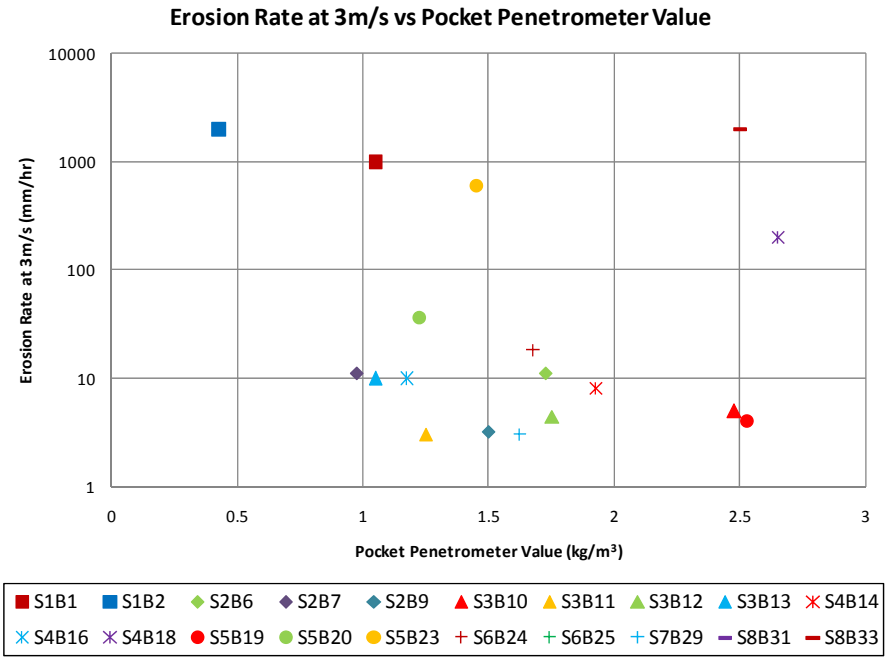

Fig. 231. Erosion rate at 3 m/s vs. Pocket Penetrometer values

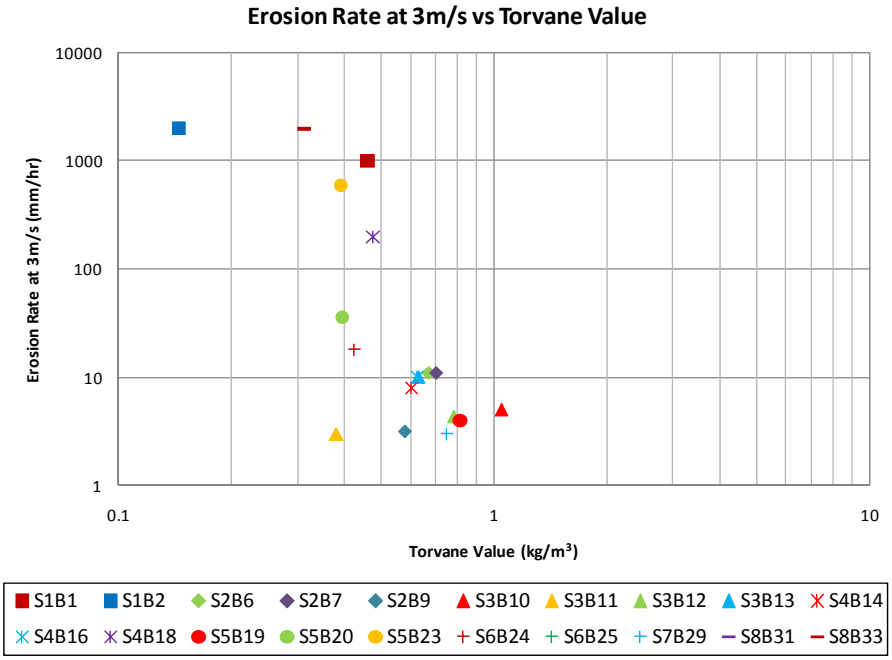

Fig. 232. Erosion rate at 3 m/s vs. Torvane values

No correlations were found for critical velocity, however, both erosion category and erosion rate at 3 m/s seem to be tied to the Torvane values. For both graphs (Figs. 227 and 229), as the Torvane reading increases, the erodibility of the soil decreases. This is shown by and increasing erosion category and decreasing erosion rate.

While all of these correlations give insight into the relationships of soil erodibility and various other parameters, they do not take into account site conditions that have proven to be very important. Site characterization is not only based on the soil properties and behaviors at the site, but also on things such as vegetative cover and low lying areas or seepage that can lead to concentrated flows. As shown by these results, all soils erode. No matter how resistant a soil is, under the right flow velocities and duration of overtopping it may erode enough to lead to progressive failure of an earthen embankment.

8. POCKET ERODOMETER EROSION CATEGORIES

Because of the many different factors that interact in the erosion phenomenon, it is important to be able to get a "real time" field or in situ erosion value for a given soil. Sample disturbance, density, and water content are all variables that affect the erosion rate and must be considered before tests are performed. It is extremely important to get at least a field estimate of the erosion rate of a given soil at the time of sampling for situations in which erosion values are needed. By the time the soil has reached the lab for testing, there is a chance the some of the previously mentioned variables will have changed. A quick field estimate of erosion rate is a beneficial supplement to any field in situ or lab testing performed and can provide an inexpensive check for possible erosion issues.

Because of the importance of site specific erosion data, there is a need for a method that can efficiently test the erosion resistance of a particular soil. In the last 20 years, several devices have been developed in an effort to quantify how erosive a soil is. These devices were discussed in detail in Sections 2.5 and 2.6. These methods, whether they occur in the field or laboratory, are each unique in their respective ways, but all of them require substantial set up and preparation. It is important to be able to get a measure of erodibility in a timely manner. The idea behind the Pocket Erodometer Test (PET) is to provide a procedure and device that do not require a lot of sample preparation, the need to transport large heavy equipment out to a site, or time spent in tedious calculations or waiting for lab results. It stems from the same idea as the well known Pocket Penetrometer. Although some would argue the Pocket Penetrometer's

legitimacy, most engineering and geotechnical drilling companies record this value and while they would not use it for design, it is considered a preliminary estimate of strength of the material.

The PET is a regulated mini jet impulse generating device or simply stated, a squirt gun. The jet is aimed at the face of the sample and the water impulses carve an erosion hole that increases with depth each time the trigger is squeezed. The depth of the hole (mm) in the surface of the sample is recorded and compared to an erodibility chart to determine the erodibility category of the soil. This erosion category allows the engineer to make preliminary decisions in erosion related work.

8.1 Initial Stages of Development

Many different options were considered during the development of the Pocket Erodometer including the most appropriate device, velocities of different devices, direction of application, distance from the face of the sample, and repeatability from one tester to another. Both cohesive and cohesionless soils were tested during the development stages to make sure the procedure would work for any material. Porcelain clay was used as a standard. This type of clay is a low plasticity clay which was made into approximately 7.5 cm diameter samples using a pug mill. These samples represent a common Shelby tube sample taken by most drilling companies.

8.1.1 The Device

The size and type of the device was the first consideration. The apparatus needed to be small and easy to carry to a site, but still have enough power to cause erosion with a few number of squeezes. Garden sprayers were initially considered because of their ability to be pressurized. The trigger could be held for a defined number of seconds, and an erosion rate could be measured. After testing the device on a few samples they were ruled out because of complexity, size, and weight. Also, the amount of water and force of the jet stream were extremely too high. The end of the sample was left saturated and the depth of erosion was much too large in only a few seconds leaving the sample unusable for any further testing. Spray bottles were also tested, but the variability from one squeeze to another ruled them out as well. The water gun was deemed as the most appropriate tool because of its size, weight, and simplicity.

A number of different water guns were tested in order to get an idea of the water jet needed to get a measureable amount of erosion to occur in a reasonable number of squeezes. Guns with a lower velocity had to be squeezed at least 50 times to get erosion to occur in some samples. After several tests, it became clear that this number of squeezes was extremely too large. The smallest waster guns had the largest force of water jet and worked ideally because of their size and weight. The guns were also checked to make sure that a complete test could be run before having to refill. The small guns had a capacity of approximately 60 squeezes before air started to be pumped into the line. The actual velocity for the water guns was found by a very simple calibration method discussed in a following section. The water gun with a velocity of

approximately 8 m/s was used during the initial calibration steps. Fig. 233 shows an actual picture of the gun used during the test development. These were purchased at Wal-Mart in a pack of 8 for about $0.40 a piece.

Fig. 233. PET apparatus

8.1.2 Direction of Application and Distance from Surface

The direction the water was aimed was also a concern. Initially, the sample was held vertically with the Pocket Erodometer pointed down at the surface of the sample, but after a few tests it was determined that the particles of soil fell back into the hole rather than being washed away. There was some fear that the hole created would vary from soil type to soil type because the more sandy particles weigh more and would fall back into the hole leading to erroneous results. Also, the hole filled with water and the force of the jet was dissipated in the water instead of on the soil surface leading to variable results. Shooting the guns vertically allowed water to enter the line after only a few squeezes so the same force was not exerted each time.

The method decided on was to hold the sample or place the sample horizontal on a flat surface and aim the device horizontally at the end of the sample. The soil particles are washed from the hole and gravity helps clear the hole of water and soil so that each water impulse strikes a similar surface. This is shown in Fig. 234.

Fig. 234. PET with horizontal orientation

The distance between the end of the Pocket Erodometer and the soil surface was also taken into consideration. Too far away it was difficult to continuously shoot the jet in the same hole and the hole widened instead of deepened. Too close and it was hard to tell what was happening. The best distance was decided after several trials to be 5 cm.

8.1.3 Methods

Initially, the PET was designed to determine the number of water impulses/squeezes for 5 mm of erosion to occur. For some soils it was very difficult to reach 5 mm of erosion and for a few it was impossible even using the highest velocity device. The test procedure was then adjusted to a set number of squeezes and a

measured erosion depth. The depth of the hole was measured with the back end of a digital caliper. The series of pictures in Fig. 235 shows snapshots of the test progression.

Fig. 235. Snapshots of PET procedure

After testing several soil types, the number of squeezes was set at 20. An increased number of squeezes showed little increased benefit after a point for two different types of soil (Fig. 236).

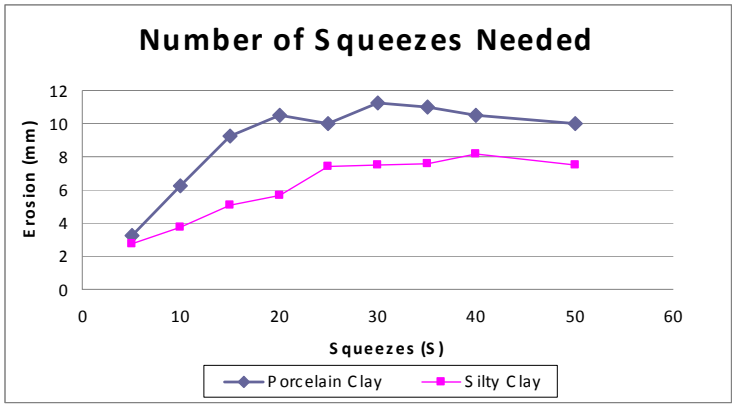

Fig. 236. Number of squeezes, S vs. erosion depth, Z

8.1.4 Repeatability

Another concern was the variability in the test from one person to another. Several testers were chosen to see whether or not there was any difference in the results. Each person performed a test to see how far the water traveled from the end of the gun when held at a given height, as well as a full test on the porcelain clay using the PET procedure. Both tests had variable results from person to person. It became obvious that there was a great effect based on how quickly the trigger was pulled, and so it was necessary to develop a calibration procedure so that each tester could develop the same velocity jet stream. After the calibration procedure, each subject was able to reproduce similar results to those shown above.

8.1.5 Velocity Calibration

A very simple calibration method was used to determine the approximate velocity of the purchased water guns. The same method was used to guarantee each tester was generating the appropriate velocity for each squeeze. As mentioned above, many different styles of guns were purchased all with different velocities. It was important to obtain the specific velocity of the particular device chosen for the Pocket Erodometer. After determining the velocity for the Pocket Erodometer, a pack containing eight of the same guns were tested and found to have a mean of 7.5 m/s and a standard deviation of 1.2 m/s (Table 25).

Table 25. Comparison of similar purchased water guns

Gun	Height (in)	Avg. Distance (in)	Avg. Velocity (ft/s)	Avg. Velocity (m/s)
1	48	169.5	28.3	8.6
2	48	153.3	25.6	7.8
3	48	155.8	26.0	7.9
4	48	134.5	22.5	6.9
5	48	171.0	28.6	8.7
6	48	102.3	17.1	5.2
7	48	125.8	21.0	6.4
8	48	164.5	27.5	8.4
JLB	48	156.8	26.2	8.0
			Mean =	7.5
			Standard Deviation =	1.2

The calibration procedure employs the use of the particle motion equations and while it neglects several variables and may not give the exact velocity, it does give a standard that can be reproduced and can ensure similar use of the Pocket Erodometer from person to person. An area at least 4 m in length must be cleared for the testing area. The calibration can be run outside, but variables such as wind which are neglected in the equations can affect the results. The ideal situation is a concrete floor area of proper length. A table or other stable object can be used as a base for the gun so that it is at a constant height throughout the calibration process. The Pocket Erodometer should be placed on the table pointed so that the water stream travels horizontally. The tester should squeeze the trigger 20 times at a rate of 1 squeeze per second. Because the water stream is not a single particle there will be some scatter in how far the water travels horizontally before hitting the ground (Fig. 237).

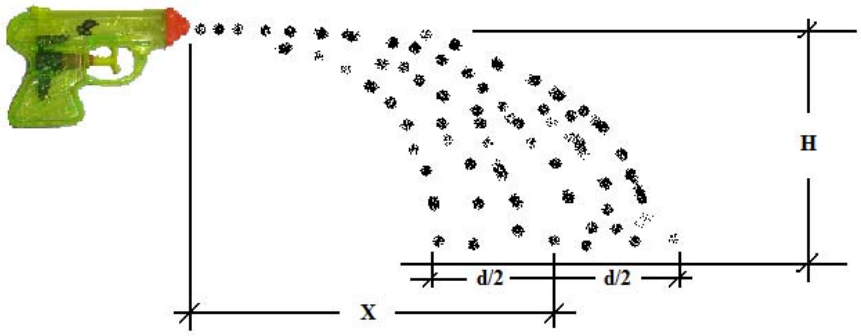

Fig. 237. Schematic of calibration dimensions

The distance should be marked at the two ends of the majority of the water on the floor surface. The extreme outliers should be ignored. These end values are averaged and then value is used in the particle motion equations:

$$x = v_{0x}\, t \tag{54}$$

$$H = \frac{1}{2} g t^2 \tag{55}$$

where x and H are defined on Fig. 237, v_{0x} is the horizontal nozzle velocity, t is the time and g is the acceleration due to gravity. Eliminating t between Eq. 54 and 55 gives:

$$v_{0x} = \frac{x}{\sqrt{\frac{2H}{g}}} \tag{56}$$

These steps can be used as a way to judge the amount of force to pull the trigger with before a test is run, and it is recommended that the procedure is done each day before testing begins to ensure similar results from day to day. The distance, X, needed

for the corresponding height can be taped off on the floor and the tester can pull the trigger multiple times to get a feel for the force needed to obtain the correct velocity.

8.1.6 Calibration Comparison with EFA Using Porcelain Clay

Once the device and the methods for the PET were developed, porcelain clay samples were used as a standard for calibration and comparison to the EFA results. The porcelain clay was essentially a low plasticity Kaolinite clay prepared by vacuum extrusion. In order to obtain meaningful results from the Pocket Erodometer tests the erosion depth was compared to the erosion rate versus velocity chart developed for the EFA. This chart displays six erosion categories ranging from very high erodibility to non-erosive. After the calculation of the velocity of the Pocket Erodometer, it was determined that one velocity would not be sufficient to span all of the possible erosion categories. Because of the relationship between nozzle diameter and velocity, the same guns were able to be made to have different velocities by widening the hole diameter at the exit point. A total of three different velocities (4 m/s, 6 m/s, 8 m/s) were chosen in order to span five of the six categories. The sixth category is for extremely resistant materials that cannot be realistically tested using the Pocket Erodometer.

Ten trials of the PET were run for each velocity Pocket Erodometer. For each test, the Pocket Erodometer was held 5 cm from the surface of the soil sample and 20 squeezes were performed at a rate of 1 squeeze per second. The erosion depth, Z, for each was recorded and the average was taken along with the standard deviation to check the variability of the test.

8.2 EFA and PET Midwest Levee Comparison

The PET was also performed on samples from the Midwest levees (Fig. 238). In order to make a comparison to the EFA, the erosion depth found from the PET must be converted to an approximate erosion rate. The length of time of the water impulse on the soil surface was estimated to be 0.5 seconds for each squeeze and 10 seconds total for each trial. The PET results were then compared with EFA results on the same samples in order to develop the PET erosion categories (Fig. 239). The samples from the Midwest levees were samples S1B2, S3B12, S5B19, and S6B25. The levee samples were all high plasticity clays except for S6B25 which was a poorly graded clean sand.

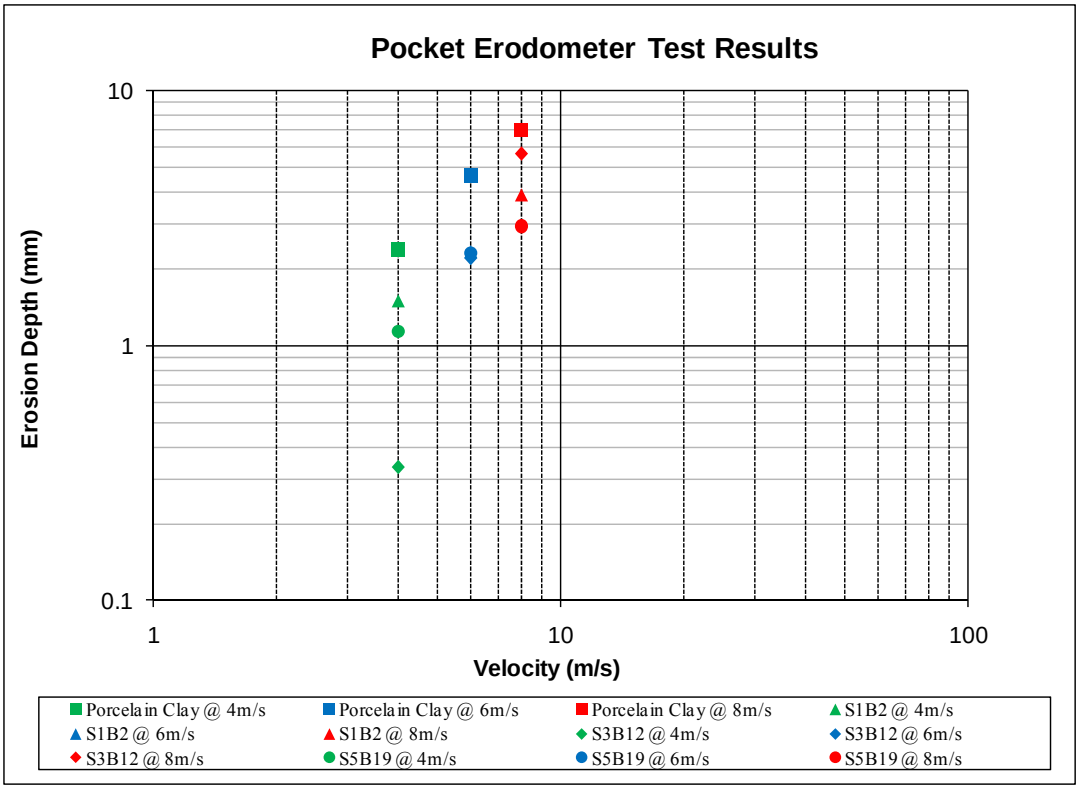

Fig. 238. PET results for porcelain clay and Midwest Levee data

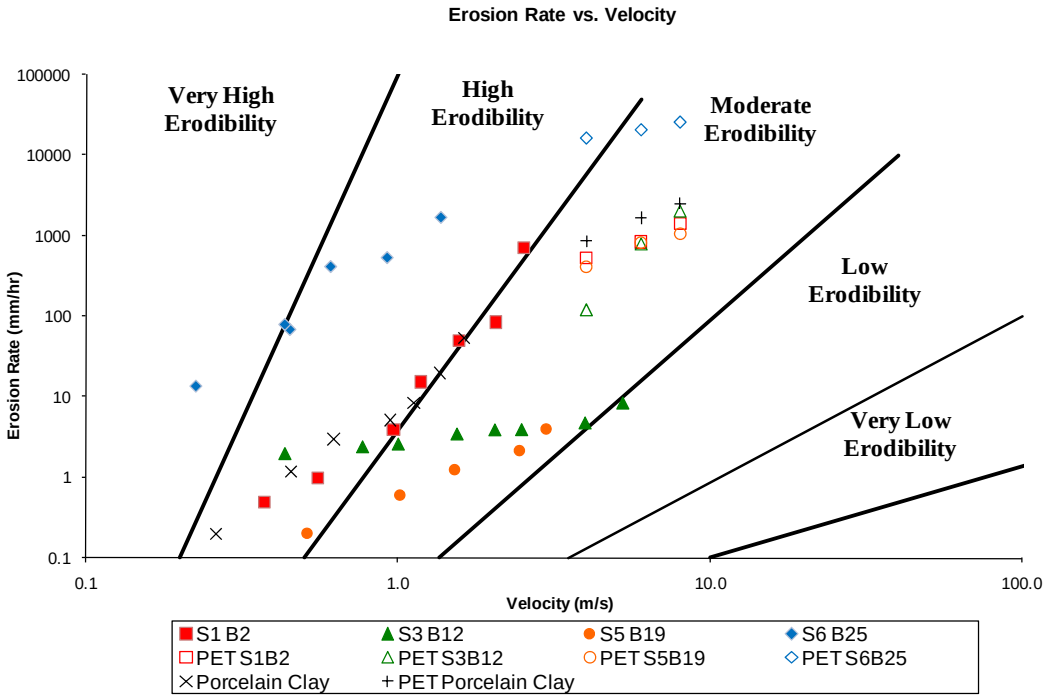

Fig. 239. EFA and PET comparison for Midwest Levee data

The points obtained with the PET plotted as an extension of the EFA erosion function for some of the samples. There is some discrepancy in two of the samples, however, both methods result in similar erodibility categories. It is likely that obtaining the PET erosion rate in that fashion is quite crude.

8.3 Pocket Erodometer Category Development

To avoid having to plot the results from the PET on the EFA erodibility chart while in the field, categories were developed based on the erosion depths for each PET (Fig. 240). The bold values shown on the chart represent the erosion depth, Z, in millimeters that defines the erodibility category of a given sample. These categories are based on the 8 m/s velocity test with the Pocket Erodometer. This velocity was chosen

because it showed the most measureable difference in the hole depths for the tested samples. The recommendations in Fig. 240 are based on a limited number of PET's and should be used with caution until further tests are done to corroborate these early results.

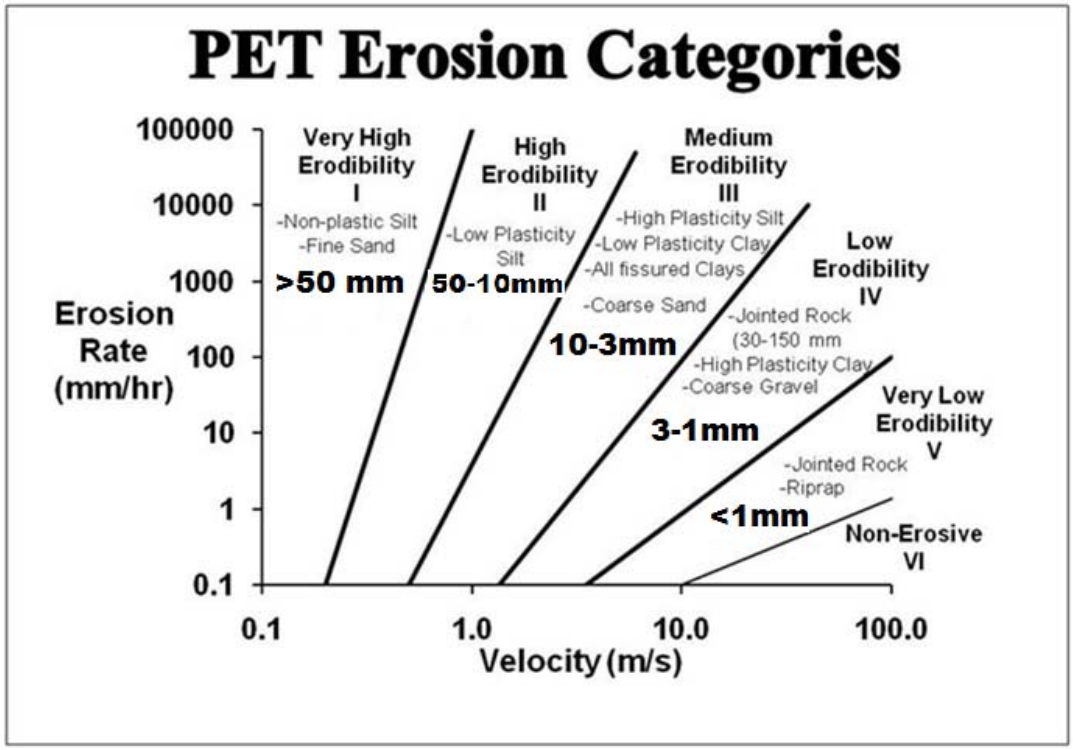

Fig. 240. PET erosion categories

The erosion categories determined by both the EFA erodibility chart and the PET erodibility chart are compared in Table 26. The values found using the PET agree reasonably well with those determined by the EFA tests. A difference of one category can be expected with the simple PET tests compared with the more expensive EFA test.

Table 26. Category comparison

Sample	Depth, Z	EFA Category	PET Category
Porcelain Clay	7	2	3
S1B2	4	2-3	3
S3B12	5.5	3	3
S5B19	3	3	3
S6B25	63	1-2	2

8.4 Recommended Pocket Erodometer Test Procedure

This test can be run on an extruded sample or on the exposed end of an un-extruded sample or yet on a reconstructed or compacted sample. It is recommended that the calibration steps be taken before beginning each testing session to ensure a proper velocity of 8 m/s for each test.

1. Place the sample horizontally either on a flat surface or by holding it in your hand.
2. Smooth the surface to remove any uneven soil. You want to begin with a smooth and vertical surface, so that it is easy to measure the erosion depth.
3. Hold the Pocket Erodometer (PE) pointed at the smooth end of the sample, 50 mm away from the face.
4. Keeping the jet of water from the PE aimed at a constant location, squeeze the trigger 20 times at a rate of 1 squeeze per second, forming an indentation in the surface of the sample. Each squeeze should fully compress the trigger and then the trigger should be fully released before it is re-compressed.

5. Using the end of a digital caliper or an appropriate measuring tool, measure the depth of the hole created.
6. The test should be repeated several times each in a different location and an average should be used to ensure a good estimate.
7. Determine the erosion category using Fig. 240.

8.5 Further Midwest Levee PET Evaluation

PETs were run on the remaining Midwest Levee samples. These samples were left over from the previous run EFA tests. The goal was to get EFA and PET categories for as close to similar sample conditions as possible. The category results from the PETs were compared to those obtained from the EFA (Fig. 241). The previous developed chart (Fig. 240) was used to determine the PET categories. As discussed above, there are several different ways to obtain the EFA categories. They can be taken as an average value across the erosion function or they can be based on the category the most number of points falls in. Both methods were considered. There is some discrepancy in the categories found for both methods (Table 27). Because of the way the numerical category system was developed, there is actually a range of numbers that get assigned to one main category label. When considering the range of the PET categories, the numbers seem to correlate quite well, except for those in PET categories 4 and 5. During the testing procedures for Samples S2B6, S2B7, S2B9, and S3B10 there was little erosion noticeable to the eye. All of the Midwest Levee samples had been in a humidity controlled room for several months between the EFA and PET testing. These

samples in particular seemed to have a much lower water content that would be expected after running the EFA tests on the sample. This could be the reason for the lower PET depth values and thus overestimated categories. Also, it may be that the PET boundary values need to be adjusted for categories 4 and 5. More testing is needed to determine which case it truly is. This work is still underway.

Table 27. Midwest Levee PET comparison

Sample No.	PET Depth, Z	EFA Category	PET Category	PET Category Span	Category based on Points
S1B1	3.58	2.6	3	2.5-3.5	3
S1B2	4	2.7	3	2.5-3.5	3
S2B6	0.425	3	5	4.5-5.5	3
S2B7	0.325	2.6	5	4.5-5.5	3
S2B9	0.2	3.4	5	4.5-5.5	4
S3B10	0.1	3.2	5	4.5-5.5	3
S3B11	1.13	3	4	3.5-4.5	3
S3B12	2.14	3.2	4	3.5-4.5	3
S3B13	2.225	2.8	4	3.5-4.5	3
S4B14	13.875	3.3	2	1.5-2.5	3
S4B16	1.45	3	4	3.5-4.5	3
S5B19	3	3.2	3	2.5-3.5	3
S5B20	3.14	3.1	3	2.5-3.5	3
S6B25	63	1.7	1	0.5-1.5	2
Porcelain Clay	7	2	3	2.5-3.5	2

The time duration of each impulse was recalculated by using a digital camera. The Pocket Erodometer was aimed and shot at a stationary metal plate. The number of frames that the water was shown impacting the plate was divided by the number of frames per second that the camera records at. This time was then converted to hours.

The erosion depth values from the PET were converted to erosion rates using the new calculated time. Fig. 241 shows the PET and EFA data.

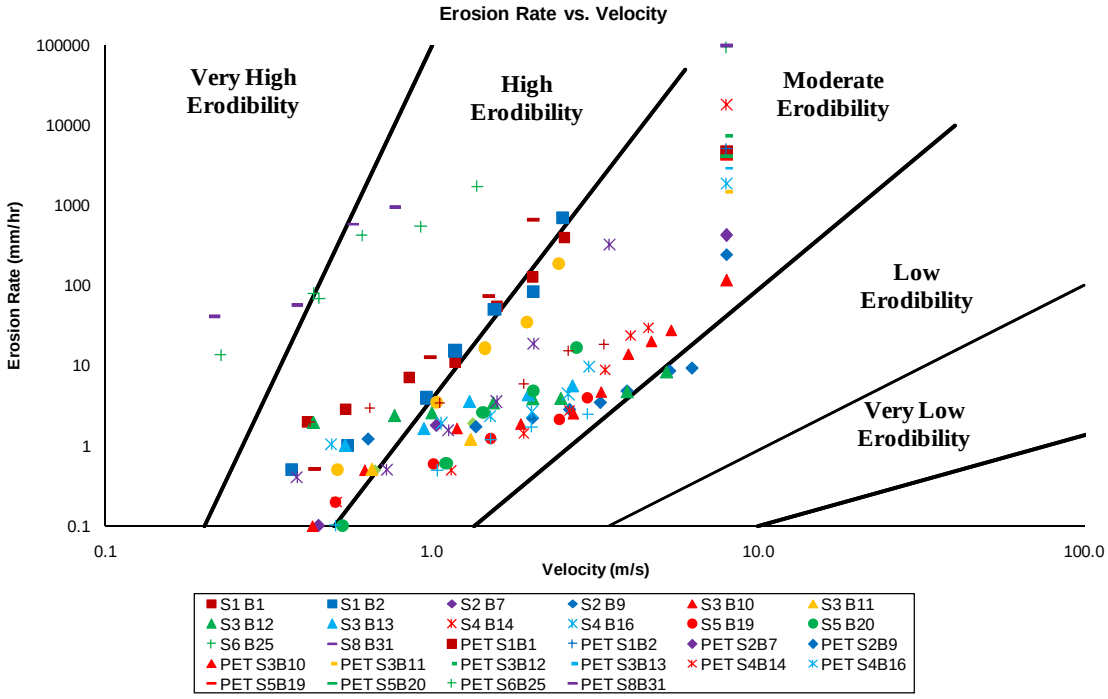

Fig. 241. EFA and PET results for Midwest Levee samples

Most of these values plot as extensions of the EFA data. Several of the PET values, however, overestimate the erodibility of the more resistant soils. One issue with the PET is that it may depend on the location the sample is tested at. Some areas are larger clumps of material and are more resistant to erosion. During several of the tests, larger clumps of material would be dislodged with only a few squeezes leading to higher rates of erosion. Similar to the previous correlations, PET values were plotted for D_{50} (Fig. 242), PI (Fig. 243), relative compaction (Fig. 244), max dry density (Fig. 245), percent clay (Fig. 246), percent passing the No. 200 sieve (Fig. 247), percent clay fraction (Fig. 248), and activity (Fig. 249).

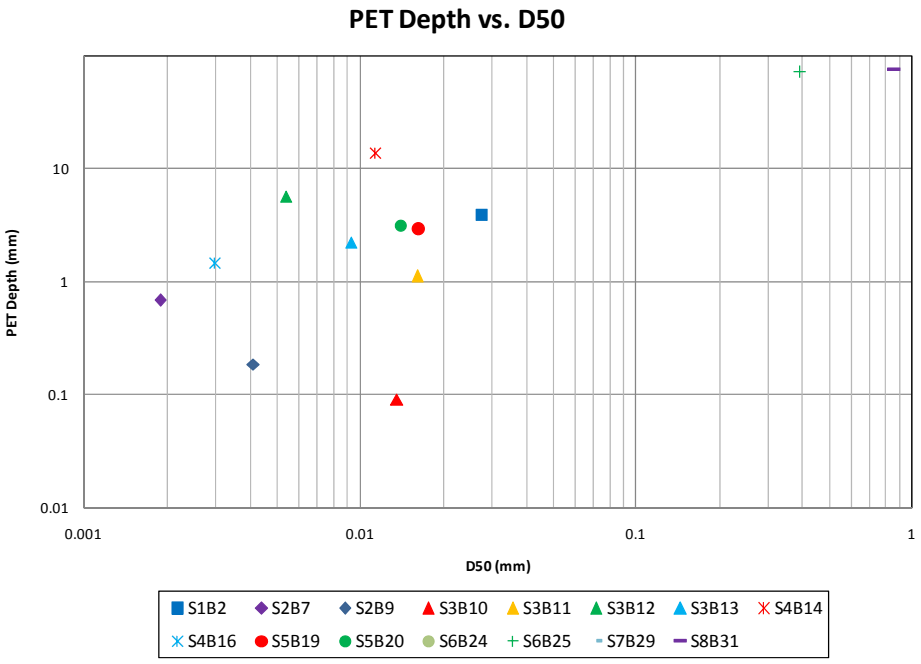

Fig. 242. PET depth vs. D_{50}

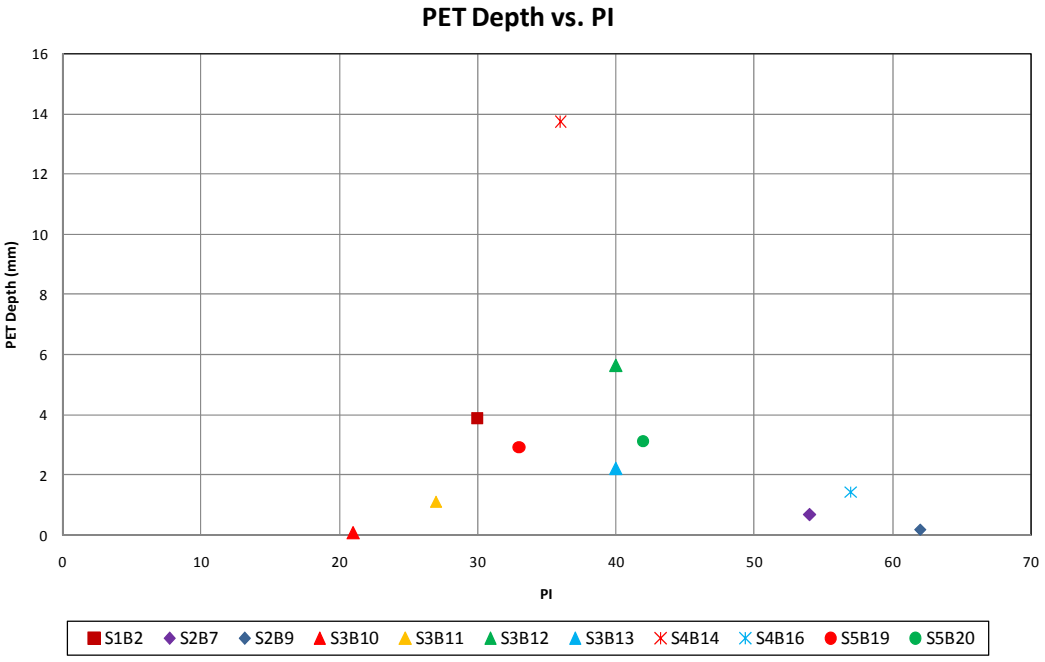

Fig. 243. PET depth vs. PI

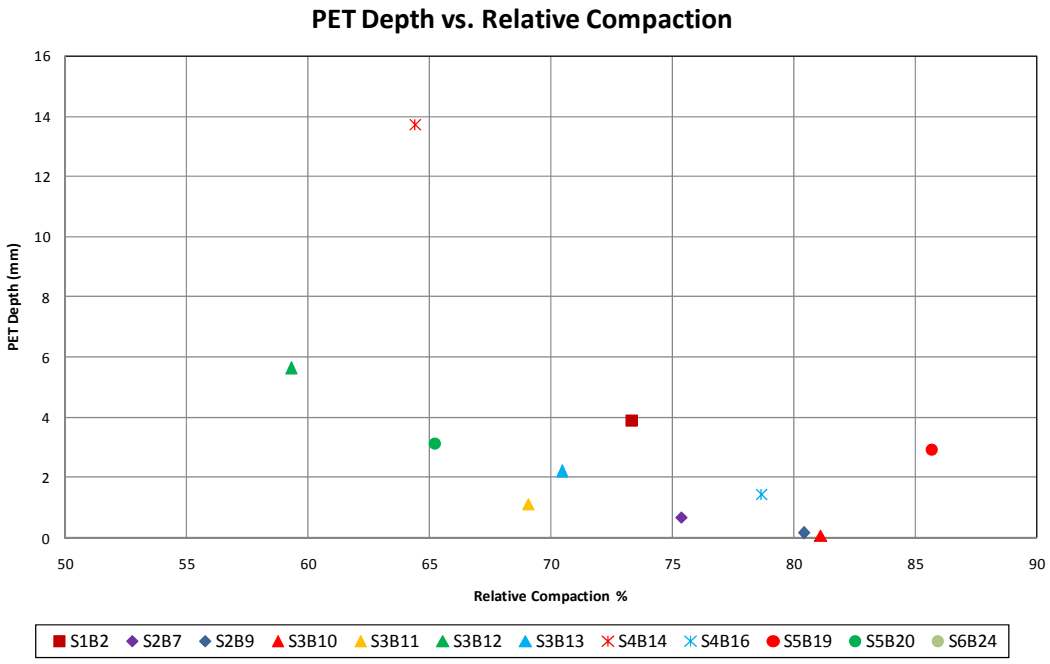

Fig. 244. PET depth vs. percent relative compaction

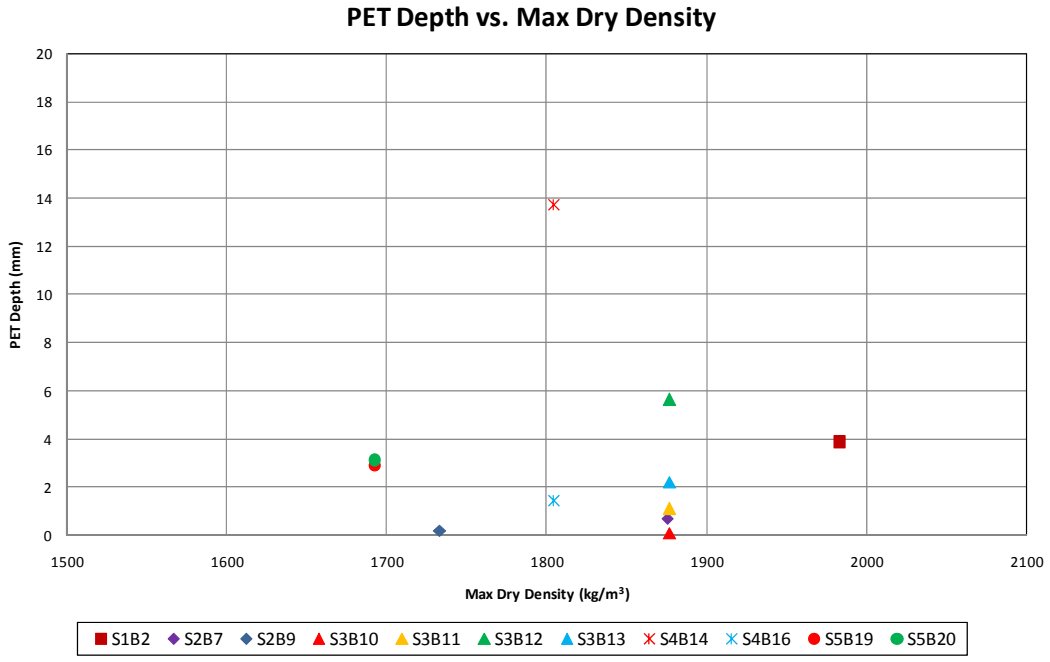

Fig. 245. PET depth vs. max dry density

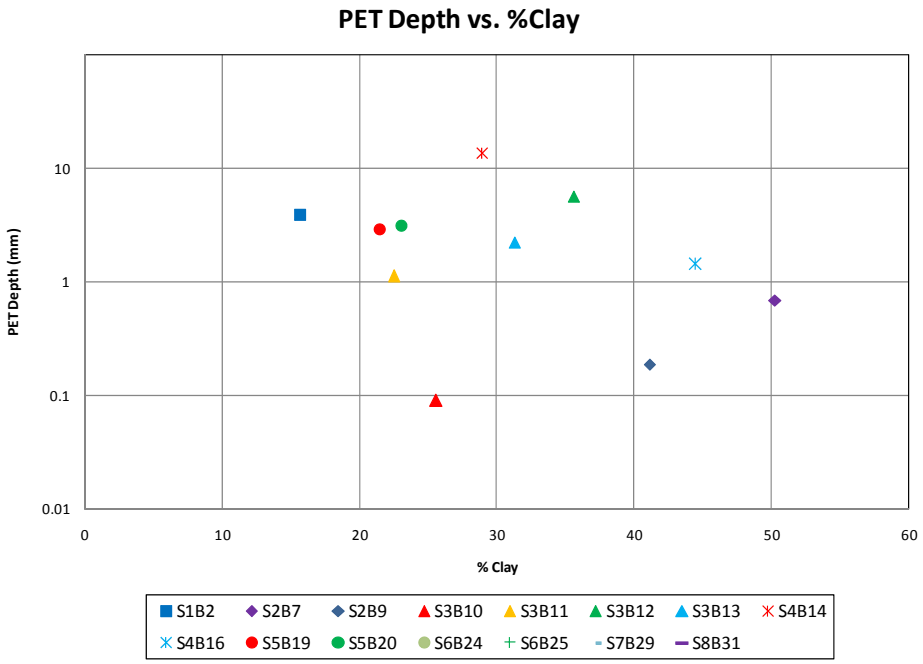

Fig. 246. PET depth vs. percent clay

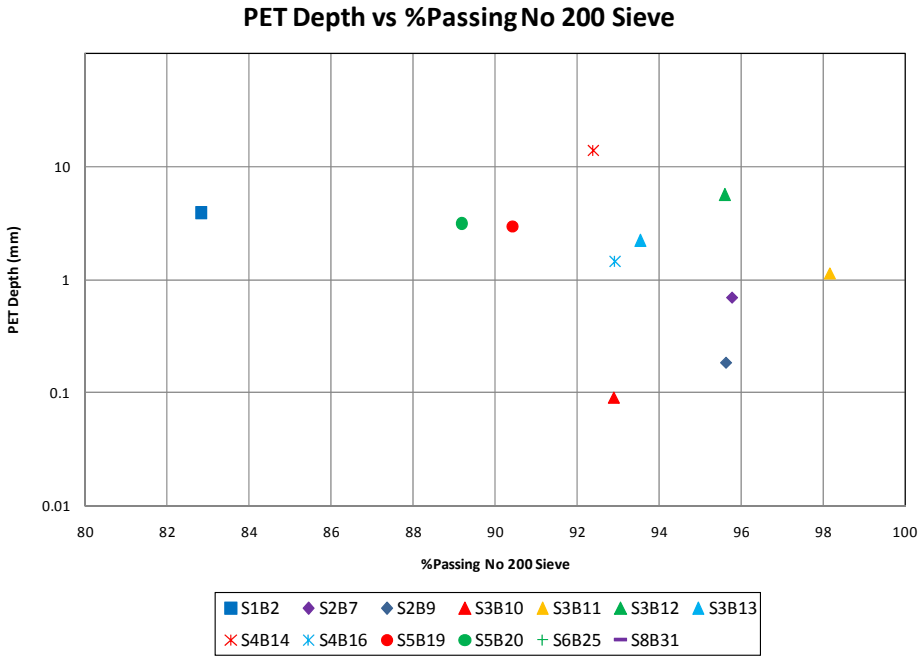

Fig. 247. PET depth vs. percent passing No. 200 sieve

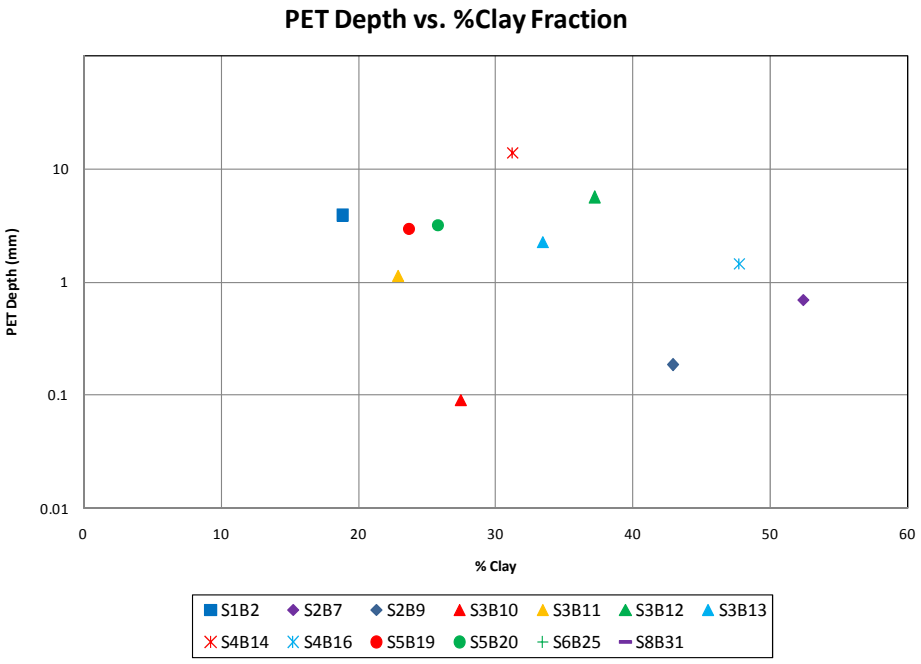

Fig. 248. PET depth vs. percent clay fraction

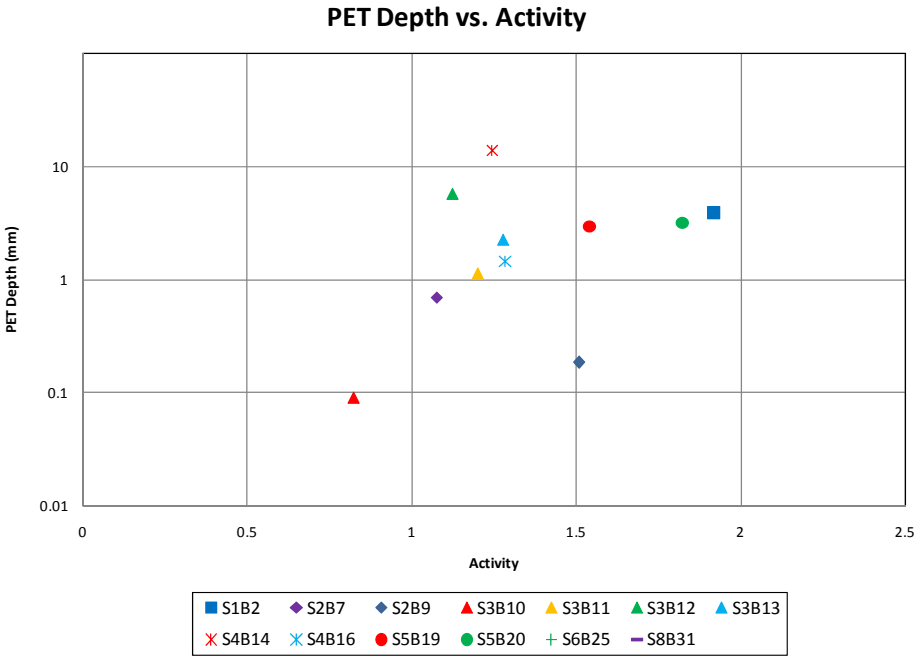

Fig. 249. PET depth vs. activity

While the results are much more scattered than the EFA correlations, the plots of D_{50} (Fig. 242), percent clay (Fig. 246), and activity (Fig. 249) show similar trends as before. PET depths were also plotted with the erosion rate at 3 m/s (Fig. 250) and erosion category (Fig. 251). Fig. 250 shows that as soils increase in erosion rate at 3 m/s they also have increasing PET depths. This proves that while the PET is a very simplified method, it still gives useful data.

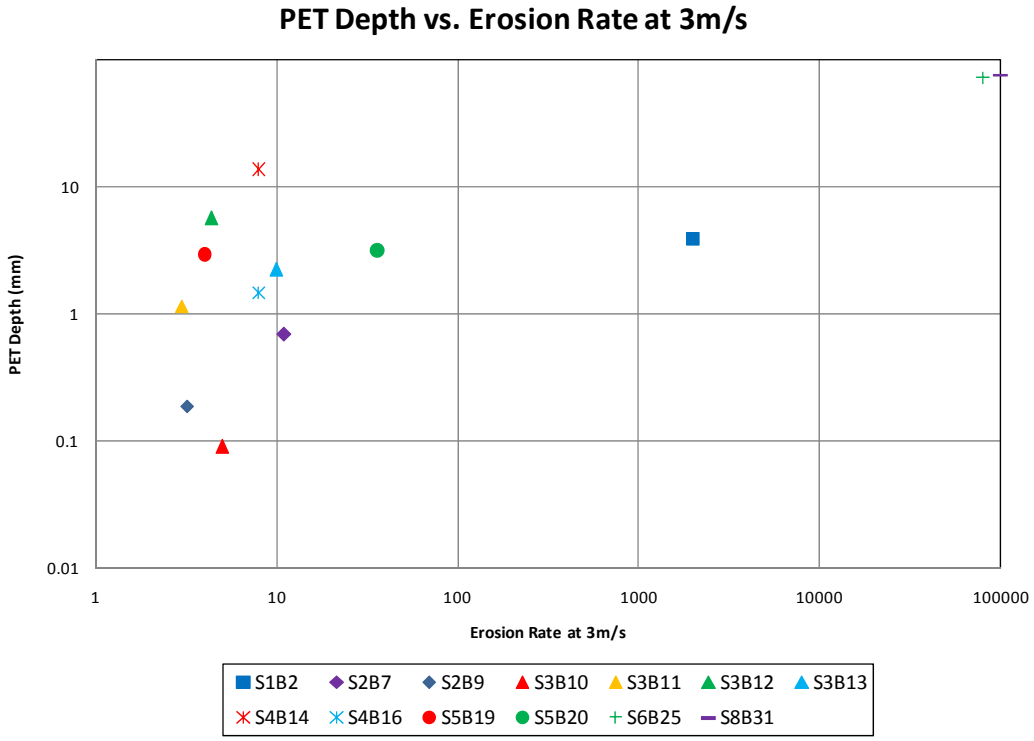

Fig. 250. PET depth vs. erosion rate at 3 m/s

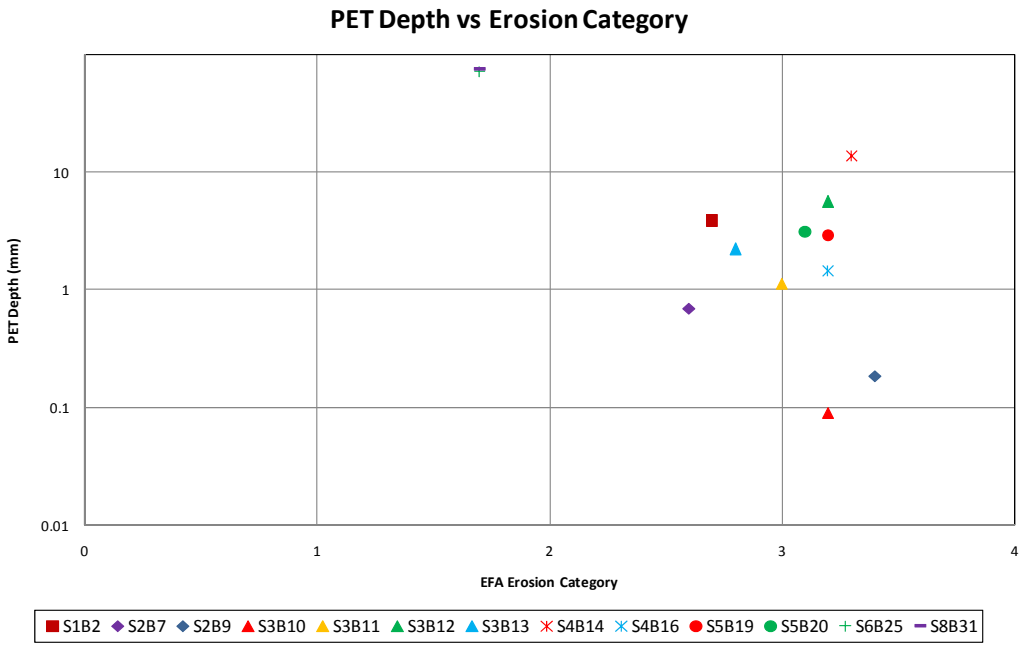

Fig. 251. PET depth vs. EFA erosion category

9. VEGETATION INVESTIGATION

Many types of armoring are available to help protect the soils comprising the levees from erosion including: concrete slabs, rip-rap, turf-reinforced mats, and grass. Of these, grass or vegetative cover is the most common. While the other options are more effective, they are costly and unrealistic for agricultural levee systems as large as those found in the Midwest. Often times in field studies, the characterization of the vegetative/grass cover present on the earthen levee side slopes is ignored or omitted from the overall analysis. The influence of this vegetative armor and the added erosion-resistance it provides are key aspects in understanding and correctly characterizing the overall performance of the levee during overtopping conditions.

9.1 Field Investigation and Sample Collection

During the field reconnaissance, bulk samples of levee grass cover were obtained for classification. The samples were chosen based on visual observations, taking into account location, root type, stem and blade width, and species in general. Samples representative of each site were collected and photographs of the general area and any distinctive grasses were taken. The samples and photographs were reviewed by several faculty members specializing in warm-season grasses in the Soil and Crop Science department at Texas A&M University (Drs. Russell Jessup, Richard White, and Byron Burson). The photographs and samples were reviewed and several grass species were identified. Additional consult from a cool-season grass specialist was obtained from Mr. Jerry Kaiser, the Plant Specialist for the Elsberry Plant Materials Center in Elsberry,

Missouri. This center is part of the U.S. Department of Agriculture (USDA) and the Natural Resources Conservation Service (NRCS). Table 28 summarizes the species of plants found at each site. The following sections introduce the types of grasses commonly found in the Midwest, how they are identified, and a more in depth discussion of the site visits.

Table 28. Common names of grasses at each site

Site	Grasses Identified	Common Nomenclature
Winfield - Pin Oak	Setaria pumila	Foxtail
	Digitaria Sanguinalis	Crabgrass
Bryants Creek	Setaria pumila	Foxtail
	Festuca arundinacea	Tall Fescue
Brevator	Phalaris arundinacea	Reed Canarygrass
	Panicum Virgatum	Switchgrass
	Bromus inermis	Smooth Brome
	Setaria pumila	Foxtail
Kickapoo	Festuca arundinacea	Tall Fescue
	Panicum Virgatum	Switchgrass
Norton Woods	Panicum Virgatum	Switchgrass
Indian Graves	Setaria pumila	Foxtail
Two Rivers	Setaria pumila	Foxtail

9.2 Introduction to Grasses of the Midwest

There are essentially two main categories of grasses: warm-season and cool-season grasses each being suited for different climates and thus locations in the US (Fig. 252). From those categories come other designations and descriptions such as turf grass, bunch grass, and range grass. Turf grasses create a mat-like sod while bunch grasses, as the name implies, tend to bunch at the roots leaving voids and bare surface. Turf grasses

are what are commonly found in lawns while range grasses are grown generally for agricultural purposes.

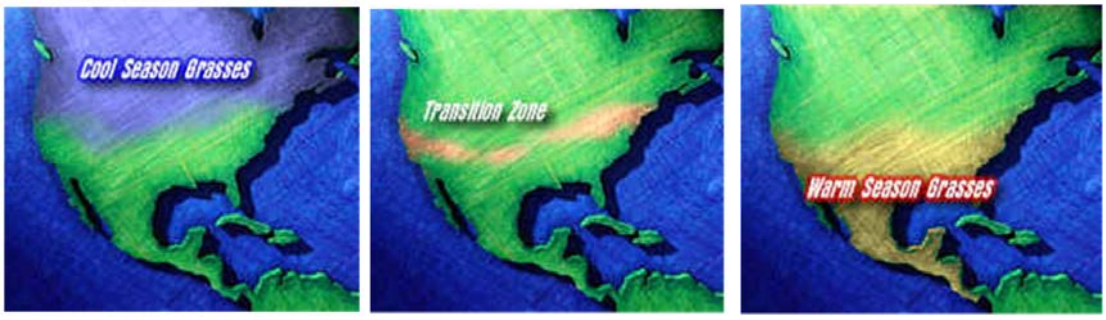

Fig. 252. Grass seasonal zones (American Lawns 2009)

The sites visited during the Midwest Levee investigation fall in the cool-season zone as well as the transitional zone. Turf grasses common to the cool-season include: Bentgrass, Kentucky Bluegrass, Rough Bluegrass, Red Fescue, and both Annual and Perennial Ryegrass. In the transition zone, there are difficulties with both the warm-season and cool-season type grasses depending on the location. Turf grasses common to the transition zone include: Kentucky Bluegrass, Tall Fescue, Perennial Ryegrass, Thermal Blue, and Zoysia.

9.3 How Grasses Are Identified (Bigelow 2009)

Types or species of vegetation are identified by a combination of distinctive markings or traits such as flowers, seed heads, and blade type. Unfortunately for most species, there is no one characteristic that can be used to sufficiently identify the grass. The first step is to make sure that the grass is a grass and not a sedge or rush. Grasses have their leaves in ranks of two, while sedges and rushes have their leaves arranged in

ranks of three. Sedges also have triangular shaped stems. Both sedges and rushes form a poor-quality turf and are generally considered weeds.

The next step is to determine the vernation, or the orientation of a newly emerging leaf. They will either be rolled or folded for most turf grasses. Once this is determined, the leaf blade is examined. There are several characteristics of the different parts of a leaf that are used to describe the grass in question. Also, the shape of the leaf blade is extremely important. The blade tip can be either pointed, rounded, or boat-shaped. Bluegrasses have a boat shaped leaf tip, while Ryegrasses generally have pointed leaf tips and glossy undersides.

Probably the most informative part of a grass is the seedhead or inflorescence. Most species have distinct features that show clearly in the inflorescence. However, grasses only have inflorescences for a very small fraction of the year, and mowing and other maintenance often removes this critical feature. As the last step used to identify grasses, growth habits are studied. Certain grasses either spread out forming a dense mat-like sod or they tend to form tussocks.

Successful identification depends on a combination of the items listed. The methods used in the Midwest Levee vegetation identification were less than ideal, but were dependent on the conditions available. As mentioned above, the inflorescence is an important feature and critical in identifying some species. Many of the grasses either did have a developed inflorescence or it had been mowed at the time of sampling, making it very difficult to identify several of the features listed. Also, the grasses were sampled several months after the flood events and new grass plants could have either been

introduced to the sites or induced to germinage from existing seed banks by the flood waters. In extreme flood conditions, many grasses are drowned and other invasive "weed-like" grasses are allowed to take over an area. This could be the case in several of the areas sampled.

The samples taken were also under somewhat extreme conditions and by the time identification was attempted, the grass samples were wilted and several of their distinguishing characteristics were damaged. Most of the identification was done through photographs taken during the site visits. While not ideal, this method still allows for the characterization of several of the most prominent species as well as their density and coverage.

9.4 Field Observations

9.4.1 Winfield - Pin Oak

Fig. 253 shows the vegetative cover present on the levee at the Winfield site. This site was identified to contain foxtail and crabgrass. While the ground cover looks somewhat substantial in the figure, most of the grasses present were more annual weeds rather than perennial sod-forming grasses. Such weeds tend to form clumps, leaving spaces where the soil surface is bare. In several areas there was little or no coverage.

Fig. 253. Winfield – Pin Oak vegetative cover

Foxtail is a summer annual with a very distinctive inflorescence (American Lawns 2009). The plant forms in tuft-like groupings and often develops in areas of sparse coverage by turf grasses. This leads to the conclusion that the ground coverage was not too dense because of the ability of the foxtail to intrude. Crabgrass is an annual grass generally found in the warmer climates. This "weed" is highly invasive and can dominate an area, but because it is an annual plant it will die out with a good freeze. None of the grasses identified at this site are what would be considered "good" protective armoring.

9.4.2 Bryants Creek

Fig. 254 shows the vegetative cover present on the levee at the Bryants Creek site. This site was identified to contain Tall Fescue and Foxtail. The ground cover in the area shown was relatively consistent, however, there were still patches of bare surface.

Essentially, the root density was low even though the coverage was good. The levees had been mown by the time of sampling, making it difficult to document the grasses at the time of flooding. Most of the vegetation present was Tall Fescue which is a perennial turf-grass. In conversations with Mr. Kaiser, he mentioned that there had been a previous over-seeding of Tall Fescue on several of the levees in the area.

Fig. 254. Bryants Creek vegetative cover

Fescues are cool-season bunch type grasses which are generally more drought and wear resistant than other cool-season grasses, such as bluegrass or ryegrass (American Lawns 2009). Fescues also tend to have deeper root systems than some of the other similar grasses. Tall Fescues can become very thick and are often used as pasture grasses. Even though the traditional fescues are more bunch forming, there are new turf-type varieties of Tall Fescue that are becoming more popular.

9.4.3 Brevator

Fig. 255 shows the vegetative cover present on the levee at the Brevator site. The Brevator site was unique in the fact that it was overtopped for three days without failing. The only signs of erosion were at a box culvert which was mostly due to seepage through a crack in the concrete structure (Fig. 256). During an interview with a nearby resident Mr. James Piper, it was noted that the grass was approximately 1 m tall at the time of flooding. The overtopping waters forced the grass to lay down essentially creating a barrier on top of the soil surface. The EFA tests show that the soil alone would not have resisted the velocities for the period of overtopping that occurred. Therefore, some benefit was gained from the vegetation on the levee. Several different varieties of plants were identified at this site including: Switchgrass, Smooth Brome, Reed Canarygrass, and Foxtail. The ground cover was consistent and root density was also much higher at this site than any of the previous sites. There were some locations; however, that were not covered with living grass at the time of sampling. It appeared these locations are where the excess flood waters and resulting anoxic root zone had killed the grass. Most of the grasses present were moderately sod forming. There was also broad leaf plants found on the land side of the levee that were more than likely a result of transported seeds from the waters. At the locations where the broad leaf plants were found the ground cover was less than substantial, but because the grass was 1 m at the time of flooding, these areas may have been protected. The vegetation found around the box culvert was mostly determined to be weeds probably left by the flooding water.

Fig. 255. Brevator vegetative cover

Fig. 256. Brevator vegetative cover at seepage point

Because this site performed extremely well under the given conditions, a more in depth investigation of the grasses present was done. Switchgrass is a native warm-season perennial grass which has very high yields and is resistant to many pests and

diseases (Bransby 2009). Switchgrass also does well in flood and drought conditions and it is very tolerant of poor soil quality. Because Switchgrass is a perennial grass, it comes back from year to year with little or no required maintenance. There are essentially two types of Switchgrass: upland and low land. Upland types grow up to 2 m and are usually found in well-drained areas. Lowland types can reach up to 3 m high and are generally found in bottom areas with heavier soils. Switchgrasses have large, permanent root systems that can reach depths of over 3 m. It also has many fine, temporary roots that improve the soil quality. Even though Switchgrass tends to grow in clumps, it is a slowly spreading type grass. In the Midwest, Switchgrass tends to develop long rhizomes or underground stems that grow horizontally and interconnect forming a thick dense sod. One of the greatest benefits of Switchgrass is its ability to be used in energy production. This technology is becoming more and more common in the US.

Reed Canarygrass or *Phalaris arundinacea* is a tall growing cool-season perennial grass which is native to many of the northern states (Sheafer 2008; Washington 2008). It is particularly well adapted to saturated or nearly saturated soils, but where standing water does not persist for an extremely long period of time. The ideal conditions for this grass typically occur in ditches or channels, levees, and river dikes. During the investigation, Mr. Piper also remarked that some of the other grasses present had been killed by the water, but the Canarygrass remained alive. This species of grass spreads by underground stems called rhizomes and forms a solid sod. It is resistant to both flooding and drought and winter freezing, making it excellent for many conditions experienced in the Midwest. The grass can tolerate soils with a pH range

from 4.9 to 8.2, but it is not particularly tolerant to saline soils. The grass creates a dense arrangement of strands that provides excellent erosion protection. If allowed to grow to a height greater than 1ft, it is suspected the grass would perform as barrier like discussed above and would protect the soils from the rushing waters.

One of the weaknesses of Reed Canarygrass is that it may require two weeks to germinate and break the surface and it is not a highly competitive species. It may take time and attention to introduce this species to other levee systems, but once established will prove to provide many erosion benefits. Although used for hay and forage in some areas, certain varieties are not particularly palatable to livestock. New low-alkaloid varieties offer improved forage yield and animal performance.

Smooth Brome or *Bromus inermis*, is a cool-season perennial grass which spreads by rhizomes and is sod-forming (Bush 2006). Depending on the region, this species can be either native or introduced. It is often used for hay for livestock and is similar to alfalfa or other legumes. The stems can reach over 1 m high. Smooth Brome has a distinct inflorescence that is approximately 10 cm long and has panicles with ascending branches. It has a massive root system and is a sod-forming grass. It has been used successfully for critical area planting and grassed waterways as long as there is plenty of water.

Each of these three grasses performs well in the Midwest climates and have root systems that spread to create thick mat-like sods. Also noted at the site, was the far distance the trees were from the levee. Trees have root systems that can reach for large distances and penetrate the levee systems leaving paths along which water can seep

through. It is highly probable that this site only experienced the overtopping waters and was not also impacted by any seepage effects. In that sense, the vegetative cover could be the main reason the site survived.

9.4.4 Kickapoo

Fig. 257 shows the vegetative cover present on the levee at the Kickapoo site. This site was identified to contain Tall Fescue and Switchgrass. While the ground cover looks somewhat substantial in the figure, there were a large number of weeds present. As in the previous cases, these could have become more dominant after the flooding. Even though the site had better erosion-preventative grasses, the breach location was more than likely caused by the lower roadway and road base material. Several locations along the same levee were overtopped and resisted erosion well. Therefore, the vegetative cover in area may have proved to be more beneficial if it were not for the low section.

Fig. 257. Kickapoo vegetative cover

9.4.5 Norton Woods

Fig. 258 shows the vegetative cover present on the dry side slope of the levee at the Norton Woods site, while Fig. 259 shows the levee crest area. This site was identified to contain mostly Switchgrass; however, the presence of other "weed-like" plants are also seen in Fig. 258. At the time of the site visit, the grass was very tall at just under 1 m in some areas. The ground cover was substantial in many locations; however, at the toe and on the downhill slope there were less dense areas of predominantly weeds and broad leaf plants. As before, this may be a result of the standing water and the floodwaters themselves killing the grasses that were there prior to the overtopping.

Fig. 258. Norton Woods vegetative cover at dry side slope of levee

Fig. 259. Norton Woods vegetative cover at levee crest

9.4.6 Indian Graves and Two Rivers

Fig. 260 shows the vegetative cover present on the levee at the Indian Graves and Two Rivers sites. Both of these sites were sand shell levees with no established vegetative cover. This site was identified to contain foxtail which was more than likely introduced by the flood waters. Sand shells such as these do not provide the proper conditions to encourage plant growth or root development. The sand allows the water to drain rather quickly leaving the shallow roots dry and killing the plants. No influence of vegetative cover was considered at these sites.

Fig. 260. Indian Graves (left) and Two Rivers (right) vegetation

9.5 Qualities of Good Vegetation Systems

The idea of the correct vegetative system for levees is one of great debate. Some argue the importance of woody and herbaceous vegetation for levee stability and erosion resistance benefit, while others claim larger rooted plants allow for the development of seepage paths and are detrimental to levees. USACE requires the removal of all large root vegetation on levees in some areas and recommends that there be no trees within 15 ft (5 m) of all levees. This is based on a combination of maintenance and seepage reasons. Proper regular maintenance is difficult with trees on the levees and in the event of a breach, trees or large shrubs can create additional obstacles which slow down work and impede the remediation process. Tree roots, as with all other encroachments, can allow the development of seepage paths through. These tunnels can weaken the levee structurally, and a combination of seepage and overtopping waters can be detrimental to

the dry side slope and toe of the levee. Also, live roots remove existing moisture from the interior of the levee which can cause shrinkage and cracking. These cracks provide the perfect paths for water to infiltrate and travel. In the case of dispersive clays, any cracks increase erosion rates much more than what would occur normally for a non-dispersive clay. In the sites observed during the Midwest Levee investigation, six of the seven main breaches visited had trees on or adjacent to the levees. Within the breached areas, there were tree roots found in at least half of the sites. The following series of pictures in Fig. 261 shows the sites where tree roots were found within the breach area.

Fig. 261. Midwest Levee sites with tree roots in breach area

Furthermore, if a tree or large plant is actually on the levee and it falls over, the root ball can rip out an entire section of the levee (Fig. 262). Trees can die and fall over naturally or can be forced over by rushing waters. Also, debris carried by the flood waters can impact the trees causing them to be overturned. Whatever the case, the removal of a chunk of the levee material leaves a weakened section of the levee and a possible low area where flood waters can concentrate and ultimately fail the levee. Fig. 263 shows the trees and shrubs adjacent to the Bryants Creek levee. The photograph shows many trees that have been pushed over and uprooted from the force of the water.

Fig. 262. Vegetation on a levee (Deretsky 2009)

Fig. 263. Trees pushed over from flood waters

On the other hand, some light vegetation and grasses are beneficial in preventing surface erosion from overtopping and even wave action. USACE encourages vegetation for flood damage reduction projects provided it is limited "to a good growth of sod maintained with grass, from 2-12 in (5.1-30.5 cm) in height, substantially free of weeds and bare spots" (Riley 2007). The main reason the heights are stated is also based on proper maintenance issues. With shorter grass, any signs of seepage or any surface slides in need of repair are more easily noticed. It is in the opinion of the author of this thesis that the grass should be allowed to grow higher during the seasonal flood periods. As discussed above, the correct types and concentrations of grasses on levees has been shown to withstand large erosive forces in overtopping events. The Brevator site discussed previously is a good example of the benefits of the appropriate grass cover.

The types of grasses that have proven to be beneficial in preventing erosion have strong mat-like root systems (Ming-Han Li 2008). Perennial grasses also provide

persistent ground and below-ground structures such as crowns and rhizomes to further stabilize the soil structure. The roots are the key component in providing strength. Root structures that are adequately deep, but that also spread horizontally to form a firm and intertwined sod are ideal. Also, dense consistent coverage resists the effects of water flow and anchors the soil down. Many native grasses tend to clump in root groups allowing for spots of uncovered and unprotected soil and possible erosion. Complete grass coverage needs to be maintained in order to be effective in controlling erosion. Grasses that are not completely dense in nature can also be allowed to grow to taller heights. As in the Brevator case, the tall grass is pushed over and creates a protective barrier between the soil and the water.

The blade type may also have an effect on the erosion prevention capabilities of certain types of grasses. Wider blade grasses tend to have slightly more ability to reduce the flow velocities. When taller broad blade grasses are pushed over they create overlapping sheet-like layers that create a protective mat, once again serving as a barrier between the soil and water.

9.6 Native versus Introduced

There are benefits for both native and introduced grass types. Even if non-native grasses are chosen because of their erosion prevention qualities and are introduced to these levee systems, there is always a tendency for the native vegetation to “choke” out the imported grasses if they are not properly maintained. Mowing natives will reduce root mass and can lead to clumps of root systems, which is not desired. Most adapted

grasses require mowing to keep them below 0.3 m tall, so that the native grasses do not take over. The extra maintenance required for non-native grasses is not preferred, but may be necessary.

With many levee systems, the soils are compacted to a specified density. Many grasses, especially natives, have a hard time developing a root system in highly compacted soils. This can lead to clumped masses and patches which is not desirable. It is important to note that the top-soil containing the root systems is often compacted to a much less degree than the actual embankment materials.

9.7 Existing Practice – USACE and NRCS

The USACE Engineering and Design Manual Number 1110-2-301(USACE 2000) provides the guidelines and criteria for the design of landscape plantings and vegetation maintenance for floodwalls, levees, and embankment dams. This document is a safe design guide rather than a requirement for vegetation near or on the levees. USACE limits any vegetation other than grasses to at least 5 m from the edge of the levee base as described by the engineer. They also require a root free zone, 1 m in width, along the face of the levee to provide a margin of safety between expected plant root depth and the designed embankment section. This document also states that the selection of plants is based on prepared lists from the Division and District landscape architects. While the document describes the proper way to achieve aesthetically pleasing yet safe vegetative landscaping near the levees, it does not give any specific guidelines on grass types or coverage characteristics.

The NRCS, however, has several specification documents and standards that provide detailed guidelines for the establishment and maintenance of erosion prevention grasses. The Conservation Practice Standard CODE 342 (NRCS 2007) gives the criteria and steps to establishing permanent vegetation on sites that have high erosion rates due to water as well as other conditions. This document gives general site investigation criteria and fertilization schemes and should be used simultaneously with the Missouri Agronomy Specification Vegetation Establishment, Herbaceous Seeding CODE 723 (NRCS 2008). This particular document facilitates the establishment of permanent herbaceous vegetation by providing species selections, site preparation, and seeding specifications. A list of vegetation species for different climate zones is given along with their corresponding ratings in erosion control, wildlife habitat, wet soil tolerance, and drought tolerance. Reed Canarygrass, Smooth Brome, and Tall Fescue are all listed as having excellent erosion control qualities, while Switchgrass is rated as good. This detailed guide has been attached in Appendix 9 for further reference.

9.8 Review of Research by Others

According to Temple et al. (1987), three components are responsible for the flow resistance in an open channel: viscous drag on the soil surface, pressure drag in the non vegetal areas due to roughness, and drag on the vegetal elements. Drag on the vegetal components dominates the flow resistance for most grass-lined channels. There are essentially three main flow regions of importance for a given channel. Low flows are defined at depths lower than the deflected grass height. Intermediate flows are when the

flow depth is greater than the deflected height of the grass. Large flows are defined as flow depths much greater than the deflected height of the grass. Most practical problems are concerned with the intermediate flows. At these flow depths, the vegetal elements tend to align themselves with the flow. The vegetal parameters expected to be the most dominate are the number of stems in an area and the length of each stem. As the elements align with the flow the leaf structure becomes less important. The flow resistance can be expressed in terms of Manning's "n." As the depth or discharge increases, the thickness of the boundary zone dominated by vegetal action decreases as well as Manning's "n."

Temple et al. (1987) also note that soil particle detachment often begins at low enough stresses to be withstood by the vegetation without significant damage. As the particles of soil are removed, the vegetation is undercut and the weaker vegetation is removed, decreasing the density and uniformity of the cover. This increased roughness leads to higher stresses at the soil/water interface and an increased erosion rate. The vegetative cover should be as dense and uniform as possible to prevent this action. Temple et al. (1987) also describes a detailed design of open channels considering grass lining, however, the methods and equations are somewhat dated.

Levee performance under wave action and overtopping has been a major area of interest in the Netherlands after the disaster of 1953 in which many levees failed from inner slope shearing following overtopping. Similar to the US, grassed clay dike revetments are the most common type of armoring (Fig. 264). The primary purpose of

this vegetation is to prevent erosion caused by hydraulic forces (Seijffert & Verheij 1998).

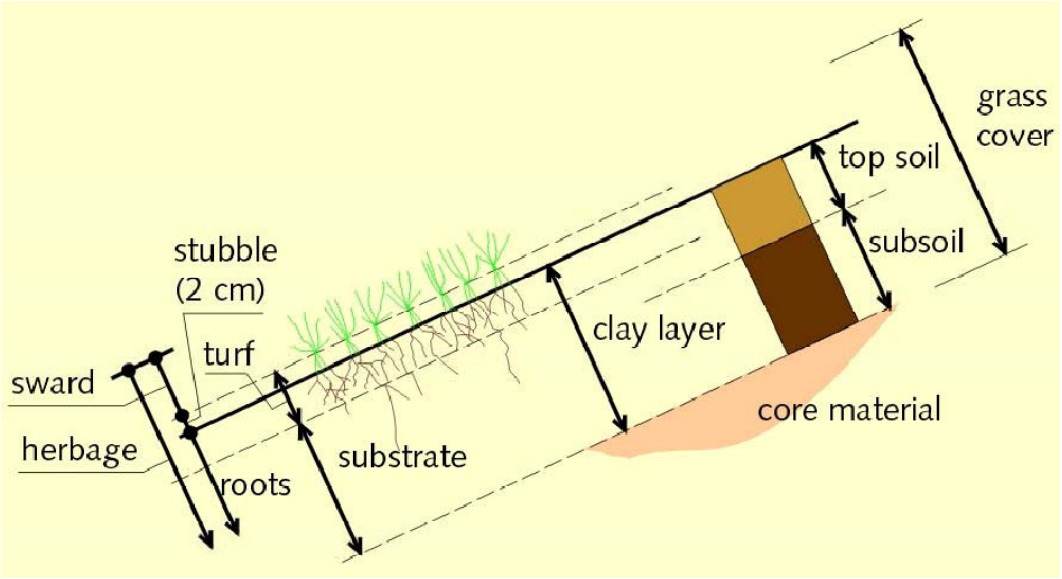

Fig. 264. Cross-section of a grass covered revetment (Muijs 1999)

The strength of the revetment is based mainly on its ability to withstand wave action and surface flows that may result during overtopping. In general, levees are subjected to the highest velocities and therefore forces at spillway type areas. Normal grass cover can resist velocities up to 2 m/s with little or no erosion, however, higher velocities can become problematic (Fig. 265). This chart shows the importance of the duration of the overtopping. As the number of hours of overtopping increases, the benefit gained from having increased vegetative cover is not as substantial. For normal flooding events like those experienced in the Midwest it is not unreasonable to assume that the overtopping lasts for 20 hours. Velocities at the toe of a levee can be over 6 m/s. This point plots much higher than the limiting cases shown below.

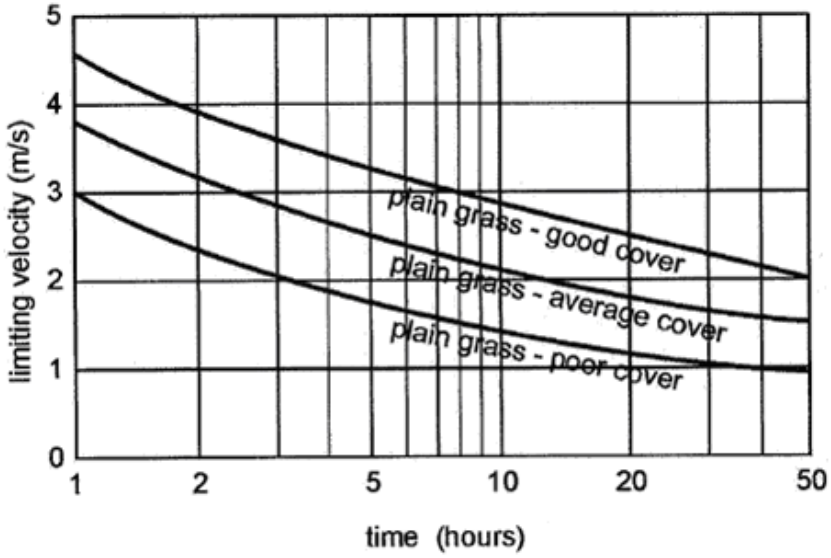

Fig. 265. Limiting velocities for plain grass (Seijffert & Verheij 1998)

Most of the resistance to erosion is due to a thick dense root system just under the soil surface (Seijffert & Verheij 1998). The hydraulic loading depends highly on the slope and geometry of the levee. Steep slopes tend to concentrate forces, while flatter slopes tend to reduce hydraulic forces on the revetment. Numerous other tests relating to the strength of grass covers have been carried out. These tests have considered variables such as, root length, percentage of surface covered, and soil properties (Seijffert & Verheij 1998).

Muijs (1999) notes that the resistance of grass cover to erosion can be controlled by how it is implemented and managed. Sod becomes much more resistant to erosion as the root density increases. The roots connect the small soil particles and prevent them from being washed away. By ensuring a relatively low level of nutrients in the soil, the grasses are forced to invest in their root systems. In a laboratory experiment, a managed grass cover over a highly erosion resistant clay was found to be resistant to erosion

caused by 1.35 m high waves for many hours. This resistance is mainly due to the sod. A structured clay with little root penetration under the sod was eroded 15 to 50 times faster than the well developed sod.

Extensive work has also been done on the topic of surface erosion at Texas A&M University by Dr. Ming-Han Li and others. Most of the focus of these studies, however, has been on warm-climate grasses native or well suited to the Texas climate. This work has been primarily applied to common roadway embankments found at overpasses and in channel flow. Full scale tests have been carried out for performance of slope protections according to ASTM D6459. Current work is being done to develop and review the bench scale testing for ECTC shear and ECTC slope. Fig. 266 gives an example of the Texas Transportation Institute facilities used in large scale surface erosion testing.

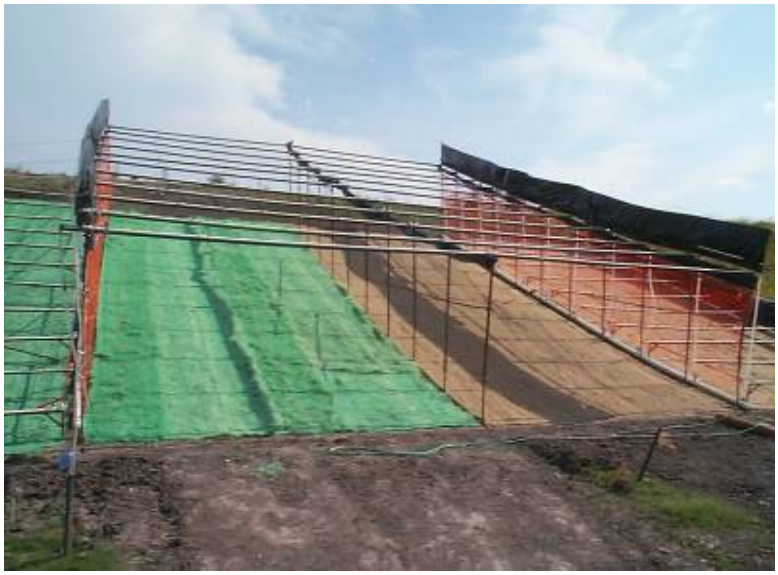

Fig. 266. Texas Transportation Institute slope erosion testing (Ming-Han Li 2008)

Work is also being done in the research and implementation of geo-synthetics and other similar products. Turf reinforcing mats (TRMs) have proven to be beneficial in helping vegetative establishment and then providing additional anchoring for the mature plants. These mats are long term non-biodegradable mats made of synthetic or natural fibers and netting. They provide solutions on steep slopes and channels where the flow conditions exceed the capacity of vegetation only.

9.9 Recommendations

The ideal option for erosion prevention on these agricultural levees is to find a locally-adapted or native grass that requires little maintenance and possess the performance characteristics discussed above. A thicker blade perennial grass with a mat-like root system that provides full coverage is preferred. Also, the moisture and flood conditions are also an issue. Some grasses are not appropriate for areas where prolonged wetting is expected, while others do not do well in drought conditions. The degree of compaction must also be considered. Some grasses do not perform well in highly compacted soils.

The grasses found at the Brevator site seemed to satisfy all of these criteria. The recommended grasses includes: Switchgrass, Tall Fescue, and Reed Canarygrass. In addition, Kentucky Bluegrass was recommended by the members of the Soil and Crop Science Department because of its preferred qualities and sod-forming characteristics. Switchgrass is also being researched as a bio-fuel plant. It may be beneficial in the near future to plant Switchgrass on the levees and harvest it for bio-fuel production. The

monetary funds received from the harvest could help offset some of the yearly maintenance costs.

A percent coverage of at least 90 percent is desirable. It is also recommended by the author of this thesis that the grasses on the levee be allowed to grow to taller heights during the flood season. The above plot (Fig. 265) shows that, while most of the erosion prevention depends on the root system, it is not always adequate for the magnitude and duration of flows experienced during overtopping flood events. There is great benefit gained from the taller grasses as they are pushed over to form a protective barrier over the soil surface. This also helps with less than perfect root densities that can be expected on agricultural levees. For the Midwest, the main flood season is reduced to late spring and early summer. The grasses on the levee and near the toe should be allowed to remain at least 0.5 m tall during this time. Not only does this increase the erosion protection, it also can lower some maintenance costs.

10. EROSION MATRIX

Because erosion is such a complicated phenomenon which depends on the interaction of many variables, an erosion matrix was developed in an effort to compare the variables determined through lab testing and field observation. The variables were chosen based on the highest degrees of influence on the performance of a given levee system.

10.1 Two Site Matrix

In an initial step, a matrix only comparing two sites was created (Table 29). Two samples and site locations were chosen based on the tested material properties, site conditions, and performance. S2B9 represents a sample which tested as one of the highest resistant to erosion, highest PI, had decent grass cover, but still failed. S3B11 was chosen because it is a slightly more erosive soil, has a lower PI, had lower relative compaction, had excellent grass cover, and was not affected by the overtopping waters. This smaller matrix was used to test different cutoff values and determine the most useful properties.

10.2 Midwest Levee Matrix

Once the two site matrix was created, a larger matrix containing all the Midwest Levee samples tested was made (Table 30). The blank spaces are where no data was obtained.

Table 29. Two site erosion matrix

Sample	D_{50} less than 0.015 mm	Plasticity Index over 25	% Relative Compaction over 80	Grass Armoring Good/Fair/Poor	% Clay over 25	% Passing No. 200 over 90	Activity less than 1.3	Torvane over 0.5 kg/m^3	Erosion Rate @ 3 m/s under 10 mm/hr	No Tree Roots within 20 m	PET Depth less than 3 mm	PASS/FAIL
S2B9	YES	YES	YES	FAIR	YES	YES	NO	YES	YES	NO	YES	FAIL
S3B11	NO	YES	NO	GOOD	NO	YES	YES	NO	YES	YES	YES	PASS

Table 30. Midwest Levee erosion matrix

Sample	D_{50} less than 0.015 mm	Plasticity Index over 25	% Relative Compaction over 80	Grass Armoring Good/Fair/Poor	% Clay over 25	% Passing No. 200 over 90	Activity less than 1.3	Torvane over 0.5 kg/m^3	Erosion Rate @ 3 m/s under 10 mm/hr	Tree Roots farther than 20 m	PET Depth less than 3 mm	PASS/FAIL
S1B1	NO	YES	NO	FAIR	NO	NO	NO	NO	NO	NO	NO	FAIL
S1B2	NO	YES	NO	FAIR	NO	NO	NO	NO	NO	NO	NO	FAIL
S2B6	YES	YES	NO	FAIR	YES	NO	YES	YES	NO	NO	YES	FAIL
S2B7	YES	YES	NO	FAIR	YES	YES	YES	YES	NO	NO	YES	FAIL
S2B9	YES	YES	YES	FAIR	YES	YES	NO	YES	YES	NO	YES	FAIL
S3B10	YES	NO	YES	GOOD	YES	YES	YES	YES	YES	YES	YES	PASS
S3B11	NO	YES	NO	GOOD	NO	YES	YES	NO	YES	YES	YES	PASS
S3B12	YES	YES	NO	GOOD	YES	YES	YES	YES	YES	YES	YES	PASS
S3B13	YES	YES	NO	GOOD	YES	YES	YES	YES	YES	YES	YES	PASS
S4B14	YES	YES	NO	FAIR	YES	YES	YES	YES	YES	NO	NO	FAIL
S4B16	YES	YES	NO	FAIR	YES	YES	YES	YES	YES	NO	YES	FAIL
S4B18	NO	YES	NO	FAIR	NO	NO	NO	NO	NO	NO		FAIL
S5B19	NO	YES	YES	FAIR	NO	YES	NO	YES	YES	NO	YES	FAIL
S5B20	YES	YES	NO	FAIR	NO	NO	NO	NO	NO	NO	NO	FAIL
S5B23	NO	YES	NO	FAIR	NO	YES	NO	NO	NO	NO		FAIL
S6B24	NO	YES	NO	POOR				NO	NO	NO		FAIL
S6B25		NO	NO	POOR	NO	NO			NO		NO	FAIL
S6B26	YES	YES	YES	POOR	NO	YES	NO			NO		FAIL
S7B29	NO	YES	NO	POOR	NO	NO	NO	YES	YES	NO		FAIL
S7B30	NO	NO		POOR	NO	NO						FAIL
S8B31	NO	NO		POOR	NO	NO			NO	NO	NO	FAIL
S8B32	NO	NO		POOR	NO	NO						FAIL
S8B33	NO	YES		POOR	NO	NO	NO	NO	NO	NO		FAIL
S8B35	NO	NO		POOR	NO	NO	NO			NO		FAIL

11. SUMMARY AND CONCLUSIONS

Many different factors influence the erosion phenomenon. Proper documentation of overtopping induced erosion is a complicated issue involving the collection and analysis of time-sensitive field data. Personal observations during and after the breaching provide a qualitative explanation of the failure mechanisms. The analysis of collected samples can help give an insight into the relationship between erodibility and soil properties such as, D_{50}, percent clay, and activity. By combining the effects of the soil properties and the site conditions, a better estimate of whether a site will fail during a flood event can be made.

The goal of the Midwest Levee reconnaissance was to gather perishable data in an effort to provide a comprehensive overview at each breach location. Laboratory testing was conducted to document the soil properties and site conditions and determine the erosion properties of the soils. This data was used to create an erosion matrix and a simplified method to identify potential erosion issues.

To predict how a site will perform during a particular flood event, there are three main inputs: the flood conditions, the site conditions, and the soil properties. Precipitation is a natural event that the engineer has no way of changing. The rain runoff drains into streams and rivers and finally into the Mississippi where it is carried south. Over time, the runoff caries sediment into the river and the riverbed can rise if not properly dredged. Any obstruction in the river or increase in riverbed height can reduce the capacity of the river. It is recommended that the river be dredged even more than it is currently dredged by USACE. Any increase in the volume capacity of the river can

decrease the height of waters the levees would be subjected to in a flood event. Also, the excess material can be used in levee construction or other construction processes. The factors determined to be the most important for the flood event is the depth of overtopping and the duration of overtopping. Long periods of overtopping can be detrimental to levees no matter what soil properties or site conditions exist.

As the areas behind the levees are developed, the floodplain areas become at greater risk of flooding. This risk can be reduced by having designated floodplain areas and sacrificial breach zones. This was seen during the 2008 Midwest floods though it was not on purpose. The breached levees upstream saved the city of St. Louis from what could have been catastrophic flood levels. Emergency breach areas could be implemented to save such cities in future flood events.

The site geometry and any imperfections can be very important factors in the performance of a levee system. At the specific site, any low spots or potential seepage paths can concentrate the flow and can be detrimental to the levee. The highest velocity flows are experienced at the toe of the levee and the change in geometry can cause large amounts of turbulence and therefore, erosion. More gradual slopes lessen this effect and increase the cross-section width also reducing seepage potential.

The vegetative cover is the single most important condition at a site. Grasses of the proper species, root density, and height can greatly reduce erosion at a site. As seen in the Brevator case, vegetative armor can prevent failure of a levee comprised of less resistant soils for long periods of overtopping. Recommended grasses include: Switchgrass, Smooth Brome, Reed Canarygrass, and Tall Fescue. It is also

recommended that these type grasses are allowed to grow at least 0.5 m tall during the flood season. Trees and woody rooted shrubs can also be harmful to levees as seen in the Winfield case. It is recommended that all trees and large root plants be removed from the levee and that roots are not allowed to grow within 10 m of the levee toe.

The erosion resistance of the materials comprising the levee is also important. However, for long periods of overtopping there are very few soils in existence that would not fail without the help from vegetative cover and other conditions. Many comparisons were made in an effort to determine those variables that most influence the erosion performance of a soil. From the correlations, it was determined that erodibility is a function of grain size, relative compaction, clay content, and activity. Devices like the Torvane and Pocket Erodometer can also be used to get a quick field estimate of erosion.

While these correlations and field devices can give insight into an erodibility value, they are no substitute for site specific erosion analysis with laboratory equipment such as the Erosion Function Apparatus. Soil behavior is highly nonlinear and the entire erosion function is needed to get an accurate measure of erodibility of a soil.

Erosion due to overtopping is a complicated, multi-variable process that is not fully understood. More work is needed to narrow down the relationships between erosion and the other variables considered in this thesis. The erosion matrix can be a very useful tool in the future to help predict whether or not a site will withstand a given flood, but it should be refined as further developments in these correlations are made.

REFERENCES

AlQaser, G.N. (1991). “Progressive failure of an overtopped embankment.” Ph.D. dissertation, Colorado State Univ., Fort Collins, Colo.

American Lawns (2009). “Types of American grass.” < http://www.american-lawns.com/grasses/grasses.html > (July 10, 2009).

ASCE. (2009). "Report card for American infrastructure." *Levees.* Washington, D.C. <http://www.infrastructurereportcard.org/fact-sheet/levees > (Apr. 11, 2009).

Bigelow, C. (2009). "How to identify a turfgrass.", Department of Agronomy, Purdue University. < http://www.agry.purdue.edu/turf/tool/instructions/instructions.htm>

Blaisdell, F. W., Clayton, L. A., Hebaus, G. G., (1981). “Ultimate dimensions of local scour.” *Journal of Hydraulics Division, ASCE*, 107(3), 327 – 337.

Bransby, D. (2009). “Switchgrass profile.” Auburn University. <http://bioenergy.ornl.gov/papers/misc/switchgrass-profile.html > (Jun. 11, 2009).

Briaud, J. (2008). “Case histories in soil and rock erosion: Woodrow Wilson bridge, Brazos River meander, Normandy cliffs, and New Orleans levees.” *Journal of Geotechnical and Geoenvironmental Engineering*, 134(10), 1424 – 1447.

Briaud, J., Chen, H., Govindasamy, A., and Storesund, R. (2008). "Levee erosion by overtopping in New Orleans during the Katrina Hurricane." *Journal of Geotechnical and Geoenvironmental Engineering*, 134, 618 – 627.

Briaud J.-L., Chen, H. C. Kwak K., Han S-W., Ting F., (2001). “Multiflood and multilayer method for scour rate prediction at bridge piers.” *Journal of Geotechnical and Geoenvironmental Engineering*, 127(2), 105-113.

Briaud, J. L., Chen, H-C., Li, Y., & Nurtjahyo, P. (2004). “SRICOS-EFA method for complex piers in fine-grianed soils.” *Journal of Geotechnical and Geoenvironmental Engineering*, 130(11), 1180 – 1191.

Bush, T. (2006). “Plant fact sheet: Smooth Brome.” USDA – NRCS. <http://plants.usda.gov/factsheet/doc/fs_brin2.doc> (Mar. 12, 2009).

Cao Y., Wang J. , Briaud J.L., Chen H.C., Li Y., Nurtjahyo P. (2002). “EFA tests and the influence of various factors on the erodibility of cohesive soils.” *Proc. of the First Int. Conf. on Scour of Foundations*, Texas A&M University, Dept. of Civil Engineering, College Station.

Chapuis, R. P., and Gatien, T. (1986). "An improved rotating cylinder technique for quantitative measurements of the scour resistance of clays." *Can. Geotech. J.*, 23, 83–87.

Cheng, A. (2008). “New Orleans levee and floodwall construction and retrofitting.” *Proc. from National Taiwan Ocean Univ.* Taiwan, Nov. 27, 2008 (July 25, 2009).

Deretsky, Z. (2009). "Researchers Release Final Report on New Orleans Levees." National Science Foundation. <http://www.nsf.gov/news/news_images.jsp?cntn_id=107007&org=NSF > (Aug. 20, 2009).

Discovery Channel (2009) "Flood." Raging Planet series. <http://dsc.discovery.com/videos/raging-planet-flood/> (July 30, 2009)

Digital Map Store. (2005). “Iowa County Map – Iowa Map.” Digital Map Store LLC, Uniontown, PA. <http://county-map.digital-topo-maps.com/iowa-county-map.gif> (March 15, 2009).

Federal Emergency Management Agency (FEMA) (2005). Photo by Bob McMillan. <http://www.fema.gov/photodata/original/15613.jpg> (Aug. 20, 2009).

Fell, R., Wan, C. F., Cyganiewicz, J., & Foster, M. (2003). “Time for development of internal erosion and piping in embankment dams.” *Journal of Geotechnical and Geoenvironmental Engineering*, 129(4), 307 – 314.

Fread, D.L. (1988). “BREACH: An erosion model for earthen dam failures.” National Weather Service, National Oceanic and Atmospheric Administration, Silver Spring, Md.

Gerritsen, H. (2006). “The 1953 dike failures in The Netherlands.” *Geo-Strata*, 8(2), 18-21; 37.

Hanson, G. (2001). “Field and laboratory jet testing method for determining cohesive material erodibility.” *Proceedings of the Seventh Federal Interagency Sedimentation Conference,* Reno, Nevada.

Hanson, G. J. & Cook, K. R. (2004). “Apparatus, test procedures, and analytical methods to measure soil erodibility in situ.” *Applied Engineering in Agriculture*, 20(4), 455 – 462.

Hanson, G., & Simon, A. (2001). “Erodibility of cohesive streambeds in the loess area of the midwestern USA.” *Hydrological Processes*, 15(1), 23 – 38.

Hassan, M., Morris, M., Hanson, G., Lakhal, K. (2004). "Breach formation: Laboratory and numerical modeling of breach formation." *Proc. Dam Safety 2004, Association of State Dam Safety Officials* (ASDSO), CD-ROM. Lexington, KY.

Hughes, S. (2008). "Estimation of combined wave and storm surge overtopping at earthen levees." USACE – ERDC. CHETN

Hughes, S., and Nadal, N. (2009). "Shear stress estimates for combined wave and surge overtopping at earthen levees." USACE – ERDC. CHETN

Illinois State Geological Survey (SGS) (2009). "Geologic maps." <http://www.isgs.uiuc.edu/maps-data-pub/maps.shtml > (June 1, 2009).

Interagency Floodplain Management Task Force (1994) "Report to the administration floodplain management task force-sharing the challenge: Floodplain management into the 21st century." p. 191

Interagency Levee Policy Review Committee (ILPRC) (2006). "The national levee challenge: Levees and the FEMA map modernization initiative." *Stakeholder Committee Report on Levees*. <http://www.fema.gov/plan/prevent/fhm/lv_report.shtm#4 > (March 4, 2009).

Interagency Performance Evaluation Team (IPET) (2006). "Losses" *IPET Task Force-USACE*. < http://www.usace.army.mil/CECW/Pages/ipet_presentations.aspx >

Iowa Department of Natural Resources (DNR) (2009). General Geology. <http://www.igsb.uiowa.edu/service/geology.htm > (June 3, 2009).

Johnson, G.P., Holmes, R.R., and Waite, L.A. (2003). "The Great Flood of 1993 on the Upper Mississippi River – 10 Years Later." USGS.

Larson, Lee W. (1996) "The great USA flood of 1993." *Proc. of the IAHS Conference*, June 24-28, 1996, Anaheim, California.

Leclair, M. (2009). "Literature review and analysis of erosion testing methods." Master of Engineering report, Texas A&M University, College Station, TX.

Li, Ming-Han. (2008). Personal communication and presentation, Texas A&M University, College Station. Dec. 12, 2008.

Martindale, B., Osman, P., Hoelscher Engineering. "Why the concerns with levees; They're safe, right?" *Levee Issues in Illinois and the National Levee Challenge Recommendations.* <www.illinoisfloods.org/documents/IAFSM_Levee%20Article.pdf > (June 7, 2009).

McCave, I.N. (1971). “Sand waves in the North Sea off the coast of Holland.” *Marine Geology*, 10, 199-225.

Missouri Department of Natural Resources (DNR) (2009). “Geology and land survey.” <http://www.dnr.mo.gov/geology/ > (May 25, 2009).

Mitchell, G. E. (1900). "Millions appropriated for levees." *The Irrigation Age*, XV1v.

Muijs, J.A. (1999). “Grass cover as a dike revetment.” *Technical Advisory Committee for Flood Defence (TAW).* <http://www.tawinfo.nl/engels/downloads/GrassasDikeCover.pdf >

National Climatic Data Center (NCDC) (2009). NOAA satellite and information service. <http://www.ncdc.noaa.gov/oa/ncdc.html >

National Committee on Levee Safety (NCLS) (2009). “Recommendations for a national levee safety program.” <http://ciasce.asce.org/news-article/report-congress-recommendations-national-levee-safety-program> 9-17.

National Information and Technology Centre for Transport and Infrastructure (CROW) (2000), “Standard RAW regulations,” The Netherlands.

National Oceanic and Atmospheric Administration (1994). “Natural disaster survey report, The great flood of 1993.”

Natural Resources Conservation Service (NRCS) (2007). “Critical area planting: CODE 342” Conservation Practice Standard. Sept. 2007.

Natural Resources Conservation Service (NRCS) (2008). “Vegetation establishment, herbaceous seeding: CODE 723” Missouri Agronomy Specification. April 2008.

O'Brien, G. (2002). "Making the Mississippi River over again: The development of river control in Mississippi." *Mississippi History Now*, Mississippi Historical Society.

Partrac Ltd. (2009). Sediment cohesive strength meter. Glasgow, UK.

Paterson, D.M. (1989). “Short term changes in the erodibility of intertidal cohesive sediments related to the migratory behavior of epipelic diatoms. *Limnology and Oceanography,* 34, 223-234.

PBS (2001). “Fatal flood.” <http://www.pbs.org/wgbh/amex/flood/filmmore/index.html> (June 11, 2009).

Phoon, K. (2008). “Reliability of levee systems.” *Reliability-based design in geotechnical engineering: computations and applications*, Wolff T.F. ed., Taylor & Francis, London, 449-459.

Pollen, N., and Shields, F. D. "Effects of removal of riparian vegetation on levee stability on the Sacramento River." *American Geophysical Union Fall Meeting*, San Francisco, CA.

Powledge, G.R., and Dodge, R.A. (1985). “Overtopping of mall dams: An alternative for dam safety.” *Proc. Specialty Conf.: Hydraulics and Hydrology in the Small Computer Age.* ASCE, Hydraulics Division, Reston, VA, 1071-1076.

Ralston, D.C. (1987). “Mechanics of embankment erosion during overflow.” *Proc. 1987 Nat. Conf.on Hydraulic Engineering,* ASCE, Hydraulics Division, Reston, VA, 733-738.

Regazzoni, P.L., Marot, D., Courivaud, J. R., Hanson, G., Wahl, T. (2008) “Soils erodibility: A comparison between the jet erosion test and the hole erosion test.” *Proceedings of the Inaugural International Conference of the Engineering Mechanics Institute*, Minneapolis, Minnesota, 1 – 7.

Riley, D.T. (2007). “Memorandum for major subordinate commands and districts: Interim vegetation guidance for control of vegetation on levees.” USACE, Washington, D.C.

Rogers, J.D. (2009). “Post-flood reconnaissance: Upper Mississippi River flooding of 2008.” *Proc. of Natural Hazard Mitigation Institute: Finding the Balance Between Floods, Flood Protection, and River Navigation.* St. Louis Univ., Nov. 11, 2008.

Schaper, J. (2009). “The geology of Missouri.” <http://members.socket.net/~joschaper/geo.html > (May 27, 2009).

Seijffert, J.W. and Verheij, H.J. (1998). “Grass covers and reinforcement measures.” Chapter 14, *Dikes and revetments: Design maintenance and safety assessment*, K.W. Pilarczyk, ed., RWS-DWW, Delft, The Netherlands.

Sheaffer, C. C., Marten, G. C., Rabas, D. L., Martin, N. P., and Miller, D. W. (1990). "Reed canarygrass." Minnesota Agricultural Experiment Station. University of Minnesota Extension, St. Paul, MN.

Stallings, E.A.(1994). *Hydrometeorlogical analysis of the great flood of 1993*: Department of Commerce. National Weather Service, National Oceanographic and Atmospheric Administration, Silver Spring, MD.

Storesund, R., Bea, R. G., Bernhardt, M. L., Briaud, J.-L., Franken, D., et al. (2009). "2008 Midwest levee performance investigation: Summary of initial field reconnaissance." University of California at Berkeley, Texas A&M Univ., Missouri S&T.

Temple, D.M., Hanson, G.J., Neilsen, M.L., and Cook, K.R. (2005). "Simplified breach analysis model for homogeneous embankments Part I. Background and model components." *Proc. 2005 U.S. Society on Dams Annual Meeting and Conference*, United States Society on Dams, Salt Lake City, UT, 151-161.

Temple, D.M., Robinson, K.M., Ahring, R.M., and Davis, A.G. (1987). *Stability design of grass-lined open channels.* U.S. Government Printing Office, Washington, DC.

Tolhurst, T., Black, K., Shayler, S., Mather, S., Black, I., Baker, K., and Paterson, D. (1999). "Measuring the in situ erosion shear stress of intertidal sediments with the Cohesive Strength Meter (CSM)." *Estuarine, Coastal and Shelf Science*, 49(2), 281-294.

Tucker, S. (2009). "So you live behind a levee; The whole story." Master of Engineering report, Texas A&M University, College Station, TX.

U.S. Army Corps of Engineers (2000). "Guidelines for landscape planting and vegetation management at floodwalls, levees, and embankment dams: EM 1110-2-301." US Army Corps of Engineers, Washington, D.C. Jan. 1, 2000.

U.S. Army Corps of Engineers (2004). "History of the Mississippi River and Tributaries Project." K. Gibbs, ed., New Orleans. <www.mvn.usace.army.mil/pao/bro/misstrib.htm> (Feb. 25, 2009).

U.S. Army Corps of Engineers (2007). "Memphis district flood risk management." <www.mvm.usace.army.mil/floodcontrol/levees/levees.htm> (Aug. 2, 2009).

U.S. Army Corps of Engineers (2008). "Corps map assists in flood fight on Mississippi." *Quad-Cities Online*. June 18, 2008. <http://www.qconline.com/archives/qco/display.php?id=391730 > (Jan. 12, 2009).

U.S. Army Corps of Engineers (2009a). "Typical levee design." <http://www.mvp.usace.army.mil/docs/flood_fight2009/4Emergency_Levee_Construction_Monitoring_2009_JRL.pdf > (June 13, 2009).

U.S. Army Corps of Engineers (2009b). “Headquarters history-flood.” <http://www.usace.army.mil/history/pages/brief/07-development/flood-lg.jpg > (July 21, 2009).

U.S. Geological Survey (USGS) (2006). Scientific assessment and strategy team (SAST) website. <http://edc.usgs.gov/sast/ > (March 14, 2009).

U.S. Geological Survey (USGS) (2007). Upper Mississippi. <http://www.umesc.usgs.gov/rivers/upper_mississippi/select_a_reach.html> (March 14, 2009).

U.S. Geological Survey (2008). Suspended sediment database: Daily values of suspended sediment and ancillary data. <http://co.water.usgs.gov/sediment/conc.frame.html> (July 29, 2009).

U.S. Geological Survey (USGS) (2009). “Water watch: Animation of flood and high flow condition maps.” <http://waterwatch.usgs.gov/?m=flood&r=mo&w=real%2Canimation&ym=200806 >

van Heerden, I. (2007). "The failure of the New Orleans levee system following Hurricane Katrina and the pathway forward." *Public Administration Review*, 67(s1), 24-35.

Wan, C. F. & Fell, R. (2004a). Laboratory tests on the rate of piping erosion of soils in embankment dams. *Geotechnical Testing Journal*, 27(3). (April 29, 2009) <http://65.209.24.102/DOWNLOAD/GTJ11903-DL.17235-1.pdf>

Wan, C. F. & Fell, R. (2004b). Investigation of rate of erosion of soils in embankment dams. *Journal of Geotechnical and Geoenvironmental Engineering*, 130(4), 373 – 380.

Washington State Department of Ecology. (2008). "Non-native freshwater plants: Reed Canarygrass." <http://www.ecy.wa.gov/Programs/wq/plants/weeds/aqua011.html> (November 28, 2008)

White, C.M., and Gayed, Y.K. (1943). “Hydraulic models of breached earthen banks.” *The Civil Engineer in War,* Vol 3, 181-200.

Wurbs, R.A. and James, W.P. (2002). *Water Resources Engineering*. Prentice-Hall, Upper Saddle River, NJ.

APPENDIX 1. MIDWEST LEVEE SAMPLE LOG

Sample No.	Site	Date	Time	H/V	GPS - N	GPS - W	Pushed or Driven	Pocket Pen	TorVane	Location
S1B1	Winfield	9/29/2008	10:40am	H			D	1.0, 1.1	0.45, 0.47	North side of breach, 41" below crest, crest centerline, into the exposed core of existing levee
S1B2	Winfield	9/29/2008		V			P	0.45, 1.1, 0.4, 0.35, 0.75	0.15, 0.14	North side of breach, 91" below crest surface, slightly East of crest centerline
S1B3	Winfield	9/29/2008		H			D	1.75, 2.1	0.3, 0.29	South side of breach, 106" below crest surface, East of crest centerline
S1B4	Winfield	9/29/2008		V			P	1.2, 1.3	0.21, 0.3	South side of breach, 156" below crest surface, slightly East of crest centerline
S1B5	Winfield	9/29/2008		H			P/D	0.6, 0.7	0.15, 0.2, 0.11	South side of breach, 34" below crest, crest centerline, into exposed core of existing levee
S1Bag 1	Winfield	9/29/2008								?
S1Bag 2	Winfield	9/29/2008								?
S1Grass 1	Winfield	9/29/2008								?
S2B6	Bryants Creek	9/29/2008	2:50pm	H	39.25225	90.77829	D	1.9, 1.55	0.75, 0.59	East side of breach, 58" below crest surface, into exposed end of existing levee
S2B7	Bryants Creek	9/29/2008		V	39.25229	90.77817	P/D	0.75, 1.0, 1.2	0.6, 0.8	East side of breach, 18" below crest surface, on surface of remaining end
S2B8	Bryants Creek	9/29/2008		V			P/D	1.6, 0.5(fissured), 1.0	0.46, 0.51	Midway between breach ends, 10' below crest surface, estimated core at point of breach
S2B9	Bryants Creek	9/29/2008		H			D	1.45, 1.55	0.6, 0.56	Midway between breach ends, 10' below crest surface, side of estimated core at point of breach
S3B10	Brevator	9/30/2008	10:00am	V	38.96272	90.71165	D	2.35, 2.6	1.075, 1.025	Crest Centerline of levee, no breach, just south of "1st" culvert
S3B11	Brevator	9/30/2008		V	38.96272	90.71171	D	1.2, 1.3	0.33, 0.43	West toe, horizontal from B10, 10' below crest
S3B12	Brevator	9/30/2008		V	38.95773	90.71169	P/D	1.75, 1.75	0.7, 0.86	Crest Centerline of levee, no breach, North of "2nd" culvert, cracked box culvert allowed seepage
S3B13	Brevator	9/30/2008		V	38.95773	90.71176	P/D	1.1, 1.0	0.56, 0.7	West toe, horizontal from B12, 10' below crest
S3Bag 5	Brevator	9/30/2008								Taken at S3B10
S3Bag 6	Brevator	9/30/2008								Taken at S3B11
S3Bag 7	Brevator	9/30/2008								Taken at S3B12
S3Bag 8	Brevator	9/30/2008								Taken at S3B13
S3Grass 3	Brevator	9/30/2008								Taken at S3B10, covering Levee
S3Grass 4	Brevator	9/30/2008								Taken at S3B12, S3B13
S4B14	Kickapoo	9/30/2008	12:40pm	V	39.18476	90.74287	P/D	2.1, 1.75	0.61, 0.6	South side of breach, crest centerline @ crest elevation
S4B15	Kickapoo	9/30/2008		V	39.18481	90.74298	P/D	1.1, 0.85	0.41, 0.45	South side of breach, West toe, 9' below crest
S4B16	Kickapoo	9/30/2008		H	39.1848	90.74282	P/D	1.1, 1.25	0.6, 0.65	South side of breach, 74" below crest surface, mid cross-section, centerline, clayey material
S4B17	Kickapoo	9/30/2008		V	39.18522	90.7429	P/D	2.1, 2.0	0.72, 0.64	North side of breach, crest surface, crest centerline
S4B18	Kickapoo	9/30/2008		V	39.18522	90.74293	P/D	2.5, 2.8	0.45, 0.5	North side of breach, 9' below crest surface, West toe
S4Bag 9	Kickapoo	9/30/2008								Taken at S4B14
S4Bag 10	Kickapoo	9/30/2008								Taken at S4B15
S4Bag 11	Kickapoo	9/30/2008								Taken at S4B16 (clayey material)
S4Bag 12	Kickapoo	9/30/2008								Taken at S4B17
S4Bag 13	Kickapoo	9/30/2008								Taken at S4B18
S4Grass5	Kickapoo	9/30/2008								
S4Grass6	Kickapoo	9/30/2008								Taken at south side of breach
S5B19	Norton Woods	9/30/2008	3:30pm	V	39.13479	90.7202	P/D	2.75, 2.3	0.875, 0.75	South side of breach, crest centerline @ crest elevation
S5B20	Norton Woods	9/30/2008		V	39.13475	90.72027	P/D	1.25, 1.2	0.4, 0.39	South side of breach, West toe, 10' below crest elevation
S5B21	Norton Woods	9/30/2008		H	39.13531	90.72055	D	1.5, 1.45	0.65, 0.65	North side of breach, 5.5' below crest surface, mid cross-section, East of centerline of crest
S5B22	Norton Woods	9/30/2008		V	39.13533	90.72061	P/D	1.35, 1.25	0.5, 0.51	North side of breach, crest centerline @ crest elevation
S5B23	Norton Woods	9/30/2008		V	39.13533	90.72066	P/D	1.4, 1.5	0.37, 0.41	North side of breach, West toe, 10' below crest elevation

S5Bag 14	Norton Woods	9/30/2008								Taken at S5B19
S5Bag 15	Norton Woods	9/30/2008								Taken at S5B20
S5Bag 16	Norton Woods	9/30/2008								Taken at S5B21
S5Bag 17	Norton Woods	9/30/2008								Taken at S5B22
S5Bag 18	Norton Woods	9/30/2008								Taken at S5B23
S4Grass 7	Norton Woods	9/30/2008								
S6B24	Indian Graves North	10/1/2008	3:30pm	V	40.00128	91.45029	P/D	1.75, 1.6	0.45, 0.4	North side of breach, 74" below crest (not push-up), West of centerline of crest, clay core
S6B25	Indian Graves North	10/1/2008		V	40.00135	91.45022	P	Sand	Sand	North side of breach, 12" below crest surface, in sand shell, East of centerline of crest
S6B26	Indian Graves North	10/1/2008		V	40.00119	91.45047	P/D	2.0, 2.5, 2.25	0.87, 0.7	North side of breach, 15' below crest surface, West toe, clay core material (out in breach area)
S6Bag 19	Indian Graves North	10/1/2008								Taken at S6B24
S6Bag 20	Indian Graves North	10/1/2008								Taken at S6B25
S6Bag 21	Indian Graves North	10/1/2008								Taken at S6B26
S6Grass 8	Indian Graves North	10/1/2008								Taken at toe of levee
S6B27	Indian Graves North	10/2/2008	11:00am	V			P/D	1.25, 1.5	0.5, 0.53	South side of breach, 8' below crest surface, West of centerline
S6B28	Indian Graves North	10/2/2008		V			P	Sand	Sand	South side of breach, 3' below crest surface, East of centerline, in sand shell
S7B29	Indian Graves South	10/2/2008		V			D	1.5, 1.75	0.8, 0.7	South side of breach, near pump, clay core
S7B30	Indian Graves South	10/2/2008		V			D?	Sand	Sand	South side of breach, Sand shell
S7Grass 9	Indian Graves South	10/2/2008								Taken at toe of levee
S8B31	Two Rivers	10/3/2008		V	41.09392	91.06867	P	Sand	Sand	East side of breach, crest centerline at crest elevation
S8B32	Two Rivers	10/3/2008		V	41.09387	91.0685	P			East side of breach, South side toe, 6' below crest elevation
S8B33	Two Rivers	10/3/2008		V	41.0938	91.07021	P/D	2.5, 2.5	0.25, 0.375	Breach area, 15' below crest surface, North of centerline of crest, 250' from East side breach
S8B34	Two Rivers	10/3/2008		V	41.09378	91.07007	P/D	0.75, 0.7	0.15, 0.15	Breach area, 17' below crest surface, centerline of crest, 200' from East side breach
S8B35	Two Rivers	10/3/2008		V	41.09?	90.06?	Auger			East side of breach, 128" below crest, Hand auger through sand, south side midway up slope
S8Bag 31	Two Rivers	10/3/2008								Taken at S8B31
S8Bag 32	Two Rivers	10/3/2008								Taken at S8B32
S8Bag 33	Two Rivers	10/3/2008								Taken at S8B33

APPENDIX 2. MIDWEST LEVEE INDEX

	Water Content																		
Sample	Mtin (g)	Mtin+wet (g)	Mtin+dry (g)	Mw (g)	Ms (g)	water content %	Mtube (g)	Mtube+soil (g)	Msoil (g)	h1 (mm)	h2 (mm)	h (mm)	Recovery %	Idiam (mm)	Odiam (mm)	Volume ($m^{3)}$	Mass Density (kg/m^3)	Total Unit Weight (kN/m^3)	Dry Mass Density (kg/m^3)	Dry Unit Weight (kN/m^3)
S1B1	36.72	85.93	78.93	7.00	42.21	16.58	586.01	1335.85	749.84	49.67	106.00	155.67	68.09	72.10	76.48	4.33E-04	1732.78	17.00	1486.29	14.58
S1B2	29.36	53.09	48.08	5.01	18.72	26.76	589.70	1546.76	957.06	29.75	127.92	157.67	81.13	71.91	76.44	5.19E-04	1842.40	18.07	1453.42	14.26
S1B3	22.32	36.08	33.82	2.26	11.50	19.65	578.59	1460.20	881.61	42.67	111.67	154.33	72.35	71.86	76.44	4.53E-04	1946.47	19.09	1626.78	15.96
S1B4	1.04	13.99	11.48	2.51	10.44	24.04	578.59	1082.24	503.65	97.00	58.33	155.33	37.55	71.91	76.44	2.37E-04	2126.10	20.86	1714.01	16.81
S1B5	22.22	35.70	32.92	2.78	10.70	25.98	578.59	1440.62	862.03	42.33	113.67	156.00	72.86	71.40	76.35	4.55E-04	1894.28	18.58	1503.62	14.75
S2B6	21.96	35.87	32.70	3.17	10.74	29.52	578.51	1231.87	653.36	68.11	86.39	154.50	55.91	72.00	76.37	3.52E-04	1857.59	18.22	1434.26	14.07
S2B7	22.12	38.72	34.80	3.92	12.68	30.91	568.84	1325.78	756.94	53.17	100.73	153.90	65.45	71.90	76.36	4.09E-04	1850.61	18.15	1413.60	13.87
S2B8	22.06	35.95	31.65	4.30	9.59	44.84	578.59	1354.56	775.97	48.33	107.67	156.00	69.02	71.92	76.72	4.37E-04	1774.25	17.41	1224.99	12.02
S2B9	22.50	45.69	39.69	6.00	17.19	34.90	578.93	1358.53	779.60	52.19	101.81	154.00	66.11	72.02	76.34	4.15E-04	1879.80	18.44	1393.43	13.67
S3B10	22.59	52.01	47.02	4.99	24.43	20.43	581.63	1397.60	815.97	45.00	109.33	154.33	70.84	72.00	76.34	4.45E-04	1832.85	17.98	1521.97	14.93
S3B11	30.69	69.81	61.11	8.70	30.42	28.60	576.95	1249.81	672.86	54.67	99.00	153.67	64.43	72.06	76.35	4.04E-04	1666.68	16.35	1296.02	12.71
S3B12	22.32	40.25	35.88	4.37	13.56	32.23	562.27	1318.65	756.38	25.21	126.29	151.50	83.36	71.99	76.29	5.14E-04	1471.52	14.44	1112.87	10.92
S3B13	22.19	41.19	36.60	4.59	14.41	31.85	557.34	1287.54	730.20	46.90	102.77	149.67	68.67	72.02	76.05	4.19E-04	1743.97	17.11	1322.66	12.98
S4B14	30.59	56.31	49.38	6.93	18.79	36.88	584.07	1332.03	747.96	39.21	115.46	154.67	74.65	72.01	76.39	4.70E-04	1590.49	15.60	1161.95	11.40
S4B15	22.31	39.54	34.84	4.70	12.53	37.51	578.59	1461.30	882.71	31.00	124.00	155.00	80.00	71.86	76.22	5.03E-04	1755.22	17.22	1276.43	12.52
S4B16	22.80	55.49	47.61	7.88	24.81	31.76	580.94	1342.85	761.91	55.97	100.03	156.00	64.12	72.01	76.39	4.07E-04	1870.35	18.35	1419.50	13.93
S4B17	22.33	35.17	31.81	3.36	9.48	35.44	578.59	1281.18	702.59	47.67	102.33	150.00	68.22	71.98	76.07	4.16E-04	1687.22	16.55	1245.70	12.22
S4B18	23.46	51.75	45.45	6.30	21.99	28.65	572.48	1258.08	685.60	56.04	97.46	153.50	63.49	72.22	76.10	3.99E-04	1717.37	16.85	1334.93	13.10
S5B19	22.56	44.03	39.28	4.75	16.72	28.41	580.56	1322.12	741.56	56.92	97.58	154.50	63.16	72.10	76.27	3.98E-04	1861.57	18.26	1449.72	14.22
S5B20	21.97	46.22	38.96	7.26	16.99	42.73	583.98	1192.22	608.24	60.94	94.40	155.33	60.77	72.17	76.40	3.86E-04	1574.98	15.45	1103.46	10.82
S5B21	23.54	38.17	35.13	3.04	11.59	26.23	578.59	1481.41	902.82	33.67	119.67	153.33	78.04	71.90	76.30	4.86E-04	1858.32	18.23	1472.18	14.44
S5B22	22.10	42.18	37.61	4.57	15.51	29.46	578.59	1279.57	700.98	53.00	101.67	154.67	65.73	71.69	76.36	4.10E-04	1708.29	16.76	1319.50	12.94
S5B23	22.11	50.07	41.94	8.13	19.83	41.00	579.35	1147.10	567.75	56.26	98.24	154.50	63.59	72.14	76.43	4.02E-04	1414.06	13.87	1002.89	9.84
S6B24	37.70	71.21	63.73	7.48	26.03	28.74	578.71	1550.71	972.00	23.67	132.17	155.83	84.81	72.13	75.98	5.40E-04	1799.96	17.66	1398.18	13.72
S6B25	31.49	57.80	56.22	1.58	24.73	6.39	578.80	1635.11	1056.31	0.00	155.00	155.00	100.00	72.02	76.31	6.31E-04	1672.88	16.41	1572.41	15.43
S6B26	1.04	7.80	6.31	1.49	5.27	28.27	578.59	1343.10	764.51	56.00	99.67	155.67	64.03	72.02	76.31	4.06E-04	1882.94	18.47	1467.92	14.40
S6B27	22.03	39.99	37.19	2.80	15.16	18.47	578.59	1623.08	1044.49	5.00	149.00	154.00	96.75	72.13	76.63	6.09E-04	1715.52	16.83	1448.07	14.21
S6B28	22.12	47.83	47.37	0.46	25.25	1.82	578.59	1608.16	1029.57	0.00	154.33	154.33	100.00	71.97	76.34	6.28E-04	1639.85	16.09	1610.51	15.80
S7B29	22.16	52.89	46.55	6.34	24.39	25.99	592.56	1442.87	850.31	39.57	119.76	159.33	75.17	72.03	76.28	4.88E-04	1742.36	17.09	1382.88	13.57
S7B30	22.35	51.91	45.80	6.11	23.45	26.06	578.59	1609.78	1031.19	0.00	154.33	154.33	100.00	71.97	76.34	6.28E-04	1642.43	16.11	1302.94	12.78
S8B31	22.40	59.47	58.26	1.21	35.86	3.37	575.59	1629.76	1054.17	1.20	153.30	154.50	99.22	72.12	76.27	6.26E-04	1683.36	16.51	1628.41	15.97
S8B32	22.44	51.88	50.82	1.06	28.38	3.74	578.59	1611.91	1033.32	0.00	156.00	156.00	100.00	71.97	76.34	6.35E-04	1628.24	15.97	1569.61	15.40
S8B33	22.55	44.65	40.80	3.85	18.25	21.10	584.49	1770.79	1186.30	6.17	149.17	155.33	96.03	72.00	76.32	6.07E-04	1953.48	19.16	1613.16	15.83
S8B34	22.01	41.04	37.87	3.17	15.86	19.99	578.59	1778.65	1200.06	1.00	152.00	153.00	99.35	71.34	76.39	6.08E-04	1975.16	19.38	1646.14	16.15
S8B35							Hand Augured													

Sample	% Relative Compaction	2 µm	-200	% Clay Fraction	Activity	d_{50} (mm)	LL	PL	PI	USCS Classification	
S1B1	74.96	15.646	82.82	18.89	1.92	0.0705	NP	NP	NP	ML	*Used values obtained from S1B2 hydrometer
S1B2	73.30	15.646	82.82	18.89	1.92	0.0232	55	25	30	CH	
S1B3	82.05					--	--	--	--	--	** Used average tube weight
S1B4	86.23					0.0276	--	--	--	--	** Used average tube weight
S1B5	75.84					--	--	--	--	--	** Used average tube weight
S2B6	76.47	42.427	89	47.67	1.15	--	--	--	--	--	
S2B7	75.37	50.218	95.78	52.43	1.08	--	--	--	--	--	
S2B8	70.69					0.0038	71	22	49	CH	** Used average tube weight
S2B9	80.41	41.098	95.63	42.98	1.51	0.0019	78	24	54	CH	
S3B10	81.10	25.523	92.9	27.47	0.82	--	--	--	--	--	
S3B11	69.06	22.484	98.16	22.91	1.20	0.0041	88	26	62	CH	
S3B12	59.30	35.6	95.6	37.24	1.12	0.0136	41	20	21	CL	
S3B13	70.48	31.293	93.55	33.45	1.28	0.0162	50	23	27	CL	
S4B14	64.40	28.911	92.4	31.29	1.25	0.0054	66	26	40	CH	
S4B15	70.74					0.0093	64	24	40	CH	** Used average tube weight
S4B16	78.67	44.413	92.92	47.80	1.28	0.0114	64	28	36	CH	
S4B17	69.04					--	--	--	--	--	** Used average tube weight
S4B18	73.99	12.488	78.68	15.87	2.64	0.0030	81	24	57	CH	
S5B19	85.67	21.431	90.42	23.70	1.54	--	--	--	--	--	
S5B20	65.21	23.045	89.18	25.84	1.82	0.0302	57	24	33	CH	
S5B21	77.23					0.0163	55	22	33	CH	** Used average tube weight
S5B22	77.98					0.0141	70	28	42	CH	** Used average tube weight
S5B23	59.27	21.427	93.98	22.80	2.10	--	--	--	--	--	
S6B24	77.06					--	--	--	--	--	
S6B25	--		1.48			0.0179	72	27	45	CH	
S6B26	80.90	21.979	94.09	23.36	2.05	--	48	20	28	ML/CL	**Used average tube weight
S6B27	79.81					0.3927	N/A	N/A	N/A	SP	** Used average tube weight
S6B28	88.76					0.0112	60	25	35	CH	** Used average tube weight, ID, and OD
S7B29	68.86	23.719	76.63	30.95	1.52	--	--	--	--	--	
S7B30	--		0.26			--	--	--	--	--	** Used average tube weight, ID, and OD
S8B31	--		0.69			0.0189	54	18	36	CH	
S8B32	--		2.31			0.6238	NP	NP	NP	SP	** Used average tube weight, ID, and OD
S8B33	--	7.285	83.04	8.77	3.71	0.8602	NP	NP	NP	SP	
S8B34	--					0.7375	NP	NP	NP	SP	** Used average tube weight
S8B35	--	5.166	33.49	15.43	1.94	0.0261	50	23	27	CH	

APPENDIX 3. PARTICLE SIZE DETERMINATION

HYDROMETER AND SIEVE ANALYSIS (ASTM D 422)

Hydrometer Analysis

Project Name:	Midwest Levees	Boring No.:	S1Bulk1
Location:	Winfield	Depth:	
Description:	Brown sandy clay	Date:	01/09/09

Hygroscopic water content

Can No.	1
Wet Wt + Tare (g)	17.32
Dry Wt + Tare (g)	15.41
Tare Wt (g)	0.99
Moisture Content (%)	13.25
Correction Factor =	0.883

Hydrometer Type:	151H	
Mass of air dry soil =	162.96	g
Specific Gravity =	2.71	
Mass of oven dry soil =	143.900	g

Start Time	Elapsed Time	Actual Reading	Composite Correction	Corrected Reading	Temperature (degrees C)	Effective Hyd. Depth	K	Diameter of particle (mm)	Percent finer in suspension (%)
2:33 PM	0	1.042	0.004	1.038	16.9	5.185	0.014	--	41.850
	0.067	1.042	0.004	1.038	16.9	5.185	0.014	0.121	41.850
	0.25	1.041	0.004	1.037	16.9	5.450	0.014	0.064	40.749
	0.5	1.039	0.004	1.035	16.9	5.979	0.014	0.048	38.546
	1	1.035	0.004	1.031	16.9	7.037	0.014	0.036	34.141
	1.5	1.033	0.004	1.029	16.9	7.566	0.014	0.031	31.938
	2	1.031	0.004	1.027	16.9	8.095	0.014	0.028	29.736
	5	1.025	0.004	1.021	16.9	9.682	0.014	0.019	23.128
	15	1.02	0.004	1.016	16.9	11.005	0.014	0.012	17.621
	30	1.017	0.004	1.013	16.9	11.798	0.014	0.009	14.317
	60	1.015	0.004	1.011	16.9	12.327	0.014	0.006	12.115
	120	1.014	0.004	1.01	16.9	12.592	0.014	0.004	11.013
	240	1.013	0.004	1.009	16.9	12.856	0.014	0.003	9.912
	480	1.013	0.004	1.009	16.9	12.856	0.014	0.002	9.912
	1140	1.012	0.004	1.008	16.9	13.121	0.014	0.001	8.811

Sieve Analysis of Coarse Fraction Weight of Soil Sieved = 66.81 g

Sieve No.	Weight of Sieve (g)	Weight of Sieve + soil (g)	Weight of Retained (%)	Percentage Retained (%)	Percentage Passed (%)	Particle Size (mm)
10	606.96	606.96	0.00	0.00	100.00	2
40	339.42	339.46	0.04	0.03	99.97	0.425
80	317.51	328.37	10.86	7.55	92.43	0.18
100	337.55	346.44	8.89	6.18	86.25	0.15
200	340.91	384.71	43.80	30.44	55.81	0.075
-200	479.43	482.55	3.12	2.17	53.64	
		Total W =	*66.71*			

Combined	
Particle Size (mm)	Percent Passing (%)
2.000	100.000
0.425	99.972
0.180	92.425
0.150	86.247
0.075	55.810
0.064	40.749
0.048	38.546
0.036	34.141
0.031	31.938
0.028	29.736
0.019	23.128
0.012	17.621
0.009	14.317
0.006	12.115
0.004	11.013
0.003	9.912
0.002	9.912
0.001	8.811

D50 = 0.0705 mm

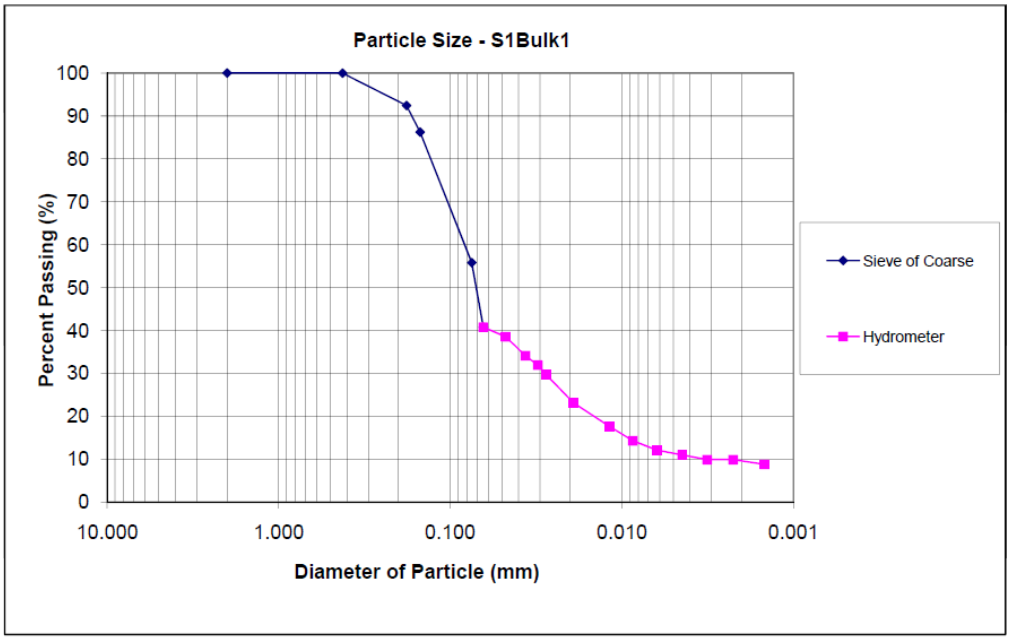
Particle Size - S1Bulk1
Percent Passing (%)
100
90
80
70
60
50
40
30
20
10
0
10.000
1.000
0.100
0.010
0.001
Diameter of Particle (mm)
Sieve of Coarse
Hydrometer

Hydrometer Analysis

Project Name:	Midwest Levees	Boring No.:	S1Bulk2
Location:	Winfield	Depth:	
Description:	Dk brown sandy clay	Date:	01/09/09

Hygroscopic water content

Can No.	1
Wet Wt + Tare (g)	18.43
Dry Wt + Tare (g)	14.79
Tare Wt (g)	0.98
Moisture Content (%)	26.36
Correction Factor =	0.791

Hydrometer Type:	151H	
Mass of air dry soil =	104.58	g
Specific Gravity =	2.71	
Mass of oven dry soil =	82.765	g

Start Time	Elapsed Time	Actual Reading	Composite Correction	Corrected Reading	Temperature (degrees C)	Effective Hyd. Depth	K	Diameter of particle (mm)	Percent finer in suspension (%)
2:41pm	0	1.041	0.005	1.036	16.9	5.450	0.014	--	60.933
	0.067	1.041	0.005	1.036	16.9	5.450	0.014	0.124	68.933
	0.25	1.04	0.005	1.035	16.9	5.714	0.014	0.066	67.018
	0.5	1.039	0.005	1.034	16.9	5.979	0.014	0.048	65.104
	1	1.036	0.005	1.031	16.9	5.772	0.014	0.036	59.359
	1.5	1.034	0.005	1.029	16.9	7.301	0.014	0.030	55.530
	2	1.033	0.005	1.028	16.9	7.566	0.014	0.027	53.615
	5	1.028	0.005	1.023	16.9	8.888	0.014	0.018	44.041
	15	1.023	0.005	1.018	16.9	10.211	0.014	0.011	34.467
	30	1.02	0.005	1.015	16.9	11.005	0.014	0.008	28.722
	60	1.018	0.005	1.013	16.9	11.534	0.014	0.006	24.893
	120	1.017	0.005	1.012	16.9	11.798	0.014	0.004	22.978
	240	1.015	0.005	1.01	16.9	12.327	0.014	0.003	19.148
	480	1.015	0.005	1.01	16.9	12.327	0.014	0.002	19.148
	1140	1.014	0.005	1.009	16.9	12.592	0.014	0.001	17.233

Sieve Analysis of Coarse Fraction Weight of Soil Sieved = 14.09 g

Sieve No.	Weight of Sieve (g)	Weight of Sieve + soil (g)	Weight of Retained (%)	Percentage Retained (%)	Percentage Passed (%)	Particle Size (mm)
10	607.00	607.00	0.00	0.00	100.00	2
40	339.61	339.76	0.15	0.18	99.82	0.425
80	317.51	320.43	2.92	3.53	96.29	0.18
100	337.54	339.58	2.04	2.46	93.83	0.15
200	340.89	348.90	8.01	9.68	84.15	0.075
-200	479.43	480.33	0.90	1.09	83.06	
		Total W =	*14.02*			

Combined	
Particle Size (mm)	Percent Passing (%)
2.000	100.000
0.425	99.819
0.180	96.291
0.150	93.826
0.075	84.148
0.048	65.104
0.036	59.359
0.030	55.530
0.027	53.615
0.010	44.041
0.011	34.467
0.008	28.722
0.006	24.893
0.004	22.978
0.003	19.148
0.002	19.148
0.001	17.233

D50 = 0.0232 mm

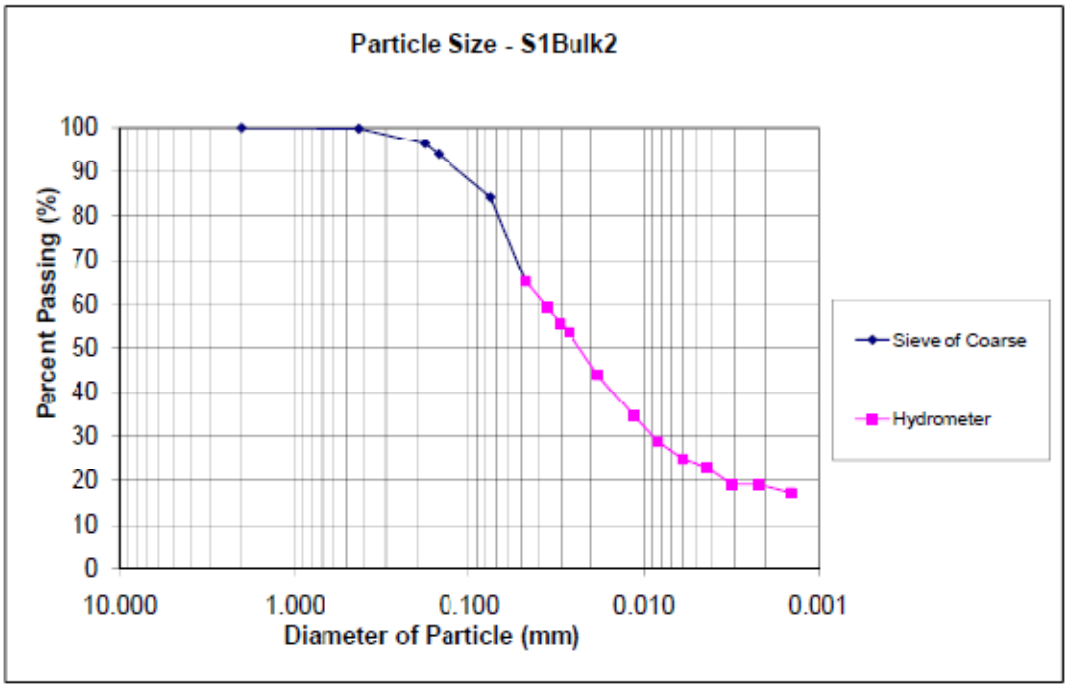
Particle Size - S1Bulk2
Percent Passing (%)
100
90
80
70
60
50
40
30
20
10
0
10.000
1.000
0.100
0.010
0.001
Diameter of Particle (mm)
Sieve of Coarse
Hydrometer

Hydrometer Analysis

Project Name:	Midwest Levees	Boring No.:	S1B2
Location:	Winfield	Depth:	
Description:	Dk brown clay	Date:	01/12/09

Hygroscopic water content

Can No.	1
Wet Wt + Tare (g)	19.19
Dry Wt + Tare (g)	15.13
Tare Wt (g)	1.02
Moisture Content (%)	28.77
Correction Factor =	0.777

Hydrometer Type:	151H	
Mass of air dry soil =	78.26	g
Specific Gravity =	2.71	
Mass of oven dry soil =	60.773	g

Start Time	Elapsed Time	Actual Reading	Composite Correction	Corrected Reading	Temperature (degrees C)	Effective Hyd. Depth	K	Diameter of particle (mm)	Percent finer in suspension (%)
1:46 PM	0	1.037	0.004	1.033	17.8	6.508	0.013	--	86.055
	0.067	1.035	0.004	1.031	17.8	7.037	0.013	0.138	80.839
	0.25	1.033	0.004	1.029	17.8	7.566	0.013	0.074	75.624
	0.5	1.03	0.004	1.026	17.8	8.359	0.013	0.055	67.801
	1	1.027	0.004	1.023	17.8	9.153	0.013	0.041	59.978
	1.5	1.025	0.004	1.021	17.8	9.682	0.013	0.034	54.762
	2	1.024	0.004	1.02	17.8	9.946	0.013	0.030	52.154
	5	1.02	0.004	1.016	17.8	11.005	0.013	0.020	41.724
	15	1.016	0.004	1.012	17.8	12.063	0.013	0.012	31.293
	30	1.014	0.004	1.01	17.8	12.592	0.013	0.009	26.077
	60	1.013	0.004	1.009	17.8	12.856	0.013	0.006	23.469
	120	1.011	0.004	1.007	17.8	13.385	0.013	0.004	18.254
	240	1.011	0.004	1.007	17.8	13.385	0.013	0.003	18.254
	480	1.01	0.004	1.006	17.8	13.650	0.013	0.002	15.646
	1140	1.01	0.004	1.006	17.8	13.650	0.013	0.001	15.646

Sieve Analysis of Coarse Fraction Weight of Soil Sieved = 11.3 g

Sieve No.	Weight of Sieve (g)	Weight of Sieve + soil (g)	Weight of Retained (%)	Percentage Retained (%)	Percentage Passed (%)	Particle Size (mm)
10	606.89	606.89	0.00	0.00	100.00	2
40	339.13	339.22	0.09	0.15	99.85	0.425
80	317.49	318.81	1.32	2.17	97.68	0.18
100	337.52	338.75	1.23	2.02	95.66	0.15
200	340.89	348.69	7.80	12.83	82.82	0.075
-200	479.40	480.28	0.88	1.45	81.37	
		Total W =	*11.32*			

Combined	
Particle Size (mm)	Percent Passing (%)
2.000	100.000
0.425	99.852
0.180	97.680
0.150	95.656
0.075	82.821
0.074	75.624
0.055	67.801
0.041	59.978
0.034	54.762
0.030	52.154
0.020	41.724
0.012	31.293
0.009	26.077
0.006	23.469
0.004	18.254
0.003	18.254
0.002	15.646
0.001	15.646

D50 = 0.0276 mm

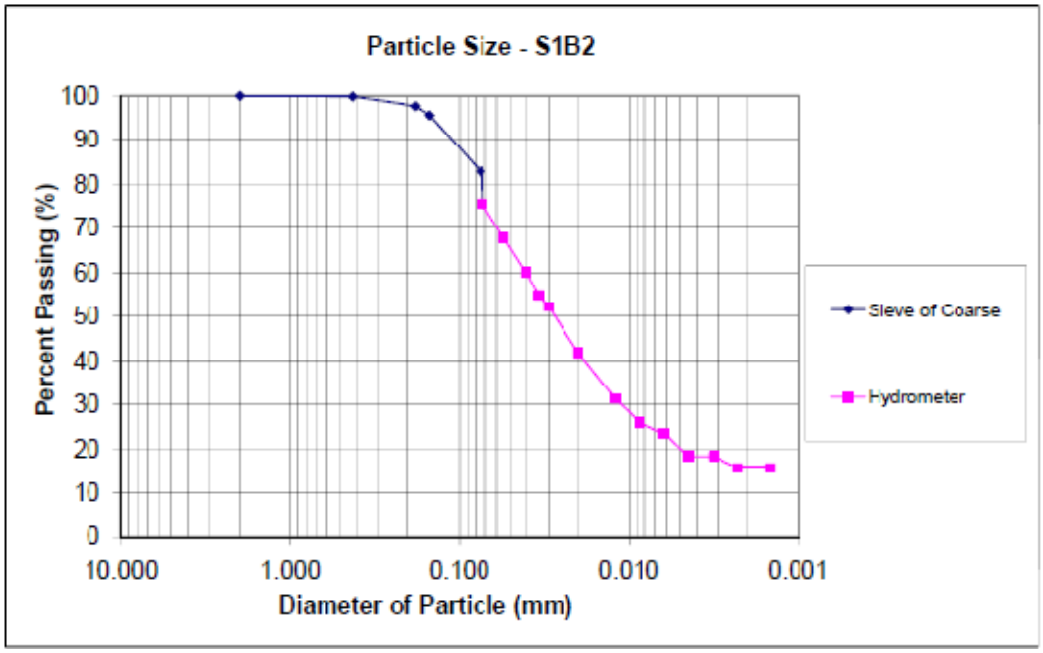
Particle Size - S1B2
Percent Passing (%)
100
90
80
70
60
50
40
30
20
10
0
10.000
1.000
0.100
0.010
0.001
Diameter of Particle (mm)
Sieve of Coarse
Hydrometer

Hydrometer Analysis

Project Name:	Midwest Levees	Boring No.:	S2B6
Location:	Brian's Creek	Depth:	58"
Description:	Gray clay w/tan seams	Date:	01/12/09

Hygroscopic water content

Can No.	1
Wet Wt + Tare (g)	15.86
Dry Wt + Tare (g)	12.68
Tare Wt (g)	1.01
Moisture Content (%)	27.25
Correcion Factor =	0.786

Hydrometer Type.	151H	
Mass of air dry soil =	75.41	g
Specific Gravity =	2.75	
Mass of oven dry soil =	59.262	g

Start Time	Elapsed Time	Actual Reading	Composite Correction	Corrected Reading	Temperature (degrees C)	Effective Hyd. Depth	K	Diameter of particle (mm)	Percent finer in suspension (%)
2:16pm	0	1.036	0.005	1.031	17.8	6.772	0.013	--	82.202
	0.067	1.034	0.005	1.029	17.8	7.301	0.013	0.139	76.899
	0.25	1.033	0.005	1.028	17.8	7.566	0.013	0.073	74.247
	0.5	1.033	0.005	1.028	17.8	7.566	0.013	0.052	74.247
	1	1.032	0.005	1.027	17.8	7.830	0.013	0.037	71.595
	1.5	1.032	0.005	1.027	17.8	7.830	0.013	0.030	71.595
	2	1.031	0.005	1.026	17.8	8.095	0.013	0.027	68.944
	5	1.03	0.005	1.025	17.8	8.359	0.013	0.017	66.292
	15	1.028	0.005	1.023	17.8	8.888	0.013	0.010	60.989
	30	1.027	0.005	1.022	17.8	9.153	0.013	0.007	58.337
	60	1.026	0.005	1.021	17.8	9.417	0.013	0.005	55.685
	120	1.024	0.005	1.019	17.8	9.946	0.013	0.004	50.382
	240	1.023	0.005	1.018	17.8	10.211	0.013	0.003	47.730
	480	1.021	0.005	1.016	17.8	10.740	0.013	0.002	42.427
	1140	1.02	0.005	1.015	17.8	11.005	0.013	0.001	39.775

Sieve Analysis of Coarse Fraction — Weight of Soil Sieved = 2.6 g

Sieve No.	Weight of Sieve (g)	Weight of Sieve + soil (g)	Weight of Retained (%)	Percentage Retained (%)	Percentage Passed (%)	Particle Size (mm)
10	606.94	607.13	0.19	0.32	99.68	2
40	339.24	339.98	0.74	1.25	98.43	0.425
80	317.50	319.86	2.36	3.98	94.45	0.18
100	337.56	338.30	0.74	1.25	93.20	0.15
200	340.90	343.39	2.49	4.20	89.00	0.075
-200	479.42	479.86	0.44	0.74	88.25	
		Total W =	*6.96*			

Combined	
Particle Size (mm)	Percent Passing (%)
2	99.679
0.425	98.431
0.18	94.448
0.15	93.200
0.075	88.998
0.052	74.247
0.037	71.595
0.030	71.595
0.027	68.944
0.017	66.292
0.010	60.989
0.007	58.337
0.005	55.685
0.004	50.382
0.003	47.730
0.002	42.427
0.001	39.775

D50 = 0.0038 mm

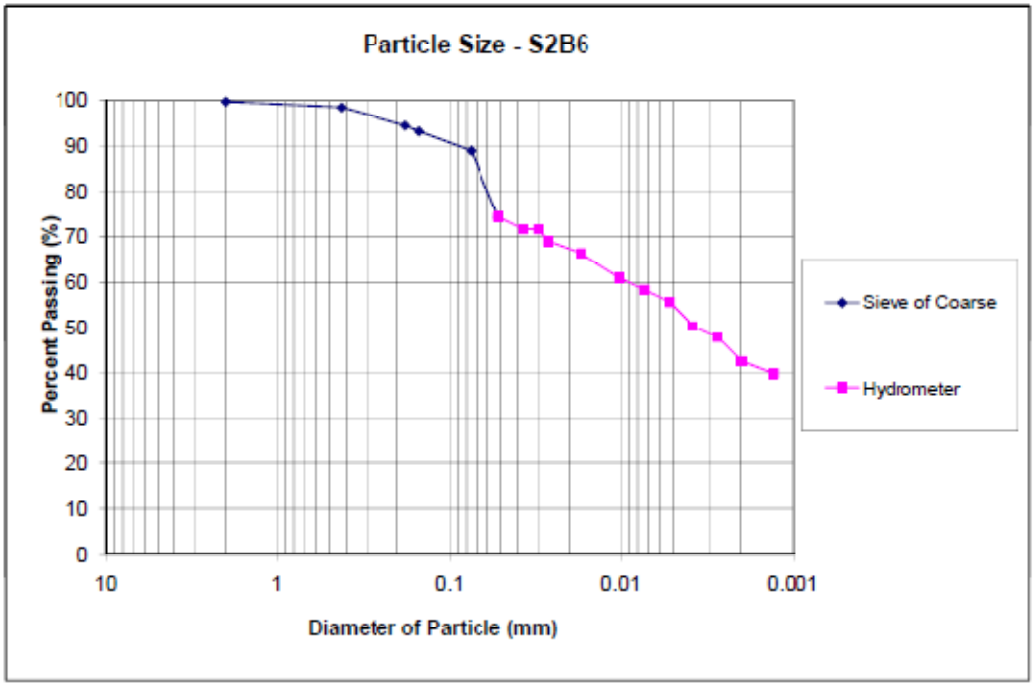
Particle Size - S2B6
Percent Passing (%)
100
90
80
70
60
50
40
30
20
10
0
10
1
0.1
0.01
0.001
Diameter of Particle (mm)
Sieve of Coarse
Hydrometer

Hydrometer Analysis

Project Name:	Midwest Levees	Boring No.:	S2E7
Location:	Brian's Creek	Depth:	18"
Description:	Clay, gray-dk gray w/tan and red/br seams	Date:	01/12/09

Hygroscopic water content

Can No.	1
Wet Wt + Tare (g)	18.18
Dry Wt + Tare (g)	13.45
Tare Wt (g)	1.02
Moisture Content (%)	38.05
Correction Factor =	0.724

Hydrometer Type:	151H	
Mass of air dry soil =	82.08	g
Specific Gravity =	2.75	
Mass of oven dry soil =	59.455	g

Start Time	Elapsed Time	Actual Reading	Composite Correction	Corrected Reading	Temperature (degrees C)	Effective Hyd. Depth	K	Diameter of particle (mm)	Percent finer in suspension (%)
2:09pm	0	1.038	0.005	1.033	17.8	6.243	0.013	--	87.220
	0.067	1.038	0.005	1.033	17.8	6.243	0.013	0.128	87.220
	0.25	1.038	0.005	1.033	17.8	6.243	0.013	0.066	87.220
	0.5	1.038	0.005	1.033	17.8	6.243	0.013	0.047	87.220
	1	1.038	0.005	1.033	17.8	6.243	0.013	0.033	87.220
	1.5	1.037	0.005	1.032	17.8	6.508	0.013	0.028	84.577
	2	1.037	0.005	1.032	17.8	6.508	0.013	0.024	84.577
	5	1.035	0.005	1.03	17.8	7.037	0.013	0.016	79.291
	15	1.033	0.005	1.028	17.8	7.566	0.013	0.009	74.005
	30	1.031	0.005	1.026	17.8	8.095	0.013	0.007	68.719
	60	1.029	0.005	1.024	17.8	8.624	0.013	0.005	63.433
	120	1.027	0.005	1.022	17.8	9.153	0.013	0.004	58.147
	240	1.025	0.005	1.02	17.8	9.682	0.013	0.003	52.861
	480	1.024	0.005	1.019	17.8	9.946	0.013	0.002	50.218
	1140	1.022	0.005	1.017	17.8	10.476	0.013	0.001	44.932

Sieve Analysis of Coarse Fraction — Weight of Soil Sieved = 2.6 g

Sieve No.	Weight of Sieve (g)	Weight of Sieve + soil (g)	Weight of Retained (%)	Percentage Retained (%)	Percentage Passed (%)	Particle Size (mm)
10	606.91	606.91	0.00	0.00	100.00	2
40	339.16	339.79	0.63	1.06	98.94	0.425
80	317.50	318.38	0.88	1.48	97.46	0.18
100	337.54	337.71	0.17	0.29	97.17	0.15
200	340.89	341.72	0.83	1.40	95.78	0.075
-200	479.42	479.74	0.32	0.54	95.24	
		Total W =	*2.83*			

Combined	
Particle Size (mm)	Percent Passing (%)
2.000	100.000
0.425	98.940
0.180	97.460
0.150	97.174
0.075	95.778
0.047	87.220
0.033	87.220
0.028	84.577
0.024	84.577
0.016	79.291
0.009	74.005
0.007	68.719
0.005	63.433
0.004	58.147
0.003	52.861
0.002	50.219
0.001	44.932

D50 = 0.0019 mm

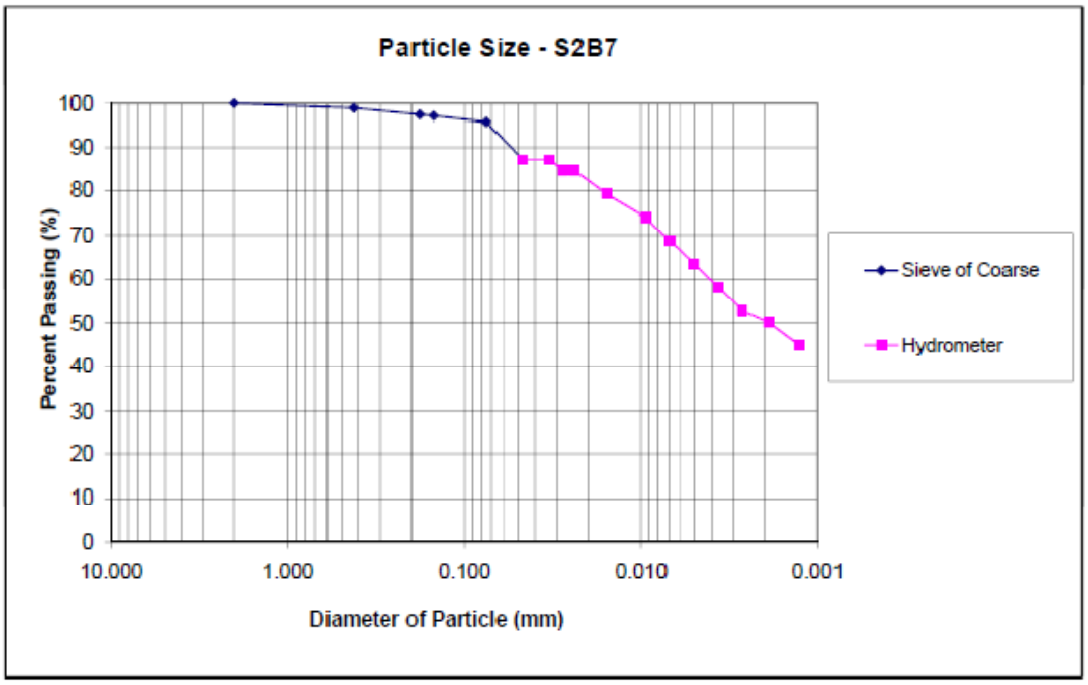
Particle Size - S2B7
Percent Passing (%)
100
90
80
70
60
50
40
30
20
10
0
10.000
1.000
0.100
0.010
0.001
Diameter of Particle (mm)
Sieve of Coarse
Hydrometer

Hydrometer Analysis

Project Name:	Midwest Levees	Boring No.:	S2B9
Location:	Brian's Creek	Depth:	10'
Description:	Gray clay, stiff, hard to break up	Date:	01/15/09

Hygroscopic water content

Can No.	1
Wet Wt + Tare (g)	16.05
Dry Wt + Tare (g)	12.21
Tare Wt (g)	1.01
Moisture Content (%)	34.29
Correction Factor =	0.715

Hydrometer Type:	151H	
Mass of air dry soil =	77.18	g
Specific Gravity =	2.74	
Mass of oven dry soil =	57.474	g

Start Time	Elapsed Time	Actual Reading	Composite Correction	Corrected Reading	Temperature (degrees C)	Effective Hyd. Depth	K	Diameter of particle (mm)	Percent finer in suspension (%)
2:53pm	0	1.035	0.005	1.03	22	7.037	0.013	--	82.195
	0.067	1.034	0.005	1.029	22	7.301	0.013	0.136	79.456
	0.25	1.034	0.005	1.029	22	7.301	0.013	0.070	79.456
	0.5	1.033	0.005	1.028	22	7.566	0.013	0.050	76.716
	1	1.033	0.005	1.028	22	7.566	0.013	0.036	76.716
	1.5	1.032	0.005	1.027	22	7.830	0.013	0.030	73.976
	2	1.032	0.005	1.027	22	7.830	0.013	0.026	73.976
	5	1.031	0.005	1.026	22	8.095	0.013	0.017	71.236
	15	1.029	0.005	1.024	22	8.624	0.013	0.010	65.756
	30	1.027	0.005	1.022	22	9.153	0.013	0.007	60.277
	60	1.025	0.005	1.02	22	9.682	0.013	0.005	54.797
	120	1.023	0.005	1.018	22	10.211	0.013	0.004	49.317
	240	1.021	0.005	1.016	22	10.740	0.013	0.003	43.838
	480	1.02	0.005	1.015	22	11.005	0.013	0.002	41.098
	1140	1.018	0.005	1.013	22	11.534	0.013	0.001	35.618

Sieve Analysis of Coarse Fraction Weight of Soil Sieved = 3.05 g

Sieve No.	Weight of Sieve (g)	Weight of Sieve + soil (g)	Weight of Retained (%)	Percentage Retained (%)	Percentage Passed (%)	Particle Size (mm)
10	606.89	606.89	0.00	0.00	100.00	2
40	339.12	339.38	0.26	0.45	99.55	0.425
80	317.49	318.15	0.66	1.15	98.40	0.18
100	337.56	337.78	0.22	0.38	98.02	0.15
200	340.91	342.28	1.37	2.38	95.63	0.075
-200	479.41	479.82	0.41	0.71	94.92	
		Total W =	*2.92*			

Combined	
Particle Size (mm)	Percent Passing (%)
2.000	100.000
0.425	99.548
0.180	90.099
0.150	98.017
0.075	95.633
0.036	76.716
0.030	73.976
0.026	73.976
0.017	71.236
0.010	65.756
0.007	60.277
0.005	54.797
0.004	49.317
0.003	43.838
0.002	41.098
0.001	35.618

D50 = 0.0041 mm

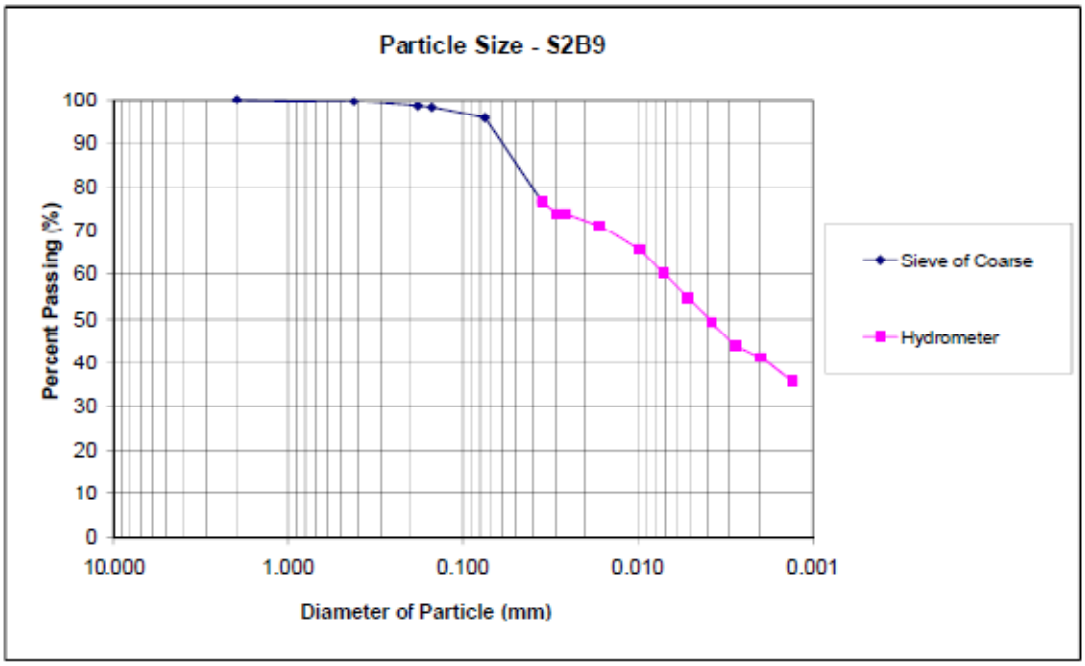
Particle Size - S2B9
Percent Passing (%)
100
90
80
70
60
50
40
30
20
10
0
10.000
1.000
0.100
0.010
0.001
Diameter of Particle (mm)
Sieve of Coarse
Hydrometer

Hydrometer Analysis

Project Name:	Midwest Levees	Boring No.:	S3B10
Location:	Brevator	Depth:	Crest Surface
Description:	Gray clay, stiff, roots present	Date:	01/12/09

Hygroscopic water content

Can No.	1
Wet Wt + Tare (g)	16.84
Dry Wt + Tare (g)	14.24
Tare Wt (g)	0.98
Moisture Content (%)	19.61
Correction Factor =	0.836

Hydrometer Type:	151H	
Mass of air dry soil =	82.05	g
Specific Gravity =	2.69	
Mass of oven dry soil =	68.599	g

Start Time	Elapsed Time	Actual Reading	Composite Correction	Corrected Reading	Temperature (degrees C)	Effective Hyd. Depth	K	Diameter of particle (mm)	Percent finer in suspension (%)
1:57pm	0	1.04	0.004	1.036	17.8	5.714	0.013	--	83.531
	0.067	1.039	0.004	1.035	17.8	5.979	0.013	0.128	81.211
	0.25	1.038	0.004	1.034	17.8	6.243	0.013	0.067	78.891
	0.5	1.038	0.004	1.034	17.8	6.243	0.013	0.048	78.891
	1	1.036	0.004	1.032	17.8	6.772	0.013	0.035	74.250
	1.5	1.035	0.004	1.031	17.8	7.037	0.013	0.029	71.930
	2	1.034	0.004	1.03	17.8	7.301	0.013	0.026	69.609
	5	1.029	0.004	1.025	17.8	8.624	0.013	0.018	58.008
	15	1.023	0.004	1.019	17.8	10.211	0.013	0.011	44.088
	30	1.021	0.004	1.017	17.8	10.740	0.013	0.008	39.445
	60	1.019	0.004	1.015	17.8	11.269	0.013	0.006	34.805
	120	1.017	0.004	1.013	17.8	11.798	0.013	0.004	30.164
	240	1.016	0.004	1.012	17.8	12.063	0.013	0.003	27.844
	480	1.015	0.004	1.011	17.8	12.327	0.013	0.002	25.523
	1140	1.014	0.004	1.01	17.8	12.592	0.013	0.001	23.203

Sieve Analysis of Coarse Fraction Weight of Soil Sieved = 5.73 g

Sieve No.	Weight of Sieve (g)	Weight of Sieve + soil (g)	Weight of Retained (%)	Percentage Retained (%)	Percentage Passed (%)	Particle Size (mm)
10	606.88	607.41	0.53	0.77	99.23	2
40	339.12	341.46	2.34	3.41	95.82	0.425
80	317.46	318.42	0.96	1.40	94.42	0.18
100	337.51	337.68	0.17	0.25	94.17	0.15
200	340.90	341.77	0.87	1.27	92.90	0.075
-200	479.40	480.23	0.83	1.21	91.69	
		Total W =	*5.70*			

Combined	
Particle Size (mm)	Percent Passing (%)
2.000	99.227
0.425	95.818
0.180	94.417
0.150	94.169
0.075	92.901
0.048	78.891
0.035	74.250
0.029	71.930
0.020	69.609
0.018	58.008
0.011	44.088
0.008	39.445
0.006	34.805
0.004	30.164
0.003	27.844
0.002	25.523
0.001	23.203

D50 = 0.0136 mm

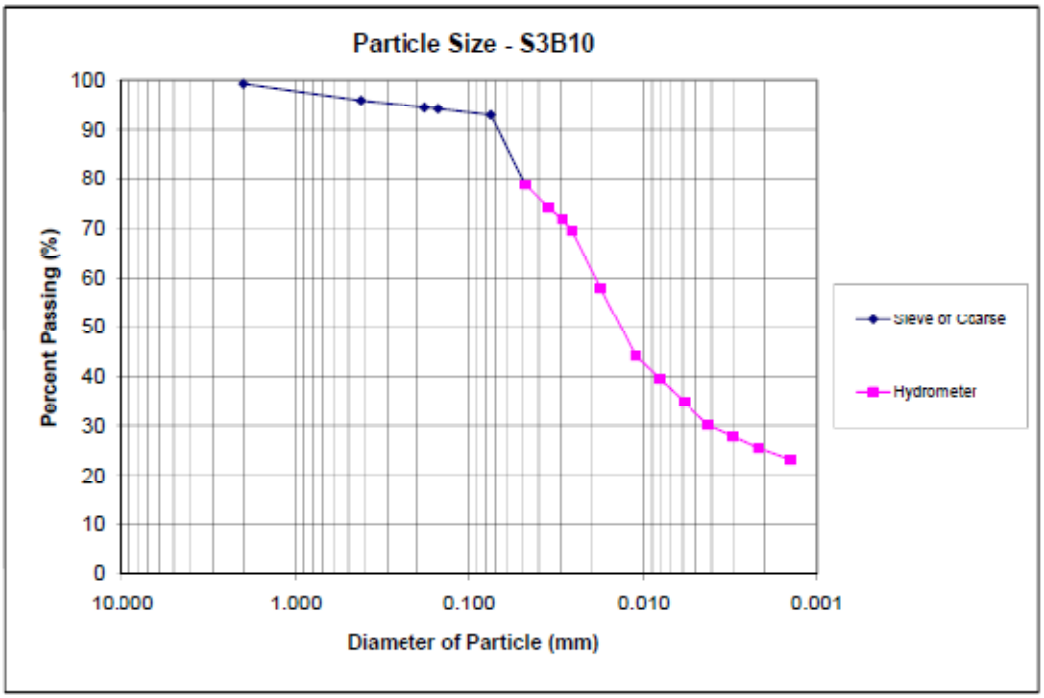
Particle Size - S3B10
Percent Passing (%)
100
90
80
70
60
50
40
30
20
10
0
10.000
1.000
0.100
0.010
0.001
Diameter of Particle (mm)
Sieve or Coarse
Hydrometer

Hydrometer Analysis

Project Name	Midwest Levees	Boring No.:	S3B11
Location:	Brevator	Depth:	10'
Description:	Gray clay, stiff	Date:	01/06/09

Hygroscopic water content

Can No.	1
Wet Wt + Tare (g)	15.06
Dry Wt + Tare (g)	12.28
Tare Wt (g)	1
Moisture Content (%)	24.65
Correction Factor =	0.802

Hydrometer Type:	151H	
Mass of air dry soil =	88.24	g
Specific Gravity =	2.69	
Mass of oven dry soil =	70.793	g

Start Time	Elapsed Time	Actual Reading	Composite Correction	Corrected Reading	Temperature (degrees C)	Effective Hyd. Depth	K	Diameter of particle (mm)	Percent finer in suspension (%)
2:15pm	0	1.04	0.004	1.036	16.9	5.714	0.014	--	80.943
	0.067	1.039	0.004	1.035	16.9	5.979	0.014	0.133	78.694
	0.25	1.039	0.004	1.035	16.9	5.979	0.014	0.068	78.694
	0.5	1.037	0.004	1.033	16.9	6.508	0.014	0.051	74.198
	1	1.036	0.004	1.032	16.9	6.772	0.014	0.038	71.949
	1.5	1.034	0.004	1.03	16.9	7.301	0.014	0.031	67.452
	2	1.032	0.004	1.028	16.9	7.830	0.014	0.028	62.956
	5	1.028	0.004	1.024	16.9	8.888	0.014	0.019	53.962
	15	1.023	0.004	1.019	16.9	10.211	0.014	0.012	42.720
	30	1.02	0.004	1.016	16.9	11.005	0.014	0.008	35.975
	60	1.018	0.004	1.014	16.9	11.534	0.014	0.006	31.478
	120	1.016	0.004	1.012	16.9	12.063	0.014	0.004	26.981
	240	1.015	0.004	1.011	16.9	12.327	0.014	0.003	24.733
	480	1.014	0.004	1.01	16.9	12.592	0.014	0.002	22.484
	1140	1.012	0.004	1.008	16.9	13.121	0.014	0.002	17.987

Sieve Analysis of Coarse Fraction Weight of Soil Sieved = 1.45 g

Sieve No.	Weight of Sieve (g)	Weight of Sieve + soil (g)	Weight of Retained (%)	Percentage Retained (%)	Percentage Passed (%)	Particle Size (mm)
10	606.94	607.01	0.07	0.10	99.90	2
40	339.30	339.80	0.50	0.71	99.19	0.425
80	317.49	317.74	0.25	0.35	98.84	0.18
100	337.52	337.60	0.08	0.11	98.73	0.15
200	340.90	341.30	0.40	0.57	98.16	0.075
-200	479.42	479.57	0.15	0.21	97.95	
		Total W =	*1.45*			

Combined	
Particle Size (mm)	Percent Passing (%)
2.000	99.901
0.425	99.195
0.180	98.842
0.150	98.729
0.075	98.164
0.051	74.198
0.038	71.949
0.031	67.452
0.020	62.956
0.019	53.962
0.012	42.720
0.008	35.975
0.006	31.478
0.004	26.981
0.003	24.733
0.002	22.484
0.002	17.987

D50 = 0.0162 mm

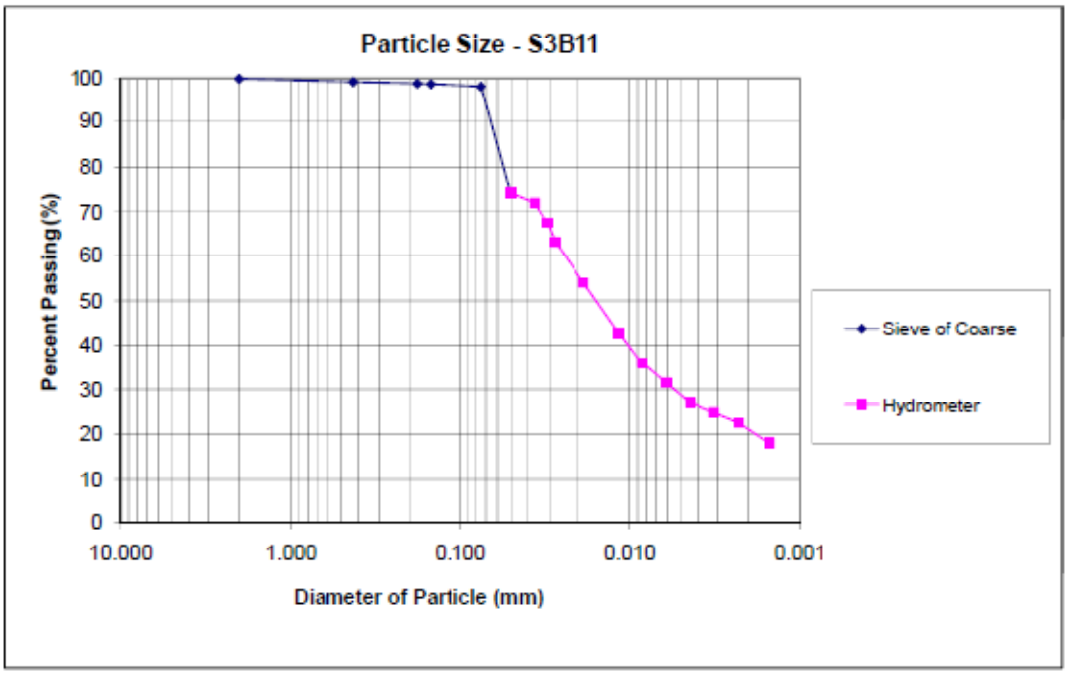
Particle Size - S3B11
Percent Passing (%)
100
90
80
70
60
50
40
30
20
10
0
10.000
1.000
0.100
0.010
0.001
Diameter of Particle (mm)
Sieve of Coarse
Hydrometer

Hydrometer Analysis

Project Name	Midwest Levees	Boring No.:	S3B12
Location:	Brevator	Depth:	Crest Surface
Description:	Gray clay, stiff, roots present	Date:	01/15/09

Hygroscopic water content

Can No.	1
Wet Wt + Tare (g)	16.64
Dry Wt + Tare (g)	14.14
Tare Wt (g)	1.02
Moisture Content (%)	19.05
Correction Factor =	0.840

Hydrometer Type:	151H	
Mass of air dry soil =	85.17	g
Specific Gravity =	2.69	
Mass of oven dry soil =	71.538	g

Start Time	Elapsed Time	Actual Reading	Composite Correction	Corrected Reading	Temperature (degrees C)	Effective Hyd. Depth	K	Diameter of particle (mm)	Percent finer in suspension (%)
2:36pm	0	1.042	0.004	1.038	22	5.185	0.013	--	84.549
	0.067	1.042	0.004	1.038	22	5.185	0.013	0.118	84.549
	0.25	1.041	0.004	1.037	22	5.450	0.013	0.061	82.324
	0.5	1.04	0.004	1.036	22	5.714	0.013	0.045	80.099
	1	1.04	0.004	1.036	22	5.714	0.013	0.031	80.099
	1.5	1.039	0.004	1.035	22	5.979	0.013	0.026	77.874
	2	1.039	0.004	1.035	22	5.979	0.013	0.023	77.874
	5	1.036	0.004	1.032	22	6.772	0.013	0.015	71.199
	15	1.029	0.004	1.025	22	8.624	0.013	0.010	55.625
	30	1.028	0.004	1.024	22	8.888	0.013	0.007	53.400
	60	1.026	0.004	1.022	22	9.417	0.013	0.005	48.950
	120	1.024	0.004	1.02	22	9.946	0.013	0.004	44.500
	240	1.022	0.004	1.018	22	10.476	0.013	0.003	40.050
	480	1.02	0.004	1.016	22	11.005	0.013	0.002	35.600
	1140	1.019	0.004	1.015	22	11.269	0.013	0.001	33.375

Sieve Analysis of Coarse Fraction Weight of Soil Sieved = 3.41 g

Sieve No.	Weight of Sieve (g)	Weight of Sieve + soil (g)	Weight of Retained (%)	Percentage Retained (%)	Percentage Passed (%)	Particle Size (mm)
10	606.88	607	0.12	0.16774199	99.832258	2
40	339.1	340.49	1.39	1.94301139	97.8892466	0.425
80	317.48	318.4	0.92	1.28602193	96.6032247	0.18
100	337.53	337.67	0.14	0.19569899	96.4075257	0.15
200	340.9	341.48	0.58	0.81075296	95.5967727	0.075
-200	479.4	479.74	0.34	0.47526897	95.1215038	
		Total W =	*3.40*			

Combined	
Particle Size (mm)	Percent Passing (%)
2.000	99.832
0.425	97.889
0.180	96.603
0.150	96.408
0.075	95.597
0.045	80.099
0.031	80.099
0.026	77.874
0.023	77.074
0.015	71.199
0.010	55.625
0.007	53.400
0.005	48.950
0.004	44.500
0.003	40.050
0.002	35.600
0.001	33.375

D50 = 0.0054 mm

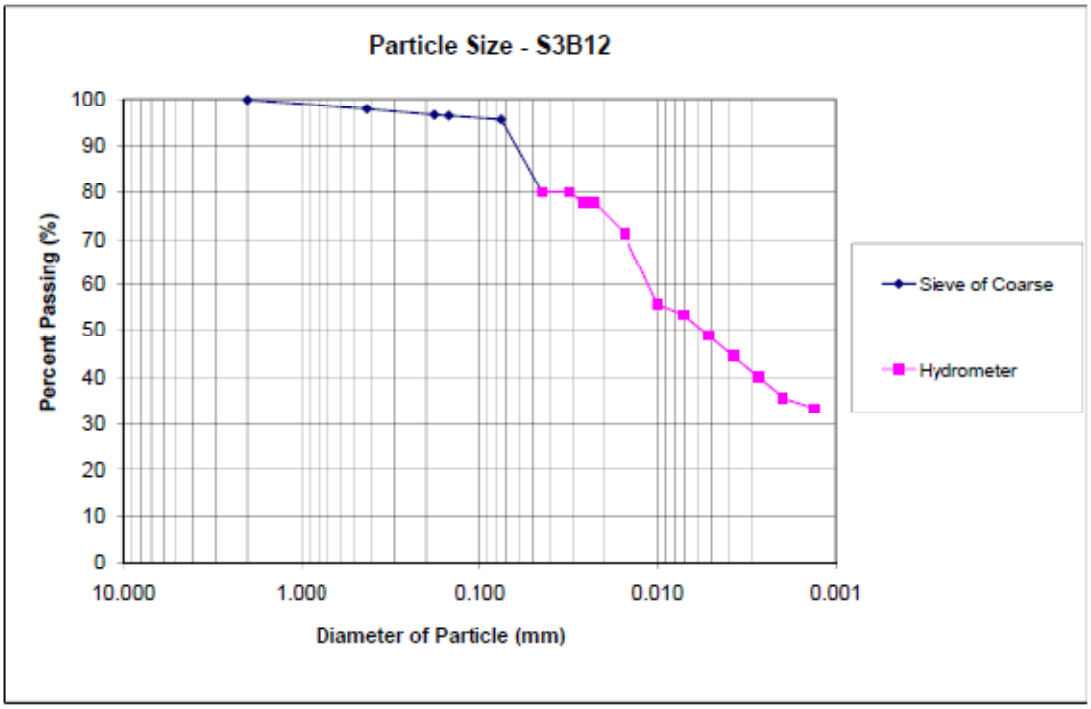
Particle Size - S3B12
Percent Passing (%)
100
90
80
70
60
50
40
30
20
10
0
10.000
1.000
0.100
0.010
0.001
Diameter of Particle (mm)
Sieve of Coarse
Hydrometer

Hydrometer Analysis

Project Name:	Midwest Levees	Boring No.:	S3B13
Location:	Brevator	Depth:	10'
Description:	Gray clay, stiff	Date:	01/15/09

Hygroscopic water content

Can No.	1
Wet Wt + Tare (g)	16.23
Dry Wt + Tare (g)	12.58
Tare Wt (g)	0.98
Moisture Content (%)	31.47
Correction Factor =	0.761

Hydrometer Type:	151H	
Mass of air dry soil =	66.87	g
Specific Gravity =	2.69	
Mass of oven dry soil =	50.865	g

Start Time	Elapsed Time	Actual Reading	Composite Correction	Corrected Reading	Temperature (degrees C)	Effective Hyd. Depth	K	Diameter of particle (mm)	Percent finer in suspension (%)
2:41pm	0	1.032	0.004	1.028	22	7.830	0.013	--	87.620
	0.067	1.03	0.004	1.026	22	8.359	0.013	0.147	81.362
	0.25	1.03	0.004	1.026	22	8.359	0.013	0.076	81.362
	0.5	1.029	0.004	1.025	22	8.624	0.013	0.055	78.232
	1	1.028	0.004	1.024	22	8.888	0.013	0.039	75.103
	1.5	1.027	0.004	1.023	22	9.153	0.013	0.033	71.974
	2	1.027	0.004	1.023	22	9.153	0.013	0.028	71.974
	5	1.024	0.004	1.02	22	9.946	0.013	0.019	62.586
	15	1.021	0.004	1.017	22	10.740	0.013	0.011	53.198
	30	1.019	0.004	1.015	22	11.269	0.013	0.008	46.939
	60	1.017	0.004	1.013	22	11.798	0.013	0.006	40.681
	120	1.016	0.004	1.012	22	12.063	0.013	0.004	37.552
	240	1.015	0.004	1.011	22	12.327	0.013	0.003	34.422
	480	1.014	0.004	1.01	22	12.592	0.013	0.002	31.293
	1140	1.013	0.004	1.009	22	12.856	0.013	0.001	28.164

Sieve Analysis of Coarse Fraction Weight of Soil Sieved = 3.5 g

Sieve No.	Weight of Sieve (g)	Weight of Sieve + soil (g)	Weight of Retained (%)	Percentage Retained (%)	Percentage Passed (%)	Particle Size (mm)
10	606.89	607.09	0.20	0.39	99.61	2
40	339.11	340.57	1.46	2.87	96.74	0.425
80	317.45	318.34	0.89	1.75	94.99	0.18
100	337.54	337.65	0.11	0.22	94.77	0.15
200	340.87	341.49	0.62	1.22	93.55	0.075
-200	479.39	479.58	0.19	0.37	93.18	
		Total W =	*3.47*			

Combined	
Particle Size (mm)	Percent Passing (%)
2.000	99.607
0.425	96.736
0.180	94.987
0.150	94.770
0.075	93.552
0.055	78.232
0.039	75.103
0.033	71.974
0.028	71.974
0.019	62.586
0.011	53.198
0.008	46.939
0.006	40.681
0.004	37.552
0.003	34.422
0.002	31.293
0.001	28.164

D50 = 0.0093 mm

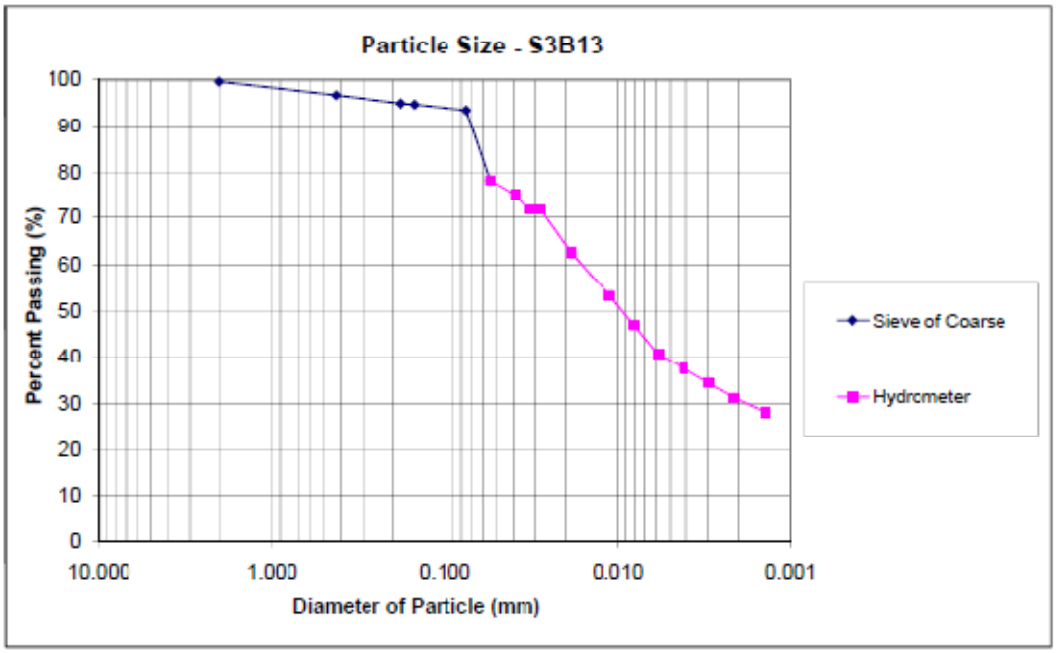
Particle Size - S3B13
Percent Passing (%)
100
90
80
70
60
50
40
30
20
10
0
10.000
1.000
0.100
0.010
0.001
Diameter of Particle (mm)
Sieve of Coarse
Hydrometer

Hydrometer Analysis

Project Name:	Midwest Levees	Boring No.:	S4B14
Location:	Kickapoo	Depth:	Crest Surface
Description:	Gray clay, roots present	Date:	01/08/09

Hygroscopic water content

Can No.	1
Wet Wt + Tare (g)	15.8
Dry Wt + Tare (g)	10.17
Tare Wt (g)	1.01
Moisture Content (%)	61.46
Correcion Factor =	0.619

Hydrometer Type:	151H	
Mass of air dry soil =	70.96	g
Specific Gravity =	2.7	
Mass of oven dry soil =	43.948	g

Start Time	Elapsed Time	Actual Reading	Composite Correction	Corrected Reading	Temperature (degrees C)	Effective Hyd. Depth	K	Diameter of particle (mm)	Percent finer in suspension (%)
2:24pm	0	1.026	0.004	1.022	16.9	9.417	0.014	--	79.505
	0.067	1.025	0.004	1.021	16.9	9.682	0.014	0.164	75.892
	0.25	1.024	0.004	1.02	16.9	9.946	0.014	0.086	72.278
	0.5	1.024	0.004	1.02	16.9	9.946	0.014	0.061	72.278
	1	1.024	0.004	1.02	16.9	9.946	0.014	0.043	72.278
	1.5	1.023	0.004	1.019	16.9	10.211	0.014	0.035	68.664
	2	1.023	0.004	1.019	16.9	10.211	0.014	0.031	68.664
	5	1.021	0.004	1.017	16.9	10.740	0.014	0.020	61.436
	15	1.018	0.004	1.014	16.9	11.534	0.014	0.012	50.594
	30	1.017	0.004	1.013	16.9	11.798	0.014	0.009	46.980
	60	1.015	0.004	1.011	16.9	12.327	0.014	0.006	39.753
	120	1.014	0.004	1.01	16.9	12.592	0.014	0.004	36.139
	240	1.012	0.004	1.008	16.9	13.121	0.014	0.003	28.911
	480	1.012	0.004	1.008	16.9	13.121	0.014	0.002	28.911
	1140	1.011	0.004	1.007	16.9	13.385	0.014	0.001	25.297

Sieve Analysis of Coarse Fraction Weight of Soil Sieved = 4.25 g

Sieve No.	Weight of Sieve (g)	Weight of Sieve + soil (g)	Weight of Retained (%)	Percentage Retained (%)	Percentage Passed (%)	Particle Size (mm)
10	606.93	606.93	0.00	0.00	100.00	2
40	339.26	339.29	0.03	0.07	99.93	0.425
80	317.50	318.40	0.90	2.05	97.88	0.18
100	337.55	337.95	0.40	0.91	96.97	0.15
200	340.90	342.91	2.01	4.57	92.40	0.075
-200	479.42	480.06	0.64	1.46	90.94	
		Total W =	*5.98*			

Combined	
Particle Size (mm)	Percent Passing (%)
2.000	100.000
0.425	99.932
0.180	97.884
0.150	96.974
0.075	92.400
0.043	72.278
0.035	68.664
0.031	68.664
0.020	61.436
0.012	50.594
0.009	46.980
0.006	39.753
0.004	36.139
0.003	28.911
0.002	28.911
0.001	25.297

D50 = 0.0114 mm

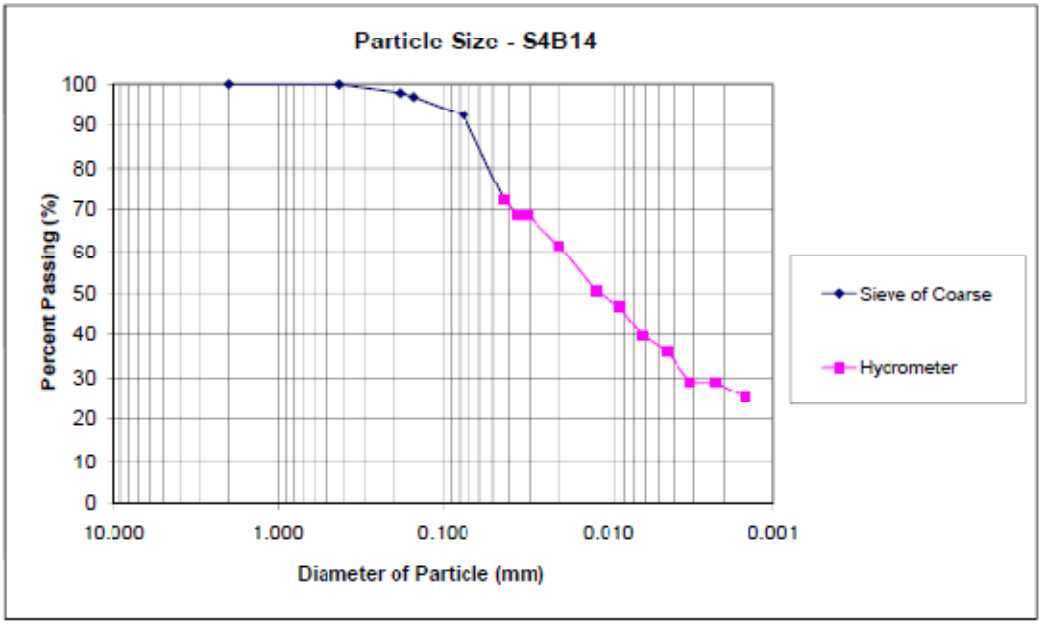
Particle Size - S4B14
Percent Passing (%)
100
90
80
70
60
50
40
30
20
10
0
10.000
1.000
0.100
0.010
0.001
Diameter of Particle (mm)
Sieve of Coarse
Hycrometer

Hydrometer Analysis

Project Name:	Midwest Levees	Boring No.:	S4B'6
Location:	Kickapoo	Depth:	74"
Description:	Gray clay	Date:	01/12/09

Hygroscopic water content

Can No.	1
Wet Wt + Tare (g)	17.88
Dry Wt + Tare (g)	13.71
Tare Wt (g)	1
Moisture Content (%)	32.81
Correction Factor =	0.753

Hydrometer Type:	151H	
Mass of air dry soil =	75.99	g
Specific Gravity =	2.7	
Mass of oven dry soil =	57.218	g

Start Time	Elapsed Time	Actual Reading	Composite Correction	Corrected Reading	Temperature (degrees C)	Effective Hyd Depth	K	Diameter of particle (mm)	Percent finer in suspension (%)
1:52pm	0	1.038	0.004	1.034	17.8	6.243	0.013	--	94.377
	0.067	1.037	0.004	1.033	17.8	6.508	0.013	0.133	91.601
	0.25	1.036	0.004	1.032	17.8	6.772	0.013	0.070	88.825
	0.5	1.036	0.004	1.032	17.8	6.772	0.013	0.049	88.825
	1	1.035	0.004	1.031	17.8	7.037	0.013	0.036	86.049
	1.5	1.034	0.004	1.03	17.8	7.301	0.013	0.030	83.273
	2	1.034	0.004	1.03	17.8	7.301	0.013	0.026	83.273
	5	1.032	0.004	1.028	17.8	7.830	0.013	0.017	77.722
	15	1.029	0.004	1.025	17.8	8.624	0.013	0.010	69.395
	30	1.027	0.004	1.023	17.8	9.153	0.013	0.007	63.843
	60	1.025	0.004	1.021	17.8	9.682	0.013	0.005	58.291
	120	1.023	0.004	1.019	17.8	10.211	0.013	0.004	52.740
	240	1.022	0.004	1.018	17.8	10.476	0.013	0.003	49.964
	480	1.02	0.004	1.016	17.8	11.005	0.013	0.002	44.413
	1140	1.019	0.004	1.015	17.8	11.269	0.013	0.001	41.637

Sieve Analysis of Coarse Fraction — Weight of Soil Sieved = 4.43 g

Sieve No.	Weight of Sieve (g)	Weight of Sieve + soil (g)	Weight of Retained (%)	Percentage Retained (%)	Percentage Passed (%)	Particle Size (mm)
10	606.91	606.95	0.04	0.06990857	99.9300914	2
40	339.18	339.7	0.52	0.90881145	99.02128	0.425
80	317.5	318.49	0.99	1.73023719	97.2910428	0.18
100	337.37	338.03	0.46	0.80394859	96.4870942	0.15
200	340.9	342.94	2.04	3.56533723	92.921757	0.075
-200	479.45	479.82	0.37	0.6466543	92.2751027	
		Total W =	*4.42*			

Combined Particle Size (mm)	Combined Percent Passing (%)
2.000	99.930
0.425	99.021
0.180	97.291
0.150	96.487
0.075	92.922
0.049	88.825
0.036	86.049
0.030	83.273
0.026	83.273
0.017	77.722
0.010	69.395
0.007	63.843
0.005	58.291
0.004	52.740
0.003	49.964
0.002	44.413
0.001	41.637

D50 = 0.0030 mm

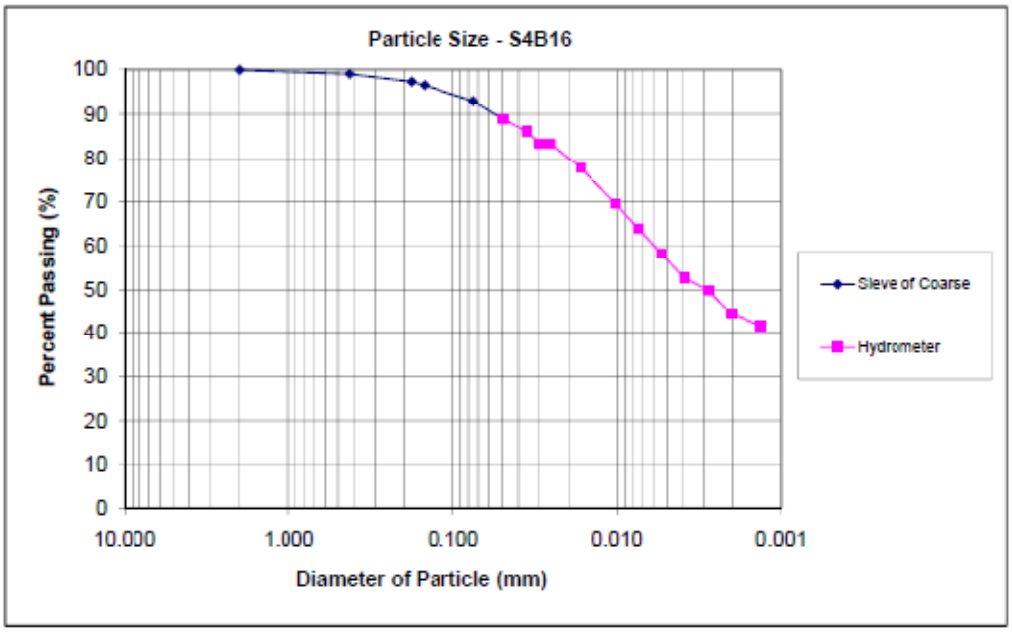
Particle Size - S4B16
Percent Passing (%)
100
90
80
70
60
50
40
30
20
10
0
10.000
1.000
0.100
0.010
0.001
Diameter of Particle (mm)
Sieve of Coarse
Hydrometer

Hydrometer Analysis

Project Name	Midwest Levees	Boring No.:	S4B18
Location:	Kickapoo	Depth:	9'
Description:	Clay, dk gray/brown, sandy	Date:	01/15/09

Hygroscopic water content

Can No.	1
Wet Wt + Tare (g)	14.2
Dry Wt + Tare (g)	11.23
Tare Wt (g)	1.02
Moisture Content (%)	29.09
Correction Factor =	0.775

Hydrometer Type:	151H	
Mass of air dry soil =	82.09	g
Specific Gravity =	2.7	
Mass of oven dry soil =	63.592	g

Start Time	Elapsed Time	Actual Reading	Composite Correction	Corrected Reading	Temperature (degrees C)	Effective Hyd. Depth	K	Diameter of particle (mm)	Percent finer in suspension (%)
2:58pm	0	1.036	0.005	1.031	22	6.772	0.013	--	77.424
	0.067	1.032	0.005	1.027	22	7.830	0.013	0.142	67.434
	0.25	1.03	0.005	1.025	22	8.359	0.013	0.078	62.439
	0.5	1.029	0.005	1.024	22	8.624	0.013	0.055	59.941
	1	1.026	0.005	1.021	22	9.417	0.013	0.040	52.449
	1.5	1.025	0.005	1.02	22	9.682	0.013	0.033	49.951
	2	1.023	0.005	1.018	22	10.211	0.013	0.030	44.956
	5	1.02	0.005	1.015	22	11.005	0.013	0.019	37.463
	15	1.016	0.005	1.011	22	12.063	0.013	0.012	27.473
	30	1.015	0.005	1.01	22	12.327	0.013	0.008	24.976
	60	1.013	0.005	1.008	22	12.856	0.013	0.006	19.980
	120	1.012	0.005	1.007	22	13.121	0.013	0.004	17.483
	240	1.011	0.005	1.006	22	13.385	0.013	0.003	14.985
	480	1.01	0.005	1.005	22	13.650	0.013	0.002	12.488
	1140	1.01	0.005	1.005	22	13.650	0.013	0.001	12.488

Sieve Analysis of Coarse Fraction — Weight of Soil Sieved = 14.4 g

Sieve No.	Weight of Sieve (g)	Weight of Sieve + soil (g)	Weight of Retained (%)	Percentage Retained (%)	Percentage Passed (%)	Particle Size (mm)
10	606.89	606.92	0.03	0.01717595	99.952821	2
40	339.12	340.27	1.15	1.80841147	98.1444126	0.425
80	317.46	320.25	2.79	4.38736348	93.7570491	0.18
100	337.54	339.17	1.63	2.56322669	91.1938224	0.15
200	340.88	348.84	7.96	12.5173524	78.67647	0.075
-200	479.42	480.28	0.86	1.35237727	77.3240927	
		Total W =	*14.42*			

Combined	
Particle Size (mm)	Percent Passing (%)
2.000	99.953
0.425	98.144
0.180	93.757
0.150	91.194
0.075	78.676
0.055	59.941
0.040	52.449
0.033	49.951
0.030	44.956
0.019	37.463
0.012	27.473
0.008	24.976
0.006	19.980
0.004	17.483
0.003	14.985
0.002	12.488
0.001	12.488

D50 = 0.0302 mm

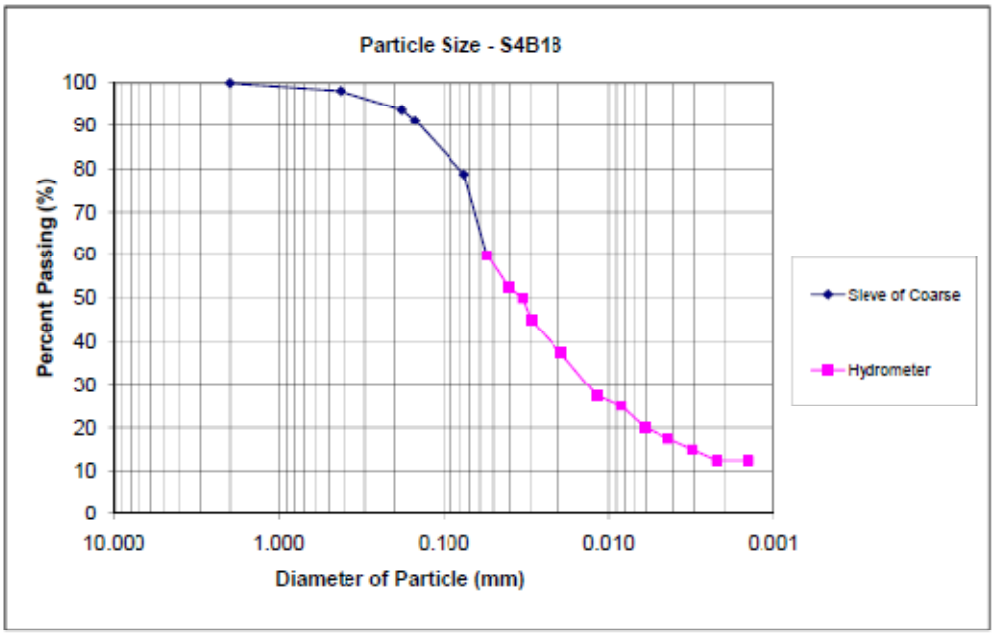
Particle Size - S4B13
Percent Passing (%)
100
90
80
70
60
50
40
30
20
10
0
10.000
1.000
0.100
0.010
0.001
Diameter of Particle (mm)
Sieve of Coarse
Hydrometer

Hydrometer Analysis

Project Name:	Midwest Levees	Boring No.:	S5B19
Location:	Norton Woods	Depth:	Crest Surface
Description:	Clay, dk brown, some sand, a lot of roots	Date:	01/12/09

Hygroscopic water content

Can No.	1
Wet Wt + Tare (g)	18.76
Dry Wt + Tare (g)	15.36
Tare Wt (g)	0.98
Moisture Content (%)	23.64
Correction Factor =	0.809

Hydrometer Type:	151H	
Mass of air dry soil =	82.47	g
Specific Gravity =	2.7	
Mass of oven dry soil =	66.700	g

Start Time	Elapsed Time	Actual Reading	Composite Correction	Corrected Reading	Temperature (degrees C)	Effective Hyd. Depth	K	Diameter of particle (mm)	Percent finer in suspension (%)
2:04pm	0	1.04	0.005	1.035	19.7	5.714	0.013	--	83.341
	0.067	1.04	0.005	1.035	19.7	5.714	0.013	0.125	83.341
	0.25	1.038	0.005	1.033	19.7	6.243	0.013	0.067	78.579
	0.5	1.036	0.005	1.031	19.7	6.772	0.013	0.049	73.818
	1	1.034	0.005	1.029	19.7	7.301	0.013	0.036	69.054
	1.5	1.032	0.005	1.027	19.7	7.830	0.013	0.031	64.292
	2	1.031	0.005	1.026	19.7	8.095	0.013	0.027	61.911
	5	1.027	0.005	1.022	19.7	9.153	0.013	0.018	52.386
	15	1.022	0.005	1.017	19.7	10.476	0.013	0.011	40.480
	30	1.02	0.005	1.015	19.7	11.005	0.013	0.008	35.718
	60	1.017	0.005	1.012	19.7	11.798	0.013	0.006	28.574
	120	1.016	0.005	1.011	19.7	12.063	0.013	0.004	26.193
	240	1.015	0.005	1.01	19.7	12.327	0.013	0.003	23.812
	480	1.014	0.005	1.009	19.7	12.592	0.013	0.002	21.431
	1140	1.013	0.005	1.008	19.7	12.856	0.013	0.001	19.049

Sieve Analysis of Coarse Fraction Weight of Soil Sieved = 6.61 g

Sieve No.	Weight of Sieve (g)	Weight of Sieve + soil (g)	Weight of Retained (%)	Percentage Retained (%)	Percentage Passed (%)	Particle Size (mm)
10	606.89	606.89	0.00	0.00	100.00	2
40	339.08	339.44	0.36	0.54	99.46	0.425
80	317.46	318.02	0.56	0.84	98.62	0.18
100	337.51	337.72	0.21	0.31	98.31	0.15
200	340.86	346.12	5.26	7.89	90.42	0.075
-200	479.41	479.84	0.43	0.64	89.78	
		Total W =	*6.82*			

Combined	
Particle Size (mm)	Percent Passing (%)
2.000	100.000
0.425	99.460
0.180	98.621
0.150	98.306
0.075	90.420
0.049	73.816
0.036	69.054
0.031	64.292
0.027	61.911
0.018	52.386
0.011	40.480
0.008	35.718
0.006	28.574
0.004	26.193
0.003	23.812
0.002	21.431
0.001	19.049

D50 = 0.0163 mm

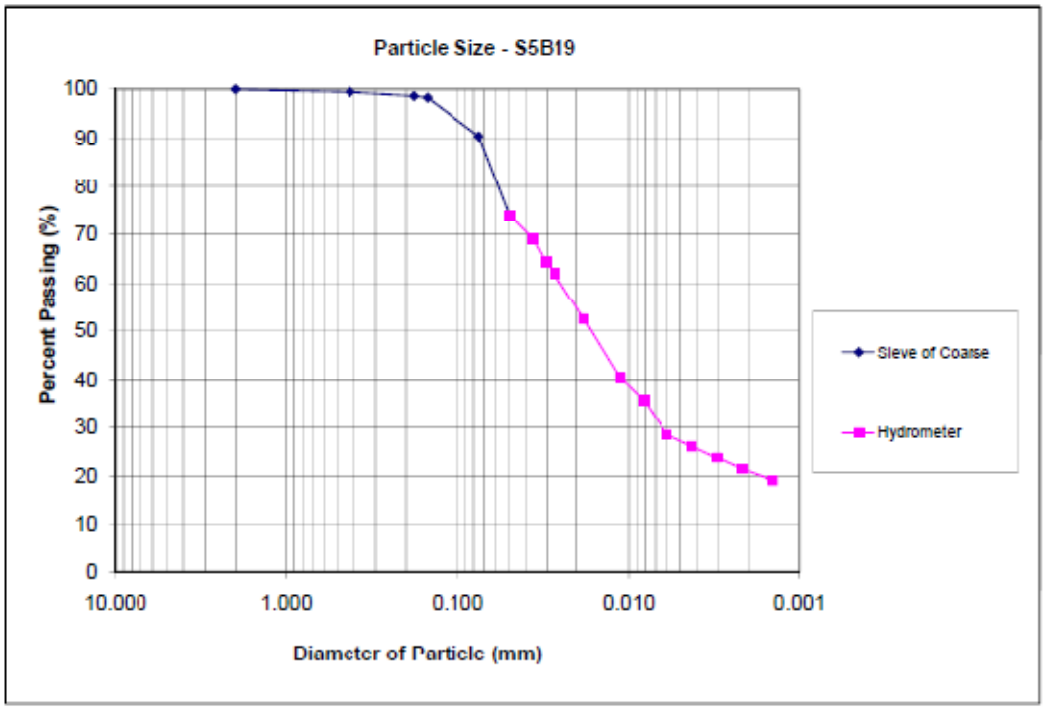
Particle Size - S5B19
Percent Passing (%)
100
90
80
70
60
50
40
30
20
10
0
10.000
1.000
0.100
0.010
0.001
Diameter of Particle (mm)
Sieve of Coarse
Hydrometer

Hydrometer Analysis

Project Name:	Midwest Levees	Boring No.:	S5B20
Location:	Norton Woods	Depth:	10'
Description:	Clay, gray/brown w/se yellow/brown sand	Date:	01/15/09

Hygroscopic water content

Can No.	1
Wet Wt + Tare (g)	14.41
Dry Wt + Tare (g)	10.99
Tare Wt (g)	1
Moisture Content (%)	34.23
Correcion Factor =	0.745

Hydrometer Type:	151H	
Mass of air dry soil =	83.26	g
Specific Gravity =	2.7	
Mass of oven dry soil =	62.026	g

Start Time	Elapsed Time	Actual Reading	Composite Correction	Corrected Reading	Temperature (degrees C)	Effective Hyd. Depth	K	Diameter of particle (mm)	Percent finer in suspension (%)
2:46pm	0	1.037	0.004	1.033	22	6.508	0.013	--	84.500
	0.067	1.034	0.004	1.03	22	7.301	0.013	0.137	76.818
	0.25	1.032	0.004	1.028	22	7.830	0.013	0.073	71.697
	0.5	1.031	0.004	1.027	22	8.095	0.013	0.053	69.136
	1	1.029	0.004	1.025	22	8.624	0.013	0.039	64.015
	1.5	1.028	0.004	1.024	22	8.888	0.013	0.032	61.454
	2	1.027	0.004	1.023	22	9.153	0.013	0.028	58.894
	5	1.025	0.004	1.021	22	9.682	0.013	0.018	53.773
	15	1.022	0.004	1.018	22	10.476	0.013	0.011	46.091
	30	1.02	0.004	1.016	22	11.005	0.013	0.008	40.970
	60	1.016	0.004	1.012	22	12.063	0.013	0.006	30.727
	120	1.016	0.004	1.012	22	12.063	0.013	0.004	30.727
	240	1.015	0.004	1.011	22	12.327	0.013	0.003	28.167
	480	1.013	0.004	1.009	22	12.856	0.013	0.002	23.045
	1140	1.012	0.004	1.008	22	13.121	0.013	0.001	20.485

Sieve Analysis of Coarse Fraction — Weight of Soil Sieved = 7.32 g

Sieve No.	Weight of Sieve (g)	Weight of Sieve + soil (g)	Weight of Retained (%)	Percentage Retained (%)	Percentage Passed (%)	Particle Size (mm)
10	606.89	607.02	0.13	0.20958984	99.7904102	2
40	339.11	339.83	0.72	1.16080529	98.6296049	0.425
80	317.46	318.61	1.15	1.85406401	96.7755409	0.18
100	337.54	337.73	0.19	0.30632362	96.4692172	0.15
200	340.92	345.44	4.52	7.28727767	89.1819396	0.075
-200	479.42	480.07	0.65	1.04794922	88.1339903	
		Total W =	*7.36*			

Combined	
Particle Size (mm)	Percent Passing (%)
2.000	99.790
0.425	98.630
0.180	96.776
0.150	96.469
0.075	89.182
0.053	69.136
0.039	64.015
0.032	61.454
0.028	58.894
0.018	53.773
0.011	46.091
0.008	40.970
0.006	30.727
0.004	30.727
0.003	28.167
0.002	23.045
0.001	20.485

D50 = 0.0141 mm

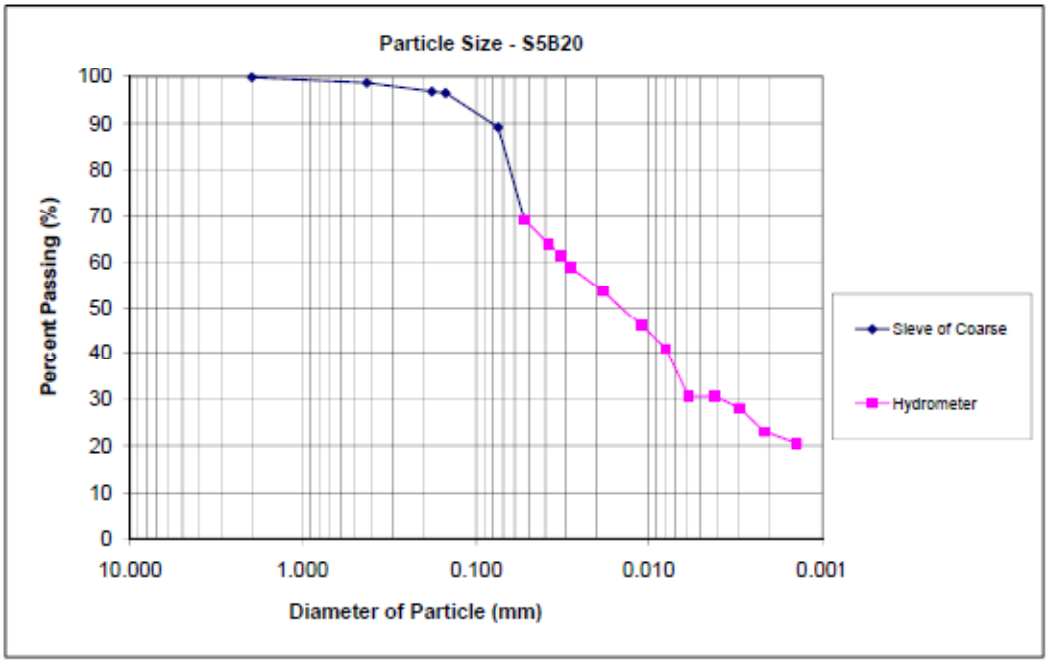
Particle Size - S5B20
Percent Passing (%)
100
90
80
70
60
50
40
30
20
10
0
10.000
1.000
0.100
0.010
0.001
Diameter of Particle (mm)
Sieve of Coarse
Hydrometer

Hydrometer Analysis

Project Name:	Midwest Levees	Boring No.:	S5B23
Location:	Norton Woods	Depth:	10'
Description:	Clay	Date:	01/15/09

Hygroscopic water content

Can No.	1
Wet Wt + Tare (g)	16.45
Dry Wt + Tare (g)	12.8
Tare Wt (g)	0.98
Moisture Content (%)	30.88
Correction Factor =	0.764

Hydrometer Type:	151H	
Mass of air dry soil =	77.61	g
Specific Gravity =	2.7	
Mass of oven dry soil =	59.299	g

Start Time	Elapsed Time	Actual Reading	Composite Correction	Corrected Reading	Temperature (degrees C)	Effective Hyd. Depth	K	Diameter of particle (mm)	Percent finer in suspension (%)
3:04pm	0	1.034	0.005	1.029	22	7.301	0.013	--	77.673
	0.067	1.031	0.005	1.026	22	8.095	0.013	0.145	69.638
	0.25	1.03	0.005	1.025	22	8.359	0.013	0.076	66.959
	0.5	1.029	0.005	1.024	22	8.624	0.013	0.055	64.281
	1	1.028	0.005	1.023	22	8.888	0.013	0.039	61.602
	1.5	1.027	0.005	1.022	22	9.153	0.013	0.032	58.924
	2	1.027	0.005	1.022	22	9.153	0.013	0.028	58.924
	5	1.024	0.005	1.019	22	9.946	0.013	0.019	50.889
	15	1.021	0.005	1.016	22	10.740	0.013	0.011	42.854
	30	1.02	0.005	1.015	22	11.005	0.013	0.008	40.175
	50	1.017	0.005	1.012	22	11.798	0.013	0.006	32.140
	120	1.016	0.005	1.011	22	12.063	0.013	0.004	29.462
	240	1.014	0.005	1.009	22	12.592	0.013	0.003	24.105
	480	1.013	0.005	1.008	22	12.856	0.013	0.002	21.427
	1140	1.012	0.005	1.007	22	13.121	0.013	0.001	18.749

Sieve Analysis of Coarse Fraction Weight of Soil Sieved = 4.08 g

Sieve No.	Weight of Sieve (g)	Weight of Sieve + soil (g)	Weight of Retained (%)	Percentage Retained (%)	Percentage Passed (%)	Particle Size (mm)
10	606.89	606.96	0.07	0.11804652	99.8819535	2
40	339.1	339.45	0.35	0.59023261	99.2917209	0.425
80	317.49	318.24	0.75	1.26478416	98.0269367	0.18
100	337.53	337.7	0.17	0.28668441	97.7402523	0.15
200	340.91	343.14	2.23	3.7606249	93.9796274	0.075
-200	479.4	479.95	0.55	0.92750838	93.052119	
		Total W =	*4.12*			

Combined	
Particle Size (mm)	Percent Passing (%)
2.000	99.882
0.425	99.292
0.180	98.027
0.150	97.740
0.075	93.980
0.055	64.281
0.039	61.602
0.032	58.924
0.028	58.924
0.019	50.889
0.011	42.854
0.008	40.175
0.006	32.140
0.004	29.462
0.003	24.105
0.002	21.427
0.001	18.749

D50 = 0.0179 mm

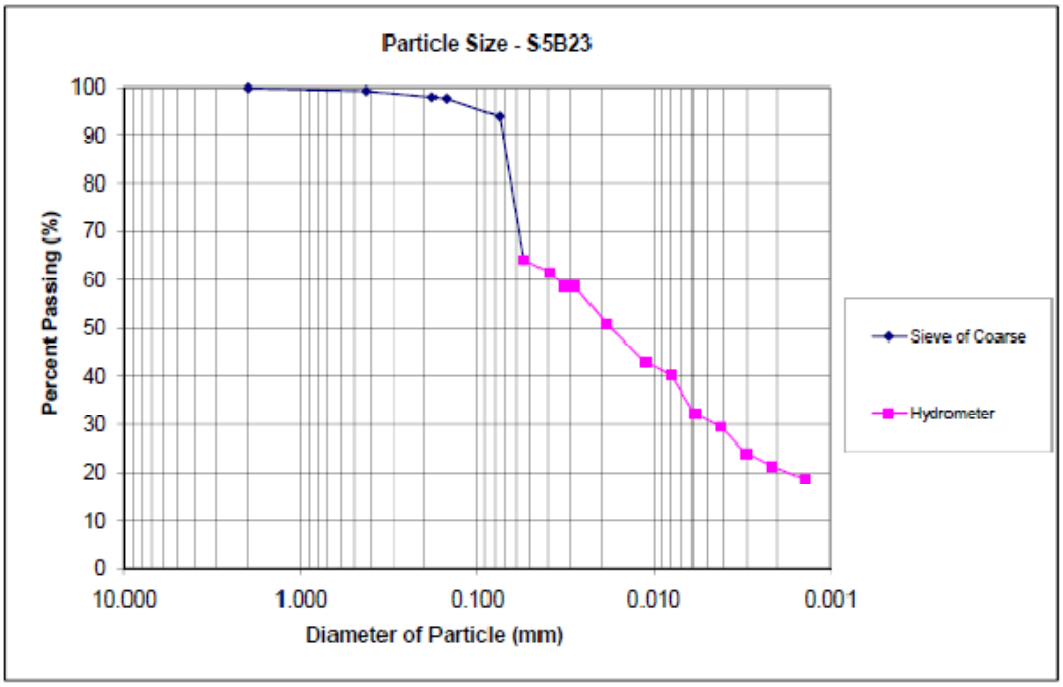
Particle Size - S5B23
Percent Passing (%)
100
90
80
70
60
50
40
30
20
10
0
10.000
1.000
0.100
0.010
0.001
Diameter of Particle (mm)
Sieve of Coarse
Hydrometer

Sieve Analysis

Project Name:	Midwest Levees	Boring No.:	S6B25
Location:	Indian Graves	Depth:Depth:	Levee Shell
Description:	Poorly graded clean sand, tan/brown	Date:	01/05/09

Sieve No.	Weight of Sieve (g)	Weight of Sieve + soil (g)	Weight of Retained (%)	Percentage Retained (%)	Percentage Passed (%)	Particle Size (mm)
4	468.94	473.71	4.77	0.54	99.46	4.75
10	451.91	470.88	18.97	2.14	97.32	2
40	345.57	725.01	379.44	42.82	54.50	0.425
80	317.54	751.03	433.49	48.92	5.57	0.18
100	337.66	352.75	15.09	1.70	3.87	0.15
200	341.07	362.23	21.16	2.39	1.48	0.075
Pan	479.50	492.63	13.13	1.48		

Total Weight of Soil = 886.05

				Cc =	0.81
			D50 = 0.3927	Cu =	2.68
D10 = 0.19		D30 = 0.28	D60 = 0.51		

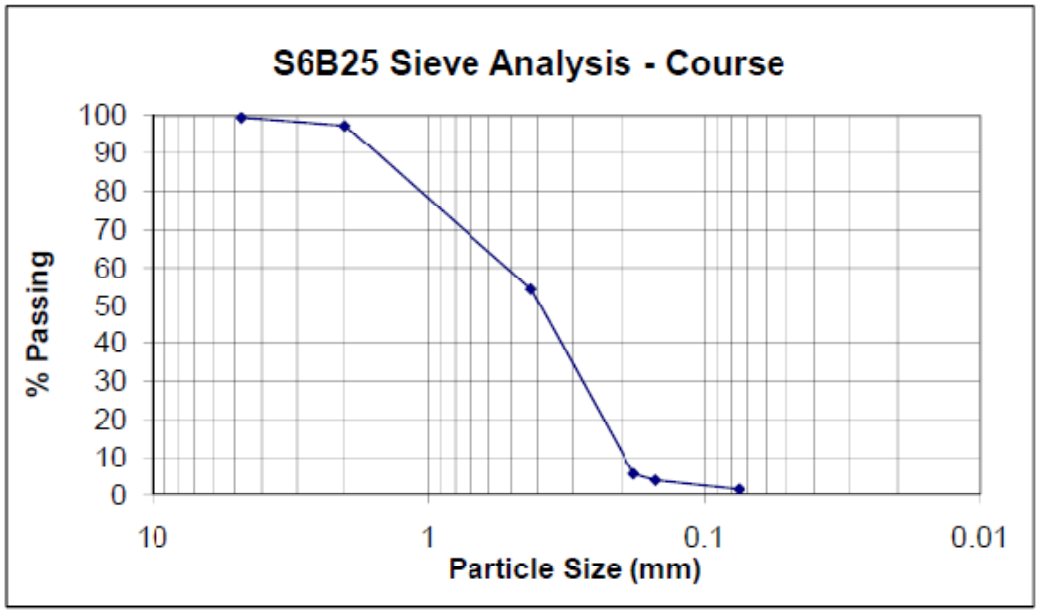

Hydrometer Analysis

Project Name:	Midwest Levees	Boring No.:	S6B26
Location:	Indian Graves - Main	Depth:	15'
Description:		Date:	01/25/09

Hygroscopic water content

Can No.	1
Wet Wt + Tare (g)	18.18
Dry Wt + Tare (g)	14.38
Tare Wt (g)	1.01
Moisture Content (%)	28.42
Correction Factor =	0.779

Hydrometer Type:	151H	
Mass of air dry soil =	73.92	g
Specific Gravity =	2.72	
Mass of oven dry soil =	57.560	g

Start Time	Elapsed Time	Actual Reading	Composite Correction	Corrected Reading	Temperature (degrees C)	Effective Hyd. Depth	K	Diameter of particle (mm)	Percent finer in suspension (%)
4:55pm	0	1.033	0.004	1.029	19.7	7.566	0.013	--	79.874
	0.067	1.032	0.004	1.028	19.7	7.830	0.013	0.145	76.926
	0.25	1.032	0.004	1.028	19.7	7.830	0.013	0.075	76.926
	0.5	1.032	0.004	1.028	19.7	7.830	0.013	0.053	76.926
	1	1.031	0.004	1.027	19.7	8.095	0.013	0.038	74.179
	1.5	1.031	0.004	1.027	19.7	8.095	0.013	0.031	74.179
	2	1.03	0.004	1.026	19.7	8.359	0.013	0.027	71.432
	5	1.027	0.004	1.023	19.7	9.153	0.013	0.018	63.190
	15	1.022	0.004	1.018	19.7	10.476	0.013	0.011	49.453
	30	1.019	0.004	1.015	19.7	11.269	0.013	0.008	41.211
	60	1.017	0.004	1.013	19.7	11.798	0.013	0.006	35.716
	120	1.015	0.004	1.011	19.7	12.327	0.013	0.004	30.221
	240	1.013	0.004	1.009	19.7	12.856	0.013	0.003	24.726
	480	1.012	0.004	1.008	19.7	13.121	0.013	0.002	21.979
	1140	1.011	0.004	1.007	19.7	13.385	0.013	0.001	19.232

Sieve Analysis of Coarse Fraction — Weight of Soil Sieved = 3.5 g

Sieve No.	Weight of Sieve (g)	Weight of Sieve + soil (g)	Weight of Retained (%)	Percentage Retained (%)	Percentage Passed (%)	Particle Size (mm)
10	606.88	606.89	0.01	0.02	99.98	2
40	339.09	339.60	0.51	0.89	99.10	0.425
80	317.48	319.35	1.87	3.25	95.85	0.18
100	496.77	497.05	0.28	0.49	95.36	0.15
200	340.91	341.64	0.73	1.27	94.09	0.075
-200	479.40	479.53	0.13	0.23	93.87	
		Total W =	*3.53*			

Combined	
Particle Size (mm)	Percent Passing (%)
2.000	99.983
0.425	99.097
0.180	95.848
0.150	95.361
0.075	94.093
0.053	76.926
0.038	74.179
0.031	74.179
0.027	71.432
0.018	63.190
0.011	49.453
0.008	41.211
0.006	35.716
0.004	30.221
0.003	24.726
0.002	21.979
0.001	19.232

D50 = 0.0112 mm

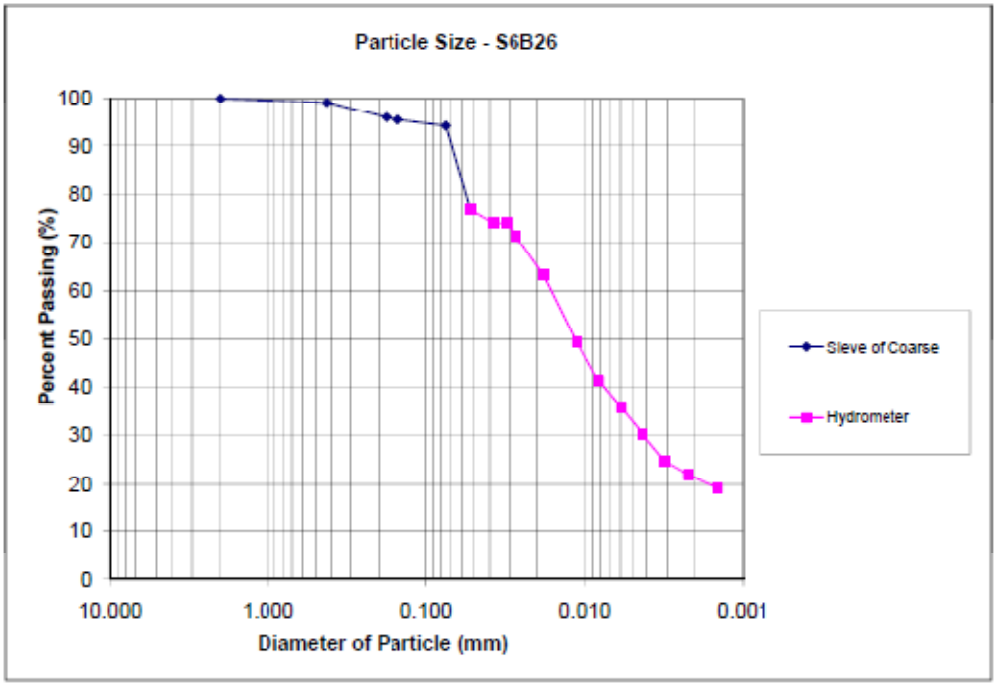
Particle Size - S6B26
Percent Passing (%)
100
90
80
70
60
50
40
30
20
10
0
10.000
1.000
0.100
0.010
0.001
Diameter of Particle (mm)
Sieve of Coarse
Hydrometer

Hydrometer Analysis

Project Name	Midwest Levees	Boring No.:	S7B29
Location:	Indian Graves - South(pump house)	Depth:	Clay core
Description:	Clay	Date:	01/25/09

Hygroscopic water content

Can No.	1
Wet Wt + Tare (g)	15.13
Dry Wt + Tare (g)	12.68
Tare Wt (g)	0.98
Moisture Content (%)	23.50
Correction Factor =	0.810

Hydrometer Type:	151H	
Mass of air dry soil =	73.19	g
Specific Gravity =	2.78	
Mass of oven dry soil =	59.261	g

Start Time	Elapsed Time	Actual Reading	Composite Correction	Corrected Reading	Temperature (degrees C)	Effective Hyd. Depth	K	Diameter of particle (mm)	Percent finer in suspension (%)
5:05pm	0	1.031	0.004	1.027	19.7	8.095	0.013	--	71.157
	0.067	1.029	0.004	1.025	19.7	8.624	0.013	0.150	65.886
	0.25	1.029	0.004	1.025	19.7	8.624	0.013	0.077	65.886
	0.5	1.028	0.004	1.024	19.7	8.888	0.013	0.055	63.251
	1	1.027	0.004	1.023	19.7	9.153	0.013	0.040	60.615
	1.5	1.026	0.004	1.022	19.7	9.417	0.013	0.033	57.980
	2	1.025	0.004	1.021	19.7	9.682	0.013	0.029	55.344
	5	1.023	0.004	1.019	19.7	10.211	0.013	0.019	50.074
	15	1.02	0.004	1.016	19.7	11.005	0.013	0.011	42.167
	30	1.018	0.004	1.014	19.7	11.534	0.013	0.008	36.896
	60	1.016	0.004	1.012	19.7	12.063	0.013	0.006	31.625
	120	1.015	0.004	1.011	19.7	12.327	0.013	0.004	28.990
	240	1.014	0.004	1.01	19.7	12.592	0.013	0.003	26.355
	480	1.013	0.004	1.009	19.7	12.856	0.013	0.002	23.719
	1140	1.012	0.004	1.008	19.7	13.121	0.013	0.001	21.084

Sieve Analysis of Coarse Fraction — Weight of Soil Sieved = 14.1 g

Sieve No.	Weight of Sieve (g)	Weight of Sieve + soil (g)	Weight of Retained (%)	Percentage Retained (%)	Percentage Passed (%)	Particle Size (mm)
10	606.89	607.66	0.77	1.30	98.70	2
40	339.09	341.66	2.57	4.34	94.36	0.425
80	317.48	324.89	7.41	12.50	81.86	0.18
100	496.76	498.07	1.31	2.21	79.65	0.15
200	340.91	342.70	1.79	3.02	76.63	0.075
-200	479.41	479.69	0.28	0.47	76.16	
		Total W =	*14.13*			

Combined	
Particle Size (mm)	Percent Passing (%)
2.000	98.701
0.425	94.364
0.180	81.860
0.150	79.649
0.075	76.629
0.055	63.251
0.040	60.615
0.033	57.980
0.029	55.344
0.019	50.074
0.011	42.167
0.008	36.896
0.006	31.625
0.004	28.990
0.003	26.355
0.002	23.719
0.001	21.084

D50 = 0.0189 mm

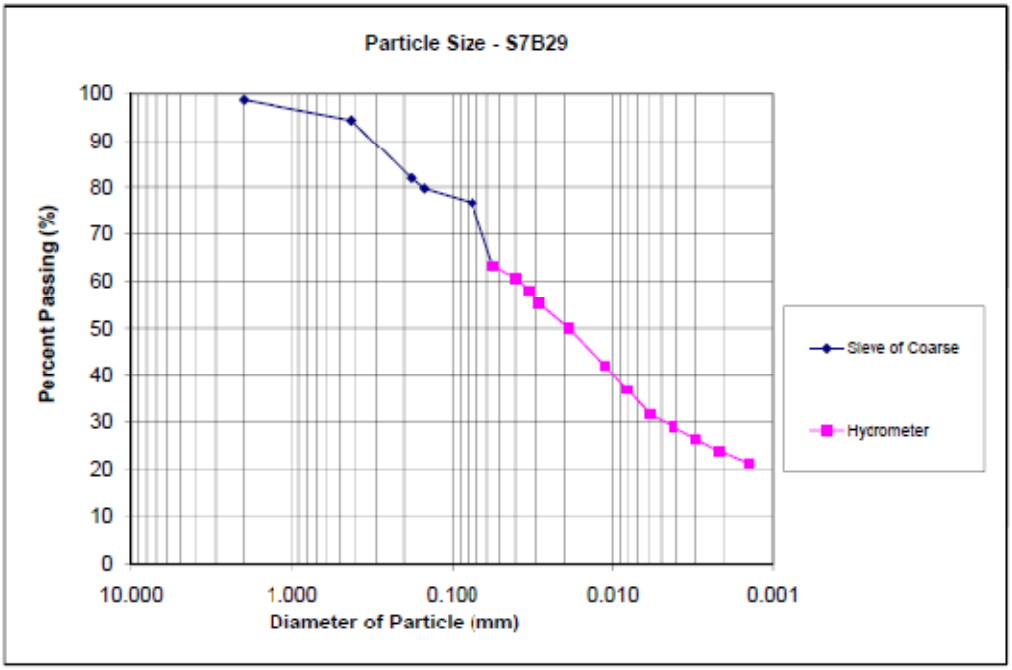
Particle Size - S7B29
Percent Passing (%)
100
90
80
70
60
50
40
30
20
10
0
10.000
1.000
0.100
0.010
0.001
Diameter of Particle (mm)
Sieve of Coarse
Hycrometer

Sieve Analysis

Project Name:	Midwest Levees	Boring No.:	S7B30
Location:	Indian Graves - South (Pump House)	Depth:Depth:	Levee Shell
Description:	Poorly graded clean sand, tan/brown	Date:	01/05/09

Sieve No.	Weight of Sieve (g)	Weight of Sieve + soil (g)	Weight of Retained (%)	Percentage Retained (%)	Percentage Passed (%)	Particle Size (mm)
4	468.92	498.55	29.63	2.79	97.21	4.75
10	606.82	657.87	51.05	4.80	92.42	2
40	339.06	938.94	599.88	56.39	36.03	0.425
80	317.55	677.30	359.75	33.82	2.21	0.18
100	337.56	344.92	7.36	0.69	1.52	0.15
200	340.90	354.29	13.39	1.26	0.26	0.075
Pan	479.45	482.25	2.80	0.26		

Total Weight of Soil = 1063.86

Cc = 0.88

D50 = 0.6238

Cu = 3.33

D10 = 0.21 D30 = 0.36 D60 = 0.7

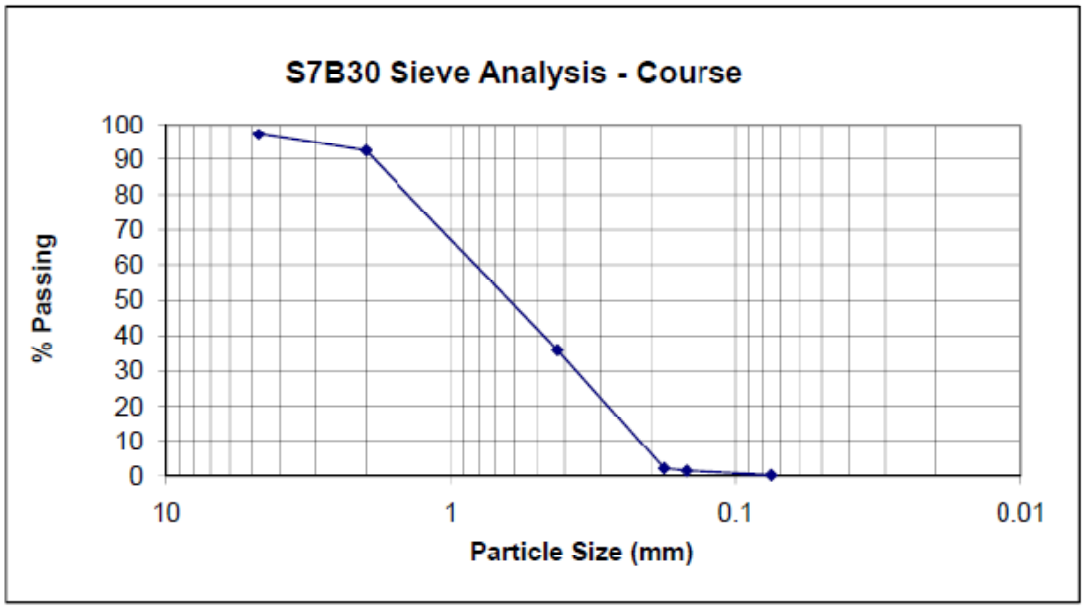

Sieve Analysis

Project Name:	Midwest Levees	Boring No.:	S8B31
Location:	Two Rivers	Depth:Depth:	Levee Shell
Description:	Poorly graded clean sand, tan/brown	Date:	01/05/09

Sieve No.	Weight of Sieve (g)	Weight of Sieve + soil (g)	Weight of Retained (%)	Percentage Retained (%)	Percentage Passed (%)	Particle Size (mm)
4	463.83	498.54	34.71	3.36	96.64	4.75
10	607.03	706.29	99.26	9.59	87.05	2
40	339.33	1042.92	703.59	68.01	19.04	0.425
80	317.53	498.08	180.55	17.45	1.58	0.18
100	337.57	340.63	3.06	0.30	1.29	0.15
200	340.92	347.10	6.18	0.60	0.69	0.075
Pan	479.44	486.59	7.15	0.69		

Total Weight of Soil = 1034.5

D10 =	0.26	D30 =	0.44	D50 =	0.8602
				D60 =	1.1

Cc = 0.68

Cu = 4.23

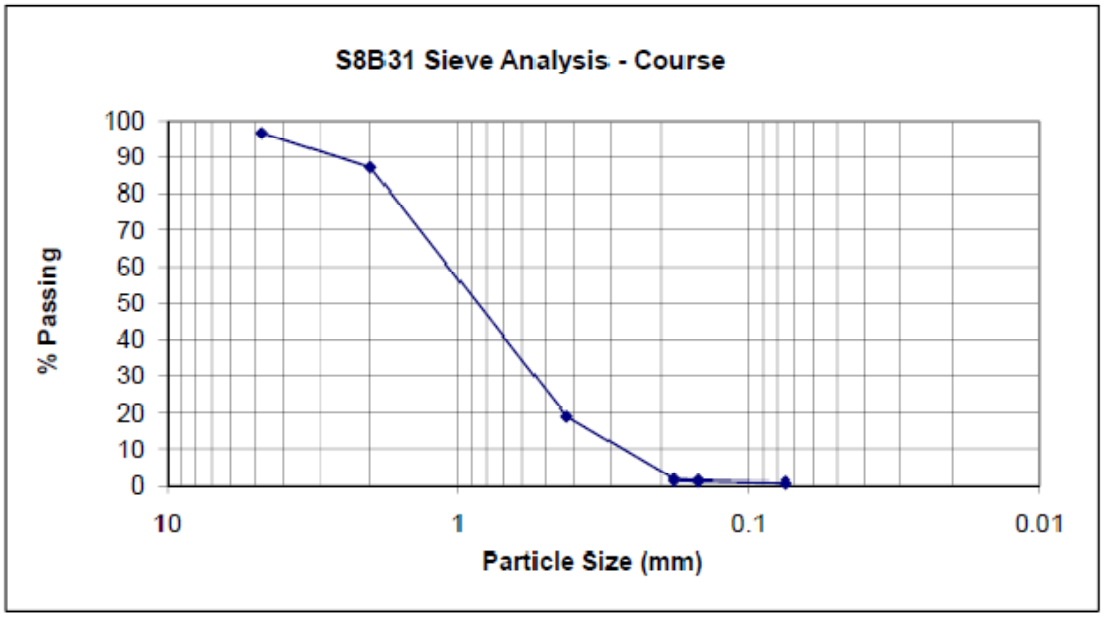

Sieve Analysis

Project Name:	Midwest Levees	Boring No.:	S8B32
Location:	Two Rivers	Depth:Depth:	Levee Shell, toe
Description:	Poorly graded clean sand, tan/brown	Date:	01/05/09

Sieve No.	Weight of Sieve (g)	Weight of Sieve + soil (g)	Weight of Retained (%)	Percentage Retained (%)	Percentage Passed (%)	Particle Size (mm)
4	468.88	496.40	27.52	3.38	96.62	4.75
10	606.93	668.59	61.66	7.58	89.04	2
40	339.24	832.54	493.30	60.61	28.43	0.425
80	317.54	510.06	192.52	23.66	4.77	0.18
100	337.57	343.60	6.03	0.74	4.03	0.15
200	340.92	354.95	14.03	1.72	2.31	0.075
Pan	479.46	498.23	18.77	2.31		

Total Weight of Soil = 813.83

D10 = 0.21 D30 = 0.44 D50 = 0.7375 Cc = 0.97
D60 = 0.95 Cu = 4.52

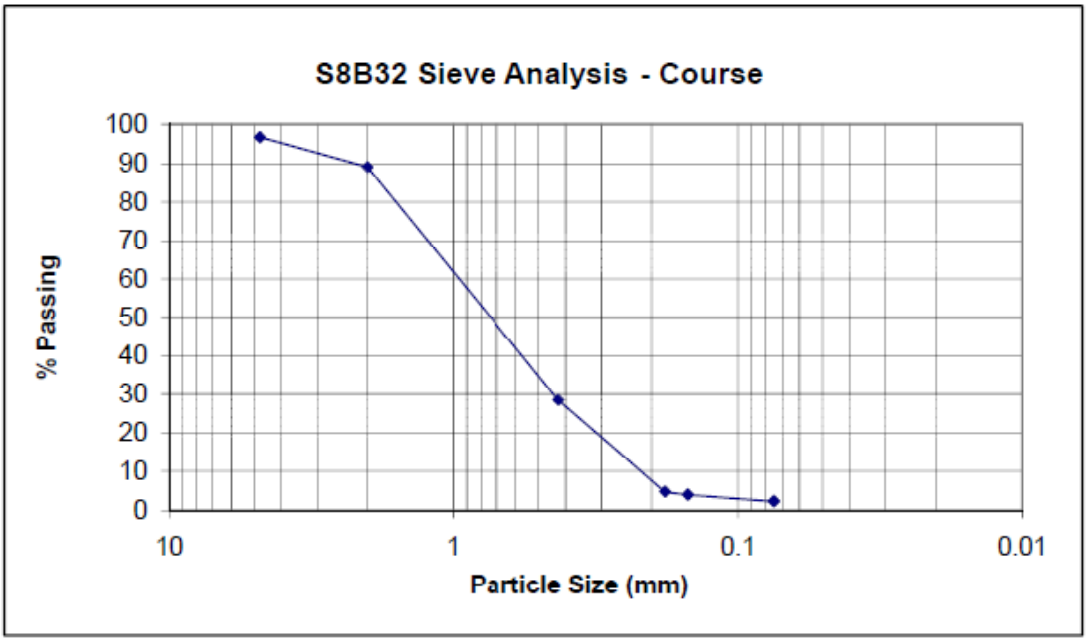

Hydrometer Analysis

Project Name	Midwest Levees	Boring No.:	S8B33
Location:	Two Rivers	Depth:	15'
Description:	Clay with silt/sand	Date:	01/25/09

Hygroscopic water content

Can No.	1
Wet Wt + Tare (g)	18.93
Dry Wt + Tare (g)	14.45
Tare Wt (g)	1
Moisture Content (%)	33.31
Correction Factor =	0.750

Hydrometer Type:	151H	
Mass of air dry soil =	87.19	g
Specific Gravity =	2.7	
Mass of oven dry soil =	65.405	g

Start Time	Elapsed Time	Actual Reading	Composite Correction	Corrected Reading	Temperature (degrees C)	Effective Hyd. Depth	K	Diameter of particle (mm)	Percent finer in suspension (%)
5:00pm	0	1.036	0.004	1.032	19.7	6.772	0.013	--	77.706
	0.067	1.035	0.004	1.031	19.7	7.037	0.013	0.138	75.278
	0.25	1.033	0.004	1.029	19.7	7.566	0.013	0.074	70.421
	0.5	1.032	0.004	1.028	19.7	7.830	0.013	0.053	67.993
	1	1.029	0.004	1.025	19.7	8.624	0.013	0.039	60.708
	1.5	1.027	0.004	1.023	19.7	9.153	0.013	0.033	55.851
	2	1.026	0.004	1.022	19.7	9.417	0.013	0.029	53.423
	5	1.021	0.004	1.017	19.7	10.740	0.013	0.020	41.281
	15	1.016	0.004	1.012	19.7	12.063	0.013	0.012	29.140
	30	1.014	0.004	1.01	19.7	12.592	0.013	0.009	24.283
	60	1.012	0.004	1.008	19.7	13.121	0.013	0.006	19.427
	120	1.011	0.004	1.007	19.7	13.385	0.013	0.004	16.998
	240	1.009	0.004	1.005	19.7	13.914	0.013	0.003	12.142
	480	1.007	0.004	1.003	19.7	14.443	0.013	0.002	7.285
	1140	1.006	0.004	1.002	19.7	14.708	0.013	0.002	4.857

Sieve Analysis of Coarse Fraction Weight of Soil Sieved = 11.78 g

Sieve No.	Weight of Sieve (g)	Weight of Sieve + soil (g)	Weight of Retained (%)	Percentage Retained (%)	Percentage Passed (%)	Particle Size (mm)
10	606.89	606.90	0.01	0.02	99.98	2
40	339.11	339.86	0.75	1.15	98.84	0.425
80	317.47	321.05	3.58	5.47	93.36	0.18
100	496.81	498.14	1.33	2.03	91.33	0.15
200	340.90	346.32	5.42	8.29	83.04	0.075
-200	479.40	479.91	0.51	0.78	82.26	
		Total W =	*11.60*			

Combined	
Particle Size (mm)	Percent Passing (%)
2.000	99.985
0.425	98.838
0.180	93.364
0.150	91.331
0.075	83.044
0.053	67.993
0.039	60.708
0.033	55.851
0.029	53.423
0.020	41.281
0.012	29.140
0.009	24.283
0.006	19.427
0.004	16.998
0.003	12.142
0.002	7.285
0.002	4.857

D50 = 0.0261 mm

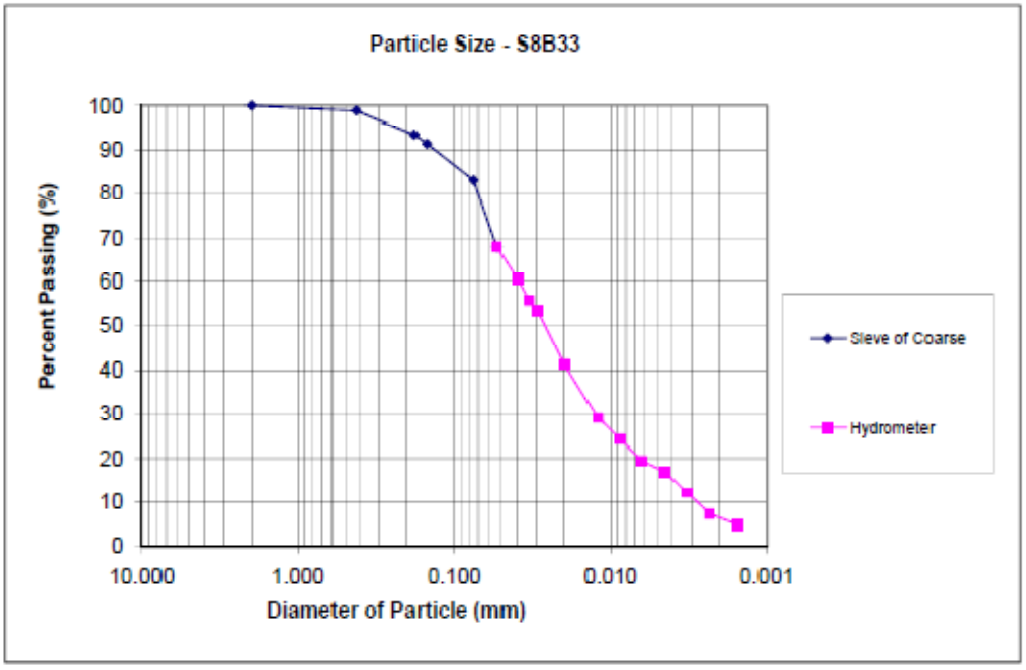
Particle Size - S8B33
Percent Passing (%)
100
90
80
70
60
50
40
30
20
10
0
10.000
1.000
0.100
0.010
0.001
Diameter of Particle (mm)
Sieve of Coarse
Hydrometer

Hydrometer Analysis

Project Name:	Midwest Levees	Boring No.:	S8B35
Location:	Two Rivers	Depth:	128", hand augered
Description:	Clay-very sandy	Date:	01/25/09

Hygroscopic water content

Can No.	1
Wet Wt + Tare (g)	16.48
Dry Wt + Tare (g)	14.48
Tare Wt (g)	1.02
Moisture Content (%)	14.86
Correction Factor =	0.871

Hydrometer Type:	151H	
Mass of air dry soil =	105.94	g
Specific Gravity =	2.7	
Mass of oven dry soil =	92.235	g

Start Time	Elapsed Time	Actual Reading	Composite Correction	Corrected Reading	Temperature (degrees C)	Effective Hyd. Depth	K	Diameter of particle (mm)	Percent finer in suspension (%)
5:11pm	0	1.027	0.005	1.022	19.7	9.153	0.013	--	37.383
	0.067	1.023	0.005	1.018	19.7	10.211	0.014	0.174	30.995
	0.25	1.022	0.005	1.017	19.7	10.476	0.014	0.091	29.273
	0.5	1.021	0.005	1.016	19.7	10.740	0.014	0.065	27.551
	1	1.02	0.005	1.015	19.7	11.005	0.014	0.047	25.329
	1.5	1.019	0.005	1.014	19.7	11.269	0.014	0.038	24.107
	2	1.019	0.005	1.014	19.7	11.269	0.014	0.033	24.107
	5	1.016	0.005	1.011	19.7	12.063	0.014	0.022	18.941
	15	1.013	0.005	1.008	19.7	12.856	0.014	0.013	13.776
	30	1.011	0.005	1.006	19.7	13.385	0.014	0.009	10.332
	60	1.011	0.005	1.006	19.7	13.385	0.014	0.007	10.332
	120	1.01	0.005	1.005	19.7	13.650	0.014	0.005	8.610
	240	1.009	0.005	1.004	19.7	13.914	0.014	0.003	6.888
	480	1.008	0.005	1.003	19.7	14.179	0.014	0.002	5.166
	1140	1.007	0.005	1.002	19.7	14.443	0.014	0.002	3.444

Sieve Analysis of Coarse Fraction Weight of Soil Sieved = 61.85 g

Sieve No.	Weight of Sieve (g)	Weight of Sieve + soil (g)	Weight of Retained (%)	Percentage Retained (%)	Percentage Passed (%)	Particle Size (mm)
10	606.90	607.54	0.64	0.69	99.31	2
40	339.09	344.10	5.01	5.43	93.87	0.425
80	317.47	361.25	43.78	47.47	46.41	0.18
100	496.75	501.82	5.07	5.50	40.91	0.15
200	340.90	347.75	6.85	7.43	33.49	0.075
-200	479.40	479.87	0.47	0.51	32.98	
		Total W =	*61.82*			

Combined	
Particle Size (mm)	Percent Passing (%)
2.000	99.306
0.425	93.874
0.180	46.409
0.150	40.912
0.075	33.485
0.065	27.551
0.047	25.329
0.038	24.107
0.033	24.107
0.022	18.941
0.013	13.776
0.009	10.332
0.007	10.332
0.005	8.610
0.003	6.888
0.002	5.166
0.002	3.444

D50 = 0.1921 mm

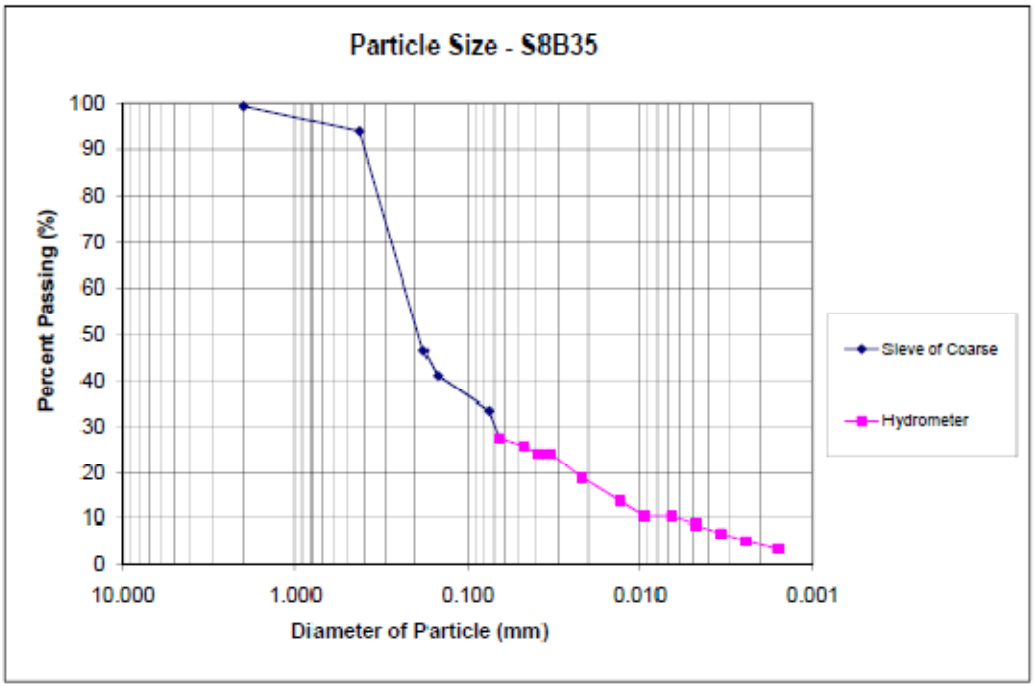
Particle Size - S8B35
Percent Passing (%)
100
90
80
70
60
50
40
30
20
10
0
10.000
1.000
0.100
0.010
0.001
Diameter of Particle (mm)
Sieve of Coarse
Hydrometer

APPENDIX 4. ATTERBERG LIMITS

ASTM D 4318

Project Name:	Midwest Levees	Boring No.:	S1Bulk2
Location:	Winfield	Depth:	
Description:	Dk brown sandy clay	Date:	12/19/08

LIQUID LIMIT DETERMINATION Method A (Multipoint)

Can No.	1	2	3	4	
Wet Wt + Tare (g)	58.74	46.41	55.28	27.73	
Dry Wt + Tare (g)	45.83	37.87	43.69	18.62	
Tare Wt (g)	22.36	22.14	22.52	1.04	
Moisture Content (%)	55.01	54.29	54.75	51.82	
No. of Blows	20	27	24	36	
Limit Limit (LL) - *Method B*	54	55	54	54	

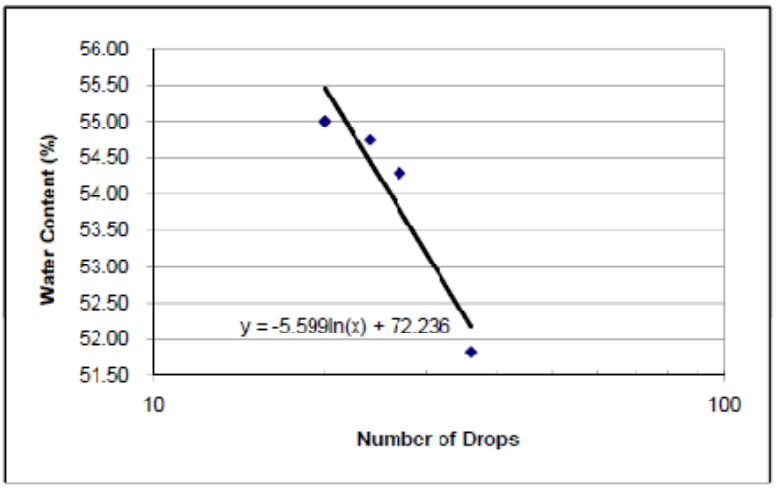

Liquid Limit =	55
Plastic Limit =	25
Plasticity Index =	30

Estimated % of Mat. Retained on the No. 40 Sieve _____

PLASTIC LIMIT DETERMINATION

Can No.	1T	3T		
Wet Wt + Tare (g)	28.79	29.07		
Dry Wt + Tare (g)	27.55	27.63		
Tare Wt (g)	22.41	22.12		
Wt. of Dry Soil (g)	5.14	5.51	0	0
Wt. of Water (g)	1.24	1.44	0	0
Trial Plastic Limit	*24.1*	*26.1*		
PLASTIC LIMIT (PL)	25.1			

Date Tested: 12/19/09 Tested by: MB

Project Name:	Midwest Levees	Boring No.:	S2B6
Location:	Brian's Creek	Depth:	58"
Description:	Gray clay w/tan seams	Date:	01/07/09

LIQUID LIMIT DETERMINATION Method A (Multipoint)

Can No.	1	2	3	4	
Wet Wt + Tare (g)	51.56	51.87	54.57	30.48	
Dry Wt + Tare (g)	39.9	39.59	41.21	18.04	
Tare Wt (g)	22.53	22.2	22.7	1	
Moisture Content (%)	67.13	70.62	72.18	73.00	
No. of Blows	32	26	23	21	
Limit Limit (LL) - *Method B*	69	71	71	71	

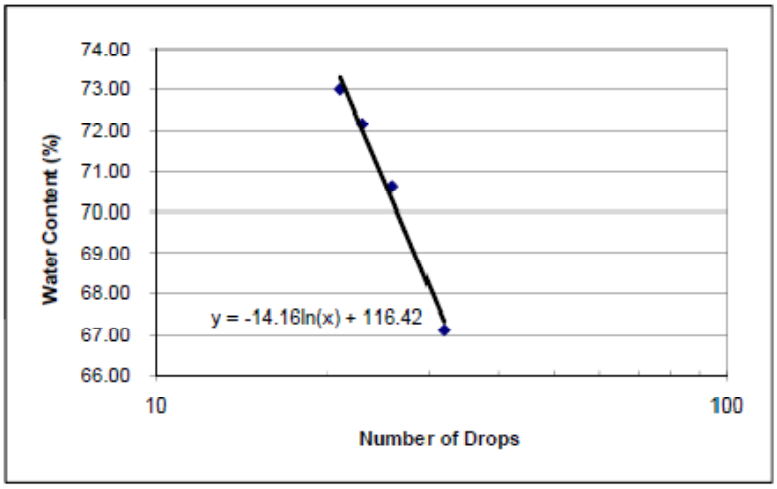

Liquid Limit =	71
Plastic Limit =	22
Plasticity Index =	49

Estimated % of Mat. Retained on the No. 40 Sieve _____

PLASTIC LIMIT DETERMINATION

Can No.	PL1	PL2		
Wet Wt + Tare (g)	30.08	30.35		
Dry Wt + Tare (g)	28.66	28.9		
Tare Wt (g)	22.16	22.42		
Wt. of Dry Soil (g)	6.5	6.48	0	0
Wt. of Water (g)	1.42	1.45	0	0
Trial Plastic Limit	*21.8*	*22.4*		
PLASTIC LIMIT (PL)	22.1			

Date Tested: 01/07/09 Tested by: MB

Project Name:	Midwest Levees	Boring No.:	S2B7
Location:	Brian's Creek	Depth:	18"
Description:	Clay, gray-dk gray w/tan and red/br seams	Date:	01/06/09

LIQUID LIMIT DETERMINATION Method A (Multipoint)

Can No.	1	2	3	4	
Wet Wt + Tare (g)	37.32	63.17	56.52	22.85	
Dry Wt + Tare (g)	30.96	52.45	44.65	13.29	
Tare Wt (g)	22.57	38.94	29.66	0.99	
Moisture Content (%)	75.80	79.35	79.19	77.72	
No. of Blows	31	19	21	23	
Limit Limit (LL) - *Method B*	78	77	78	77	

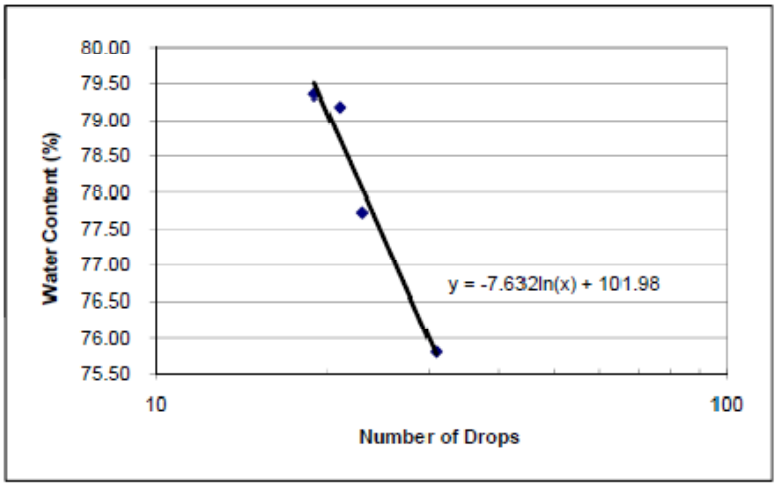

Liquid Limit =	78
Plastic Limit =	24
Plasticity Index =	54

Estimated % of Mat. Retained on the No. 40 Sieve _____

PLASTIC LIMIT DETERMINATION

Can No.	PL1	PL2		
Wet Wt + Tare (g)	30.54	28.49		
Dry Wt + Tare (g)	29.17	27.28		
Tare Wt (g)	23.26	22.51		
Wt. of Dry Soil (g)	5.91	4.77	0	0
Wt. of Water (g)	1.37	1.21	0	0
Trial Plastic Limit	*23.2*	*25.4*		
PLASTIC LIMIT (PL)	24.3			

Date Tested: 01/06/09 Tested by: MB

Project Name:	Midwest Levees	Boring No.:	S2B9
Location:	Brian's Creek	Depth:	10'
Description:	Gray clay, stiff, hard to break up	Date:	01/07/09

LIQUID LIMIT DETERMINATION Method A (Multipoint)

Can No.	1	2	3	4	
Wet Wt + Tare (g)	24.57	25.46	32.29	31.9	
Dry Wt + Tare (g)	13.59	14	17.5	17.18	
Tare Wt (g)	0.97	0.99	0.96	0.96	
Moisture Content (%)	87.00	88.09	89.42	90.75	
No. of Blows	26	24	23	18	
Limit Limit (LL) - *Method B*	87	88	89	87	

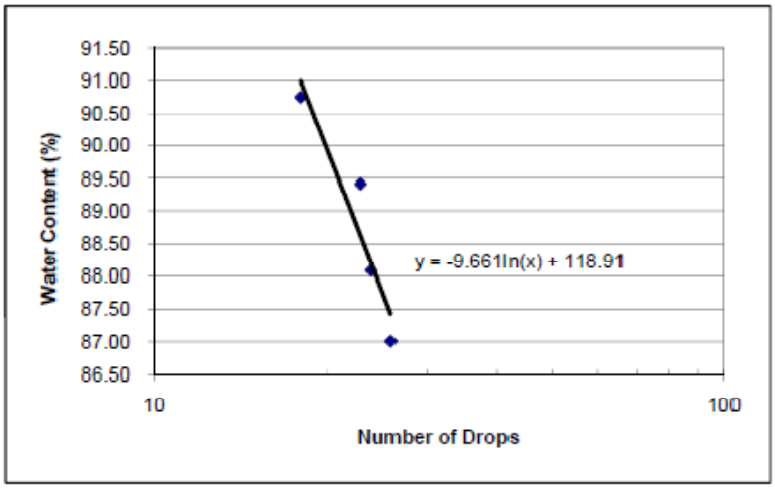

Liquid Limit =	88
Plastic Limit =	26
Plasticity Index =	62

Estimated % of Mat. Retained on the No. 40 Sieve _____

PLASTIC LIMIT DETERMINATION

Can No.	PL1	PL2		
Wet Wt + Tare (g)	28.74	28.71		
Dry Wt + Tare (g)	27.34	27.38		
Tare Wt (g)	22.05	22.33		
Wt. of Dry Soil (g)	5.29	5.05	0	0
Wt. of Water (g)	1.4	1.33	0	0
Trial Plastic Limit	*26.5*	*26.3*		
PLASTIC LIMIT (PL)	26.4			

Date Tested: 01/07/09 Tested by: MB

Project Name:	Midwest Levees	Boring No.:	S3B10
Location:	Brevator	Depth:	Crest Surface
Description:	Gray clay, stiff, roots present	Date:	12/17/08

LIQUID LIMIT DETERMINATION Method A (Multipoint)

Can No.	1	2	3	4	
Wet Wt + Tare (g)	54.66	58.66	63.32	34.88	
Dry Wt + Tare (g)	44.98	48.4	51.46	25.18	
Tare Wt (g)	21.99	23.18	22.34	0.98	
Moisture Content (%)	42.11	40.68	40.73	40.08	
No. of Blows	21	25	27	31	
Limit Limit (LL) - *Method B*	41	41	41	41	

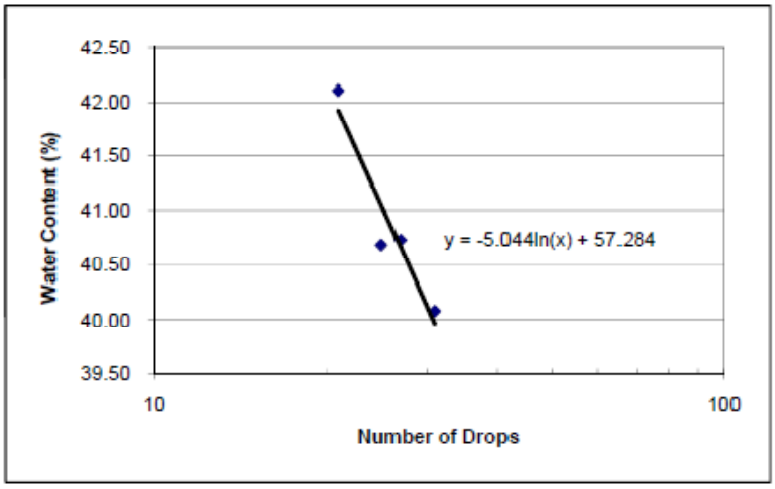

Liquid Limit =	41
Plastic Limit =	20
Plasticity Index =	21

Estimated % of Mat. Retained on the No. 40 Sieve _____

PLASTIC LIMIT DETERMINATION

Can No.	PL1	PL2		
Wet Wt + Tare (g)	28.38	28.78		
Dry Wt + Tare (g)	27.34	27.71		
Tare Wt (g)	22.19	22.43		
Wt. of Dry Soil (g)	5.15	5.28	0	0
Wt. of Water (g)	1.04	1.07	0	0
Trial Plastic Limit	*20.2*	*20.3*		
PLASTIC LIMIT (PL)	20.2			

Date Tested: 12/17/08 Tested by: MB

Project Name:	Midwest Levees	Boring No.:	S3B11
Location:	Brevator	Depth:	10'
Description:	Gray clay, stiff	Date:	01/05/09

LIQUID LIMIT DETERMINATION Method A (Multipoint)

Can No.	1	2	3	4	
Wet Wt + Tare (g)	44.7	51.4	54.96	24.77	
Dry Wt + Tare (g)	37.16	41.59	44.58	17.05	
Tare Wt (g)	22.33	22.12	22.48	1	
Moisture Content (%)	50.84	50.39	46.97	48.10	
No. of Blows	21	24	31	26	
Limit Limit (LL) - *Method B*	50	50	48	48	

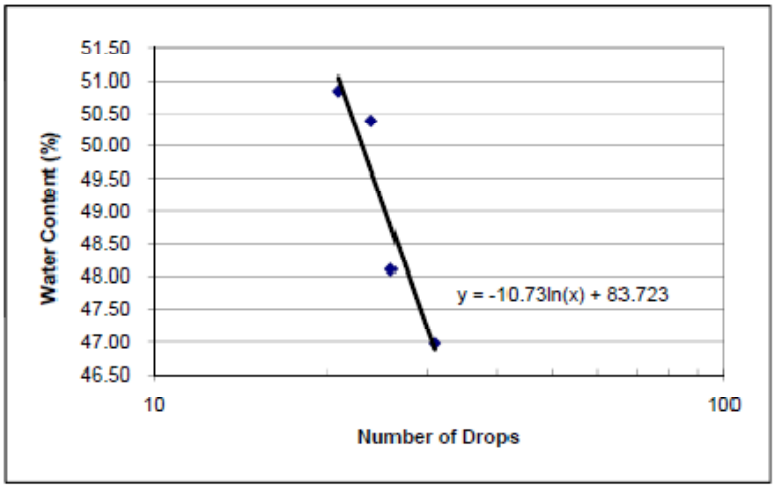

Liquid Limit =	50
Plastic Limit =	23
Plasticity Index =	27

Estimated % of Mat. Retained on the No. 40 Sieve _____

PLASTIC LIMIT DETERMINATION

Can No.	PL1	PL2		
Wet Wt + Tare (g)	28.94	28.61		
Dry Wt + Tare (g)	27.73	27.37		
Tare Wt (g)	22.44	22.11		
Wt. of Dry Soil (g)	5.29	5.26	0	0
Wt. of Water (g)	1.21	1.24	0	0
Trial Plastic Limit	*22.9*	*23.6*		
PLASTIC LIMIT (PL)	23.2			

Date Tested: 01/05/09 Tested by: MB

Project Name:	Midwest Levees	Boring No.:	S3B12
Location:	Brevator	Depth:	Crest Surface
Description:	Gray clay, stiff, roots present	Date:	12/17/08

LIQUID LIMIT DETERMINATION Method A (Multipoint)

Can No.	1	2	3	4	
Wet Wt + Tare (g)	49.44	48.16	54.98	26.75	
Dry Wt + Tare (g)	38.85	37.75	41.73	16.44	
Tare Wt (g)	22.56	22.23	22.6	1.02	
Moisture Content (%)	65.01	67.07	69.26	66.86	
No. of Blows	27	25	19	26	
Limit Limit (LL) - *Method B*	66	67	67	67	

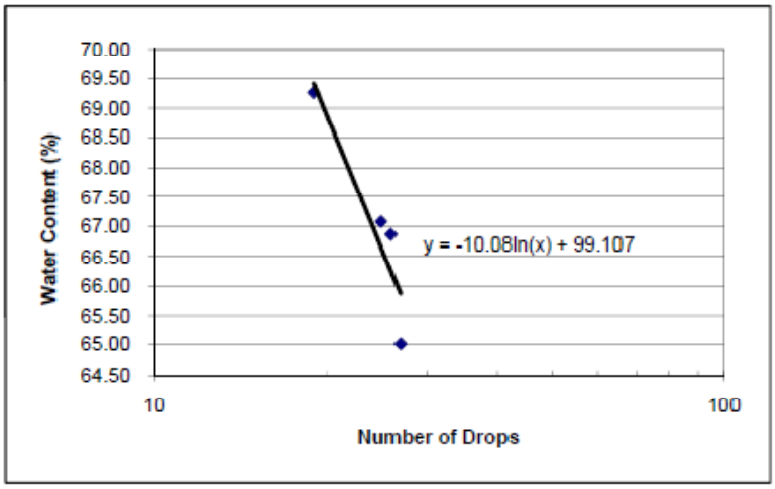

Liquid Limit = 66

Plastic Limit = 26

Plasticity Index = 40

Estimated % of Mat. Retained on the No. 40 Sieve

PLASTIC LIMIT DETERMINATION

Can No.	PL1	PL2		
Wet Wt + Tare (g)	30.47	28.41		
Dry Wt + Tare (g)	28.79	27.12		
Tare Wt (g)	22.4	22.17		
Wt. of Dry Soil (g)	6.39	4.95	0	0
Wt. of Water (g)	1.68	1.29	0	0
Trial Plastic Limit	*26.3*	*26.1*		
PLASTIC LIMIT (PL)	26.2			

Date Tested: 12/17/08 Tested by: MB

Project Name:	Midwest Levees	Boring No.:	S3B13
Location:	Brevator	Depth:	10'
Description:	Gray clay, stiff	Date:	01/05/09

LIQUID LIMIT DETERMINATION Method A (Multipoint)

Can No.	1	2	3	4	
Wet Wt + Tare (g)	57.91	54.15	48.09	29.06	
Dry Wt + Tare (g)	44.21	42.38	37.94	17.9	
Tare Wt (g)	22.49	23.46	22.13	0.99	
Moisture Content (%)	63.08	62.21	64.20	66.00	
No. of Blows	25	30	25	21	
Limit Limit (LL) - *Method B*	63	64	64	65	

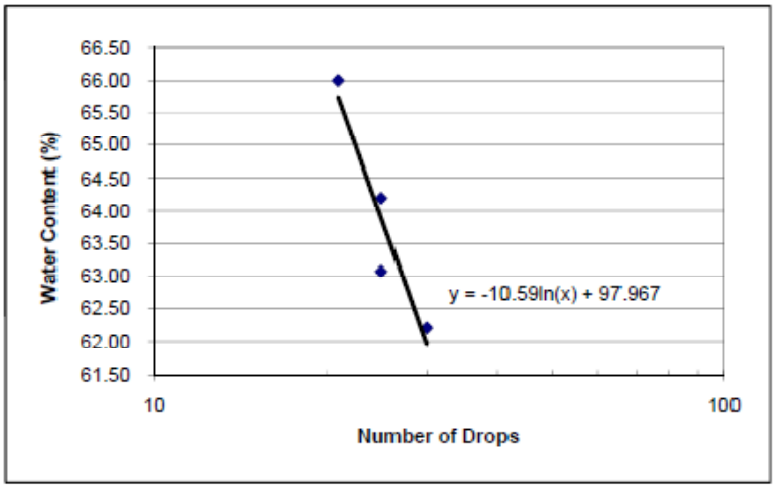

Liquid Limit = 64

Plastic Limit = 24

Plasticity Index = 40

Estimated % of Mat. Retained on the No. 40 Sieve

PLASTIC LIMIT DETERMINATION

Can No.	PL1	PL2		
Wet Wt + Tare (g)	28	29.33		
Dry Wt + Tare (g)	26.84	27.96		
Tare Wt (g)	21.98	22.11		
Wt. of Dry Soil (g)	4.86	5.85	0	0
Wt. of Water (g)	1.16	1.37	0	0
Trial Plastic Limit	*23.9*	*23.4*		
PLASTIC LIMIT (PL)	23.6			

Date Tested: 01/05/09 Tested by: MB

Project Name:	Midwest Levees	Boring No.:	S4B14
Location:	Kickapoo	Depth:	Crest Surface
Description:	Gray clay, roots present	Date:	12/20/08

LIQUID LIMIT DETERMINATION Method A (Multipoint)

Can No.	1	2	3	4	
Wet Wt + Tare (g)	52.3	47.94	51.13	25.78	
Dry Wt + Tare (g)	40.39	38.2	39.97	16.12	
Tare Wt (g)	21.92	23.13	22.32	1	
Moisture Content (%)	64.48	64.63	63.23	63.89	
No. of Blows	26	23	37	30	
Limit Limit (LL) - *Method B*	65	64	66	65	

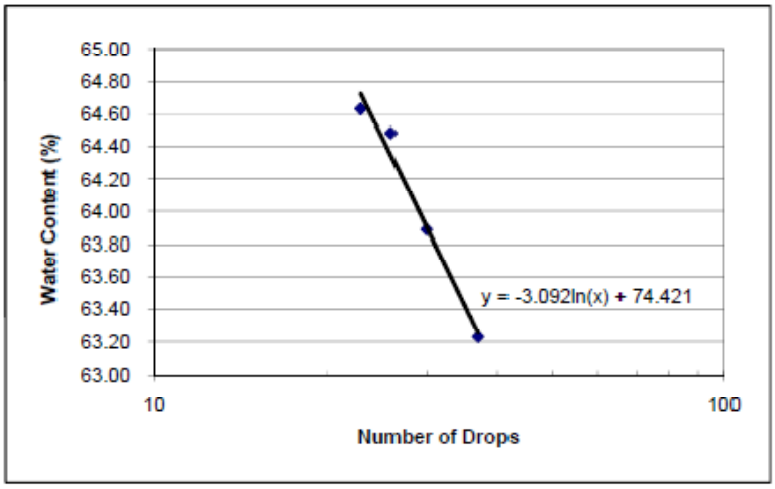

Liquid Limit =	64
Plastic Limit =	28
Plasticity Index =	36

Estimated % of Mat. Retained on the No. 40 Sieve _____

PLASTIC LIMIT DETERMINATION

Can No.	PL1	PL2		
Wet Wt + Tare (g)	30.71	30.87		
Dry Wt + Tare (g)	28.86	29.04		
Tare Wt (g)	22.15	22.39		
Wt. of Dry Soil (g)	6.71	6.65	0	0
Wt. of Water (g)	1.85	1.83	0	0
Trial Plastic Limit	*27.6*	*27.5*		
PLASTIC LIMIT (PL)	27.5			

Date Tested: 12/20/08 Tested by: MB

Project Name:	Midwest Levees	Boring No.:	S4B16
Location:	Kickapoo	Depth:	74"
Description:	Gray clay	Date:	12/20/08

LIQUID LIMIT DETERMINATION Method A (Multipoint)

Can No.	1	2	3	4	
Wet Wt + Tare (g)	49.46	49.55	26.43	28.43	
Dry Wt + Tare (g)	37.96	37.33	14.76	16.36	
Tare Wt (g)	22.55	22.18	1.05	0.97	
Moisture Content (%)	74.63	80.66	85.12	78.43	
No. of Blows	30	28	19	26	
Limit Limit (LL) - *Method B*	76	82	82	79	

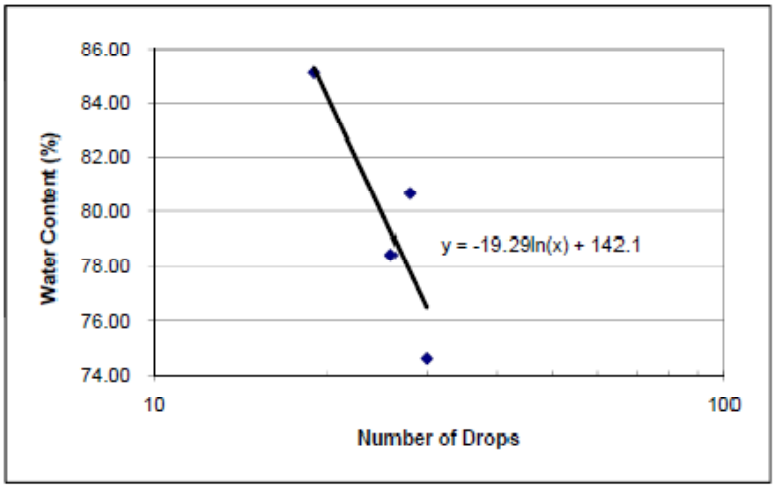

Liquid Limit = 81

Plastic Limit = 24

Plasticity Index = 57

Estimated % of Mat. Retained on the No. 40 Sieve

PLASTIC LIMIT DETERMINATION

Can No.	PL1	PL2		
Wet Wt + Tare (g)	28.85	29		
Dry Wt + Tare (g)	27.57	27.68		
Tare Wt (g)	22.4	22.17		
Wt. of Dry Soil (g)	5.17	5.51	0	0
Wt. of Water (g)	1.28	1.32	0	0
Trial Plastic Limit	*24.8*	*24.0*		
PLASTIC LIMIT (PL)	24.4			

Date Tested: 12/20/08 Tested by: MB

Project Name:	Midwest Levees	Boring No.:	S4B18
Location:	Kickapoo	Depth:	9'
Description:	Clay, dk gray/brown, sandy	Date:	12/22/08

LIQUID LIMIT DETERMINATION Method A (Multipoint)

Can No.	1	2	3	4	
Wet Wt + Tare (g)	51.36	50.3	57.75	33.59	
Dry Wt + Tare (g)	40.58	39.97	44.81	21.31	
Tare Wt (g)	22.42	22.17	20.4	1	
Moisture Content (%)	59.36	58.03	53.01	60.46	
No. of Blows	22	25	29	21	
Limit Limit (LL) - *Method B*	58	58	54	59	

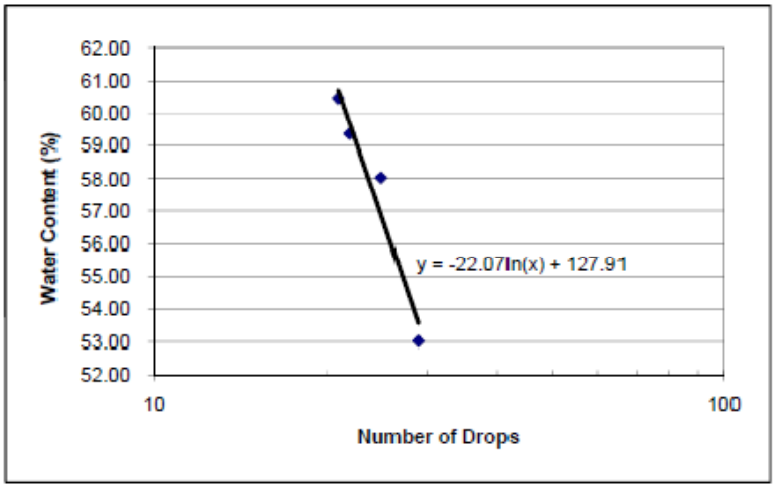

Liquid Limit =	57
Plastic Limit =	24
Plasticity Index =	33

Estimated % of Mat. Retained on the No. 40 Sieve _____

PLASTIC LIMIT DETERMINATION

Can No.	PL1	PL2		
Wet Wt + Tare (g)	29.25	28.63		
Dry Wt + Tare (g)	27.93	27.36		
Tare Wt (g)	22.56	22.12		
Wt. of Dry Soil (g)	5.37	5.24	0	0
Wt. of Water (g)	1.32	1.27	0	0
Trial Plastic Limit	*24.6*	*24.2*		
PLASTIC LIMIT (PL)	24.4			

Date Tested: 12/22/08 Tested by: MB

Project Name:	Midwest Levees	Boring No.:	S5B19
Location:	Norton Woods	Depth:	Crest Surface
Description:	Clay, dk brown, some sand, a lot of roots	Date:	01/13/09

LIQUID LIMIT DETERMINATION Method A (Multipoint)

Can No.	1	2	3	4	
Wet Wt + Tare (g)	37.75	33.79	34.55	37.57	
Dry Wt + Tare (g)	32.3	29.62	30.28	32.12	
Tare Wt (g)	22.48	22.17	22.56	22.24	
Moisture Content (%)	55.50	55.97	55.31	55.16	
No. of Blows	23	21	22	26	
Limit Limit (LL) - *Method B*	55	55	54	55	

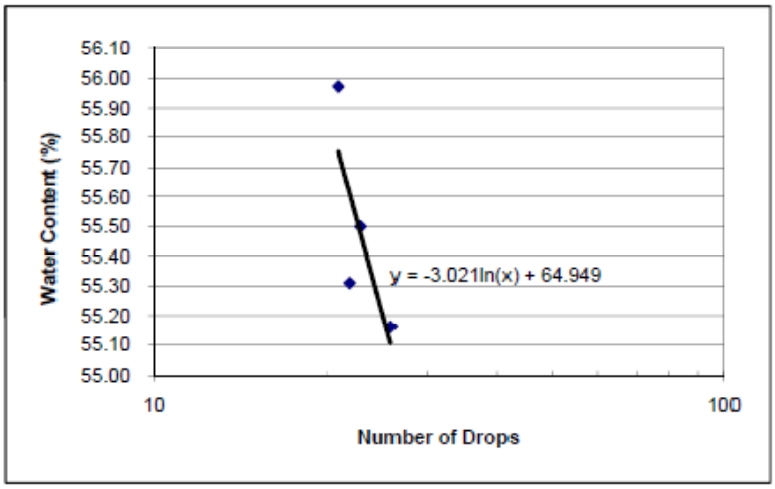

Liquid Limit = 55

Plastic Limit = 22

Plasticity Index = 33

Estimated % of Mat. Retained on the No. 40 Sieve

PLASTIC LIMIT DETERMINATION

Can No.	PL1	PL2		
Wet Wt + Tare (g)	28.29	28.13		
Dry Wt + Tare (g)	27.17	27		
Tare Wt (g)	22.12	21.98		
Wt. of Dry Soil (g)	5.05	5.02	0	0
Wt. of Water (g)	1.12	1.13	0	0
Trial Plastic Limit	*22.2*	*22.5*		
PLASTIC LIMIT (PL)	22.3			

Date Tested: 01/13/09 Tested by: ST Checked by: MB

Project Name:	Midwest Levees	Boring No.:	S5B20
Location:	Norton Woods	Depth:	10'
Description:	Clay, gray/brown w/se yellow/brown sand	Date:	01/13/09

LIQUID LIMIT DETERMINATION Method A (Multipoint)

Can No.	1	2	3	4	
Wet Wt + Tare (g)	48.5	49.15	53.87	26.37	
Dry Wt + Tare (g)	37.82	38.64	40.65	15.75	
Tare Wt (g)	22.49	23.46	22.11	1	
Moisture Content (%)	69.67	69.24	71.31	72.00	
No. of Blows	25	28	23	20	
Limit Limit (LL) - *Method B*	70	70	71	70	

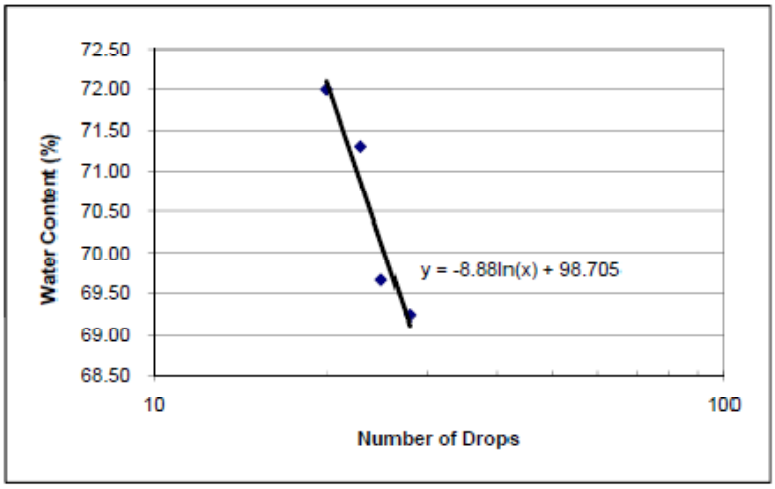

Liquid Limit =	70
Plastic Limit =	28
Plasticity Index =	42

Estimated % of Mat. Retained on the No. 40 Sieve _____

PLASTIC LIMIT DETERMINATION

Can No.	PL1	PL2		
Wet Wt + Tare (g)	28.98	28.49		
Dry Wt + Tare (g)	27.5	27.11		
Tare Wt (g)	22.4	22.17		
Wt. of Dry Soil (g)	5.1	4.94	0	0
Wt. of Water (g)	1.48	1.38	0	0
Trial Plastic Limit	*29.0*	*27.9*		
PLASTIC LIMIT (PL)	28.5			

Date Tested: 01/13/09 Tested by: MB

Project Name:	Midwest Levees	Boring No.:	S5B23
Location:	Norton Woods	Depth:	10'
Description:	Clay	Date:	01/07/09

LIQUID LIMIT DETERMINATION Method A (Multipoint)

Can No.	1	2	3	4	
Wet Wt + Tare (g)	29.13	30.77	27.43	23.21	
Dry Wt + Tare (g)	17.25	18.33	16.41	13.87	
Tare Wt (g)	0.97	1.02	0.98	0.98	
Moisture Content (%)	72.97	71.87	71.42	72.46	
No. of Blows	21	25	28	26	
Limit Limit (LL) - *Method B*	71	72	72	73	

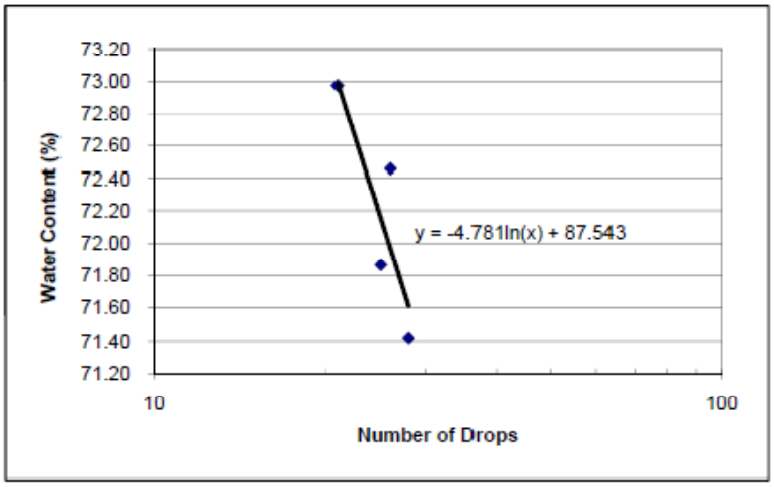

Liquid Limit = 72

Plastic Limit = 27

Plasticity Index = 45

Estimated % of Mat. Retained on the No. 40 Sieve

PLASTIC LIMIT DETERMINATION

Can No.	PL1	PL2		
Wet Wt + Tare (g)	39.58	44.97		
Dry Wt + Tare (g)	37.81	43.69		
Tare Wt (g)	31.32	38.93		
Wt. of Dry Soil (g)	6.49	4.76	0	0
Wt. of Water (g)	1.77	1.28	0	0
Trial Plastic Limit	*27.3*	*26.9*		
PLASTIC LIMIT (PL)	27.1			

Date Tested: 01/07/09 Tested by: MB

Project Name:	Midwest Levees	Boring No.:	S6B24
Location:	Indian Graves - Main	Depth:	74"
Description:	Clay-sandy	Date:	12/17/08

LIQUID LIMIT DETERMINATION Method A (Multipoint)

Can No.	1	2	3	4	
Wet Wt + Tare (g)	60.24	50.16	57.64	33.61	
Dry Wt + Tare (g)	47.88	41.39	46.32	23.02	
Tare Wt (g)	22.45	23.23	22.58	0.99	
Moisture Content (%)	48.60	48.29	47.68	48.07	
No. of Blows	19	24	28	23	
Limit Limit (LL) - *Method B*	47	48	48	48	

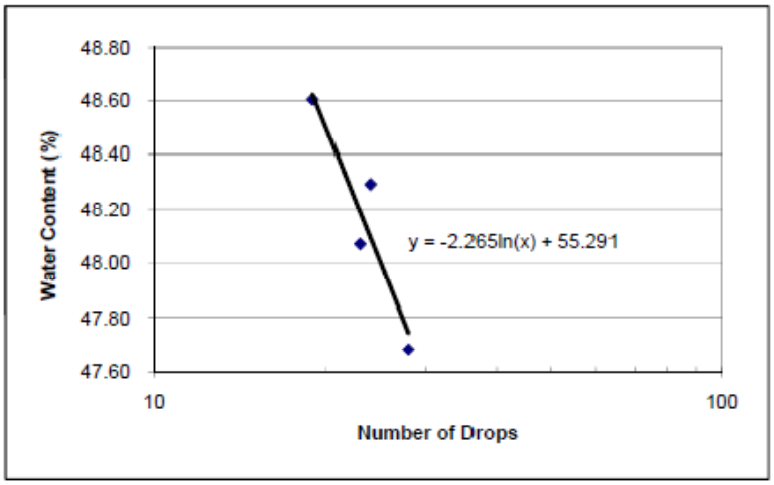

Liquid Limit = 48

Plastic Limit = 20

Plasticity Index = 28

Estimated % of Mat. Retained on the No. 40 Sieve

PLASTIC LIMIT DETERMINATION

Can No.	PL1	PL2		
Wet Wt + Tare (g)	28.31	29.87		
Dry Wt + Tare (g)	27.27	28.6		
Tare Wt (g)	21.98	22.12		
Wt. of Dry Soil (g)	5.29	6.48	0	0
Wt. of Water (g)	1.04	1.27	0	0
Trial Plastic Limit	*19.7*	*19.6*		
PLASTIC LIMIT (PL)	19.6			

Date Tested: 12/17/08 Tested by: MB

Project Name:	Midwest Levees	Boring No.:	S6B26
Location:	Indian Graves - Main	Depth:	15'
Description:		Date:	01/12/09

LIQUID LIMIT DETERMINATION Method A (Multipoint)

Can No.	1	2	3	4	
Wet Wt + Tare (g)	44.71	56.91	47.59	29.48	
Dry Wt + Tare (g)	36.62	44.35	38.09	18.91	
Tare Wt (g)	22.55	23.45	22.13	0.97	
Moisture Content (%)	57.50	60.10	59.52	58.92	
No. of Blows	34	26	23	27	
Limit Limit (LL) - *Method B*	60	60	59	59	

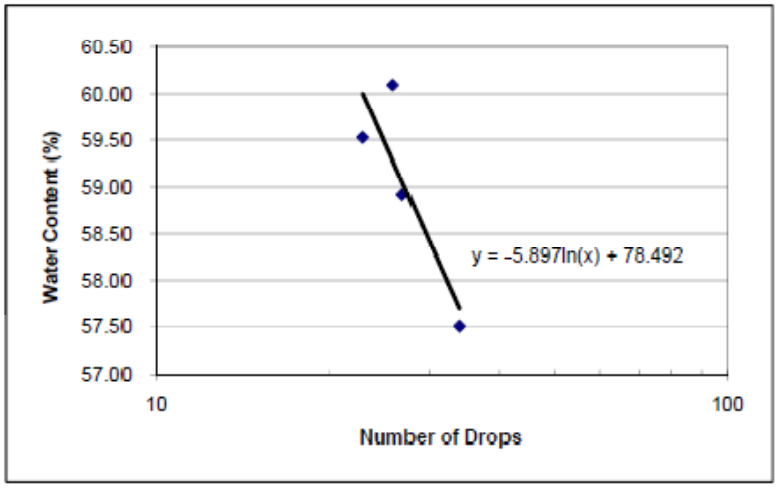

Liquid Limit =	60
Plastic Limit =	25
Plasticity Index =	35

Estimated % of Mat. Retained on the No. 40 Sieve

PLASTIC LIMIT DETERMINATION

Can No.	PL1	PL2		
Wet Wt + Tare (g)	28.46	28.24		
Dry Wt + Tare (g)	27.24	27.05		
Tare Wt (g)	22.4	22.17		
Wt. of Dry Soil (g)	4.84	4.88	0	0
Wt. of Water (g)	1.22	1.19	0	0
Trial Plastic Limit	*25.2*	*24.4*		
PLASTIC LIMIT (PL)	24.8			

Date Tested: 01/12/09 Tested by: MB

Project Name:	Midwest Levees	Boring No.:	S7B29
Location:	Indian Graves - South(pump house)	Depth:	Clay core
Description:	Clay	Date:	01/21/09

LIQUID LIMIT DETERMINATION Method A (Multipoint)

Can No.	1	2	3	4	
Wet Wt + Tare (g)	30.07	54.2	56.18	63.29	
Dry Wt + Tare (g)	19.86	43.04	44.7	48.56	
Tare Wt (g)	0.98	22.49	23.43	22.17	
Moisture Content (%)	54.08	54.31	53.97	55.82	
No. of Blows	25	26	28	24	
Limit Limit (LL) - *Method B*	54	55	55	56	

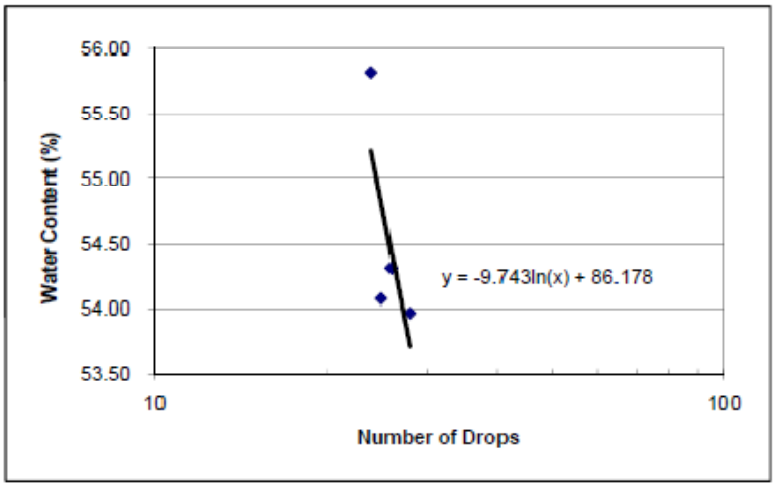

Liquid Limit =	54
Plastic Limit =	18
Plasticity Index =	36

Estimated % of Mat. Retained on the No. 40 Sieve _____

PLASTIC LIMIT DETERMINATION

Can No.	PL1	PL2		
Wet Wt + Tare (g)	28.88	28.91		
Dry Wt + Tare (g)	27.82	27.87		
Tare Wt (g)	21.96	22.2		
Wt. of Dry Soil (g)	5.86	5.67	0	0
Wt. of Water (g)	1.06	1.04	0	0
Trial Plastic Limit	*18.1*	*18.3*		
PLASTIC LIMIT (PL)	18.2			

Date Tested: 01/21/09 Tested by: MB

Project Name:	Midwest Levees	Boring No.:	S8B33
Location:	Two Rivers	Depth:	15'
Description:	Clay	Date:	01/21/09

LIQUID LIMIT DETERMINATION Method A (Multipoint)

Can No.	1	2	3	4	
Wet Wt + Tare (g)	48.91	49.13	54.27	32.47	
Dry Wt + Tare (g)	40.03	40.15	43.72	22.18	
Tare Wt (g)	22.44	22.21	22.57	1.04	
Moisture Content (%)	50.48	50.06	49.88	48.68	
No. of Blows	19	23	21	26	
Limit Limit (LL) - *Method B*	49	50	49	49	

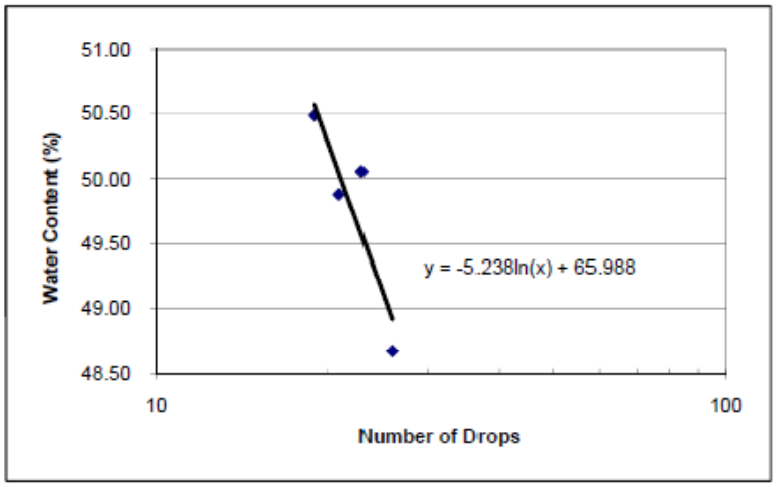

Liquid Limit = 50

Plastic Limit = 23

Plasticity Index = 27

Estimated % of Mat. Retained on the No. 40 Sieve

PLASTIC LIMIT DETERMINATION

Can No.	PL1	PL2		
Wet Wt + Tare (g)	28.06	28.28		
Dry Wt + Tare (g)	26.91	27.13		
Tare Wt (g)	21.97	22.11		
Wt. of Dry Soil (g)	4.94	5.02	0	0
Wt. of Water (g)	1.15	1.15	0	0
Trial Plastic Limit	*23.3*	*22.9*		
PLASTIC LIMIT (PL)	23.1			

Date Tested: 01/21/09 Tested by: MB

Project Name:	Midwest Levees	Boring No.:	S8B35
Location:	Two Rivers	Depth:	128", hand augered
Description:	Clay-very sandy	Date:	01/21/09

LIQUID LIMIT DETERMINATION Method A (Multipoint)

Can No.	1	2	3	4	
Wet Wt + Tare (g)	29.77	31.03	41.6	37.77	
Dry Wt + Tare (g)	23.26	24.4	32.76	29.5	
Tare Wt (g)	1.01	0.99	0.99	0.99	
Moisture Content (%)	29.26	28.32	27.82	29.01	
No. of Blows	18	25	28	26	
Limit Limit (LL) - *Method B*	28	28	28	29	

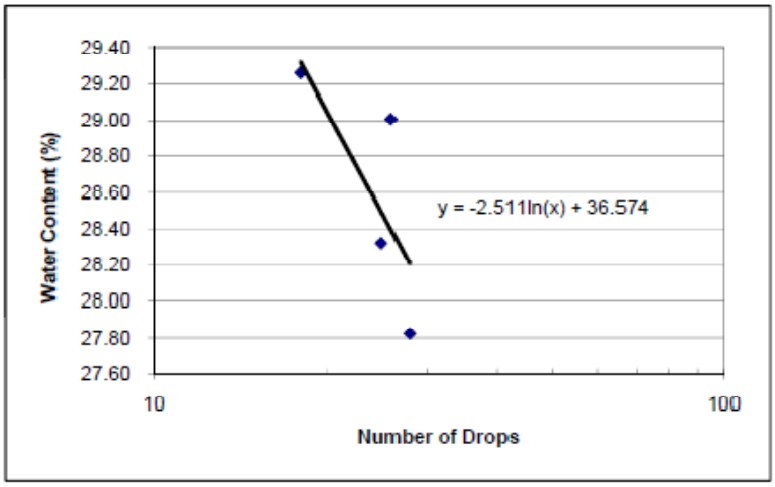

Liquid Limit =	28
Plastic Limit =	18
Plasticity Index =	10

Estimated % of Mat. Retained on the No. 40 Sieve _____

PLASTIC LIMIT DETERMINATION

Can No.	PL1	PL2		
Wet Wt + Tare (g)	46.36	40.85		
Dry Wt + Tare (g)	44.11	39.8		
Tare Wt (g)	31.4	34.3		
Wt. of Dry Soil (g)	12.71	5.5	0	0
Wt. of Water (g)	2.25	1.05	0	0
Trial Plastic Limit	*17.7*	*19.1*		
PLASTIC LIMIT (PL)	18.4			

Date Tested: 01/21/09 Tested by: MB

APPENDIX 5. COMPACTION CURVES

ASTM D 1557

Modified Proctor Calibration Test

COMPACTION TEST

Project: Midwest Levees **Site:** Winfield-Pin Oak

Sample No.: S1Bulk2

Method of Test:

☐ Standard ASTM D-698
☐ Method A ☐ Method B ☐ Method C

☑ Modified ASTM D-1557
☑ Method A ☐ Method B ☐ Method C
☐ Small Volume Version

☐ Tex-114-E ☐ Part I ☐ Part II

Sieve Size	Est. % Ret.
7/8-in.	
3/4-in.	
3/8-in.	
1/4-in.	
No. 4	

Mold Diam.: ☑ 4-in. ☐ 6-in.
Mold Designation:

Mold Volume (cf): 0.0333
Rammer Type: ☑ Manual ☐ Mechanical

Hammer Wt.: ☐ 5.5-lbs ☑ 10-lbs
No. of Layers: ☐ 3 ☐ 5 ☑ other
Blows/Layer: ☑ 25 ☐ 56 ☐ other
Prep. Method: ☐ wet ☑ dry

Oversize Corr. Needed: ☐ yes ☑ no

Mold + wet soil (g)	4356.75	4423.44	4345.66	4469.76	4377.11	4444.98	
Mold tare (g)	2384.23	2384.23	2384.23	2384.23	2384.23	2385.23	
Wet soil (g)	1972.52	2039.21	1961.43	2085.53	1992.88	2059.75	
Wet unit weight (pcf)	130.46	134.87	129.72	137.93	131.80	136.23	
Target Water (%)	11	15	18	13	10	12	
Water Added (%)	4	8	11	6	3	5	
Tin no.	1	2	3	5	4	6	
Tin + wet soil (g)	49.74	42.30	47.94	46.60	47.67	45.54	
Tin + dry soil (g)	46.98	39.67	43.88	43.83	45.18	43.30	
Weight of water	2.76	2.63	4.06	2.77	2.49	2.24	
Tin weight (g)	22.45	22.16	22.11	22.35	22.33	23.53	
Dry soil (g)	24.53	17.51	21.77	21.48	22.85	19.77	
Water content (%)	11.25	15.02	18.65	12.90	10.90	11.33	
Dry unit weight	117.26	117.26	109.33	122.18	118.85	122.36	
Dry unit weight (kN/m^3)	18.43	18.43	17.18	19.20	18.68	19.23	
Dry Density (kg/m^3)	1878.38	1878.27	1751.36	1957.08	1903.84	1960.06	

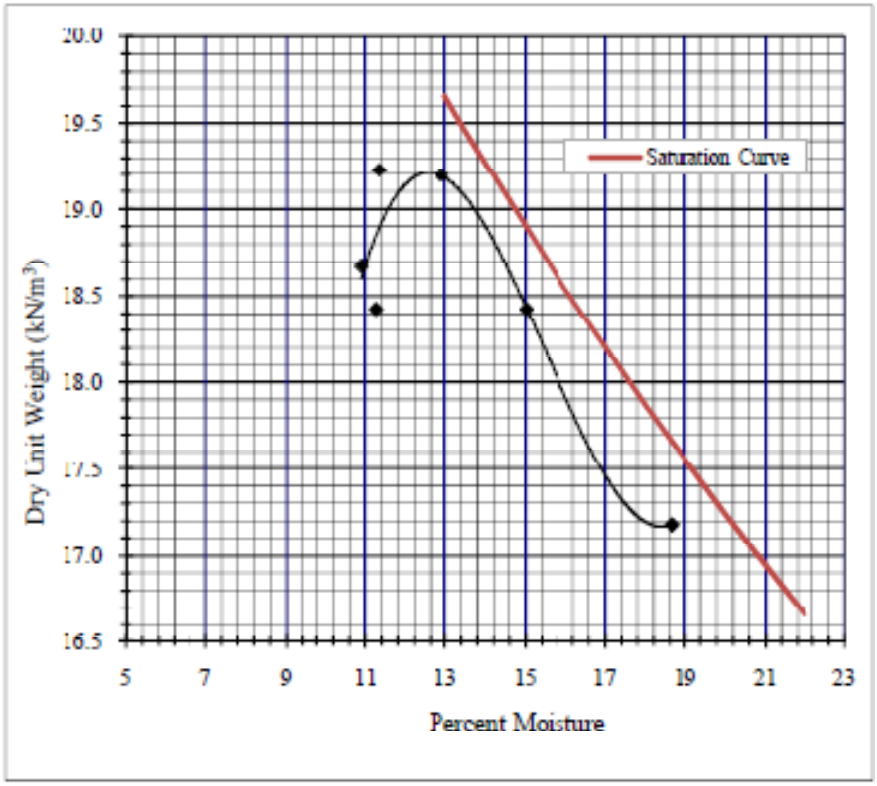

Max Density = 1957.19 Max Unit Weight = 19.2

Wopt = 12.5

Saturation Curve S.G. = 2.71

Water content (%)	Dry unit weight (kN/m^3)
13.00	19.66
13.50	19.46
14.00	19.27
16.00	18.54
18.00	17.87
20.00	17.24
22.00	16.66

COMPACTION TEST

Project: Midwest Levees **Site:** Winfield-Pin Oak

Modified Proctor - Small Volume Mold **Sample No.:** S1Bulk2

Method of Test:

☐ Standard ASTM D-698
☐ Method A ☐ Method B ☐ Method C

☑ Modified ASTM D-1557
☐ Method A ☐ Method B ☐ Method C
☑ Customized Small Volume Version

☐ Tex-114-E ☐ Part I ☐ Part II

Sieve Size	Est. % Ret.
7/8-in.	
3/4-in.	
3/8-in.	
1/4-in.	
No. 4	

Mold Diam.: ☑ 4-in. ☐ 6-in.
Mold Designation:

Mold Volume (cf): 0.0080
Rammer Type: ☑ Manual ☐ Mechanical

Hammer Wt.: ☐ 5.5-lbs ☑ 10-lbs
No. of Layers: ☐ 3 ☐ 5 ☑ other
Blows/Layer: ☐ 25 ☐ 56 ☑ other
Prep. Method: ☐ wet ☑ dry

Oversize Corr. Needed: ☐ yes ☑ no

Mold + wet soil (g)	652.89	667.55	651.15	701.52	676.19	693.94	
Mold tare (g)	199.18	199.18	199.18	199.18	199.18	199.18	
Wet soil (g)	453.71	468.37	451.97	502.34	477.01	494.76	
Wet unit weight (pcf)	125.03	129.07	124.55	138.43	131.45	136.34	
Target water %	11	14	18	13	10	12	
Water Added (%)	4	7	11	6	3	5	
Tin no.	A	B	C	D	E	F	
Tin + wet soil (g)	47.05	46.68	47.42	41.19	49.19	51.24	
Tin + dry soil (g)	44.73	43.51	43.41	39.00	46.68	48.10	
Weight of water (g)	2.32	3.17	4.01	2.19	2.51	3.14	
Tin weight (g)	21.95	22.21	22.26	22.41	22.44	22.00	
Dry soil (g)	22.78	21.30	21.15	16.59	24.24	26.10	
Water content (%)	10.18	14.88	18.96	13.20	10.35	12.03	
Dry unit weight (pcf)	113.47	112.35	104.70	122.29	119.12	121.70	
Dry unit weight (kN/m^3)	17.83	17.65	16.45	19.22	18.72	19.12	
Dry Density (kg/m^3)	1817.67	1799.67	1677.13	1958.87	1908.07	1949.47	

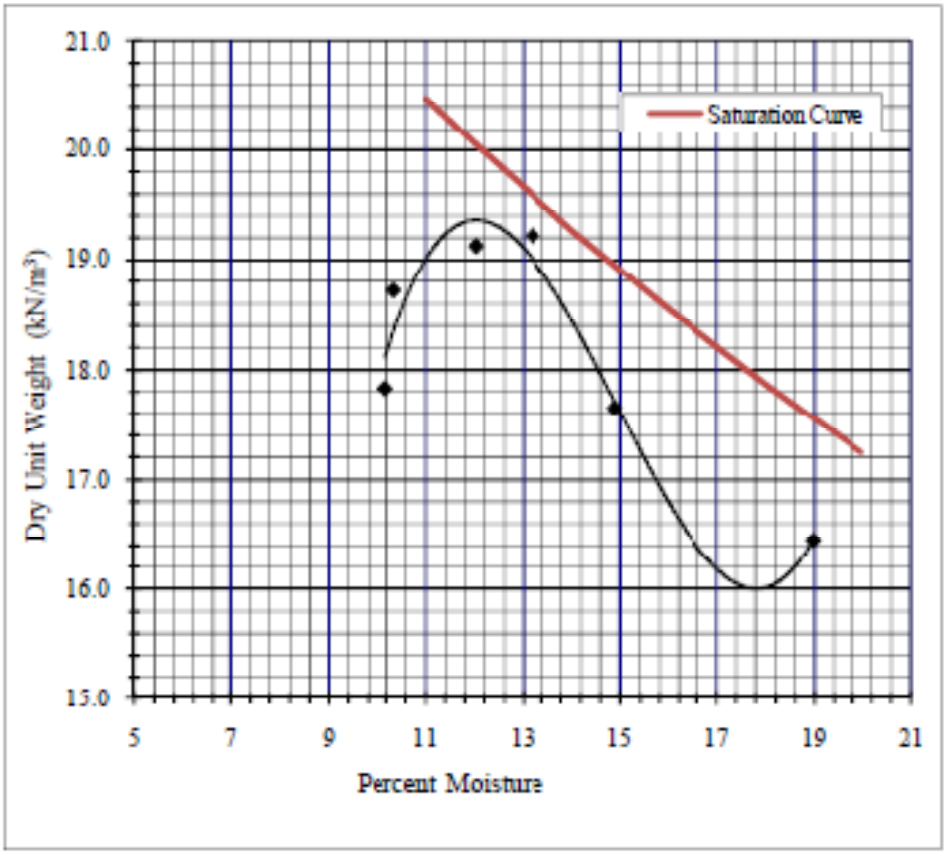

Max Density = 1977.57 Max Unit Weight = 19.4

Wopt – 12

Saturation Curve S.G. = 2.71

Water content (%)	Dry unit weight (kN/m³)
11.00	20.48
12.00	20.06
14.00	19.27
16.00	18.54
18.00	17.87
19.00	17.55
20.00	17.24

COMPACTION TEST

Project: Midwest Levees **Site:** Kickapoo

Modified Proctor - Small Volume Mold **Sample No.:** S1B4

Method of Test:

☐ Standard ASTM D-698
☐ Method A ☐ Method B ☐ Method C

☑ Modified ASTM D-1557
☐ Method A ☐ Method B ☐ Method C
☑ Customized Small Volume Version

☐ Tex-114-E ☐ Part I ☐ Part II

Sieve Size	Est. % Ret.
7/8-in.	
3/4-in.	
3/8-in.	
1/4-in.	
No. 4	

Mold Diam.: ☑ 4-in. ☐ 6-in.
Mold Designation:

Mold Volume (cf): 0.0080
Rammer Type: ☑ Manual ☐ Mechanical

Hammer Wt.: ☐ 5.5-lbs ☑ 10-lbs
No. of Layers: ☐ 3 ☐ 5 ☑ other
Blows/Layer: ☐ 25 ☐ 56 ☑ other
Prep. Method: ☐ wet ☑ dry

Oversize Corr. Needed: ☐ yes ☑ no

Mold + wet soil (g)	650.35	675.4	702.71	688.44	698.84		
Mold tare (g)	199.18	199.18	199.18	199.18	199.18		
Wet soil (g)	451.17	476.22	503.53	489.26	499.66		
Wet unit weight (pcf)	124.33	131.23	138.76	134.83	137.69		
Target water %	7	9	11	14	13		
Water Added (%)	5	7	9	12	11		
Tin no.	1	2	3	4	5		
Tin + wet soil (g)	9.69	9.53	8.72	9.42	12.23		
Tin + dry soil (g)	9.12	8.83	7.92	8.37	10.97		
Weight of water (g)	0.57	0.70	0.80	1.05	1.26		
Tin weight (g)	1.00	0.99	1.00	0.98	1.01		
Dry soil (g)	8.12	7.84	6.92	7.39	9.96		
Water content (%)	7.02	8.93	11.56	14.21	12.65		
Dry unit weight (pcf)	116.18	120.48	124.38	118.05	122.23		
Dry unit weight (kN/m^3)	18.26	18.93	19.55	18.55	19.21		
Dry Density (kg/m^3)	1860.95	1929.85	1992.38	1891.03	1957.94		

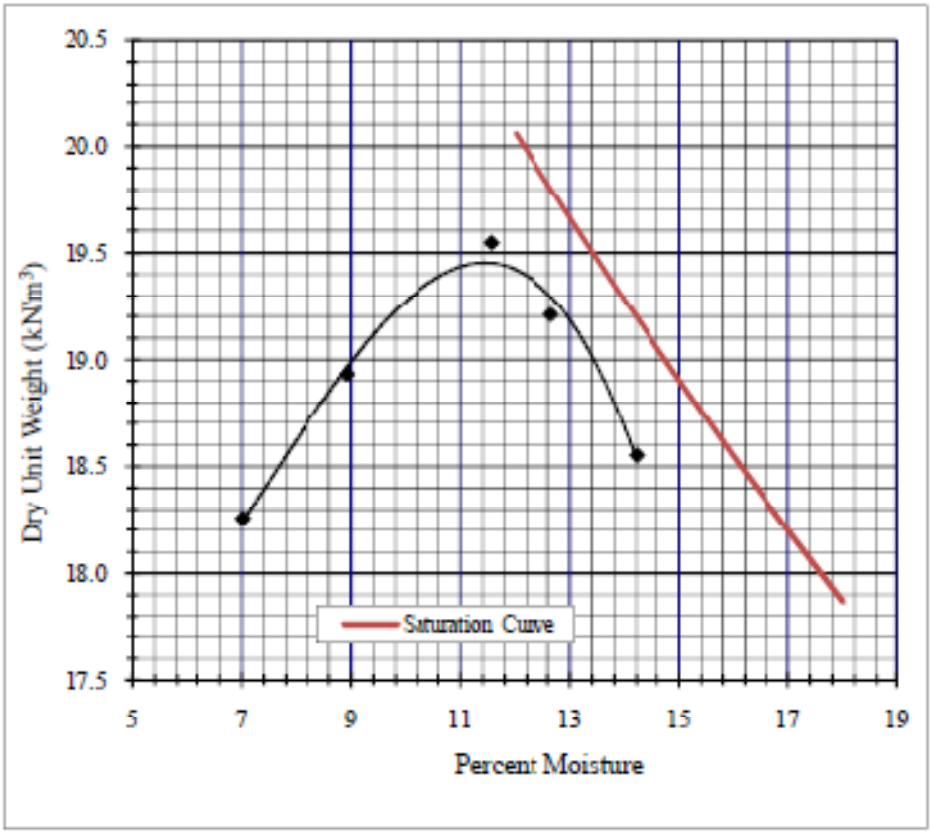

Max Density = 1987.77 Max Unit Weight = 19.5

Wopt = 11.4

Saturation Curve S.G. = 2.71

Water content (%)	Dry unit weight (kN/m^3)
12.00	20.06
13.00	19.66
14.00	19.27
15.00	18.90
16.00	18.54
17.00	18.20
18.00	17.87

COMPACTION TEST

Project: Midwest Levees **Site:** Kickapoo

Modified Proctor - Small Volume Mold **Sample No.:** S2B6

Method of Test:

☐ Standard ASTM D-698
☐ Method A ☐ Method B ☐ Method C

☑ Modified ASTM D-1557
☐ Method A ☐ Method B ☐ Method C
☑ Customized Small Volume Version

☐ Tex-114-E ☐ Part I ☐ Part II

Sieve Size	Est. % Ret.
7/8-in.	
3/4-in.	
3/8-in.	
1/4-in.	
No. 4	

Mold Diam.: ☑ 8-in. ☐ 6-in.
Mold Designation:

Mold Volume (cf): 0.0080
Rammer Type: ☑ Manual ☐ Mechanical

Hammer Wt.: ☐ 5.5-lbs ☑ 10-lbs
No. of Layers: ☐ 3 ☐ 5 ☑ other
Blows/Layer: ☐ 25 ☐ 56 ☑ other
Prep. Method: ☐ wet ☑ dry

Oversize Corr. Needed: ☐ yes ☑ no

Mold + wet soil (g)	692.3	625.83	687.14	696.26	672.95		
Mold tare (g)	199.18	199.18	199.18	199.18	199.18		
Wet soil (g)	493.12	426.65	487.96	497.08	473.77		
Wet unit weight (pcf)	135.89	117.57	134.47	136.98	130.56		
Target water %	18	12	14	18	20		
Water Added (%)	16	10	12	16	18		
Tin no.	A	B	C	D	E		
Tin + wet soil (g)	36.80	33.84	36.20	37.11	39.46		
Tin + dry soil (g)	34.60	32.47	34.30	35.02	36.43		
Weight of water (g)	2.20	1.37	1.90	2.09	3.03		
Tin weight (g)	22.12	22.03	22.13	22.40	22.43		
Dry soil (g)	12.48	10.44	12.17	12.62	14.00		
Water content (%)	17.63	13.12	15.61	16.56	21.54		
Dry unit weight (pcf)	115.53	103.93	116.31	117.52	107.33		
Dry unit weight (kN/m^3)	18.15	16.33	18.28	18.47	16.87		
Dry Density (kg/m^3)	1850.54	1664.87	1863.11	1882.48	1719.25		

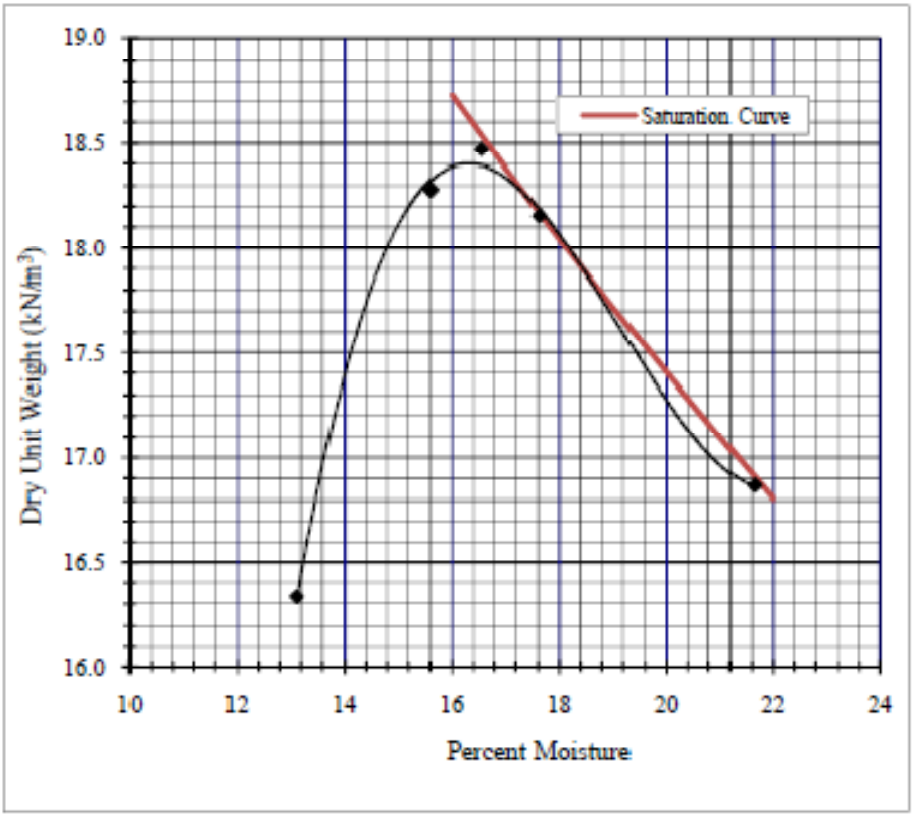

Max Density = 1875.64 Max Unit Weight = 18.4

Wopt = 16.4

Saturation Curve S.G. = 2.75

Water content (%)	Dry unit weight (kN/m^3)
16.00	18.73
17.00	18.38
18.00	18.05
19.00	17.72
20.00	17.40
21.00	17.10
22.00	16.81

COMPACTION TEST

Project: Midwest Levees **Site:** Kickapoo

Modified Proctor - Small Volume Mold **Sample No.:** S2B9

Method of Test:

☐ Standard ASTM D-698
☐ Method A ☐ Method B ☐ Method C

☑ Modified ASTM D-1557
☐ Method A ☐ Method B ☐ Method C
☑ Customized Small Volume Version

☐ Tex-114-E ☐ Part I ☐ Part II

Sieve Size	Est. % Ret.
7/8-in.	
3/4-in.	
3/8-in.	
1/4-in.	
No. 4	

Mold Diam.: ☑ 4-in. ☐ 6-in.
Mold Designation:

Mold Volume (cf): 0.0080
Rammer Type: ☑ Manual ☐ Mechanical

Hammer Wt.: ☐ 5.5-lbs ☑ 10-lbs
No. of Layers: ☐ 3 ☐ 5 ☑ other
Blows/Layer: ☐ 25 ☐ 56 ☑ other
Prep. Method: ☐ wet ☑ dry

Oversize Corr. Needed: ☐ yes ☑ no

Mold + wet soil (g)	660.07	633.52	671.7	661.99	620.18	654.06	
Mold tare (g)	199.18	199.18	199.18	199.18	199.18	199.18	
Wet soil (g)	460.89	434.34	472.52	462.81	421	454.88	
Wet unit weight (pcf)	127.01	119.69	130.21	127.54	116.02	125.35	
Target water %	20	16	22	18	15	23	
Water Added (%)	18	14	20	16	13	21	
Tin no.	2	1	3	4	5	6	
Tin + wet soil (g)	34.22	30.23	32.85	34.57	33.80	35.83	
Tin + dry soil (g)	32.15	29.12	30.97	32.64	32.30	33.53	
Weight of water (g)	2.07	1.11	1.88	1.93	1.50	2.30	
Tin weight (g)	22.20	22.46	22.15	22.33	22.35	23.55	
Dry soil (g)	9.95	6.66	8.82	10.31	9.95	9.98	
Water content (%)	20.80	16.67	21.32	18.72	15.08	23.05	
Dry unit weight (pcf)	105.14	102.59	107.34	107.43	100.82	101.87	
Dry unit weight (kN/m^3)	16.52	16.12	16.87	16.88	15.84	16.01	
Dry Density (kg/m^3)	1684.12	1643.39	1719.34	1720.83	1614.94	1631.87	

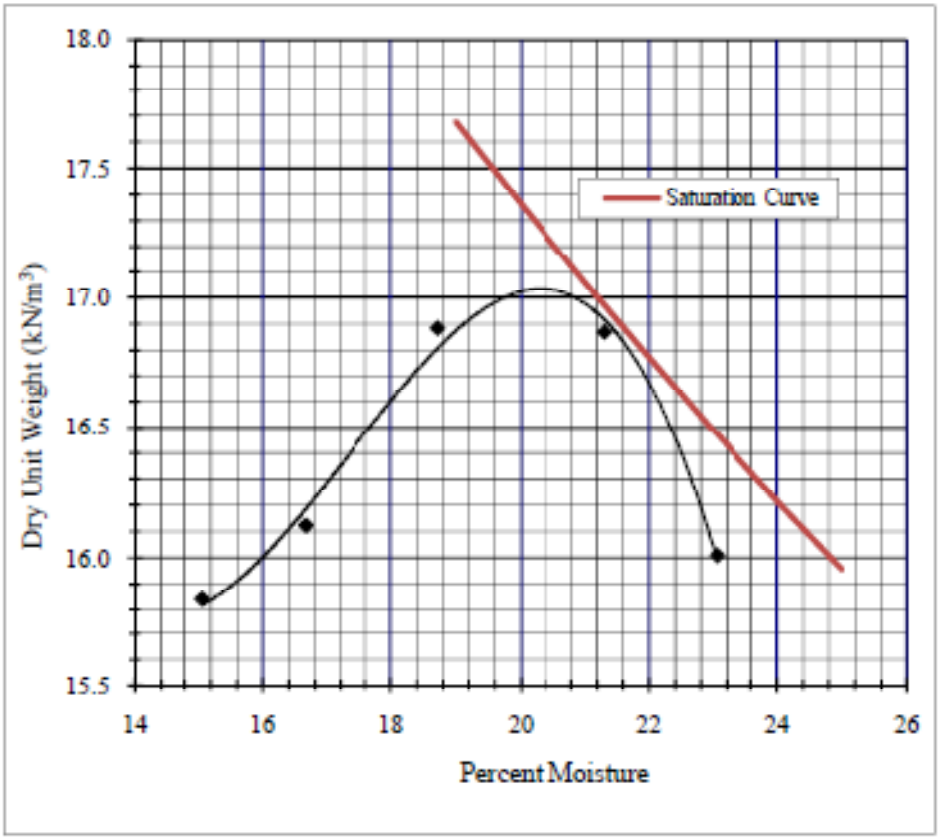

Max Density = 1732.93 Max Unit Weight = 17

Wopt = 20.1

Saturation Curve S.G. = 2.74

Water content (%)	Dry unit weight (kN/m^3)
19.00	17.68
20.00	17.36
21.00	17.06
22.00	16.77
23.00	16.49
24.00	16.22
25.00	15.95

COMPACTION TEST

Project: Midwest Levees **Site:** Norton Woods

Modified Proctor - Small Volume Mold **Sample No.:** S3B12

Method of Test:

☐ Standard ASTM D-698
☐ Method A ☐ Method B ☐ Method C

☑ Modified ASTM D-1557
☐ Method A ☐ Method B ☐ Method C
☑ Customized Small Volume Version

☐ Tex-114-E ☐ Part I ☐ Part II

Sieve Size	Est. % Ret.
7/8-in.	
3/4-in.	
3/8-in.	
1/4-in.	
No. 4	

Mold Diam.: ☑ 8-in. ☐ 6-in.
Mold Designation:

Mold Volume (cf): 0.0080
Rammer Type: ☑ Manual ☐ Mechanical

Hammer Wt.: ☐ 5.5-lbs ☑ 10-lbs
No. of Layers: ☐ 3 ☐ 5 ☑ other
Blows/Layer: ☐ 25 ☐ 56 ☑ other
Prep. Method: ☐ wet ☑ dry

Oversize Corr. Needed: ☐ yes ☑ no

Mold + wet soil (g)	595.92	648.61	670.01	676.73	672.76	682.07	672.69
Mold tare (g)	199.18	199.18	199.18	199.18	199.18	199.18	199.18
Wet soil (g)	396.74	449.43	470.83	477.55	473.58	482.89	473.51
Wet unit weight (pcf)	109.33	123.85	129.75	131.60	130.51	133.07	130.49
Target water %	10	12	16	18	15	18	21
Water Added (%)	6	8	12	14	11	14	17
Tin no.	1	2	4	5	F	E	5
Tin + wet soil (g)	42.91	49.34	43.84	46.85	38.64	39.79	41.48
Tin + dry soil (g)	40.77	46.21	40.66	42.99	36.40	37.18	38.23
Weight of water (g)	2.14	3.13	3.18	3.86	2.24	2.61	3.25
Tin weight (g)	22.45	22.18	22.35	22.33	22.03	22.44	22.37
Dry soil (g)	18.32	24.03	18.31	20.66	14.37	14.74	15.86
Water content (%)	11.68	13.03	17.37	18.68	15.59	17.71	20.49
Dry unit weight (pcf)	97.90	109.58	110.55	110.88	112.91	113.05	108.30
Dry unit weight (kN/m^3)	15.38	17.22	17.37	17.42	17.74	17.77	17.02
Dry Density (kg/m^3)	1568.14	1755.27	1770.82	1776.18	1808.58	1810.94	1734.72

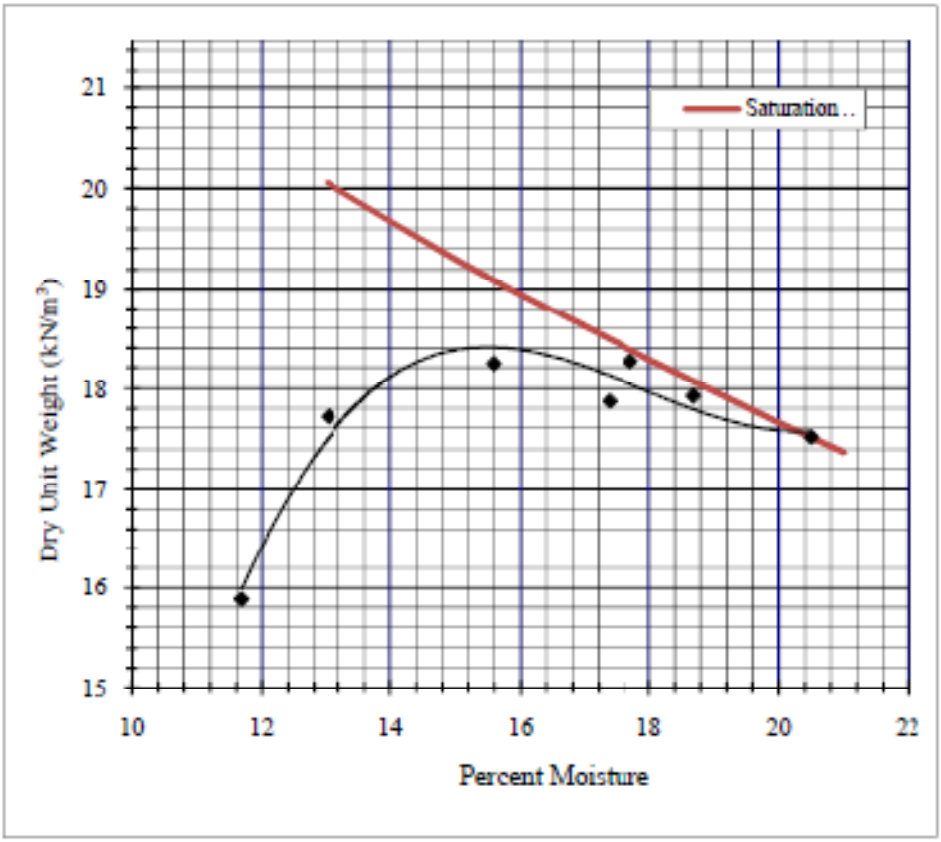

Max Density = 1875.64 Max Unit Weight = 18.4

Wopt = 15.6

Saturation Curve S.G. = 2.69

Water content (%)	Dry unit weight (kN/m³)
13.00	19.55
14.00	19.17
15.00	18.80
16.00	18.45
18.00	17.78
20.00	17.16
21.00	16.86

COMPACTION TEST

Project: Midwest Levees **Site:** Kickapoo

Modified Proctor - Small Volume Mold **Sample No.:** S4B18

Method of Test:

☐ Standard ASTM D-698
☐ Method A ☐ Method B ☐ Method C

☑ Modified ASTM D-1557
☐ Method A ☐ Method B ☐ Method C
☑ Customized Small Volume Version

☐ Tex-114-E ☐ Part I ☐ Part II

Sieve Size	Est. % Ret.
7/8-in.	
3/4-in.	
3/8-in.	
1/4-in.	
No. 4	

Mold Diam.: ☑ 8-in. ☐ 6-in.
Mold Designation:

Mold Volume (cf): 0.0080
Rammer Type: ☑ Manual ☐ Mechanical

Hammer Wt.: ☐ 5.5-lbs ☑ 10-lbs
No. of Layers: ☐ 3 ☐ 5 ☑ other
Blows/Layer: ☐ 25 ☐ 56 ☑ other
Prep. Method: ☐ wet ☑ dry

Oversize Corr. Needed: ☐ yes ☑ no

Mold + wet soil (g)	644.09	675.38	670.02	674.18	671.74		
Mold tare (g)	199.18	199.18	199.18	199.18	199.18		
Wet soil (g)	444.91	476.2	470.84	475	472.56		
Wet unit weight (pcf)	122.61	131.23	129.75	130.90	130.22		
Target water %	12	16	14	18	20		
Water Added (%)	10	14	12	16	18		
Tin no.	A	B	6	D	E		
Tin + wet soil (g)	38.74	42.12	36.44	32.56	32.25		
Tin + dry soil (g)	36.77	39.28	34.71	31.04	30.72		
Weight of water (g)	1.97	2.84	1.73	1.52	1.53		
Tin weight (g)	22.12	22.04	23.56	22.39	22.44		
Dry soil (g)	14.65	17.24	11.15	8.65	8.28		
Water content (%)	13.45	16.47	15.52	17.57	18.48		
Dry unit weight (pcf)	108.07	112.67	112.32	111.33	109.91		
Dry unit weight (kN/m^3)	16.98	17.70	17.65	17.50	17.27		
Dry Density (kg/m^3)	1731.16	1804.77	1799.24	1783.39	1760.66		

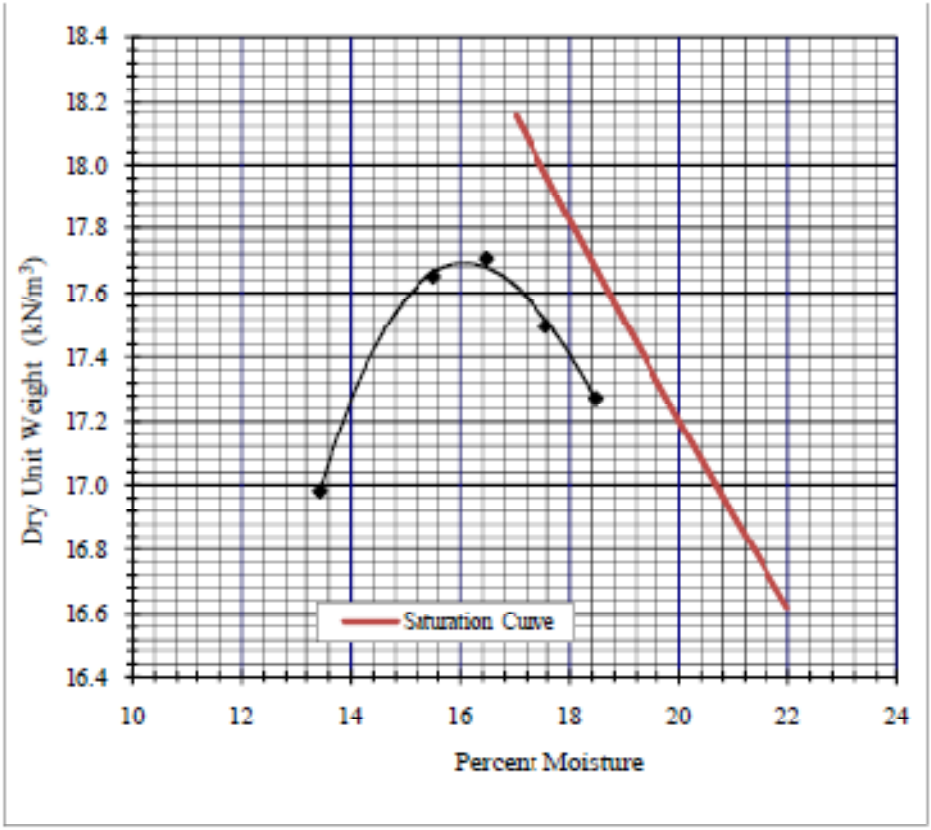

Max Density = 1804.28 Max Unit Weight = 17.7

Wopt = 16

Saturation Curve S.G. = 2.70

Water content (%)	Dry unit weight (kN/m^3)
17.00	18.15
18.00	17.82
19.00	17.51
20.00	17.20
21.00	16.90
22.00	16.62

COMPACTION TEST

Project: Midwest Levees **Site:** Kickapoo

Modified Proctor - Small Volume Mold **Sample No.:** S5B21

Method of Test:

☐ Standard ASTM D-698
☐ Method A ☐ Method B ☐ Method C

☑ Modified ASTM D-1557
☐ Method A ☐ Method B ☐ Method C
☑ Customized Small Volume Version

☐ Tex-114-E ☐ Part I ☐ Part II

Sieve Size	Est. % Ret.
7/8-in.	
3/4-in.	
3/8-in.	
1/4-in.	
No. 4	

Mold Diam.: ☑ 8-in. ☐ 6-in.
Mold Designation:
Mold Volume (cf): 0.0080
Rammer Type: ☑ Manual ☐ Mechanical

Hammer Wt.: ☐ 5.5-lbs ☑ 10-lbs
No. of Layers: ☐ 3 ☐ 5 ☑ other
Blows/Layer: ☐ 25 ☐ 56 ☑ other
Prep. Method: ☐ wet ☑ dry

Oversize Corr. Needed: ☐ yes ☑ no

Mold + wet soil (g)	652.03	681.1	694.35	672.13	678.91		
Mold tare (g)	199.18	199.18	199.18	199.18	199.18		
Wet soil (g)	452.85	481.92	495.17	472.95	479.73		
Wet unit weight (pcf)	124.79	132.80	136.46	130.33	132.20		
Target water %	11	13	15	17	16		
Water Added (%)	9	11	13	15	14		
Tin no.	A	B	C	D	E		
Tin + wet soil (g)	33.67	36.85	37.56	36.03	40.16		
Tin + dry soil (g)	32.44	35.05	35.58	34.00	37.52		
Weight of water (g)	1.23	1.80	1.98	2.03	2.64		
Tin weight (g)	22.10	22.04	22.11	22.33	22.45		
Dry soil (g)	10.34	13.01	13.47	11.67	15.07		
Water content (%)	11.90	13.84	14.70	17.40	17.52		
Dry unit weight (pcf)	111.53	116.66	118.97	111.02	112.49		
Dry unit weight (kN/m^3)	17.53	18.33	18.69	17.45	17.68		
Dry Density (kg/m^3)	1786.48	1868.77	1905.69	1778.37	1801.98		

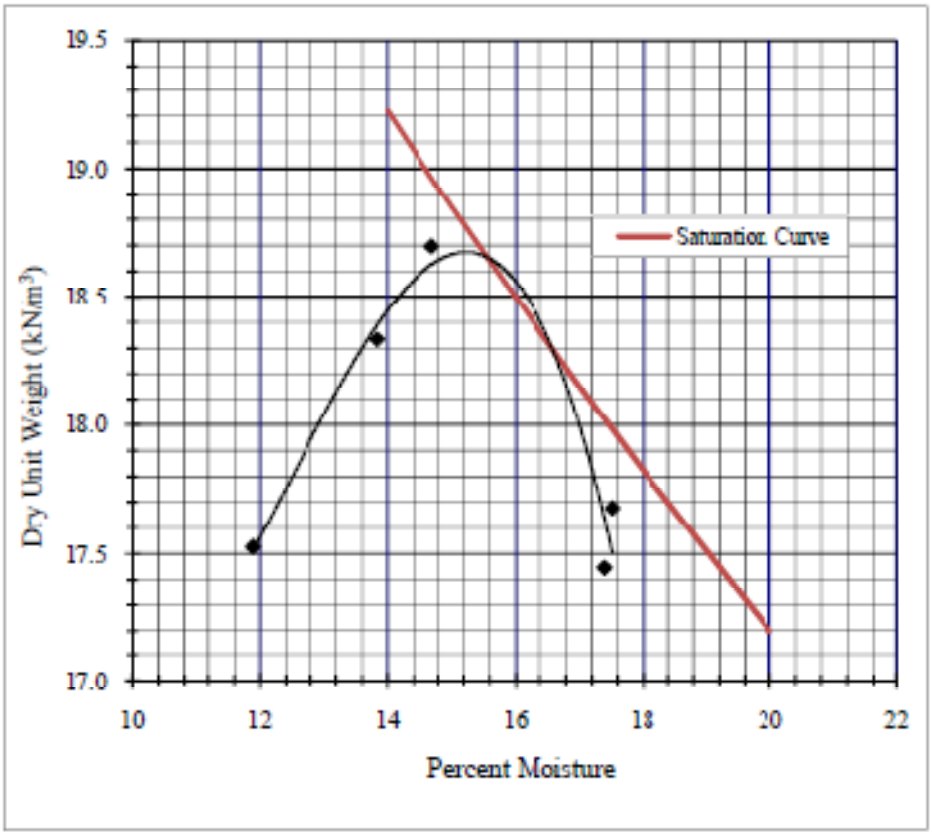

Max Density = 1906.22 Max Unit Weight = 18.7

Wopt = 15.2

Saturation Curve S.G. = 2.70

Water content (%)	Dry unit weight (kN/m^3)
14.00	19.22
15.00	18.85
16.00	18.50
17.00	18.15
18.00	17.82
18.00	17.82
20.00	17.20

COMPACTION TEST

Project: Midwest Levees **Site:** Norton Woods

Modified Proctor - Small Volume Mold **Sample No.:** S5B23

Method of Test:

☐ Standard ASTM D-698
☐ Method A ☐ Method B ☐ Method C

☑ Modified ASTM D-1557
☐ Method A ☐ Method B ☐ Method C
☑ Customized Small Volume Version

☐ Tex-114-E ☐ Part I ☐ Part II

Sieve Size	Est. % Ret.
7/8-in.	
3/4-in.	
3/8-in.	
1/4-in.	
No. 4	

Mold Diam.: ☑ 4-in. ☐ 6-in.
Mold Designation:

Mold Volume (cf): 0.0080
Rammer Type: ☑ Manual ☐ Mechanical

Hammer Wt.: ☐ 5.5-lbs ☑ 10-lbs
No. of Layers: ☐ 3 ☐ 5 ☑ other
Blows/Layer: ☐ 25 ☐ 56 ☑ other
Prep. Method: ☐ wet ☑ dry

Oversize Corr. Needed: ☐ yes ☑ no

Mold + wet soil (g)	650.58	649.71	615.61	631.52	631.19	650.82	
Mold tare (g)	199.18	199.18	199.18	199.18	199.18	199.18	
Wet soil (g)	451.4	450.53	416.43	432.34	432.01	451.64	
Wet unit weight (pcf)	124.39	124.15	114.76	119.14	119.05	124.46	
Target water %	19	17	12	13	15	22	
Water Added (%)	17	15	10	11	13	20	
Tin no.	A	B	C	D	E	F	
Tin + wet soil (g)	43.15	46.91	44.72	37.13	42.24	41.14	
Tin + dry soil (g)	39.77	43.27	42.05	35.25	39.63	37.41	
Weight of water (g)	3.38	3.64	2.67	1.88	2.61	3.73	
Tin weight (g)	22.11	22.05	22.20	22.41	22.41	22.02	
Dry soil (g)	17.66	21.22	19.85	12.84	17.22	15.39	
Water content (%)	19.14	17.15	13.45	14.64	15.16	24.24	
Dry unit weight (pcf)	104.41	105.98	101.15	103.92	103.38	100.18	
Dry unit weight (kN/m^3)	16.41	16.65	15.90	16.33	16.25	15.74	
Dry Density (kg/m^3)	1672.49	1697.56	1620.29	1664.72	1656.01	1604.73	

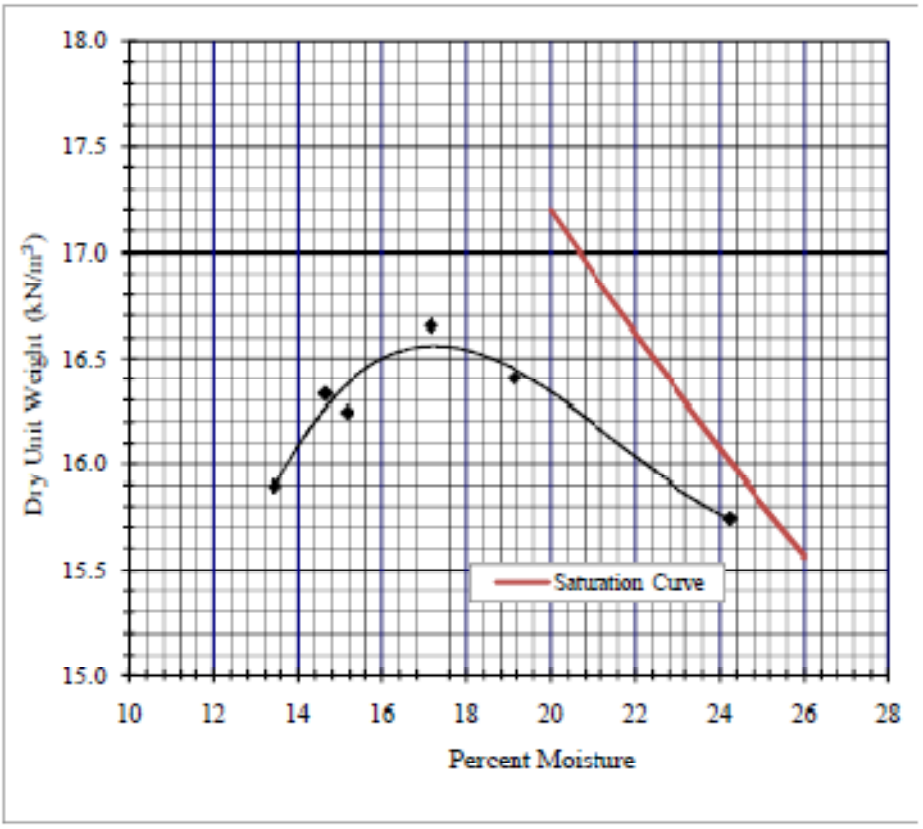

Max Density = 1692.15 Max Unit Weight = 16.6

Wopt = 17

Saturation Curve S.G. = 2.70

Water content (%)	Dry unit weight (kN/m^3)
20.00	17.20
21.00	16.90
22.00	16.62
24.00	16.07
25.00	15.81
26.00	15.56

COMPACTION TEST

Project: Midwest Levees **Site:** Kickapoo

Modified Proctor - Small Volume Mold **Sample No.:** S6B26

Method of Test:

☐ Standard ASTM D-698
☐ Method A ☐ Method B ☐ Method C

☑ Modified ASTM D-1557
☐ Method A ☐ Method B ☐ Method C
☑ Customized Small Volume Version

☐ Tex-114-E ☐ Part I ☐ Part II

Sieve Size	Est. % Ret.
7/8-in.	
3/4-in.	
3/8-in.	
1/4-in.	
No. 4	

Mold Diam.: ☑ 8-in. ☐ 6-in.
Mold Designation:

Mold Volume (cf): 0.0080
Rammer Type: ☑ Manual ☐ Mechanical

Hammer Wt.: ☐ 5.5-lbs ☑ 10-lbs
No. of Layers: ☐ 3 ☐ 5 ☑ other
Blows/Layer: ☐ 25 ☐ 56 ☑ other
Prep. Method: ☐ wet ☑ dry

Oversize Corr. Needed: ☐ yes ☑ no

Mold + wet soil (g)	667.15	652.65	683.47	662.98	681.14		
Mold tare (g)	199.18	199.18	199.18	199.18	199.18		
Wet soil (g)	467.97	453.47	484.29	463.8	481.96		
Wet unit weight (pcf)	128.96	124.96	133.46	127.81	132.82		
Target water %	16	14	18	21	19		
Water Added (%)	14	12	16	19	17		
Tin no.	1	2	3	4	5		
Tin + wet soil (g)	34.81	32.95	37.10	36.41	41.84		
Tin + dry soil (g)	33.04	31.58	34.91	33.98	38.74		
Weight of water (g)	1.77	1.37	2.19	2.43	3.10		
Tin weight (g)	22.40	22.17	22.11	22.31	22.34		
Dry soil (g)	10.64	9.41	12.80	11.67	16.40		
Water content (%)	16.64	14.56	17.11	20.82	18.90		
Dry unit weight (pcf)	110.57	109.08	113.96	105.78	111.70		
Dry unit weight (kN/m^3)	17.37	17.14	17.91	16.62	17.55		
Dry Density (kg/m^3)	1771.11	1747.34	1825.46	1694.50	1789.28		

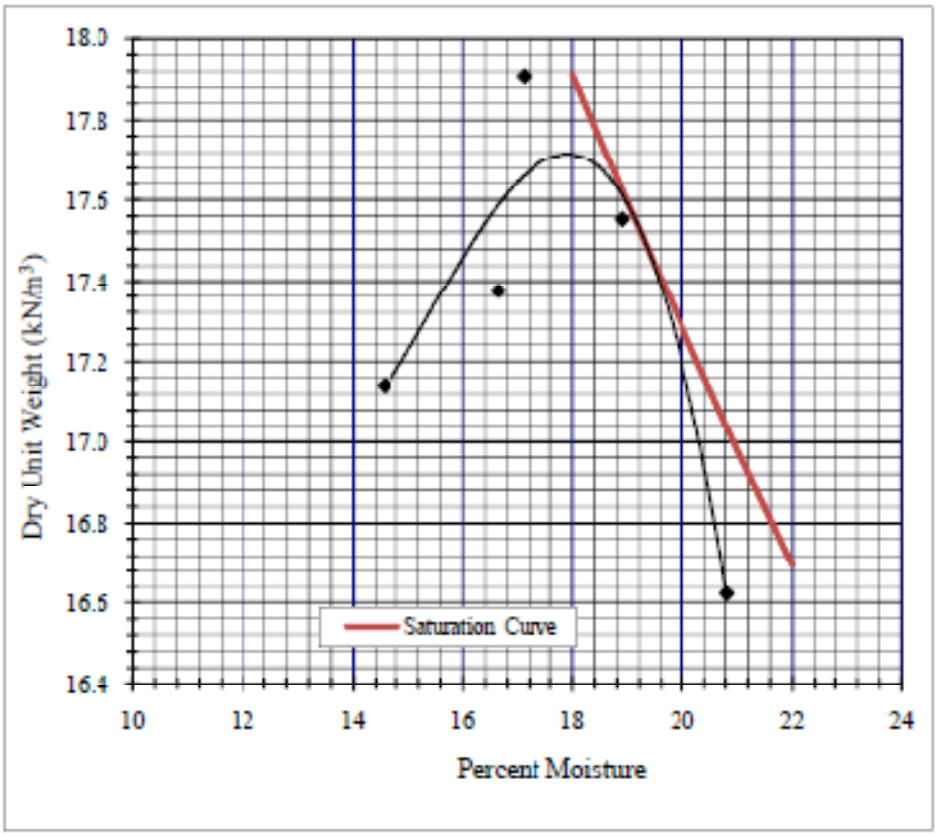

Max Density = 1804.28 Max Unit Weight = 17.7

Wopt = 18

Saturation Curve S.G. = 2.72

Water content (%)	Dry unit weight (kN/m³)
18.00	17.91
18.50	17.75
19.00	17.59
19.50	17.44
20.00	17.28
21.00	16.98
22.00	16.69

COMPACTION TEST

Project: Midwest Levees **Site:** Norton Woods

Modified Proctor - Small Volume Mold **Sample No.:** S7B29

Method of Test:

☐ Standard ASTM D-698
☐ Method A ☐ Method B ☐ Method C

☑ Modified ASTM D-1557
☐ Method A ☐ Method B ☐ Method C
☑ Customized Small Volume Version

☐ Tex-114-E ☐ Part I ☐ Part II

Sieve Size	Est. % Ret.
7/8-in.	
3/4-in.	
3/8-in.	
1/4-in.	
No. 4	

Mold Diam.: ☑ 6-in. ☐ 6-in.
Mold Designation:

Mold Volume (cf): 0.0080
Rammer Type: ☑ Manual ☐ Mechanical

Hammer Wt.: ☐ 5.5-lbs ☑ 10-lbs
No. of Layers: ☐ 3 ☐ 5 ☑ other
Blows/Layer: ☐ 25 ☐ 56 ☑ other
Prep. Method: ☐ wet ☑ dry

Oversize Corr. Needed: ☐ yes ☑ no

Mold + wet soil (g)	675.72	710.76	689.79	697.54	715.79		
Mold tare (g)	199.18	199.18	199.18	199.18	199.18		
Wet soil (g)	476.54	511.58	490.61	498.36	516.61		
Wet unit weight (pcf)	131.32	140.98	135.20	137.33	142.36		
Target water %	10	14	16	12	14		
Water Added (%)	8	12	14	10	12		
Tin no.	1	2	3	4	5		
Tin + wet soil (g)	41.98	43.07	42.16	54.87	41.75		
Tin + dry soil (g)	39.95	40.46	39.32	51.32	39.39		
Weight of water (g)	2.03	2.61	2.84	3.55	2.36		
Tin weight (g)	22.45	22.18	22.11	22.32	22.37		
Dry soil (g)	17.50	18.28	17.21	29.00	17.02		
Water content (%)	11.60	14.28	16.50	12.24	13.87		
Dry unit weight (pcf)	117.67	123.36	116.05	122.36	125.03		
Dry unit weight (kN/m^3)	18.49	19.39	18.24	19.23	19.65		
Dry Density (kg/m^3)	1884.92	1976.10	1858.92	1959.96	2002.75		

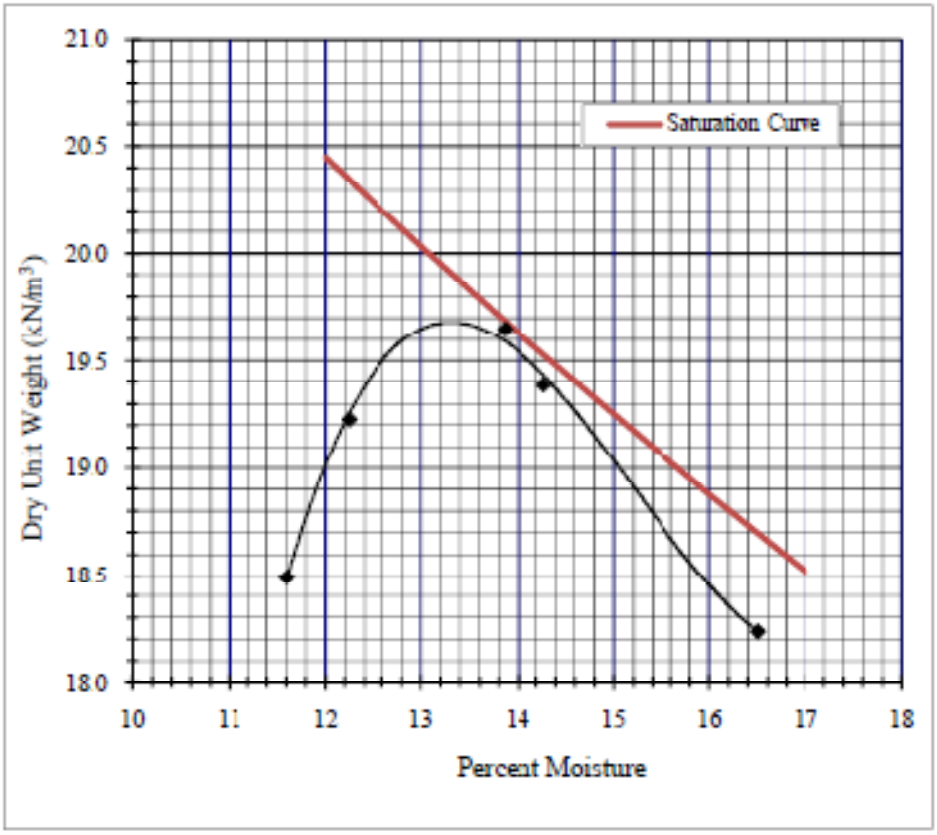

Max Density = 2008.15 Max Unit Weight = 19.7

Wopt = 13.2

Saturation Curve S.G. = 2.78

Water content (%)	Dry unit weight (kN/m^3)
12.00	20.45
13.00	20.03
14.00	19.63
16.00	18.88
17.00	18.52

APPENDIX 6. SPECIFIC GRAVITY

ASTM D 854

Pycnometer Calibration ASTM D854

Pycnometer Only		1	2	3	4	5
Reading	1	96.55	106.67	98.54	99.85	93.88
	2	96.56	106.68	98.55	99.86	93.87
	3	96.56	106.67	98.55	99.84	93.86
	4	96.57	106.67	98.55	99.84	93.87
	5	96.56	106.68	98.55	99.86	93.87
	Avg	96.56	106.67	98.55	99.85	93.87
	Std Dev	0.01	0.01	0.00	0.01	0.01

Temp	19.7
Density	0.99827

Pycnometer & Water		1	2	3	4	5
Reading	1	345.63	356.2	347.79	348.97	343.02
	2	345.73	356.12	347.77	349.05	343
	3	345.66	356.11	347.78	349.04	343.01
	4	345.67	356.14	347.8	349.01	343.04
	5	345.7	356.13	347.75	349.07	342.99
	Avg	345.68	356.14	347.78	349.03	343.01
	Std Dev	0.038341	0.035355	0.019235	0.038987	0.019235

		1	2	3	4	5
Volume		249.5117	249.9624	249.6819	249.5517	249.5718
		249.6018	249.8723	249.6519	249.6218	249.5617
		249.5317	249.8723	249.6619	249.6319	249.5818
		249.5317	249.9023	249.6819	249.6018	249.6018
		249.5718	249.8823	249.6319	249.6419	249.5517
	Avg	249.55	249.90	249.66	249.61	249.57
	Std Dev	0.036395	0.037881	0.02125	0.035699	0.019269

SPECIFIC GRAVITY ANALYSIS

Pycnometer Only		1	2	3	4	5
Reading	1	96.55	106.67	98.54	99.85	93.88
	2	96.56	106.68	98.55	99.86	93.87
	3	96.56	106.67	98.55	99.84	93.86
	4	96.57	106.67	98.55	99.84	93.87
	5	96.56	106.68	98.55	99.86	93.87
Avg		96.56	106.674	98.548	99.85	93.87
Std Dev		0.01	0.01	0.00	0.01	0.01

Temp	23	22.1	22.5	22.3	22.2	23.6
Density	0.99754	0.99775	0.99766	0.9977	0.99773	0.9974
K	0.99933	0.99954	0.99766	0.9995	0.99952	0.99919

		Mass P&S	Mass P	MP&W	Mass Bowl	MDry +B	Mdry	Gs @t	Gs @ 20		Mdry+B	Mdry	Gs@20
Reading	1	367.65	96.56	345.5485	297.28	331.6	34.32	2.808853	2.80756	S6B26	332.02	34.74	2.747477
23	2	378.15	106.674	356.0117	386.02	420.6	34.58	2.779357	2.778079	S5B21	421.11	35.09	2.708045
	3	370.02	98.548	347.6463	291.45	326.26	34.81	2.799072	2.797784	S1B4	326.8	35.35	2.722951
	4	371.76	99.85	348.8984	277.21	312.67	35.46	2.814648	2.813353	S2B9	313.09	35.88	2.754836
	5	365.02	93.87	342.8785	357.2	392.08	34.88	2.738163	2.736903	S3B12	392.4	35.2	2.694329
						[hot]					[cooled]		
TAKE 2	2	377.91	106.67	356.00	385.94	420.22	34.28	2.77229	2.770904	S1B4	420.76	34.82	2.69689
22.3	5	365.6	93.87	342.87	277.21	313.13	35.92	2.724104	2.722742	S5B21	313.45	36.24	2.68202
	1	368.39	96.56	345.54	413.47	449.26	35.79	2.76669	2.765307	S6B26	449.84	36.37	2.68964
	3	370.54	98.55	347.64	277.2	312.95	35.75	2.783015	2.781623	S2B9	313.36	36.16	2.726611
	5	364.58	93.87	342.87	297.28	331.35	34.07	2.757367	2.755989	S3B12	331.88	34.6	2.683852
						[hot]					[cooled]		
SAND	1	383.04	96.56	345.53	297.35	356.96	59.61	2.697767	2.691454	SAND	357.49	60.14	2.651778
22.5						[hot]					[cooled]		
OTTAWA	1	382.93	96.56	345.5435	297.36	357.14	59.78	2.669522	2.668241	OTTAWA	357.5	60.14	2.641839
22.2						[hot]				ASTM C778	[cooled]		
										Gs=2.65			
OTTAWA	1	383.39	96.56	345.4612	297.37	357.67	60.3	2.695433	2.69325		358.18	60.81	2.655491
23.6						[hot]					[cooled]		

Cooled Avg		Hot Avg
2.7186	S6B26	2.7864
2.6950	S5B21	2.7504
2.7099	S1B4	2.7843
2.7407	S2B9	2.7975
2.6891	S3B12	2.7464

OTTAWA SAND AVG	
HOT	COOLED
2.68074543	2.648665

APPENDIX 7. EFA RESULTS

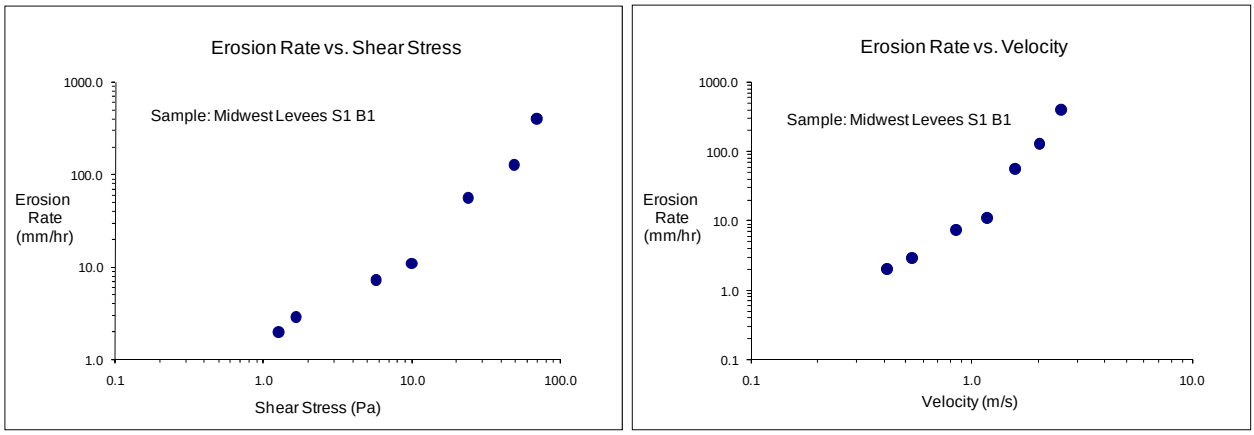

EFA RESULTS: S1B1 – WINFIELD PIN OAK

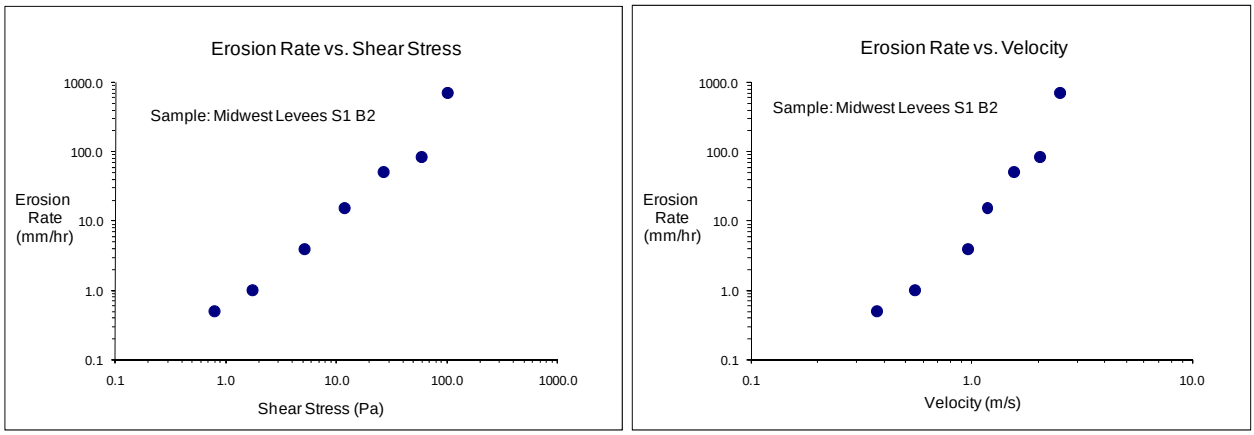

EFA RESULTS: S1B2 – WINFIELD PIN OAK

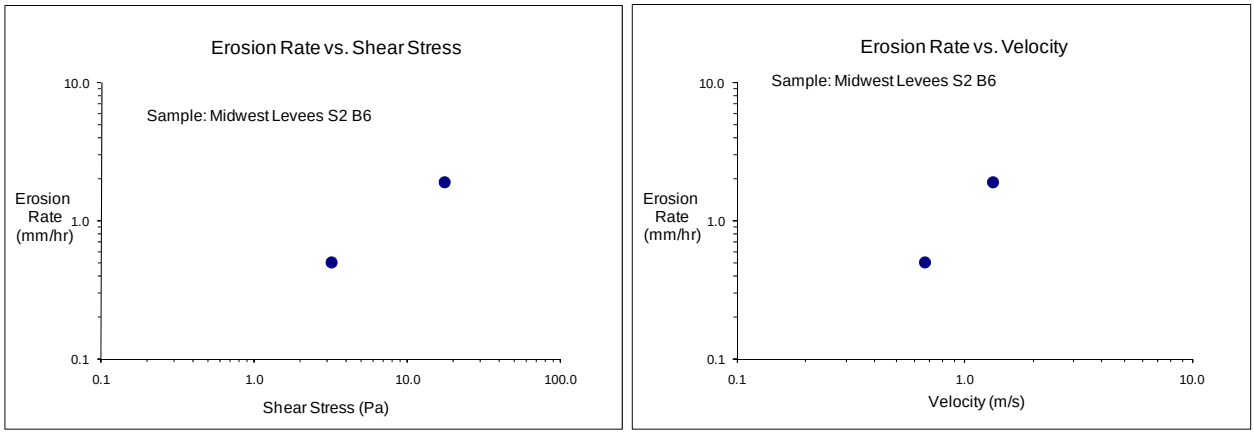

EFA RESULTS: S2B6 – BRYANTS CREEK

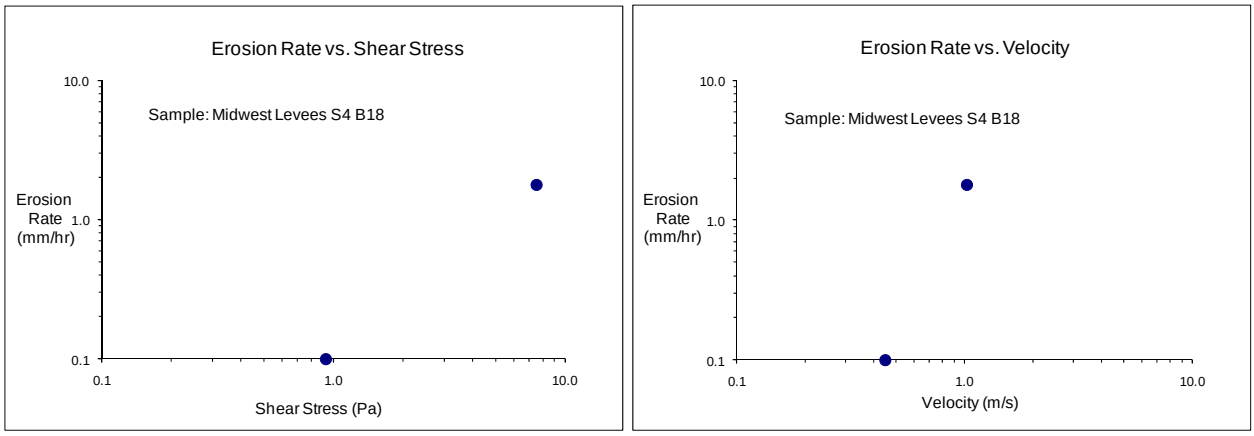

EFA RESULTS: S2B7 – BRYANTS CREEK

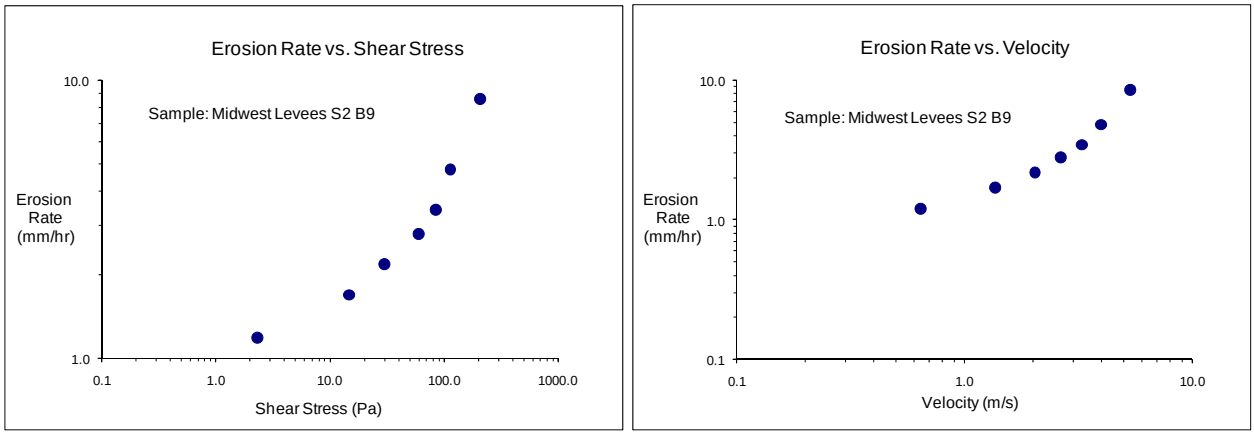

EFA RESULTS: S2B9 – BRYANTS CREEK

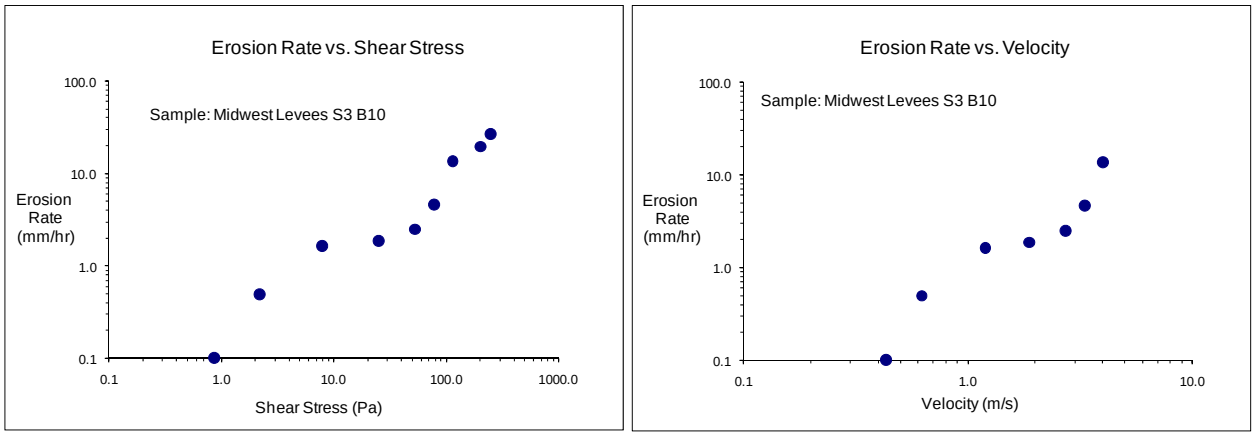

EFA RESULTS: S3B10 – BREVATOR

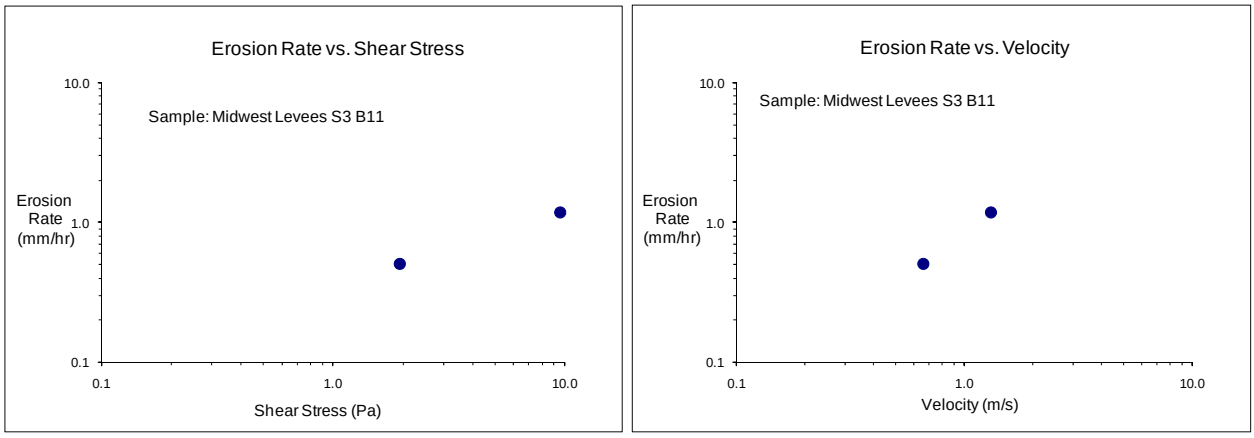

EFA RESULTS: S3B11 – BREVATOR

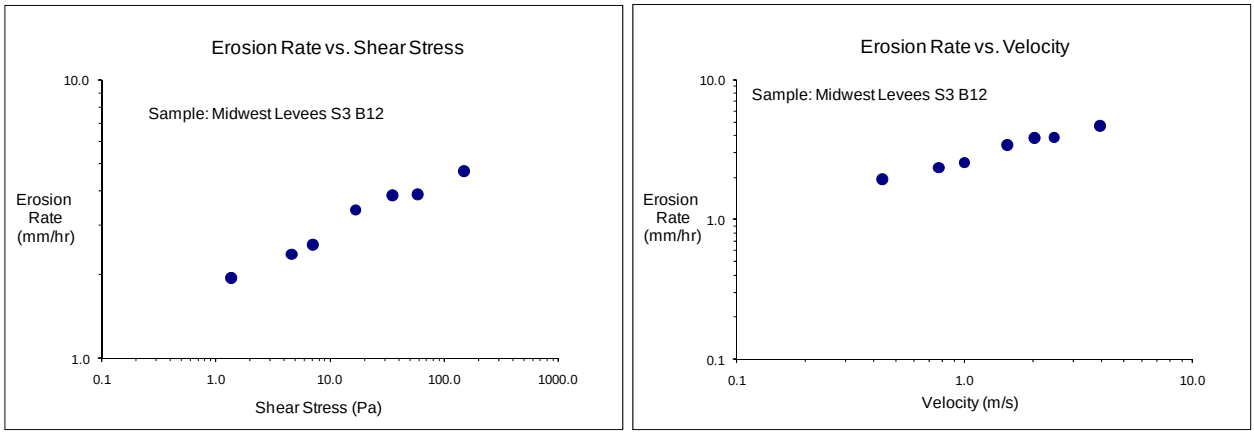

EFA RESULTS: S3B12 – BREVATOR

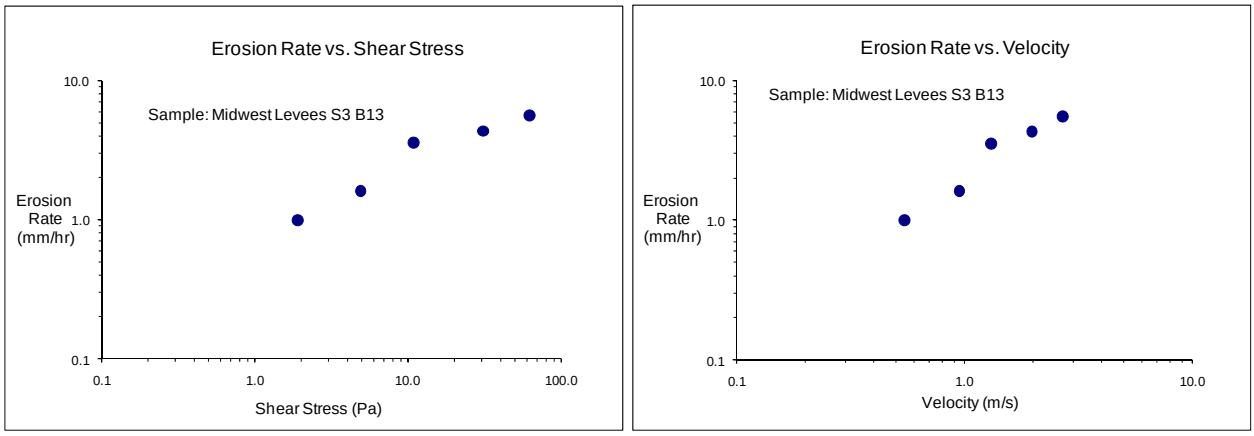

EFA RESULTS: S3B13 – BREVATOR

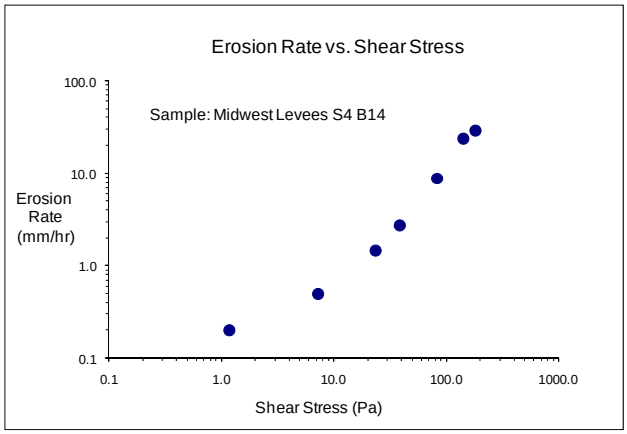

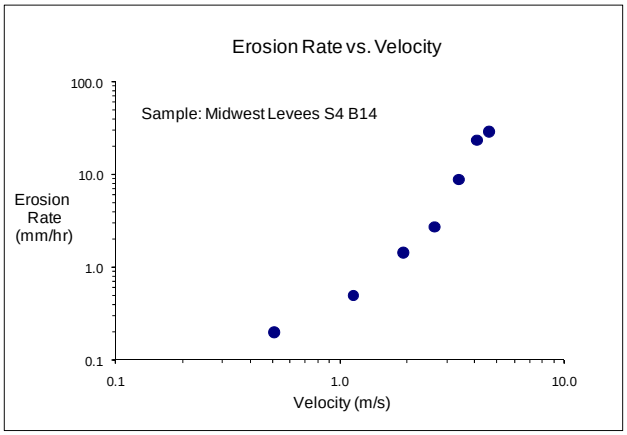

EFA RESULTS: S4B14 – KICKAPOO

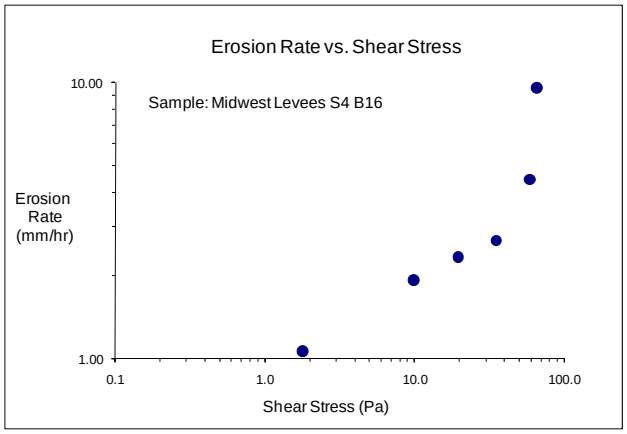

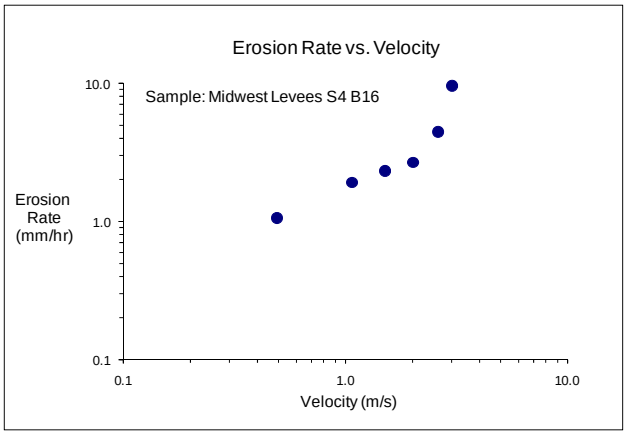

EFA RESULTS: S4B16 – KICKAPOO

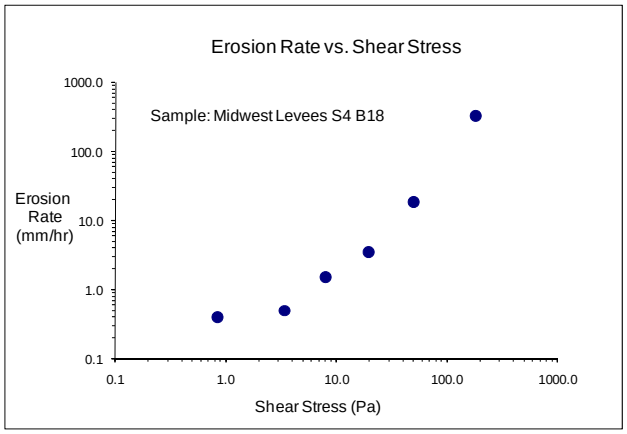

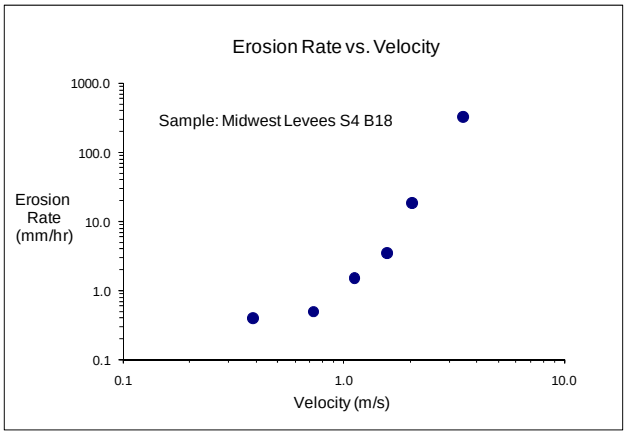

EFA RESULTS: S4B18 – KICKAPOO

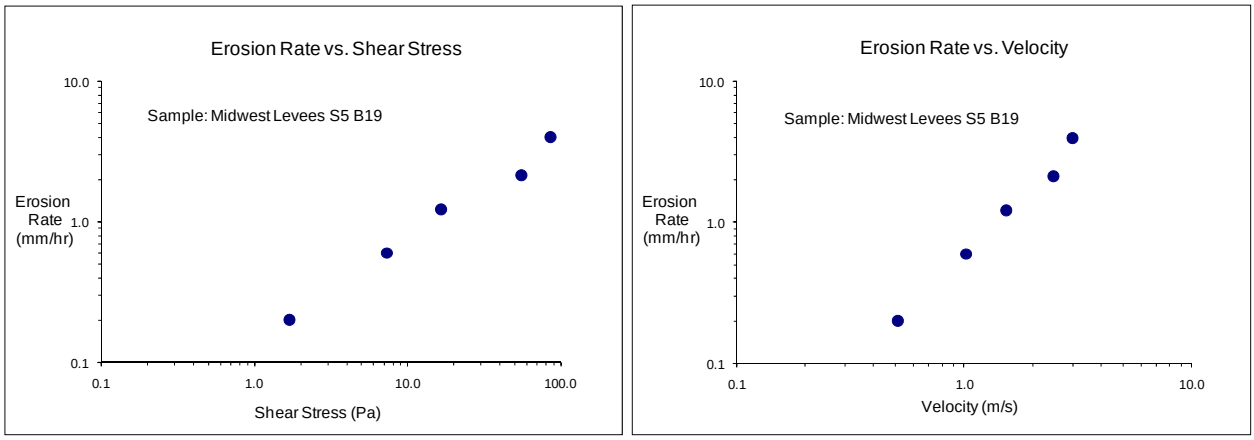

EFA RESULTS: S5B19 – NORTON WOODS

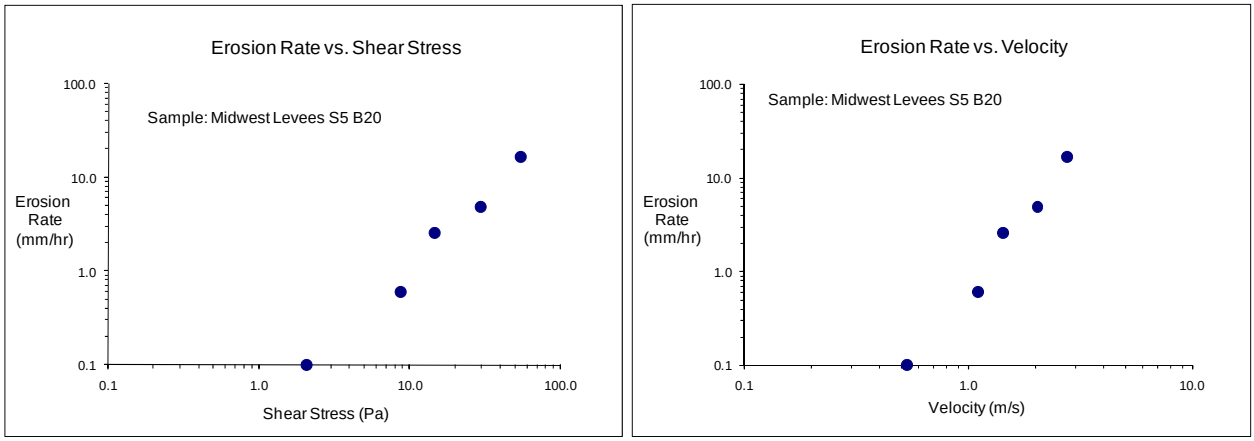

EFA RESULTS: S5B20 – NORTON WOODS

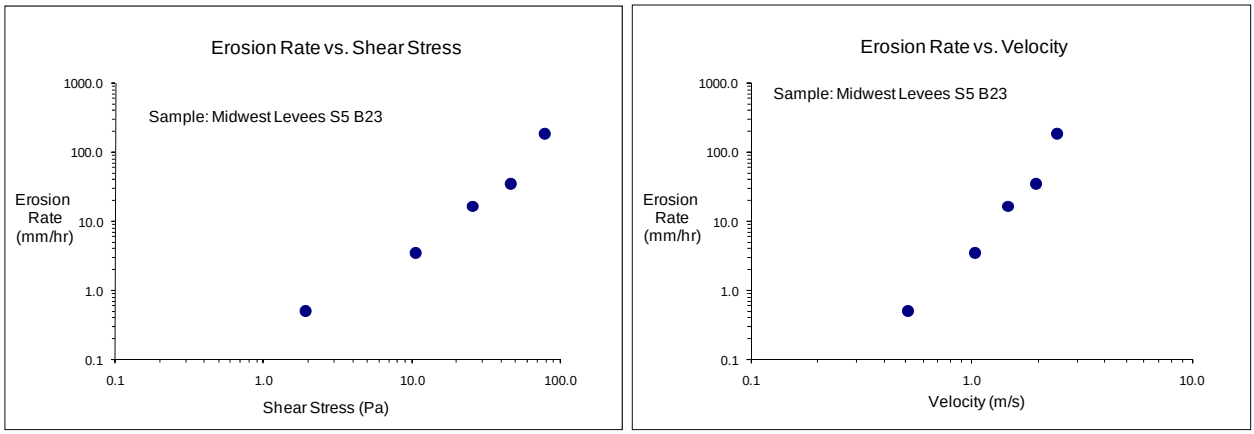

EFA RESULTS: S5B23 – NORTON WOODS

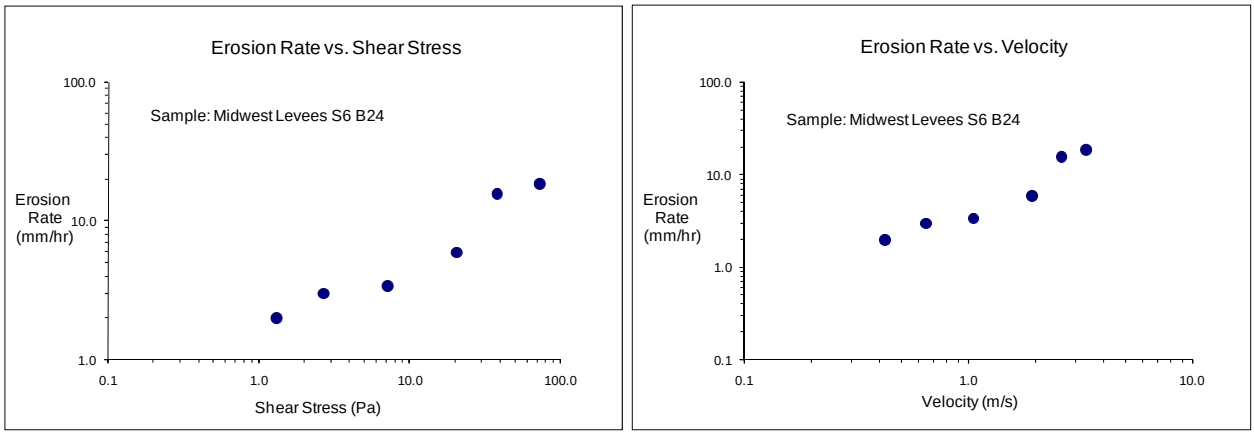

EFA RESULTS: S6B24 – INDIAN GRAVES NORTH

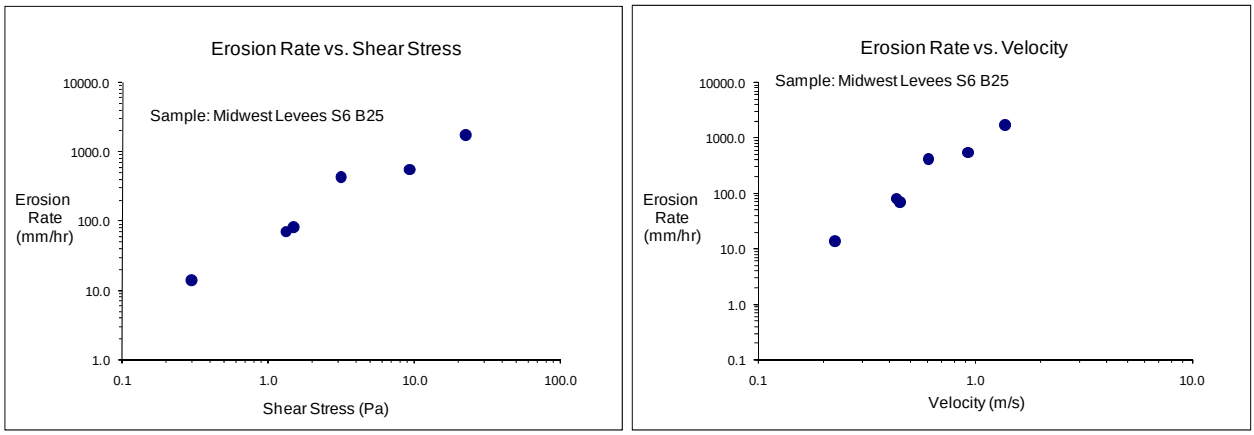

EFA RESULTS: S6B25 – INDIAN GRAVES NORTH

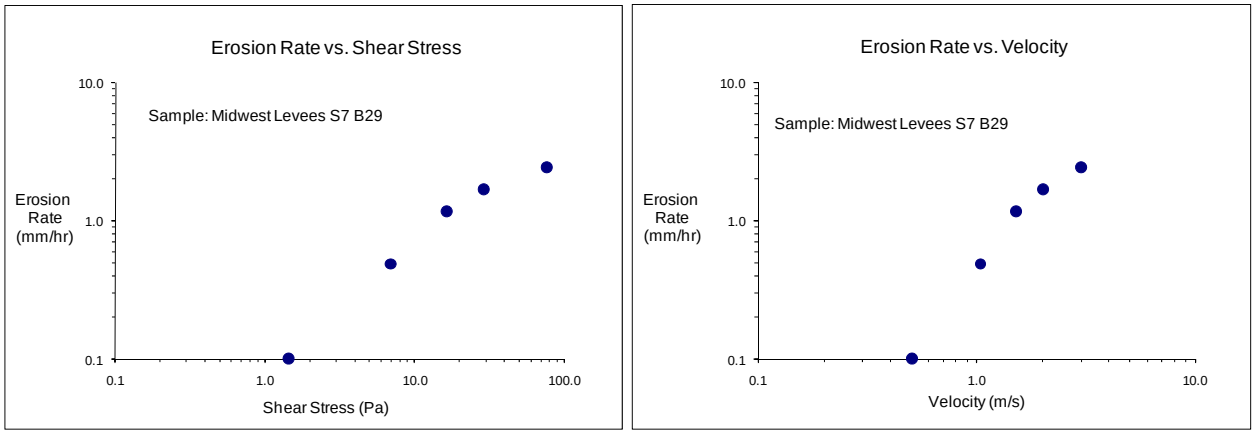

EFA RESULTS: S7B29 – INDIAN GRAVES SOUTH

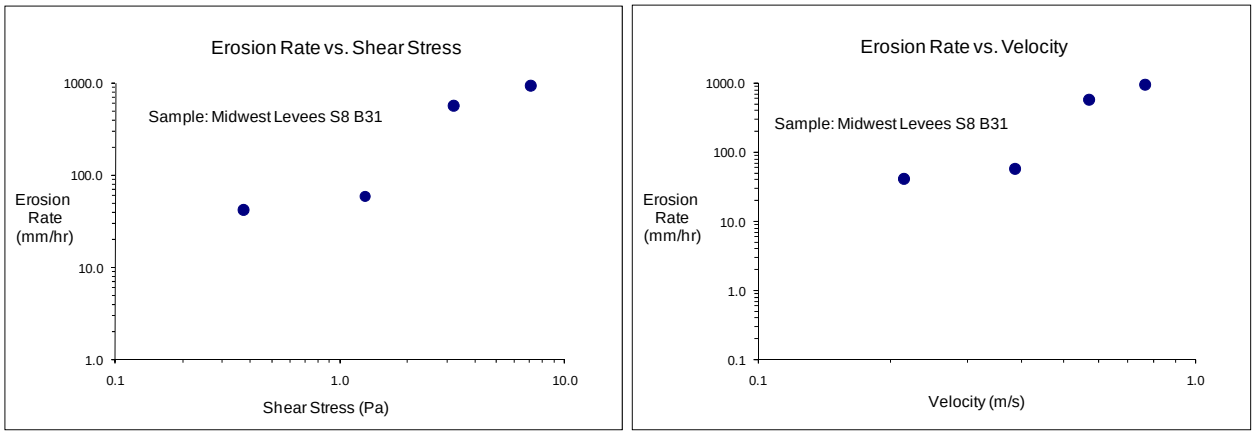

EFA RESULTS: S8B31 – TWO RIVERS

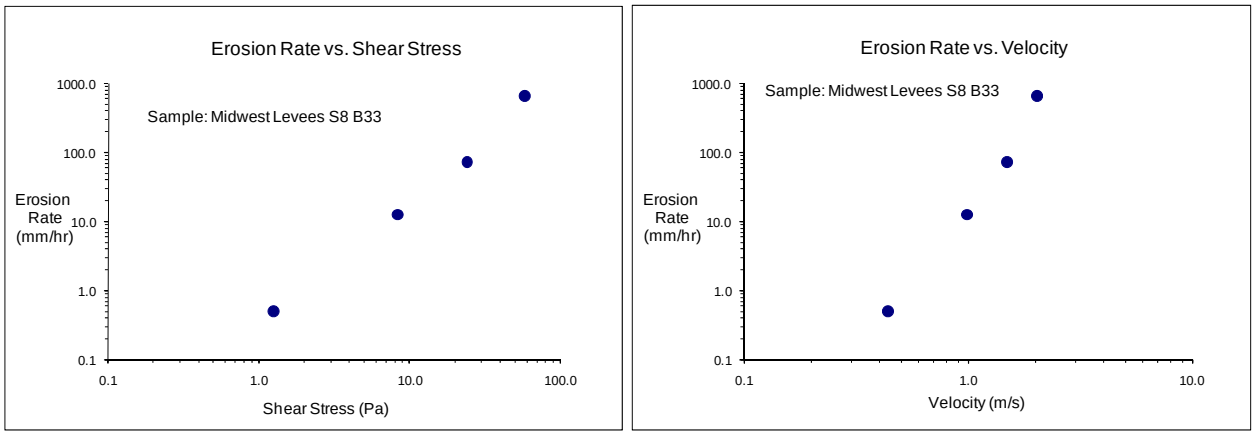

EFA RESULTS: S8B33 – TWO RIVERS

APPENDIX 8. ADDITIONAL PHOTOGRAPHS

WINFIELD – PIN OAK

Winfield breach looking South.

Winfield breach looking North.

Tree roots shown in the missing levee section.

Tree roots and scour pool at Winfield breach.

Person shown for scale of breach height.

Measuring depth of sample from levee crest height – S1B5.

Measuring depth of sample from levee crest height – S1B4.

Breach height well over 2 meters.

Eroded area looking West.

Scour area looking East at Mississippi River and bordering cliffs.

Vertically pushed sample – S1B2.

Foundation debris washed into tree.

Scour hole around tree base.

High water marks on trees.

Field opposite of levee with levee material deposited from flood waters.

Scour area from main flow path of water.

Cliffs bordering East side of the Mississippi River.

Northeast view of breach and scour area.

Southeast view of breach and scour area.

Winfield - Pin Oak S1B5

BRYANTS CREEK

Flooded field adjacent to levee.

Breach area looking East.

Breach area and temporary repaired levee looking West.

Temporary repaired levee with LIDAR station set up on top.

Boat and depth finder to record bathymetry data.

Temporary levee and scour area looking East.

Temporary levee and scour area looking West.

Accessing scour pool for bathymetry readings.

Plastic sheets placed during temporary levee repair to aid in erosion prevention.

Adjacent trees and brush washed over from flood waters.

Trees adjacent to levee section.

Recording bathymetry data in scour pool.

Edge of the East side of the breach – S2B6.

Sampling in estimated original levee core – S2B9.

Temporary repaired levee and plastic sheeting.

Scour Pool.

Pushing the tube for sample S2B7 near the levee crest.

Breach and scour area.

Levee vegetative cover – Tall Fescue.

Levee vegetative cover – Tall Fescue and Foxtail.

Scour area and adjacent field.

Trees and brush opposite major scour area showing the high force of the water.

Existing original levee material and scour area.

Existing original levee material and scour area.

LIDAR and bathymetry setup.

Oxidized soil in original levee material.

Remaining toe of original levee looking North.

Remaining toe of original levee looking East.

Zoomed in view of remaining toe of original levee.

Additional scour zone opposite of small pond.

View of both scour zones.

Breach area looking Northeast.

Levee material and scattered vegetation.

Main scour zone in background with vegetation in foreground.

Levee vegetation and scour pool in background.

Section of temporary repaired levee which has been rocked.

Levee side slope vegetative cover.

BREVATOR

Land side slope vegetative cover and corn stalks.

Vegetative cover and water shown at land side levee toe.

View of levee system.

Ponding water at land side toe.

Culvert and gate structure.

Exit point of gate structure.

Gate structure in the partial up position.

Gate structure on wet side of levee.

Area where samples S3B10 and S3B11 were taken looking North.

Vegetative cover on majority of levee section.

Side slope showing the brown grasses were killed by the floodwaters.

Scour area due to seepage through a crack in the culvert box.

Exit point of culvert 1.

Area adjacent to culvert 1 exit.

Vegetation near seepage point.

Scour hole from seepage through crack in culvert.

Scour hole.

Scour hole.

Examining scour hole.

Scour hole.

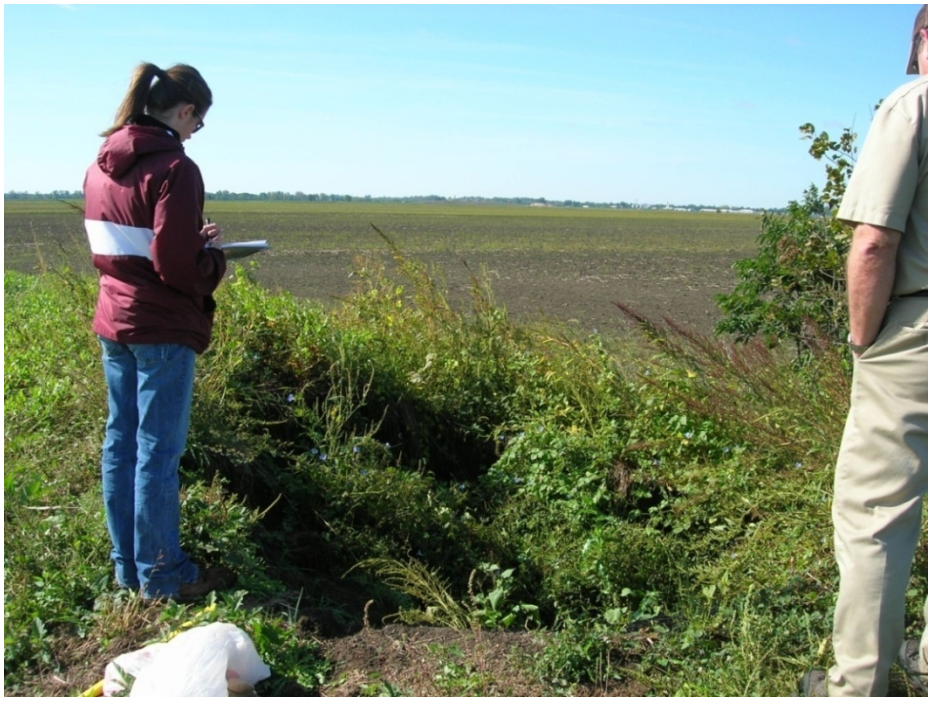

Documenting scour hole.

Vegetative cover adjacent to scour hole.

Levee system looking North.

Levee system looking South.

KICKAPOO

Kickapoo - S4B16.

Pushing the tube flush – S4B16.

Bulk samples taken at each tube sample location.

Elevated house on river side of levee.

Breach area and temporary new road path lower than adjacent levee crest.

New road path to replace the previous one located in the breach zone.

North side of breach showing trees on levee and the new road.

Breach and scour pool looking West.

Scour area looking West.

South end of levee and scour pool.

Breach and scour pool looking West.

Scour area looking Northeast.

Scour area looking West.

Showing high water marks on pole.

High water marks shown relative to elevated home.

Scour pool opposite of elevated house looking East.

Scour area looking West.

Scour pool looking West.

North end of breach showing tree roots within levee section.

Breach area looking West showing tree roots within existing levee section.

North end of breach showing trees on levee and lower road section.

View of North section of levee.

Scour pool.

Scour pool and levee looking South.

Remaining South end of levee section and scour pool.

Breach area looking West.

View of adjacent river which breaks off and later rejoins the Mississippi River.

Levee side slope vegetation.

Close up of levee vegetative cover.

Vegetative cover along levee crest and side slopes.

Flooded roadway near the Kickapoo levee.

NORTON WOODS

View of breach and adjacent field upon approach.

Breach and scour pool area looking Southeast.

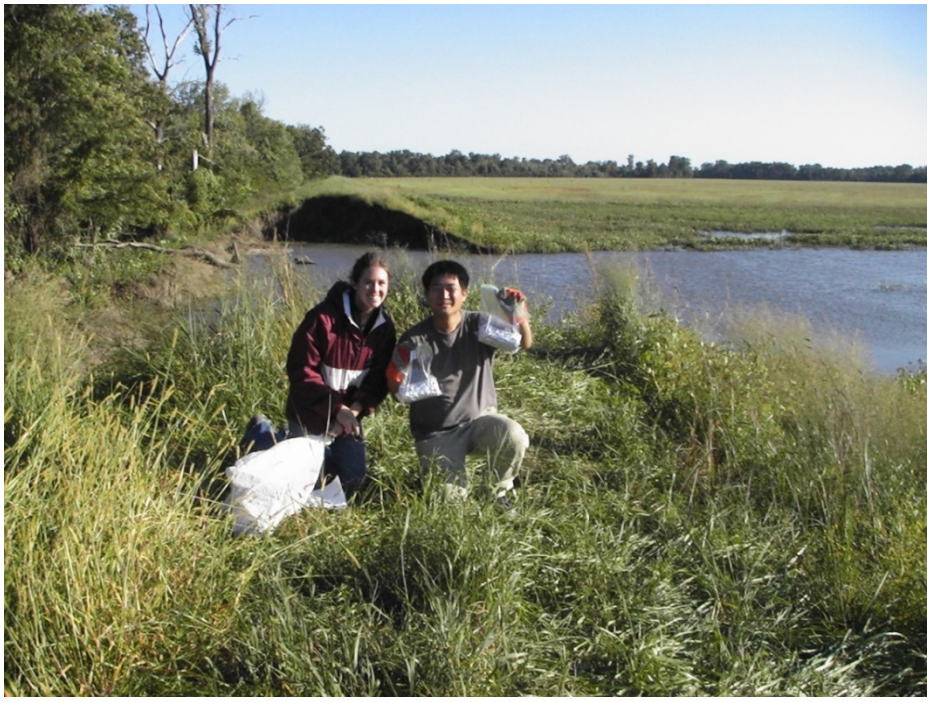

Sample collection on North end of existing levee.

Remaining toe of original levee looking Southeast.

Remaining North end of original levee.

Scour area in adjacent field.

Bathymetry readings.

Depth finder device used for bathymetry readings.

Existing levee toe on river side of the levee.

Existing material at levee toe.

Existing material at levee toe.

Vegetative cover on North side levee crest.

Vegetative cover on North side of levee side slope.

Levee vegetation on side slope.

Side slope vegetative cover.

Levee system and vegetative conditions looking North.

INDIAN GRAVES NORTH

Sand shell/clay core levee system looking South.

Levee sand shell material.

Sand shell/clay core levees looking South.

Sand ripples from flowing water.

Sand shell and clay core levee system.

Indian Graves breach zone looking South.

Indian graves breach zone looking South.

Scour pool looking West.

Sour pool looking West toward Mississippi river.

Scour pool looking Northwest.

North end of remaining levee section.

Taking bathymetry readings of scour depth.

Remaining levee material within scour zone.

Levee system looking North.

Levee system looking North showing push up.

Indian Graves North – S6B25.

Remaining North end of original levee.

Remaining North end of original levee taken from river side of levee.

Remaining North end of original levee looking East.

North end of existing levee and scour pool.

Indian Graves S6B26 taken in estimated original levee core material.

Indian Graves S6B26 taken in estimated original levee core material.

North end of remaining levee showing the location of S6B24.

Scour pool and remaining levee material.

Scour pool and remaining levee material looking West.

Trees and brush adjacent to levee shown pushed over from the rushing water.

Sand deposited into the adjacent field.

Push up height relative to person.

Existing material and vegetation.

View of North end of breach looking West.

Scour area and tree line looking Northwest.

Scour area looking West.

Scour area looking Southwest.

Breach and scour area looking South.

Scour area looking Southeast.

River side slope of levee and vegetative cover.

TWO RIVERS

Hand auger used for S8B35.

Hand auger used for S8B35.

Sample taken in existing material S8B34, expected to be native material.

View of S8B34 relative to remaining East end of levee.

Vertical sample taken at S8B33.

Scour pool looking East.

Sand shell sample taken at S8BB31.

Sand shell sample taken at S8BB31.

Breach and scour zone looking West.

Breach zone looking Southwest.

Levee breach viewed from existing East end of levee.

View of scour pool and breached levee system looking Southwest.

Rock levee armoring on land side slope of existing levee.

Temporary rock levee used to keep floodwater from carving a new path.

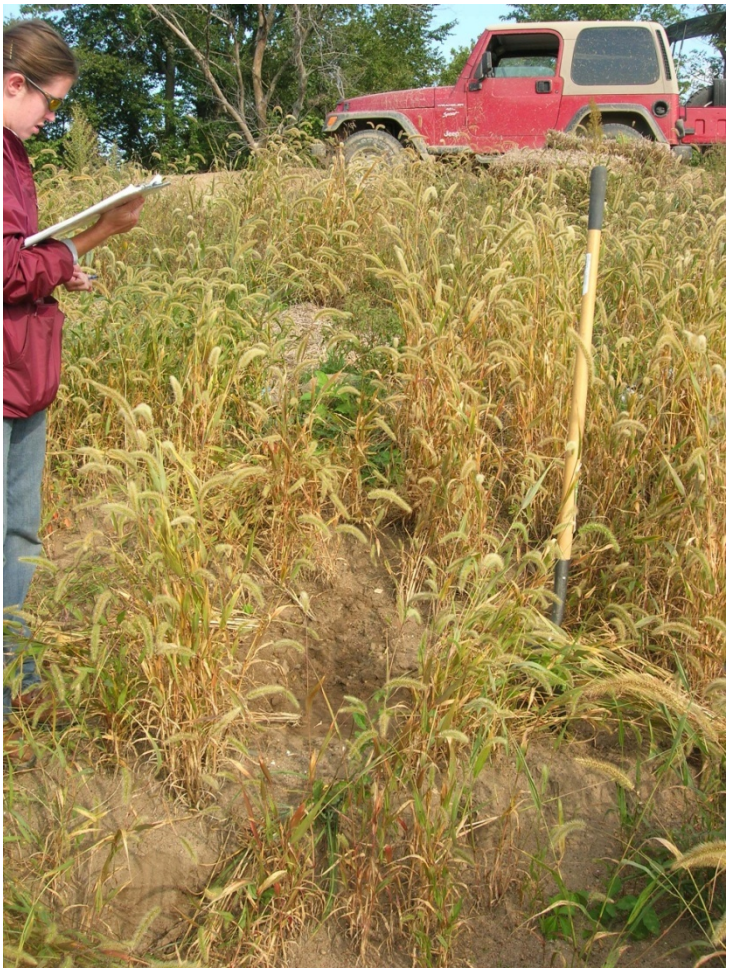

Foxtail found on the land side slope of remaining levee.

MISCELLANEOUS PHOTOGRAPHS

Other sand shell levees in the area.

Other sand shell levees in the area.

Small breach area.

Tree roots in small breach area.

Tree roots in small breach area.

Small breach area.

Small erosion area adjacent to roadway.

Small erosion area adjacent to roadway with tree roots shown.

Levee area near Lock and Dam 25.

APPENDIX 9. NRCS MISSOURI AGRONOMY SPECIFICATION

NATURAL RESOURCES CONSERVATION SERVICE
MISSOURI AGRONOMY SPECIFICATION

VEGETATION ESTABLISHMENT, HERBACEOUS SEEDING

CODE 723

GENERAL

This item of work shall consist of providing the species selection, site preparation, timing and manner of seeding, and facilitating practices for the establishment of permanent herbaceous vegetation. This specification is the criteria to be applied for the following conservation practice standards:

CONSERVATION COVER (327)
CRITICAL AREA PLANTING (342)
PASTURE AND HAYLAND PLANTING (512)
UPLAND WILDLIFE HABITAT MANAGEMENT (645)

The current version of Missouri SeedRate may be used to generate a seeding recommendation and to document the proper completion of the conservation practice. SeedRate creates a JS-AGRON-25 form that will be the record of planning and application for the conservation practice standards listed above. If SeedRate is not available, simple computations will be used to calculate the seeding rate for each species.

SPECIES SELECTION

Adapted Species - Species selected must be adapted to the site (soils, Pasture Suitability Group, wet soil conditions, drought tolerance, etc.) and expected growing conditions as well as the expected use and management of the vegetation. When erosion control is a primary purpose, the mixture must contain at least 60 percent perennial grasses.

Mixtures are usually desired over monoculture plantings. Where the primary use is for grazing management, legumes shall not exceed 50 percent of the mixture. If the primary planned use is hay production and the site is highly erodible, the mixture shall not exceed 75 percent legumes.

Where wildlife habitat is the resource objective, refer to the UPLAND WILDLIFE HABITAT MANAGEMENT (645) conservation practice standard for criteria.

Site Conditions – Plant species and cultivars shall be selected based on:

1) climatic conditions such as annual precipitation, seasonal precipitation distribution, length of growing season, humidity levels, temperature extremes, wind, and solar radiation;
2) soil condition and position attributes such as pH, available water holding capacity, aspect, drainage class, inherent fertility, salinity or alkalinity, flooding or ponding, and levels of toxic elements that may be present such as selenium or aluminum; and
3) resistance to disease and insects common to the site or location.

Use – Select species and cultivars that are desirable for the planned use and address the resource concerns.

Companion Crop – A companion crop may be established prior to or at the same time as a permanent seeding of grass, forbs, and/or legumes. The companion crop will be selected and managed to minimize competition with the permanent seeding. Approved companion crops are:

1) Redtop may be planted on erodible sites along with warm season grasses that are slow to establish. A seeding rate not to exceed 1.0 pound per acre pure live seed may be added to the full seeding rate of the planned warm season grasses, forbs, and legumes.

2) Spring Oats may be planted at a rate not to exceed 25 pounds per acre of high quality, relatively weed-free seed (feed-grade oats are suitable if they are clean). When the permanent seed is drilled in one operation along with the oats, the planting depth will be ½ -inch or less. Note: Oats seeded in the fall will winter-kill and not mature. Oats seeded earlier in the year must not be allowed to mature because of competition with the permanent seeding species. Clip, harvest, or flash-graze when the oats are in the milk stage; manage the stand as often as necessary to keep the canopy from becoming competitive.

3) Winter Wheat may be used ONLY where topsoil has been removed and the permanent vegetation is being established on subsoils. Wheat may be planted at a rate not to exceed 25 pounds per acre of high quality, relatively weed-free seed. Clip, harvest, or flash-graze when the wheat is in the milk stage; suppress the wheat cover as often as necessary to keep the canopy from becoming competitive with the permanent species.

SEEDING RATES

1) Based on Use – The seeding rates vary for each separate species as determined by the pure live seed needed for select uses. Refer to Table 1 for the specific base rates required for each of the seeding practices. The four conservation practices supported by this specification have four separate and distinct multipliers for the base rates in Missouri.

The CONSERVATION COVER (327) practice standard requires a seeding rate that represents 100 percent of the desired plant cover for erosion control. The base rate will be adequate for erosion control while providing quality habitat for wildlife. The base rate also applies to seedings under the UPLAND WILDLIFE HABITAT MANAGEMENT (645) practice standard unless there is an exception for specific mixes in the standard.

The CRITICAL AREA PLANTING (342) practice standard is usually applied on cut and fill construction sites. Herbaceous vegetation cannot be successfully established on these sites with the CONSERVATION COVER (327) or PASTURE AND HAYLAND PLANTING (512) practices. The CRITICAL AREA PLANTING rate is designed to supply additional seed to the site and allow natural selection to reduce the number of surviving seedlings. The seeding rate is 200 percent of the base rate in Table 1 (base rate times 2).

The PASTURE AND HAYLAND PLANTING (512) practice standard requires a seeding rate for the establishment of a production field either for grazing or hay harvesting. This 512 rate is the desired seeding rate for establishing adequate ground cover on relatively undisturbed sites and represents 125 percent of the base rate (base rate times 1.25).

Reduced seeding rates for the UPLAND WILDLIFE HABITAT MANAGEMENT (645) practice may be applied on non-highly erodible lands (NHEL) that do NOT have an erosion problem. Erosion rates from wind and water must remain within tolerable limits (T) after seeding, and concentrated flow erosion must be controlled. The seeding rate is 75 percent of the base rate (base rate times 0.75). This option for reduced seeding rates does not apply to wildlife field borders. Refer to Table 1 in the UPLAND WILDLIFE HABITAT MANAGEMENT (645) standard for the recommended species and seeding rates of wildlife field border.

These base rates and specific adjustments by conservation practice (practice multiplier) will be used whenever the soil, site conditions, equipment and management conditions are adequate for the establishment of the desired stand of grass, legumes, and forbs under each of the seeding practices.

TABLE 1: BASE SEEDING RATES - POUNDS PURE LIVE SEED PER ACRE

Species	Base Rate (100%)	Erosion Control Rating	Wildlife Habitat Rating	Wet Soil Tolerance Rating	Drought Tolerance Rating
Cool Season Legumes:					
Birdsfoot Trefoil	5.0	Fair	Fair	Low	Medium
Alsike Clover	3.2	Good	Good	High	Low
Ladino Clover	3.0	Good	Fair	Medium	Low
Red Clover	6.1	Fair	Fair	None	Low
Kura Clover	7.0	Fair	Fair	None	Low
Alfalfa	7.5	Fair	Excellent	None	High
Warm Season Legumes:					
Common Lespedeza[1/]	7.5	Poor	Excellent	Low	High
Illinois Bundleflower	14.5	Fair	Excellent	None	Medium
Partridge Pea[1/]	26.8	Fair	Excellent	None	Medium
Roundhead Bushclover	6.3	Poor	Good	None	High
Showy Ticktrefoil	10.0	Fair	Excellent	None	High
Cool Season Grasses:					
Canada Wildrye	15.3	Good	Excellent	Low	Medium
Virginia Wildrye[2/]	15.0	Good	Excellent	Medium	Medium
Kentucky Bluegrass	2.2	Good	Good	Low	Low
Orchardgrass	4.2	Fair	Excellent	None	Medium
Perennial Ryegrass	7.3	Poor	Good	None	Low
Redtop	1.7	Good	Good	Medium	Low
Reed Canarygrass	4.8	Excellent	Poor	High	Medium
Smooth Brome	8.0	Excellent	Fair	Low	Medium
Tall Fescue	8.0	Excellent	Poor	Low	High
Timothy	3.1	Good	Excellent	Low	Low
Warm Season Grasses:					
Bermudagrass	2.1	Excellent	Poor	Low Medium	High
Big Bluestem[2/]	8.0	Fair	Good	Medium	High
Oldworld Bluestem	2.5	Good	Poor	None	High
Composite Dropseed	2.3	Fair	Good	None	High
Eastern Gamagrass[2/]	8.0	Poor	Good	Medium	Medium
Indiangrass[2/]	7.8	Fair	Excellent	Low	Medium
Little Bluestem[2/]	6.4	Good	Excellent	None	High
Sideoats Grama[2/]	7.5	Good	Excellent	None	Medium
Southern Crabgrass[1/]	2.2	Poor	Poor	Low	Low
Switchgrass[2/]	4.7	Good	Good	Medium	Medium
Warm Season Forbs:					
Grayhead Coneflower	3.6	Poor	Good	None	Medium
Pale Purple Coneflower	16.4	Poor	Fair	None	Medium
Ox-eye Falsesunflower	11.3	Poor	Fair	None	High
Wild Bergamot	1.4	Poor	Fair	High	Low

[1/] These species are annual species; plant early in the growing season to allow seedset to occur. Check to make sure that the use of these species meets the local environmental conditions and any program requirements prior to planning in the seed mixture.

[2/] Locally adapted cultivars or ecotypes of these native species will be planted in Missouri. Refer to Table 2 of this specification for a listing of acceptable cultivars.

TABLE 2: NATIVE GRASS SPECIES CULTIVARS FOR USE IN MISSOURI

Grass Species	Cultivar	Area of Adaptation	Source of Collection
Native Cool Season Grasses			
Virginia Wildrye	Cuivre River	Statewide	Eastern Missouri
	O'Ma'Ha	North of I-70	East and Northeast Nebraska
Native Warm Season Grasses			
Big Bluestem	Rountree	Statewide	Western Iowa
	OZ-70	South of I-70	Southern Missouri, Southern Illinois, Northern Arkansas, and Eastern Oklahoma
	Kaw	Statewide	Eastern Kansas
	Pawnee	North of I-70	North Central Kansas and South Central Nebraska
	Champ	Statewide	North Central Nebraska
Little Bluestem	Aldous	Statewide	Eastern Kansas
	Cimarron	South of I-70, sandy sites only	Southwest Kansas and Oklahoma Panhandle
	Camper	North of I-70	North Central Kansas and South Central Nebraska
Eastern Gamagrass	Pete	Statewide	Kansas and Oklahoma
	PMK-24	Statewide	Kansas and Oklahoma
Sideoats Grama	El Reno	Statewide	Central Oklahoma
	Trailway	Statewide	North Central Nebraska
Indiangrass	Rumsey	Statewide	Southern Illinois
	Osage	Statewide	Eastern and Central Kansas and Oklahoma
	Cheyenne	Statewide	Western Oklahoma
	Nebraska 54	North of I-70	Nebraska
Switchgrass	Cave-In-Rock	Statewide	Southern Illinois
	Blackwell	Statewide	North Central Oklahoma
	Alamo	Lowland Sites – South of I-70	South Central Texas
	Kanlow	Lowland Sites - Statewide	East Central Oklahoma
	Pathfinder	North of I-70	North Central and South Central Nebraska
	Trailblazer	North of I-70	Selection from Pathfinder
	Nebraska 28	North of I-70	North Central Nebraska

2) Based on Method – When it is possible to properly place the seed and obtain good seed to soil contact, less seed is needed on the site to establish a full stand. This condition is represented by the base rate in Table 1 times the rate adjustment factor for each separate practice.

Certain broadcast seeding methods only offer a fair chance of adequate stand establishment. Broadcast planting methods that do not ensure uniform seed distribution and provide adequate seed to soil contact (firm soil and shallow placement of seed) meet the criteria. This site condition is represented by a method adjustment factor times the base rate in Table 1. The broadcast rates should be the base rate times 1.50 (50 percent increase in seed for the broadcast method) times practice adjustment factor of 0.75, 1.0, 1.25, or 2.0 for the specific conservation practice standard that applies.

NRCS MOFOTG
April 2008

3) Based on Mix – The amount of seed needed will vary based on the percentage of each species in the desired mix that is planned and applied to the site. Use SeedRate to calculate the amount of seed needed to apply the minimum seed to meet the practice criteria. Each conservation practice requires a different minimum amount of seed due to the different conservation purposes. Declare the desired percentage for each species in SeedRate.

An example of the seeding rate calculations for Use, Method, and Mixture follows the formula: Base Rate from Table 1 x Use (%) x Method(%) x Mix (%) = Seeding Rate. For seeding Birdsfoot Trefoil as a Critical Area Planting using broadcast methods and 20 percent of the mix, the formula would be:

5.0 PLS pounds/acre x 200% x 150% x 20% = 3.0 pounds/acre seeding rate

4) Based on Existing Stand – SeedRate allows a planner to calculate the seed needed to complete an interseeding practice. Interseeding is a process to plant a portion of the desired stand without removing or destroying all the established plants currently occupying the site. The interseeding rate will be based on 50 percent of the stand surviving site preparation and 50 percent of the stand being established from seed.

SITE PREPARATION

Weed Control – Competitive vegetation will be controlled on the site prior to seeding. Mechanical, chemical, or biological means will be employed to remove undesirable vegetation. Herbicides and/or tillage may be used to retard the growth of existing cover in an interseeding operation.

Surface Conditions – Prior to seedbed preparation, shape the site sufficiently to permit the use of tillage and seeding equipment. A firm, weedfree seedbed is required for all seedings. The seedbed will be made firm by rolling or culti-packing prior to seeding. The seedbed is firm if you can walk on it without sinking in more than one-half inch.

On highly erodible soils where soil erosion is likely to occur, particular attention to seedbed preparation and/or to the use of companion crops for protection during the erosive establishment period is encouraged. A no till establishment procedure should be used. Herbicides will be needed to control existing vegetation and suppress weedy competition. Always follow the herbicide label. The seedbed will be made firm by culti-packing or rolling prior to seeding when tillage is used for site preparation.

Where erosion is not a concern, a clean-tilled seedbed may be used. Firm the seedbed prior to planting grasses, legumes, or forbs.

For no till seeding into an existing pasture or hayland field, prescribed burning, herbicides, heavy grazing, close mowing, or some combination of these treatments will be used to weaken the existing stand, control weedy species, and/or prevent seed production during the growing season prior to seeding. Timing of herbicide applications shall be based on the growth stage of the targets species or specie being controlled. Adequate time for decomposition of root crowns should be provided so that good soil to seed contact may be obtained at planting time

When planning a no till seeding into heavy crop residue, remove some of the residue cover prior to planting. This may be accomplished by grazing, baling, shredding, or prescribed burning. Drills equipped with residue management attachments or aggressive coulters may be required to cut through or move heavy residue.

Surface Conditions for Construction or Critical Areas – Cover fine textured soils (greater than 40% clay) and coarse textured soils (sands, loamy sands) with a minimum of six (6) inches of topsoil after construction is complete. Topsoil shall be the highest quality surface soil available at

the site. Topsoil shall be free of brush, rocks, and other large materials to the extent that it is not detrimental to the establishment and maintenance of desired plants. Soil materials from drained ponds or surface material from an erosive area will not be used. If available topsoil material is no better than the material to be covered, do not apply topsoil.

Prepare a seedbed, incorporate lime and fertilizer, and plant or cover seed with mechanical operations on slopes where it is safe to operate equipment. Use appropriate methods to prepare a seedbed, control weeds, incorporate fertilizer, and achieve seed to soil contact of the permanent seeding or temporary cover where slopes are too steep for safe vehicle operation. All slopes must be smooth and free of rills or gullies.

Moisture in Soil Profile – Soil moisture shall be adequate for the germination and establishment of the desired vegetation. Plan seedings to be planted prior to the portion of the year when adequate precipitation is likely to occur. Follow required planting dates in Table 3 discussed below.

SOIL FERTILITY

Follow the criteria in the NUTRIENT MANAGEMENT (590) practice standard to apply fertilizer and soil amendments for stand maintenance.

The CRITICAL AREA PLANTING (342) practice standard allows an option to use all-inclusive fertilizer and limestone application rates for stand establishment. If seeding is being applied for wildlife habitat, see the UPLAND WILDLIFE HABITAT MANAGEMENT (645) practice standard.

The following criteria apply to any seeding standard where a soil test will be used to determine the fertility and effective neutralizing material needed for establishment of the vegetative stand:

- the application of fertilizer and soil amendments shall be based on a current soil test (less than 4 years old) taken since the last application of lime or fertilizer. Applied amounts shall be within the larger of ten (10) percent or ten (10) pounds per acre of the recommended amounts. Requirements for the application of nitrogen, phosphate, and potash may be waived when the soil test recommendation for each individual nutrient is less than 25 pounds per acre and the total amount of fertilizer material to be applied is less than 50 pounds per acre. Agricultural lime requirements of 600 pounds or less of effective neutralizing material (ENM) may be waived.
- on grass and legume plantings where no nitrogen is recommended and only where the vendor cannot provide a fertilizer blend without nitrogen, up to 30 pounds per acre of nitrogen may be applied.
- if lime or fertilizer is required for establishment, applications shall be appropriately placed and timed prior to seeding to be effective. Lime and fertilizer shall be applied prior to seeding and incorporated during tillage operations. To establish a legume crop, lime shall be applied at least three months prior to planting. On no till plantings containing legumes where incorporation with tillage cannot be accomplished, lime shall be applied at least 6 months prior to the seeding date. This advance time requirement (3 to 6 months prior to seeding) may be waived for mixes containing:
  1) alfalfa when the pH is equal to or more than 5.7 (salt) or 6.2 (water);
  2) warm season legumes when the pH is equal to or more than 5.2 (salt) or 5.7 (water); or
  3) all other legumes when the pH is equal to or more than 5.5 (salt) or 6.0 (water).

  Applications of liming materials in excess of 4 tons per acre can be applied in split applications with approximately half of the lime requirement being properly placed and timed prior to the seeding and the remainder applied within 2 years following the planting date.

PLANTING DATES

Specific planting dates are required for successful completion of vegetation establishment. Refer to Table 3 for acceptable and optimal planting dates.

TABLE 3: PLANTING DATES[1/]

Plantings with a dominance of:	Spring Planting Period	Summer or Fall Planting Period	Dormant Season Planting Period
Cool Season Grasses and Legumes in Northern Missouri[1/]:			
Acceptable Dates	Mar 16 – May 31	Aug 01 – Oct 15[2/]	Dec 01 – Mar 15
Optimal Dates	Mar 16 – Apr 30	Aug 16 – Sep 15	
Cool Season Grasses and Legumes in Southern Missouri[1/]:			
Acceptable Dates	Mar 01 – May 15	Aug 16 – Oct 15[2/]	Dec 16 – Feb 29
Optimal Dates	Mar 01 – Apr 15	Sep 01 – Sep 30	
Warm Season Grasses, Legumes, and Forbs in Northern Missouri[1/]:			
Acceptable Dates	Mar 16 – Jun 30		Nov 16 – Mar 15
Optimal Dates	Apr 16 – Jun 15		
Warm Season Grasses, Legumes, and Forbs in Southern Missouri[1/]:			
Acceptable Dates	Mar 01 – Jun 15		Dec 01 – Feb 29
Optimal Dates	Apr 01 – May 31		

[1/] Planting dates are based on plant suitability zones. Northern Missouri is all counties north of Bates, Henry, Benton, Morgan, Moniteau, Cole, Osage, Gasconade, Franklin, and St. Louis Counties. Southern Missouri is all counties including and south of those listed.

[2/] Mixtures containing legume species will be planted by September 15 in Northern Missouri and the Ozark Highlands and September 30 in the rest of Southern Missouri.

Critical Area Planting Date Exemption - A special exemption on seeding dates may be used with CRITICAL AREA PLANTING (342) mixtures of cool-season grasses. These mixtures may be planted from June 1 through July 31 in Northern Missouri or from May 16 through August 15 in Southern Missouri only when the following conditions exist:

1) soil moisture on the site is at field capacity at time of seeding;
2) planting rates are increased by an additional 50 percent
3) an adequate, firm, and weed-free seedbed has been prepared;
4) seed is planted at a depth of ¼ inch or less with a grassland drill or similar quality seeding equipment; and
5) mulching material is applied following the planting operation according to the MULCHING (484) practice standard.

PLANTING METHOD

Drill or Planter Methods – Plant the seed mixture with a grassland drill, grain drill, or packer seeder at the proper depth. Drills shall be capable of properly metering and placing the size and kind of seed being planted. Desired seeding depth shall be between 1/8 and 1/4 inch for all species except eastern gamagrass which will be planted to a depth of 1 to 1½ inches. Set the drill or seeder at shallower depths (1/8 inch) for small seeds or planting on heavier soils. Plant large seeds at the deeper depth (1/4 inch) or when planting on sandy soil.

Broadcast Planting Methods – Spread the seed on the soil surface in any manner that applies adequate seed to the entire area. Rolling or packing after spreading the seed will be required for any broadcast seeding that occurs outside of the dormant seeding period. Seed may be broadcast on the soil surface without a mechanical operation to cover the seed where it is too steep for safe vehicle operation or where surface obstructions hinder mechanical operations.

SEED QUALITY

Only viable, high quality and adapted seed will be used. All seed shall have a current seed test within 10 months of the planting date that lists germination, purity, and hard seed as a percentage for determining pure live seed and lists the percent of weed seed present that meets State seed quality law standards. Seed must be clean and relatively free of weed seed and other contaminants. Seed that has become wet, moldy, or otherwise damaged in transit or storage is not acceptable. Certified seed is preferred but not required.

INOCULATION OF LEGUMES

Legume seed shall be inoculated with the proper, viable *Rhizobium* bacteria species prior to planting. Pre-inoculated seed shall be planted prior to the expiration date on the inoculum tag or be re-inoculated with the appropriate inoculum within 24 hours prior to seeding. Inoculated seed will not be exposed to direct sunlight.

Inoculation of legumes may be waived when a current pasture inventory (JS-AGRON-24 or similar inventory) shows that the legume species to be seeded occupies more than 5 percent of the vegetative cover on the site.

SPECIAL PLANTING METHODS

Sprigging – Planting sprigs, rhizomes, stolons, or cuttings of bermudagrass, prairie cordgrass, and reed canarygrass may provide quicker and easier cover than planting seed. The planting rate will be a minimum of 20 bushels of sprigs per acre. The following steps will be required:

1) Plant only in a moist, fertile, weed-free seedbed.
2) Plant reed canarygrass (only in the spring) and bermudagrass (spring or summer season by June 15) to take advantage of available precipitation and the growing season. Plant prairie cordgrass only with dormant rhizomes in early spring or as vegetative rooted plants by May 31.
3) Plant pure live sprigs as soon as possible after harvesting within the same day if possible or within 24 hours of digging the sprigs.
4) Plant sprigs at least 2 inches deep to ensure placement in soil moisture, but leave tips of green leaves above the ground.
5) Firm soil around the sprigs to obtain good soil to sprig contact.
6) Control weeds with selective herbicides applied immediately after planting.
7) Fertilize to hasten good ground coverage as soon as new stolons or rhizomes are evident.

Sodding for CRITICAL AREA PLANTING (342) – Apply fertilizer and lime according to a current soil test. Incorporate lime and fertilizer to a depth of 2 or 3 inches, and firm the site with a cultipacker, roller, or similar tool. The site must be relatively smooth to apply sod.

Wet the soil surface to a depth of 2 inches or more prior to laying the sod. Only moist, fresh sod shall be used. Lay sod as soon as possible after delivery to the site. Begin laying the sod from the lower end of any slope. On steep slopes the use of ladders will speed up the laying operation and limit damage to the sod.

Sod strips shall be laid at right angles to the flow of water. Stagger the joints between sod pieces. Fill any open joints with topsoil. Tamp and roll laid sod to ensure a solid contact of the sod rootmass with the moist soil surface.
On steep sites or when anticipating overland flow, sod shall be held in place by woven wire, wooden pegs, wire staples, or similar material designed for this use. Pegs or staples will be a minimum of 10 inches long.

Recently laid sod should be irrigated until moisture penetrates the soil layer beneath the sod.

Apply sod during the growing season and no later than October 1.

ESTABLISHMENT PERIOD

Weed Control – Weeds and companion crops will be controlled by herbicides, mowing, clipping, or controlled grazing prior to becoming competitive with the species planted. Competing species should be controlled depending upon their density, prior to becoming 12 inches tall, but always before viable seed set. Weed control procedures will be performed as often as necessary to ensure that stands are not reduced due to excessive competition.

VITA

Michelle Lee Bernhardt
Zachry Dept. of Civil Engineering
Texas A&M University
College Station, TX 77843

Email Address: mlb02c@tamu.edu

Education: B.S., Civil Engineering, Texas A&M University, May 2008
Focus: Structural Engineering
M.S., Civil Engineering, Texas A&M University, December 2009
Focus: Geotechnical Engineering

Certifications: Engineer in Training (E.I.T.) License

Experience:
Department of Civil Engineering – Dr. Jean-Louis Briaud, Texas A&M University, College Station, TX - Research Assistant (Oct. 2008 – Oct. 2009)
Project: 2008 Midwest Levee Failure Investigation

- Participated in Field Reconnaissance and sample collection
- Conducted Laboratory testing to determine soil index properties and erosion properties
- Analyzed field and laboratory findings

U.S. Army Corps of Engineers – Les Perrin, Southwest District office, Fort Worth, TX – Engineering Intern

Teaching Assistantship – Department of Civil Engineering – Dr. Giovanna Biscontin, Texas A&M University - Introduction to Geotechnical Engineering

- Instructed and assisted with laboratory testing
- Worked with undergraduate students on soil mechanics problems and laboratory procedures

Activities and Leadership: Geo-Institute President - TAMU GSO
Tau Beta Pi Engineering Honor Society
Chi Epsilon Engineering Honor Society
American Society of Civil Engineers (ASCE) Member